CT- and MR-Guided Interventions in Radiology

Andreas H. Mahnken
Jens Ricke
Editors

Springer

CT- and MR-Guided Interventions in Radiology

Andreas H. Mahnken · Jens Ricke (Eds.)

CT- and MR-Guided Interventions in Radiology

Springer

Editors

Dr. Andreas H. Mahnken
Department of Diagnostic Radiology
University Hospital
RWTH Aachen University
Pauwelsstraße 30
52074 Aachen, Germany
mahnken@rad.rwth-aachen.de

Dr. Jens Ricke
Department of Radiology
and Nuclear Medicine
University Hospital Magdeburg
Leipziger Straße 44
39120 Magdeburg, Germany
jens.ricke@med.ovgu.de

ISBN 978-3-540-73084-2 e-ISBN 978-3-540-73085-9

DOI 10.1007/978-3-540-73085-9

Library of Congress Control Number: 2008939149

Cover design: Frido Steinen, eStudio Calamar, Spain
Production: le-tex publishing services oHG, Leipzig

Printed on acid-free paper

9 8 7 6 5 4 3 2 1

springer.com

Foreword

Interventional radiology has become a most attractive subspecialty in radiology owing to continuous growth over the past 30 years. New instruments, innovative techniques, and new imaging modalities were the basis of such a remarkable development. Computed tomography (CT), magnetic resonance (MR) imaging, and ultrasound have emerged as important techniques for nonvascular interventions such as percutaneous biopsy, drainage, ablation, and neurolysis. Different organs, diseases, and lesions can be approached in this way for the treatment and management of tumors, fluid collections, and pain. The various chapters in this book cover a comprehensive spectrum of nonvascular interventions guided by CT or MR imaging and reflect the high expertise of European specialists in this field. A special section is devoted to interventional oncology as an emerging field of radiology.

I am particularly happy that Andreas Mahnken from our institution at Aachen University is continuing our traditional focus in interventional radiology and has realized this project together with Jens Ricke from Magdeburg.

I am sure that there is a need and an important market for such a book. Interventional radiologists should recognize and find their role in this promising clinical and scientific field. This book will contribute its share and represents a most valuable source of information and guidance. I extend my best wishes for the great success of this textbook and I am sure it will have a place on the shelf of every interventional radiologist.

Aachen University Hospital

Rolf W. Günther MD
Chairman of the Department of Radiology

Contents

Part IV Economics in Interventional Radiology

Contributors

Reto Bale, MD
SIP – Department for Microinvasive Therapy
Department of Radiology
Medical University Innsbruck
Anichstraße 35
6020 Innsbruck, Austria
E-mail: reto.bale@i-med.ac.at

Alexander Beck MD
Charité Campus-Virchow-Klinikum
Klinik für Strahlenheilkunde
Augustenburger Platz 1
13353 Berlin, Germany
E-mail: alexander.beck@charite.de

Philipp G.C. Begemann, MD
Department of Diagnostic
and Interventional Radiology
University Medical Center Hamburg-Eppendorf
Martinistraße 52
20246 Hamburg, Germany
E-mail: p.begemann@uke.uni-hamburg.de

Oliver Beuing, MD
Department of Neuroradiology
University Hospital Magdeburg
Leipziger Straße 44
39120 Magdeburg, Germany
E-mail: oliver.beuing@med.ovgu.de

Deniz Bilecen, MD
Interventional Radiology
University of Basel
Petersgraben 4
4031 Basel, Switzerland
E-mail: dbilecen@uhbs.ch

Mathias Bosch, MD
Boston Scientific Corp. – Germany
Daniel-Goldbach-Straße 17–27
40880 Ratingen, Germany
E-mail: mathias.bosch@bsci.com

Roland Bruening, MD
Roentgeninstitut Asklepios Klinik Barmbek
Ruebenkamp 220
22999 Hamburg, Germany
E-mail: r.bruening@asklepios.com

Arno Buecker, MD, MSc
Department of Diagnostic
and Interventional Radiology
University Hospital Saarland
Kirrbergerstraße 1
66421 Homburg, Germany
E-mail: arno.buecker@uks.eu

Philipp Bruners, MD
Applied Medical Engineering
Helmholtz-Institute
RWTH Aachen University
Pauwelsstraße 20
52074 Aachen, Germany
E-mail: bruners@hia.rwth-aachen.de

Stephan Clasen, MD
Department of Diagnostic
and Interventional Radiology
Eberhard-Karls-University Tübingen
Hoppe-Seyler-Straße 3
72076 Tübingen, Germany
E-mail: stephan.clasen@med.uni-tuebingen.de

Markus Düx, MD
Department of Radiology and Neuroradiology
Krankenhaus Nordwest
Steinbacher Hohl 2–26
60488 Frankfurt am Main, Germany
E-mail: duex.markus@khnw.de

Katrin Eichler, MD
University of Frankfurt/Main
Department of Diagnostic
and Interventional Radiology
Theodor-Stern-Kai 7
60590 Frankfurt am Main, Germany
E-mail: k.eichler@em.uni-frankfurt.de

Roman Fischbach, MD
Department of Radiology
Asklepios Klinik Altona
Paul-Ehrlich-Straße 1
22763 Hamburg, Germany
E-mail: Roman Fischbach@ak-altona.lbk-hh.de

Thomas Helmberger, MD
Department of Diagnostic
and Interventional Radiology and Nuclear Medicine
Klinikum Bogenhausen
Englschalkinger Straße 77
81925 Munich, Germany
E-mail: thomas.helmberger@kh-bogenhausen.de

Susanne Hengst, MD
Charité Campus-Virchow-Klinikum
Klinik für Strahlenheilkunde
Augustenburger Platz 1
13353 Berlin, Germany
E-mail: susanne.hengst@charite.de

Dietrich Henzler, MD, PhD
Departments of Anesthesia and Critical Care
Dalhousie University, Halifax
Health Science Centre
1278 South Park St., 10 West Victoria
Halifax, Nova Scotia, B3H 2Y9, Canada
Email: mail@d-henzler.de

Jan Hoeltje, MD
Roentgeninstitut Asklepios Klinik Barmbek
Ruebenkamp 220
22999 Hamburg, Germany
E-mail: j.hoeltje@asklepios.com

Ralf Torsten Hoffmann, MD
Department of Clinical Radiology
Großhadern Campus
Ludwig-Maximilians-University Munich
Marchioninistraße 15
81377 Munich, Germany
Email: thoffma@med.uni-muenchen.de

Christian Hohl, MD
Institute of Diagnostic and Interventional Radiology
Helios Klinikum Siegburg
Ringstrasse 49
53721 Siegburg, Germany
E-mail: christian-hohl@helios-kliniken.de

Dagmar Honnef, MD
Department of Radiology
University Hospital, RWTH Aachen University
Pauwelsstraße 30
52074 Aachen, Germany
E-mail: honnef@rad.rwth-aachen.de

Norbert Hosten, MD
Department of Diagnostic Radiology
and Neuroradiology
Ernst Moritz Arndt University
Ferdinand-Sauerbruch-Straße
17485 Greifswald, Germany
E-mail: hosten@uni-greifswald.de

Augustinus Ludwig Jacob, MD
Interventional Radiology
University of Basel
Petersgraben 4
CH-4031 Basel, Switzerland
E-mail: ajacob@uhbs.ch

Kerstin Jungnickel, PhD
Department of Radiology and Nuclear Medicine
University Hospital Magdeburg
Leipziger Straße 44
39120 Magdeburg, Germany
E-Mail: kerstin.jungnickel@med.ovgu.de

Bruno Kastler, MD, MSc
Department of Radiology
and Laboratoire d'imagerie et d'ingéniérie
University of Besançon
CHU Minjoz
25030 Besançon, France
E-mail: b.kastler@noos.fr

Marcus Katoh, MD
Department of Diagnostic
and Interventional Radiology
University Hospital Saarland
Kirrbergerstraße 1
66421 Homburg, Germany
E-mail: marcus.katoh@uks.eu

Sebastian Kos, MD, MBA
Interventional Radiology
University Hospital Basel
Petersgraben 4
CH-4031 Basel, Switzerland
E-mail: koss@uhbs.ch

Gabriele A. Krombach, MD
Department of Diagnostic Radiology
University Hospital, RWTH Aachen University
Pauwelsstraße 30
52074 Aachen, Germany
E-mail: krombach@rad.rwth-aachen.de

Thomas Lehnert, MD
Department of Diagnostic
and Interventional Radiology
University of Frankfurt/Main
Theodor-Stern-Kai 7
60590 Frankfurt am Main, Germany
E-mail: thomas.lehnert@kgu.de

Andreas Lubienski, MD
Radiology Health Care Center Minden
Ringstraße 44
32427 Minden, Germany
E-mail: andreas_lubienski@yahoo.com

Martin G. Mack, MD
Department of Diagnostic
and Interventional Radiology
University of Frankfurt/Main
Theodor-Stern-Kai 7
60590 Frankfurt am Main, Germany
E-mail: martinmack@arcor.de

Andreas H. Mahnken, MD, MBA
Department of Diagnostic Radiology
University Hospital, RWTH Aachen University
Pauwelsstraße 30
52074 Aachen, Germany
E-mail: mahnken@rad.rwth-aachen.de

Dirk Meister
University of Frankfurt/Main
Department of Diagnostic
and Interventional Radiology
Theodor-Stern-Kai 7
60590 Frankfurt am Main, Germany
E-mail: dirk@housefiles.de

Peter Messmer, MD
Consultant Trauma Surgeon
Emergency and Trauma Center
Rashid Hospital
PO Box 4545
Dubai, U.A.E.
E-mail: peter.messmer@aoalumni.org

Bernard Meyer, MD
Charité – Campus Benjamin Franklin
Klinik und Hochschulambulanz
für Radiologie und Nuklearmedizin (CC6)
Hindenburgdamm 30
12200 Berlin, Germany
E-mail: Bernhard.Meyer@Charite.de

Konrad Mohnike, MD
Department of Radiology and Nuclear Medicine
University Hospital Magdeburg
Leipziger Straße 44
39120 Magdeburg, Germany
E-mail: konrad.mohnike@med.ovgu.de

Michael F Murphy, MD
Anesthesiology
Dalhousie University
10 West Victoria, 1278 South Park St.
Halifax, Nova Scotia, B3H 2Y9, Canada
Email: michael.murphy@cdha.nshealth.ca

Philippe L. Pereira, MD
Department of Radiology and Nuclear Medicine
Klinikum am Gesundbrunnen
Am Gesundbrunnen 20–26
74078 Heilbronn, Germany
Email: philippe.pereira@slk-kliniken.de

Uta Preim, MD
Department of Radiology and Nuclear Medicine
University Hospital Magdeburg
Leipziger Straße 44
39120 Magdeburg, Germany
E-Mail: uta.preim@med.ovgu.de

Ulf Redlich, MD
Department of Radiology and Nuclear Medicine
University Hospital Magdeburg
Leipziger Straße 44
39120 Magdeburg, Germany
E-Mail: ulf.redlich@med.ovgu.de

Jens Ricke, MD
Department of Radiology and Nuclear Medicine
University Hospital Magdeburg
Leipziger Straße 44
39120 Magdeburg, Germany
E-mail: jens.ricke@med.ovgu.de

Christian Rosenberg, MD
Department of Diagnostic Radiology
and Neuroradiology
Ernst Moritz Arndt University
Ferdinand-Sauerbruch-Straße
17485 Greifswald, Germany
E-mail: christian.rosenberg@uni-greifswald.de

Arnd-Oliver Schäfer, MD
Department of Diagnostic Radiology
University Hospital Freiburg
Hugstetter Straße 55
79106 Freiburg, Germany
E-Mail: arnd-oliver.schaefer@uniklinik-freiburg.de

Günther Schneider, MD
Department of Diagnostic
and Interventional Radiology
University Hospital Saarland
Kirrbergerstraße 1
66421 Homburg, Germany
E-mail:
dr.guenther.schneider@uniklinikum-saarland.de

Jens-Peter Staub, MD
Department VIII – Radiology
Bundeswehrkrankenhaus Ulm
Oberer Eselsberg 40
89081 Ulm, Germany
E-mail: jens.staub@t-online.de

Christoph Gregor Trumm, MD
Department of Clinical Radiology
Großhadern Campus
Ludwig-Maximilians-University Munich
Marchioninistraße 15
81377 Munich, Germany
Email: christoph.trumm@med.uni-muenchen.de

Bernd Turowski, MD
Department of Neuroradiology
Institute of Diagnostic Radiology
Heinrich-Heine-University Düsseldorf
Moorenstraße 5
40225 Düsseldorf, Germany
E-mail: bernd.turowski@uni-duesseldorf.de

Thomas J. Vogl, MD
Department of Diagnostic
and Interventional Radiology
University of Frankfurt/Main
Theodor-Stern-Kai 7
60590 Frankfurt am Main, Germany
E-mail: t.vogl@em.uni-frankfurt.de

Markus Völk, MD
MVZ Theresientor
Stadtgraben 10
94315 Straubing, Germany
E-mail: markus.voelk@web.de

Frank K. Wacker, MD
The Russell H. Morgan Department of Radiology
and Radiological Science
Johns Hopkins School of Medicine
600 North Wolfe St.
Baltimore, MD 21287, USA
E-mail: fwacker1@jhmi.edu

Gerlig Widmann, MD
SIP – Department for Microinvasive Therapy
Department of Radiology
Medical University Innsbruck
Anichstraße 35
6020 Innsbruck, Austria
E-mail: gerlig.widmann@i-med.ac.at

Gero Wieners, MD
Department of Radiology and Nuclear Medicine
University Hospital Magdeburg
Leipziger Straße 44
39120 Magdeburg, Germany
E-mail: gero.wieners@med.ovgu.de

Joachim Ernst Wildberger, MD
Department of Radiology
University Hospital Maastricht
PO Box 5800
NL 6202 AZ Maastricht, The Netherlands
E-mail: j.wildberger@mumc.nl

Kai Wilhelm, MD
Department of Radiology
University Hospital Bonn
Sigmund-Freud-Straße 25
53127 Bonn, Germany
E-mail: kai.wilhelm@ukb.uni-bonn.de

Part I
Basics

Pre- and Postinterventional Imaging

1

Marcus Katoh, Günther Schneider and Arno Bücker

Contents

1.1 Introduction

Every intervention starts with the visualization of the target organ or lesion and the path to the chosen target. In principle, any imaging modality that gives images with adequately high spatial resolution and contrast can be used for pre- and postinterventional imaging. The image contrast needed encompasses visualization of the target lesion as well as the surrounding anatomy, particularly critical structures along the intended needle path. This is a prerequisite for defining the ideal path to the lesion and for monitoring the interventional procedure. During the intervention real-time imaging would be the ideal solution, but near real-time imaging usually will suffice.

X-ray fluoroscopy provides real-time images with high spatial resolution. Until now, X-ray fluoroscopy in combination with iodine contrast medium application has been regarded as the gold standard for vascular intervention. It is also used for guiding musculoskeletal procedures such as percutaneous osteosynthesis or arthrography. For other indications, however, X-ray fluoroscopy is less suited to monitor interventions owing to the low intrinsic soft-tissue contrast and the lack of three-dimensional information in projection images.

Similar to X-ray fluoroscopy, ultrasound offers very fast images with high spatial resolution. In addition, contrast agents can be applied to improve image contrast or to acquire dynamic perfusion information (Wells 2006; Delorme et al. 2006). However, the field of view is limited. Furthermore, bone and air may impair the visualization of the target as they prevent ultrasound penetration. Moreover, ultrasound monitoring of hyperthermal ablation procedures is limited owing to air bubbles caused by vaporization. Therefore, ultrasound guidance is mostly used for superficial lesions that can be easily reached without the risk of injuring adjacent organs or vessels. Dedicated interventional ultrasound probes with a central perforation may be used, which allow the accurate delineation and positioning of dedicated interventional devices.

In contrast, cross-sectional imaging modalities such as computed tomography (CT) and magnetic resonance (MR) imaging provide excellent overviews with the capability of three-dimensional reconstructions due to the volumetric data set. Intestinal or vascular structures can be clearly identified. In addition, the same slice orientation can be imaged multiple times, which in turn allows for precise planning of the path to the lesion even in deeper areas of the body. This chapter deals with general considerations for pre- and postinterventional imaging and provides the basic knowledge for successful peri-interventional CT and MR imaging.

Mahnken/Ricke (Eds.), *CT- and MR-Guided Interventions in Radiology*

1.2 Materials and Techniques

1.2.1 Preinterventional CT Imaging

For preinterventional CT imaging, one should consider the patient's orientation and position if the lesion site is already known; e.g., the patient should be moved to the left of the CT gantry if the right liver lobe is going to be targeted. In addition, the table should be lowered to gain space above the patient. This allows for use of longer instruments and avoids collision of instruments with the gantry during controls, which is of particular interest in obese patients. Oral or rectal contrast medium application should be used to delineate adjacent intestinal structures; however, barium-containing contrast agents should not be used so as to avoid potential complications such as barium peritonitis (de Feiter et al. 2006). In addition, intravenous contrast medium application might be necessary (sometimes even repetitively) to visualize arterial and venous vessels or to better delineate the lesion. Contrast medium is also invaluable to identify hyperperfused lesions or vascular tumors, which may represent contraindications for biopsies (Fig. 1.1).

In general, routine CT protocols and reconstructions, which are used for daily diagnosis, can be used for preinterventional CT imaging.

For thoracic and abdominal lesions, a spiral CT scan should be performed with a minimum slice thickness of approximately 5 mm and an increment of approximately 4 mm. For cervical and peripheral bone or soft-tissue lesions the reconstructed slice thickness and increment should not exceed 3 and 2 mm, respectively. Sequential CT techniques are not recommended to avoid misregistration of the lesion owing to varying breathing volumes and consequently different organ and lesion positions in-between different breath-holds. The breathing commands should be the same as required for later intervention. In practice, examinations during expiration are more favorable as expiration allows the patient to hold the position of the diaphragm at the same level more easily.

After scanning, different reconstructions are required depending on the lesion site. For thoracic lesions, e.g., data need to be reconstructed using soft-tissue (widow width approximately 350 HU; level approximately 50 HU) as well as lung (widow width approximately 1500 HU; level approximately −600 HU)

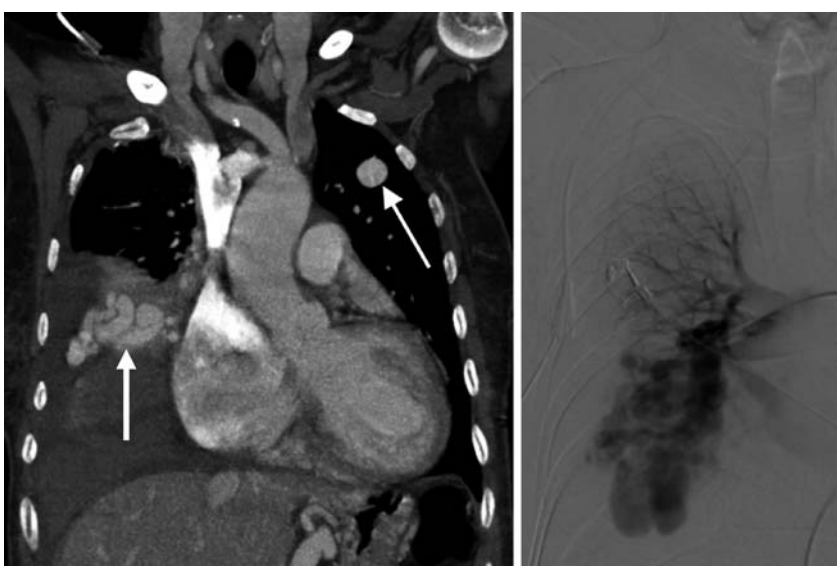

Fig. 1.1 Coronal reconstruction of an intravenous contrast-enhanced spiral computed tomography (CT) data set demonstrating multiple pulmonary arteriovenous malformations (*arrows*) in a 75-year-old female patient (*left*). Prior to this control CT, the patient underwent CT-guided biopsy (without contrast medium application) on the right side as a solid tumor was suspected. This intervention led to massive bleeding. The corresponding X-ray angiography shows nicely the extension of the arteriovenous malformation (*right*)

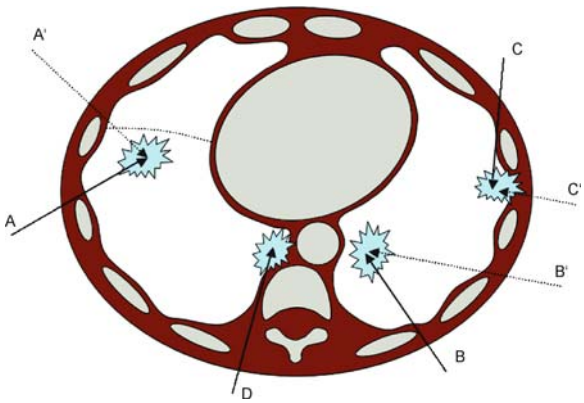

Fig. 1.2 A cross-sectional image at the level of the heart illustrating some aspects that should be considered to reach pulmonary lesions. The pleura should be passed only once (*A*) instead of multiple times (*A′*). Another access should be chosen (*B*) if a vessel is located behind the lesion (*B′*). For subpleural lesions, an indirect access is more favorable (*C*) than a direct path (*C′*) to decrease the risk of a pneumothorax. Passing the pleura can often be completely avoided for mediastinal and paramediastinal/paravertebral lesions (*D*)

algorithms to evaluate the proximity to vessels and pleural space.

For thoracic lesions, one may consider the following points (Fig. 1.2):

- For pulmonary lesions, the cranial border of the ribs should be used as an entry point to avoid injury of the intercostal artery.
- The pleura (including the horizontal and oblique fissures) should be passed only once in order to keep the risk of pneumothorax as low as possible.
- Lesions in front of a vessel should be targeted from the side (tangential orientation of the biopsy path toward the vessel) to avoid accidental vessel injury.
- Subpleural lesions should be targeted tangentially to the pleura. Furthermore, an aspiration biopsy should be performed rather than a cutting biopsy to avoid pneumothorax.
- Mediastinal and paramediastinal/paravertebral lesions may be reached without passing the pleura; mediastinal widening by injection of NaCl solution can be helpful.

For abdominal lesions, one may consider the following points:

- In the case of subphrenic lesions, one should avoid passing the pleura.
- Subcapsular liver lesions should be targeted indirectly (passing normal liver parenchyma first) to avoid abdominal bleeding.
- Renal and especially splenic lesions are prone to bleeding.
- The stomach can be passed if a lesion is located behind it.

For lesions of the upper or lower extremities, one may consider the following points:

- If a malignant lesion is expected, only the compartment in which the lesion is located should be opened/passed.
- The path of intervention, e.g., for biopsy should be the same as the potential operative access in order to allow easy resection of the biopsy path in the case of malignant lesions prone to metastases along the biopsy path.

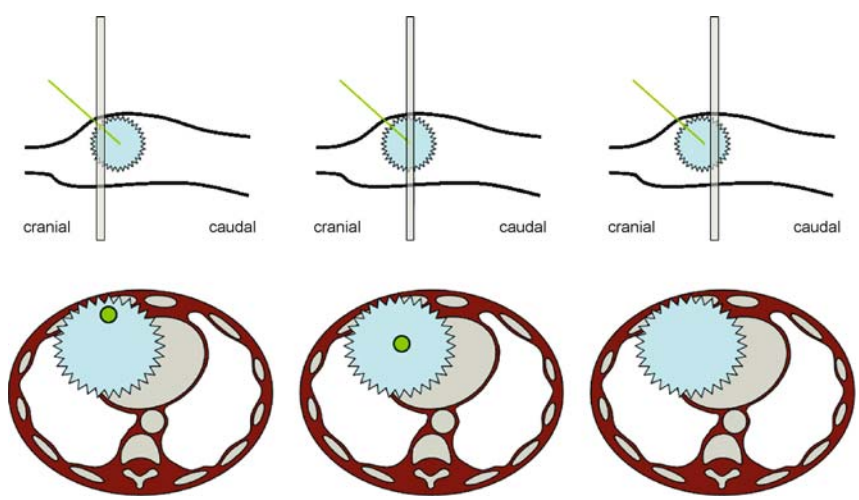

Fig. 1.3 The position of a needle (*green line*) inside a target lesion (*blue*, *upper row*). Repositioning of the axial slices (*gray*) will allow one to exactly locate the tip of an interventional instrument on the axial images (*lower row*). Note the fact that an axial slice through the tip of a needle will look very similar

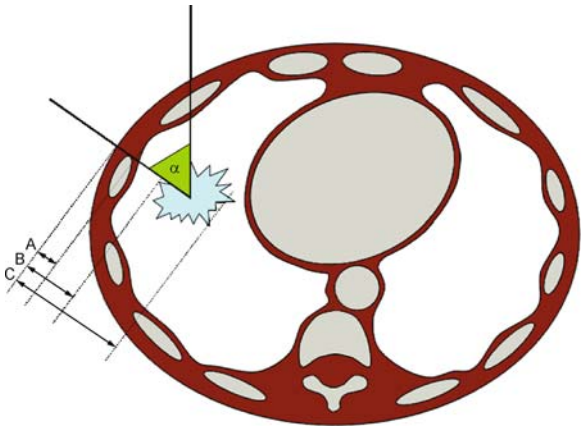

Fig. 1.4 A cross-sectional image at the level of the heart demonstrating the measurements that should be performed before intervention: angle between a vertical line (alternatively a horizontal line) and a line connecting the entry point and the lesion (α), the distance from the skin to the pleura (or peritoneum) (*A*), the distance from the skin to the beginning of the lesion (*B*), and the distance from the skin to the end of the lesion (*C*)

In general, intervention is simplified if the access to the lesion is planned parallel to the gantry as the whole instrument can be visualized at once on one axial slice. Otherwise, the instrument (particularly the tip of the instrument) must be identified by acquiring multiple axial slices along the instrument (Fig. 1.3).

If an adequate image slice was chosen for intervention, the following points should be determined (Fig. 1.4):

- Slice position.
- Angle between a horizontal/vertical line and a line connecting the entry point and the lesion.
- Distance from the skin to the pleura, peritoneum, liver capsule, or any other structure in need of thorough local anesthesia.
- Distance from the skin to the beginning of the lesion.
- Distance from the skin to the end of the lesion.

1.2.2 Postinterventional CT Imaging

Immediately after the intervention, a control scan should be performed. An additional contrast medium application is usually not necessary.

The following issues should be confirmed or ruled out (Fig. 1.5):

- Pneumothorax;
- Bleeding;
- Position of the drainage or other materials.

Even if there is no obvious complication, it has to be decided on a case-by-case basis whether to carry out follow-up examination, e.g., chest X-ray, 2 and 4 h after thoracic interventions to rule out pneumothorax and intraparenchymal or pleural hemorrhage. Postinterventional hemoptysis might be observed in some cases. Hemoptysis, however, should significantly decrease within the next few hours. Massive bleeding as defined by hemoptysis of more than 200 ml in 1 h requires immediate control.

After abdominal interventions, ultrasound can sufficiently identify bleeding or free abdominal fluid. In patients with impaired echoic window, a repeat CT scan might be considered. In some cases the hemoglobin level might be controlled.

1.2.3 Preinterventional MR Imaging

Besides imaging without ionizing radiation, MR imaging offers advantages such as high soft-tissue contrast, multiplanar imaging without reconstructions, and the ability to measure multiple physical or functional parameters, including flow, perfusion, diffusion, and temperature. Space for intervention, however, is more limited in a MR scanner than in a CT scanner. The bore diameter of a commercial closed-bore MR scanner is about 60 cm; therefore, patient accessibility is limited, which may complicate some MR interventions, and orientation as well as positioning of the patient must be considered more carefully. To overcome the drawback of limited space, open-bore systems were developed with a vertical or a horizontal gap between the magnets (Lamb and Gedroyc 1997; Adam et al. 1998). Depending on the magnet design, space is infinite at least in one direction, offering wide lateral or frontal access. Obese and particularly claustrophobic patients appreciate these open-bore scanners. Advantages exist also for pediatric or emergency patients who require ventilation. To date, the field strength of a commercial open-bore system is limited to a maximum of 1.0 T [GE, Signa Ovation HD (0.35 T); Toshiba,

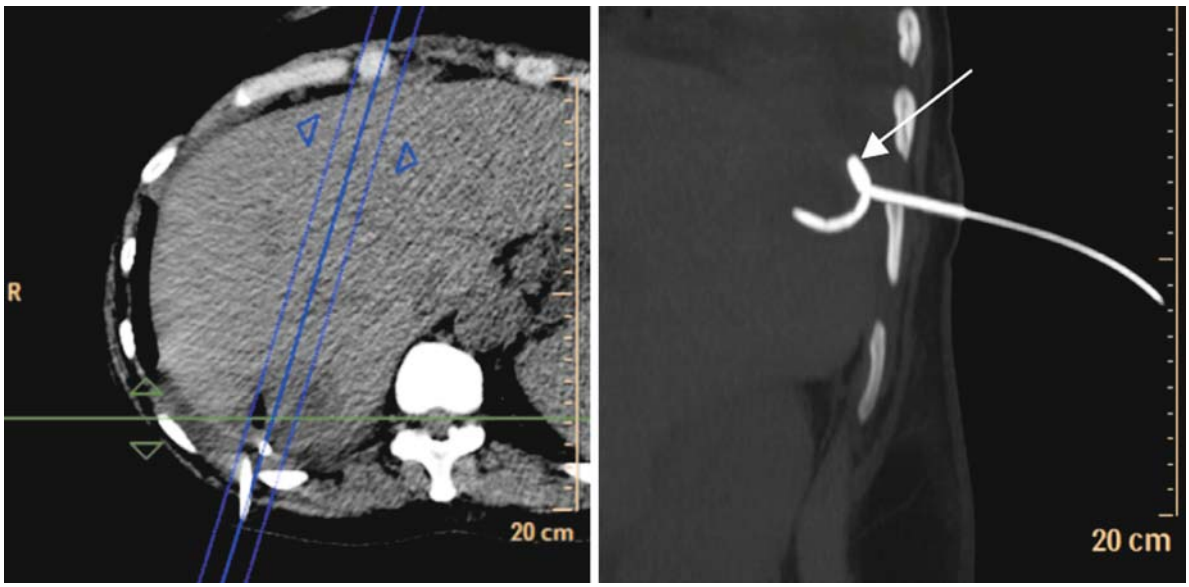

Fig. 1.5 Control CT after insertion of a drainage catheter for the treatment of a liver abscess. The *left image* shows an axial image at the level of the abscess (*arrow*). The corresponding parasagittal maximum intensity projection reconstruction on the *right* demonstrates that the drainage passes the pleura with a loop in it

Opart (0.35 T); Philips, Panorama HFO (1.0 T)]. An alternative scanner design has been provided by Siemens (Espree), offering a short-bore 1.5-T system with a bore length of only 125 cm and a bore width of 68 cm.

Even though MR-guided interventions have the potential to replace high-cost, open surgery procedures, the realization is still limited to a few research centers. The most promising clinical application for MR-guided intervention seems to be for brain, breast, liver, prostate, and bone, which will be discussed in detail later in this book.

In principle, every sequence type and image weighting (T1, T2, proton density, diffusion weighing, and fiber tracking) can be used that delineates the lesion in question with adequately high spatial resolution and contrast. Besides sufficient in-plane resolution, slice thickness is of considerable significance. Image slices should be thin enough to delineate the lesion accurately but thick enough to obtain reasonable signal-to-noise ratios i.e., 3–5 mm. Three-dimensional imaging or overlapping slice techniques are preferable while gaps between the slices should be avoided. If two-dimensional imaging techniques are applied, the same sequence should be acquired in two different slice orientations to visualize the lesion.

For thoracic and abdominal lesions, breath-hold maneuvers are necessary to prevent respiratory motion artifacts and spatial misregistrations. Moreover, respiratory motion correction techniques (e.g., navigator, respiratory sensor) can be applied to perform MR imaging during free breathing and to increase spatial resolution.

Considering the appearance of malignant lesions using MR imaging, which are mostly hyperintense on T2-weighed and hypointense on T1-weighed sequences, T2-weighed sequences are more favorable for preinterventional and interventional imaging as dark instruments are better distinguishable from usually hyperintense pathologic lesions.

For localizing alien elements, "passive" visualization based on signal void due to spin replacement and susceptibility artifacts is usually used (Bakker et al. 1997). Magnetic susceptibility describes the degree to which a substance becomes magnetized in response to an external magnetic field, resulting in local field disturbances. This effect is influenced by several factors. In general, stronger magnetic fields cause more (or more severe) artifacts (Frahm et al.

1996). Gradient-echo sequences are sensitive to susceptibility artifacts particularly with increasing echo time. In contrast, susceptibility artifacts are decreased in spin-echo (SE) sequences owing to the refocusing pulses. Furthermore, the size of susceptibility artifacts is greatly affected by the orientation within the magnetic field and the choice of the frequency- and phase-encoding direction (Ladd et al. 1996). (This is discussed in more detail in Chap. 3.) Hence, T2-weighed SE or fast imaging using turbo-spin-echo (TSE) sequences might be a suitable imaging technique for planning the intervention. Alternatively, steady-state free-precession (SSFP) imaging can be performed, which provides a high signal-to-noise ratio and image contrast, which is characterized by T2/T1. SSFP has the added advantage that this sequence is flow-compensated owing to the symmetric shape of the gradient pulses in all three spatial coordinates.

In some cases, intravenous contrast medium administration might be necessary to better delineate the extension of the lesion. The choice of contrast agent will be determined by the longest-lasting effect of contrast enhancement of the particular agent.

The most important benefit of MR imaging over CT is the ability to acquire images in any arbitrary orientation. However, even with MR imaging, intervention can be controlled more easily and safely if one of the main axes (axial, coronal, or sagittal) is used for intervention guidance.

If an adequate image slice was chosen, the same measurements as in CT should be performed to control every step during intervention.

1.2.4 Postinterventional MR Imaging

While the patient remains in the magnet, MR imaging should be performed to rule out potential complications such as acute bleeding using T2-weighted SE/TSE or SSFP sequences. Using the same sequence, one can also confirm treatment efficacy or the position of materials such as drainage and markers.

Chest X-ray and ultrasound can be performed in addition to MR imaging, comparable to the follow-up after CT-guided intervention.

Summary

There are various imaging modalities available for pre- and postinterventional imaging as well as for interventional navigation.

X-ray fluoroscopy, which provides real-time images with high spatial resolution, is regarded as the gold standard for vascular intervention and is also used for some musculoskeletal procedures. The soft-tissue contrast, however, is very limited.

Ultrasound also provides real-time images with high spatial resolution. The indications for ultrasound-guided interventions, however, are restricted by bone, air, and the small field of view.

CT is widely accessible and provides an excellent overview with the capability of three-dimensional reconstructions due to the volumetric data. In addition, intestinal or vascular structures can be clearly identified using iodine contrast medium. CT is the most valuable imaging modality for abdominal and particularly thoracic targets. Image quality can be impaired by metal artifacts.

MR imaging provides a similar overview to and even better soft-tissue contrast than CT. It has the added advantage of multiplanar imaging without reconstructions. Patient access and space for intervention, however, is more limited owing to a smaller bore size. In addition, the availability of MR scanners is much more restricted. Therefore, MR-guided interventions are still limited to a few research centers.

Key Points

- For pre- and postinterventional imaging as well as for interventional navigation the imaging modality should be used that visualizes the lesion or the target organ best.
- CT is suited to navigate abdominal and particularly thoracic interventions. MR imaging needs to be applied where high soft-tissue contrast is mandatory and for lesions only visible by this technique, namely, breast lesions.
- Patient position and breathing depth should be considered before imaging to allow correct planning and safe access to the lesion.
- Using CT, oral, rectal, or intravenous contrast medium application might be necessary to visualize adjacent organs or vessels. Data reconstruction with different (soft-tissue, lung, bone) algorithms can be helpful to plan the access route.
- For MR-guided interventions T2-weighed SE or TSE sequences as well as SSFP sequences are very suitable for distinguishing target lesions from instruments.
- After intervention, conventional X-ray or ultrasound examination can be used to rule out complications such as pneumothorax or bleeding.

References

Adam G, Bucker A, Glowinski A et al. (1998) Interventionelle MR-Tomographie: Gerätekonzepte. Radiologe 38:168–172

Bakker CJ, Hoogeveen RM, Hurtak WF et al. (1997) MR-guided endovascular interventions: susceptibility-based catheter and near-real-time imaging technique. Radiology 202:273–276

de Feiter PW, Soeters PB, Dejong CH (2006) Rectal perforations after barium enema: a review. Dis Colon Rectum 49:261–271

Delorme S, Krix M, Albrecht T (2006) Ultraschallkontrastmittel – Grundlagen und klinische Anwendung. Rofo 178:155–164

Frahm C, Gehl HB, Melchert UH et al. (1996) Visualization of magnetic resonance-compatible needles at 1.5 and 0.2 Tesla. Cardiovasc Intervent Radiol 19:335–340

Ladd ME, Erhart P, Debatin JF et al. (1996) Biopsy needle susceptibility artifacts. Magn Reson Med 36:646–651

Lamb GM, Gedroyc WM (1997) Interventional magnetic resonance imaging. Br J Radiol 70:S81–S88

Wells PN (2006) Ultrasound imaging. Phys Med Biol 51:R83–R98

CT-Guided Interventions – Indications, Technique, Pitfalls

2

Philipp G.C. Begemann

Contents

2.1 Introduction

Over the last 30 years (Haaga 2005), computed tomography (CT) has developed into a well-accepted and widely used guiding tool for a broad range of percutaneous interventions. It can be used either as an alternative to sonography or fluoroscopy or if interventions cannot be done under sonographic or fluoroscopic guidance.

In general, CT-guided interventions may be divided into diagnostic interventions and therapeutic interventions, although there are overlaps.

Typical diagnostic interventions are biopsies, which can be done as aspiration or fine-needle biopsies, punch biopsies, or drill biopsies, depending on the region, the access, or the material that has to be biopsied. Aspiration or fine-needle biopsies are used to acquire either liquid material for a microbiological analysis to search for infection or superinfection (Fig. 2.1a,b), for example, in patients with acute pancreatitis, or to obtain material for cytologic examination, for example, in small pulmonary nodules or in regions that cannot be reached or safely approached with punch biopsies. The latter is carried out if larger amounts of tissue are needed for pathologic or histologic examinations, for example, punch biopsies of lymph nodes or soft-tissue masses to identify or classify tumors before treatment (Fig. 2.1c–e) or to search for remaining living tumor cells after chemotherapy in persistent lymph nodes or tumor masses. Punch biopsies can also be done in parenchymal organs or large pulmonary or pleural masses. Drill biopsies are usually done in bones to classify bone tumors or soft-tissue tumors within bones (Fig. 2.1f–g).

Further diagnostic interventions that can be done under CT guidance include discographies or localization techniques, for example, coil or wire placement prior to video-assisted thoracoscopy surgery of small lung nodules (Fig. 2.2d–f) or before partial nephrectomy of small renal cell carcinomas or suspect renal lesions (Fig. 2.6).

Drainages are partly diagnostic, partly therapeutic. Most drainages are done to evacuate abscesses as an established alternative method to surgical intervention (Fig. 2.2a–c). But also other liquid-filled structures can be drained, such as bilioma, hematoma, seroma, urinoma, cysts, pseudocysts, pleural effusion or empyema, the renal pelvis, and the urinary bladder. Depending on the access path, drainages can generally be placed in two different ways. Either with the trocar technique, where the fluid collection is punctured directly with the drainage placed on a mandrin with a cutting edge (Fig. 2.2b) or with the Seldinger

Mahnken/Ricke (Eds.), *CT- and MR-Guided Interventions in Radiology*

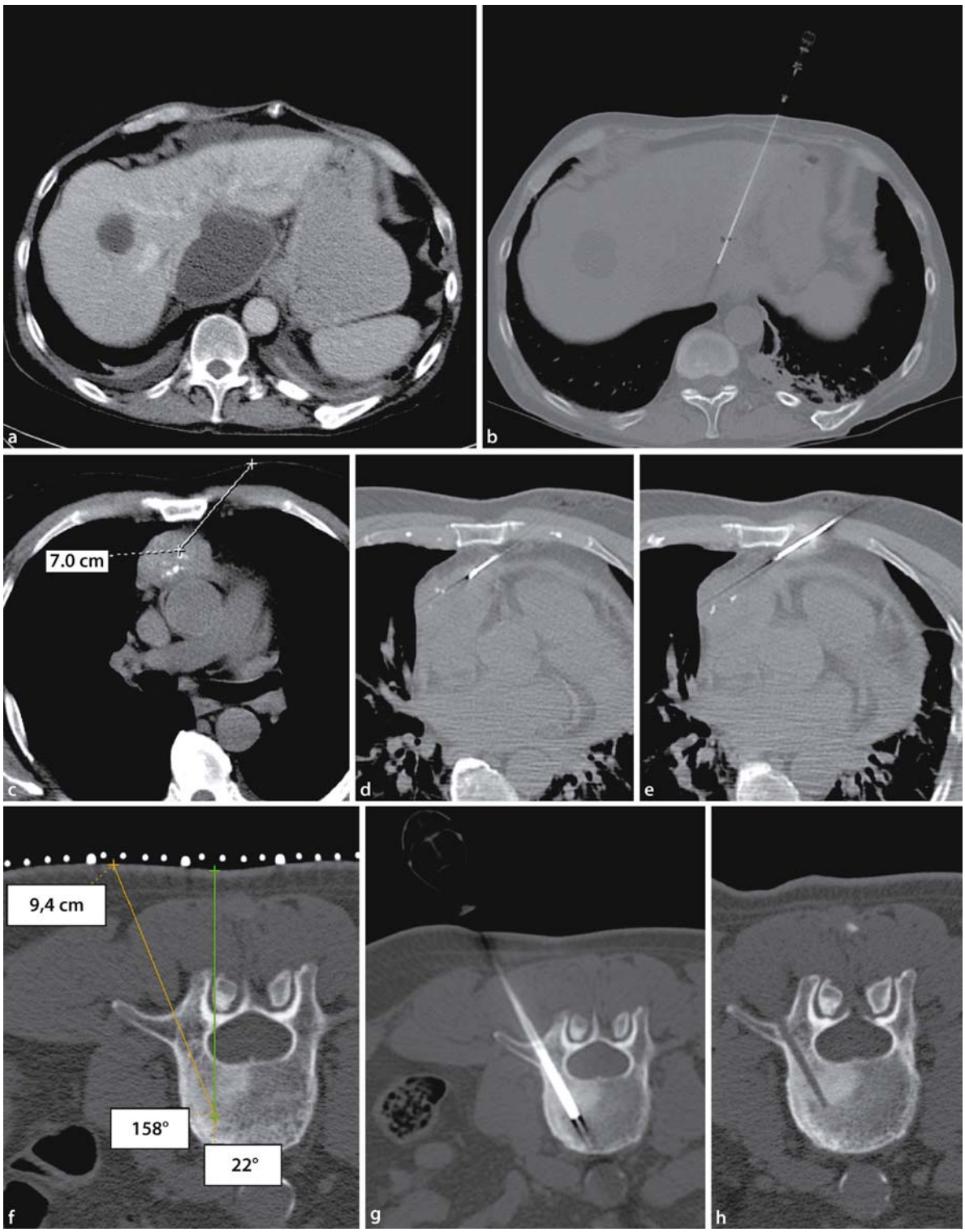

Fig. 2.1 **a**,**b** A fine-needle aspiration of a liquid structure behind the left liver lobe after liver surgery, which turned out to be a seroma without superinfection. **c**–**e** An example of a punch biopsy of a retrosternal mass, turning out to be a squamous cell carcinoma. **f**–**h** A drill biopsy of a bone metastasis in a vertebral body (L3)

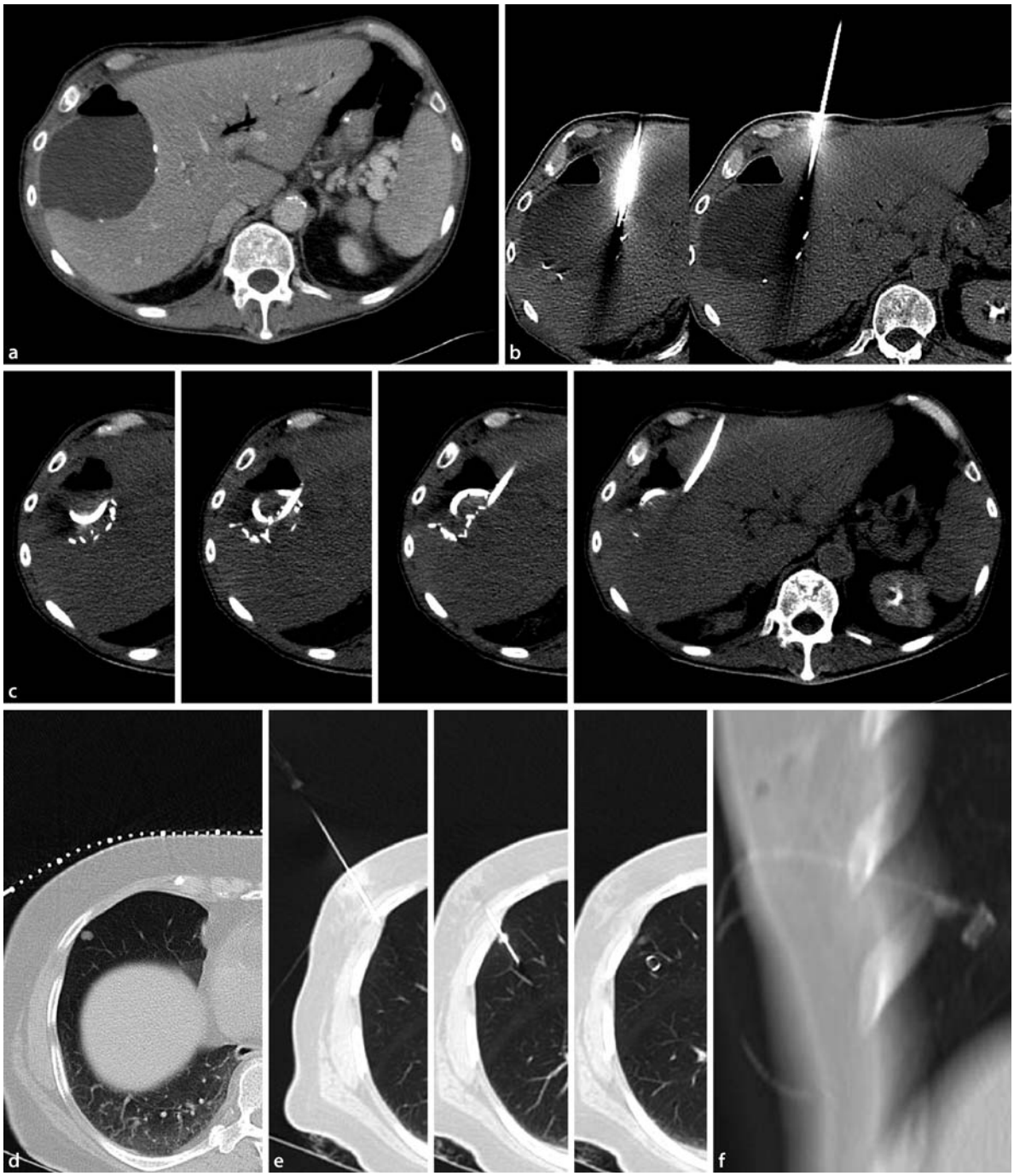

Fig. 2.2 **a**–**c** The drainage of a large liver abscess after surgery. The 12-F drainage catheter was placed with the trocar technique. **d**–**f** An example of a localization of a small lung nodule before video-assisted thoracoscopy surgery (**f** is a sagittal multiplanar reformation)

technique, where the fluid collection is first punctured with a thin hollow needle before a guide wire is placed within the collection. Finally the drainage catheter is inserted over the wire.

Hyperthermal tumor therapy, including radiofrequency ablation or laser interstitial thermal therapy, percutaneous ethanol injection, or local radiation therapy can be performed under CT guidance as

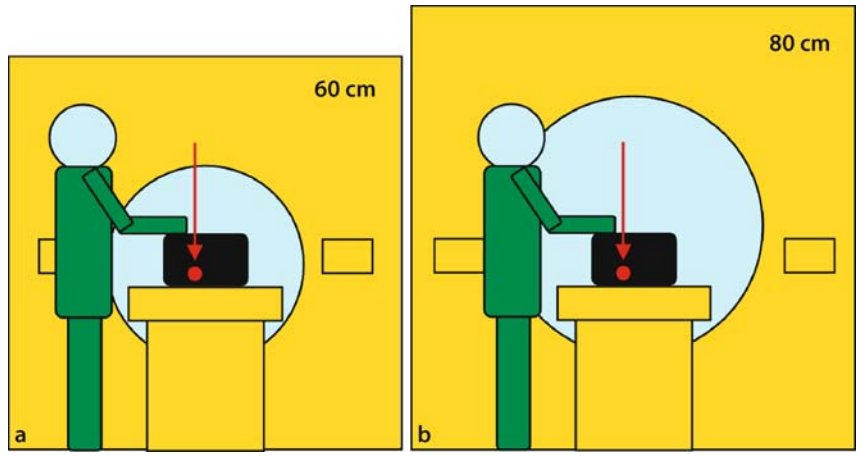

Fig. 2.3a,b The space in the bore when using a diameter of 60 cm and a diameter of 80 cm. **a** The device shown (*red arrow*, for example, a drainage on a trocar) could not be placed within the bore to control the localization or to use computed tomography (CT) fluoroscopic guidance. Using a CT scanner with a larger bore (**b**) can overcome this limitation

curative or palliative tumor therapy for primary or metastatic tumors in virtually all regions of the body.

Another large field of therapeutic interventions is pain management by the use of neurolysis or injection therapy of local anesthesia with or without corticoids. CT-guided thermal ablation of osteoid osteoma could even be established as a curative treatment of choice. Many other skeletal interventions are also routinely performed under CT guidance, including vertebroplasty and osteoplasty as well as percutaneous osteosynthesis, for example, percutaneous screw insertion of the pelvis after divulsion of the iliosacral joint. Cysts or parasitic cysts can be sclerosed with CT guidance, and even CT-guided gastrostomies are routinely done now. The different types of intervention, their indications, and typical examples are summarized in Table 2.1 (Feuerbach et al. 2003).

2.2 Materials and Techniques

2.2.1 General Equipment

Generally every type of CT scanner (single slice or multislice) can be used for CT-guided interventions. There should be enough space in the scanner room for the radiologist, one or two assistants, the sterile table with the required instruments, and possible further equipment (for example, for anesthesia or even general anesthesia, radiofrequency generators, etc.). Some interventions, e.g., complex CT-guided skeletal interventions, require even more space to achieve definite sterile conditions. This needs to be considered when selecting the room for the planned procedure.

Before every intervention, the scanner room has to be carefully cleaned and disinfected with antibacterial, antifungal, and/or antiviral agents, especially the CT table and the gantry.

A movable instrument table has to be covered with sterile sheets and equipped with syringes of different size (5, 10, and 20 ml) with and without Luer-Lock, hypodermic, and 20G syringe needles for local anesthesia, anesthetics, saline solution, sterile pads, sterile clear tape to cover the CT gantry's control panel, and sterile sheets for interventional purposes. Furthermore, the procedure-specific materials such as puncture needles, drainages, sample tubes, and specific drugs need to be placed on the table. The radiologist has to perform a medical hand washing and wear a surgical cap and mask, sterile gloves, as well as a lead apron. In complex interventions as well as in all skeletal interventions, the interventionalist needs to wear a sterile coat.

2.2.2 Desirable Equipment

Different technical specifications or technical tools make the procedure easier or even safer. A list of desirable equipment for successful CT-guided interventions is given below:

- Multislice CT scanners with wide detector arrays are preferable, since detectors with a width of, for example, 16 × 1.5 mm (24 mm) or 64 × 0.625 mm (40 mm) are mostly able to cover the whole range

Table 2.1 Overview of the most common computed tomography (CT) guided interventions and their indications

Type of intervention	Indications	Examples
Fine-needle biopsy	Cytology	Small lymph nodes (<1 cm) Pulmonary nodules Difficult access (i.e., transgastral) Suspected malignant efusion
	Microbiology	Suspected superinfection
Punch biopsy	Histology	Lymph nodes Solid masses
Drill biopsy	Histology	Bones Bone tumors Soft tissue tumors within bones
Drainages	Microbiology Therapy	Every type of superinfected fluid collection Abscess Necrosis Fluid collections (bilioma, seroma, etc.) (Gastrostomy)
Localization techniques	Surgery preparation	Lung nodules before video-assisted thoracoscopy surgery Intraparenchymal kidney tumors
Tumor/ablation therapy	Palliative or curative tumor therapy	Primary cancers (hepatocellular carcinoma, renal cell carcinoma, lung cancer, etc.) Metastasis (liver, kidney, adrenal, lung, etc.)
Neurolysis	Pain therapy	Tumor-induced pain (sympathetic chain, ganglion celiacum, etc.) Neuralgia [Gasserian (trigeminal) ganglion, etc.]
Anesthesia injection	Pain therapy	Periradicular therapy (disc herniation, etc.)
Skeletal Interventions	Trauma therapy	Vertebroplasty, scaroplasty, percutaneous screw insertions, etc.

of the intervention site in the *z*-direction. This not only permits one to easily recognize needle deviations into cranial and caudal direction, but also permits adaptation of the puncture direction to organ shift during the intervention.

- A monitor within the scanner room is almost mandatory for the radiologist to monitor the procedure.
- A foot pedal to start sequential scans or fluoroscopy makes the radiologist more independent during the procedure and helps to speed up the intervention.
- The patient table can be either moved after covering the control panel with sterile clear tape or pushed directly after manually releasing the table. Newer CT systems also offer a complete control panel fixed at the side of the patient table, where all scanner actions can be carried out by the radiologist under sterile conditions.
- CT scanners with a larger bore (Fig. 2.3), for example, 85 cm, are very practical for CT-guided interventions since they at least partly overcome the narrowness of normal-size CT scanners with a typical gantry bore of 70 cm. CT scanners with a big gantry bore are offered by different CT vendors, e.g., Philips (Brilliance CT Big Bore, 85-cm bore size, 60-cm true scan field, 16-slice configuration), Siemens (Somatom Sensation Open, 82-cm bore size, 50-cm scan field of view, 24- or 40-slice configuration), Toshiba (Aquilion Large Bore, 90-cm bore size, 70-cm field of view, 16-slice configuration), and GE Healthcare (LightSpeed RT, 80-cm bore size, four-slice configuration).
- For difficult double-angulated interventions the use of commercially available tracking systems can be considered (see Chap. 7).
- Another CT tool made to improve safety, especially in less compliant patients, is CT fluoroscopy, as described later.

A typical CT room suitable for CT interventions is shown in Fig. 2.4 with a 64-slice CT scanner with a foot pedal and a monitor within the scanner room. Additionally the system is capable of performing CT fluoroscopy.

Fig. 2.4 A typical CT scanner room suitable for CT interventions equipped with a 64-slice CT scanner with a foot pedal, a monitor, and the option to perform fluoroscopic interventions

2.2.3 CT-Guided Puncture – Step by Step

CT-guided punctures follow a very similar course of action as is described in theory and in a sample procedure where a CT-guided localization of a renal tumor is described (Fig. 2.3).

The general course of a CT-guided intervention is as follows:

1. The first mandatory step is the review of the radiological examinations that have been done to the patient so far. It is the decision of the radiologist whether he/she will perform the puncture or if alternative approaches (i.e., surgery) have to be considered. If the puncture is determined, the patient needs to be informed about the course, the risks, and the possible complications of the procedure (Table 2.2) optimally the day before the procedure. Depending on local laws, written consent may be required.
2. The knowledge of the patient's blood clotting capabilities (International Normalized Ratio, INR, platelet count, previous taking of platelet inhibitors, i.e., aspirin) is obligatory before starting the procedure. Generally the INR should be below 1.7 and the platelet count above 50 000/mm^3.
3. Before the procedure, the CT room should be cleaned and the sterile table prepared.
4. The patient is placed on the CT table in a position that facilitates the preinterventionally determined access route. For most interventions a spiral scan of the region of the intended procedure is done for further planning. The scan can be done with or without the use of contrast material to identify vascular structures and/or areas of abnormal or pathologic contrast enhancement behavior. Furthermore, it has to be decided whether the procedure has to be done in inspiration, expiration, or free breathing, depending on the area and the compliance of the patient. Ideally a radiopaque grid has already been fixed on the patient's skin (Fig. 2.1f). The access path of the intervention can be assessed either on the axial images or on multiplanar reformations if procedures are needed to be angulated to the *z*-direction. Preferably, the intervention is planned in a plane perpendicular to the *z*-axis, which makes the procedure much easier to perform and to monitor. If double-angulated punctures are necessary, a tilted gantry can be used for surveillance to provide images parallel to the direction of the intervention.

Table 2.2 Main risks and complications of CT-guided interventions

General complications	Drug reaction due to local anesthesia
	Nerve lesion with numbness or paralysis
	Infection, abscess, sepsis
	Bleeding, hematoma
	Surgery
	Death
Procedure-specific complications	
Thoracic procedures	Pneumothorax
	Air embolism (arterial and venous) with arterial infarction (i.e., myocardial infarction, stroke)
Abdominal procedures	Pneumothorax (upper abdomen)
	Injury of parenchymal organs of the abdomen (i.e. liver, spleen, kidneys)
	Arteriovenous fistula in parenchymal organs
	Injury of the intestine
	Peritonitis
Osseous procedures	Fracture
	Osteomyelitis
Tumor ablation	Large necrosis with resulting sepsis
	Injury of adjacent organs or structures
	Bleeding

5. The pathway of the puncture can be measured (length and angle; Fig. 2.1e).
6. The radiologist performs a medical hand washing and dresses with a surgical cap and mask and sterile gloves. A sterile coat is used in complex as well as in all skeletal interventions. The skin area of the procedure is disinfected and the patient covered with sterile sheets.
7. After another disinfection of the skin, local anesthesia is performed. Using the syringe needle for the local anesthesia, one approaches the intended target for the first time. This step can already be done with CT guidance using the techniques described below. Careful local anesthesia is mandatory for the patient, especially in bone punctures.
8. After the target has been reached with the anesthesia needle, the procedure is repeated with the interventional device (i.e., drainage, puncture device, RF ablation device, etc.). If a thicker device is used, a small incision of the skin using a scalpel is necessary.
9. After the procedure has finished, the skin lesion is bandaged. A CT scan of the target region is performed to exclude complications and, if necessary, to control the position of drainage catheters, coils, or localization needles.
10. Depending on the procedure, the patient should typically maintain bed rest for 3–6 h, ideally lying on the punctured site. During that time he or she should be regularly monitored. After pulmonary punctures at least one chest X-ray should be performed to exclude pneumothorax (see Chap. 1). After punctures in the upper abdomen a chest X-ray can be considered depending on the course of the intervention. In difficult interventions, a further CT scan may be required in the short follow-up. In patients with reduced blood clotting capabilities or after punctures with a bleeding risk, further controls of the blood hemoglobin are needed.

Generally two different techniques of CT surveillance are used:

1. *Sequential scans*: Whenever it is necessary to control the position of the puncture device, the patient is moved into the CT gantry, positioned according to the laser marker, and sequential scans of the region are performed either by the technician or by the radiologist using the foot pedal. With use of multislice CT, with every sequential scan, several images with a width of approximately 2–5 mm can be displayed on the monitor. If small lesions are punctured, the slice thickness has to be adjusted accordingly, so as not to miss the lesion owing to partial volume artifacts. Every interventional step between the sequential scans is planned on the preinterventionally acquired images. The navigation of the puncture device can be done either as a freehand procedure or with the help of one or two assistants if angulated or double-angulated procedures have to be done. The angles are measured on the previous scans. In angulated procedures one assistant is positioned either opposite the radiologist or at the bottom of the CT table and monitors the angulation using a goniometer. In the case of a double-angulated procedure, two assistants are positioned opposite the radiologist and at the bottom of the CT table (Fig. 2.5).
2. *CT fluoroscopy*: Real-time fluoroscopic cross-sectional images are generated when the performing radiologist presses the foot pedal, and the pathway and direction of the puncture device can be directly observed. One to four images can be displayed on the monitor; the slice thickness of the fluoroscopic images can be chosen according to the scanner specifications. The procedure has to be performed within the CT bore. To avoid extensive doses to the radiologist's hand, different scanner-specific dose-saving tools and needle holders are available.

As a pictorial sample procedure, a CT-guided localization of a small renal mass is described:

1. On an initial CT scan, a suspect, 2-cm noncystic renal lesion with irregular contrast material enhancement is diagnosed in the dorsomedial parenchyma of the right kidney which does not bulge out the renal surface. Instead of total nephrectomy, organ-sparing surgery was planed, and it was requested to localize the tumor prior to surgery (Fig. 2.6a). It was decided to use a breast lesion coil to be placed directly behind the tumor in the perirenal fat.
2. The patient is placed on the CT table in a way that there is good access to the target region. In this case, the patient was placed in prone position.

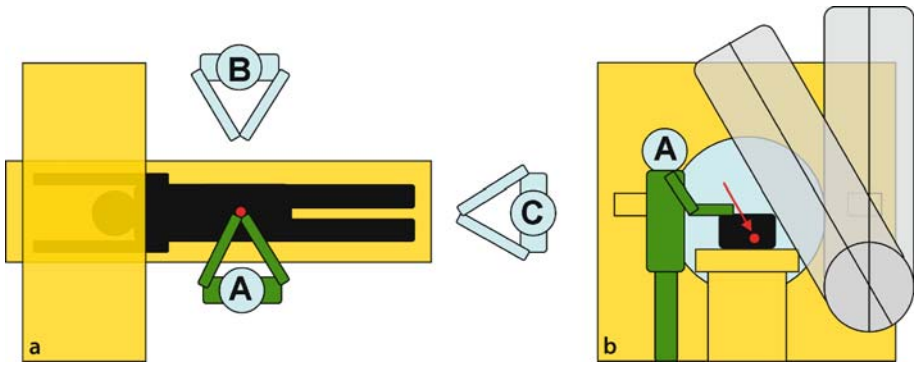

Fig. 2.5 **a** The positions of the radiologist (A) and two assistants (B and C) for a goniometer-guided double-angulated procedure. **b** The view of assistant C with the goniometer and the accordingly angulated puncture device

3. A contrast-enhanced (spiral) scan is done to plan the procedure (Fig. 2.6b). In this example, the easiest way to reach the perirenal fat next to the tumor would be from dorsal paravertebral direction. Since the dorsal pulmonary recessus is behind the lesion, and a transpleural puncture should be avoided, either an angulated caudocranial access or lateral access is possible. To stay in the *xy*-plane without angulation in the *z*-direction, it was decided to use the lateral access. The distance from the skin to the lesion and the entrance angle are measured.
4. Local anesthesia is performed with a 7-cm 22G needle (Fig. 2.6c) and the direction is controlled.
5. After incision of the skin, it was changed to an 18G hollow needle. With use of sequential CT scans for image guidance, the needle tip was placed directly behind the renal lesion (Fig. 2.6d).
6. A breast localization coil was positioned directly behind the tumor via the hollow needle (Fig. 2.6e,f).
7. The postinterventional spiral scan excluded immediate complications such as pneumothorax (Fig. 2.6g) or bleeding and showed coil localization directly behind the tumor also in the multiplanar reformations (Fig. 2.6h).

2.2.4 Pitfalls

To avoid unwanted incidents such as bleeding, infection, pneumothorax, or nerve injury the following precautions have to be taken:

- The whole procedure has to be performed under sterile conditions to prevent intervention-related iatrogenic infections especially in skeletal interventions.
- The patient's blood clotting capabilities must be known to prevent bleeding.
- Before the intervention starts, the initially acquired CT images have to be analyzed carefully to identify the safest path to the target. Extensive knowledge of the anatomy of the region of intervention is mandatory to avoid injury of neural structures or blood vessels, especially arteries. Transpleural pathways to access targets, for example, within the liver or kidneys, should be avoided to prevent pneumothorax or spreading of infection or tumor from the abdomen into the thorax. Transgastral fine-needle biopsies or punctures for pain therapy are generally possible, but the patient has to be fasting and peri-interventional antibiotics should be administered. The same holds true for the passage of the small bowels (see Chap. 6).
- The direction of the puncture should not head towards organs sensitive to damage, i.e., aorta, coronary arteries, etc., especially when performing punch biopsies.
- In order to avoid contact of the puncture device with the gantry, especially when long devices are used, the procedure should be done with the patient table in the lowest position in order to gain more space in the gantry bore. This is even more important if the patient is positioned on his/her side, for example, on the left side, if the liver is punctured.
- Interventions of the lung or breath-dependent organs have to be done with careful agreement with the patient to prevent failed puncture. If this is not

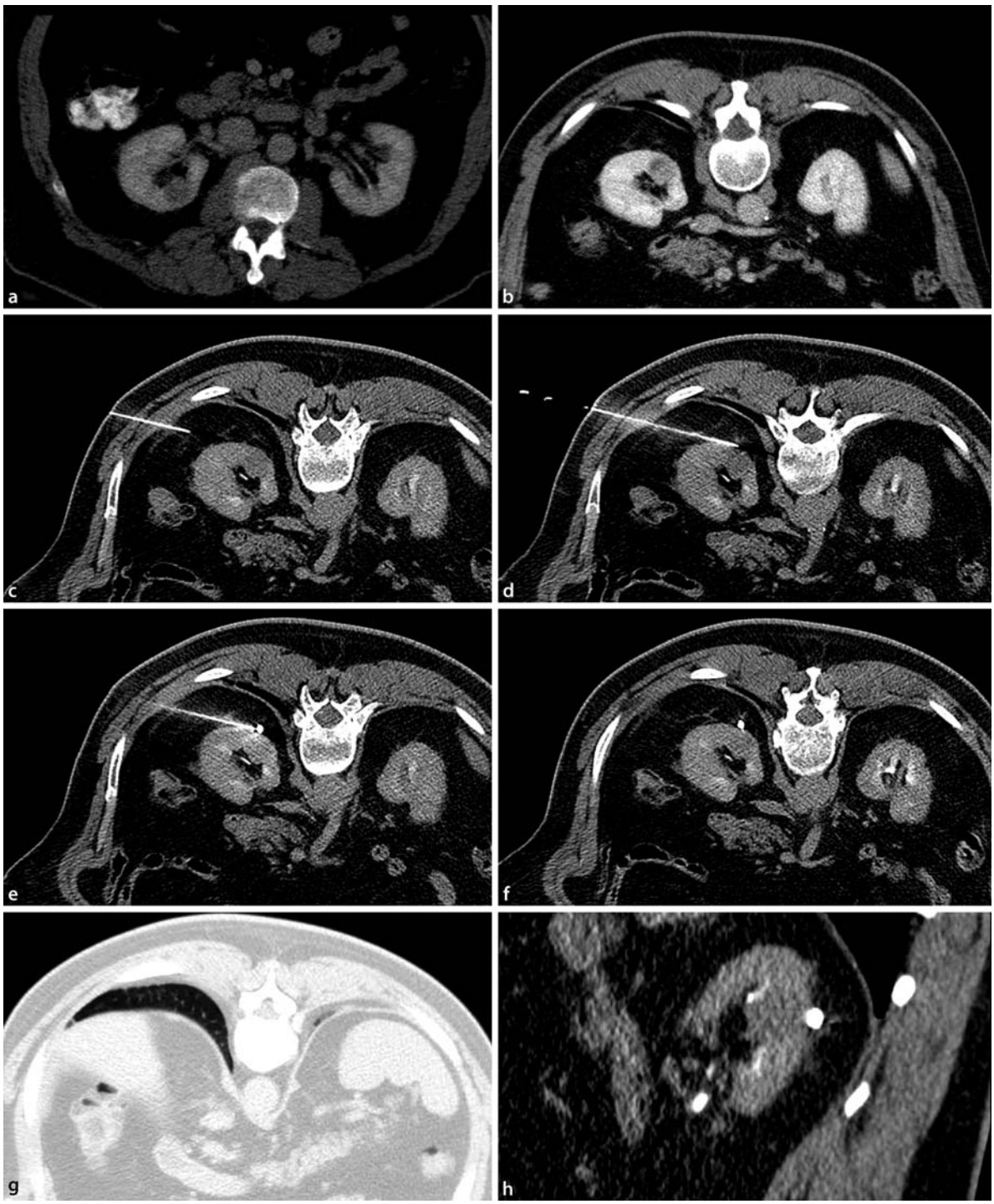

Fig. 2.6a–h The localization procedure of a small renal tumor before organ-sparing surgery. The complete procedure is described in the text

possible, the use of CT fluoroscopy helps to avoid repeated punctures.

- Biopsies or drainages of parenchymal organs should be done with parenchymal bridging of the access path to prevent bleeding or spreading of infection into the peritoneum or retroperitoneum.
- Liver punctures in patients with ascites should be avoided, if possible, owing to a higher bleeding risk, especially in patients with liver cirrhosis. Preinterventional drainage directly prior to the intervention may be used to provide safe access to the target without interposition of fluid.
- If large tumor masses are biopsied, samples from the center and from the periphery of the tumor have to be taken to gain enough, reliable material for histologic workup, since many tumors are necrotic at their center.

2.2.5 Radiation Dose

A relevant disadvantage of CT guidance is the exposure of the patient and the interventionalist to radiation. The dose which will be administered to the patient shows broad variations and can be effectively influenced by the interventionalist. Since there are usually previous CT or magnetic resonance images, the planning scan as well as the control scan after finishing the procedure should be limited to the minimum scan range needed. The dose settings (kilovolts and milliampere seconds) should be limited to an acceptable level to identify the important structures and to monitor complications, especially in the sequential scans or CT fluoroscopy. The number of sequential scans and the time of CT fluoroscopy should be kept as low as possible.

Summary

CT offers the possibility to safely guide interventions. CT is widely available and generally CT interventions can be performed with every type of scanner. No special interventional equipment is needed, which is an important advantage over magnetic resonance guidance. The radiation exposure during CT-guided interventions has to be mentioned and every procedure should be performed in a dose-saving manner.

Key Points

- CT is a widely available tool to monitor interventions.
- The patients have to be informed about the complications and the patient's blood clotting capabilities must be known.
- The procedures have to be done under sterile conditions.
- Knowledge of the anatomy and accurate planning of the procedure are mandatory to avoid complications.
- After the procedure the patients have to be carefully monitored.

References

Feuerbach S, Schreyer A, Schlottmann K (2003) Standards in radiographically guided biopsies – indications, techniques, complications. Radiologie Up2date 3:207–223

Haaga JR (2005) Interventional CT: 30 years' experience. Eur Radiol 15(Suppl 4):D116–D120

MR-Guided Interventions – Indications, Technique, Pitfalls

3

Arno Bücker and Marcus Katoh

Contents

3.1 Introduction

Different techniques have proved to be valuable for guidance of interventional procedures, namely, ultrasound, computed tomography (CT), and magnetic resonance (MR) imaging. For many indications all these techniques are "me too" alternatives. If there is no medical reason to prefer one imaging modality over another, factors such as availability, simplicity, and cost are of great importance. Looking at any of those cofactors, it is evident that MR imaging is the least likely method to be initially favored for guidance of interventional procedures. In this chapter only nonvascular interventions will be considered, such as imaging-guided punctures/markings, drainages, and tumor ablations. Each radiologist performing any of these procedures should be familiar not only with the standard techniques of ultrasound and CT guidance, but also with guidance technique exploiting the imaging features of MR imaging. This is true despite the fact that there are so far only rare indications which definitely require MR imaging as a guidance tool. But some lesions which are only detectable by MR imaging require MR guidance or MR-guided localization and marking (Solomon et al. 2002). Among these, breast lesions are the most common and the continuously growing role of MR imaging in this field will lead to an increase in the numbers of breast lesions which can only be biopsied or marked by MR guidance.

3.2 Materials and Techniques

3.2.1 MR Scanner

The ideal MR scanner will allow complete open access to the patient. Current MR scanners do not allow for this, but there is a distinct difference between closed-bore and open-bore MR scanners (Adam et al. 1998). The best patient access so far is offered by a magnet which consists of two halves; the space between the two halves can be occupied by the interventionalist. This double-doughnut concept creates a field strength of 0.5 T in the imaging area, demonstrating the fact that MR scanners offering better patient access usually have lower field strengths ranging from 0.064 to 1 T. MR scanners with filed strengths up to 3 T have been evaluated for MR guidance of interventions (Paley et al. 2001).

Considering high image quality along with high imaging speed as a demand for interventional MR

imaging, the need for surface coils is obvious. While they are not always necessary, they will offer advantages such as better signal-to-noise ratio and the ability to apply parallel imaging techniques. Many surface coils are ring coils allowing access to the imaged area through the open center part of the surface coil. In addition, dedicated devices are available for MR-guided breast interventions (Floery and Helbich 2006), although the ability to perform MR-guided breast interventions with standard surface coils has been proved (Daniel et al. 1998). Even dedicated robotic systems have been developed to perform the intervention inside a high-field closed-bore MR scanner (Kaiser et al. 2000). Whether the additional investment in a dedicated interventional coil is justified will depend on the numbers of interventions performed at one institution and on the skill of the interventionalist.

If one considers vascular interventions, the need for fast imaging capabilities requires preferably high-field-strength MR scanners (Buecker et al. 2002b; Mahnken et al. 2004b; Spuentrup et al. 2002), although midfield systems have been used since the very beginning to perform vascular interventions as well (Wildermuth et al. 1997). Looking at nonvascular interventions, patient access might be of more importance than imaging speed. Furthermore, lower field strength will lead to smaller susceptibility artifacts, which can be advantageous when metallic instruments are used (Frahm et al. 1996a; Gehl et al. 1996). Consequently, punctures and biopsies have been performed on a wide range of MR scanners from low to high field, proving that all of these scanners can be used to reliably perform MR-guided interventions (Adam et al. 1999; Barentsz 1997; Buecker et al. 1998; Frahm et al. 1996b; Hall et al. 1999b; Heywang-Kobrunner et al. 2000). Therefore, individual factors of the single institution will influence the choice of the field strength more than the fact that MR-guided interventions are being planned for the future.

When planning interventions within the MR room, one should ensure there are double doors to allow shielded access to the scanning room even during image acquisition. Furthermore, an in-room monitor and console will be very helpful. Any change of geometry data of an imaging sequence with on-the-flight angulation of the imaging slice should be possible from within the MR room without the need for the usually applied time-consuming preparation phases of standard diagnostic imaging sequences. Furthermore, switching between different sequences should be possible as well and the orientation of the actual imaging plane should be indicated on images of other orientation. This should allow easy planning of the imaged slice through any desired path, allowing for visualization of the imaged interventional instrument in its full length. For nonvascular interventions a reliable means of communication from within the MR room to the console outside might seem a possible alternative, but the noise of any imaging sequence will make this task quite difficult to achieve. Considering the generally available options of all major vendors for in-room equipment, direct manipulation of imaging sequences inside the MR room should be standard for any MR scanner when interventions are being performed.

3.2.2 Imaging Sequence – General Considerations

The originally very slow technique of MR imaging has by now developed into a technique allowing even for real-time control of vascular interventions with a high temporal resolution while maintaining a combination of adequate spatial resolution and good contrast (Buecker et al. 2002a). Considering nonvascular interventions, fast spin echo sequences and gradient echo sequences have been initially applied for this purpose (Adam et al. 1997). Owing to the contrast between vessels and surrounding tissue and the speed of steady-state free-precession sequences, this technique is widely used for MR guidance of vascular interventions (Duerk et al. 1998). One disadvantage of steady-state free-precession imaging is the substantial noise produced by this technique, causing not only problems for communication but also discomfort to the anxious patient. In general, the ideal sequence for MR guidance of biopsy procedures encompasses the following features:

1. Good contrast between the lesion and the interventional instrument;
2. Sufficiently high temporal and spatial resolution to visualize all lesions to be targeted and to be performed during an easy patient breath-hold if not faster;

3. Sufficient field of view to avoid back folding, enabling switching of phase and frequency encoding directions;
4. Preferably low acoustic noise;
5. Preferably no additional hardware requirements.

T2-weighted sequences will usually be advantageous compared with T1-weighted sequences because the susceptibility artifact of metallic instruments causes a signal drop on all sequences. The same is true for signal void caused by nonmetallic objects such as ceramic instruments. The usually high signal intensity of pathologic lesions on T2-weighted images yields a good contrast between low-signal instrument and high-signal lesion (Fig. 3.1) (Bucker et al. 1997).

Many so-called real-time imaging sequences have been published. Considering the imaging frames of 15 per second for a video, this demand is rarely ever met by MR imaging sequences. But nonvascular interventions do not require such a high temporal resolution. Considering the greater importance of high contrast and high spatial resolution, some imaging time should be invested in these parameters. Nonetheless, an easy patient breath-hold should be the maximum time needed to acquire an image or an image series. Imaging rates of one image every 10–15 s fulfill this requirement. But looking at the length of a procedure, the demand for faster imaging becomes obvious. The shorter the acquisition time for a single image, the shorter the time of discomfort for the patient and the lower the risk of inadvertent misplacement of a biopsy needle owing to patient movement – not to speak of the procedure time and the related cost.

Using the current software implementations, one could easily adapt the imaging sequence to each single indication and the patient's compliance. But, in general, it will be better for the interventionalist to be familiar with *one* imaging sequence and its contrast and spatial resolution. Therefore, one should try to establish two general biopsy sequences which are suitable for all interventions; one imaging sequence should be T2-weighted and the other T1-weighted to allow easy switching between these two contrasts depending on the lesion's characteristics. Later it will be discussed how different imaging parameters along with the field strength influence the appearance of our instruments and tips will be given for how to set up the ideal imaging sequences for the individual situation of each institution.

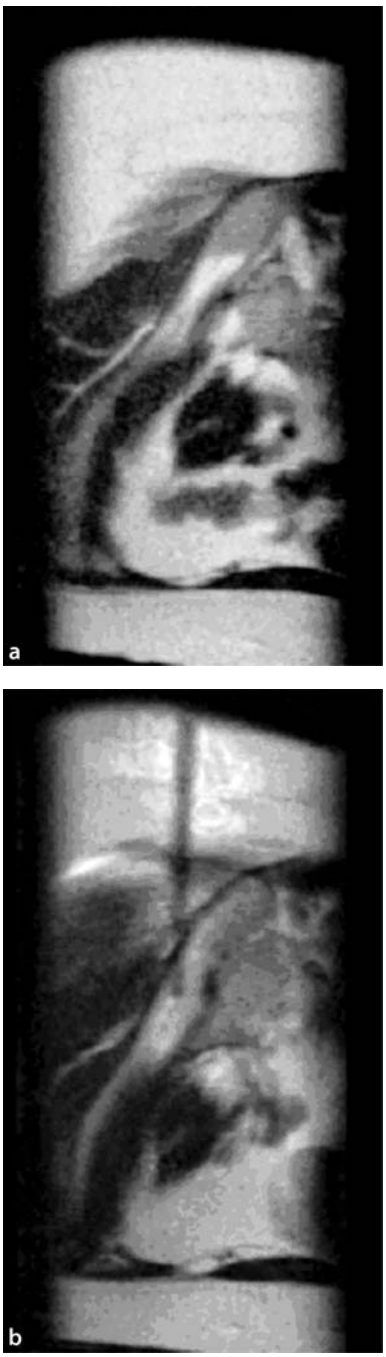

Fig. 3.1 A region of bone marrow edema of the pelvis on a T2-weighted image acquired in 600 ms (**a**). A 14G bone drill was used to biopsy this lesion (**b**), which turned out to be a chronic osteomyelitis. Excellent contrast between the lesion and the instrument is achieved on the T2-weighted image

The susceptibility artifact of a metallic instrument will depend on the relationship of its axis to the phase and frequency encoding direction. Switching of phase

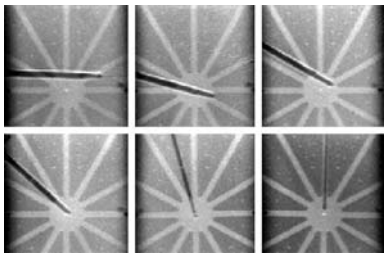

Fig. 3.2 The orientation of an 18 G needle positioned in a water bath is changed stepwise from horizontal to vertical. The change of needle position from the first to the last image is identical in its influence on the susceptibility artifact to switching the phase and frequency encoding direction

and frequency encoding is easily possible without any changes to the imaging contrast or imaging speed if the initially acquired field of view is large enough to cover the complete area of interest. This in turn allows for fast changing of the artifact size of metallic instruments (Fig. 3.2).

During any biopsy procedure the patient has to tolerate an individual amount of stress due to the pain induced and especially due to the unknown situation. Any additional stress factors should be avoided for the patient's sake but also to ensure the optimal compliance. Time is of the essence here as mentioned earlier. Another stress factor is acoustic noise and this should not be neglected, because many patients describe the noise as the most unpleasant experience of an MR imaging examination, second only to the limited space inside the magnet bore. Therefore, quieter imaging sequences are preferable if no other disadvantages such as reduced image contrast or speed outweigh these. In addition, very loud imaging sequences such as from steady-state free-precession techniques, for example, can hinder any communication quite dramatically.

MR imaging allows different ways to visualize instruments, and these can be divided into active and passive methods of instrument visualization (Coutts et al. 1998; Sathyanarayana et al. 2007; Schulz et al. 1999; Staubert et al. 2000; Wildermuth et al. 1998). An in-depth discussion of all the different methods is beyond the scope of this chapter; however, most of the time one will focus on passive methods for nonvascular interventions.

In short, active methods use one or even more microcoils fixed to the interventional instrument – usually its tip. Using the MR scanner, one determines the positions of the micro coils and these are projected either onto a previously acquired road-map image or onto an anatomic image acquired during the determination of the microcoil position (Buecker et al. 2002b; Wildermuth et al. 1998). This technique requires a modification of the interventional instrument by attaching a microcoil. In addition, the original active visualization technique required the connection of the microcoil to the scanner. This sophisticated technique makes a simple procedure such as MR-guided biopsy quite complicated and further safety concerns arise, which are beyond the scope of this book. Additional changes to the MR scanner and the software are needed as well. Newer techniques of active visualization exploit so-called fiducial markers (Coutts et al. 1998), which do not require a connection of the interventional instrument to the MR scanner. But still changes to the software are needed to visualize and localize the fiducial marker.

In contrast to the active methods, passive visualization of an instrument is done without any hardware or software changes. The interventional instrument is displayed directly on the acquired anatomic image.

3.2.3 Imaging Sequence – How to Influence the Appearance of Metallic Instruments and Susceptibility Artifacts

Many interventional instruments still consist of metal. Metals have to be nonferromagnetic in order not to be attracted by the strong magnetic field of the MR scanners. This is the case for *most* modern implants, which consist of stainless steel, Nitinol alloys, or titanium to name a few. But is any nonferromagnetic device MR-safe or MR-compatible? There is some confusion concerning these terms. The Food and Drug Administration offered the following definitions:

MR-compatible: This term indicates that the device, when used in the MR environment, is MR-safe and has been demonstrated neither to significantly affect the quality of the diagnostic information nor to have its operations affected by the MR device.

MR-safe: This term indicates that the device, when used in the MR environment, has been demonstrated to present no additional risk to the patient, but may affect the quality of the diagnostic information.

According to these definitions a device can not be named MR-compatible without stating the MR environment (namely, the field strength) and the MR imaging indication. A stainless steel coronary stent may be MR-compatible according to the abovementioned definition for a functional MR examination of the heart, but it will be "only" MR-safe for imaging of the coronary arteries.

Another safety concern in the MR environment is caused by the nature of metals, which are electrically conducting. Depending on the length of the conducting material and the field strength of the MR scanner, an interventional instrument can act as an antenna. Substantial heating of metallic guide wires has been shown to occur during in vitro and in vivo experiments. The radiofrequency energy used to create the MR images can be fed into the instrument if the instrument is in resonance with the radiofrequency power applied. There is no agreement among physicists of different groups on the minimum length at which these safety concerns may appear. The minimal length for occurrence of resonance of a conductive wire is given as 29 cm by one group (Nitz et al. 2001) and 117 cm by another (Armenean et al. 2004). But even for 29 cm the length of biopsy needles is below the lowest critical threshold for MR scanners with a magnet strength of 1.5 T or less.

In the following it will be explained how to manipulate susceptibility artifacts (Ladd et al. 1996). Depending on the field strength, a large artifact might be advantageous compared with a smaller one. While this can be true for low-field-strength MR scanners, usually the opposite holds for higher-field-strength MR scanners, requiring minimization of susceptibility artifacts to optimally visualize a metallic instrument and a pathologic lesion. Consequently, the principles will be explained but no generally true recommendations as to the imaging sequence parameters to be used can be given.

Spin echo sequences will, in general, yield a smaller susceptibility artifact compared with gradient echo sequences (Fig. 3.3). The susceptibility artifact of a gradient echo sequence will be greatly influenced by the echo time used; the shorter the echo time, the smaller the accompanying artifact (Fig. 3.4).

The orientation of any metallic instrument to the main magnetic field influences the size of the instrument in the image (Fig. 3.2). Usually the ideal approach of a needle to a lesion is predefined and cannot be altered. Nonetheless, one has to be aware of this effect and the possible change of artifact size. Furthermore, a complete switch of phase and frequency encoding direction can be easily achieved, allowing for a substantial change of the size of susceptibility artifacts. This is demonstrated by the first and last images in Fig. 3.2, which differ in the orientation of the

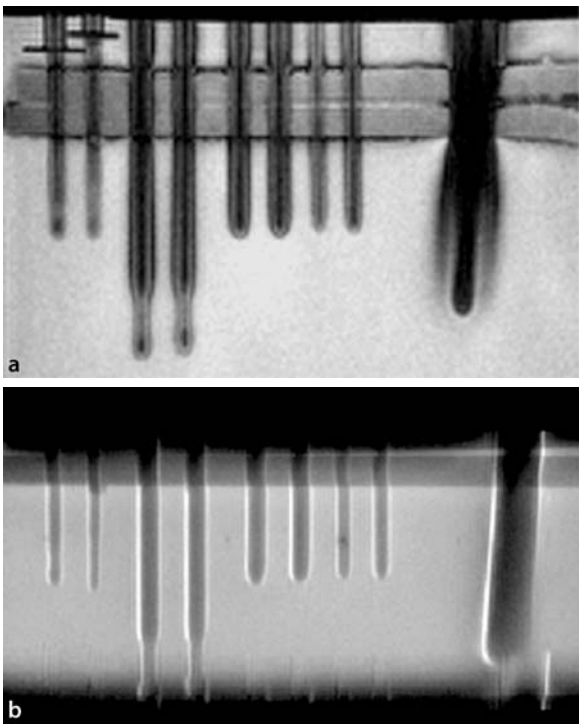

Fig. 3.3a,b Different magnetic resonance (MR) compatible biopsy needles (18 G Tru-Cut, 14 G Tru-Cut, 18 G biopsy, and 22 G biopsy needles) and one non-MR-compatible 22 G needle (*last needle on the right*) are imaged in a water bath with a gradient echo sequence (**a**) and a spin echo sequence (**b**)

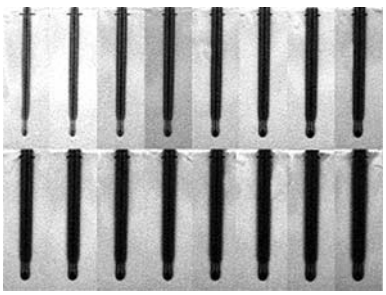

Fig. 3.4 Gradient echo images of a 14 G biopsy needle acquired with stepwise increase of echo time from 1.5 ms for the *left of the upper row* to 20 ms for the *right of the lower row* (**a**) (1.5, 2, 3, 4, 5, 6, 7, 8, 9, 10, 11, 12, 13, 14, 15, 20 ms)

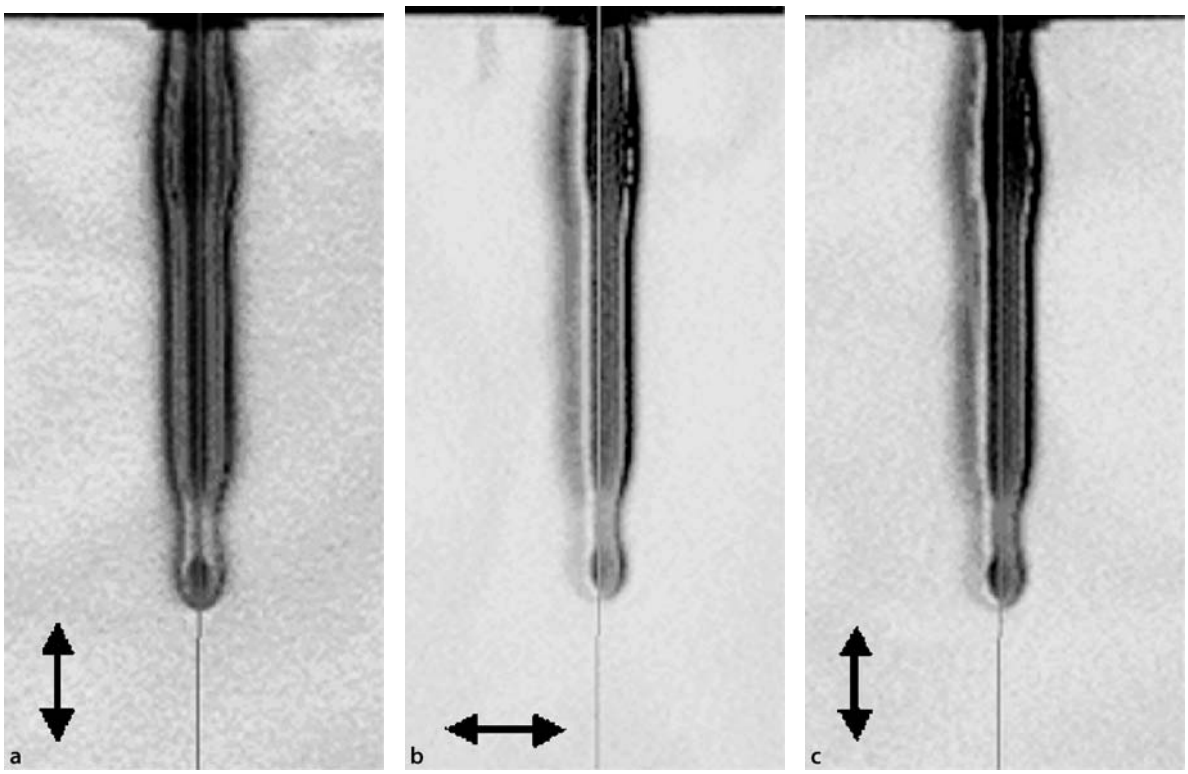

Fig. 3.5a–c Gradient echo images of a 14G needle in a water bath demonstrating the effect of shifting the susceptibility artifact about the true center of the needle, which is marked by the *vertical line*. **a** Image acquired without any partial *k*-space strategies. **b** Image acquired with 65% echo readout (partial echo). **c** Image acquired with partial *k*-space filling of 65%. The *black arrows* indicate the phase encoding direction

biopsy needle to the main magnetic field; the change of this orientation is equivalent to switching the phase and frequency encoding direction of the imaging sequence.

In order to achieve faster imaging methods a reduction of the echo readout or partial filling of *k*-space is sometimes used. If these techniques are applied to sequences used to guide interventions, one has to be aware of a slight change of the form of susceptibility artifacts. One half of the susceptibility artifact surrounding the metallic instrument will be reduced. While this can be easily detected in an experimental setup imaging a needle within a water bath (Fig. 3.5), it might be much more difficult to visualize with an anatomic background. Usually the needle will be in the center of the signal drop and imaging artifact caused by the difference in susceptibility. This is no longer true when applying partial echo or half Fourier imaging sequences (Fig. 3.5). The amount of metal will also influence the artifact size. Sometimes this parameter can be changed by removing/inserting a mandrel into a needle.

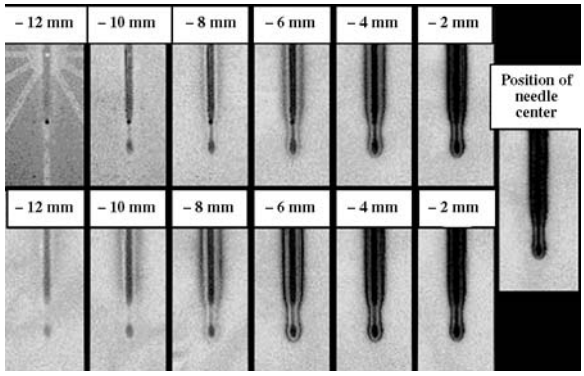

Fig. 3.6 Gradient echo images acquired with a slice thickness of 10 mm are moved in a 2-mm stepwise fashion about the physical center of the biopsy needle positioned in a water bath

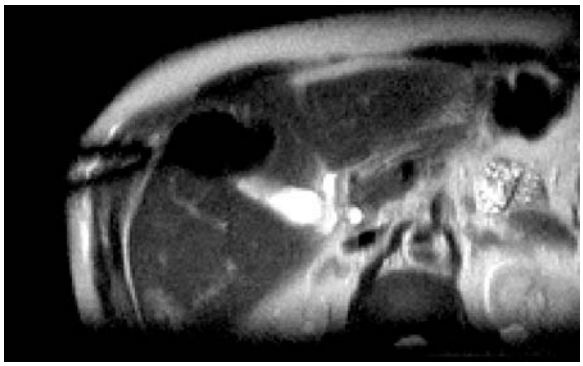

Fig. 3.7 Ice ball formation around two cryoprobes in the liver as depicted on a T2-weighted image acquired in 600 ms (LoLo technique). (Image courtesy of J. Tacke, Passau Hospital, Germany)

So far, we have only looked at the appearance of the interventional instrument within the imaged slice. The three-dimensional artifact is symmetrically oriented around the physical position of the needle (Fig. 3.6); therefore, the needle is not centered at the slice position where the needle shape can be depicted best. Instead the largest artifact will define the image where the needle is centered exactly in the middle of the imaging plane (Fig. 3.6).

3.2.4 Imaging Sequence – Dedicated Temperature Measurements

Tumor ablation is an increasingly widespread therapy. Different hyperthermal ablation techniques as well as cryoablation are in routine clinical use. Cryotherapy can be easily controlled by MR imaging because the growing ice ball is clearly visualized on standard MR images (Fig. 3.7). The best correlation between the necrotic area and the depicted size of the area of signal

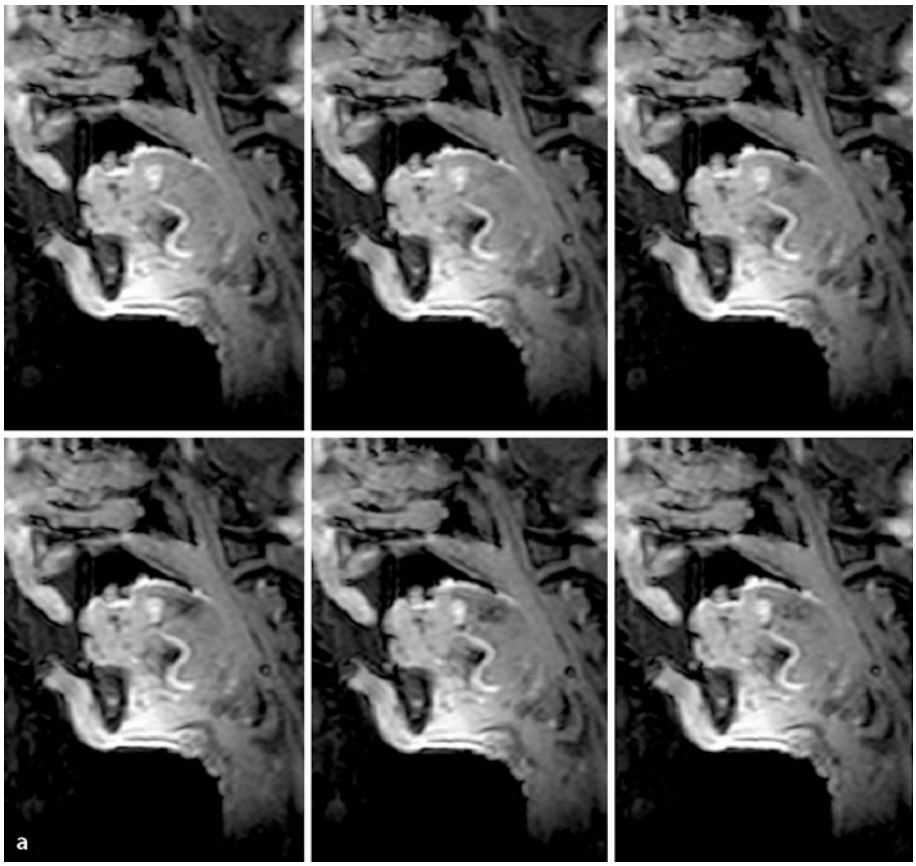

Fig. 3.8a It is difficult to depict the temperature increase around a laser fiber on these T1-weighted gradient echo images. A slight drop in signal intensity can be seen around the laser tip positioned in the tongue base tumor

void seen on MR images is achieved with T2-weighted spin echo images (Tacke et al. 2001). Few clinical studies have been reported on the topic of MR-guided cryosurgery (Mogami et al. 2007; Morin et al. 2004). This is probably due to the fact that radiofrequency ablation leads to larger lesions than does cryoablation with identically sized instruments.

Hyperthermal ablation is performed with radiofrequency, laser, microwaves, or focused ultrasound probes (de Jode et al. 1999; Furusawa et al. 2007; Hynynen et al. 1997; Kurumi et al. 2007; Mueller-Lisse and Heuck 1998; Steiner et al. 1998; Vogl et al. 2007). Beside some technical problems for the use of radiofrequency and microwave generators within the MR environment, the visualization of temperature changes by MR is in general possible. Qualitatively this can be achieved by T1-weighted images (Fig. 3.8a), but the control of thermal ablation is not sufficient using the signal drop seen on T1-weighted images. Exploiting the inherent physical properties of the MR technique one can also semi-quantitatively image temperature changes (Fig. 3.8b). These MR techniques are very prone to movement artifacts. Newer real-time sequences for temperature measurements have been developed (de Senneville et al. 2007). The first clinical trials for MR-guided focused ultrasound treatment of breast lesions (Furusawa et al. 2007) and uterine fibroids (Stewart et al. 2006) have been performed.

3.3 Indications

The relatively complicated technique of MR imaging, the availability, and the cost prohibit widespread use of MR guidance for interventions which can be controlled by other imaging modalities such as ultrasound

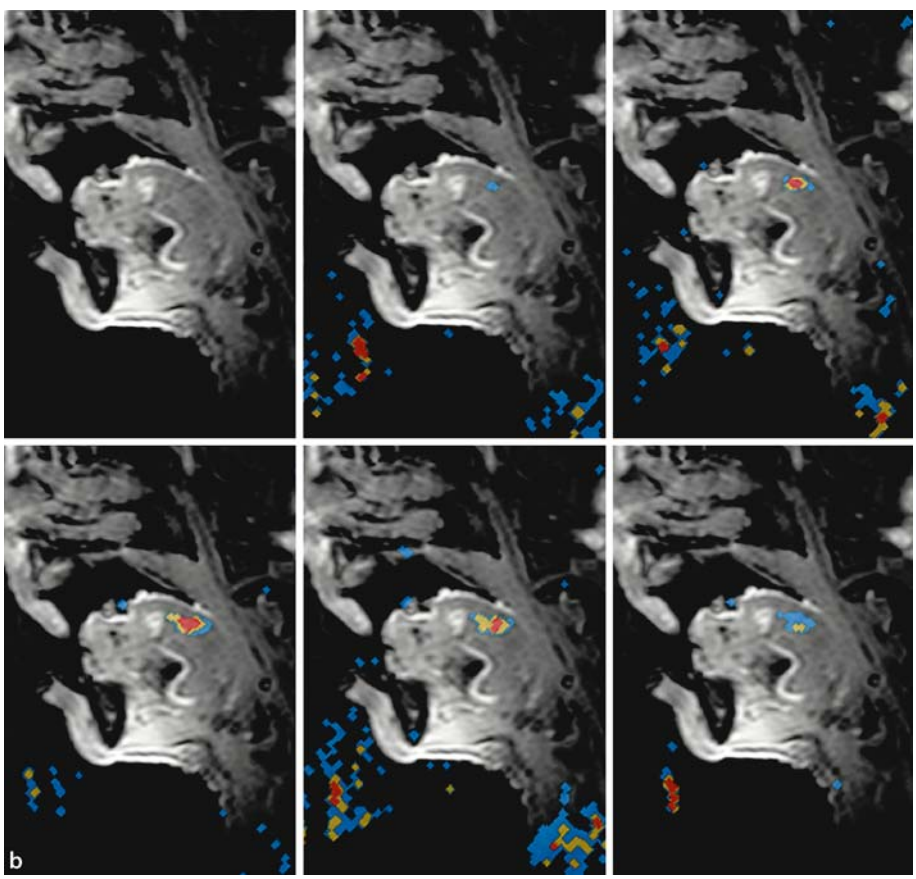

Fig. 3.8b Using the temperature-dependent change of the phase information of the same MR images, one can project a semiquantitative depiction of the temperature changes onto the anatomic images

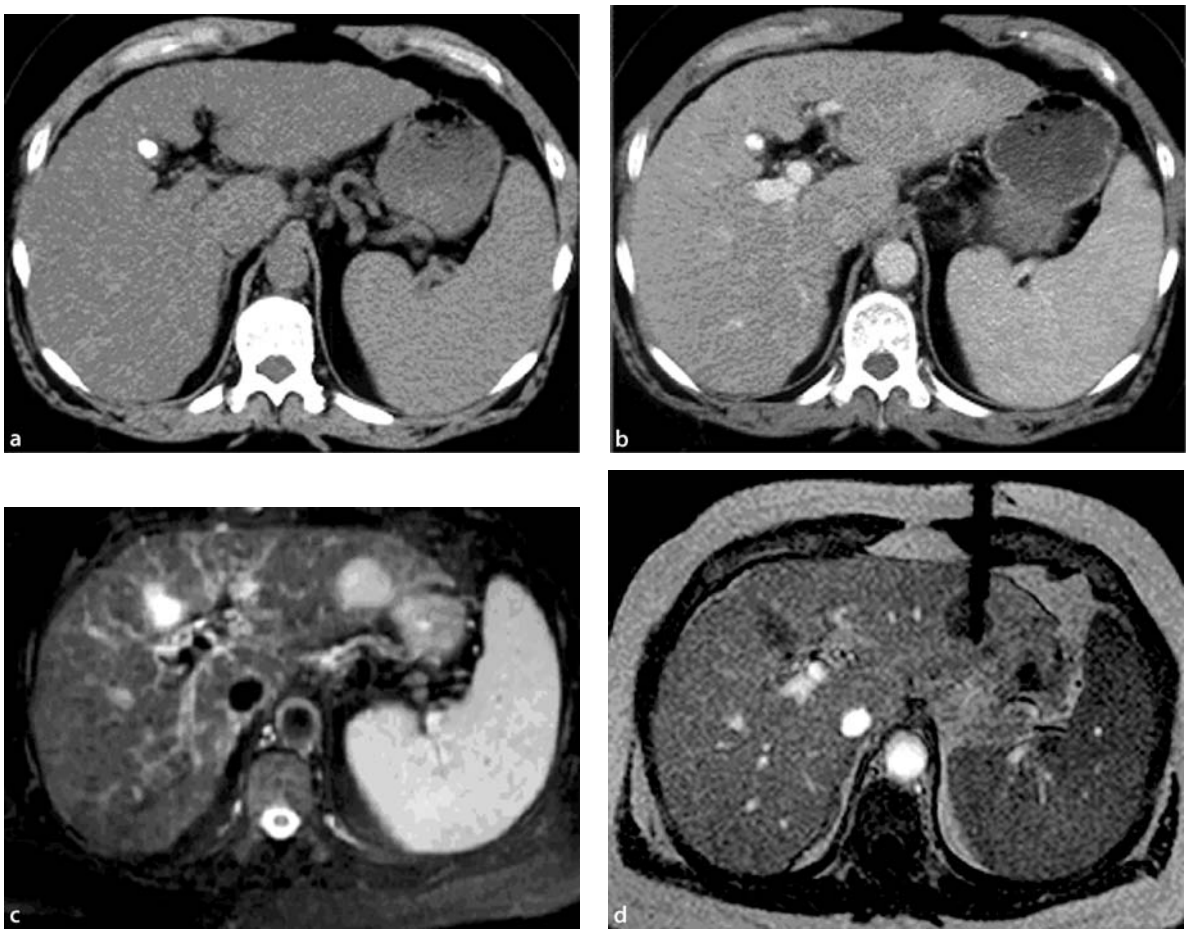

Fig. 3.9a–d A liver tumor was initially overlooked on the computed tomography images (**a**, **b**). It is clearly visualized on the T2-weighted imaged (**c**) and was biopsied using a T1-weighted gradient echo sequence (**d**). Histologically, the tumor proved to be a hepatocellular carcinoma

or CT. But there are lesions which can only be seen by MR imaging and consequently can only be biopsied by this technique. Seldom, this is the case for tumors of the liver (Fig. 3.9), but the most common lesions only visible by MR imaging are breast lesions. MR offers the means for simple biopsies and markings (Fig. 3.10) (Dershaw 2000; Heywang-Kobrunner et al. 2000), but also the possibility of excisional biopsies (Gould et al. 1998). MR-guided brain biopsies have been performed and have been proved to be superior to stereotactic brain biopsy (Hall et al. 1999a). Bone marrow lesions can be very well visualized by MR imaging, and consequently MR guidance for these lesions can be performed as well (Neuerburg et al. 1998) (Fig. 3.1).

The necessary instruments for biopsies as well as for preoperative marking are now available (Flory and Helbich 2006). Beside metallic instruments, nonmetallic devices have been tested as well (Reichenbach et al. 2000), but so far they have not replaced metallic instruments. Dedicated breast biopsy devices exist which fixate the breast and allow an approach from the lateral side (deSouza et al. 1995; Fischer et al. 1995). Techniques without the need for any additional devices have been described as well (Daniel et al. 1998). Usually the procedures are performed with the patient outside the magnet bore, with the advance of the interventional instrument being controlled by placing the patient in the scanner bore after advancing the instrument blindly. But au-

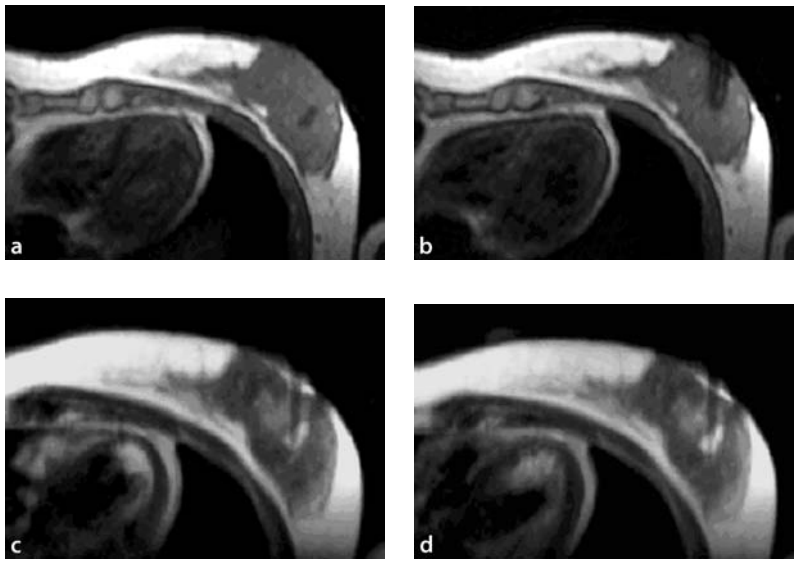

Fig. 3.10a–d T1-weighted gradient echo image without contrast agent depicts a breast lesion which showed a pathologic fast uptake of contrast agent, suggesting a malignant tumor (**a**). Using a T1-weighted gradient echo sequence, the localization wire causes a susceptibility artifact large enough to hide the lesion (**b**). Changing to a T2-weighted spin echo sequence nicely depicts the needle (**c**) and the marking wire (**d**) within the lesion, which was successfully removed operatively and turned out to be a fibroadenoma

tomated devices have been developed which can be used via remote control and allow the patient to be kept all the time inside the magnet bore, thereby allowing continuous control of the procedure (Kaiser et al. 2000).

Ablative therapy is so far not a standard indication for MR guidance. The treatment of uterine fibroids and breast lesions by focused ultrasound requires a direct control of this minimally invasive technique. In this field, MR guidance has been shown to be invaluable, leading to dedicated focused ultrasound probes integrated into MR tables (Gedroyc and Anstee 2007).

MR-guided focused ultrasound treatment of breast lesions (Furusawa et al. 2007) and uterine fibroids (Stewart et al. 2006) has been performed clinically so far. Other techniques of thermoablation such as laser and radiofrequency therapy have been applied with MR guidance as well (Mahnken et al. 2004a; Meister et al. 2007; Reither et al. 2000), but for this field it is not clear if a broader clinical indication will arise, because standard treatment without direct control of heat spreading is widely available and performed already (Pereira 2007). Treatment of renal tumors with cryoablation (Mogami et al. 2007), radiofrequency therapy (Lewin et al. 2004), or microwave therapy (Kurumi et al. 2007) has been performed under MR guidance, but the clinical value of all the different available techniques for different indications remains to be proved.

MR imaging is also used for intraoperative guidance of surgical procedures and has been successfully exploited clinically for neurosurgery and endoscopic sinus surgery (Alexander et al. 1995; Buchfelder et al. 2000; Hall et al. 1998; Hsu et al. 1998; Rubino et al. 2000). In the field of clinical neurosurgery complication rates were found to be acceptable (Hall et al. 2000).

Summary

Despite the fact that MR guidance is cost-intensive compared with ultrasound and CT guidance, there is a growing role for MR-guided interventions. Obviously, tumors only visible by MR imaging such as breast lesions are one major indication. But beyond this, the imaging feature of MR imaging allowing temperature measurements has been developed to a state allowing for clinical use. Especially thermal ablation

therapies – and among these focused ultrasound – are controlled by MR imaging and offer a truly noninvasive combination of ablation therapy. Clinically the combination of focused ultrasound and MR guidance is used for breast lesions and uterine leiomyomas, but a growing spread of indications can be expected with further development of focused ultrasound techniques which will allow even the noninvasive penetration of bone.

Key Points

- There are dedicated interventional MR scanners with dedicated software.
- The susceptibility artifacts of metallic instruments can be influenced by changing the imaging sequence; the following parameters lead to smaller susceptibility artifacts:
  1. Spin echo instead of gradient echo sequence;
  2. Shorter echo time for gradient echo sequences;
  3. Smaller amount of metal (remove mandrel);
  4. Orientation of the length of the instrument parallel to the frequency encoding direction;
  5. Lower main magnetic field.
- Compatibility
  1. MR-compatible means MR-safe without affecting the image quality (depends on the main magnetic field) and indication;
  2. MR-safe instruments can affect the image quality, but are still safe to use (depends on the main magnetic field).
- Visualization
  1. Passive visualization: direct visualization of an instrument in the MR image;
  2. Active visualization: use of dedicated microcoils to calculate the position of the microcoil and project this position onto the previously acquired MR image.
- There is no one, optimal imaging sequence for MR guidance.
- MR imaging can depict temperature changes, thereby allowing for control of temperature ablation, which is especially useful for focused ultrasound therapy.
- The most demanding indication for MR guidance of nonvascular interventions is breast lesions only visible by MR imaging.

References

Adam G, Neuerburg J, Bücker A et al. (1997) Interventional magnetic resonance. Initial clinical experience with a 1.5-tesla magnetic resonance system combined with c-arm fluoroscopy. Invest Radiol 32:191–197

Adam G, Bücker A, Glowinsku A et al. (1998) Interventionelle MR Tomographie: Gerätekonzepte. Radiologe 38:168–172

Adam G, Bücker A, Nolte-Ernsting C et al. (1999) Interventional MR imaging: percutaneous abdominal and skeletal biopsies and drainages of the abdomen. Eur Radiol 9:1471–1478

Alexander E 3rd, Kooy HM, van Herk M et al. (1995) Magnetic resonance image-directed stereotactic neurosurgery: use of image fusion with computerized tomography to enhance spatial accuracy. J Neurosurg 83:271–276

Armenean C, Perrin E, Armean M et al. (2004) RF-induced temperature elevation along metallic wires in clinical magnetic resonance imaging: influence of diameter and length. Magn Reson Med 52:1200–1206

Barentsz JO (1997) MR intervention in the pelvis: an overview and first experiences in MR-guided biopsy in nodal metastases in urinary bladder cancer. Abdom Imaging 22:524–530

Buchfelder M, Ganslandt O, Fahlbusch R et al. (2000) Intraoperative magnetic resonance imaging in epilepsy surgery. J Magn Reson Imaging 12:547–555

Bucker A, Adam G, Neuerburg JM et al. (1997) MR-gesteuerte Biopsie mit einer hochauflösenden schnellen T2-gewichteten Turbospinechosequenz „LoLo“: erste klinische Erfahrungen. Rofo 167:491–495

Buecker A, Adam G, Neuerburg JM et al. (1998) MR-guided biopsy using a T2-weighted single-shot zoom imaging sequence (local look technique). J Magn Reson Imaging 8:955–959

Buecker A, Spuentrup E, Grabitz R et al. (2002a) Magnetic resonance-guided placement of atrial septal closure device in animal model of patent foramen ovale. Circulation 106:511–515

Buecker AG, Neuerburg JM et al. (2002b). Simultaneous real-time visualization of the catheter tip and vascular anatomy for MR-guided PTA of iliac arteries in an animal model. J Magn Reson Imaging 16:201–208

Coutts GA, Gilderdale DJ, Chui M et al. (1998) Integrated and interactive position tracking and imaging of interventional tools and internal devices using small fiducial receiver coils. Magn Reson Med 40:908–913

Daniel BL, Birdwell RL, Ikeda DM et al. (1998) Breast lesion localization: a freehand, interactive MR imaging-guided technique. Radiology 207:455–463

de Jode MG, Vale JA, Gedroyc WM (1999) MR-guided laser thermoablation of inoperable renal tumors in an open- configuration interventional MR scanner: preliminary clinical experience in three cases. J Magn Reson Imaging 10:545–549

Dershaw DD (2000) Equipment, technique, quality assurance, and accreditation for imaging-guided breast biopsy procedures. Radiol Clin North Am 38:773–789

de Senneville BD, Mougenot C, Moonen CT (2007) Real-time adaptive methods for treatment of mobile organs by MRI-controlled high-intensity focused ultrasound. Magn Reson Med 57:319–330

deSouza NM, Kormos DW, Krausz T et al. (1995) MR-guided biopsy of the breast after lumpectomy and radiation therapy using two methods of immobilization in the lateral decubitus position. J Magn Reson Imaging 5:525–528

Duerk JL, Lewin JS, Wendt M et al. (1998) Remember true FISP? A high SNR, near 1-second imaging method for T2-

like contrast in interventional MRI at .2 T. J Magn Reson Imaging 8:203–208
Fischer U, Vosshenrich R, Döler W et al. (1995) MR imaging-guided breast intervention: experience with two systems. Radiology 195:533–538
Floery D, Helbich TH (2006) MRI-guided percutaneous biopsy of breast lesions: materials, techniques, success rates, and management in patients with suspected radiologic-pathologic mismatch. Magn Reson Imaging Clin N Am 14:411–425
Frahm C, Gehl HB, Melchert UH et al. (1996a) Visualization of magnetic resonance-compatible needles at 1.5 and 0.2 Tesla. Cardiovasc Intervent Radiol 19:335–340
Frahm C, Gehl HB, Weiss HD et al. (1996b) Technik der MRT-gesteuerten Stanzbiopsie im Abdomen an einem offenen Niederfeldgerät: Durchführbarkeit und erste klinische Ergebnisse. Rofo 164:62–67
Furusawa H, Namba K, Nakahara H et al. (2007) The evolving non-surgical ablation of breast cancer: MR guided focused ultrasound (MRgFUS). Breast Cancer 14:55–58
Gedroyc WM, Anstee A (2007) MR-guided focused ultrasound. Expert Rev Med Devices 4:539–547
Gehl HB, Frahm C, Schimmelpenning H et al. (1996) Technik der MRT gesteuerten abdominellen Drainage an einem offenen Niederfeldmagneten: Durchführbarkeit und erste Ergebnisse. Rofo 165:70–73
Gould SW, Lamb G, Lomax D et al. (1998) Interventional MR-guided excisional biopsy of breast lesions. J Magn Reson Imaging 8:26–30
Hall WA, Martin AJ Liu H et al. (1998) High-field strength interventional magnetic resonance imaging for pediatric neurosurgery. Pediatr Neurosurg 29:253–259
Hall WA, Liu H, Martin AJ et al. (1999a) Comparison of stereotactic brain biopsy to interventional magnetic resonance-imaging-guided brain biopsy. Stereotact Funct Neurosurg 73:148–153
Hall WA, Martin AJ, Liu H et al. (1999b) Brain biopsy using high-field strength interventional magnetic resonance imaging. Neurosurgery 44:807–814
Hall WA, Liu H, Martin AJ et al. (2000) Safety, efficacy, and functionality of high-field strength interventional magnetic resonance imaging for neurosurgery. Neurosurgery 46:632–642
Heywang-Kobrunner SH, Heinig A, Pickuth D et al. (2000) Interventional MRI of the breast: lesion localisation and biopsy. Eur Radiol 10:36–45
Hsu L, Fried MP, Jolesz FA (1998) MR-guided endoscopic sinus surgery. AJNR Am J Neuroradiol 19:1235–1240
Hynynen K, Vykhodtseva NI, Chung AH et al. (1997) Thermal effects of focused ultrasound on the brain: determination with MR imaging. Radiology 204:247–253
Kaiser WA, Fischer H, Vagner J et al. (2000) Robotic system for biopsy and therapy of breast lesions in a high-field whole-body magnetic resonance tomography unit. Invest Radiol 35:513–519
Kurumi Y, Tani T, Naka S et al. (2007) MR-guided microwave ablation for malignancies. Int J Clin Oncol 12:85–93
Ladd ME, Erhart P, Debatin JF et al. (1996) Biopsy needle susceptibility artifacts. Magn Reson Med 36:646–651
Lewin JS, Nour SG, Connell CF et al. (2004) Phase II clinical trial of interactive MR imaging-guided interstitial radiofrequency thermal ablation of primary kidney tumors: initial experience. Radiology 232:835–845
Mahnken AH, Buecker A, Spuentrup E et al. (2004a) MR-guided radiofrequency ablation of hepatic malignancies at 1.5 T: initial results. J Magn Reson Imaging 19:342–348
Mahnken AH, Chalabi K, Jalali F et al. (2004b) Magnetic resonance-guided placement of aortic stents grafts: feasibility with real-time magnetic resonance fluoroscopy. J Vasc Interv Radiol 15:189–195
Meister D, Hubner F, Mack M et al. (2007) MR-Thermometrie bei 1,5 Tesla zur thermischen Ablation mittels laserinduzierter Thermotherapie. Rofo 179:497–505
Mogami T, Harada J, Kishimoto K et al. (2007) Percutaneous MR-guided cryoablation for malignancies, with a focus on renal cell carcinoma. Int J Clin Oncol 12:79–84
Morin J, Traore A, Dionne G et al. (2004) Magnetic resonance-guided percutaneous cryosurgery of breast carcinoma: technique and early clinical results. Can J Surg 47:347–351
Mueller-Lisse UG, Heuck AF (1998) Steuerung und Monitoring von fokalen Thermotherapien mit der Magnetresonanztomographie. Radiologe 38:200–209
Neuerburg JM, Adam G, Buecker A et al. (1998) MRI-guided biopsy of bone in a hybrid system. J Magn Reson Imaging 8:85–90
Nitz WR, Oppelt A, Renz W et al. (2001) On the heating of linear conductive structures as guide wires and catheters in interventional MRI. J Magn Reson Imaging 13:105–114
Paley M, Mayhew JE, Martindale AJ et al. (2001) Design and initial evaluation of a low-cost 3-Tesla research system for combined optical and functional MR imaging with interventional capability. J Magn Reson Imaging 13:87–92
Pereira PL (2007) Actual role of radiofrequency ablation of liver metastases. Eur Radiol 17:2062–2070
Reichenbach JR, Wurdinger S, Pfleiderer SO et al. (2000) Comparison of artifacts produced from carbon fiber and titanium alloy needles at 1.5 T MR imaging. J Magn Reson Imaging 11:69–74
Reither K, Wacker F, Ritz JP et al. (2000) Laserinduzierte Thermotherapie (LITT) von Lebermetastasen in einem offenen 0,2 T MRT. Rofo 172:175–178
Rubino GJ, Farahani K, McGill D et al. (2000) Magnetic resonance imaging-guided neurosurgery in the magnetic fringe fields: the next step in neuronavigation. Neurosurgery 46:643–654
Sathyanarayana S, Aksit P, Arepally A et al. (2007) Tracking planar orientations of active MRI needles. J Magn Reson Imaging 26:386–391
Schulz T, Schneider JP, Winkel A et al. (1999) Der MR-Track-Pointer. Ein wiederverwendbares Instrument zur Lokalisation bei Interventionen. Rofo 171:244–248
Solomon SB, Bohlman ME, Choti MA (2002) Percutaneous gadolinium injection under MR guidance to mark target for CT-guided radiofrequency ablation. J Vasc Interv Radiol 13:419–421
Spuentrup E, Ruebben A, Schaeffter T et al. (2002) Magnetic resonance – guided coronary artery stent placement in a swine model. Circulation 105:874–879
Staubert A, Vester M, Tronnier VM et al. (2000) Interventional MRI-guided brain biopsies using inductively coupled surface coils. Magn Reson Med 43:278–283

Steiner P, Botnar R, Dubno B et al. (1998) Radio-frequency-induced thermoablation: monitoring with T1-weighted and proton-frequency-shift MR imaging in an interventional 0.5-T environment. Radiology 206:803–810

Stewart EA, Rabinovici J, Tempany CM et al. (2006) Clinical outcomes of focused ultrasound surgery for the treatment of uterine fibroids. Fertil Steril 85:22–29

Tacke J, Adam G, Haage P et al. (2001) MR-guided percutaneous cryotherapy of the liver: in vivo evaluation with histologic correlation in an animal model. J Magn Reson Imaging 13:50–56

Vogl TJ, Lehnert T, Eichler K et al. (2007) Adrenal metastases: CT-guided and MR-thermometry-controlled laser-induced interstitial thermotherapy. Eur Radiol 17:2020–2027

Wildermuth S, Debatin JF, Leung DA et al. (1997) MR imaging-guided intravascular procedures: initial demonstration in a pig model. Radiology 202:578–583

Wildermuth S, P Erhart, Leung DA et al. (1998) Aktive Instrumentenführung in der Interventionellen MR-Tomographie: Einführung eines neuen Konzept. Rofo 169:77–84

Radiation Protection During CT-Guided Interventions

4

Kerstin Jungnickel

Contents

4.1 Introduction

Computed tomography (CT) fluoroscopy combines the benefit of a perfect localization of CT with real-time-imaging of conventional fluoroscopy. However, the major concern is the exposure of the patient and the operator to radiation. CT employs a highly collimated beam with a much higher dose rate than conventional fluoroscopy. During CT-guided interventions, two aspects have to be considered:

1. The skin dose of the patient can potentially be very high because the same slice is scanned again and again.
2. The operator is always in the direct vicinity of the gantry. Specifically in the fluoroscopy mode the interventionalist's skin on his/her hand is endangered when it is in the direct beam.

Two modes are established in CT intervention: a sequential mode with one image acquired after the other, to verify the needle position as well as the path to the target; and CT fluoroscopy with a continuous scan during the whole procedure, potentially leading to higher radiation exposure than the sequential mode.

4.2 Dose Considerations

During CT interventions the tube current is usually reduced to about 50 mA. Some operators even work with 10 mA (Paulson et al. 2001), as long as the image quality is sufficient for guiding the intervention. The image quality is directly related to the detector dose and thus to the tube current–time product. Leaving the rotation time constant, a reduction of the tube current–time product results in a loss of image quality. Different from the situation with diagnostic images, this can be tolerated for CT fluoroscopy. The voltage is usually set to 120 kV. The mean fluoroscopy time is about 120 s, but depending on the method and the routine of the operator as well as on the general difficulty of the intervention, the time can vary drastically (Silverman et al. 1999).

4.2.1 Patient Dose

The typical dose rate within the beam (120 kV, 50 mA) at the patient's skin is about 5 mSv/s (300 mSv/min) (Nawfel et al. 2000). A rather long intervention with an exposure time of 7 min would lead to a critical threshold of 2 Sv for deterministic effects on the skin (Table 4.1). The effective dose rate of the patient is about 1% of the dose rate at the skin (Hohl et al. 2008). For

Table 4.1 Estimation of computed tomography fluoroscopy time when the threshold of the deterministic effect and the dose limit for skin is reached (scan parameters 120 kV, 50 mA, 10-mm collimation)

Threshold of deterministic effects at the skin (2 Gy) reached after	7 min
Dose limit for skin/hand for occupational exposure (500 mSv per year) reached after	2 min/200 min (inside/outside direct beam)

a mean fluoroscopy time of 2 min this would lead to an effective dose of 6 mSv. This is a dose similar to that which would be delivered during a diagnostic CT examination.

4.2.2 Operator Dose

For the operator the dose limits for occupational exposure must be considered. The dose limit for the hand is 500 mSv per year. If the interventionalist exposes his/her hand in the beam, the dose received is equal to the dose to the patient's skin, which, given the average values quoted earlier, is about 5 mSv/s. If the operator's hand is not in the direct beam, the dose obviously is much less. A few centimeters away from the beam the radiation exposure of the interventionalist is limited only to the scattering generated in the patient. The dose rate rapidly drops from a few millisieverts per second within the beam to 40–50 µSv/s at a distance of 10 cm from the gantry (Nawfel et al. 2000; Stoeckelhuber et al. 2005). If the interventionalist's hand is in the direct beam, he/she reaches the dose limit after less than 2 min! If the hand is not in the direct beam, the dose limit is reached after 200 min – e.g., 100 interventions with a duration of 2 min each.

The dose limit for the effective dose for occupational exposure is 20 mSv per year. Our unpublished data reveal that the dose rate at the usual position of the interventionalist next to the gantry is about 2 µSv/s, leading to an effective dose of about 0.02 mSv for a 2-min intervention if the operator wears a lead apron (0.35 mm). This calculation includes the significantly reduced shielding of the lead aprons at 120 kV as compared with 80 kV. X-rays of 120 kV are more penetrating and thus lead to absorption of less than 90% by the lead apron (80 kV: 97%). Thus, the amount of radiation which penetrates the lead apron and reaches the interventionalist is greater than in conventional fluoroscopy by a factor of 3. The dose limit for the effective dose is reached after 2000 min – e.g., 1000 interventions with a duration of 2 min each.

The radiation exposure of the eyes, with the lenses being at risk of cataract formation, is another aspect to be considered carefully. In the literature, the threshold for detectable opacity of the lenses is estimated at 500–2000 mSv, and for visual impairment at 5000 mSv (Hidajat et al. 2006; Britton and Wholey1988); hence, eye protection is crucial at CT intervention. The dose limit for the eye lens for occupational exposure is 150 mSv per year. With a dose rate of 2 µSv/s the limit is reached after 1500 min (without protective goggles) – e.g., 750 interventions with a duration of 2 min each.

4.3 Radiation Protection in General

The distance to the gantry and the patient (the patient scatters radiation) should be maximized (Fig. 4.1). This is especially important for the assistant operator, nurse, or anesthesiologist, who works at the other side of the gantry. Scattering from the patient's body is the dominant source of radiation to the interventionalist. Lead protection applied as a lead cover to the patient greatly reduces exposure of the in-room personnel such as the interventionalist and the technician. It should thus be applied with care before the patient is covered with sterile drape. A dose meter under the lead apron has to be worn inside the scanner room. The interventionalist should wear a ring dose meter in addition because it is possible that his/her hand will be highly exposed. The ALARA principle states that radiation as low as reasonably achievable should be used (ICRP 1991). A dose reduction, simply by minimizing voltage, current, collimation, and fluoroscopy duration, is always recommended. Reducing the tube voltage from 140 to 120 kV results in a reduction of radiation exposure of more than 30% (Rogalla and Juran 2004). There is a linear dependence between dose and tube current–time product, so using 50 mA instead of 100 mA will lead to half the dose. The same holds for the collimation: a slice thickness of 5 mm will yield half the dose as one of 10 mm. If the scanning param-

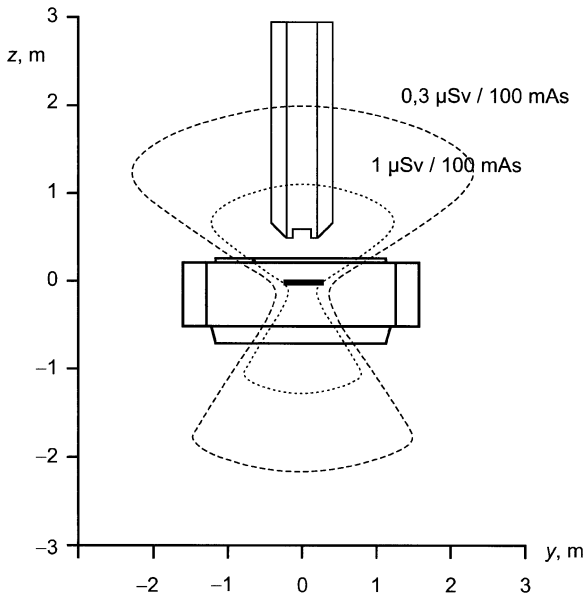

Fig. 4.1 Isodose distribution around a computed tomography scanner. (Courtesy of Siemens)

eters are optimized, the dose will be directly proportional to the fluoroscopy time.

4.4 Radiation Protection by Technical Means

A technical approach to reduce radiation exposure of the interventionalist's hand is to interrupt the radiation when the X-ray tube is in the upper segment of the gantry (usually between 10- and 2-o'clock position). This gated fluoroscopy leads to a significantly lower dose because the hand is never in the unattenuated beam (Hohl et al. 2008). However, keeping the hand out of the gantry is still highly recommended! A dose display which the interventionalist can glance at is very useful. Optimal would be a display of the patient's skin dose as a percentage of potential skin dose hazard (2 Gy), of the overall tube current–time product, and a time scale. An acoustic or optical warning signal can also be highly useful.

4.5 Radiation Protection of the Interventionalist

X-ray protection of the operator is similar to that for other fluoroscopic interventions. A lead apron with 0.35-mm lead equivalent must be worn. A thyroid shield and protective goggles must be used as well because of the proximity to the gantry. To protect the operator from the radiation scattered by the patient a lead drape should always be placed on the patient close to the scan plane. In this way the scatter radiation is reduced by more than 70% (Nawfel et al. 2000; Stoeckelhuber et al. 2005). To avoid deterministic skin effects at the hand, a needle holder is recommended. This is an effective way to protect the hand from the primary beam during the intervention and thus to reduce the skin dose by a factor of a 100 (see earlier). A plastic instead of a metal needle holder should be used to avoid metal artifacts in the image. Protective gloves which shield about 50% of the radiation and have sufficient tactility may be used in addition.

Summary

As long as the operator performs fewer than about 1000 biopsies a year, the effective dose and therefore the stochastic effect of radiation is likely to be a minor problem. The main attention has to be drawn to deterministic effects on the patient's and the operator's skin. The dose limit for occupational exposure of the hand is 500 mSv per year. If the operator's hand is frequently hit by the direct beam, this limit is easily reached. In addition, the eye lenses are exposed to scatter radiation. This effect depends directly on the distance between the interventionalist and the gantry and/or the patient, and is thus specifically threatening during CT fluoroscopy.

Key Points

- Be aware! CT interventions potentially deliver very high doses to the interventionalist, support personnel, and the patient.
- Reduce the dose delivered by careful validation of the voltage, current, and fluoroscopy time.
- Use sequential images and intermittent fluoroscopy if possible.
- Use a needle holder.
- Always wear appropriate protection including (undamaged) lead aprons, thyroid shielding, and, often underestimated, always use protective goggles to avoid cataract formation of your eye lenses.

References

Britton CA, Wholey MH (1988) Radiation exposure of personnel during digital subtraction angiography. Cardiovasc Intervent Radiol 11:108–110

Hidajat N, Wust P, Felix R et al. (2006) Radiation exposure to patient and staff in hepatic chemoembolization: risk estimation of cancer and deterministic effects. Cardiovasc Intervent Radiol 29(5):791–796

Hohl C, Suess C, Wildberger JE et al. (2008) Dose reduction during CT fluoroscopy: phantom study of angular beam modulation. Radiology 246:519–525

ICRP (1991) Recommendations of the International Commission on Radiological Protection. ICRP publication 60. Pergamon, Oxford

Nawfel RD, Philip FJ, Silverman SG et al. (2000) Patient and personnel exposure during CT fluoroscopy-guided interventional procedures. Radiology 216:180–184

Paulson EK, Sheafor DH, Enterline DS et al. (2001) CT fluoroscopy-guided interventional procedures: techniques and radiation dose to radiologists. Radiology 220:161–167

Rogalla P, Juran R (2004) CT-Durchleuchtung. Radiologe 44:671–675

Silverman SG, Tuncali K, Adams DF et al. (1999) CT-fluoroscopy-guided abdominal interventions: techniques, results, and radiation exposure. Radiology 212:673–681

Stoeckelhuber BM, Leibecke T, Schulz E et al. (2005) Radiation dose to the radiologist's hand during continuous CT fluoroscopy-guided interventions. Cardiovasc Intervent Radiol 28:589–594

Medical Management of the Patient

5

Dietrich Henzler and Michael Murphy

Contents

5.1 Introduction

Substantial progress has been made in the practice of interventional radiology. Such gains would not be possible without adequate medical management of patients. Their well-being may be threatened by such procedures, many of which exceed several hours' duration, during which time they need to remain totally immobile. Certain procedures may be painful or impose the risk of substantial complications. The patient population subjected to these procedures is tending to the extremes of life: the very young and the very old. These patients tend to be fragile and at times noncompliant with the demands of the procedure.

This chapter provides an overview of the monitoring techniques that may be used, medications that may prove useful, and the limitations of self-administered sedation.

Before embarking on these discussions, it is crucial that all involved in the planning for these suites understand the requirements imposed by health care organizations, specialty societies, and building codes with respect to anesthetizing locations. Issues such as the location of piped gas outlets, electrical safety, and air exchanges per hour must be incorporated in the plan to ensure that sedation or occasional anesthesia can be performed in these areas and remain within the applicable laws and standards.

5.2 Materials and Techniques

5.2.1 Monitoring

Ensuring the patient's hemodynamic and respiratory stability may be a major challenge during these procedures, particularly for patients at the extremes of age. Proximity and access to the patient may be limited owing to positioning within the scanner. These factors easily distract one's attention from the monitors, suggesting the need for a second physician or an experienced nurse in the event a timely response to hemodynamic or respiratory deterioration is required. Table 5.1 gives information on recommended monitoring.

5.2.1.1 Hemodynamic Monitoring

Basic hemodynamic monitoring is obligatory for all interventional procedures, particularly in patients un-

Mahnken/Ricke (Eds.), *CT- and MR-Guided Interventions in Radiology*

Table 5.1 Recommended monitoring in sedated patients

	Technique	Normal range
Oxygenation	Pulse oximetry	SpO_2 > 96% on room air
Ventilation	Capnography	10–14 breaths/min, $EtCO_2$ 40–50 mmHg (vol%)
Blood pressure, noninvasive	Noninvasive blood pressure	110–150 systolic, MAP 60–90 (adult)
Heart rate, arrhythmia, ischemia	ECG	Heart rate 60–100, no QRS/ST changes compared with preprocedural ECG
Sedation and analgesia depth	Verbal response	Mild sedation

SpO_2 O_2 saturation, *$EtCO_2$* end-tidal CO_2, *MAP* mean arterial pressure, *ECG* electrocardiogram

dergoing lengthy procedures and those with the following needs or suffering from the following conditions:

- Patients requiring sedation
- Patients with severe claustrophobia
- Patients with labile circulation
- Patients with significant coronary heart disease or arrhythmias

Basic hemodynamic monitoring includes a three-lead electrocardiogram (ECG) and noninvasive blood pressure measurement. It should be noted that built-in ECG devices in computed tomography (CT) and magnetic resonance imaging (MRI) scanners are for cardiac imaging triggering purposes only and may not be approved to monitor and diagnose arrhythmias or ST-segment changes. Separate monitors are recommended, and the output signal of these monitors can be transmitted directly to the scanner for cardiac triggering purposes. In MRI, only one set of ECG leads with short cables and specially approved ECG electrodes may be used to avoid the risk of inflicting burns on the patient when the magnetic field is activated and to prevent image disturbance.

Automatic noninvasive measurement is recommended for accurately and reliably determining blood pressure. Advantages include (1) more time for staff to attend to other tasks, (2) timed repetition of blood pressure measurements, and (3) continuous display of the blood pressure and other parameters (e.g., systolic, diastolic, and mean blood pressure; pulse rate), depending on the machinery.

Modern noninvasive machines employ a detection system based on an oscillometric principle, whereby the blood pressure is electronically determined from the pulse amplitude. The shortcomings of the noninvasive blood pressure technique are those of any cuff measurement technique and usually involve patients with obese arms, uncooperative moving patients, and those with very high or very low blood pressure. Even with these limitations, automatic machines are more accurate, precise, and reliable than auscultation in patients (Murphy and Thompson 2002).

5.2.1.2 Monitoring of Respiration

Respiratory depression is a particular concern in patients undergoing procedural sedation. Unrecognized hypoxia and hypercarbia demand close respiratory monitoring. Patients at particular risk include:

- The massively obese
- Those with manifest or suspected sleep apnea
- The very young and the very old
- Those with pre-existing pulmonary disease
- Those with pre-existing heart disease such as congestive heart failure, particularly those that are orthopneic

Clinically, respiration is monitored by auscultating breathing sounds and visually observing chest and abdominal excursion. These methods are imprecise and require supplementation with technologies that monitor oxygenation and ventilation of the patient.

Hemoglobin Oxygen Saturation

Hemoglobin oxygen saturation (SpO_2) is monitored by the use of pulse oximetry; it is obligatory for every sedated patient and in unsedated patients during invasive or interventional procedures. Transmission oximetry is based on differences in the optical transmission spectrum of oxygenated and deoxygenated hemoglobin, so misleading values may be obtained in the presence of abnormal hemoglobins

Table 5.2 Expected changes in SpO_2 after apnea and recovery

	Time to desaturation (<90%) after apnea	Time to restoration of SpO_2>95% after start of mechanical ventilation
Healthy adult, breathing room air	120–180 s	3–20 min[a]
Healthy adult, breathing 100% O_2	180–600 s	≈ 25 s
Morbid obesity, pregnancy, 100%	60–180 s	≈ 40 s
Children, breathing 100% O_2	22–45 s	≈ 30 s
Small children (0–2 years), breathing 100% O_2	20–30 s	≈ 20 s

[a]With unassisted spontaneous breathing

(e.g., methemoglobinemia, as seen with topical benzocaine use, or carboxyhemoglobinemia; Murphy and Thompson 2002). Further limitations to the value of pulse oximetry exist with severe vasoconstriction (e.g., shock, hypothermia), excessive movement, synthetic fingernails and nail polish, and severe anemia. Erroneously high readings (about 3–5%) and a higher incidence of failure to detect signals have also been reported in dark-skinned races.

Be aware that owing to the sigmoid shape of the O_2 dissociation curve large changes in the arterial partial oxygen pressure (PaO_2) can occur without much impact on SpO_2 until a saturation of 90% (a PaO_2 of 65 mmHg) is reached, after which small decreases in PaO_2 result in large decreases in SpO_2. While it may take 5–8 min after apnea for SpO_2 to decrease to 95%, rapid desaturation below 70% might occur within less than 1 min; in small children in less than 30 s! Note that once desaturation has occurred, SpO_2 might continue to fall for 10–15 s even with adequate oxygenation and ventilation and it may take 1–2 min for SpO_2 to rise (Table 5.2) (Heier et al. 2001; Xue et al. 1996; Tanoubi 2006).

Desaturation is more likely to occur in patients with reduced functional residual capacity (the "oxygen reservoir" remaining in the lung at the end of a normal tidal expiration), such as with infants, obese patients, or pregnant women. The administration of oxygen during procedural sedation for invasive procedures is a double-edged sword in that oxygen saturations may remain normal, even in the face of apnea for some time, in effect masking the fact that ventilation has ceased. The addition of end-tidal carbon dioxide ($EtCO_2$) monitoring (see the next section) in these patients aids in the detection of apnea in cases where oxygen administration fails to reveal it.

End-Tidal Carbon Dioxide

Monitoring of $EtCO_2$ will detect clinically occult hypoventilation and is mandatory in all patients at risk for respiratory depression. This includes patients with pre-existing pulmonary diseases, older patients, and patients needing deeper sedation to ensure compliance (confused patients, children) or pain control during invasive procedures.

Capnography is the graphic record of instantaneous CO_2 concentrations in the respired gases during a respiratory cycle. Capnometry is the measurement and display of CO_2 concentrations on a visual display and the usual concentration displayed is the $EtiCO_2$ concentration (Murphy and Thompson 2002).

In sedated, spontaneously breathing patients (as opposed to intubated patients) the sampling catheter is incorporated into a nasal prong oxygen delivery apparatus. These devices often also display the respiratory rate as well as the $EtCO_2$ concentration.

Hypoventilation (rising $EtCO_2$ concentration, slowing or cessation of respiratory rate) can be detected early by these devices, prompting immediate corrective interventions (e.g., stimulation of breathing, bag mask ventilation, or sedating agent reversal). Examples of different capnography traces are given in Fig. 5.1.

5.2.1.3 Equipment Issues in the MRI Suite

Several manufacturers offer "MRI-compatible" monitoring equipment. However, this sometimes refers only to the technical shielding of the monitor against harm from the magnet and does not necessarily include demagnetization. These pieces of equipment must not be brought into the room on a portable trolley, but

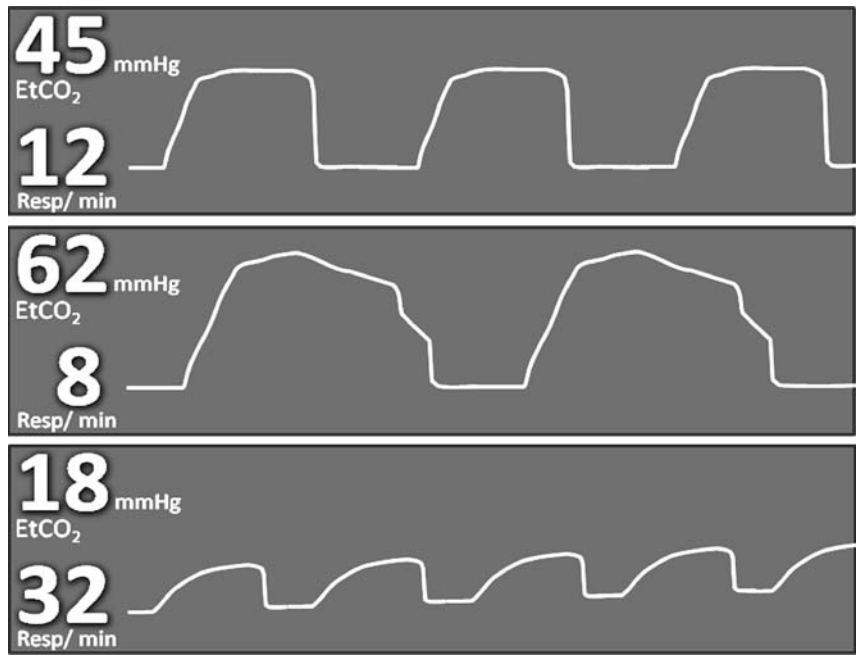

Fig. 5.1 Typical traces of exhaled CO_2: normal (*top*); opioid breathing (*middle*); shallow breathing in deep sedation with slowly increasing levels of CO_2 (*bottom*)

have to be installed firmly attached to the wall outside the magnetic field. Equipment not labeled as MRI-compatible may not function properly (i.e., artifacts, misreadings, wrong values) if it is installed inside the MRI room.

When purchasing monitoring equipment it is important to consider whether procedures will be preformed under deep sedation or general anesthesia (see the next section for indications), in which case more portable and compatible (with the anesthesia machine) devices may be required.

5.2.2 Sedation

5.2.2.1 Definitions

The terminology of sedation has undergone considerable evolution over the years. Different medical and dental specialties have used imprecise terms to describe what is being done. It is essential that the lexicon be firmly established and agreed upon in order to ensure unambiguous communication across specialty lines and among practitioners of the same specialty. This is particularly important to investigators as they attempt to make "apples to apples" comparisons and to the readers of such studies for the same reason.

The consciousness continuum spans cognition from "awake and alert" to "death." The continuum is arbitrarily punctuated by points defined as closely as possible by the clinical appearance of the patient (American Society of Anesthesiologists 2004a). As it currently stands:

1. Minimal sedation (anxiolysis; sometimes referred to as "conscious sedation") is a drug-induced state during which patients respond normally to verbal commands. Although cognitive function and coordination may be impaired; ventilatory and cardiovascular functions are unaffected.
2. Moderate sedation/analgesia is a drug-induced depression of consciousness during which patients respond purposefully to verbal commands, either alone or accompanied by light tactile stimulation. No interventions are required to maintain a patent airway, and spontaneous ventilation is adequate. Cardiovascular function is usually maintained.
3. Deep sedation/analgesia is a drug-induced depression of consciousness during which patients cannot be easily aroused but respond purposefully following repeated or painful stimulation. The ability to independently maintain ventilatory function may be impaired. Patients may require assistance in maintaining a patent airway, and sponta-

neous ventilation may be inadequate. Cardiovascular function is usually maintained.

4. General anesthesia is a drug-induced loss of consciousness during which patients are not arousable, even by painful stimulation. The ability to independently maintain ventilatory function is often impaired. Patients often require assistance in maintaining a patent airway, and positive-pressure ventilation may be required because of depressed spontaneous ventilation or drug-induced depression of neuromuscular function. Cardiovascular function may be impaired. General anesthesia generally involves the presence of an anesthesiologist.

5.2.2.2 The Consciousness Continuum

It is generally agreed that an individual administering procedural analgesia and sedation ought to be capable of managing one level beyond the level desired. For example, if one is attempting to produce moderate sedation, one ought to be competent to manage the physiological concomitants of deep sedation. Having said that, it is well known that individuals have different, and at times unpredictable, responses to the medications employed to produce procedural sedation and analgesia.

5.2.2.3 Sedation, Analgesia, and Dissociation

Sedation and analgesia, for the most part, are separate issues (Murphy 2006a). Sedative hypnotics do not possess analgesic activity, and in fact may be antianalgesic. The apparatus of pain transmission is not interrupted by even very deep levels of sedative hypnosis, leading to "wind-up" and postprocedural pain transmission facilitation.

Parenteral analgesic agents ordinarily employed in procedural sedation and analgesia possess different degrees of sedating side effects (e.g., morphine, sufentanil) that may be useful in managing individual patients. However, employing an opioid as the primary agent to achieve sedation is rather like attempting to insert a round peg in a square hole: it can be done, but it is a poor fit and often at the expense of ventilatory drive.

Ketamine is an agent that in a dose-dependent fashion produces sedation, amnesia, analgesia, and hypnosis, followed by dissociation. The dissociated state is unique in that patients do not respond to surgical stimuli (i.e., they appear as though they are under general anesthesia), but maintain and protect their airway, and maintain ventilation, hemodynamics, and muscle tone (catalepsy) provided the dose of ketamine is reasonable. In a quantitative sense they are much like patients in the moderate sedation/analgesia category. So, although qualitatively and cognitively these patients fit the general anesthesia definition, from a "safety" perspective they conform to the moderate sedation/analgesia definition. This state is called "dissociative sedation" (Murphy 2006a).

5.2.2.4 Clinical Approach to Sedation

The best advice is to pre-emptively determine how deeply sedated the patient will need to be to accomplish what is required in a manner acceptable to the patient. Further, consider the reserve of the patient and whether or not it is sufficient to withstand the effects of the medications that are contemplated, balanced against the stimulation to be inflicted by the procedure. Consider the aspiration risk, particularly if a deeply sedated or general anesthetic state may supervene. In the final analysis, one must be confident that sedation and analgesia can be safely and effectively undertaken in a manner that is acceptable to the patient and that referral for general anesthesia is unnecessary.

In summary, select the desired state, select the most appropriate medications to get the patient to that end point, and administer them by the safest route. Take into account whether or not the procedure will inflict pain. The following are common end points:

- Minimal sedation (e.g., a mildly anxious patient for a CT scan): PO dosing is acceptable and usual.
- Moderate sedation for nonpainful procedures (e.g., substantially anxious patients for CT and MRI scanning): intravenous titration using "titratable drugs" (see later) is safest, with the probable exception of ketamine.
- Moderate sedation and analgesia for painful procedures: Select a "titratable" opioid (e.g., fentanyl) and titrate it intravenously to establish an acceptable level of analgesia; then utilize a "titratable" sedative hypnotic to titrate the patient to the moderate sedation end point. Avoiding the practice of alternating small doses of sedative hypnotic agents with small doses of opioids, in the author's ex-

Table 5.3 Sedative drugs

	Dose range	Time to maximum effect	Duration of action	Side effects
Midazolam[a]	0.03 mg/kg i.v. Repeat dose 1 mg i.v.	2 min	10–30 min	Paradoxical reaction, apnea
Diazepam (lipid)	5–10 mg i.v.	10 min	20–40 min	Paradoxical reaction, active metabolites >100 h!
Propofol[a]	0.5–1 mg/kg i.v. bolus or 2–4 mg/kg/h infusion	30–60 s maintenance	4–6 min 5–10 min after discontinuation	Apnea!
Etomidate	0.1–0.2 mg/kg i.v.	20–30 s	3–5 min	Apnea, adrenocortical depression, do not repeat

[a] Only half the does may be sufficient in patients older than 60 years.

Table 5.4 Analgesic drugs

	Dose range	Time to maximum effect	Duration of action	Side effects
Morphine	2.5–10 mg i.v.	2–5 min	4–6 h	Apnea, nausea
Hydromorphone	10–20 µg/kg i.v.	5 min	3–4 h	Apnea, nausea
Piritramide	0.1–0.15 mg/kg i.v.	2–5 min	5–8 h	Apnea, nausea
Fentanyl	1–2 µg/kg i.v.	≈ 60 s	20–30 min	Apnea, nausea
Remifentanil	0.05–0.25 µg/kg/min infusion	2–4 min	2–3 min	Apnea, thoracic rigidity
Ketamine (racemic)[a]	0.5–1 mg/kg i.v.	≈ 60 s	10–20 min	Dysphoria, hallucination, hypersalivation, apnea

[a] For (*S*)-ketamine use half the dose of racemic ketamine.

perience, reduces the risk of sudden and unpredictable apnea. Alternatively, employ ketamine intravenously or by mouth.

The use of single doses of any class of medication (sedative hypnotic, opioid, and ketamine) by any route (intravenous, by mouth, intramuscular, subcutaneously, per rectum) is inherently more dangerous (respiratory and cardiovascular depression) than a measured intravenous titration to a defined end point. Some agents have a broader safety profile (ketamine) than others (midazolam, propofol) and some are intermediate in risk (chloral hydrate).

"Titratable" drugs are safer and preferable for intravenous titration to a moderate sedation end point. These drugs have a rapid onset, rapid offset, and a clearly identifiable effect on a dose-by-dose basis (e.g., fentanyl, propofol, ketamine–propofol combinations).They permit one to adjust both the dose and the dosage interval, in a safe and effective manner. Medications such as diazepam are difficult to titrate and midazolam is of intermediate ease, possessing as much as a 2-min delay to peak effect profile.

Remember to evaluate the "physiologic reserve" of the patient (Murphy (2006b). For the most part one will be titrating to a "CNS" end point, i.e., degree of sedation and adequacy of analgesia. However, some patients will be too sick or unstable (e.g., a hypotensive patient in ventricular tachycardia; decompensated chronic obstructive pulmonary disease, COPD, patient) to use the CNS end point and titration will be against ventilatory (e.g., hypoxia, hypercarbia) or cardiovascular (e.g., hypotension) end points. In the very ill, one will use only an amnestic (e.g., a small dose of midazolam) to obtund memory as higher doses may lead to further decompensation.

Administration of the drugs and monitoring should not be undertaken by the same individual performing the procedure if sedation beyond anxiolysis is induced.

A sedated patient must not be left unattended, because the level of sedation can deepen suddenly owing to delayed drug effects or temporary cessation of stimuli!

Drugs commonly used for sedation are benzodiazepines, chloral hydrate, barbiturates, propofol, and etomidate. For dosages and characteristics refer to Table 5.3. Drugs commonly used for analgesia are opioids, ketamine, and nonstreoidal anti-inflammatory substances. For dosages and characteristics refer to Table 5.4.

5.2.2.5 Side Effects of Sedation

A freely running and well-secured intravenous cannula is mandatory in all cases. Sedatives should be given intravenously, with some exceptions in children for rectal or nasal application. Oral medication should be given only for baseline analgesic or as premedication. Subcutaneous injections are obsolete, since unreliable resorption may lead to a delayed effect or even the maximum of significant drug levels after the procedure in unmonitored situations.

Respiratory Depression

Opioids act at the central and peripheral opioid μ-receptors, which results in pain relief, nausea, and respiratory depression. It may take up to 15 min after intravenous administration for them to reach their maximum (analgesic and respiration depressant) effect. This may or may not be associated with a decreased level of consciousness. Mild levels of respiratory depression will result in a reduced respiratory rate with deep breaths. Typically, patients will respond when verbally addressed. With higher doses the respiratory rate decreases further, ultimately leading to apnea. The dose response is very much dependent on age and pre-existing medical conditions.

The same opioid dose might be insufficient for pain control in a 40-year-old healthy patient but lead to apnea in a 75-year-old patient.

Patients who are maintained on opioid medication for chronic pain may require higher doses for effective pain control during the procedural sedation as ought to be expected. The dose must be titrated to the desired level of pain control and respiratory function. Note that there are cases where pain control cannot be reached without significant respiratory depression, up to and including apnea. An anesthesiologist may be the best option for patients such as this.

Airway Obstruction

With deepening sedation, especially when opioids and sedative hypnotics are used together, the muscles of the tongue and the upper airway may relax, leading to upper-airway obstruction. This obstruction may be relieved by pulling the mandible forward (Esmarch's procedure) or by employing an oropharyngeal airway (see Sect. 5.3.6).

Confusion

Small doses of any sedative hypnotic agent such as the benzodiazepines, barbiturates, and alcohols (e.g., propofol) are known to produce a "paradoxical" reaction characterized by hyperactivity and agitation. The incidence has been reported to happen in up to 10% of patients, mostly children and the elderly. A milder degree of confusion (disorientation, ataxia, restlessness) is not uncommon. Repetitive dosing of this class of medications may improve or worsen the agitation, in the latter case causing one to abort the procedure. The most appropriate course of action when confronted by this situation may be to switch agent class.

Hemodynamic Compromise

Hemodynamic compromise is rare in procedural sedation except perhaps in the most fragile of patients or those patients with incipient hemodynamic instability (e.g., those where sympathic tone is reduced or peripheral vasoplegia exists or those with decreased cardiac reserve).

5.3 Medical Management

5.3.1 Preparations

In adult patients the presedation preparation is similar to that undertaken prior to any surgical procedure or administration of a general anesthetic. A detailed history evaluating the reserve of the vital organ systems

(CNS, cardiovascular, and respiratory) as well as that of any chronic disease, of previous interventions, and current medication and allergies should be taken in advance. No food should be permitted up to 6 h before a planned procedure owing to the risk of aspiration of gastric contents, though clear fluids are permitted up to 2 h before.

5.3.1.1 Which Patients Should Be Managed by Anesthesia?

Depending on availability, the organizational structure of the hospital, and the emergency training level of the radiologist, the indication for an anesthesia consult could be liberal or restrictive. The degree of anxiety, the intensity of procedural pain to be endured, or the duration of a procedure that demands total immobility will define the need for and the depth of procedural sedation and analgesia. Patient tolerance for all of these factors must also be factored into the decision. Some patients with cardiac or pulmonary insufficiency may experience severe dyspnea when lying supine, in which case one ought to contemplate an anesthesia consult. Patients with significant sleep apnea should receive special attention during the procedure and should be admitted as an inpatient overnight to a monitored bed according to the hospital's policy.

5.3.1.2 Premedication

Anxiolytic medication may be administered orally to patients who need them. The following benzodiazepines have reasonably quick onset times and relatively short durations of action. Typical doses in adults are:

- Oxazepam, 10 mg p.o.
- Diazepam, 5 mg p.o.
- Lorazepam, 0.5–1 mg p.o., or sublingually if a more rapid onset is desired

Benzodiazepines should not be given as premedication in patients with significant respiratory impairment (e.g., COPD, pulmonary fibrosis, progressive muscular weakness) owing to their muscle-relaxing effects. An alternative may be clonidine (1.5–2 µg/kg body weight p.o.).

Patients at risk for aspiration (chronic reflux, hiatal hernia, gastroparesis, obesity) should additionally receive 150–300 mg ranitidine or a proton-pump inhibitor.

Medications the patient takes chronically should generally be continued as usual, with the exception of oral antidiabetics, insulin, and angiotensin-converting-enzyme inhibitors/AT-2 blockers in a combination of more than antihypertensives. Patients with insulin-dependent diabetes should have an endocrine or anesthesia consult to set up a specific insulin regimen. Any rescue medication carried by the patient (e.g., nitro spray, bronchodilating puffers) should remain immediately available during the patient's entire stay.

5.3.2 Conduct of Sedation

5.3.2.1 Administrative Matters

It is highly advisable to reach agreement with the institution's anesthesia department on which cases/procedures ought to require anesthesia consult. Standard operating procedures should be crafted in cooperation with the department of anesthesia and rendered to written form, including:

- Preparative issues (e.g., patient selection criteria, *nil per os* status, presedation evaluation parameters, etc.)
- Resuscitation equipment to be immediately available
- Which physicians are credentialed to perform sedation and how that credentialing is to occur (Murphy 2006a)
  - The numbers, roles, and responsibilities of ancillary personnel to be present during the procedure
  - Medications and dosages to be employed
  - Monitoring to be employed
  - Discharge criteria
  - Incident recognition and reporting
  - Quality assurance program

5.3.2.2 Setup of Sedation

Every patient should have an intravenous infusion established with normal saline or Ringer's solution. Monitoring leads and oxygen delivery tubing should be secured to the table outside the scanner and tested for adequacy in the final scanning position.

5.3.2.3 Sedation

The choice of drug depends on availability and the preference and experience of the sedating physician.

Of note some drugs may take some time following intravenous administration to reach their peak effect, rendering them difficult to use in situations where titration to a physiological or psychological end point is desirable. Premature administration of subsequent doses of medication before the peak effect of the initial dose has had its effect runs the risk of "stacking doses" and a potentially dangerous accumulation of drug!

A short-acting benzodiazepine (e.g., midazolam) may be administered at the start of the procedure to relieve procedure-related anxiety. For deeper sedation or for anticipated painful interventions such medications may be combined with a medium-length-acting opioid (morphine, hydromorphone, piritramide). However, it must be emphasized that these classes of medications are synergistic in effect and may produce hypoventilation and apnea. Vigilance and monitoring are essential. Fentanyl is a short-acting opioid that may be used in small doses (1 µg/kg i.v.) before the actual puncture or in lieu of longer-acting medications such as morphine for shorter procedures (up to 30 min). The final dose of fentanyl should be titrated to the effect, remembering that the context-sensitive half-time lengthens with repeat doses (danger of accumulation).

Repeat doses of midazolam are seldom necessary in procedures shorter than 30 min. If more sedation is needed during the procedure, small repeat doses of propofol (0.1–0.2 mg/kg i.v.) can be given alternatively without risk of accumulation, but with the risk of transient apnea. Each dose will calm the patient for approximately 3–10 min and should be administered under close respiration monitoring only. For a standard sedation regimen, see Fig. 5.2.

Supplemental Oxygen

Oxygen should always be administered during sedation to prevent alveolar hypercarbia in occult hypoventilation. With nasal prongs and maximum flow no fraction of inspired oxygen concentration higher than 60% can be achieved. Patients requiring higher fractions of inspired oxygen should be managed by anesthesia consult.

New Concepts

Special solutions are possible in collaboration with anesthesia and acute pain services. For example, a patient-controlled analgesia can be used for focused interventions (embolization, radiofrequency ablation) at distal sites without severe pain stimulus, e.g., bone or uterus.

5.3.3 Adjunctive Treatment

Ordinarily, less medication is required if the patient is reassured and informed of what to expect. Continuing

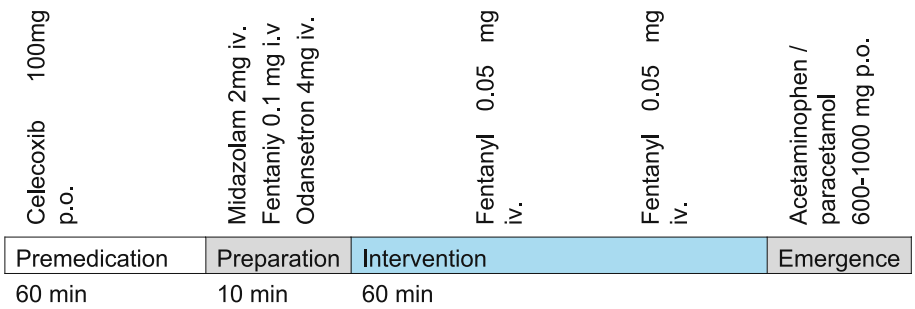

Fig. 5.2 Standard sedation regimen. For a 40-year-old, 75-kg adult without significant comorbidities the regimen represents an example of how sedation might occur for a radiofrequency ablation of a tibial tumor. It is contemplated that local anesthetic agents are infiltrated for needle punctures. One ought to administer lower doses in older patients and young children, at least initially until a dose–response characteristic is identified (e.g., how much sedation did the initial dose of midazolam deliver and how long did it take to produce a peak effect following intravenous administration). For sedation of children, refer to the text

reassuring verbal contact is crucial, particularly in children, the elderly, and those who are mentally challenged.

Pre-emptive analgesia may be of benefit when administered before a painful intervention to attenuate the perception of pain. This is generally felt to be more effective than a reactive strategy. Agents such as ibuprofen (400–800 mg p.o.), naproxen (500 mg p.o.) or COX-II inhibitors (celecoxibe 100–200 mg p.o., etoricoxibe 60–90 mg p.o.) should be considered, recognizing their risk profiles.

In the event that significant hypertension related to sympathetic activation due to stress or insufficient pain control occurs, adjunctive treatment is best with small doses of β-blockers (e.g., 5–20 mg labetalol intravenously titrated, 1–5 mg metoprolol intravenously titrated).

In very anxious patients or in patients with a history of nausea after sedation/anesthesia a prophylactic dose of antiemetics is indicated).

5.3.4 Postsedation Care

Standards have been set by the American Society of Anesthesiologists (2004b) for postanesthesia care, and these should be applied accordingly. These mandate inter alia that:

- All patients who have received [...] monitored anesthesia care shall receive appropriate postanesthesia management.
- The patient's condition shall be evaluated continually [...] post sedation.
- A physician is responsible for the discharge of the patient.

Monitoring of blood pressure, heart rate, oxygen saturation, and CO_2 must be continued until the effects of sedation have dissipated.

A health care professional must be in continuous attendance to respond to alarms, assist the patient, and call for medical assistance if required. The patient can be transferred to an unmonitored, but supervised area if:

- Hemodynamics and respiration are stable at preprocedural levels.
- The patient is awake and orientated.
- There is no acute pain.

Postprocedural pain management must take into account the fact that sedative and opioid medications employed during the sedation will be present at some level for days after discharge. The doses of oral and parenteral agents should be adjusted accordingly. All patients in the recovery phase should be monitored for at least 30 min following a dose of opioid medication.

After the procedure acetaminophen/paracetamol (500–1000 mg i.v./p.o.), ketorolac (30 mg i.v.), parecoxib (40 mg i.v.), or metamizole sodium (1000 mg slowly i.v. or p.o.) are usually effective to provide sufficient analgesia. For patients suffering from chronic pain the hospital's chronic pain service should be consulted prior to the procedure. Additional analgesic medication should be given if pain cannot be controlled by nonopioid substances. Medium-length-acting opioids are preferred (repeat doses of piritramide 1.5–3 mg i.v., hydromorphone 0.2–0.4 mg i.v., or morphine 0.5–1 mg i.v.). If pain cannot be controlled with usual doses, other reasons have to be excluded, e.g., liver capsule hematoma after radiofrequency ablation of liver tumors.

5.3.4.1 Respiratory and Cardiovascular Issues

Postprocedural bronchospasm in known asthmatics or COPD patients should be managed with head elevation, supplemental oxygen, and effective pain control. Bronchodilators such as salbutamol (two puffs, repeated every 2 min until relief is obtained) are indicated as are intravenously administered prednisolone (250 mg) or methylprednisolone (20 mg) for resistant or severe cases.

In the event that these symptoms do not improve with treatment, one ought to consider other disorders, such as:

- Congestive heart failure, pulmonary edema, or hypervolemia
- Pulmonary embolism
- Upper-airway obstruction, aspiration, atelectasis, or pneumothorax

The most frequent causes of postprocedural hypertension are unrecognized pain and inadvertent withholding of chronic antihypertensive medication. After effective treatment of pain, which is often denied by the patient, the patient's usual medication should be given by mouth. If viewed to be dangerous, hyperten-

sion may be managed (i.e., to avoid postinterventional bleeding) with the following medication:

- Nitro spray: two puffs (0.8 mg) sublingually, repeat after 2 min if there is no effect
- Ca-channel blockers: nifedipine or nitredipine (10 mg) sublingually
- Vasodilators: urapidil (10–50 mg) intravenously titrated
- β-Blockers: labetalol (5–20 mg) intravenously titrated or metoprolol (1–5 mg) intravenously titrated

The most frequent cause of postprocedural hypotension is unrecognized hypovolemia due to insufficient fluid resuscitation or occult blood loss. If after a fluid bolus of 10–20 ml/kg (in adults) hypotension persists, occult bleeding from the intervention site has to be ruled out by ultrasound or repeat CT scan.

5.3.4.2 Nausea and Vomiting

Nausea can result from opioid medication, accumulation of gastric secretions or air in the stomach, vestibular irritation, or visceral nerve irritation, e.g., peritoneal or liver capsule tension. The treatments of choice are intravenous serotonin antagonists (owing to their minor sedating side effects) such as:

- Tropisetron, 2.5–5 mg i.v.
- Odansetron, 4–8 mg i.v., repeated after 12 h if needed

In children, dimenhydrinate is a good alternative, because it has mild sedating and antianxiety effects.

5.3.4.3 Patient Discharge

The patient can be discharged if:

- Consciousness, hemodynamics, and respiration remain stable at preprocedural levels for 30 min.
- The patient had tolerated some clear fluids and a light snack.
- The patient can sit unaided.
- The patient had voided.
- The patient's pain is controlled.

Under no circumstances should the patient be permitted to operate a motor vehicle for 24 h after a procedure involving sedation. Cases of fatal car accidents after interventions employing only light sedation have been reported, leading to the conviction of the treating physician. Patients must be discharged with a responsible caretaker and never alone.

5.3.5 Special Considerations in Children

Children under the age of 3 years (under 6 years if preterm born) and/or examinations lasting more than 120 min should be managed by specially qualified staff or with anesthesia staff in attendance only. Several aspects have to be considered in general regarding the sedation of pediatric patients (Kretz 2006):

- There is no "safe" sedation recipe that obviates the need for close monitoring of the infant patient!
- Smaller children require deeper levels of sedation than adults if they are required to lie still completely.
- Children tolerate pain less well than adults.
- Children are physiologically more susceptible to laryngospasm than adults.
- Some of the medications used are not approved for use in children and have to be considered as off-label use.
- Venous access is more difficult to establish than in adults, leading to the single-dose by mouth, per rectum, or intramuscular strategies. These strategies are inherently more hazardous with respect to respiratory and cardiovascular compromise than intravenous titration methods.

The following dosing schemes (see also Table 5.5) should be considered as examples only and should not be taken as recommendations. The final plan should be developed depending on the availability of drugs, personal experience, and hospital policies.

5.3.5.1 Preparations

Special attention should be given to the preparation of children. A quiet and secluded environment will remove anxiety from the children and their parents. Infections of the upper respiratory tract are not uncommon and should be carefully evaluated.

New onset of cough, pulmonary wheeze or bronchospasm, thick nasal secretions, or fever should lead to postponement of the procedure, since there is an increased risk of respiratory complications. Minor nasal secretions or congestion may be treated

Table 5.5 Pediatric medication

	Application	Initial dose	Repeat dose
Atropine	i.v.	10 µg/kg	NA
Midazolam	i.v.	30–50 µg/kg	10 µg/kg (maximum 10 mg)
	p.o.	0.5 mg/kg (maximum 8 mg)	NA
Atropine	i.v.	10 µg/kg	N/A
Propofol	i.v.	1 mg/kg	0.5–1 mg/kg
Ketamine (racemic)[a]	i.v.	1–2 mg/kg	0.5 mg/kg
	p.o., p.r.	2 mg/kg	NA
Chloral hydrate	p.o., p.r.	25–100 mg/kg	NA variable absorption
Pentobarbital	p.o., p.r.	2–6 mg/kg	NA
Acetaminophen/paracetamol	p.o., p.r.	30 mg/kg (maximum 1 g)	20 mg/kg 6-hourly
Ketorolac	i.v.	0.5 mg/kg (maximum 30 mg)	NA
Morphine	i.v.	50 µg/kg	NA
Fentanyl	i.v.	1.5 µg/kg	1.0 µg/kg
Piritramide	i.v.	0.05–0.1 mg/kg	0.05 mg/kg
Odansetron	i.v.	0.1 mg/kg (maximum 4 mg)	0.1 mg/kg after 12 h
Tropisetron	i.v.	0.2 mg/kg (maximum 5 mg)	NA
Dimenhydrinate	i.v.	1.25 mg/kg (maximum 50 mg)	4-hourly

NA not applicable
[a] For (*S*)-ketamine, use half the dose.

with nasal spray (oxymetazoline, xylometazoline) before starting the sedation to improve nasal breathing.

Many congenital and acquired conditions may complicate procedural sedation in children because they affect the reserve of vital organ systems (cardiovascular, respiratory, and neurological). Practitioners are urged to consult anesthesia or pediatrics personnel in such cases.

Intravenous access is not considered to be mandatory in otherwise healthy children for noninterventional sedation. Antimuscarinic agents (glycopyrrolate or atropine, 0.01 mg/kg) designed to reduce oral secretions may be administered at the discretion of the treating physician.

5.3.5.2 Implementation of Sedation

The following regimens have been demonstrated to be effective in pediatric patients though practitioners are urged to exercise extreme caution in the patient population mentioned in the previous section. The practice of administering large doses of sedative hypnotics prior to coming to the diagnostic facility is to be condemned. Immediate access to trained personnel, monitoring apparatus, and resuscitation equipment is crucial.

Deep sedation can be produced with:

- Cloral hydrate, 50–75 mg/kg orally or rectally (20 min prior to the procedure)
- Midazolam, 0.5 mg/kg orally (maximum 7–8 mg) (20–30 min before) or 0.1 mg/kg nasally (10 min prior to the procedure)
- Ketamine, 5–10 mg/kg orally or rectally (20–30 min prior to the procedure)

Once the child has been sedated and accepts the monitoring modalities, they must be applied immediately, and blood pressure, heart rate, SpO_2, and CO_2 should be monitored. For painful procedures acetaminophen/paracetamol or ketorolac may be administered in advance.

Table 5.4 gives an overview of commonly used medications and dosing.

Opioids should be administered with great caution to avoid respiratory depression. Repeat doses of sedation should involve short-acting substances only. Ketamine has the advantage of inducing deep sedation/analgesia without causing respiratory depression, but is known to cause unpleasant hallucinations perhaps leading to fearful behavior and noncompliance in children subjected to repeated procedures. The addition of midazolam to ketamine to induce amnesia and prevent bad dreams has been suggested, but has failed to prove its effectiveness in randomized studies.

The postprocedural care is as for the adult. Emergence reactions ranging from mild confusion to combative behavior and unremitting crying are seen not infrequently, especially after ketamine usage. Treatment options include small doses of dimenhydrinate, midazolam, or clonidine (1–2 µg/kg i.v.).

5.3.6 Emergency Care

During the procedure multiple problems have to be anticipated and one should be prepared to deal with them before patient harm supervenes. The most common life-threatening complications are hypoventilation/apnea and hypotension.

The recommendations given in the following sections cannot replace adequate emergency training, but highlight common situations/treatments only. Reference to current specialty-specific guidelines is highly recommended.

5.3.6.1 Airway Obstruction and Respiratory Distress

The sedated patient is continuously at risk of losing control of the airway, resulting in upper-airway obstruction. Pharmacologic reversal agents such as naloxone (opioid antagonist) (0.2–0.4 mg i.v.) and flumazenil (benzodiazepine antagonist) (0.1–0.5 mg i.v.) may be effective in restoring spontaneous airway maintenance and ventilation. Otherwise the practitioner is advised to call for help from those skilled in airway management and resuscitation and to proceed to manage the airway.

There are two maneuvers commonly used which have been shown in multiple studies to improve airway patency. Extension of the neck by head-tilt chin-lift is the primary maneuver used in any patient in whom cervical spine injury is not a concern. While the patient's forehead is pressed downward, the mentum is lifted with the fingertips of the other hand, which lifts the tongue from the posterior pharynx and opens the airway. The jaw-thrust also moves the tongue anteriorly with the mandible, minimizing its obstructing potential. An even more effective jaw-thrust is achieved by forcibly and fully opening the mouth to "translate" the condyles of the mandible out of the temperomandibular joint, then pushing the mandible forward (Esmarch's maneuver) with both hands bilaterally (Fig. 5.3a).

To maintain the airway, oropharyngeal and nasopharyngeal (Fig. 5.3) airways will prevent the tongue from occluding the airway and provide an open conduit for air to pass. An oropharyngeal airway should be placed whenever bag mask ventilation is contemplated (i.e., gas exchange is not restored by airway opening maneuvers). Neither of these airway devices will protect the trachea from aspiration of secretions or gastric contents.

In the event that the patient is apneic, endotracheal intubation should not be attempted by the inexperienced. Instead, securing appropriate ventilation and oxygenation utilizing bag mask ventilation is crucial. This rescue equipment must be immediately available in all sedating locations.

Once the airway has been opened, the resuscitation bag is connected to the mask and an optimal mask seal obtained. The standard adult resuscitation bag has a 1500-ml capacity. This entire volume should not be delivered as it will lead to stomach insufflation. One ought to aim to deliver 500 ml per breath (one third of an adult bag) (Schneider and Murphy 2004). The goal is effective oxygenation and ventilation. To do so one ought to deliver ten to 12 breaths per minute without exceeding the proximal and distal esophageal sphincter opening pressures of approximately 25 cm of water. High upper-airway peak inspiratory pressures result from short inspiratory times, large tidal volumes, incomplete airway opening, increased airways resistance, and decreased compliance. To minimize the potential for gastric inflation each breath ought to be delivered limiting the tidal volume to that which is sufficient to produce a visible chest rise. For the ventilation of children, pediatric resuscitation bags with smaller volumes should be used, delivering 14–20 breaths per minute of 100–300 ml to produce a visible chest rise.

If ventilation cannot be facilitated via a face mask (difficult anatomy, sealing problems, i.e., in patients with a beard), a laryngeal mask is a viable alternative (Fig. 5.3d). With the patient's head tilted, the laryngeal mask is inserted, holding it like a pen, into the supraglottic space until it moves down no further and is inflated with 10–20 ml of air. Physicians planning to use this device in emergency situations

Airway management

a) Jaw thrust (Esmarch's manoeuvre)

b) Oropharyngeal (Guedel's tube) and nasopharyngeal airway (Wendel's tube)

c) Facemask, sealed over mouth and nose utilizing the 'C-grip'or two hands

d) Laryngeal mask airway (LMA)

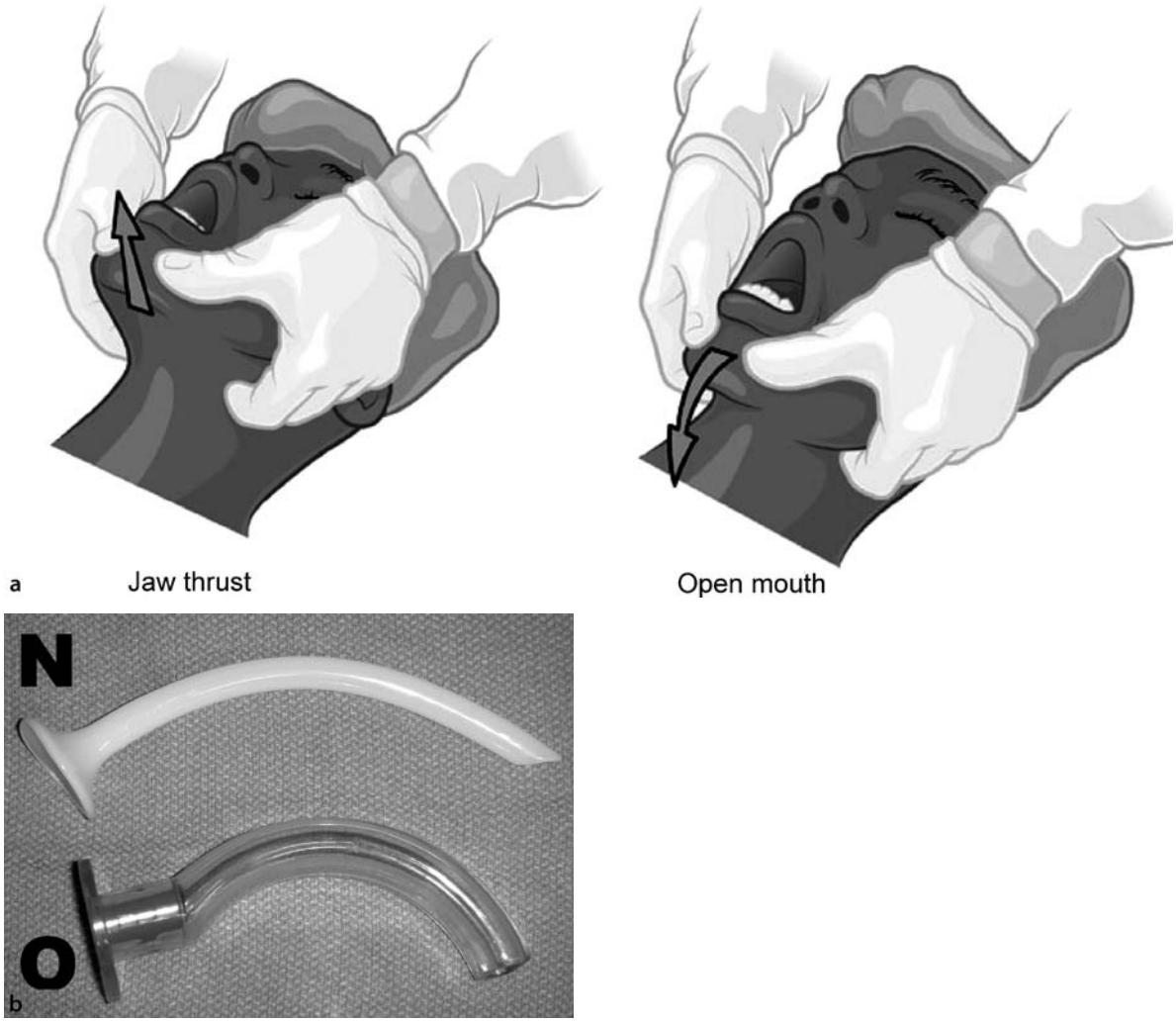

Fig. 5.3a,b Airway management: **a** jaw thrust (Esmarch's maneuver); **b** oropharyngeal airway (Guedel's tube) and nasopharyngeal airway (Wendel's tube)

should become familiar with the type and use of it beforehand.

5.3.6.2 Severe Hemodynamic Compromise

Hypotension is ordinarily easier to manage than hypoventilation. Intravenous bolus doses of balanced salt solutions (e.g., 10–20 ml/kg of Ringer's lactate or normal saline) or 5–10 ml/kg of synthetic colloidal solutions (e.g., pentastarch, tetrastarch) are the initial step in resuscitation. Small repeated doses of adrenergic agents such as ephedrine (5–10 mg i.v.), phenylephrine (0.1 mg i.v.), or cafedrin/teodrenalin (0.1 ml) are effective.

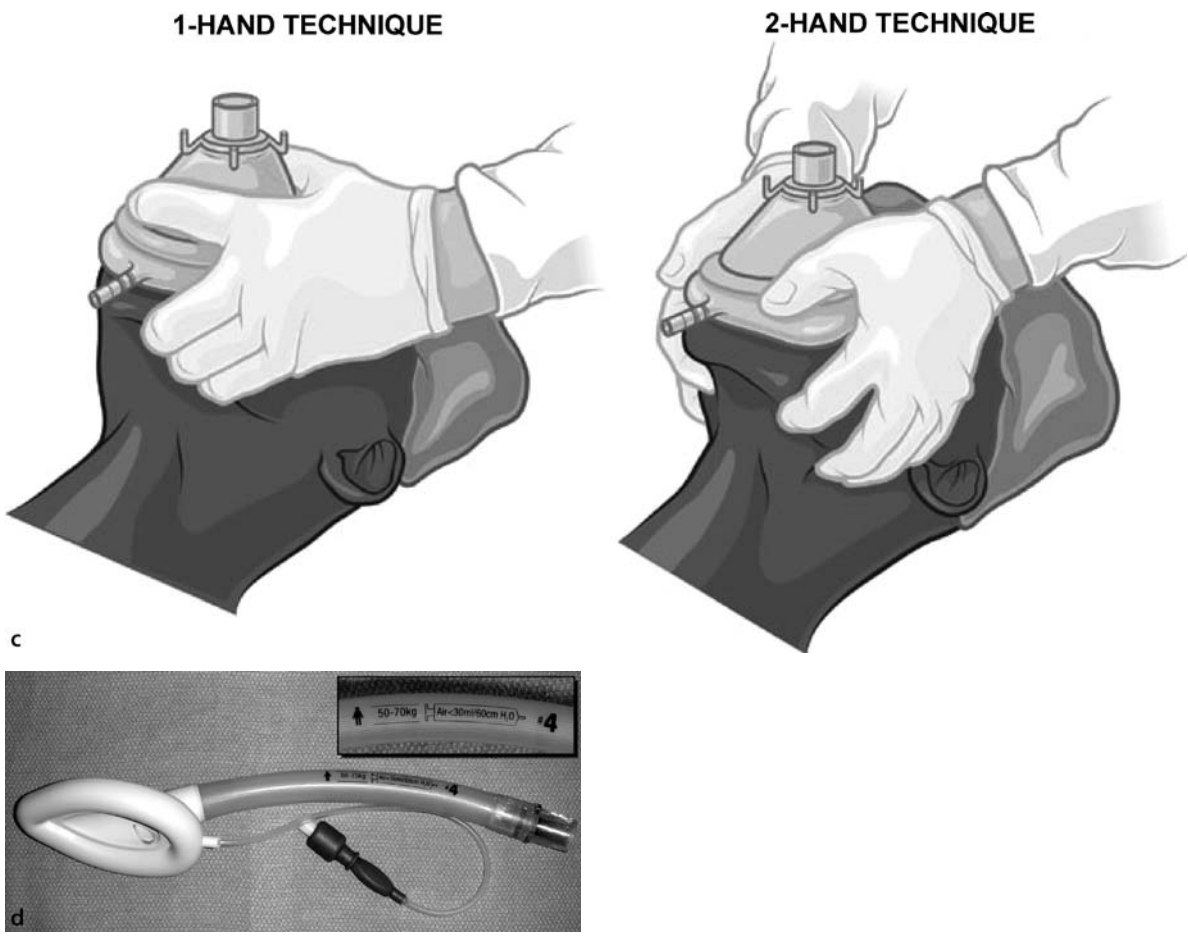

Fig. 5.3c,d Airway management: **c** face mask, sealed over the mouth and nose utilizing the "C-grip" or two hands; **d** laryngeal mask airway

5.3.6.3 Anaphylaxis

Anaphylactic reactions to sedative hypnotic agents and opioids are decidedly uncommon. However, reactions might also be caused by local anesthetics or radiographic contrast media. Anaphylactiod reactions (dose-dependent drug-induced release of histamine from immune cells) will lead to urticaria, flushing, pruritis, and, rarely, hypotension.

Anaphylaxis is defined as an immediate systemic reaction caused by immunoglobulin E mediated rapid release of potent mediators from tissue mast cells and peripheral basophils.

Immediate management includes:

- Discontinuation of antigens
- Basic life support (ABCs)
- Start of volume expansion
- Epinephrine!!!

Epinephrine ought to be administered if the patient exhibits:

- Bronchospasm, significant gastrointestinal symptoms, laryngeal edema, hypotension
- Any rapidly progressive reaction

Administration should start at 5–10 µg/min intravenous infusion.

Importantly, it must be appreciated that there is no benefit from the subcutaneous route of administration. Antihistamines should also be administered: diphenhydramine (0.5–1.0 mg/kg i.v.) or clemastine (2–4 mg i.v.) (H1-receptor blocker) and ranitidine (50 mg i.v.) (H2-receptor blocker). Bronchodilators such as 2.5 mg salbutamol in 5 ml of saline as an aerosol are employed

continuously for bronchospasm. Corticosteroids (250–500 mg prednisolone, 0.25–1 g hydrocortisone, or 1 g methylprednisolone intravenously) are also indicated. Any patient suffering from an anaphylactic reaction should be admitted as an inpatient and monitored for 24 h.

Summary

Sedation can be performed by nonanesthesiologists safely if the administrative, technical, and medication administration requirements have been fulfilled and the physician performing the sedation has adequate training in the application of sedation and emergency procedures. Patients and procedures eligible for nonanesthesiologist sedation should be determined in co-operation with one's respective anesthesia department and standard operating procedures should be formulated for emergencies.

All patients undergoing more than minimal sedation (anxiolysis only) need to be monitored for respiratory and hemodynamic deterioration with continuous pulse oximetry, capnography, ECG, and blood pressure measurements.

After determining the desired level of sedation, one should asses each patient individually for risks considering there is no standard recipe suitable for all patients. Depending on the procedure (diagnostic versus interventional) and the patient factors (e.g., age, comorbidities, level of anxiety) the sedation should be titrated with intravenous boluses of short-acting to medium-length-acting sedatives and analgesics. Small doses of midazolam for sedation and fentanyl for analgesia have been used frequently, with ketamine as an alternative.

Adjunctive treatment includes appropriate premedication, the management of hemodynamics, and postsedation nausea and pain. Special attention has to be given to airway patency and ventilation, particularly in the very young or the very old, particularly if the procedure requires deep sedation.

Sedating children mandates special caution and knowledge of pediatric physiology and pharmacology. The dosing of medication is usually done per kilogram of body weight. Chloral hydrate is an alternative agent for nonintravenous sedation.

All patients must be adequately monitored after sedation by a trained health care professional with direct access to emergency care and medical assistance until the patient has returned to preprocedural levels of performance.

Key Points

- Respiratory and hemodynamic monitoring is necessary in every sedated patient.
- Indications for general anesthesia should be established in consultation with the department of anesthesia.
- For long-duration examinations sedation is ordinarily sufficient; in painful interventions an analgesic should be added.
- Special care has to be taken in sedating children and the elderly.
- Staff performing sedation should be familiar with emergency procedures.

References

American Society of Anesthesiologists (2004a) Continuum of depth of sedation: definition of general anesthesia and levels of sedation/analgesia. Available via http://www.asahq.org/publicationsAndServices/sgstoc.htm

American Society of Anesthesiologists (2004b) Standards for postanesthesia care. Available via http://www.asahq.org/publicationsAndServices/sgstoc.htm

Heier T, Feiner JR, Lin J, Brown R et al. (2001) Hemoglobin desaturation after succinylcholine-induced apnea: a study of the recovery of spontaneous ventilation in healthy volunteers. Anesthesiology 94:754–759

Kretz FJ (ed) (2006) Anästhesie und Intensivmedizin bei Kindern, 2nd edn. Thieme, Stuttgart

Murphy MF, Thompson J (2002) Monitoring the emergency patient. In: Marx JA (ed) Rosen's emergency medicine. Mosby, Philadelphia, pp 28–32

Murphy MF (2006a) Pain management and procedural sedation: definitions and clinical applications. In: Mace SE, Ducharme J, Murphy MF (eds) Pain management and sedation: emergency department management. McGraw-Hill, New York, pp 7–14

Murphy MF (2006b) Preprocedural patient assessment and intraprocedural monitoring. In: Mace SE, Ducharme J, Murphy MF (eds) Pain management and sedation: emergency department management. McGraw-Hill, New York, pp 47–53

Schneider RE, Murphy MF (2004) Bag mask ventilation and endotracheal intubation. In: Walls RM, Murphy MF, Luten RC (eds) Manual of emergency airway management, 2nd edn. Lippincott Williams & Wilkins, Philadelphia, pp 43–69

Tanoubi I (2006) Oxygenation before anesthesia (preoxygenation) in adults. Anesthesiol Rounds 5:1–6

Xue FS, Luo LK, Tong SY et al (1996) Study of the safe threshold of apneic period in children during anesthesia induction. J Clin Anesth 8:568–574

Ways to the Target

6

Andreas Lubienski

Contents

6.1 Introduction

Cross-sectional imaging modalities such as ultrasound, computed tomography (CT), and magnetic resonance (MR) imaging are well-accepted guiding tools for interventional biopsies and therapies (Gupta and Madoff 2007). Especially CT combined with fluoroscopy is able to offer fast and safe ways to nearly any target in the human body, incorporating the major advantage of panoramic views compared with ultrasound, and therefore represents very often the guiding modality of choice (Rogalla and Juran 2004). Even targets in bones and air-containing structures (e.g., lungs) can be addressed very easily and successfully with CT guidance. In contrast, MR imaging seems to be more complex and time-consuming and therefore is usually reserved for interventional procedures in very tricky areas with the necessity of high soft-tissue contrast and in situations where CT is contraindicated (Gupta 2004). The accuracy of the puncture and the complication rates depend on the target size and site, traversing and surrounding anatomical structures, the number of biopsies, the material and puncture technique selected, and patient's cooperation (Gupta and Madoff 2007).

6.2 Materials and Techniques

6.2.1 Patient's Position

At the time of the assignment of the procedure, potential puncture routes have to be clarified on the basis of the imaging in order to assess the risks and complexity of the procedure.

Depending on the access route, the position of the patient on the examination table is chosen (prone, supine, or angulated position). For all interventions, independent of their duration or complexity, it is crucial to select a stable and comfortable position of the patient. Upholstery should be considered when necessary. Especially when CT-guided punctures of the trunk are planned, one has to take into account streak artifacts caused by the arms and therefore has to adjust the position of the arms. In order to have enough

Mahnken/Ricke (Eds.), *CT- and MR-Guided Interventions in Radiology*

room within the gantry, the table should be the lowest position possible (Gupta et al. 2004).

6.2.2 Planning of the Access Route

Depending on the diagnostics and/or expected complexity or level of risk, additional imaging is required. Usually a nonenhanced CT or MR scan is sufficient, but in special areas, such as head and neck, or parenchymal organs contrast-enhanced imaging seems to be mandatory to delineate structures at risk and/or the target itself.

To get representative biopsies one has to consider that in many cases soft-tissue tumors have necrotic tissue in the central parts, whereas viable tumor cells are located at the periphery. Owing to inflammatory changes in the vicinity of the targeted lesion, especially in lung tumors adjacent to the pleura, the needle tip should be placed preferably in the tumor part next to the hilum.

The way to the target should be as safe as possible. Traversing of sensible anatomical structures such as nerves, vessels, and/or pleural space and adjacent organs has to be avoided whenever possible. Adjusting the patient's position and additional respiratory maneuvers may be helpful to get an optimal and safe way to the target. Transparenchymal access (e.g., small bowel, stomach, liver) is possible (Figs. 6.1, 6.2) (Iguchi et al. 2007).

Usually the easiest way to the target is chosen. Thus, complexity is increased when vertical and horizontal pathways are changed into angulated or doubled-angulated access routes. Planning of such pathways is realized with multiplanar imaging and should be restricted to specially trained physicians (Gupta et al. 2005; Ohno et al. 2004).

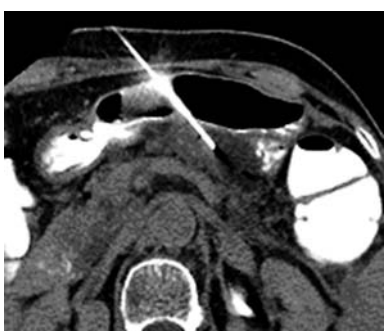

Fig. 6.1 Anterior transgastric biopsy approach to an unclear focal mass located in the pancreatic body. Biopsy revealed macrocystic pancreatic adenoma. (Courtesy of Andreas H. Mahnken, RWTH Aachen University)

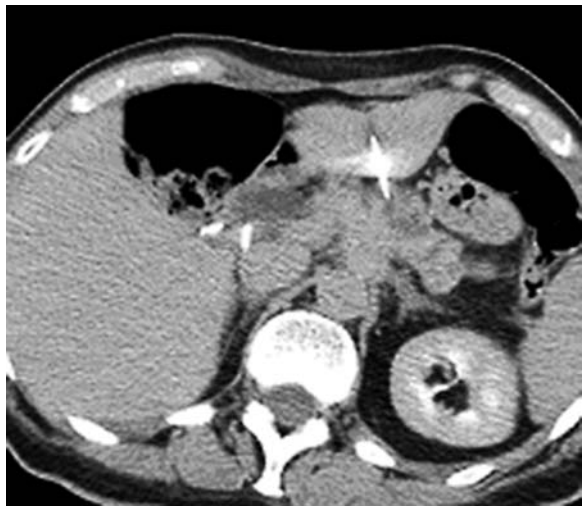

Fig. 6.2 Anterior transhepatic approach to an unclear focal mass located in the pancreatic body. Biopsy revealed a pancreatic carcinoma

6.2.3 Local Anesthesia

Typically 5–20 ml of a local anesthetic drug (e.g., 1% lidocaine) is administered subcutaneously at the puncture site (Maturen et al. 2007). On the basis of reference scans, the infiltration depth of the local anesthesia, the minimal distance between the puncture site and the target, and the maximal depth of the puncture needle before traversing a critical anatomical structure are electronically assessed.

Sufficient anesthesia of pleura, peritoneum, and periosteum is mandatory. When lung punctures are planned, anesthesia should involve but not lacerate the pleura. Repositioning of the needle before administering the anesthetic drug is required when nerves have been punctured as indicated by a sharp and sudden pain.

6.2.4 Puncture Technique

After a short intracutaneous incision the needle is advanced along the previously planned route. Depending on traversing anatomical structures, the needle is advanced directly into the target lesion without any interruption or step by step with control scans in-between.

Anatomical landmarks may help one navigate into the target. The majority of imaging-guided punctures are, of course, straightforward, and can be easily performed using either a single needle pass or coaxial systems. Whenever possible the needle is placed as exactly as possible within the imaging plane. The latter allows one to visualize the entire needle shaft and ideally the target with a single image. This ensures the needle tip is in the correct position prior to biopsy or treatment. In CT, the exact needle tip position may be confirmed by looking for the needle artifact caused by beam hardening. In MR, the signal loss and susceptibility artifacts normally permit passive tracking of the puncture device. The majority of axial needle placements may be performed with the naked eye, particularly if the patient and table are gently brought out of the gantry to remove problems of parallax which may otherwise occur if the operator is working obliquely. Alternatively, the issue of parallax may be addressed using the laser alignment of the scanner; shining the laser through both skin puncture site and needle hub to ensure correct axial needle alignment. In MR, the use of an open MR system provides almost unimpeded access to the patient and multiplanar image acquisition eases the problem of the needle alignment.

There are different techniques to address the target. In CT, the so-called angled-gantry technique uses a gantry angulation, which is set according to the planned angled approach. In reality, angles approaching 20 or 25° lead to problems of access to the patient and of effectively decreasing the gantry/patient distance, as well as being disconcerting for the patient. Following this, the CT laser alignment is then set such that the laser passes through the needle onto the skin surface; and if both the puncture site and the needle hub are confirmed to be in the line of the laser then the needle placement is automatically aligned at the correct angle. By doing this, each scan performed during needle advancement will be in the plane of the entire needle.

In CT- as well as in MR-guided interventions, there are several tricks to avoid loops of overlying bowel:

1. The first and easiest approach to solve this problem is the so-called bowel displacement technique. The first step is to compress the abdomen to displace bowel loops from the potential needle track. This is done by placing a sterile drape or sheet in a ring- or nest-shaped configuration around the site for skin puncture. This is then taped and strapped firmly to the flanks and the examination table to push into the abdomen and displace bowel loops in a manner akin to the compression cone for small-bowel studies. This allows a needle to be placed in the center of the CT or MR gantry, thus maintaining the sterile field.
2. A second method that can be used in exceptional circumstances to displace the bowel is the needle angulation technique where an initial needle is placed adjacent to the bowel loop. The needle is passed beyond the bowel loop and levered across the skin surface to displace the bowel and free up a potential passage for the second biopsy needle to be placed.
3. A third way to displace a bowel loop is to create an artificial pneumoperitoneum via an initially placed first needle in order to free up a potential passage for the second needle.
4. Finally, in cases of extreme body habitus a coaxial needle technique can be used. In such cases it is important to begin the procedure with the table set as low as possible to maximize the space available between the patient's skin surface and the inner aspect of the CT or MR gantry. The latter helps one avoid being forced to pass the needle further than one initially feels comfortable to do; remember to use a coaxial system with a short outer needle. Alternatively, of course, a short biopsy needle may be used for this purpose. When imaging confirms the short needle is in a safe position, the second needle may be placed directly adjacent and parallel to it. This allows the needle to be placed sufficiently far enough to allow the patient to be scanned with the needle in situ. The short needle may then be removed and discarded and the procedure continues as normal. After the entire procedure, a control scan of the target, including all adjacent structures, should follow in order to rule out immediate complications.

6.3 Special Techniques

6.3.1 Lung

Depending on the site of the target, one should consider the transbronchial approach (centrally located lesion) or the transpulmonal approach (peripherally

located lesion) (Fig. 6.3). To prepare for diagnostic lung surgery, a percutaneously placed marking wire (Fig. 6.4) can be released. A sufficient pulmonary reserve (O_2 pressure greater than 60 mmHg) is an important prerequisite for percutaneous lung punctures especially because of the high risk for pneumothoraces (case-dependent up to 60%). Interestingly, instillation of 0.9% NaCl solution into the puncture access during extraction of the needle seems to reduce the incidence of pneumothoraces (Billich et al. 2008). Severe lung emphysema and pulmonary hypertension are relative contraindications for the procedure. Perifocal hemorrhage and or hemorrhage along the needle path after the procedure can often be seen and are usually without any consequences. Hemoptysis is encountered in about 2–5% of all cases. Air embolism is a very rare but sometimes fatal complication (Hiraki et al. 2007).

Especially in small lesions the needle tip should be advanced in the nodule. The number of pleural passages needs to be kept as low as possible to reduce the risk of pneumothorax. Consequently, traversing two lobes on the way to the target should be avoided.

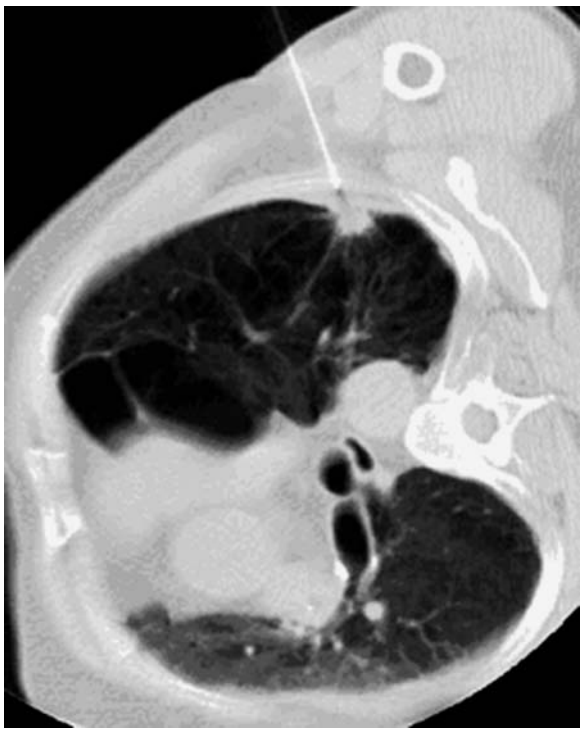

Fig. 6.3 Lateral intercostal approach to a lung cancer nodule located adjacent to the pleura with the patient being in the lateral decubitus position

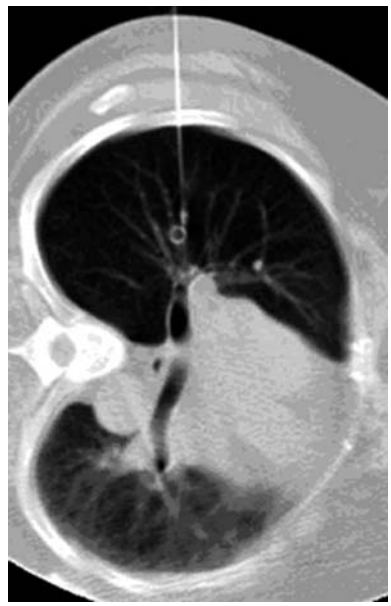

Fig. 6.4 Lateral intercostal approach to a very small lung cancer nodule located near the hilum with consecutive placement of a marking wire prior to surgery

6.3.2 Mediastinum

Depending on the site of the target within the mediastinal compartment (anterior, middle, or posterior part) the access route – anterior (Fig. 6.5) or posterior (Fig. 6.6) – is chosen. Knowledge of the exact vascular routes is absolutely mandatory to prevent probably fatal complications. Multiplanar imaging prior to the procedure may help one scrutinize the exact mediastinal anatomy (Gupta et al. 2005). A direct mediastinal approach involves placement of the needle through an extrapleural space medial to the lung to avoid transgression of the lung and pleura. The needle can be advanced through (Gupta et al. 2002a) or lateral to the sternum (Fig. 6.7), through the posterior paravertebral space (Fig. 6.6), through the suprasternal notch, or through the subxiphoid space. To minimize the risk for a pneumothorax the puncture should be performed in expiration in order to have a broader contact area at the anterior chest wall. To increase the space of the puncture channel injection of 10–50 ml 0.9% saline solution may be helpful. The latter widens the extrapleural space and creates space for the needle, permitting one to avoid passage of the pleura. Artificial pneumothorax is another safe method that provides access for CT-guided

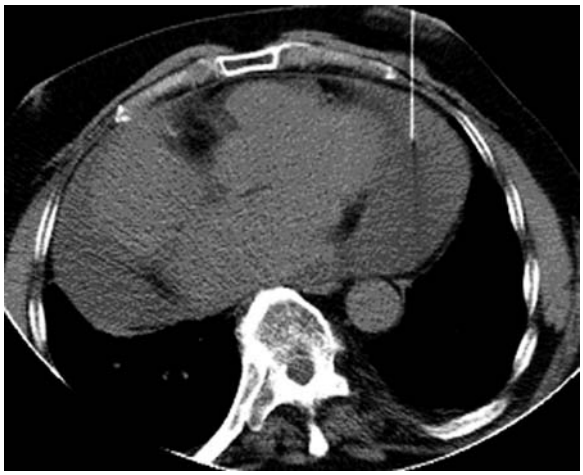

Fig. 6.5 Anterior intercostal approach to a pericardial fluid collection

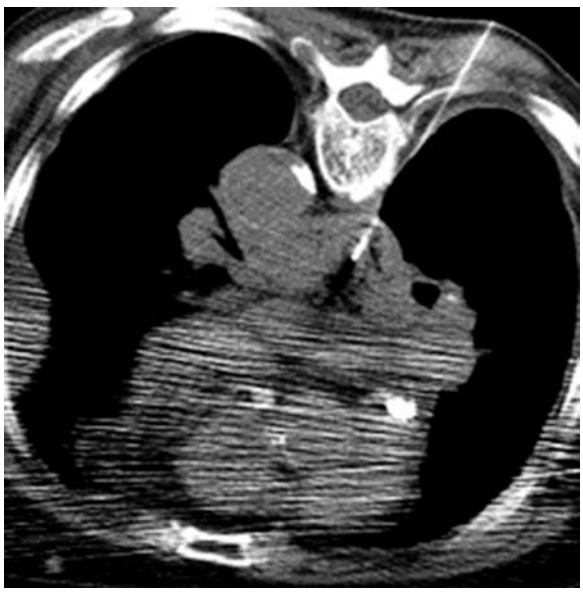

Fig. 6.6 Posterior paravertebral approach into the posterior compartment of the mediastinum in order to get tissue samples from an unclear paraesophageal mass. The needle is advanced close to the spine in order to avoid passage of the pleura and thereby reduce the risk of pneumothorax

biopsy of mediastinal lesions without traversing aerated lung (Gupta et al. 2005). The transpulmonary approach to mediastinal biopsy allows access to targets in various anterior, middle, and posterior mediastinal locations. This approach is generally used for lesions that are not accessible with an extrapleural approach.

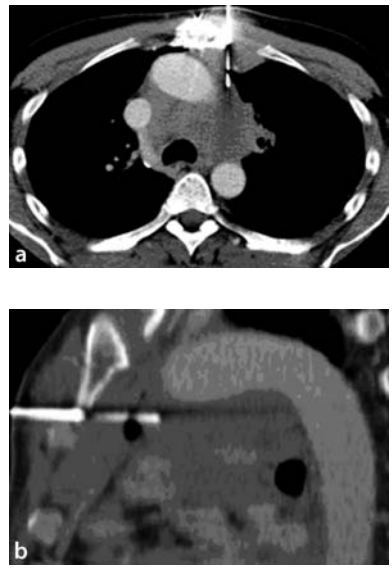

Fig. 6.7a,b Anterior parasternal approach to a mass located in the upper anterior mediastinal compartment. Biopsy revealed metastatic tumor tissue from a neuroendocrine carcinoma of unknown origin

6.3.3 Liver

In general, there are two interventional ways to the liver, transjugularly and percutaneously. Like in other areas, the way to the target is dependent on its localization within the liver. Every intrahepatic target can be approached percutaneously in a safe way with image guidance; even targets located high in the liver dome do not need a transpleural approach (Figs. 6.8, 6.9). In some situations it is useful to navigate with the help of landmarks such as gallbladder, portal vein, etc. to reach the target. One should always have a transhepatic route long enough to realize a tamponade of a hemorrhage along the puncture channel by itself. Traversing the falciform ligament or Glisson's triad should always be avoided (Stattaus et al. 2007). Passage of these structures is painful for the patient. If an intercostal approach is chosen, one should cross the rib at the top side to avoid damage to the intercostal nerve and vessels.

6.3.4 Gallbladder and Spleen

Diagnostic or therapeutic interventional procedures for the gallbladder or the spleen are very rare. When-

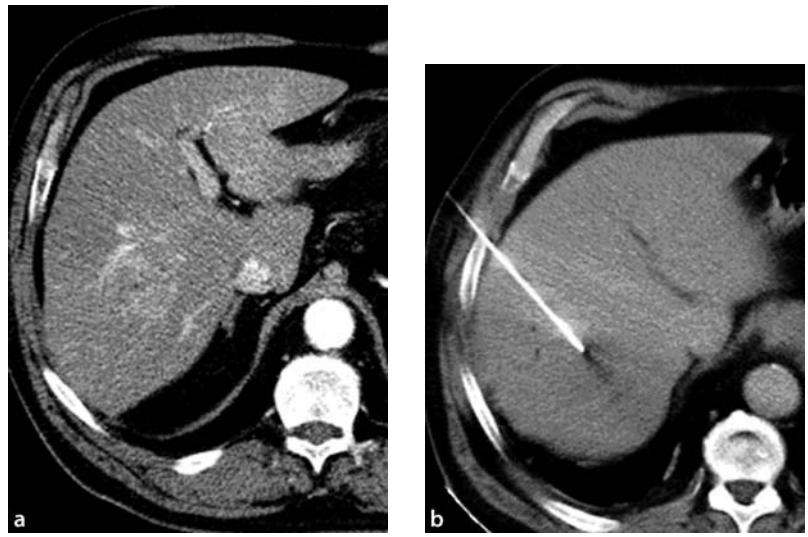

Fig. 6.8a,b Anterolateral intercostal approach to an unclear focal liver lesion enhanced slightly during arterial phase computed tomography (CT) (**a**) in liver segment 5/8 in a patient suffering from prostate cancer. Biopsy revealed a well-differentiated hepatocellular carcinoma (**b**)

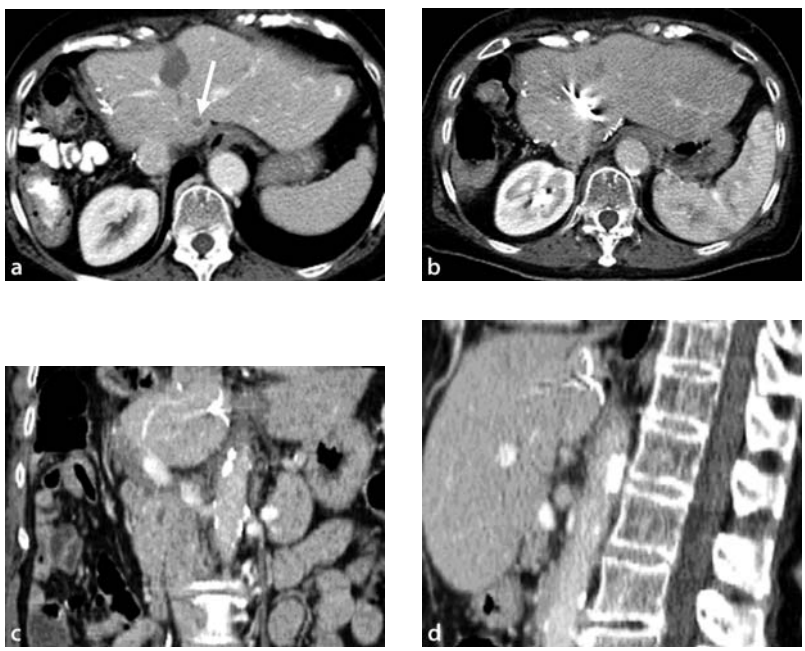

Fig. 6.9a–d Angulated outplane anterior approach to a small recurrent liver metastasis from colorectal cancer in liver segment 1 after right-sided hemihepatectomy. Preinterventional enhanced CT (**a**) demonstrates a small focal hypodense lesion within liver segment 1 (*arrow*). **b–d** The way to the target in multiplanar views with a radiofrequency (RF) probe opened in the lesion center

ever there is a process within the gallbladder exceeding the wall, the origin of the malignancy seems obvious and a minimally invasive biopsy prior to surgery is not necessary. If there is an indication for gallbladder decompression by tube placement, a transhepatic pathway should be preferred. Owing to the fact that intrasplenic lesions are often associated with malignant lymphoma, there are usually other anatomical sites where enlarged lymph nodes can be reached more easily and safely to assess the diagnosis by percutaneous biopsy. Despite a higher bleeding risk, biopsies or interventional treatments of the spleen can be per-

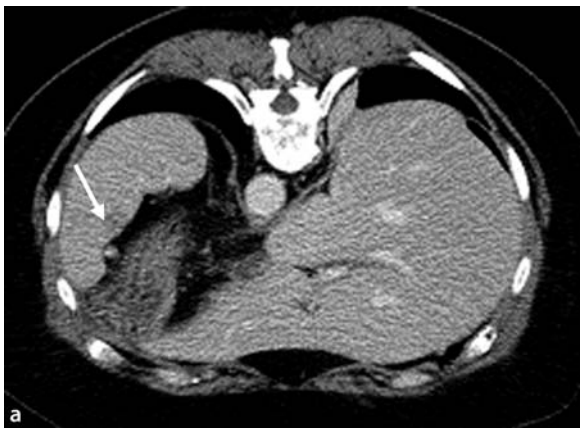

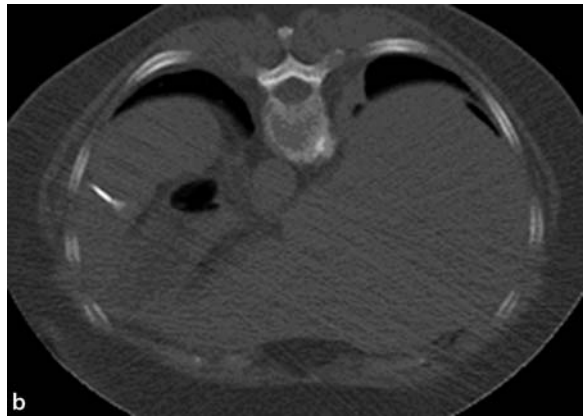

Fig. 6.10a,b Posterolateral approach to a small metastasis from colorectal cancer located near the spleenic hilum with the patient being in the prone position. Preinterventional enhanced CT (**a**) demonstrates a small focal hypodense lesion within the spleen (*arrow*). **b** The way to the target in an axial plane with an RF probe opened in the lesion center

formed in a safe way (Fig. 6.10). Sometimes postinterventional embolization of the puncture route is required (Lieberman et al. 2007). In most cases targets within the spleen can be approached via a lateral intercostal access route (Kang et al. 2007).

6.3.5 Pancreas

Pancreatic lesions are sometimes not easy to detect. Imaging protocols usually require contrast-enhanced scans or sequences to delineate focal intrapancreatic lesions. Because of this and because of the anatomical localization, punctures of the pancreas are somewhat challenging. Depending on the site of the target, several puncture routes can be chosen. Lesions in the pancreatic head or body are usually approached via an anterior pathway (Li et al. 2008). In some instances a transgastric (Fig. 6.1) or a transhepatic (Fig. 6.2) route is necessary. Lesions located in the pancreatic tail can be reached either by a lateral or by a posterior route (Figs. 6.11, 6.12). A transintestinal way to the target represents a further option. Fine-needle passage of the small bowel is usually safe. Owing to the gut flora and the subsequent risk of infection, passage of the colon should be avoided. Recent data have suggested a coaxial fine-needle aspiration biopsy with a posterior transcaval approach (Gupta et al. 2002b).

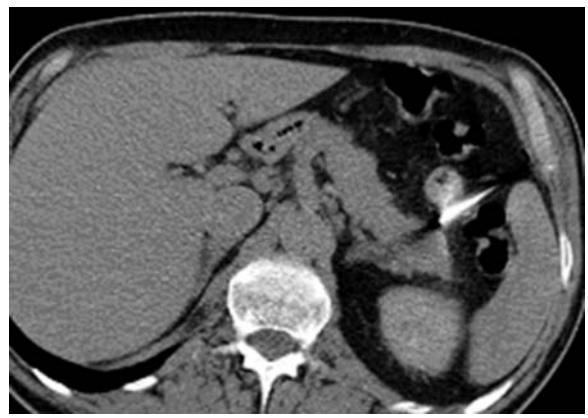

Fig. 6.11 Lateral approach to an unclear focal mass located in the pancreatic tail. Biopsy revealed metastasis from bronchial carcinoma

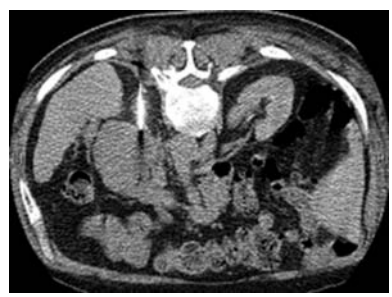

Fig. 6.12 Posterior paravertebral approach to an unclear focal mass located in the pancreatic tail. Biopsy revealed a pancreatic carcinoma

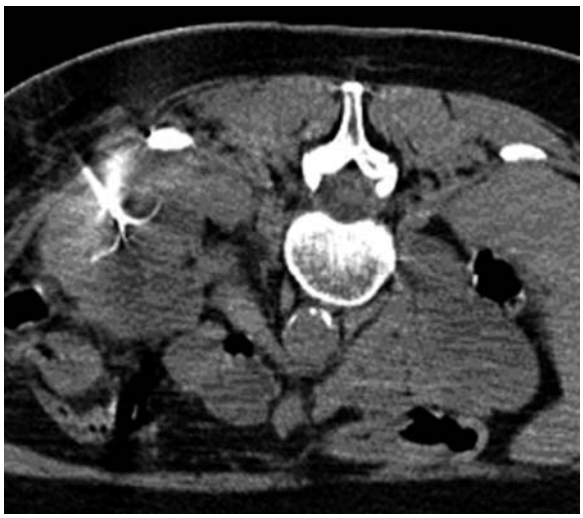

Fig. 6.13 Posterior approach to a recurrent renal cell carcinoma located in the contralateral left kidney 2 years after right-sided nephrectomy for renal cell carcinoma. Peri-interventional nonenhanced CT demonstrates a RF probe within the tumor

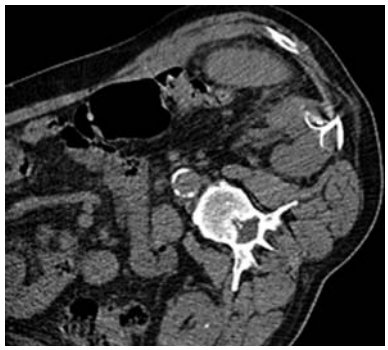

Fig. 6.14 Lateral approach to a recurrent renal cell carcinoma located in the contralateral left kidney 37 months after right-sided nephrectomy for renal cell carcinoma. Peri-interventional nonenhanced CT demonstrates a RF probe within the tumor

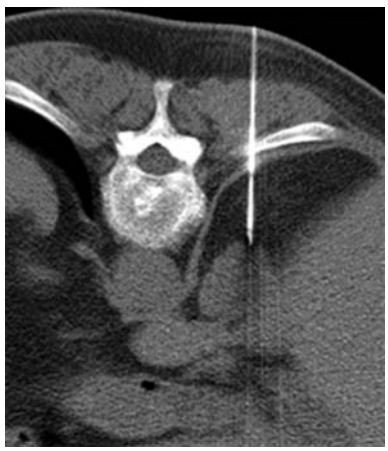

Fig. 6.15 Posterior approach to an unclear focal mass located in the right adrenal gland. Biopsy revealed metastasis from bronchial carcinoma

6.3.6 Kidney

The accuracy of percutaneous renal mass biopsy has been widely debated. Recent data have suggested that core needle biopsy is highly sensitive for the detection of renal malignancy, with relatively few nondiagnostic biopsies and very few procedure-related complications. Percutaneous renal mass biopsy significantly affects clinical management (Maturen et al. 2007). The kidneys are usually approached from a posterior route (Fig. 6.13) but can – depending on the site of the target – also be reached using a lateral approach (Fig. 6.14). In selected cases a transhepatic access to a renal target can be chosen (Iguchi et al. 2007). As renal tumors are commonly hypervascularized, puncture tract embolization may be required after renal punctures.

6.3.7 Adrenal Gland

Whenever there is an unclear focal lesion within the adrenal gland, noninvasive diagnostic tools such as MR imaging should be preferred to clarify the origin of the lesion. If this is not possible, percutaneous image-guided biopsy is a well-accepted option. Special attention has to be paid when a pheochromocytoma cannot be ruled out prior to biopsy. In such situations administration of α1- and α2-blockers is necessary to prevent a hypertensive crisis. Several ways to the target are possible, including posterior (Fig. 6.15), anterior, lateral, and transhepatic routes. Transrenal, transsplenic, or transpleural pathways should be avoided. In order to increase a paravertebral extrapleural puncture channel, physiological saline solution can be injected (Harisinghani et al. 2003).

6.3.8 Retroperitoneum and Peritoneal Cavity

The posterior approach is the standard route to lesions located within the retroperitoneum near to the aorta or the inferior vena cava (Fig. 6.16); the patient is positioned prone and a needle path via the dorsal spinal

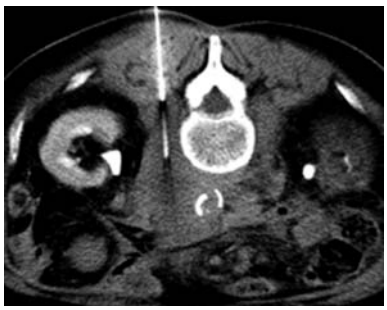

Fig. 6.16 Posterior approach via the dorsal spinal and psoas muscle to a malignant lymphoma located within the retroperitoneum near to the aorta

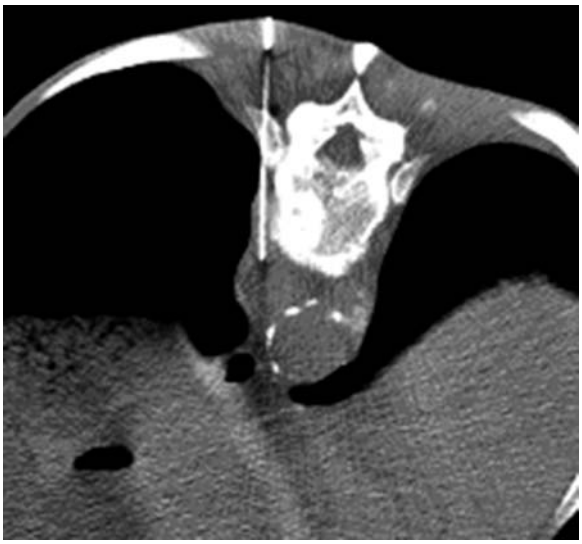

Fig. 6.17 Posterior paravertebral extrapleural approach to a malignant lymphoma located retrocrural near to the aorta

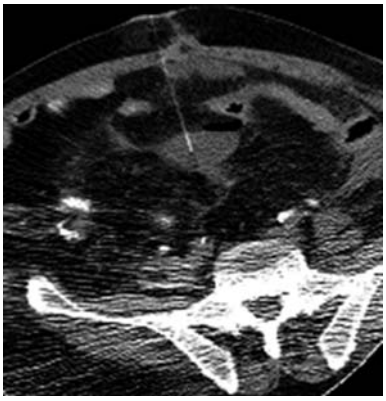

Fig. 6.18 Anterior approach to a fluid collection located in the mesenterium

and the psoas muscle is reasonable. With a strictly vertical needle path damage to the large vessels can be avoided, because the needle tends to end lateral to them. Special care must be taken regarding the ureter, which may be interposed between the target and psoas muscle. Therefore, if CT is chosen as the guiding method, the planning CT series should be acquired in the venous phase after contrast medium injection, and thereafter the ureter will be delineated for the duration of the biopsy. Alternatively 20–30 ml of contrast agent can be injected intravenously about 3–5 min prior to the intervention to label the ureter. For the pararenal approach in patients with a pararenal mass, patient position (prone, supine, right- or left-sided) and biopsy approach will be individually based on a safe access route avoiding major vascular structures as well as the pleural space. In most cases, this approach is noncritical and easy to perform. In the anterior–posterior approach in patients with a peripancreatic mass, the patient is positioned supine and the biopsy approach will be – if other ways are not available – via the left lobe of the liver. This transhepatic route requires administration of local anesthesia on both sides of the liver. In targets located near the aorta beneath the diaphragm (retrocrural) a posterior route is usually chosen (Fig. 6.17) in some cases with the necessity of angulated outplane needle paths sometimes requiring injection of 0.9% NaCl solution in order to increase the space of the puncture channel to prevent pleural laceration (Stattaus et al. 2008).

Depending on the site of the target within the peritoneal cavity, the access route is chosen. Usually a transabdominal approach through the anterior or lateral abdominal wall is suitable for nearly all intraabdominal targets (Fig. 6.18). Transintestinal pathways can be useful in some situations, but should be avoided whenever possible. The same holds true for the transaortic approach that is sometimes used for celiac plexus block. Anyhow, although these access routes are feasible options they should be limited to fine needles (20G–25G); cutting within the bowel or vessel wall needs to be avoided under any circumstance.

6.3.9 Pelvis

Access route planning for image-guided punctures within the deep pelvic space remains challenging

because vital structures such as overlying bowel, bladder, vessels, and bones as well as the uterus and adnexa, in female patients, often obstruct the projected needle path. A thorough understanding of the pelvic anatomy therefore is mandatory. There are several potential pathways to reach an intrapelvic target. They usually depend on the site of the target within the pelvic space (Gupta et al. 2004). The transabdominal approach through the lower anterior or lateral abdominal wall is suitable for lesions located either cranial to the level of the urinary bladder or anterior or lateral to the bladder. The transgluteal approach is suitable for lesions located in the presacral and perirectal regions (Fig. 6.19). In addition, targets located posterior or posterolateral to the urinary bladder and adnexal lesions can be accessed with this approach. In general, this way is used for posterior pelvic lesions in the lower part of the pelvis at the level of the greater sciatic foramen that are not accessible with an anterior approach because of intervening bowel, bladder, uterus, and iliac vessels. To avoid damage to neurovascular structures, the posterior access route should be as close as possible to the sacral bone. The anterolateral extraperitoneal approach is ideally suited for percutaneous biopsy of lesions located along the medial aspect of the iliopsoas muscle. This approach provides safe access to obturator or deep external iliac, anterior external iliac, and internal iliac targets. For presacral and posterior pelvic lesions that are not accessible by means of the transgluteal approach because either they are located above the level of the greater sciatic foramen or intervening vascular structures are present a transsacral approach might be an option. A transosseous approach through the iliac wing allows safe access to targets in close relation to the iliopsoas muscle that are not approachable by means of other routes (Schweiger et al. 2000; Yarram et al. 2007).

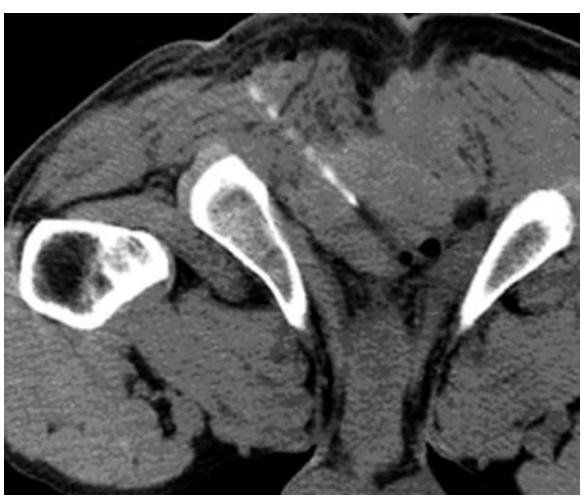

Fig. 6.19 Posterior transgluteal approach to an unclear perineal mass in a patient with a history of rectal cancer and extirpation of the rectum. Aspiration revealed hematoma

6.3.10 Bone

Each bone puncture is accompanied by an increased risk for inflammatory complications and therefore should be performed under sterile conditions. Because of this, transperitoneal approaches are contraindicated.

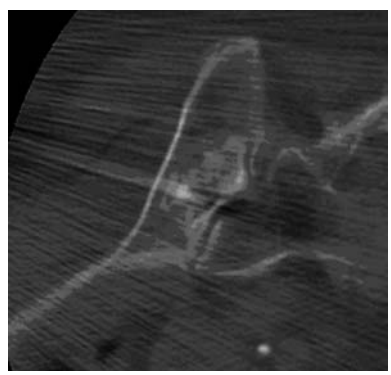

Fig. 6.20 Lateral transgluteal approach to a partially sclerotic osteolysis located in the left iliac wing. Biopsy revealed metastasis of breast cancer. Alternatively a dorsal approach would have been feasible

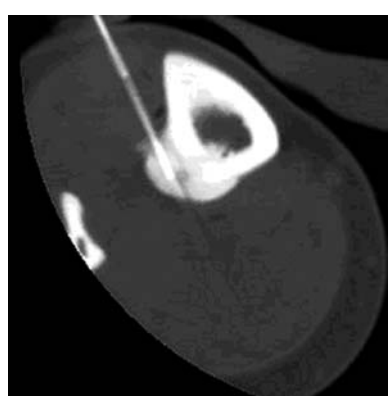

Fig. 6.21 Posterior approach for puncture of an osteoid osteoma prior to RF ablation

Prior to any bone puncture the periosteum has to be well anesthetized, avoiding sedation and narcosis when the puncture route is next to nerve structures. In peripheral bones the access route depends on the localization of the target and adjacent vascular and/or nerve structures (Figs. 6.20, 6.21, 6.22). Targets in the spine are usually approached from posterior using a transpedicular (Fig. 6.24) or extrapedicular paraspinal (Fig. 6.23) route (Tehranzadeh et al. 2007). Lesions in the cervical spine are approached using an anterior–posterior parapharyngeal route, whereas targets located in the upper cervical spine (e.g., C2) sometimes have to be accessed using a transoral approach (Reddy et al. 2005).

6.3.11 Miscellaneous

There are a lot of other targets that can be safely approached by image guidance (Figs. 6.23–6.32). The way to the target depends on the site of the target and surrounding structures at risk. In the vast majority of cases the shortest way seems to be the most appropriate and the safest. Adjusting the position of the patient according to the planned access route, including respiration maneuvers (e.g., Valsalva) (Fig. 6.30), represents a key point for successful punctures (Enoch et al. 2008; Akinci and Akhan 2005; Datta et al. 2007; Gupta et al. 2007; Boswell et al. 2007).

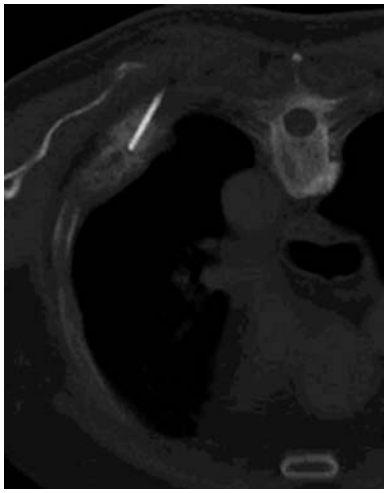

Fig. 6.22 Posterior approach to a lesion causing partially sclerotic rip destruction. The tangential direction of the puncture helps to reduce the risk of fracture and accidental injury to the pleura. Biopsy revealed metastasis of breast cancer

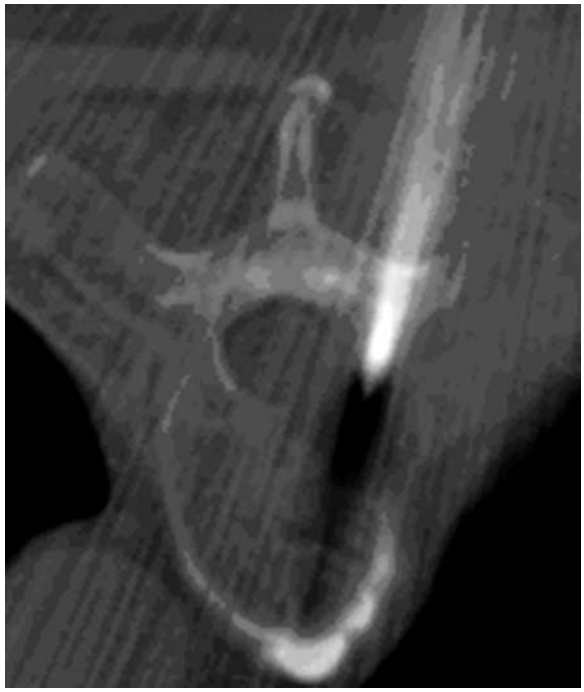

Fig. 6.23 Posterior transpedicular approach to an osteolysis in thoracic vertebra 11. Biopsy revealed metastasis of colorectal carcinoma

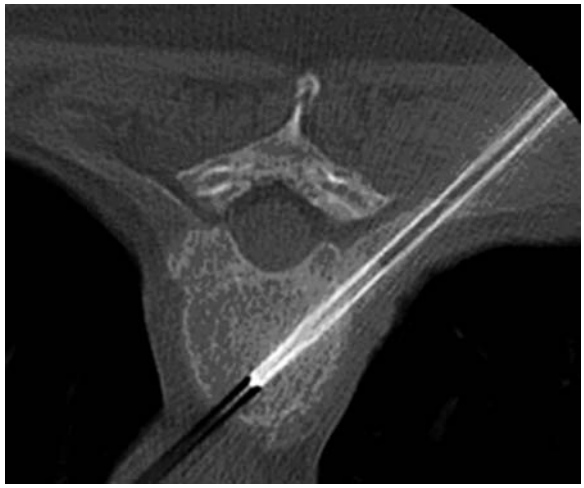

Fig. 6.24 Posterior extrapedicular approach to thoracic vertebra 9 prior to vertebroplasty. The costovertebral joint can safely be passed to access thoracic or lumbar vertebrae

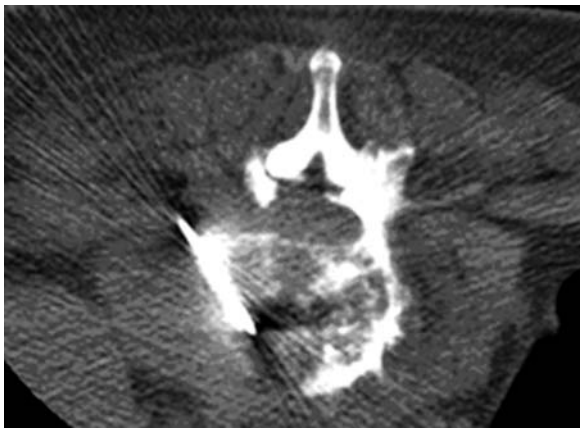

Fig. 6.23 Angulated posterior approach to the intervertebral space in septic discitis. Aspiration revealed intervertebral abscess with *Staphylococcus aureus*

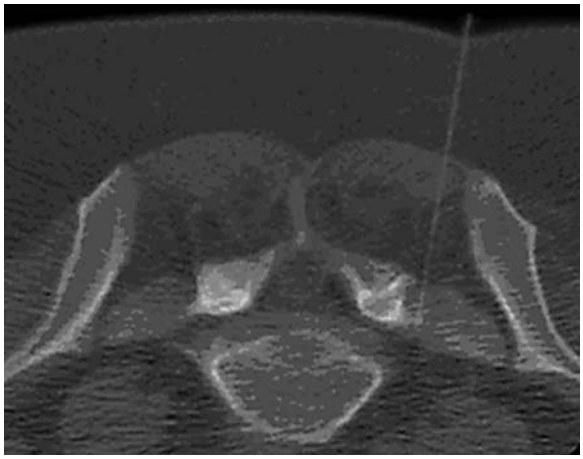

Fig. 6.24 Posterior approach to lumbar vertebra 5 for selective nerve block

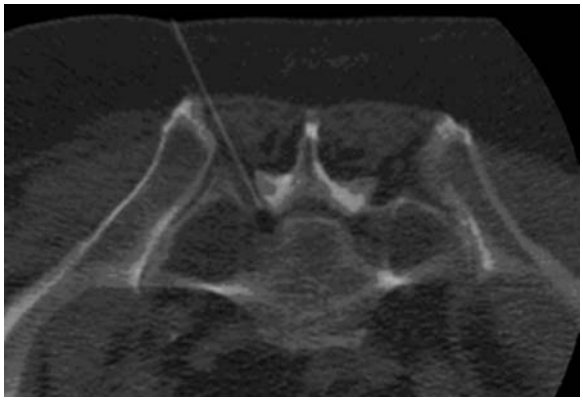

Fig. 6.25 Posterior approach to sacral vertebra 1 for selective nerve block

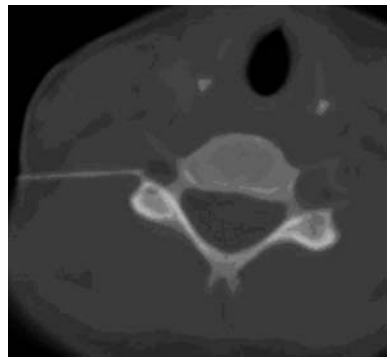

Fig. 6.26 Lateral approach to cervical vertebra 6 for selective nerve block

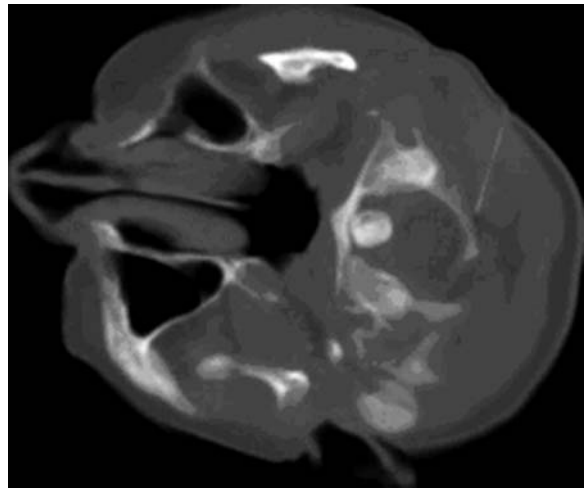

Fig. 6.27 Posterolateral approach to cervical vertebra 2 for selective nerve block

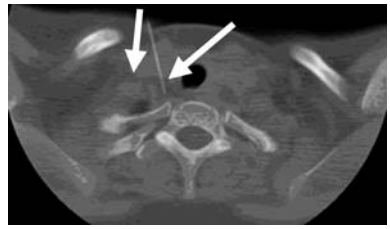

Fig. 6.28 Anterior approach for selective stellate ganglion block. Note the access route between the carotid artery (*long arrow*) and the jugular vein (*short arrow*). Valsalva maneuver was helpful to reach the target without any complication

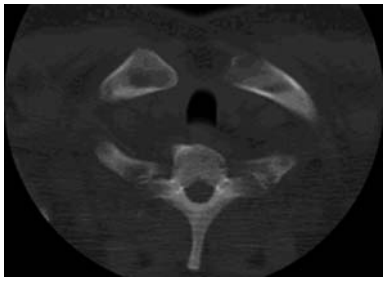

Fig. 6.29 Anterolateral approach for selective stellate ganglion block

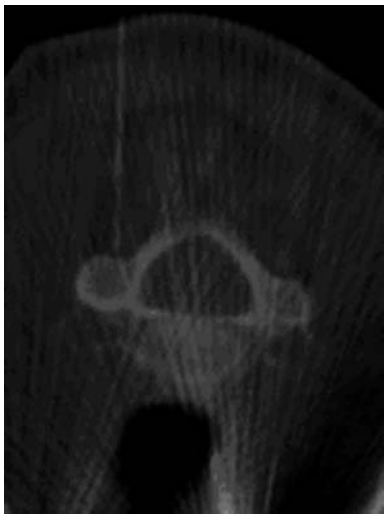

Fig. 6.30 Posterior approach for cervical facet joint block

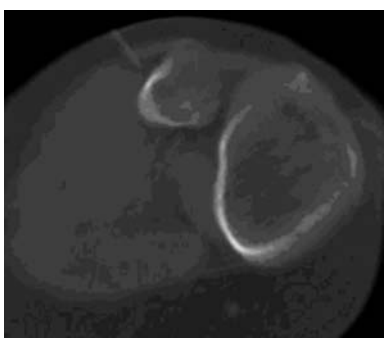

Fig. 6.31 Posterolateral approach for selective block of the common peroneal nerve

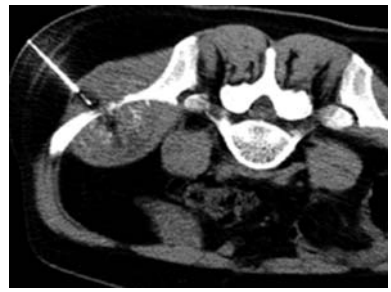

Fig. 6.32 Posterolateral, transgluteal approach to an unclear iliac mass. Biopsy revealed metastasis of a colorectal carcinoma

Summary

Virtually all regions the body may be accessed by CT- or MR-guided puncture. Depending on the region that needs to be accessed for diagnostic or therapeutic purposes, a variety of more or less safe routes are available. Depending on the anticipated route, adequate patient position and material need to be selected, while the method for image guidance should depend on lesion visibility. The figures shown only provide a glimpse at the potential access routes to different parts of the body and depending on the individual patient the access routes may vary widely. The general principle, however, is always the same: the shortest way with as little angulation as possible, avoid nerves, vessels, lung, and hollow organs, select the least traumatic puncture device that is reasonable for the anticipated task. If these basic requirements are considered, safe and successful puncture will be achieved.

Key Points

- There is no inaccessible lesion.
- Use a stable and comfortable patient position.
- Avoid angulated trajectories if possible.
- Transgastric, transhepatic, transosseous, and transvascular access routes are feasible if needed.
- Balance the risk and the benefit of the different access routes.
- Consider surgical and endovascular approaches when deciding to perform a CT- or MR-guided puncture.

References

Akinci D, Akhan O (2005) Celiac ganglia block. Eur J Radiol 55:355–361

Billich C, Muche R, Brenner G et al. (2008) CT-guided lung biopsy: incidence of pneumothorax after instillation of NaCl into the biopsy track. Eur Radiol 18:1146–1152

Boswell MV, Trescot AM, Datta S et al. (2007) Interventional techniques: evidence-based practice guidelines in the management of chronic spinal pain. Pain Physician 10:7–111

Datta S, Everett CR, Trescot AM et al. (2007) An updated systematic review of the diagnostic utility of selective nerve root blocks. Pain Physician 10:113–128

Enoch DA, Cragill JS, Laing R et al. (2008) Value of CT-guided biopsy in the diagnosis of septic discitis. J Clin Pathol 16:750–753

Gupta S (2004) New techniques in image-guided percutaneous biopsy. Cardiovasc Intervent Radiol 27:91–104

Gupta S, Madoff DC (2007) Image-guided percutaneous needle biopsy in cancer diagnosis and staging. Tech Vasc Interv Radiol 10:88–101

Gupta S, Wallace MJ, Morello FA et al. (2002a) CT-guided percutaneous needle biopsy of intrathoracic lesions by using the transsternal approach: experience in 37 patients. Radiology 222:57–62

Gupta S, Ahrar K, Morello FA Jr et al. (2002b) Masses in or around the pancreatic head: CT-guided coaxial fine-needle aspiration biopsy with a posterior transcaval approach. Radiology 222:63–69

Gupta S, Nguyen HL, Morello FA et al. (2004) Various approaches for CT-guided percutaneous biopsy of deep pelvic lesions: anatomic and technical considerations. Radiographics 24:175–189

Gupta S, Seaberg K, Wallace MF et al. (2005) Imaging-guided percutaneous biopsy of mediastinal lesions: different approaches and anatomic considerations. Radiographics 25:763–786

Gupta S, Henningsen JA, Wallace MJ et al. (2007) Percutaneous biopsy of head and neck lesions with CT guidance: various approaches and relevant anatomic and technical considerations. Radiographics 27:371–390

Harisinghani MG, Maher MM, Hahn PF et al. (2003) Predictive value of benign percutaneous adrenal biopsies in oncology patients. Clin Radiol 57:898–901

Hiraki T, Fujiwara H, Sakurai J et al. (2007) Nonfatal systemic air embolism complicating percutaneous CT-guided transthoracic needle biopsy: four cases from a single institution. Chest 132:684–690

Iguchi T, Hiraki T, Gobara H et al. (2007) Transhepatic approach for percutaneous computed-tomography-guided radiofrequency ablation of renal cell carcinoma. Cardiovasc Interv Radiol 30:765–769

Kang M, Kalra N, Gulati M et al. (2007) Image guided percutaneous splenic interventions. Eur J Radiol 64:140–146

Li L, Liu LZ, Wu QL et al. (2008) CT-guided core needle biopsy in the diagnosis of pancreatic diseases with an automated biopsy gun. J Vasc Interv Radiol 19:89–94

Lieberman S, Libson E, Sella T et al. (2007) Percutaneous image-guided splenic procedures: update on indications, technique, complications, and outcomes. Semin Ultrasound CT MR 28:57–63

Maturen KE, Nghiem HV, Caoili EM et al. (2007) Renal mass core biopsy: accuracy and impact on clinical management. AJR Am J Roentgenol 188:563–570

Ohno Y, Hatabu H, Takenaka D et al. (2004) Transthoracic CT-guided biopsy with multiplanar reconstruction image improves diagnostic accuracy of solitary pulmonary nodules. Eur J Radiol 51:160–168

Reddy AS, Hochman M, Loh S et al. (2005) CT guided direct transoral approach to C2 for percutaneous vertebroplasty. Pain Physician 8:235–238

Rogalla P, Juran R (2004) CT fluoroscopy. Radiologe 44:671–675

Schweiger GD, Yip VY, Brown BP (2000) CT fluoroscopic guidance for percutaneous needle placement into abdominopelvic lesions with difficult access routes. Abdom Imaging 25:633–637

Stattaus J, Kühl H, Hauth EA et al. (2007) Liver biopsy under guidance of multislice computed tomography: comparison of 16G and 18G biopsy needles. Radiologe 47:430–438

Stattaus J, Kalkmann J, Kuehl H et al. (2008) Diagnostic yield of computed tomography-guided coaxial core biopsy of undetermined masses in the free retroperitoneal space: single-center experience. Cardiovasc Intervent Radiol. doi:10.1007/s00270-008-9317-5

Tehranzadeh J, Tao C, Browning CA (2007) Percutaneous needle biopsy of the spine. Acta Radiol 48:860–868

Yarram SG, Nghiem HV, Higgins E et al. (2007) Evaluation of imaging-guided core biopsy of pelvic masses. AJR Am J Roentgenol 188:1208–1211

Navigated Interventions – Techniques and Indications

7

Gerlig Widmann and Reto Bale

Contents

7.1 Indications

Computer-assisted navigated interventions gain increasing importance in interventional radiology. Using frameless stereotactic navigation systems, the interventionalist can navigate a pointer and other instruments on multiplanar reconstructed images in real time and is armed with sophisticated preoperative planning, simulation, and arbitrarily angulated guided puncturing through adjustable rigid aiming devices (Bale et al. 1997, 2000, 2001, 2006; Bale and Widmann 2007).

Indications for navigated interventions include several procedures:

- Interventions where both high-precision and double-angulated access routes are needed;
- Radiofrequency (RF) ablation of large tumors/metastases requiring multiple probe positions in different locations to cover the large volume;
- RF ablation of the Gasserian ganglion in patients with trigeminal neuralgia;
- Percutaneous fixation of pelvic fractures;
- Retrograde drilling of small osteochondral lesions;
- Discography and vertebroplasty in difficult anatomical regions and conditions (scoliosis, etc.);
- Fractionated interstitial brachytherapy.

Depending on the precision needed for an interventional procedure virtually all organs and body regions from head to toe can be the subject of navigated interventions. This includes brain, nerves, liver, kidney, adrenal gland, lung, bone, and soft tissue (Goldberg et al. 2000; Gazelle et al. 2000; Bale and Widmann 2007).

7.2 Materials and Techniques

7.2.1 Material Available/Needed

Navigated interventions are best performed in an interventional treatment center and require:

1. An imaging modality;
2. A patient fixation system;
3. A surgical navigation system;
4. An image-to-patient registration technique;
5. An aiming device;
6. Puncture and treatment instruments.

7.2.1.1 Imaging Modality

In computed tomography (CT), scanners with a large gantry bore are preferred. The availability of a slid-

ing gantry is favorable. In magnetic resonance (MR) imaging, open systems are of particular value.

7.2.1.2 Patient Fixation

(Double) vacuum based immobilization devices (e.g., BodyFix®, Medical Intelligence, Schwabmünchen, Germany) allow for safe and easy patient fixation (Bale et al. 1999, 2002; Nagel et al. 2005). Such devices consist of a vacuum pump connected to different types of machine-washable pillows or plastic bags which are filled with tiny polystyrene balls.

7.2.1.3 Navigation System

Optical-based navigation systems (e.g., StealthStation® Treon™ plus, Medtronic, Louisville, USA; VectorVision® Colibri® , BrainLAB, Feldkirchen, Germany; CAPPA® IRAD, Siemens, Erlangen, Germany) are routinely used for neurosurgery, ENT surgery, and orthopedic surgery (Caversaccio et al. 1999; Grunert et al. 2002; Bale and Widmann 2007). They offer the advantage of a high technical accuracy in the range 0.1–0.4 mm (Khadem et al. 2000), convenient handling, and easy sterilization. Disadvantages are the necessity of constant visual contact between the camera array, the dynamic reference frame, and instruments and the potential susceptibility to interference through reflection of light from metallic surfaces in the operating room environment.

Electromagnetic navigation systems (e.g., AxiEM™, Medtronic, Louisville, USA; CAPPA® IRAD, Siemens, Erlangen, Germany; Percunav, Traxtal, Toronto, Canada) can reach comparable accuracy (Mascott 2005), and have the advantages of possible use of very small detector coils including angiographic catheters, navigation of flexible instruments, and no need for visual contact between the instrument and the sensor system (Schiemann et al. 2004; Wood et al. 2005; Banovac et al. 2005; Zhang et al. 2006a). However, these systems may be distorted by external magnetic fields and metal objects (Wagner et al. 2002), leading to incorrect position sensing of up to 4 mm (Birkfellner et al. 1998; Marmulla et al. 1998; Hummel et al. 2005, 2006). They may also be considered a contraindication in patients with pacemakers and cochlear implants.

7.2.1.4 Registration Technique

Point-based registration using attachable skin markers (e.g., Beekley SPOTS®, Beekley, Bristol, CT, USA) is the most widely used registration technique (Maurer et al. 1998; Fitzpatrick et al. 1998). It involves determining the coordinates of corresponding points (fiducials) in the image (manually or semiautomatically using the computer) and on the patient (with the probe of the navigation system) and computing the geometrical transformation that best aligns these points.

Automatic registration can be achieved either by a stable camera position and a calibration of the CT system (i.e., modality based navigation) (Jacob et al. 2000) or by using reflective markers that are automatically detected on the CT dataset and on the real patient (Jacob et al. 2000; Nagel et al. 2005).

7.2.1.5 Aiming Device

Most targeting devices are aligned to the preplanned virtual path by using the pointer (i.e., navigation probe) of the navigation system.

The EasyTaxis™ system (Philips Medical Systems, Best, The Netherlands) consists of a spherical alignment body (trapped ball) that rotates freely in a bearing and that can be locked by a screw (Dorward et al. 1997; Bale et al. 2001). It is connected to an adjustable mechanical arm with six degrees of freedom. The alignment body contains a large central cylindrical hole to accept a tube with an incomplete inner sleeve to place the navigation probe or other tubes for the guidance of different surgical instruments (e.g., biopsy needles and RF probes). The EasyTaxis™ system allows for separate positioning of the tip (which has to be in the virtual elongation of the pathway) and adjustment of the angulations of the probe (which has to be aligned with the virtual elongation of the path) via a trapped ball on the distal end of the mechanical arm.

The Vertek™ system (Medtronic, Louisville, USA) (Bale et al. 2006) consists of a mechanical device with two independent pivot joints. Thereby the complex rotational movement is replaced by two degrees of freedom. Owing to there being a tracked needle with a light-emitting diode at the distal part of the needle, the tip can be continuously tracked in real time during the advancement. However a possible bending of the needle would not be detected by the system.

The Atlas™ system (Medtronic, Louisville, USA) (Bale and Widmann 2007) is similar to the Vertek™ system but has the advantage of a freely adjustable mechanical guide accepting instruments with variable diameters and thus does not necessitate the use of reducing tubes.

7.2.2 Technique

7.2.2.1 (Double) Vacuum Patient Immobilization

To preserve the image-to-patient registration, the patient has to be immobilized in the intervention room, e.g., via a (double) vacuum system. The patient is positioned on a vacuum splint (plastic bags filled with polystyrene balls) and the air is evacuated, resulting in hardening of the plastic bag. If a rigid fixation is necessary (e.g., in interventions without general anesthesia) the double-vacuum fixation technique may be applied. In these cases the patient may be additionally covered with cushions filled with polystyrene balls, leaving an area for the surgical approach. Thereafter the patient and the cushions are covered by a plastic foil. When the vacuum pump is turned on, the air is evacuated from the space between the covering foil and the patient/vacuum splint to a negative pressure of about 80 mbar, resulting in a hardening. Thus, the patient is rigidly sucked on the therapy couch (Fig. 7.1).

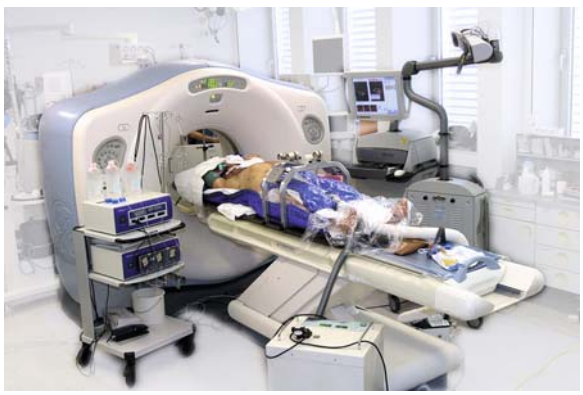

Fig. 7.1 Set-up for 3D-navigated radiofrequency (RF) ablation. The patient is immobilized by the double-vacuum immobilization. The vacuum pump can be seen in the *lower-right corner*, the camera of the navigation system in the *upper-right corner*, and the RF ablation system in the *lower-left corner*

7.2.2.2 Imaging

Most navigation systems require a continuous (volumetric) CT dataset. Gaps or overlapping slices are usually not acceptable. Tilting of the CT gantry needs to be avoided. For most cases CT slices of 3 mm or less are recommended as there is a clear correlation between voxel size and accuracy (Bucholz et al. 1993; Dorward et al. 1999; Maciunas et al. 1994). In addition, multimodal fusion with previously obtained three-dimensional MR imaging/positron emission tomography (PET)/single photon emission CT (SPECT) data may improve the planning procedure especially in lesions that are poorly visible by CT.

7.2.2.3 Planning

According to the type of intervention, a single (e.g., biopsy) or multiple (e.g., RF ablation of large metastases) puncture paths are planned using the navigation software. The trajectory planning is based on various two-dimensional and three-dimensional reconstructions of the patient's CT data and superimposed MR imaging/PET/SPECT data. By using the reconstructed longitudinal and orthogonal cuts along the planned path, one can prevent potential violation of vital structures (Fig. 7.2).

7.2.2.4 Registration

Registration markers should be broadly distributed around the volume of interest and have to be clearly indicated on the image data and the patient, respectively (West et al. 1999; Khan et al. 2006). Registration is performed by touching the real marker on the patient (Fig. 7.3) or on a reference frame and selecting the corresponding marker on the virtual three-dimensional dataset on the monitor. Automated registration technology may facilitate application (Jacob et al. 2000; Nagel et al. 2005). Respiratory motion decreases the accuracy and may require respiratory gating and affine transformation methods (Holzknecht et al. 2001; Zhang et al. 2006b). If high precision is required for interventions in organs that are sensitive to respiratory motion (the liver or the

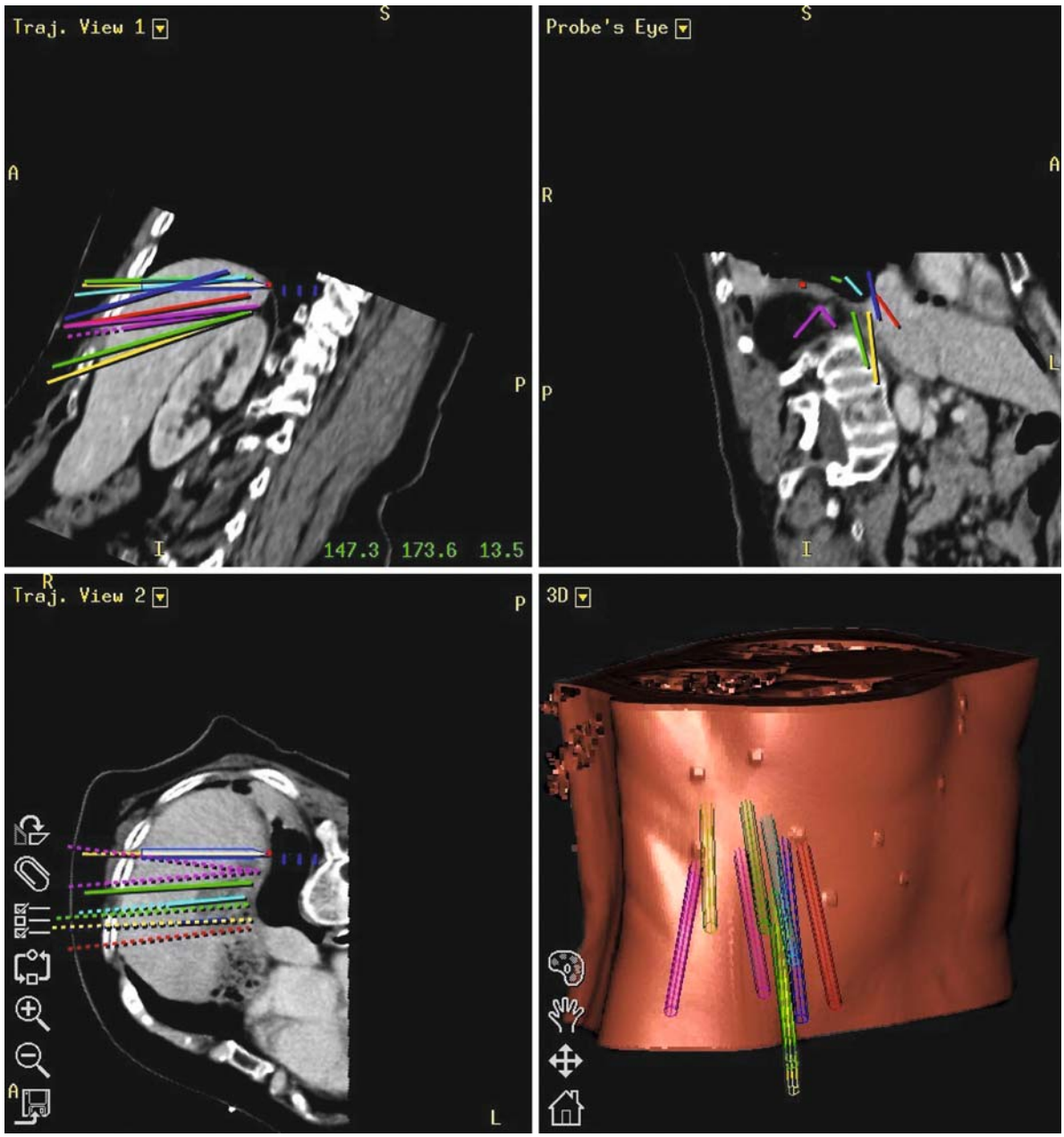

Fig. 7.2 Planning of multiple pathways on 2D reformatted and 3D computed tomography (CT) images (*lower-right quadrant*) for treating a large metastasis from colorectal carcinoma. The trajectory 0° (*upper-left quadrant*) and the trajectory 90° (*lower-left quadrant*) are planes along the needle trajectory and the probe's eye view (*upper-right quadrant*) is perpendicular to the pathway

bases of the lungs), general anesthesia may be required. The CT scans, the registration procedure, and the puncture must be performed in the same respiratory phase. By disconnection of the endotracheal tube, one can achieve a repositioning accuracy of 1–3 mm of the liver.

Fig. 7.3 Registration of the patient by touching the skin fiducials with the probe and selecting the corresponding markers on the screen (not shown)

7.2.2.5 Navigation

After unsterile registration, the puncture area is disinfected and draped. The pointer of the navigation system is introduced into the aiming device, which is adjusted according to the preplanned path using the guidance view of the navigation software. The needle is advanced through the aiming device to the preplanned depth as indicated by the navigation system (Fig. 7.4).

7.2.2.6 Control Imaging of Needle Positioning

For verification of the accuracy of the needle position, a low-dose control CT scan (with the needles in place) is obtained and fused with the planning CT scan (with the planned paths). Blending between the two datasets allows the planned paths to be superimposed on the real needles in the patient (Fig. 7.5).

7.2.2.7 Intervention

After verification of the correct needle position, the actual intervention (e.g., biopsy, RF ablation, infiltration, osteoplasty, etc.) is performed (Fig. 7.6).

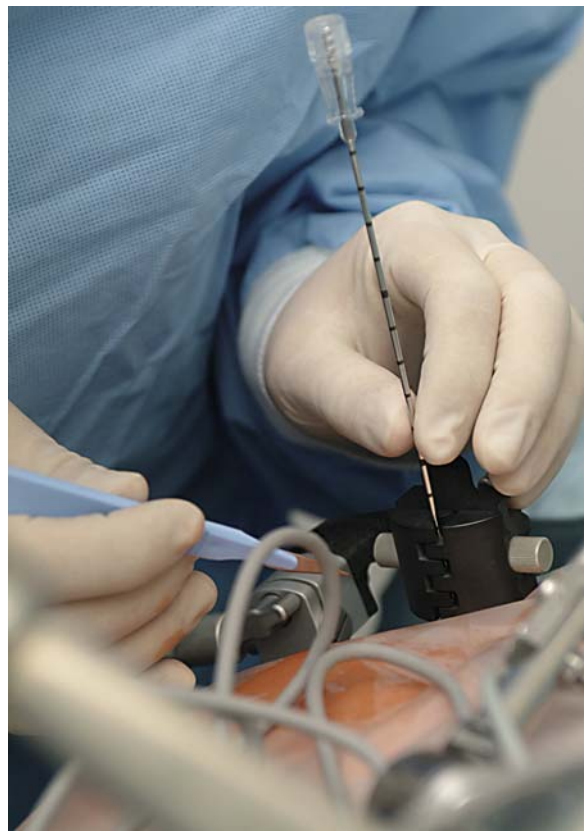

Fig. 7.4 Coaxial needle is advanced through the Atlas aiming device

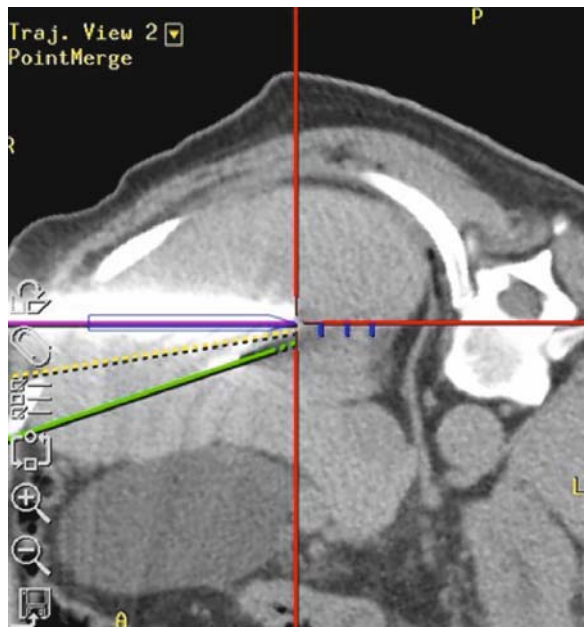

Fig. 7.5 The control CT scan is superimposed on the planning CT scan, with the pathway (*blue line*) showing precise placement

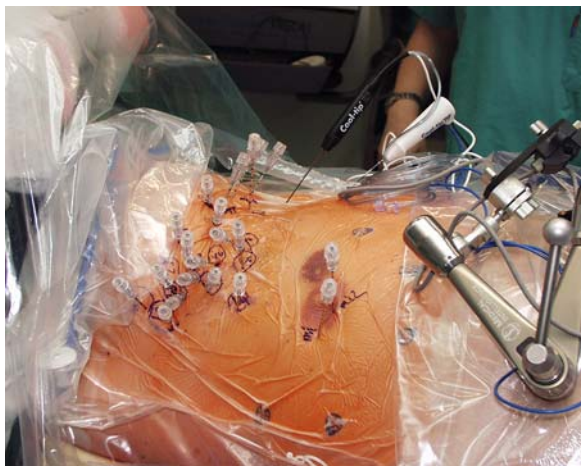

Fig. 7.6 Twenty-two coaxial needles have been introduced with 3D navigation

7.2.2.8 Control Imaging

Final control imaging may be performed to exclude intervention-related complications and to document the success of the intervention. Depending on the type of intervention, administration of contrast material or additional image registration may be needed.

7.3 Results

Navigation systems provide interactive visualization of the actual position of a probe or instrument in relation to the patient in real time with free angulations in the entire examination volume (Holzknecht et al. 2001). Usually, only a single planning CT scan and one low-dose control CT scan for confirmation of the correct needle position are required, which allows one to reduce the radiation exposure of the patient as well as of the interventionalist (Holzknecht et al. 2001). Multiple needles can be planned and placed under navigation using a single planning image dataset only (Banovac et al. 2005; Zhang et al. 2006b; Wood et al. 2007). This is especially helpful for ablation of large tumors where multiple overlapping ablation areas have to be achieved (Fig. 7.7). Compared with the current free-hand movement of needles, adjustable aiming devices enable rigid trajectory alignment and instrument guidance in three-dimensional arbitrarily oriented tracks (Germano and Queenan 1998; Holloway et al. 2005; Dorward et al. 1997; Paleologos et al. 2001; Patel and Sandeman 1997; Bale et al. 1997; Nagel et al. 2005). This technique allows one to reduce needle misplacement and repeated puncture attempts and thereby helps in achieving a predictable and reproducible result. In that way image-guided interventions become less dependent on the individual interventionalist's experience (Banovac et al. 2005). Depending on the location and the rigidity of immobilization, the laboratory accuracy of 1–2 mm can be reached in the patient.

In spite of the apparent advantages over the conventional CT-guided puncture technique, such systems are currently only rarely used by the interventional radiologist. The reasons for this are manifold and may depend on three basic requirements: knowledge about functionality of navigation systems, familiarity, and availability of such a system (Bale and Widmann 2007).

7.4 Complications

Navigated interventions include the following procedural errors (Grunert et al. 2002; Gralla et al. 2003; Mascott 2005; Mascott et al. 2006):

- *Patient fixation*: Movement in the time between image acquisition, registration, and puncture must be avoided. For interventions in the liver and lung respiratory gating may be necessary.
- *Planning*: The trajectories have to be planned in order to prevent violation of vital structures. For bone interventions an orthogonal plan to the bone surface is favored to minimize the risk of needle/pin deviation.
- *Registration*: The registration process is one of the most crucial steps in three-dimensional navigation. It requires an optimal distribution and indication of the markers on the real patient as well as a precise definition of the markers on the virtual dataset. The registration accuracy has to be checked prior to navigation.
- *Navigation*: The aiming device has to be rigidly secured before advancement of the needle. The needle position has to be controlled prior to the actual intervention.

Interventional complications depend on the anatomical region and the type of procedure and are described in detail in each procedure-specific chapter.

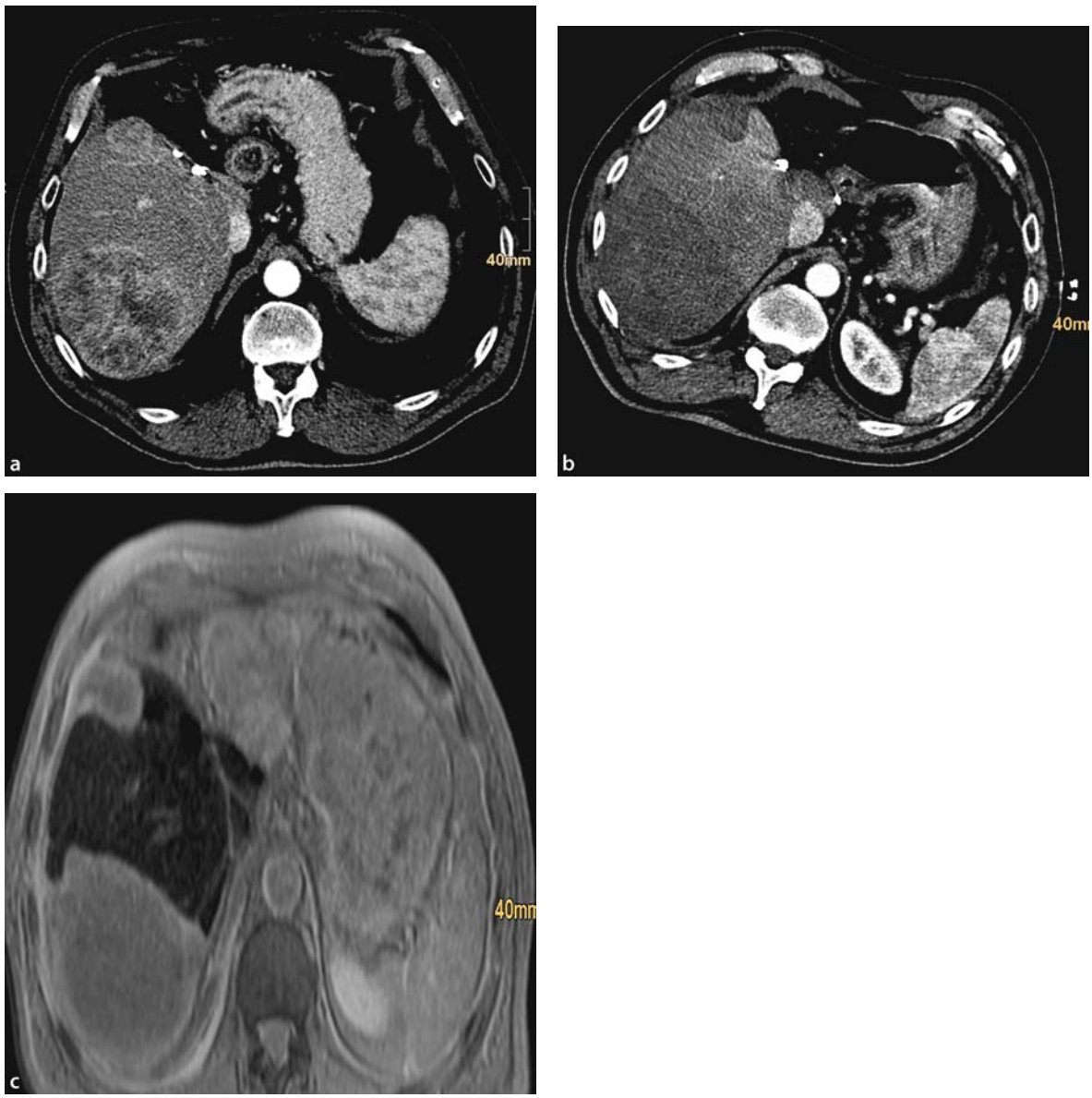

Fig. 7.7a–c RF ablation in a patient with two hepatocellular cacinomas (10 and 3 cm in diameter) and a history of left hemihepatectomy. The preinterventional CT scan shows two large contrast-enhanced tumors (**a**). Control CT after RF ablation shows the large areas of necrosis (**b**). Magnetic resonance imaging with iron particles (Resovist, Bayer-Schering Pharma, Berlin, Germany) 1 year after 3D-navigated RF ablation shows no evidence of tumor recurrence (**c**)

Summary

The spectrum of conventional CT- and MR-guided interventions is enlarged by navigated computer-assisted puncture techniques. Three-dimensionally guided puncture techniques provide a more sophisticated planning of the puncture path, because the puncture plane can be individually defined using a three-dimensional environment. Multimodal fusion imaging data for diagnostic and planning purposes in combination with fusion

of postoperative data to the initial planning data improve the interventionalist's confidence. Rigid aiming devices enhance puncture accuracy and patient safety and reduce radiation dose and "room time." Based on the advantages of navigated interventions, including their multipurpose applicability, navigation systems may represent a valuable investigation for an institution.

Key Points

The interventionalist has to be aware of the relevant procedural steps:

- Patient fixation
- Imaging
- Registration
- Navigation

The interventionalist also has to be aware of subsequent complications due to a three-dimensionally navigated approach. A check of the registration accuracy before navigation and a control CT scan to verify the correct needle placement are mandatory.

References

Bale R, Widmann G (2007) Navigated CT-guided interventions. Minim Invasive Ther Allied Technol 16196–204

Bale RJ, Vogele M, Martin A et al. (1997) VBH head holder to improve frameless stereotactic brachytherapy of cranial tumors. Comput Aided Surg 2:286–291

Bale RJ, Vogele M, Rieger M et al. (1999) A new vacuum device for extremity immobilization. AJR Am J Roentgenol 172:1093–1094

Bale RJ, Freysinger W, Gunkel AR et al. (2000) Head and neck tumors: fractionated frameless stereotactic interstitial brachytherapy-initial experience. Radiology 214:591–595

Bale RJ, Hoser C, Rosenberger R et al. (2001) Osteochondral lesions of the talus: computer-assisted retrograde drilling—feasibility and accuracy in initial experiences. Radiology 218:278–282

Bale RJ, Lottersberger C, Vogele M et al. (2002) A novel vacuum device for extremity immobilisation during digital angiography: preliminary clinical experiences. Eur Radiol 12:2890–2894

Bale RJ, Laimer I, Martin A et al. (2006) Frameless stereotactic cannulation of the foramen ovale for ablative treatment of trigeminal neuralgia. Neurosurgery 59:ONS394–ONS401

Banovac F, Tang J, Xu S et al. (2005) Precision targeting of liver lesions using a novel electromagnetic navigation device in physiologic phantom and swine. Med Phys 32:2698–2705

Birkfellner W, Watzinger F, Wanschitz F et al. (1998) Systematic distortions in magnetic position digitizers. Med Phys 25:2242–2248

Bucholz RD, Ho HW, Rubin JP (1993) Variables affecting the accuracy of stereotactic localization using computerized tomography. J Neurosurg 79:667–673

Caversaccio M, Bachler R, Ladrach K et al. (1999) The "Bernese" frameless optical computer aided surgery system. Comput Aided Surg 4:328–334

Dorward NL, Alberti O, Dijkstra A et al. (1997) Clinical introduction of an adjustable rigid instrument holder for frameless stereotactic interventions. Comput Aided Surg 2:180–185

Dorward NL, Alberti O, Palmer JD et al. (1999) Accuracy of true frameless stereotaxy: in vivo measurement and laboratory phantom studies. Technical note. J Neurosurg 90:160–168

Fitzpatrick JM, West JB, Maurer CR, Jr. (1998) Predicting error in rigid-body point-based registration. IEEE Trans Med Imaging 17:694–702

Gazelle GS, Goldberg SN, Solbiati L et al. (2000) Tumor ablation with radio-frequency energy. Radiology 217:633–646

Germano IM, Queenan JV (1998) Clinical experience with intracranial brain needle biopsy using frameless surgical navigation. Comput Aided Surg 3:33–39

Goldberg SN, Gazelle GS, Compton CC et al. (2000) Treatment of intrahepatic malignancy with radiofrequency ablation: radiologic-pathologic correlation. Cancer 88:2452–2463

Gralla J, Nimsky C, Buchfelder M et al. (2003) Frameless stereotactic brain biopsy procedures using the Stealth Station: indications, accuracy and results. Zentralbl Neurochir 64:166–170

Grunert P, Espinosa J, Busert C et al. (2002) Stereotactic biopsies guided by an optical navigation system: technique and clinical experience. Minim Invasive Neurosurg 45:11–15

Holloway KL, Gaede SE, Starr PA et al. (2005) Frameless stereotaxy using bone fiducial markers for deep brain stimulation. J Neurosurg 103:404–413

Holzknecht N, Helmberger T, Schoepf UJ et al. (2001) Evaluation of an electromagnetic virtual target system (CT-guide) for CT-guided interventions. Rofo 173:612–618

Hummel JB, Bax MR, Figl ML et al. (2005) Design and application of an assessment protocol for electromagnetic tracking systems. Med Phys 32:2371–2379

Hummel J, Figl M, Birkfellner W et al. (2006) Evaluation of a new electromagnetic tracking system using a standardized assessment protocol. Phys Med Biol 51:N205–N210

Jacob AL, Messmer P, Kaim A et al. (2000) A whole-body registration-free navigation system for image-guided surgery and interventional radiology. Invest Radiol 35:279–288

Khadem R, Yeh CC, Sadeghi-Tehrani M et al. (2000) Comparative tracking error analysis of five different optical tracking systems. Comput Aided Surg 5:98–107

Khan MF, Dogan S, Maataoui A et al. (2006) Navigation-based needle puncture of a cadaver using a hybrid tracking navigational system. Invest Radiol 41:713–720

Maciunas RJ, Galloway RL Jr, Latimer JW (1994) The application accuracy of stereotactic frames. Neurosurgery 35:682–694

Marmulla R, Hilbert M, Niederdellmann H (1998) Intraoperative precision of mechanical, electromagnetic, infrared and laser-guided navigation systems in computer-assisted

surgery. Mund Kiefer Gesichtschir 2(Suppl 1):S145-8–S145-S148

Mascott CR (2005) Comparison of magnetic tracking and optical tracking by simultaneous use of two independent frameless stereotactic systems. Neurosurgery 57:295–301

Mascott CR, Sol JC, Bousquet P et al. (2006) Quantification of true in vivo (application) accuracy in cranial image-guided surgery: influence of mode of patient registration. Neurosurgery 59:ONS146–ONS156

Maurer CR Jr, Maciunas RJ, Fitzpatrick JM (1998) Registration of head CT images to physical space using a weighted combination of points and surfaces. IEEE Trans Med Imaging 17:753–761

Nagel M, Schmidt G, Petzold R et al. (2005) A navigation system for minimally invasive CT-guided interventions. Med Image Comput Comput Assist Interv Int Conf Med Image Comput Comput Assist Interv 8:33–40

Paleologos TS, Dorward NL, Wadley JP et al. (2001) Clinical validation of true frameless stereotactic biopsy: analysis of the first 125 consecutive cases. Neurosurgery 49:830–835

Patel N, Sandeman D (1997) A simple trajectory guidance device that assists freehand and interactive image guided biopsy of small deep intracranial targets. Comput Aided Surg 2:186–192

Schiemann M, Killmann R, Kleen M et al. (2004) Vascular guide wire navigation with a magnetic guidance system: experimental results in a phantom. Radiology 232:475–481

Wagner A, Schicho K, Birkfellner W et al. (2002) Quantitative analysis of factors affecting intraoperative precision and stability of optoelectronic and electromagnetic tracking systems. Med Phys 29:905–912

West J, Fitzpatrick JM, Wang MY et al. (1999) Retrospective intermodality registration techniques for images of the head: surface-based versus volume-based. IEEE Trans Med Imaging 18:144–150

Wood BJ, Zhang H, Durrani A et al. (2005) Navigation with electromagnetic tracking for interventional radiology procedures: a feasibility study. J Vasc Interv Radiol 16:493–505

Wood BJ, Locklin JK, Viswanathan A et al. (2007) Technologies for guidance of radiofrequency ablation in the multimodality interventional suite of the future. J Vasc Interv Radiol 18:9–24

Zhang H, Banovac F, Lin R et al. (2006a) Electromagnetic tracking for abdominal interventions in computer aided surgery. Comput Aided Surg 11:127–136

Zhang X, Zheng G, Langlotz F et al. (2006b) Assessment of spline-based 2D-3D registration for image-guided spine surgery. Minim Invasive Ther Allied Technol 15:193–199

Special Considerations for Image-Guided Interventions in Pediatric Patients

8

Dagmar Honnef

Contents

8.1 Introduction

Image-guided interventions are increasingly gaining importance in interventional clinical routine. These include minimally invasive diagnostic procedures as well as percutaneous therapeutic interventions. Generally speaking, percutaneous interventions are less invasive than surgical procedures and should be considered whenever feasible, particularly in patients in whom resection of the primary tumor is not intended or possible. Compared with interventional procedures in adults, several specific features have to be taken into account for image-guided interventions in pediatric patients. Children need special care and they suffer from other diseases than grown-up patients. In general, ultrasound and magnetic resonance (MR) imaging guidance should be preferred whenever possible, because unlike computed tomography (CT) guided interventions they are not associated with radiation exposure. In this chapter special considerations for image-guided interventions in pediatric patients are presented.

8.2 Materials and Techniques

8.2.1 Preparation

Prior to any interventional procedure or a CT scan, clinical justification has to be ensured. Whenever possible the interventional radiologist who performs the procedure should talk to the parents and obtain parental consent. Antibiotics may be given prior to nephrostomy and abscess drainage or biliary procedures (Table 8.1). However, the findings of controlled studies dealing with preinterventional antibiotic treatment in children have not been published yet. The use of sedative protocols depends on the complexity of the intervention, the experience of the physician, as well as the capability of the patient to cooperate. Owing to the lack of cooperation or limited ability to cooperate, procedures are often performed with the patient under analgesic sedation or total intravenous anesthesia provided by an experienced physician (see Chap. 5). In addition, local anesthesia should be used to minimize depth of sedation during the procedure as well as postinterventional local pain.

Mahnken/Ricke (Eds.), *CT- and MR-Guided Interventions in Radiology*

Table 8.1 Suggestions for medication for interventional procedures. Dosage and selection of antibiotics should be discussed with the referring pediatrician. Special considerations may be necessary in immunoincompetent children or patients with heart diseases. The data provided on medication have been adapted to body weight

Indication	Pathogen	Antibiotics	Age	Dose in 24 h (mg/kg body weight)	Single dose
Spondylodiscitis	*Staphyloccocus aureus*	Cefuroxim or cefotiam or flucloxacillin	<12 years 3–12 months 1–12 years	150–200 mg i.v. 40–100 mg i.v. 3–8 g i.v.	3 3–4 3–4
Lung abscess	*S. aureus*	Cefuroxim or cefotiam			
Liver abscess	*Entamoeba histolytica* *Escherichia coli*	Metronidazol Tinidazol Amipicillin + aminoglycoside + metronidazol	<12 years 6–12 years	30 mg i.v. or p.o. 30 mg p.o.	3
Abscess due to appendicitis	*E. coli*, *Streptococcus*	Cefuroxim or cefotiam and metronidazol	<12 years <12 years	75–150 mg i.v. 15–30 mg i.v.	3 3
Preinterventional					
Urolgic system	*E. coli*, *Staphylococcus*	Cefuroxim or cefotiam or aminopenicillin + β-lakcamase-inhibitor	<12 years	50 mg i.v.	1
Biliary system	*E. coli*, *Streptococcus*	Cefuroxim or cefotiam or ampicillin + sulbactam	<12 years 1–12 years	50 mg i.v. 50 mg i.v.	1 1
Bone	*S. aureus*, *Staphyloccocus epidermidis*	Clindamycin[a]	<12 years	10 mg i.v.	1

[a] Clindamycin penetrates the bone.

It is recommended to perform lung biopsies in tracheal intubation and controlled ventilation because of potential complications (Bendon et al. 2005). The most common are pneumothorax and hemoptysis. Intubation helps to detect hemoptysis early and allows for effective suctioning. Furthermore it aids in achieving a more reliable needle positioning and results in fewer complications and higher diagnostic accuracy (Bendon et al. 2005). In patients with hepatic or renal failure, general anesthesia should be preferred to analgesic sedation owing to the risk of drug toxicity, hypotension, respiratory depression, and prolonged sedation (Kaye et al. 2000). Compared with adults, the surface area to body volume ratio is higher in children, which causes the child to cool down more rapidly. To prevent hypothermia especially in small children, it is recommended to use blankets during the procedure. In thoracic and abdominal imaging, the arms should be elevated as they can cause artifacts. Furthermore, irradiation of the arms should be avoided as red bone marrow is located in the extremities. Therefore, in sedated patients it might be necessary to tape the arms in this position.

Oral contrast medium application is usually not necessary, but may be helpful for detecting interenteric lesions. Diluted nonionic, low-osmolarity contrast media should be used to obviate electrolytes shift (1.5% diluted: baby 100 ml, infant 200–300 ml, schoolchild 300–500 ml) (Honnef et al. 2004). Orally administered contrast medium also helps to avoid

accidental bowel injury by mistaking the bowel for the target lesion. Depending on localization and tissue contrast, contrast medium may be applied intravenously (1–2.0 ml 300 mg/ml iodine/kg body weight).

8.2.2 Computed Tomography

Minimizing radiation exposure in CT examinations is crucial as children are more sensitive to X-rays than adults (Brenner et al. 2001). Regarding dose minimization, sequential scanning is superior to spiral data acquisition. A further tube voltage and/or tube current reduction compared with the levels used in pediatric diagnostic CT studies should be performed (Honnef et al. 2004, 2007; Siegel et al. 2004; Vock 2005). A standard CT protocol cannot be provided as the degree of radiation dose reduction depends on several factors, such as body region, tissue contrast, and lesion size. For large lesions a lower image quality can be accepted with consequently increased dose reduction. A smaller dose decrease may be possible for small lesions than recommended by the preinterventional CT protocol. Usually 80- or 100-kVp protocols should be used. The effective dose is determined by several factors, such as scan length, slice thickness, number of scans, collimation, pitch, and type of CT scanner. These factors have to be optimized for each procedure. Particularly slice thickness and collimation have to be adapted to needle and lesion size. Generally submillimeter collimation should be avoided, as it is less dose-efficient than a thicker collimation. Additional gonad shielding is recommended in male patients (Hohl et al. 2005). Different computer software systems are available for estimating the radiation dose applied (Nagel et al. 2004).

8.2.3 Magnetic Resonance Imaging

There are only few publications dealing with MR-guided interventions in children (Schulz et al. 2003, 2005). At the moment this technique is mainly used for neurosurgical procedures. MR imaging is in particular applicable to tumors, which are ill defined by ultrasound and CT as MR imaging provides a high soft-tissue contrast. It is especially useful in localizing bone marrow edema, for example, caused by medullar metastasis in Ewing's sarcoma (Schulz et al. 2003). Compared with CT, the major advantage is the lack of radiation exposure, but it is not known yet what effects exposure to the magnetic field in prolonged MR examinations may have on the pediatric body. Disadvantages of MR guidance include increased procedure duration with longer anesthesia time and higher costs as well as the limited number of open MR scanners with easy access to the patient. In general, better image quality due to fewer field inhomogeneities can be achieved with closed-bore MR-systems. These, however, hamper the access to the patient. At the moment there are only a few MR-compatible biopsy instruments available (Schulz et al. 2003) and especially in small lesions (less than 1 cm) susceptibility artifacts may complicate the instrumentation (Lewin et al. 1998). The latter is more obvious with 1.5-T than with 0.5-T MR scanners. Spin-echo sequences should be preferred to minimize susceptibility artifacts. So far, MR guidance is not considered a reliable method in thoracic biopsies (Adam et al. 1999).

8.2.4 Biopsy

Percutaneous biopsy is suited to prove the structure of most lesions. It is mandatory prior to any radiation therapy or chemotherapy. The only exception in pediatric patients is suspected malignancy in large cartilaginous tumors, because malignant transformed large cartilaginous tumors typically contain large benign parts.

The choice of the biopsy needle depends on the access, further underlying diseases (e.g., coagulopathy, lung emphysema), and lesion size. Furthermore, the assumed tumor entity has to be considered because for differentiation of pediatric tumors (small, round, or blue cell) immunohistochemical, molecular pathological, and cytogenetic analysis has to be done apart from histologic analysis. These complex analyses require a certain amount of tissue, which results in the need for a core biopsy (Hoffer 2005). Many needles are available with selectable throw lengths. These should be adapted to the individual lesion size and localization.

Fine-needle biopsy is only justified in recurrent tumors, if there is malignancy, or if a sample for microbiological analysis is obtained. For aspiration of

fluid collections 22G needles are generally adequate in neonates (Coley and Hogan 2006). Particular care has to be taken in bone biopsy. In this case sterility has to be guaranteed to avoid osteomyelitis.

8.2.5 Localization Techniques

Typical indications for preoperative lesion localization are unsuccessful pulmonary biopsies or very small, not palpable, or difficult-to-access lesions. It may also be used prior to resection of extrapulmonary lesions (Fig. 8.1). To minimize the surgical trauma, the puncture point of the needle should be agreed with the surgeon. The most common technique is the needle placement of a hookwire. An alternative method has been described by McConnell et al. (2002). They used a mixture containing 3 ml autologous blood stained with 0.3 ml methylene blue for CT-guided localization of pulmonary nodules prior to video-assisted thoracoscopic resection. Patrick et al. (2002) applied – also in children – methylene blue (0.2–0.5 ml) within the pulmonary parenchyma just beneath the pleura overlying the nodule.

8.2.6 Drainage

The choice of the drainage catheter size depends on the expected content of a fluid collection. A catheter size of 8.5 F is adequate for drainage of most fluid collections in pediatric patients (Cahill et al. 2005; Gobien et al. 1985) (Fig. 8.2). Even in pasty abscesses clogging is virtually never observed with this catheter size. For drainage in neonates, 5- or 6-F catheters are recommended, because of the small body size (Coley and Hogan 2006). A small pigtail loop should be used in small fluid collections or neonatal kidneys. When compared with adults, tissue elasticity in children is much greater and catheter insertion, especially at the abscess wall, may be difficult (Gervais et al. 2004). This problem can be overcome by use of a dilatator

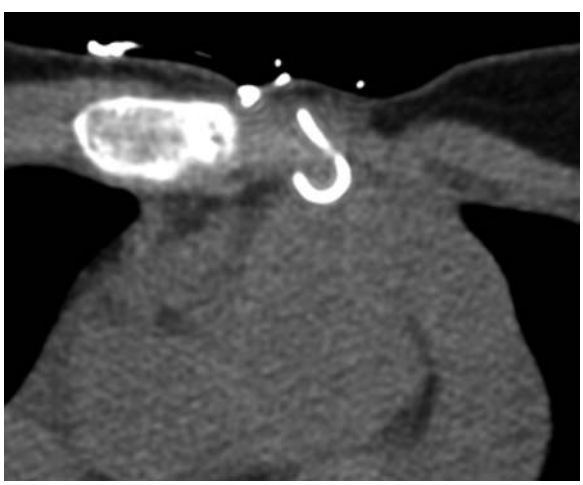

Fig. 8.1 Preoperative hookwire localization in a 17-year-old girl with Hodgkin's disease and positron emission tomography positive rest tumor in the anterior mediastinum (120 kVp, 110 mA $s_{eff.}$)

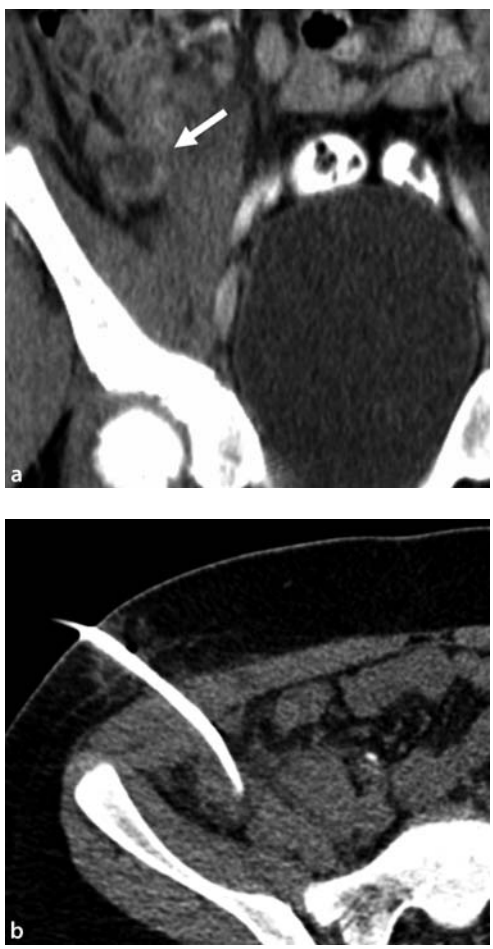

Fig. 8.2a,b Preinterventional computed tomography (CT; 100 kVp, 75 mA $s_{eff.}$) in a 12-year-old boy after appendectomy. Coronal multiplanar reformation demonstrates an abscess in the right lower abdomen (**a**; *arrow*). After successful placement of an 8.5-F drainage catheter using the trocar technique (**b**), the abscess completely resolved within 8 days, proving the success of the interventional procedure

prior to final catheter placement. Thrombolytic substances such as streptokinase (120 000 IU) or tissue plasminogen activator (2–10 mg) may be used in addition to saline instillation (Gervais et al. 2004; Kilic et al. 2002). They should be kept for 20–30 min in the abscess and then allow to drain. To date, doses of thrombolytic substances have not been standardized. The volume of normal saline should be adjusted to the size of the abscess. The volume applied should be less than the amount of fluid removed. Otherwise the abscess could be under pressure and cause sepsis. Aspiration may be sufficient only if the abscess is small (Hoffer et al. 1999) or if aspiration does not show any ichor (Cahill et al. 2005). Intravenous administration of antibiotics should always be done (Table 8.1).

Indications for nephrostomy include postoperative or congenital obstruction, massive vesicoureteral reflux, or congenital bladder problems as well as renal infection or postinterventional situations (Riccabona et al. 2002). This procedure is usually performed under ultrasound guidance (Riccabona et al. 2002), and CT or MR guidance should only be chosen if the procedure cannot be completed with ultrasound guidance.

Transgluteal as well as transabdominal and transrectal approaches have been described in pelvic drainages in infants (Cahill et al. 2005; Chung et al. 1996; Gervais et al. 2004; Jamieson et al. 1997; Pereira et al. 1996). Transrectal drainages should be performed only if it is certain that the fluid collection is infected as the approach will not be sterile. Catheter placement in interenteric abscesses should be done using the Seldinger technique with use of a 19G–22G needle, avoiding the colon (Gervais et al. 2004). Infected tumors may also be drained (Gervais et al. 2004).

8.2.7 Other Therapeutic Procedures

Aneurysmal bone cysts can be treated with injection of Ethibloc (Ethnor Laboratories, Ethicon, Norderstedt, Germany). The cyst is localized with a fine needle (21G–22G) using CT guidance (Garg et al. 2000). Thereafter a larger needle (16G) is inserted into the cyst and aspiration of blood proves the diagnosis. Before the injection of Ethibloc, contrast medium should be injected to ensure the intracavitary location of the needle and to exclude leakage into the soft tissues. Finally 4–8 ml Ethibloc is injected, depending on the size of the cyst (Garg et al. 2000). Ethibloc prevents cyst growth and induces endostal new bone formation. Particularly in septated cysts it is important to reach all parts of the cyst to avoid local recurrence. Antibiotics should be prescribed (Table 8.1). It is recommended to perform a follow-up CT after 6 months and a further reassessment after 12 months (Garg et al. 2000). Ethibloc should not be used in spinal lesions because of the possibility of leakage into the adjacent tissues or spinal vessels and potential paraplegia.

CT-guided intra-articular corticosteroid injection into inflammatory sacroiliac joints may be performed in patients with juvenile spondyloarthropathy who did not respond to oral nonsteroidal anti-inflammatory drugs. In these patients intra-articular injection of 40 mg corticosteroid (e.g., triamcinolone) is a viable treatment option in children (Fischer et al. 2003).

Radiofrequency ablation is regularly performed in pediatric patients suffering from osteoid osteoma (Cioni et al. 2004; Mahnken et al. 2006). Successful radiofrequency ablation of a small number of benign cartilaginous tumors in children has also been reported (Erickson et al. 2001; Ramnath et al. 2002). Unfortunately, there is no dedicated material available for pediatric radiofrequency ablation. Particularly shorter radiofrequency probes, which may be more appropriate for smaller pediatric patients, are not available (Brown and van Sonnenberg 2007). Further application of radiofrequency in children in the future may be for incurable painful bone metastasis as in osteosarcoma or Ewing's sarcoma. Radiofrequency ablation is also a therapeutic option in selected patients suffering from nephroblastoma (Brown et al. 2005). Hypothetically, hyperthermia may occur in children owing to a higher heat delivery relative to a smaller body volume than for adults (Brown et al. 2005). A combined CT-guided radiofrequency therapy and brachytherapy was used in a child with multiple recurrences of Wilms tumor (Ghandi et al. 2005). These strategies may be considered to obviate dialysis after nephrectomy. So far there exists no information on the long-term outcome of these therapeutic approaches.

Neurolysis is performed in the same technical way as in adults. Percutaneous celiac plexus block has been used in chronic pain refractory to medication due to chronic inflammatory bowel disease and several small-bowel resections (Tanelian and Cousins 1989) as well

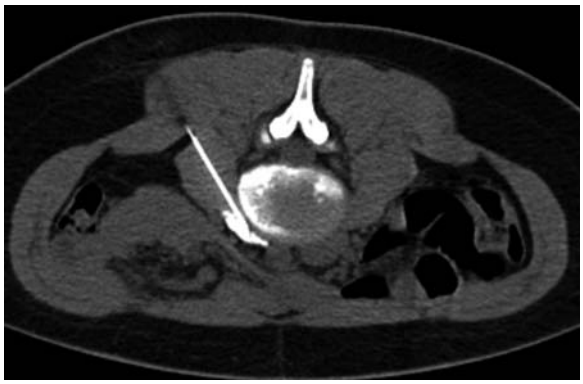

Fig. 8.3 A 16-year-old girl suffering from reflex sympathetic dystrophy of the left foot. For CT-guided (100 kVp, 50 mA $s_{eff.}$) left lumbar sympathicolysis 15 ml bupivacaine mixed with 0.5 ml contrast material for visualization of the fluid distribution was injected para-aortally at the level of lumbar vertebra 3. Immediately after the injection the patient described a warm feeling in the foot and the perfusion improved as could be seen by the change of the skin color of the foot. The procedure was repeated six times until the problems resolved permanently

as upper abdominal malignancies (Berde et al. 1990; Staats and Kost-Byerly 1995).

Reflex sympathetic dystrophy or sympathetically maintained pain syndrome is another indication for image-guided neurolysis. It is rare condition in children and differs from the adult form as it has a distinct female predilection; lower limb involvement is preferred and runs a relatively benign course. In these pediatric patients CT- or MR-guided lumbar sympathetic block can also be applied successfully (Nordmann et al. 2006) (Fig. 8.3). In children a permanent neurolysis should be avoided and never be used in the first place, even if this results in repeated interventions.

8.3 Results

8.3.1 Biopsy

Comparing fine-needle with cutting biopsies, the latter led to a significantly higher rate of specific diagnosis (83.7 vs. 38.9%) with the same complication rate (Guimaraes et al. 2003). In 75 CT-guided lung biopsies in children, 56 coaxial core biopsies and 15 fine-needle aspiration biopsies or both ($n = 4$) were performed with a major complication rate of 1.3%. Of these biopsies, 85% were diagnostic (Cahill et al. 2004). Even in small pulmonary nodules (0.5–2.0 cm) adequate cores could be obtained in 83% of cases (Connolly et al. 1999). Open lung biopsy is still considered the gold standard in interstitial lung diseases, but core biopsies were also successfully applied in children (Heyer et al. 2005; Wilkinson et al. 1999). Specificity and sensitivity of 100% was achieved in invasive aspergillosis with core biopsy, however this was associated with a 46% complication rate due to bleeding (Hoffer et al. 2001). In contrast to adults, hemoptysis as a complication of lung biopsies can be life-threatening in children, because it can lead to significant hypovolemia (Bendon et al. 2005).

Mediastinal biopsies, mainly spring-loaded core biopsies, showed 75% sensitivity and 100% specificity in children with suspected Hodgkin's disease or non-Hodgkin lymphoma (Garett et al. 2002). Aspiration of fluid collections in non-Hodgkin lymphoma or leukemia is often sufficient for diagnosis and should be preferred as it is less invasive (Garett et al. 2002).

In 90 pediatric abdominal biopsies the results for the core biopsy were significantly better than for the fine-needle biopsy with a comparable complication rate (Hugosson et al. 1999). A sensitivity of 89.6% and specificity of 100% in 202 core biopsies (15G or 18G) of solid pediatric tumors were reported (Garrett et al. 2005). Another study comparing fine-needle and core biopsy in solid tumors showed fewer differences regarding diagnostic accuracy (Sklair-Levy et al. 2001). However, in all studies fine-needle biopsy has been shown to limit the differentiation of nephroblastomatosis from nephroblastoma. Besides histologic information, percutaneous core biopsy provided additional genetic information (N-myc gene expression status, DNA Index) in up to 95% of cases with advanced neuroblastomas (Hoffer et al. 1996). In predominantly retroperitoneal punctures, 88% of the diagnoses were correct after core biopsy (14G or 18G) (Hussain et al. 2001). This result was confirmed in another series (Skoldenberg et al. 2002).

Diagnostic biopsies of solid tumors have resulted in a reported complication rate of 13.4%, with bleeding as the most common complication (Garrett et al. 2005). In percutaneous renal core biopsies in children, subcapsular hematomas were observed in up to 16% of the patients (Feneberg et al. 1998).

Percutaneous musculoskeletal biopsies are also feasible in children. Biopsy could confirm osteosarcoma in up to 94% of cases (Ahrar et al. 2004). In malignant bone tumors, passive dissemination of tumor cells

from the bone biopsy site necessitates resection of the puncture tracts; therefore, the access course should be discussed with the surgeon in advance. If there is no doubt of malignancy prior to biopsy, open surgery may be appropriate. Shin et al. (2007) demonstrated that 76% of core needle biopsies of musculoskeletal lesions were successful in children. The diagnostic success of biopsy in primary malignant tumors was 92% compared with 65% in primary benign tumors. Minor complications of 4.7% occurred from the biopsies.

In children spondylodiscitis is mainly due to hematogenous infection with *Staphyloccocus aureus* as the intervertebral discs are vascularized (Early et al. 2003). In spondylodiscitis either a fine-needle aspiration of an abscess formation or a core biopsy of the intervertebral disc or paravertebral granulation tissue is performed for microbiological analysis. Bacterial specimens can be found in up to 40% of such pediatric cases (Ventura et al. 1996); therefore, samples should only be taken in patients with suspected tuberculosis or fungal disease or in children who do not respond to intravenous antibiotic therapy or who suffer from chronic inflammation (Early et al. 2003; Ventura et al. 1996).

8.3.2 Localization Techniques

Until now large series on pulmonary needle localization in children have not been reported in the literature (Hardaway et al. 2000; Waldhausen et al. 1997). Smith et al. (1996) found needle localization is superior to intraoperative ultrasound during video-assisted thoracoscopic surgery because sonography may fail to detect superficially located lesions. As shown by Hardaway et al. (2000), one can also use hookwire localization in any other region of the body (Fig. 8.1). Successful MR-guided musculoskeletal tumor marking has been reported too (Schulz et al. 2005). Alternative techniques to preoperatively localize pulmonary nodules with methylene blue are also safe and effective especially in children with pulmonary nodules smaller than 1 cm (McConnell et al. 2002; Patrick et al. 2002).

McConnell et al. (2002) reported that 19 procedures performed in 17 children were diagnostic and 80% demonstrated malignancy. In one patient video-assisted thoracoscopic surgery had to be converted to open thoracotomy because of malfunction of the endoscopic stapler. In another study (Patrick et al. 2002) 13 procedures were completed successfully thoracoscopically. No thoracotomies were performed, and no complications were present.

8.3.3 Drainage

The success rate of image-guided percutaneous thoracic drainage with catheters is superior to that of aspiration alone (Margau et al. 2006). In 58 children with parapneumonic effusion and empyema complete resolution was achieved in 54 patients without mortality or 30-day recurrence after percutaneous intrapleural catheter placement with additional instillation of tissue plasminogen activator (Hawkins et al. 2004). Intrapleural fibrinolytic treatment with urokinase or streptokinase was effective in 80% of infants with pleural empyema after insufficient tube thoracostomy and intravenous administration of antibiotics (Kilic et al. 2002).

It is reported that 80–90% of small pulmonary abscesses can be cured with antibiotics alone (Klein and Zarka 2000). But aspiration of abscess fluid and microbiological analysis helps to perform targeted antibiotic therapy. Aspiration is only sufficient in lung abscesses with a volume below 15 ml (Hoffer et al. 1999). On the basis of the results of Hoffer et al. (1999), catheter drainage should be performed in lung abscesses with a volume of 20 ml or more or with an inner diameter of 3 cm. However, one has to consider the complication of a pleural empyema. Although interventional therapy provides diagnostic and therapeutic approached towards lung abscesses, it is less effective in necrotizing pneumonia with complications such as bronchopleural fistula, pneumatocele, and persistent pneumothorax (Hoffer et al. 1999). Preoperative drainage of congenital cystic adenomatoid malformation may be considered in children with respiratory insufficiency (Margau et al. 2006).

Renal abscesses are often caused by vesicoureteral reflux (Wippermann et al. 1991). Small renal abscesses resolve with antibiotic treatment alone, whereas larger ones can be successfully drained (Wippermann et al. 1991). In xanthogranulomatous pyelonephritis, an uncommon chronic, inflammatory disease, percutaneous drainage of the abscess and adjunctive antibiotic therapy prior to nephrectomy is recom-

mended to avoid complications (Bingöl-Kologlu et al. 2002).

The transgluteal approach to the drainage of pelvic fluid collections with image guidance has proven to be safe and effective (Cahill et al. 2005). Abscess recurrence is found in less than 5% of pediatric patients after successful drainage (Gervais et al. 2004). Ninety-one percent of children suffering from appendiceal abscess could successfully be treated with an image-guided drainage and intravenous antibiotics (Jamieson et al. 1997) (Fig. 8.2). Low-density tumors may be mistaken for an abscess. This should be considered in cases of minimal fluid drainage and little change in the appearance of the lesion (Gervais et al. 2004).

Intramuscular abscess is very rare in children. In a series of 18 children drainage of a psoas abscess proved to be a valuable alternative to surgery (Belgith et al. 2003). This procedure is also feasible in obturator muscle abscess (Orlicek et al. 2001). Absolute recommendations to guide the duration of antibiotic treatment in childhood spondylodiscitis have not been published. Parenteral antibiotics should be given between 4 and 6 weeks, followed by oral antibiotics for 1–2 weeks (Early et al. 2003) (Table 8.1). Most children improve rapidly with a 4–6-week course of antibiotics (Kayser et al. 2005). Conservative treatment is usually sufficient in spondylodiscitis with paravertebral fluid collection; however, drainage may be necessary if clinical improvement cannot be assessed (Brown et al. 2001; Garron et al. 2002).

8.3.4 Other Therapeutic Interventions

Percutaneous Ethibloc injection in aneurysmal bone cysts, mainly localized at the extremities, showed complete resolution of the lesions in 70% of patients (Garg et al. 2000); therefore, it can be an alternative to surgery (Cottalorda and Bourelle 2006). Pathologic fracture, local inflammation, and flulike illness are known complications of the procedure.

Intra-articular corticosteroid injection was effective in 87.5% of patients with juvenile spondyloarthropathy who were not responding to nonsteroidal anti-inflammatory drugs. These patients showed a significant decrease in their subjective complaints (Fischer et al. 2003). Improvement was seen about 1–2 weeks later and lasted for a mean of 12 months.

Summary

In the last few years there has been increasing interest in percutaneous image-guided interventions in children. Many interventions can be performed with ultrasound guidance, but CT- or MR-guided procedures may be needed in selected cases. Considering justified indications and correct performance of the procedures, CT- and MR-guided interventions in infants are feasible with limited risks. Apart from diagnostic procedures, therapeutic interventions (drainage, injection therapies, neurolysis, and radiofrequency ablation) are also successfully applicable in children and may help to avoid surgery. However, the published data are very heterogeneous as different localizations (e.g., chest, abdomen), tumor entities, patient ages (adults and children), interventional instruments, and imaging modalities are used in one study.

Key Points

- CT- or MR-guided interventional techniques used in adults can also be applied in children, but some special considerations have to be taken into account.
- Sedation or total intravenous anesthesia is more often necessary, because of limited cooperation. An additional local anesthesia is always recommended.
- Lung biopsies should be performed in tracheal intubation and controlled ventilation. Open lung biopsy is still considered the gold standard in interstitial lung diseases. In contrast to adults, hemoptysis as a complication of lung biopsies can be life-threatening in children because it can lead to significant hypovolemia. Aspiration of fluid collections in non-Hodgkin lymphoma or leukemia is often sufficient for diagnosis and should be preferred as it is less invasive.
- Depending on localization and tissue contrast, intravenous contrast media may be applied in CT examinations (1–1.5 mg iodine/kg body weight). Decrease of radiation exposure in CT examinations is essential (sequential scanning, tube voltage, and/or tube current reduction). Shielding may be applied.
- MR imaging is the preferred modality in biopsies of bone marrow abnormalities. However, small lesions (less than 1 cm) may not be visible owing to susceptibility artifacts.
- In pediatric small, round, or blue cell tumors core biopsy is needed to gain additional genetic information.
- A drainage catheter size of 8.5 F is adequate for drainage of most fluid collections in pediatric patients. Thrombolytic substances may be used. Catheter drainage should be considered in lung abscesses with a volume of 20 ml or more or with an inner diameter of 3 cm. For neonatal drainages, 5- or 6-F catheters are recommended. Owing to high tissue elasticity, insertion of a dilatator or catheter may be difficult.

- Conservative treatment is usually sufficient in spondylodiscitis with paravertebral fluid collection. Samples should only be taken in patients with suspected tuberculosis or fungal disease or in children who do not respond to intravenous antibiotic therapy or who suffer from a chronic course.
- Intra-articular corticosteroid injection is effective in juvenile spondyloarthropathy.
- Permanent neurolysis in children should not be used in the first place.

References

Adam G, Bücker A, Nolte-Ernsting C et al. (1999) Interventional MR-imaging: percutaneous abdominal and skeletal biopsies and drainages of the abdomen. Eur Radiol 9:1471–1478

Ahrar K, Himmerich JU, Herzog CE et al. (2004) Percutaneous ultrasound-guided biopsy in the definitive diagnosis of osteosarcoma. J Vasc Interv Radiol 15:1329–1333

Belgith M, Ben Brahim M, Jouini R et al. (2003) Psoas abscess in children based on a series of 18 cases. Prog Urol 13:1372–1375

Bendon AA, Krishnan BS, Korula G (2005) CT-guided lung biopsies in children: anesthesia management and complications. Paediatr Anaesth 15:321–324

Berde CB, Sethna NF, Fisher DE et al. (1990) Celiac plexus blockade for a 3-year-old boy with hepatoblastoma and refractory pain. Pediatrics 86:779–781

Bingöl-Kologlu M, Ciftci AO, Senocak ME et al. (2002) Xanthogranulomatous pyelonephritis in children: diagnostic and therapeutic aspects. Eur J Pediatr Surg 12:42–48

Brenner D, Elliston C, Hall E et al. (2001) Estimated risks of radiation-induced fatal cancer from pediatric CT. AJR Am J Roentgenol 176:289–296

Brown R, Hussain M, McHugh K et al. (2001) Discitis in young children. J Bone Joint Surg Br 83:106–111

Brown SD, van Sonnenberg E (2007) Issues in imaging-guided tumor ablation in children versus adults. AJR Am J Roentgenol 189:626–632

Brown SD, van Sonnenberg E, Morrison PR et al. (2005) CT-guided radiofrequency ablation of pediatric Wilms tumor in a solitary kidney. Pediatr Radiol 35:923–928

Cahill AM, Baskin KM, Kaye RD et al. (2004) CT-guided percutaneous lung biopsy in children. J Vasc Interv Radiol 15:955–960

Cahill AM, Baskin KM, Kaye RD et al. (2005) Transgluteal approach for draining pelvic fluid collections in pediatric patients. Radiology 234:893–898

Chung T, Hoffer FA, Lund DP (1996) Transrectal drainage of deep pelvic abscesses in children using a combined transrectal sonographic and fluoroscopic guidance. Pediatr Radiol 26:874–878

Cioni R, Armillotta N, Bargellini I et al. (2004) CT-guided radiofrequency ablation of osteoid osteoma: long-term results. Eur Radiol 14:1203–1208

Coley BD, Hogan MJ (2006) Image-guided interventions in neonates. Eur J Radiol 60:208–220

Connolly BL, Chait PG, Duncan DS et al. (1999) CT-guided percutaneous needle biopsy of small lung nodules in children. Pediatr Radiol 29:342–346

Cottalorda J, Bourelle S (2006) Current treatments of primary aneurysmal bone cysts. J Pediatr Orthop B 15:155–167

Early SD, Kay RM, Tolo VT (2003) Childhood diskitis. J Am Acad Orthop Surg 11:413–420

Erickson JK, Rosenthal DI, Zaleske DJ et al. (2001) Primary treatment of chondroblastoma with percutaneous radiofrequency heat ablation: report of three cases. Radiology 221:463–468

Feneberg R, Schaefer F, Zieger B et al. (1998) Percutaneous renal biopsy in children: a 27-year experience. Nephron 79:438–446

Fischer T, Biedermann T, Hermann KG (2003) Sacroiliitis in children with spondyloarthropathy: therapeutic effect of CT-guided intra-articular corticosteroid injection. Fortschr Rontgenstr 175:814–821

Ghandi S, Meech SJ, Puthawala MA et al. (2005) Combined computed tomography-guided radiofrequency ablation and brachytherapy in a child with multiple recurrences of Wilms' tumor. J Pediatr Hematol Oncol 27:377–379

Garrett KM, Hoffer FA, Behm FG et al. (2002) Interventional techniques for the diagnosis of lymphoma and leukemia. Pediatr Radiol 32:653–662

Garrett KM, Fuller CE, Santana VM et al. (2005) Percutaneous biopsy of pediatric solid tumors. Cancer 104:644–652

Garg NK, Carty H, Walsh HP et al. (2000) Percutaneous Ethibloc injection in aneurysmal bone cysts. Skeletal Radiol 29:211–216

Garron E, Viehweger E, Launay F et al. (2002) Nontuberculous-spondylodiscitis in children. J Pediatr Orthop 22:321–328

Gervais DA, Brown SD, Connolly SA et al. (2004) Percutaneous imaging-guided abdominal and pelvic abscess drainage in children. Radiographics 24:737–754

Gobien RP, Stanley JH, Schabel SI et al. (1985) The effect of drainage tube size on adequacy of percutaneous abscess drainage. Cardiovasc Intervent Radiol 8:100–102

Guimaraes AC, Chapchap P, de Camargo B et al. (2003) Computed tomography-guided needle biopsies in pediatric oncology. J Pediatr Surg 38:1066–1068

Hardaway BW, Hoffer FA, Rao BN (2000) Needle localization of small pediatric tumors for surgical biopsy. Pediatr Radiol 30:318–322

Hawkins JA, Scaife ES, Hillman ND et al. (2004) Current treatment of pediatric empyema. Semin Thorac Cardiovasc Surg 16:196–200

Heyer CM, Lemburg SP, Kagel T et al. (2005) Evaluation of chronic infectious interstitial pulmonary disease in children by low-dose CT-guided transthoracic lung biopsy. Eur Radiol 15:1289–1295

Hohl C, Mahnken AH, Klotz E et al. (2005) Radiation dose reduction to the male gonads during MDCT: the effectiveness of a lead shield. AJR Am J Roentgenol 184:128–130

Hoffer FA (2005) Interventional radiology in pediatric oncology. Eur J Radiol 53:3–13

Hoffer FA, Chung T, Diller L et al. (1996) Percutaneous biopsy for prognostic testing of neuroblastoma. Radiology 200:213–216

Hoffer FA, Bloom DA, Colin AA et al. (1999) Lung abscess versus necrotizing pneumonia: implications for interventional therapy. Pediatr Radiol 29:87–91

Hoffer FA, Gow K, Flynn PM et al. (2001) Accuracy of percutaneous lung biopsy for invasive pulmonary aspergillosis. Pediatr Radiol 31:144–152

Honnef D, Wildberger JE, Stargardt A et al. (2004) Multislice spiral CT (MSCT) in pediatric radiology: dose reduction for chest and abdomen examinations. Fortschr Rontgenstr 176:1021–1030

Honnef D, Wildberger JE, Schubert H et al. (2007) CT-guided interventions in children. Fortschr Rontgenstr 179:605–612

Hugosson CO, Nyman RS, Cappelen-Smith JM et al. (1999) Ultrasound-guided biopsy of abdominal and pelvic lesions in children. A comparison between fine-needle aspiration and 1.2 mm-needle core biopsy. Pediatr Radiol 29:31–36

Hussain HK, Kingston JE, Domizio P et al. (2001) Imaging-guided core biopsy for the diagnosis of malignant tumors in pediatric patients. AJR Am J Roentgenol 176:43–47

Jamieson DH, Chait PG, Filler R (1997) Interventional drainage of appendiceal abscesses in children. AJR Am J Roentgenol 169:1619–1622

Kaye RD, Sane SS, Towbin RB (2000) Pediatric intervention: an update – part I. J Vasc Interv Radiol 11:683–697

Kayser R, Mahlfeld K, Greulich M et al. (2005) Spondylodiscitis in childhood: results of a long-term study. Spine 30:318–323

Kilic N, Celebi S, Gurpinar A (2002) Management of thoracic empyema in children. Pediatr Surg Int 18:21–23

Klein JS, Zarka MA (2000) Transthoracic needle biopsy. Radiol Clin North Am 38:235–266

Lewin JS, Petersilge CA, Hatem SF et al. (1998) Interactive MR imaging-guided biopsy and aspiration with a modified clinical C-arm system. AJR Am J Roentgenol 170:1593–1601

Mahnken AH, Tacke JA, Wildberger JE et al. (2006) Radiofrequency ablation of osteoid osteoma: initial results with a bipolar ablation device. J Vasc Interv Radiol 17:1465–1470

Margau R, Amaral JG, Chait PG et al. (2006) Percutaneous thoracic drainage in neonates: catheter drainage versus treatment with aspiration alone. Radiology 241:223–237

McConnell PI, Feola GP, Meyers RL (2002) Methylene blue-stained autologous blood for needle localization and thoracoscopic resection of deep pulmonary nodules. J Pediatr Surg 37:1729–1731

Nagel HD, Blobel J, Brix G et al. (2004) 5 years of "concerted action dose reduction in CT" – What has been achieved and what remains done? Fortschr Rontgenstr 176:1683–1694

Nordmann GR, Lauder GR, Grier DJ (2006) Computed tomography guided lumbar sympathetic block for complex regional pain syndrome in a child: a case report and review. Eur J Pain 10:409–412

Orlicek SL, Abramson JS, Woods et al. (2001) Obturator internus muscle abscess in children. J Pediatr Orthop 21:744–748

Patrick DA, Bensard DD, Teitelbaum DH et al. (2002) Successful thoracoscopic lung biopsy in children utilizing preoperative CT-guided localization. J Pediatr Surg 37:970–973

Pereira JK, Chait PG, Miller SF (1996) Deep pelvic abscesses in children: transrectal drainage under radiologic guidance. Radiology 198:393–396

Ramnath RR, Rosenthal DI, Cates J et al. (2002) Intracortical chondroma simulating osteoid osteoma treated by radiofrequency. Skeletal Radiol 31:597–602

Riccabona M, Sorantin E, Hausegger K (2002) Imaging guided interventional procedures in paediatric uroradiology – a case based overview. Eur J Radiol 43:167–179

Schulz T, Bennek J, Schneider JP et al. (2003) MR-guided pediatric interventions – a retrospective case study. Fortschr Rontgenstr 175:1673–1681

Schulz T, Tröbs RB, Schneider JP et al. (2005) Pediatric MR-guided interventions. Eur J Radiol 53:57–66

Siegel MJ, Schmidt B, Bradly D et al. (2004) Radiation dose and image quality in pediatric CT: effect of technical factors and phantom size and shape. Radiology 233:515–422

Shin HJ, Amaral JG, Armstrong D et al. (2007) Image-guided percutaneous biopsy of musculoskeletal lesions in children. Pediatr Radiol 37:362–369

Sklair-Levy M, Lebensart PD, Applbaum YH et al. (2001) Percutaneous image-guided needle biopsy in children – summary of our experience with 57 children. Pediatr Radiol 31:732–736

Skoldenberg EG, Jakobson AA, Elvin A et al. (2002) Diagnosing childhood tumors: A review of 147 cutting needle biopsies in 110 children. J Pediatr Surg 37:50–56

Smith MB, Lobe TE, Schropp KP et al. (1996) A prospective evaluation of an endoscopic ultrasonic probe to detect intraparenchymal malignancy at pediatric thoracoscopy. J Laparoendosc Surg 6:233–237

Staats PS, Kost-Byerly S (1995) Celiac plexus blockade in a 7-year-old child with neuroblastoma. J Pain Symptom Manage 10:321–324

Tanelian D, Cousins MJ (1989) Celiac plexus block following high-dose opiates for chronic noncancer pain in a four-year-old child. J Pain Symptom Manage 4:82–85

Ventura N, Gonzalez E, Terricabras L et al. (1996) Intervertebral discitis in children: a review of 12 cases. Int Orthop 20:32–34

Vock P (2005) CT dose reduction in children. Eur Radiol 15:2330–2340

Waldhausen JH, Shaw DW, Hall DG et al. (1997) Needle localization for thoracoscopic resection of small pulmonary nodules in children. J Pediatr Surg 32:1624–1625

Wilkinson AG, Paton JY, Gibson N et al. (1999) CT-guided 14-G cutting needle lung biopsy in children: safe and effective. Pediatr Radiol 29:514–516

Wippermann CF, Schofer O, Beetz R et al. (1991) Renal abscess in childhood: diagnostic and therapeutic progress. Pediatr Infect Dis J 10:446–450

Part II
Diagnostic Interventions

Biopsy

9

Christoph Gregor Trumm and Ralf-Thorsten Hoffmann

Contents

9.1 Introduction

Image-guided percutaneous biopsy using ultrasound and computed tomography (CT) is widely established as safe method for differentiation of benign and malignant masses, while magnetic resonance (MR) imaging was only introduced as a guidance method in the mid-1990s. Most of the procedures are performed in patients with a known primary tumor to rule out metastatic malignancy, to establish the final diagnosis, or to differentiate between tumor necrosis and potential vital tumor tissue in residual lesions after therapy.5

9.2 Patient Preparation and Aftercare

Most image-guided biopsies can be performed on an outpatient basis. Informed patient consent including possible conscious sedation after detailed explanation of potential complications should be obtained at least 24 h before the intervention. A coagulation disorder should be ruled out by taking platelet levels (more than 50 000/mm^3), partial thromboplastin time (less than 50 s), prothrombin time (more than 50%), and International Normalized Ratio (1.5 or less) in all patients, especially if the lesion is located in the depth of the chest and abdomen. In superficial lesions (e.g., in the neck), direct pressure is usually sufficient for hemostasis and dedicated coagulation studies are not required. In case the patient has taken nonsteroidal anti-inflammatory drugs inhibiting platelet aggregation (e.g., acetylic salicylic acid), a core biopsy should be postponed for 7 days. In the absence of any abnormalities regarding platelet levels, partial thromboplastin time, and pro-

Table 9.1 Contraindications for computed tomography (CT) guided and magnetic resonance (MR) guided biopsy

Uncorrectable coagulation disorder
Platelets $< 50000/mm^3$ [a]
INR > 1.5 [b]
Prothrombin time (quick) $< 50\%$ [b]
Partial thromboplastin time > 50 s [c]
Intake of platelet inhibitors < 24 h before the intervention [d]
Massive ascites
Adipositas in combination with small cirrhotic liver (transjugular or surgical biopsy recommended)
Incompliant patients
Absence of a safe pathway from the skin to the target site

INR International Normalized Ratio
[a] A preprocedural platelet transfusion may be necessary.
[b] Usually due to coumarins or liver disease; coumarin withdrawal takes a few days to reverse INR. INR can also be reversed by vitamin K or fresh frozen plasma.
[c] Usually prolonged secondary to heparin or heparin-like drugs. These agents generally have short half-lives and their action can be quickly reversed.
[d] Clinical assessment should be made as to whether to proceed or reschedule the biopsy.

thrombin time, a fine-needle biopsy (20G or smaller) may be performed because the risk of hemorrhage due to nonsteroidal anti-inflammatory drugs alone is low (Table 9.1) (Cardella et al. 2003).

The majority of CT-guided biopsies can be performed under local anesthesia. Children, incompliant adult patients, or biopsies of deep abdominal lesions (e.g., pancreatic masses) represent potential exceptions. In those selected cases, sufficient analgosedation can be achieved by intravenous administration of benzodiazepines, e.g., midazolam (1 mg per dose; given in two to four doses) for anxiolysis and opioids, and fentanyl (0.02 mg per dose; given in one to five doses) for analgesia (see Chap. 5). If analgosedation is used, the patient should be monitored during the whole procedure using pulse oximetry. The nurse or radiology technician is responsible for keeping the patient compliant, while the radiologist can concentrate on the procedure. Before the intervention, the patient should be placed in a stable and comfortable position. Depending on the lesion location, supine, prone or lateral decubitus position is most commonly used.

For correlation, pre-, peri-, and postinterventional CT or MR images should be obtained in the same position during the respiratory cycle, preferably under expiration. In the case of an anterior approach, the CT or MR table is set as low as possible to leave enough room for needle insertion. Preparation of the skin area overlying the entry point of the biopsy needle includes shaving (if necessary), sterile draping, and skin disinfection.

Following CT-guided biopsy, patients are kept in the ward with vital signs observed every 15 min for 1 h. In high-risk patients, observation can be continued beyond this time, for example, with checking of vital signs every 30 min for 3 h.

After lung biopsy, the patient should lie with the puncture site down for 2 h. The two pleural layers are compressed by the weight of the lung itself and further air leakage through the pleural defect is minimized. Chest radiographs (posteroanterior) are obtained 2 and 4 h after the intervention to rule out delayed pneumothorax. If the chest radiograph of the patient in the erect position after 2 h shows a small pneumothorax, a further chest X-ray should be obtained after 4 h. In the case of pneumothorax and patient symptoms, air aspiration or a chest tube should be inserted for treatment (see Sect. 11.2).

At discharge, patients should be advised to take care of the puncture site. They are instructed to call their physician in the event of bleeding or marked swelling at the puncture site. Patients are advised not to bathe for 24 h if no dedicated waterproof bandage is used for sealing the puncture site.

9.3 CT and CT-Fluoroscopic Guidance

CT as a guiding method is especially suitable for lesions located deep under the skin surface which are not depictable or not easily depictable via ultrasound

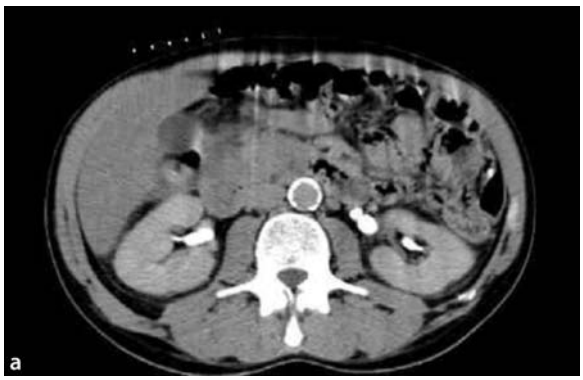

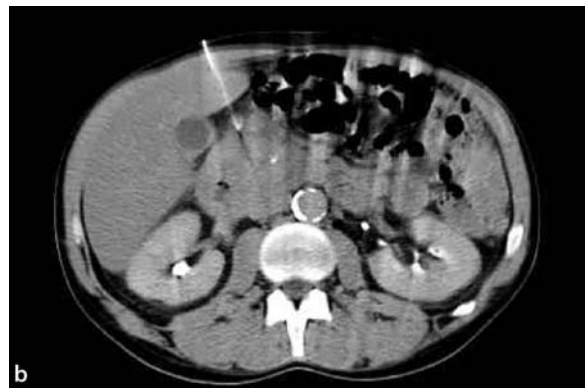

Fig. 9.1a,b Patient (supine position) with suspect mass of the pancreas head. A radiopaque grid made of 4-F catheters is taped on the patient's skin covering the intended region of needle entry before the planning computed tomography (CT) scan (**a**). An anterior transhepatic approach passing the left liver lobe was chosen for coaxial punch biopsy with an 18G Tru-Cut needle under sequential CT guidance (**b**). Histopathologic analysis revealed a pancreatic adenocarcinoma

(e.g., deep retroperitoneal, pelvic, and thoracic lesions). With some exceptions, such as liver lesions isodense to normal parenchyma in the nonenhanced CT scan, CT usually provides excellent visualization of the target lesion for biopsy, and differentiation from adjacent organs. It is generally preferable not to schedule a biopsy procedure at the same time as the first diagnostic scan. If available, recent outside films not older than 2 weeks or a separate preceding diagnostic study should be used for selection of target lesions for biopsy and planning of the access pathway. Two different techniques of CT guidance can be utilized:

9.3.1 Sequential CT Guidance

For planning of the access route, a CT scan of the region of interest is performed first. The preliminary scan can be performed without contrast if a recent diagnostic study is available and the lesion is easily visible. In the chest, a nonenhanced CT scan (slice thickness 3 mm or less) is also sufficient for detection of intrapulmonary lesions suitable for aspiration or punch biopsy. For suspect masses in the mediastinum and abdomen (intra- and retroperitoneal), a contrast-enhanced CT scan is necessary for clear differentiation of parenchymal organs, intestines, and blood vessels. Focal lesions within parenchymal organs are usually visualized during the venous phase (scan delay 50–70 s). An additional arterial phase (scan delay approximately 30 s) scan should be obtained if arteries are present along the access path (e.g., parasternal access, internal mammary artery) and in hypervascularized lesions (e.g., hepatocellular carcinoma, metastases of renal cell carcinoma).

For defining the skin entry point of the biopsy needle, a radiopaque grid is placed on the skin of the patient (Fig. 9.1a). The patient is positioned either in prone, supine, or lateral decubitus position depending on the shortest distance from the skin surface to the lesion. Then the CT scan is performed covering the region of interest. Commercially available grid-systems, or a homemade grid made from several 4–5-F catheters that are cut to a length of 15–30 cm, and taped together at intervals of 1 cm, can be used. After the planning CT scan (with the grid system taped on the skin of the patient) has been performed, the slice position showing both the lesion and the potential in-plane access route or the intended needle entry point only (double-oblique access), is chosen. The distance from the skin level of the needle entry point to the lesion is measured. The CT table is moved to the position of choice for biopsy and the needle entry point can be marked with a felt pen using the grid as well as the centering laser beam.

After skin disinfection, local anesthesia using 10–20 ml of 1–2% lidocaine hydrochloride is applied in the subcutaneous fat and down to the capsule of the parenchymal organs (e.g., the liver) or down to the

periosteum of bones, using a small 22G needle that additionally marks the entry point and intended angle of the biopsy needle. After a small skin incision with a scalpel and CT rescanning with the local anesthesia needle in the skin entry point to confirm the correct position, the biopsy needle is inserted parallel to the local anesthesia needle. Thereafter, repeated CT scans covering a short range above and below the needle entry point (e.g., 3–5 cm along the *z*-axis) are performed, and the angulation of the needle is adapted to interfering anatomical structures if necessary (Fig. 9.1b). The use of multislice spiral CT with its inherent ability to simultaneously acquire several sections is beneficial for this purpose, as it omits the need for multiple scans above and below the needle entry point. The direction of the needle in relation to the lesion can be easily detected using the streak at the needle tip. Finally, the needle is inserted into the edge of the lesion for tissue sampling.

9.3.2 CT-Fluoroscopic Guidance

Since the introduction of CT fluoroscopy (CTF) with faster image reconstruction on multislice CT scanners, real-time visualization nearly comparable to that of ultrasound is available. Cross-sectional CT images are reconstructed at reduced spatial resolution and updated continually at a rate of up to ten frames per second by using a high-speed array processor (Carlson et al. 2001). In contrast to the grid-based technique using repeated nonenhanced CT scans covering the volume of interest, the needle is visualized on an in-room monitor. The operator can dynamically adjust the needle position under single-shot or continuous CTF until the lesion is reached. The main advantages are a substantial reduction of in-room time for both the patient and the operator, and real-time visualization of critical anatomical structures such vessels along the trajectory during needle insertion. This technique is particularly helpful in the case of incompliant patients who are unable to cooperate, e.g., to hold their breath, or in regions with persistent motion as may be found close to the heart and diaphragm. In contrast to conventional CT guidance, the main disadvantage is radiation exposure of the operator (Silverman et al. 1999). The use of a grab handle for holding the needle helps to avoid the direct exposure of the operator's hand to the radiation beam during CTF. As important advantages of this technique, patient absorbed radiation dose and in-room time can be significantly reduced by 94 and 32%, respectively (Carlson et al. 2001).

9.4 CT-Guided Aspiration Biopsy

Percutaneous fine-needle aspiration biopsy (FNAB) is a well-established method to obtain an aspirate with a thin needle (20G or greater) which usually provides enough material to confirm or rule out malignancy by cytologic analysis. In most cases, a histologic diagnosis is not possible owing to an insufficient amount of material.

9.4.1 Indications

FNAB is suitable for tissue sampling of pulmonary lesions as well as neck lesions (e.g., lymph nodes) and abdominal lesions given a known primary tumor in combination with suspected metastases of the liver, lymph nodes, etc. In abdominal lesions, FNAB is preferable where direct access is precluded by surrounding organs. It is generally considered insufficient if the primary tumor is unknown.

9.4.2 Material

Fine-needle biopsies are performed with 20G–25G needles (small gauge), including various commercially available needle types and needle tip designs. The needle tip is either sharp-beveled (e.g., Chiba or spinal needle) or cutting (Turner needle, 45° bevel tip with cutting edge; Franseen needle, three-pronged needle tip; Westcott needle, slotted side-opening proximal to the needle tip; E-Z-EM needle, trough cut in the needle tip) (Lee 2004) (Fig. 9.2). Coaxial biopsy sets consist of an outer guide needle in combination with a smaller aspiration needle. Typical needle combinations for coaxial FNAB are 23G/20G or 22G/19G sets (Table 9.2).

Table 9.2 Commercially available needles for CT- and MR-guided aspiration biopsy (exemplary selection of different manufacturers and needles)

Needle type (manufacturer)	Gauge	Length (cm)[a]
Chiba (Boston Scientific, Natick, MA, USA)	22	6; 8
Franseen (Boston Scientific, Natick, MA, USA)	18; 20; 22	6; 8
Coaxial lung biopsy set Greene-Type (Boston Scientific, Natick, MA, USA)	22	6
Chiba (Cook Medical, Bloomington, IN, USA)	18–23; 25	5; 10; 15; 20
Spinal needles (Cook Medical, Bloomington, IN, USA)	18; 20; 22	10; 15
Chiba-Needle Ultra (Somatex, Teltow, Germany)	19.5; 22	9; 12; 15; 22; 28
Chiba (E-Z-EM, Lake Success, NY, USA)	18; 20; 22	10; 15; 20
Percucut cut-biopsy needle with keyhole cutting edge (E-Z-EM, Lake Success, NY, USA)	18; 19.5; 21	5; 10; 15
MR-compatible fine needles		
Mreye Chiba (Cook Medical, Bloomington, IN, USA)	20; 22	10; 20
Lufkin (E-Z-EM, Lake Success, NY, USA)	22	5

[a] Not all gauge–length combinations may be available.

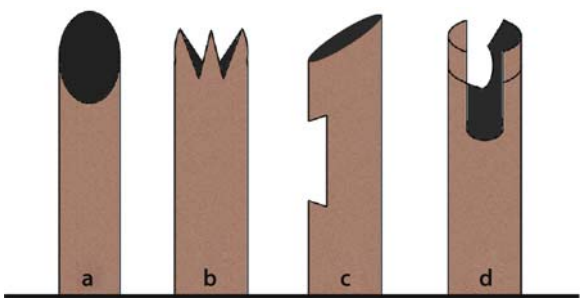

Fig. 9.2 The most common fine needle types: Turner (*a*), Franseen (*b*), Westcott (*c*), and E-Z-EM (*d*). The Turner needle is characterized by a 45° bevel with a cutting edge. The Franseen needle has a three-pronged tip. The Westcott needle contains a side-cutting trough close to its tip. The E-Z-EM needle has a trough cut within the needle tip. (Schematic according to Lee 2004)

9.4.3 Technique

9.4.3.1 General Considerations

FNAB can be performed by solely using the fine needle, by applying a coaxial approach or by using a tandem technique. The first technique is characterized by the straightforward puncture of the target lesion. This technique has some disadvantages, including limited controllability. The coaxial technique is characterized by a combination of two needles. A thicker, shorter needle is inserted down to the anterior edge of the lesion. Then a thinner, longer needle is introduced through the first needle. Multiple samples can be taken using the thinner needle without several punctures. If necessary, the larger needle can be pulled back and its angle changed to reach different areas of the lesion. With the tandem technique, first a single reference needle is introduced into the lesion. Then further needles are introduced "in tandem", i.e., parallel to the first needle without having to guide them separately.

After the appropriate needle length has been measured in the planning scan, preparation of the chosen entry site, and local anesthesia, the fine needle is inserted into the lesion under image control, i.e., repeated nonenhanced short CT scans or CTF sequences triggered by the operator. As soon as the needle has been introduced into the lesion, the trocar is removed and a 10- or 20-ml Luer-Lok syringe is connected to the proximal end of the needle, and suction is applied. The aspirated volume ranges between 3 and 5 ml for most biopsies, and should be reduced (1–2 ml) in hypervascularized lesions to avoid aspiration of larger amounts of blood. During application of suction, the needle is moved back and forth within the lesion for 10–15 s, or until the hub of the syringe becomes filled with blood. Before the needle is removed from the lesion, the suction is stopped to avoid aspiration of further tissue potentially confusing cytologic evaluation of the sample.

In hypervascularized lesions such as in the thyroid gland, nonaspiration fine-needle biopsy can alternatively be performed. The needle is introduced into the lesion without a syringe, and is moved back and forth several times.

If a cytopathologist is in the room during the biopsy procedure, he/she can give an initial statement if the tissue sample is sufficient for evaluation, or if further samples have to be taken. Otherwise the aspirated material is crossed out on a glass slide and immediately afterwards fixed with alcohol. An additional blood clot should be obtained and fixed in formalin, as this will significantly increase sensitivity for malignancy (Wildberger et al. 2003).

9.4.3.2 Special Considerations

Lung

The advantage of CT-guided lung biopsy is that the lung parenchyma and not inflated areas at the puncture site is visualized and can be used as an access path to the lesion, substantially reducing the risk of pneumothorax. Local anesthesia is applied subcutaneously. Then a coaxial needle can be inserted through the parietal pleura under suspended respiration. The operator can adjust the needle direction by withdrawing the coaxial needle to the periphery of the lung (without removing the needle outside the pleura). If the coaxial technique is used, the outer coaxial needle is inserted 2–3 mm into the edge of the lesion, providing stability during coaxial biopsies. Then the inner biopsy needle is introduced and at least two samples are obtained (Fig. 9.3).

Mediastinum

Biopsies in the mediastinum have to be performed with special respect to vascular structures (Fig. 9.4). For planning of the biopsy procedure, a contrast-enhanced CT scan is performed to rule out vascular abnormalities such as aneurysms, and to visualize the mediastinal vessels. For sampling lesions in the anterior mediastinum, an anterior parasternal approach is usually chosen. The internal mammary artery and vein that are located approximately 1 cm from the sternum have to be avoided (Fig. 9.4a). Additionally, the access path through the mediastinal fat can be widened by injection of sterile saline through a 22G needle. After distension of the anterior mediastinum, the FNAB needle can be safely introduced without passing the paramediastinal lung parenchyma (Fig. 9.4b,c). When the lesion is located in the posterior mediastinum, the paravertebral space can also be distended using sterile saline.

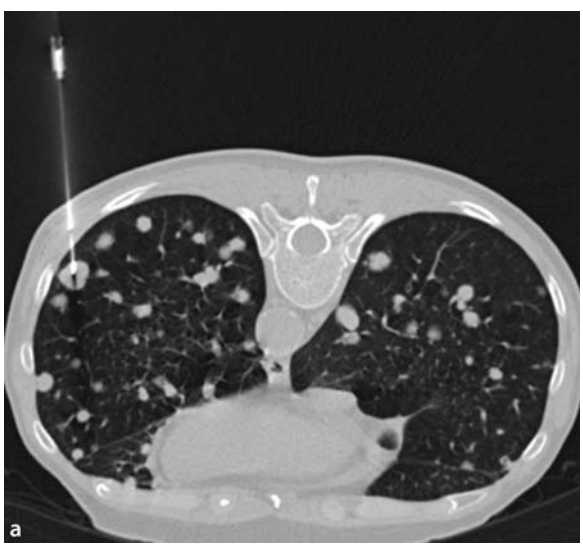

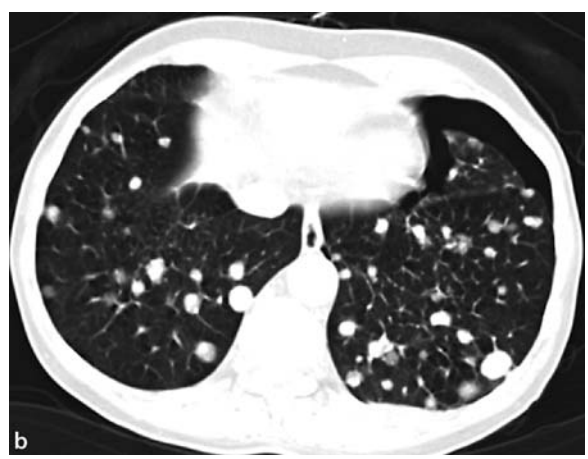

Fig. 9.3a,b Patient (prone position) with multiple lung metastases. A subpleural nodule in the left lower lobe was chosen for aspiration biopsy under CT-fluoroscopic guidance with a 19G (10-cm) needle (**a**). Postinterventional CT (supine position) showed a small pneumothorax that did not require therapy after further follow-up with X-ray (**b**). Cytologic analysis revealed pulmonary metastases of an adenocarcinoma (sigmoid colon)

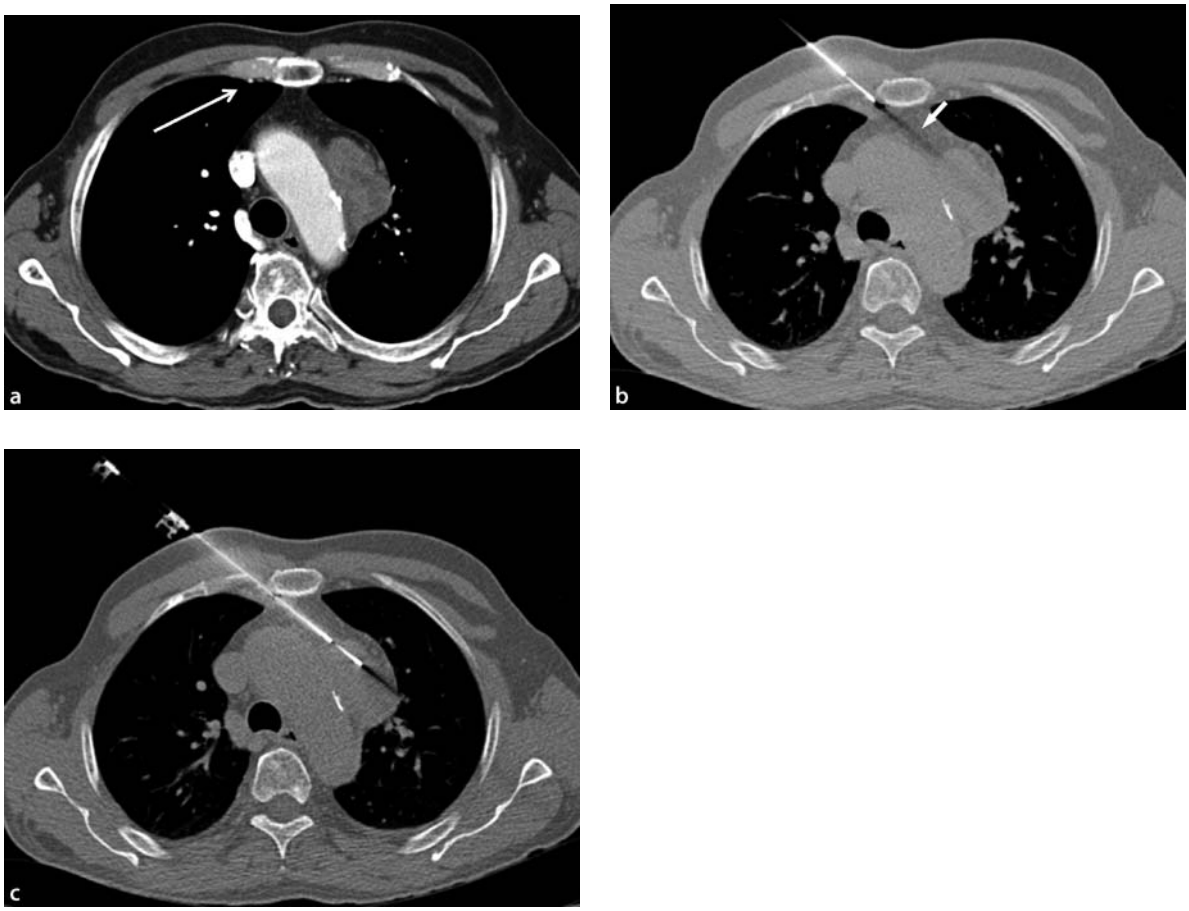

Fig. 9.4a–c Patient (supine position) with a paraaortal mass in the upper mediastinum. The preinterventional CT (arterial phase) showed the right internal mammary artery and vein (*arrow*) next to the sternum (**a**). First sterile saline was injected with a 22G needle to widen the parasternal space. Then an 18G (13-cm) Tru-Cut biopsy needle was introduced under CT-fluoroscopic guidance. Note the typical black streak artifact along the needle pathway (**b**,**c**). Histopathologic analysis revealed a mesenchymal tumor

Liver

Depending on the experience of the operator and the availability of an interventional CT unit, the majority of liver biopsies can also be performed under ultrasound guidance. If lesions in the dome of the liver cannot be visualized with ultrasound, a CT/CTF-guided (double) oblique approach may be preferable, while crossing the costophrenic sulcus should be avoided. Gantry angulation may help to access high liver lesions. Before the biopsy needle is introduced into the liver parenchyma, the capsule has to be infiltrated with local anesthetic. During penetration of the liver capsule, the patient should be asked not to breathe. Passing normal liver tissue before entering the lesion reduces the risk of relevant subcapsular or intraparenchymal bleeding due to self-tamponade occurring after the puncture. The biopsy may also be performed in a right decubitus position or under maximum expiration when the costophrenic sulcus is not inflated. The sample should normally be taken from the edge of the liver mass where the vital tumor tissue (in contrast to the central necrotic area) is located. In cases of liver lesions with large necrotic areas, a coaxial technique combining an outer cannula with the biopsy needle may be useful as the liver capsule is crossed only once.

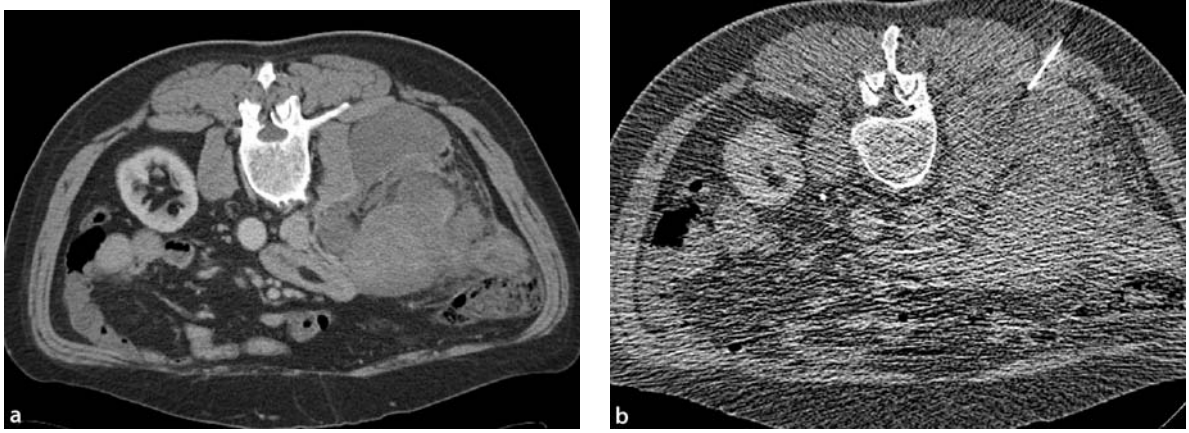

Fig. 9.5a,b Patient (prone position) with suspect retroperitoneal mass encasing the right kidney (**a**). A right posterior approach was chosen for aspiration biopsy with a 19G (10-cm) needle under CT-fluoroscopic guidance (**b**). Cytologic analysis revealed a lymphoma

Pancreas

Typically the pancreas is surrounded by various organs such as the stomach, liver, transverse colon, and kidney or major vessels. Especially needle biopsy of small suspect masses in the pancreatic head is therefore usually regarded as technically sophisticated, and CT guidance is preferred instead of ultrasound. For differentiation of the tumor from surrounding normal parenchyma or inflammation, a contrast-enhanced CT scan obtained in an arterial phase should generally be performed prior to the intervention. The most common access route is from an anterior approach and often traverses gastrointestinal structures and the mesenteric vessels, increasing the general risk of the procedure. On the other hand, with CTF transgression of vital structures can be avoided in most cases. In difficult-to-access lesions, the stomach or the small intestine may be punctured with a 20G–22G needle. Given an immunocompetent patient, FNAB traversing the gastrointestinal tract or the liver has been shown to be technically acceptable in many studies (Brandt et al. 1993; Elvin et al. 1990; Luning et al. 1985; Mueller 1993). Transhepatic, transsplenic and paracaval/transcaval approaches have also been described (Brandt et al. 1993).

If the pancreatic tumor is too scirrhous to obtain sufficient specimen in spite of several trials, usually a switch to a large-gauge core biopsy system is necessary. The colon should generally not be penetrated even with a small-gauge needle to avoid superinfection, especially if cystic pancreatic lesions containing fluid are sampled (Mueller 1993). In the case of unintended penetration, metronidazole should be administered prophylactically.

Kidney

Biopsies of the kidney are rarely performed because they are often interpreted as hemorrhagic or inconclusive, and most solid renal masses are surgically removed. Exceptional indications for biopsy are suggested lymphoma and metastasis to the kidney from another primary tumor, since these conditions are usually not treated surgically. The usual access route under CT guidance is posterior or lateral, while the renal hilum should be avoided (Fig. 9.5).

Adrenal Glands

Owing to the anatomic localization in the upper retroperitoneum, the access path for biopsy is relatively sophisticated and several approaches are possible:

- The right lateral transhepatic approach (right adrenal gland, through right liver lobe, supine position)

- The left anterior transhepatic approach (left adrenal gland, through left liver lobe, supine position)
- The angled prone approach (both adrenal glands, subcostal approach at 45°, prone position; Fig. 9.6)
- The lateral decubitus approach (the side of the patient with the adrenal lesion is placed next to the table, preventing full expansion of the ipsilateral pulmonary recessus while the overlying lung is fully expanded)

Retroperitoneum

Biopsies of retroperitoneal lesions are usually performed under CT guidance. With the most common posterior approach, the needle passes through or parallel to the psoas muscle (Figs. 9.7, 9.8). Small-gauge needles are only necessary when using an anterior approach.

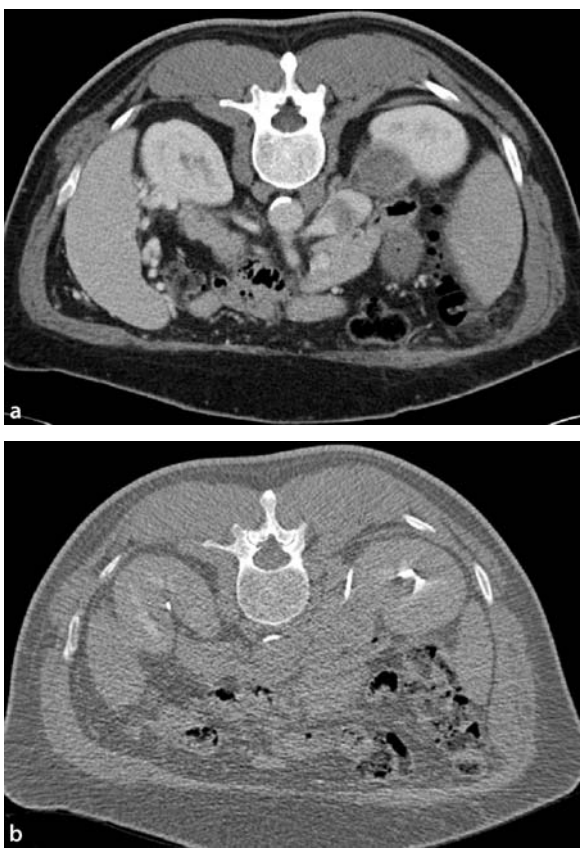

Fig. 9.6a,b Patient (prone position) with a known hepatocellular carcinoma. The preinterventional CT showed a suspect mass of the right adrenal gland (**a**). A posterior right paravertebral approach was chosen for aspiration biopsy with a 19G (13-cm) needle under CT-fluoroscopic guidance (**b**). Cytologic analysis revealed an adrenal metastasis of hepatocellular carcinoma

Pelvic Lesions

While transrectal and transvaginal biopsies are routinely guided using ultrasound, the access routes for CT-guided biopsy in the pelvis include:

- The transgluteal approach through the greater sciatic foramen
- The presacral approach through the gluteal cleft
- The anterior approach (Fig. 9.9)

For the transgluteal approach, the patient is placed in the prone position. The needle is introduced from the buttock through the greater sciatic foramen into the deep pelvis as close to the coccygeal bone as possible in order to avoid puncture of the sciatic nerve.

9.4.4 Results

9.4.4.1 Lung

In pulmonary lesions, FNAB has been reported to have diagnostic accuracy and sensitivity rates of more than 93% (Swischuk et al. 1998) and 95% (Klein et al. 1996; Laurent et al. 2000), respectively. While several authors have reported accuracy rates of less than 75% for lesions 1.0 cm or smaller (Li et al. 1996; Tsukada et al. 2000; van Sonnenberg and Casola 1988), respiratory gating (Tomiyama et al. 2000) and CTF (Irie et al. 2001) have contributed to improve success rates. The study of Irie et al. showed a reduction of procedure time using CTF (79 biopsies with 29 lesions smaller than 1.5 cm) while accuracy was not improved for the subset of patients with lesions 1 cm or smaller (Irie et al. 2001). Subpleural pulmonary nodules are often more challenging than deep lesions. Especially the ribs or scapula may potentially hinder direct access to a nodule. In the comparison of an oblique versus a right-angled access path (61 subpleural lesions) by Tanaka et al. (1996), success rates were significantly better for the oblique path (81.2%) than for the right-angled access (43.3%). With direct access, the parenchymal distance to the subpleural nodule may be less than 1 cm, not allowing one to correct the needle

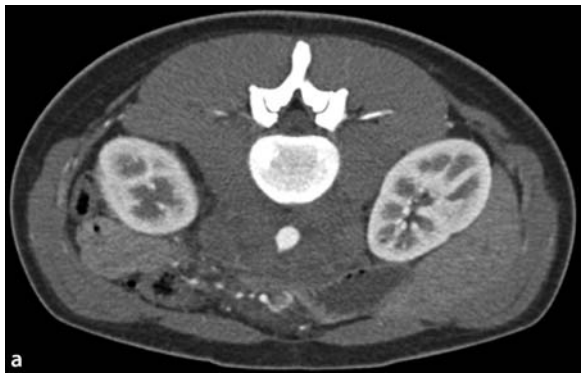

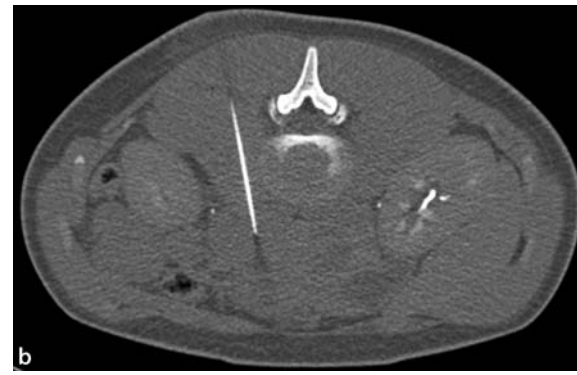

Fig. 9.7a,b Patient (prone position) with extensive paraaortal lymph node bulking (**a**). A left posterior paravertebral approach was chosen for aspiration biopsy with a 19G (15-cm) needle under CT-fluoroscopic guidance (**b**). Cytologic analysis revealed lymph node metastases of an adenocarcinoma

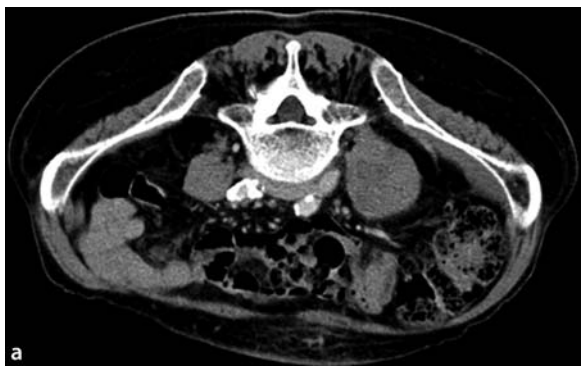

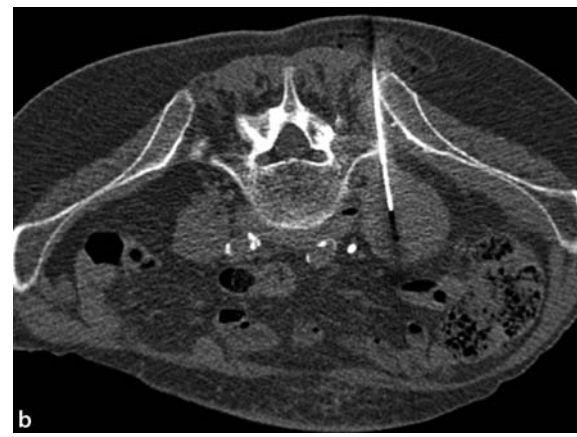

Fig. 9.8a,b Patient (prone position) with suspect mass of the right psoas muscle (**a**). A posterior paravertebral (fifth lumbar vertebra) access was chosen for Tru-Cut biopsy with an 18G (13-cm) needle under CT-fluoroscopic guidance (**b**). Histopathologic analysis revealed metastasis of ovarial carcinoma

direction without pulling it through the pleural surface again. Once a pneumothorax has occurred, usually a retraction of the lung is observed, making further sampling difficult if not impossible. A longer, tangential transparenchymal access route implies improved needle stability (Wallace et al. 2002).

9.4.4.2 Mediastinum

In 89 patients undergoing CT-guided mediastinal FNAB for lung cancer staging (50 with and 39 without core biopsy of lymph nodes with short-axis diameter greater than 1.5 cm) before mediastinoscopy, Zwischenberger et al. (2002) reported diagnostic success (cancer cell type, sarcoidosis, or caseating granulomas) in 78% of the cases, while only in nine patients lymph nodes (paraesophageal, pulmonary ligament, parasternal, and paraaortic) could not be accessed. In the study by Assaad et al. (2007) (157 mediastinal FNAB) adequate diagnostic cytologic material could be obtained in 82% of the cases, with concordance of subsequent histologic and FNAB diagnosis in 78% (53 of 68) of the corresponding cases.

9.4.4.3 Liver

FNAB in the abdomen with both ultrasound and CT guidance has been described as a safe and technically successful procedure by several authors (Ferrucci et al.

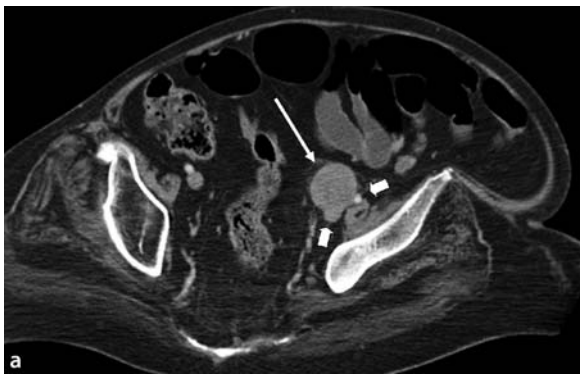

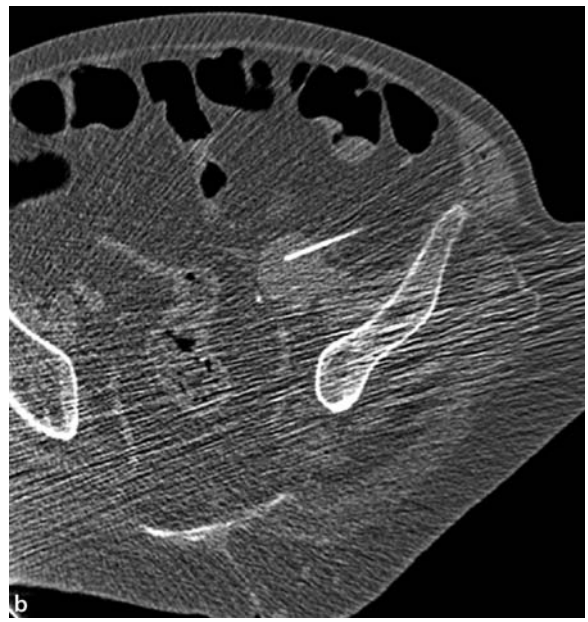

Fig. 9.9a,b Patient (supine position) with a history of diffuse large B-cell lymphoma. Preinterventional CT showed a moderately enhanced nodule (*long arrow*) next to the iliac vessels (*short arrows*) (**a**). The 18G (13-cm) Tru-Cut biopsy needle was introduced under CT-fluoroscopic guidance next to the left iliac crest through the peritoneal fat (**b**). Histopathologic analysis revealed recurrence of diffuse large B-cell lymphoma

1980; Memel et al. 1996; Smith 1991; Welch et al. 1989). CT-guided FNAB of liver lesions has been reported to have sensitivity rates of 92% and specificity rates of 96% (Luning et al. 1984).

9.4.4.4 Kidney

Most renal masses can be characterized with high accuracy by noninvasive imaging alone, and a solid non-fat-containing or complex renal mass should be considered a renal cell carcinoma until proven otherwise. Metastases to the kidney are usually small and multifocal or perinephric. Lymphomatous involvement of the kidneys also usually occurs in the setting of disseminated disease and is characterized by typical CT patterns such as multiple small masses, spread from retroperitoneal disease, diffuse infiltration, and perinephric encasement.

In a study by Brierly et al. (2000) with 49 patients undergoing FNAB for various renal masses, the sensitivity of CT-guided biopsy for the diagnosis of malignancy ranged from 89% in large solid masses to only 50% in complex cysts. Inadequate specimens were obtained in 16% of the patients. In another study, by Lechevallier et al. (2000), CT-guided renal biopsy of 63 patients had an overall accuracy of 89%. Biopsy material was not sufficient for analysis in 15 patients (21%). Unsuccessful biopsy was related to lesion size: biopsy was unsuccessful in 11 of 30 tumors (37%) of 3 cm or less, and in four of 43 tumors (9%) greater than 3 cm.

9.4.4.5 Adrenal Glands

Incidentally discovered adrenal masses (incidentalomas) are relatively frequent. Adrenal incidentalomas exceeding 1 cm in size are found in 1–5% of patients undergoing chest or abdominal CT for unrelated reasons. The risk of malignancy in patients with nonfunctioning adrenal masses is between 3.5 and 34% (Lumachi et al. 2001). Since the development of dedicated MR imaging techniques for differentiation of adrenal masses, adrenal biopsy is performed only in

exceptional cases, and benign adrenocortical nodules are the most common lesion to be found with FNAB (more than 40%).

Lumachi et al. (2003) performed a study to compare the usefulness of FNAB cytology, CT, and MR imaging in patients with nonfunctioning adrenal masses. Including 34 patients with adrenal masses incidentally discovered in a CT scan, the authors found a sensitivity and specificity of 100% for the combination of both MR imaging and FNAB. The authors recommended performing image-guided FNAB in all patients with nonfunctioning adrenal masses of 2 cm or more in size. The morbidity rate found in the study was 2.9%.

9.4.4.6 Retroperitoneum and Pelvis

Nahar Saikia et al. (2002) performed 242 aspiration biopsies of deep-seated thoracic, abdominal, and retroperitoneal lymph nodes under ultrasound ($n = 216$) and CT ($n = 26$) guidance, respectively. The diagnostic accuracy rate was 86%. In 23 patients with 26 suspect abdominal, pelvic ($n = 6$) or retroperitoneal ($n = 12$) lymph nodes, Memel et al. (1996) reported technical success, i.e., sampling of adequate tissue for cytologic or histologic evaluation, in 21 of 23 ultrasound-guided biopsies (91%). Three of 26 lymph nodes (11.5%) could not be sampled owing to poor visualization under ultrasound.

9.4.5 Complications

In the lung, apart from pneumothorax (16–44.6%) and consecutive thoracostomy tube insertion, complication rates for image-guided FNAB are low (Laurent et al. 2000; Swischuk et al. 1998; van Sonnenberg et al. 1988). Factors increasing the risk of pneumothorax are small lesion size (Cox et al. 1999; Fish et al. 1988; Kazerooni et al. 1996), increasing depth of the lesion, several passes through the pleura, and underlying pulmonary disease (Poe et al. 1984; Quon et al. 1988). Pulmonary hemorrhage and hemoptysis are observed in up to 1.4 and 1.7% of the procedures, respectively (Arslan et al. 2002). In the case of hemoptysis, the patient should lie in a lateral decubitus position on the punctured side, preventing aspiration of blood into the contralateral lung. Air embolism is also a rare complication of thoracic FNAB resulting from a direct communication between a pulmonary vein and atmospheric air. Reasons for the entry of air are the operator leaving the proximal end of the biopsy needle open after insertion into the chest, and the patient breathing deeply during the intervention. The patient should receive 100% oxygen, and should lie in the left lateral decubitus position with the head down in order to prevent cerebral embolism.

Complication rates of FNAB in the abdomen are very low. In the metaanalysis including literature data and results of questionnaires distributed in North American and European hospitals in the 1980s, Smith (1991) found mortality rates between 0.006% (63,108 biopsies) and 0.031% (16,381 biopsies) in the USA, and between 0.008 and 0.018% in European hospitals. Leading causes of death reported in Europe ($n = 33$) were hemorrhage after liver biopsy (17 of 21), and pancreatitis after pancreas biopsy (five of six). The frequency of needle tract seeding was in a range between 0.003 and 0.009% in the four questionnaires.

In hepatocellular carcinoma, given a high positive predictive value of suspicious imaging findings alone (Torzilli et al. 1999), percutaneous biopsy has a limited role. Common risks include intraperitoneal bleeding and needle tract tumor implantation. In the study of Bret et al. (1988), 2.5% of 159 patients ($n = 4$) with hepatocellular carcinoma who underwent FNAB developed serious bleeding after the procedure, and one died. Factors that may contribute to hemorrhage include tumor hypervascularization, failure of cirrhotic liver tissue to seal the needle track, free bleeding into perihepatic ascites, and coagulopathy secondary to liver dysfunction (Grant and Neuberger 1999). Needle tract implantation has a reported incidence of up to 5% (Takamori et al. 2000).

Acute pancreatitis has been described as a rare but potentially fatal complication of needle biopsy of the pancreas (Mueller et al. 1988; Smith 1991). In their series of 184 pancreatic biopsies in 178 patients, Mueller et al. (1988) reported severe postprocedure pancreatitis in five patients (3%).

As far as vascular structures are concerned, many studies have shown that the transgression of vessels, especially low-pressure veins, does not significantly elevate the complication rate (Ferrucci et al. 1980; Smith 1991; Welch et al. 1989).

Key Points

- Histopathologic analysis is not possible.
- Suitable technique in patients with a known primary tumor.
- Needle diameter 20G–25G with standard needle lengths of 5–20 cm.
- The needle should be introduced with a coaxial or tandem technique.
- Cytologic sample obtained through back-and-forth movement of needle within lesion under manual aspiration.
- Sampling of hypervascularized lesions without aspiration.
- Transgression of bowels is possible if direct access to the lesion is precluded.

9.5 CT-Guided Punch Biopsy

In comparison with aspiration biopsy, the punch biopsy (synonym, core biopsy) technique is performed either with spring-activated cutting needles (Tru-Cut) in combination with a biopsy gun or with manually activated cutting needles. This technique allows one to obtain cores of tissue with an intact histologic structure that facilitates a precise histologic diagnosis or immunohistochemical analysis.

9.5.1 Indications

Large-gauge automated needle biopsies (14G–19G) are traditionally performed in patients without a known primary tumor, in cases of potential lymphoma, and after inconclusive FNAB. Owing to the varying availability of a cytopathologist and results that are comparable to those of FNAB (or even better), in most radiology departments punch biopsy has meanwhile been established as the primary technique of choice.

9.5.2 Material

In comparison with the aspiration technique, core biopsy needles are defined by diameters of 14G–19G (large gauge), and usually by the combination with a spring-activated Tru-Cut system. The Tru-Cut biopsy needle is characterized by a trough at the distal end. First the biopsy gun fires the inner needle into the lesion, where a core of tissue falls into the trough. Then the outer needle cuts the sample lying in the trough out of the surrounding tissue and captures the sample, which can be safely removed through the outer needle or with the whole system (Fig. 9.10). When an automated Tru-Cut system is used for biopsy, the localization of the needle tip next to the lesion should be documented before taking the sample. Usually at least two samples are taken for histologic evaluation and are instantly put into 10% formalin. Different manufacturers offer either disposable all-in-one systems, or the combination of disposable biopsy needles of various diameters and lengths (up to 30 cm) with a standard multiuse gun (Table 9.3). The main advantage is cost reduction. With respect to histopathologic evaluation, the advantages of the core biopsy system are that the amount of tissue obtained is more or less constant, while the sample keeps its histologic structure. In contrast to manually handled large-gauge biopsy systems, the automated mechanism ensures a quick procedure, with the biopsy needle in the patient only for a short period of time.

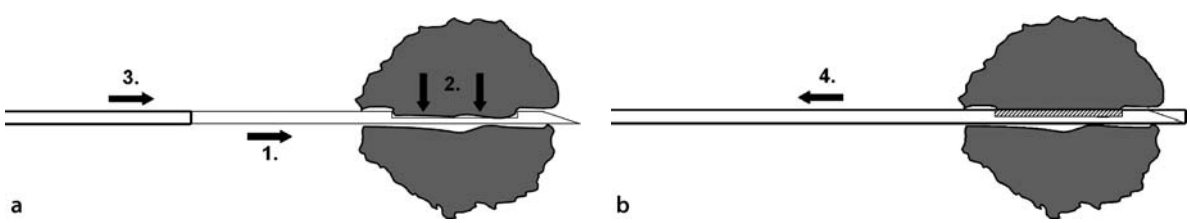

Fig. 9.10a,b The automated Tru-Cut biopsy technique: The inner needle (characterized by a trough at its end) is fired into the target lesion by the biopsy gun (*1*). A core of tissue falls into the trough (*2*). The outer needle slides across the trough and thereby cuts out the specimen (*3*). Finally, the specimen can be safely removed with the inner needle or with the whole system (*4*)

Table 9.3 Commercially available needles for CT- and MR-guided punch biopsy (exemplary selection of different manufacturers and needles)

Needle type (manufacturer)	Gauge	Length (cm)[a]
Tru-Cut manual biopsy needle (Allegiance, McGaw Park, IL, USA)	14; 18	7; 11; 15
Temno semiautomated biopsy system, adjustable cutting length (Allegiance, McGaw Park, IL, USA)[b]	14–22	6; 9; 11; 15; 20; 48
Percucut self-aspirating-type cut needle (E-Z-EM, Lake Success, NY, USA)	18; 19.5; 21	5; 10; 15
Easy Core automated biopsy system (Boston Scientific, Natick, MA, USA)	15; 18; 20	10; 15; 21; 25
Magnum reusable core biopsy gun with disposable biopsy needles (Bard Biopsy, Tempe, AZ, USA)[b]	12–20	10; 13; 16; 20; 25; 30
Max Core disposable automated biopsy needle (Bard Biopsy, Tempe, AZ, USA)	14; 16; 18; 20	10; 16; 20; 25
Monopty disposable core biopsy system (Bard Biopsy, Tempe, AZ, USA)	12; 14; 16; 18; 20	10; 16; 20
Quick Core automated biopsy needle with spring (Cook, Medical, Bloomington, IN, USA)[b]	14; 16; 18; 19; 20	6; 9; 15; 20
Biopsy-Handy (Somatex, Teltow, Germany)[b]	14–20	10; 15; 20
SABD semiautomated biopsy device (Pflugbeil, Zorneding, Germany)	14–21	11.5; 15; 20
MR-compatible core biopsy needles		
MR-compatible biopsy needles (E-Z-EM, Lake Success, NY, USA)	18; 20	5; 10; 15; 20
Magnum (Bard Biopsy, Tempe, AZ, USA)	13–14; 16	
Biopsy-Handy semiautomated biopsy system (Somatex, Teltow, Germany)	14–18	10–20
MRI Bio-Gun automated biopsy system (E-Z-EM, Lake Success, NY, USA)	14; 18	15
MRIDD BiopsyGun semiautomated biopsy system (MRI Devices Daum, Schwerin, Germany)	14–18	10–15

[a] Not all gauge–length combinations may be available.
[b] Coaxial needles available

9.5.3 Technique

Before introduction of the biopsy needle, local anesthesia is applied with a 22-gauge needle. In children, the elderly, and anxious patients intravenous anxiolysis and sedation may be used. During the intervention cardiorespiratory monitoring is needed in case of conscious sedation. After local anesthesia, a small skin incision is made at the intended needle entry point. The rest of the puncture procedure is performed in the same manner as described in Sect. 9.4.3.

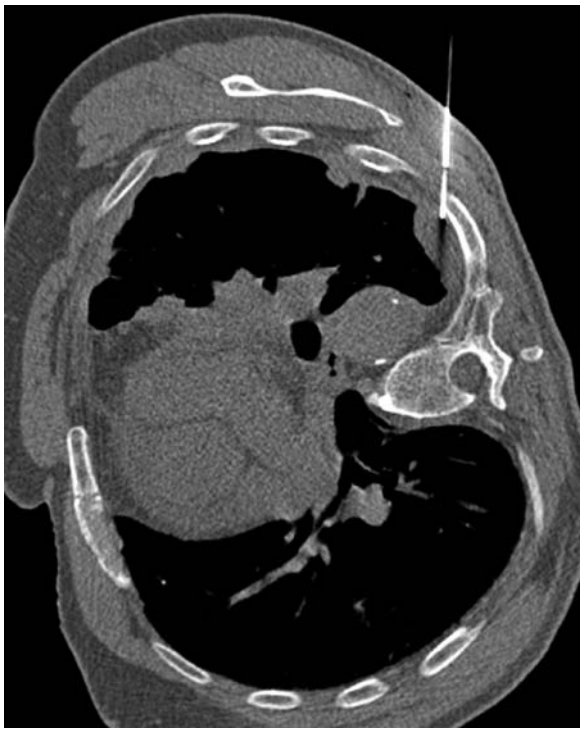

Fig. 9.11 Patient (right lateral decubitus position) with a history of asbestos exposure. Preinterventional CT showed pleural wall thickening of the left lung. An 18G (10-cm) Tru-Cut biopsy needle was introduced under CT-fluoroscopic guidance parallel to the posterior thoracic wall through an intercostal access. Histopathologic analysis revealed pleural mesothelioma

9.5.4 Results

9.5.4.1 Lung

Anderson et al. (2003) performed a study to determine diagnostic accuracy by comparing FNAB with core biopsies of 195 pulmonary lesions in 182 patients, and found a significantly higher diagnostic yield of the core biopsy technique (93%) compared with FNAB (78%). They concluded that core biopsy should be the method of choice especially if a dedicated cytopathologist is not available (Fig. 9.11). Charig and Phillips (2000) reported their results of 185 core lung biopsies in 183 patients with predominantly 18G and 20G needles. Diagnostic accuracy (93.5%) and complication rates were comparable to the published figures for FNAB.

9.5.4.2 Abdomen

In contrast to FNAB, histologic classification of liver masses is only possible with larger core biopsy systems in most cases, as true-positive findings increase from 84 to 98% (Pagani 1983) (Fig. 9.12). Regarding the ability to differentiate samples obtained with either 14- or 18-gauge needles, no significant difference was found between both large-gauge needle types (Haage et al. 1999). Automated cutting needles have

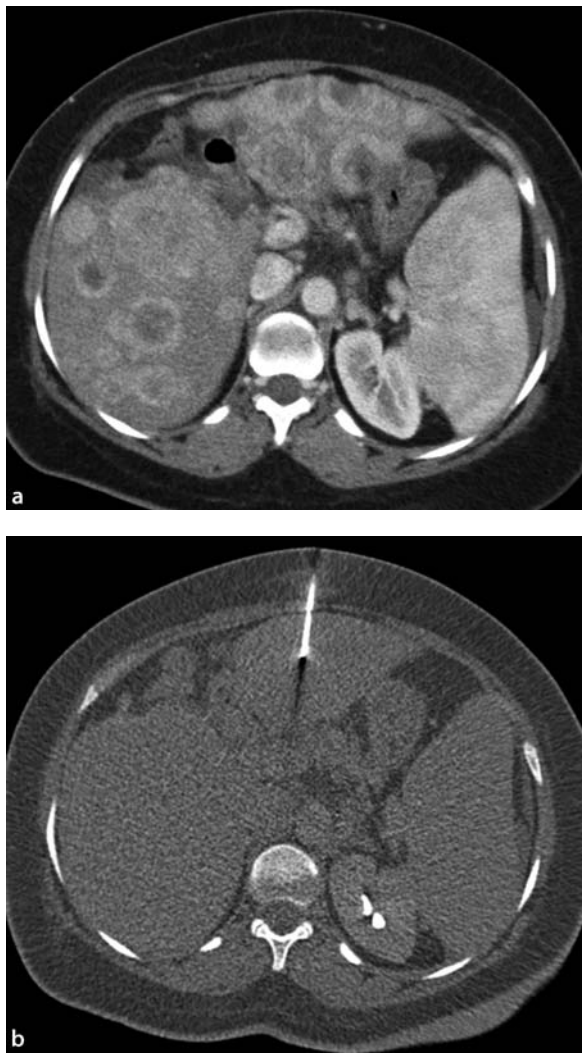

Fig. 9.12a,b Patient (supine position) with multiple hepatic rim-enhanced lesions in both liver lobes (preinterventional CT; venous phase) (**a**). An easy-to-access lesion in segment 3 was chosen for Tru-Cut biopsy with a 16G (10-cm) needle under CT-fluoroscopic guidance (**b**). Histopathologic analysis revealed hepatic metastases of gall bladder carcinoma

additionally contributed to increase the accuracy of the histologic sample (Hopper et al. 1993). Stattaus et al. conducted a study to determine the visibility of small liver lesions in 50 patients during CT-guided biopsy with 16G and 18G semiautomated biopsy needles and the influence on biopsy results. Thirty-eight patients underwent biopsy guided by nonenhanced CT (89.5% accuracy); 12 patients received contrast medium at different time points during the biopsy for better visualization, leading to reduced accuracy (75%). Overall accuracy was 86%. The authors concluded that in the case of poor visualization of liver lesions in the nonenhanced CT scan, correlation between the liver lesion and anatomical landmarks can be used to verify the correct position of the biopsy needle. In addition, interventional MR imaging has the potential to reveal lesions that are poorly visible by CT and ultrasound, providing results comparable to CT guidance: 87–94% sensitivity, 90–100% specificity, and 85–93% accuracy (Salomonowitz. 2001; Zangos et al. 2003). Numerous studies evaluated fine-needle aspiration of pancreatic masses (Gupta et al. 2002; Luning et al. 1985; Sofocleous et al. 2004), while only a few authors focused on core biopsy in the pancreas (Elvin et al. 1990; Wutke et al. 2001). For CT-guided core biopsies conducted in intraabdominal organs (liver, pancreas), the study by Wutke et al. (2001) showed sensitivity, specificity, and accuracy values of 88.4, 100, and 90.4%, respectively. CTF can furthermore help avoid penetration of vital structures by the core biopsy needle along its pathway (Fig. 9.13).

9.5.4.3 Retroperitoneum and Pelvis

In their analysis of 180 CT-guided coaxial core biopsies, Wutke et al. (2001) reported markedly higher diagnostic utility rates for non-organ-related retroperitoneal lesions (88%) than for liver and pancreatic lesions (66%). Overall sensitivity, specificity, and accuracy rates were 91.1, 100, and 93.3%, respectively. The study of Hau et al. (2002) focused on the diagnostic accuracy of both CT-guided FNAB and core biopsy of musculoskeletal lesions. The authors found an accuracy rate of 74% for the subset of core biopsies (258 procedures) in comparison with 63% for CT-guided FNAB (101 procedures). Diagnostic accuracy rates for pelvic and nonpelvic musculoskeletal lesions were 81 and 68%, respectively.

9.5.4.4 Complications

The study of Anderson et al. (2003) (see Sect. 9.5.4.1) showed an initial pneumothorax rate after the biopsy of 30%, which was reduced to 18% after 4-h follow-up. Only 2% of the patients developed clinical symptoms requiring further therapy with a chest tube. Separated pneumothorax rates according to the biopsy technique were 35% (FNAB) and 16% (core biopsy), respectively. Charig and Phillips (2000) reported pneumothoraces in 25.9% (four of 48 patients, 8.3%, requiring an intercostal drain) and small hemoptyses without pneumothorax in 7% of their patients.

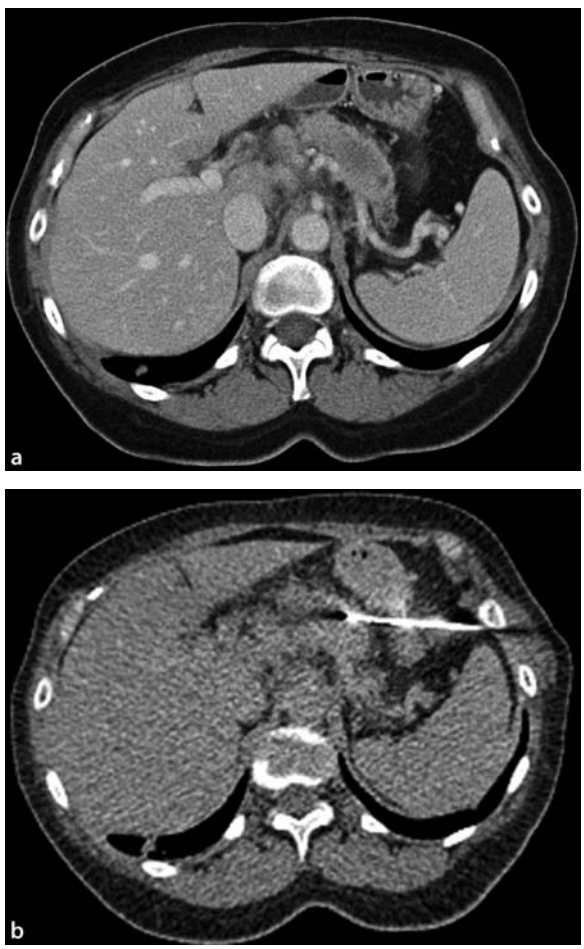

Fig. 9.13a,b Patient (supine position) with suspect pancreatic mass and pulmonary metastases. Preinterventional CT (venous phase) showed a hypodense area in the pancreatic body and tail (**a**). An intercostal left lateral access path between the spleen and the smaller gastric curvature was chosen for Tru-Cut biopsy with an 18G (13-cm) needle under CT-fluoroscopic guidance (**b**). Histopathologic analysis revealed a pancreatic adenocarcinoma

In a large retrospective multicenter study by Piccinino et al. (1986) including 68,276 liver biopsies with a Tru-Cut system, a complication rate of only 0.4% was found. Deaths after liver biopsy were rarely observed, usually owing to hemoperitoneum in patients with malignant disease or cirrhosis. The authors reported a higher rate of deaths, serious hemorrhagic complications, pneumothorax, and biliary peritonitis in biopsies performed with the Tru-Cut needle (0.003%) than with the Menghini needle (0.001%). In contrast to the analysis by Smith (1991) revealing values between 0.003 and 0.009%, the rate of tumor cell seeding after percutaneous tumor puncture of hepatocellular carcinoma has been reported to be in the range between 1% (Llovet et al. 2001) and 5% (Takamori et al. 2000). In biopsy of subcapsular lesions, the rate can even increase to 12% (Llovet et al. 2001).

9.5.5 Appraisal

CT-guided percutaneous aspiration and punch biopsy may be performed in essentially every organ system and overall complication rates are low. The success rates of an individual institution depend on the number of samples obtained, the size of the lesion, the organ in which the biopsy is performed, the experience of the local pathologist staff, the available imaging equipment, and – first and foremost – the skills of the operator. More complex situations include biopsies of lesions that are protected by overlying bone structures or that require transgression of vital organs to reach the target lesion. FNAB requires the availability of an on-site cytopathologist, while transgression of the bowels is usually possible without an increased complication rate. In comparison, punch biopsy – especially if performed with a Tru-Cut needle and an automated biopsy gun – facilitates quick histopathologic sampling in most cases with comparable complication rates.

Key Points

- Needle diameter 12G–19G.
- Standard needle lengths 5–20 cm.
- A spring-activated Tru-Cut needle is a common standard.
- The sample is usually sufficient for histopathologic analysis.
- The needle must not transgress bowels.

9.6 CT-Guided Drill Biopsy

During the past few decades, surgical (open) biopsy of musculoskeletal tumors could be gradually replaced by image-guided (closed) biopsy techniques (Bickels et al. 1999). The main advantages of image-guided percutaneous biopsy in the musculoskeletal system are reduced morbidity and costs. FNAB is often limited in bone tumors given an inadequate ability to sample the tissue matrix, while core biopsy reaches accuracy rates of 68–100% (Pramesh et al. 2001). On the other hand, in young patients with deep subcortical lesions or suspect lesions with a sclerotic rim, the core biopsy needle alone may not be sufficient to penetrate the cortical bone.

9.6.1 Indications

Indications for image-guided percutaneous bone biopsy are bone metastases and primary bone tumors. The biopsy is performed to verify that a suspected bone lesion is indeed a metastasis, or to detect the primary tumor. In patients with breast cancer, hormone sensitivity of a metastatic bone lesion can be important for adequate therapy. In suspected primary bone tumors, biopsy is only exceptionally performed for histologic evaluation with respect to the intended therapy. Special attention should be given to potential tumor seeding, and the access path for biopsy should be carefully planned together with the surgeon responsible for resection (Schweitzer et al. 1996). Another indication for percutaneous bone biopsy is suspected osseous infection with microorganisms that have to be identified before antibiotic therapy. Common contraindications are an uncorrectable coagulopathy and potential soft-tissue infection with the danger of superinfection of the bone.

9.6.2 Material

A variety of bone biopsy needles are available, ranging from sharp-threaded, drilling-type 17G needles to large-bore 8G needles (Table 9.4). For sclerotic or osteoplastic bone lesions of the spine it is advantageous

Table 9.4 Commercially available needles for CT-guided drill biopsy (exemplary selection of different manufacturers and needles)

Needle type (manufacturer)	Gauge	Length (cm)[a]
Ackermann biopsy needle set (Cook, Medical, Bloomington, IN, USA)	14	9.7; 11; 17.2; 18.5
Elson biopsy needle set (Cook, Medical, Bloomington, IN, USA)	14 (with 22G introducer and 12G coaxial needle)	17.1; 18.3
Geremia vertebral biopsy set (Cook, Medical, Bloomington, IN, USA)	16 (with 22G introducer needle)	15
Myers biopsy needle set (Cook, Medical, Bloomington, IN, USA)	14	10
Spi-Cut biopsy needle (Somatex, Teltow, Germany)[b]	12.5; 14	5; 10; 15; 20
Ostycut Bone biopsy needle (Bard Biopsy, Tempe, AZ, USA)[b]	14–17	5; 7.5; 10; 12.5; 15
Bonopty coaxial biopsy system eccentric drill penetration set (Radi Medical Systems, Uppsala, Sweden)	14	
Percucut bone biopsy needle (E-Z-EM, Lake Success, NY, USA)	17	5; 7.5; 10; 12.5; 15
Percucut coaxial sheath cut-biopsy needle with keyhole cutting edge (E-Z-EM, Lake Success, NY, USA)	19.5	15
Laredo trephine needle	8	

[a] Not all gauge–length combinations may be available.
[b] Removal of sample under aspiration.

to collect as much material as possible because these lesions are often difficult to adequately decalcify for diagnostic workup. Therefore, for sclerotic bone lesions, bone biopsy needles of 11G or larger are usually best.

When a spinal lesion is in a location that is difficult to access (e.g., a tight passage between the carotid sheath and vertebral artery in the upper cervical spine), lightweight short drilling needles may be advantageous in setting and keeping trajectories in shallow soft tissues, in contrast to larger 11G needles with heavy handles, which often throw the trajectory of the needle off course when used under CT guidance. Because the small 17G E-Z-EM needles are short and very lightweight, they can be set in shallow soft tissues during targeting and still hold their trajectory without hand support. Because they are also very sharp and threaded, they can thus be drilled deeply into the bone to obtain core samples very effectively in most cases.

9.6.3 Technique

In comparison with MR imaging, CT is inexpensive and easily available in most institutions; therefore, most bone biopsies are performed under CT guidance. First a CT scan is performed to visualize the bone lesion, and the needle entry point and access path are chosen. In the case of superficial bone biopsies without potential interference with vascular and nerve structures along the access path, a nonenhanced CT scan is usually sufficient for planning of the access route. Vessels, nerves, and visceral and articular structures should be avoided. Depending on the localization of the bone lesion, different approaches are available:

- Vertebral body: Depending on the vertebral level, the access path is anterior (cervical spine), transpedicular (Fig. 9.14) or intercostovertebral (thoracic spine) (Fig. 9.15), and transpedicular or posterolateral (lumbar spine).

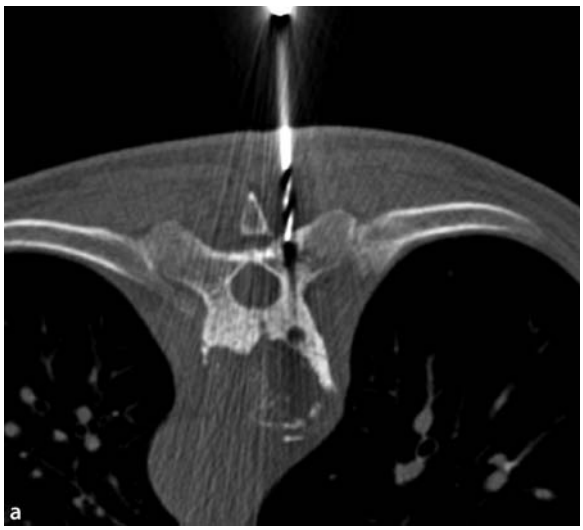

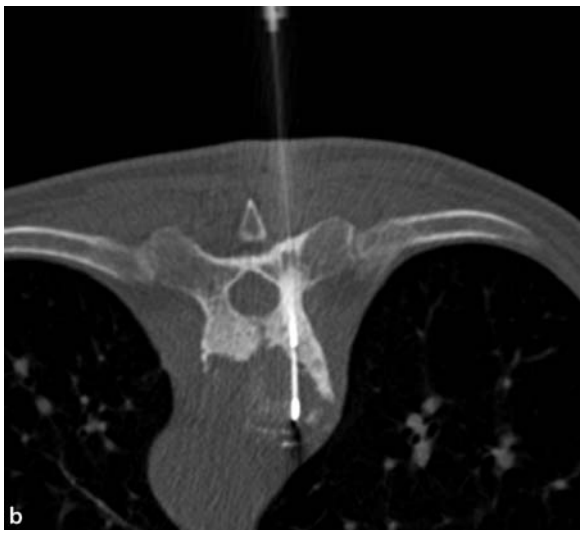

Fig. 9.14a,b Patient (prone position) with major osteolysis (anterior two thirds) of the lower thoracic vertebra showing osteosclerosis of the posterior third and both pedicles. First, transpedicular access was achieved with a surgical manual drill (**a**). Then the soft tissue sample was taken with an 18G (13-cm) Tru-Cut biopsy needle under CT-fluoroscopic guidance (**b**). Histopathologic analysis revealed a spinal metastasis of prostate carcinoma

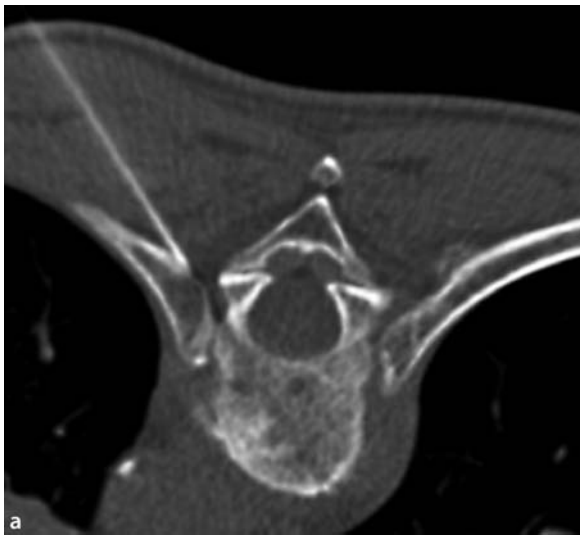

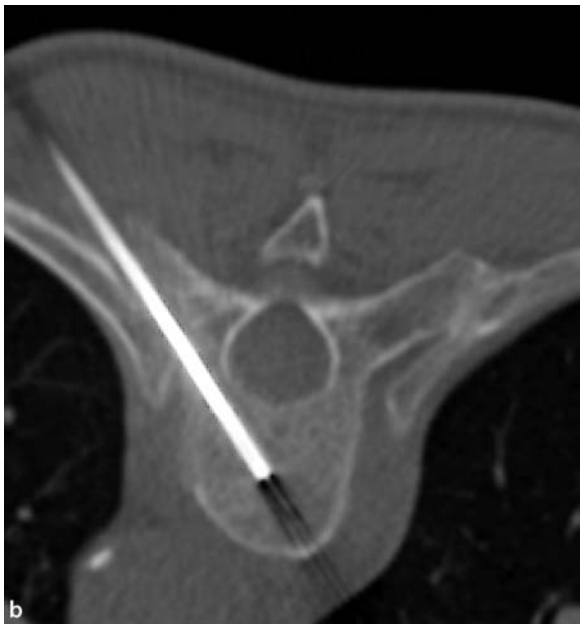

Fig. 9.15a,b Patient (prone position) with suspected spondylodiscitis in the Th°7/8 spinal segment. Preinterventional CT showed small osteolytic defects close to the upper end plate of thoracic vertebra 8. After local anesthesia with a 22G needle (**a**), a 12.5G bone biopsy needle was introduced through the left costovertebral joint (**b**). Microbiological analysis revealed spondylodiscitis due to a *Staphylococcus aureus* infection

- Pelvis: An anterior, lateral, or posterior approach (avoiding the femoral and sacral nerve plexus and the sacral canal) is used (Fig. 9.16).
- Peripheral long tubular bones: An approach orthogonal to the cortical bone is used. This reduces the risk of the biopsy needle gliding off the cortex. The shortest possible access path should be chosen in order to avoid critical structures such as vessels and nerves (Fig. 9.17).
- Flat bones (ribs, sternum, scapula): An oblique approach angle of 30–60° is chosen that provides more material for biopsy, and helps to protect the underlying structures behind the flat bone (Fig. 9.18).

The whole procedure has to be carried out under strictly sterile conditions to avoid osseous infection with subsequent osteomyelitis. Percutaneous drill biopsy is usually performed under local anesthesia or analgosedation (in incompliant patients), while pediatric bone biopsy represents an exception requiring general anesthesia. Local anesthesia is applied from the skin level down to the periosteum of the intended entry point of the biopsy needle with a 22G needle. Leaving the anesthesia needle in the skin by detaching the syringe from the needle with the needle along the intended trajectory course saves time in subsequent needle placements. The initial anesthesia

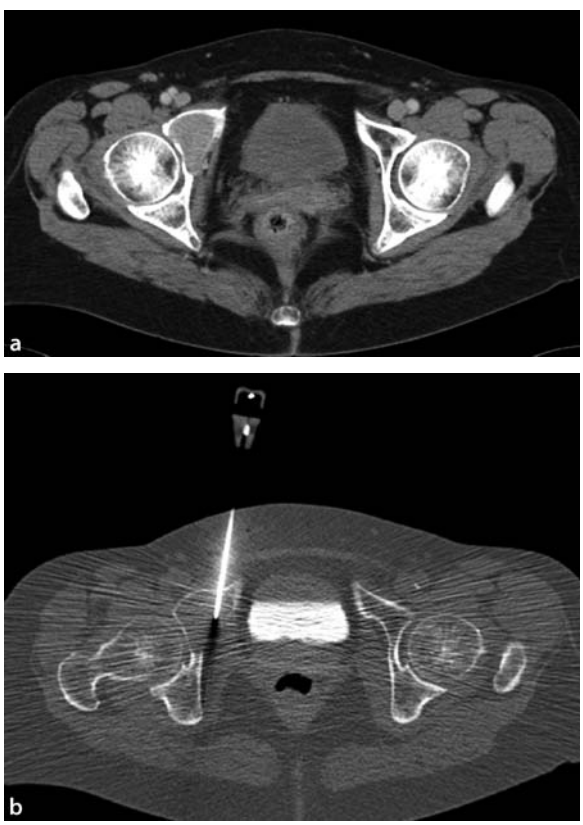

Fig. 9.16a,b Patient (supine position) with osteolysis of the anterior column of the right acetabulum (**a**). A 14G bone biopsy needle was introduced with a sterile surgical hammer avoiding the right common femoral artery and vein (**b**). Histopathologic analysis revealed multiple myeloma

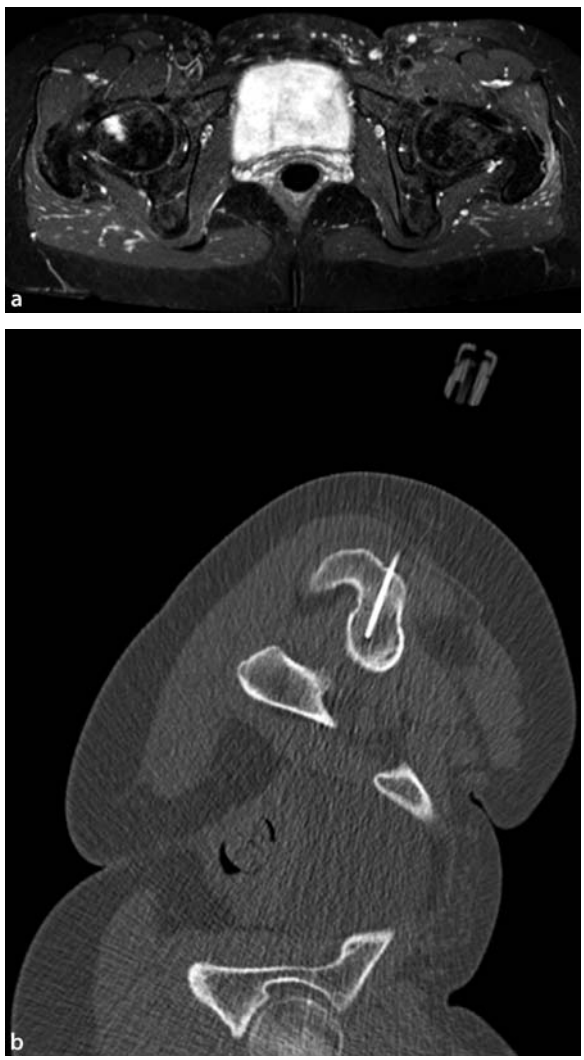

Fig. 9.17a,b Patient with a history of breast cancer and hip pain. Fat-suppressed magnetic resonance imaging (short tau inversion recovery sequence) of the pelvis showed a hyperintense lesion of the right proximal femoral neck (**a**). A 14G bone biopsy needle was introduced in a left lateral decubitus position providing stability during insertion with a surgical hammer (**b**). Histopathologic analysis revealed bone metastasis of breast cancer

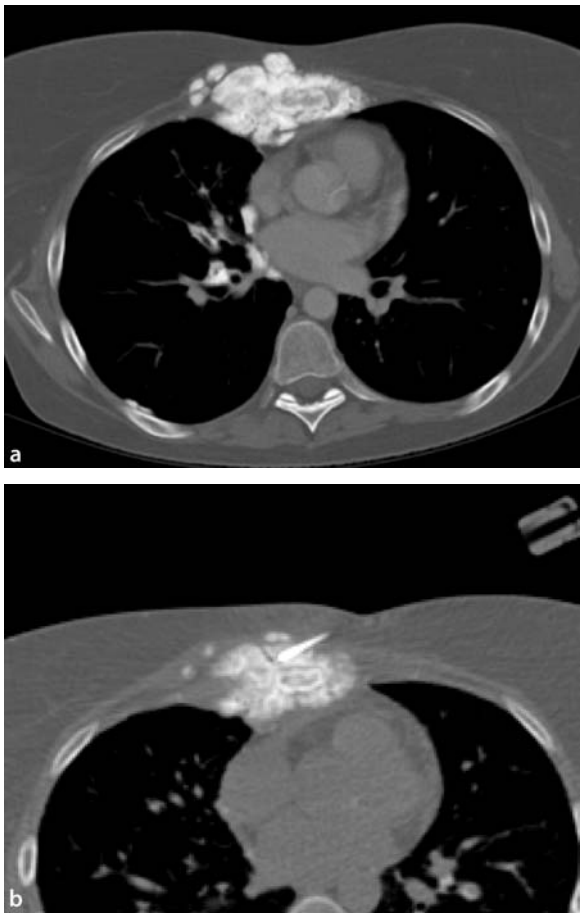

Fig. 9.18a,b Patient (supine position) with a history of Hodgkin's lymphoma and complete remission after radiochemotherapy who developed a painful swelling around the sternum. The preinterventional CT showed an osteoblastic tumor of the sternum, and calcifications in the right pulmonary hilum and pleura (**a**). A slightly oblique approach with a 12G needle was chosen for CT-guided biopsy of the sternum (**b**). Histopathologic analysis revealed an osteosarcoma

needle serves as a relative directional marker on both the images and the skin, and longer needles can subsequently be placed with positional readjustments as necessary, so that the final needle can be placed in tandem (or coaxial) fashion relative to the target zone. The biopsy needle is introduced through the cortical bone under intermittent CT/CTF control verifying the correct needle direction. The needle containing the sample is completely removed, and the sample is fixed in 10% formalin. In the case of suspected infection, the specimen is not fixed but is put directly into a sterile container for microbiological analysis. Osteolyses characterized by a soft tissue core are directly sampled using a 16G or 18G Tru-Cut biopsy needle (Fig. 9.14b). Depending on the thickness of the cortical bone and the degree of sclerosis surrounding the bone lesion, a surgical hammer in combination with the bone biopsy needle (e.g., 14G Somatex Spi-Cut, Teltow, Germany), an 8G trephine needle (e.g., Laredo type), a dedicated bone penetration set (e.g., Bonopty; Radi Medical Systems, Uppsala, Sweden), or a manual drill can be used to penetrate the cortex (Fig. 9.14a).

9.6.4 Results

In their study including 359 CT-guided bone biopsies of musculoskeletal lesions with the FNAB and core biopsy technique, Hau et al. (2002) reported accuracy rates of 63% ($n = 101$) and 74% ($n = 258$), respectively. Especially sarcomas have been shown to be undergraded with FNAB sampling only, therefore making core biopsy preferable.

Jelinek et al. (2002) reported their results in 110 primary bone tumors that were sampled under CT and fluoroscopic guidance, respectively. Correct final diagnosis could be obtained by biopsy in 88% of the patients, while the only minor complication was a small hematoma (0.9% complication rate). Dupuy et al. (1998) performed 176 CT-guided core needle biopsies and 45 fine-needle biopsies with accuracy rates of 93 and 80%, respectively, and a complication rate below 1%. The efficacy of CT-guided percutaneous biopsy in the management of spinal bone lesions has also been evaluated extensively (Renfrew et al. 1991).

In comparison with conventional CT guidance, the advantage of CTF is the online visualization, the excellent resolution of bone and the surrounding soft tissue, and the possibility to target even small lesions (Daly and Templeton 1999). The very good resolution of bone and soft tissue is furthermore able to reduce the number of complications due to misplacement of the needle. Another big advantage is the possibility to perform biopsies in an off-plane direction, enabling the physician to easily target spinal lesions of lumbar vertebra 5 or the sacrum. In the upper lumbar and thoracic regions, CTF provides a means of real-time visualization of the adjacent lung and other posteriorly located visceral organs, such as the kidneys, in

the case of a high lumbar target. In the cervical region, CTF may also be the preferred method of image guidance for biopsies because it can be used to define the positions of the jugular vein, carotid artery, vertebral artery, and pharyngeal and esophageal structures.

9.6.5 Complications

In bone lesions that are assumed to be extremely hypervascularized such as suspected metastases of renal cell carcinoma, a digital subtraction angiogram may have to be obtained prior to biopsy. Transarterial embolization or direct puncture of the lesion with injection of absorbable gelatin sponge or poly(vinyl alcohol) particles helps to prevent serious hemorrhage when samples of the lesion are taken.

When biopsies are performed in thoracic lesions, the operator should always be cautious of a possible pneumothorax; at the end of the procedure, either a follow-up CT scan or an expiratory chest radiograph should be obtained to rule out a pneumothorax. A chest tube kit should be available before biopsy of the thoracic spine.

When pushing or drilling a needle through very dense bone, and when vital structures such as the aorta, the carotid artery, or the vertebral artery are located just beyond the target zone along the trajectory path, the operator may want to use a détente technique with one hand pushing the needle toward the target and the other hand grasping the needle shaft to provide a counteraction force, to prevent piercing beyond the target area into vital structures if resistance to the needle should suddenly give way.

When delivering a bone core that is impacted within the bone biopsy needle, it is prudent to avoid pushing the core out of the needle with such force that it suddenly flies off and becomes lost. To remove a bone core from the biopsy needle, the operator should use the appropriate trocar design that is intended for such a removal.

9.6.6 Appraisal

The growing availability and inexpensiveness as well as the ability to safely access musculoskeletal structures have substantially increased the role of CT for guidance of percutaneous biopsies in comparison with other imaging modalities such as ultrasound and conventional fluoroscopy. Adjacent major vessels, nerves, and visceral structures can be avoided and the biopsy needle can be precisely positioned within the target lesion for histopathologic sampling. CT provides excellent visualization of bone with the exception of some bone marrow lesions only detectable in MR imaging. Though CTF is necessary only in selected cases, given an experienced operator using repeated single-shot CTF for needle positioning, CTF can markedly reduce both the in-room time and the radiation dose for the patient.

Key Points

- Needle diameter 8G–19G.
- Needle lengths 5–20 cm.
- Strictly sterile conditions are mandatory during the whole biopsy procedure.
- For primary bone tumors the needle pathway should lie within the surgical resection area.
- The access angle should be chosen according to the type of bone (tangential access in flat bones, orthogonal access in tubular bones).
- Access to the spine should be anterior/anterolateral in the cervical spine, intercostovertebral/transpedicular in the thoracic spine, and transpedicular/posterolateral in the lumbar spine.
- Needle insertion should be with a hand grip or a surgical hammer.
- A hand drill is preferable for access to lesions with a sclerotic rim/thickened cortical bone.

9.7 MR-Guided Biopsy

Interventional MR imaging has been adapted for guidance of biopies since the mid-1990s, utilizing nonferromagnetic biopsy needles for different field strengths from 0.2 to 1.5 T (Kariniemi et al. 2005; Lewin et al. 1996; Salomonowitz et al. 2000; Silverman et al. 1995). Technologic advances such as the introduction of open and short-bore magnet designs, the proliferation of fast imaging sequences, and the availability of MR-compatible instruments have aided the growth of this field. The advantages of MR-guided biopsy are a high soft-tissue contrast, lack of radiation exposure, and the ability to arbitrarily choose the angulation of the imaging plane for needle track

visualization. MR-guided biopsy was first introduced for abdominal (Mueller et al. 1986) and head-and-neck FNAB, and was adapted for breast and bone biopsies later.

The best design of an MR system with regard to high-quality images and low field inhomogeneity would be a spherical magnet. However, this design represents a suboptimal environment for MR-guided intervention, which requires free access to the patient. Early MR-guided biopsies and aspirations were made with conventional cylindric superconducting systems. This technique is similar to that of CT-guided procedures, in which access to the patient is limited and the patient must be withdrawn from the magnet for the manipulation of biopsy equipment, resulting in relatively long procedure times.

Three types of magnets are used clinically for MR-guided therapy:

1. Closed, short-bore cylindrical superconducting systems operating at between 1.0 and 1.5 T (Rofsky et al. 1998; Salomonowitz 2001)
2. Open, midfield ("double-donut") systems operating at 0.5 T
3. Open, low-field (biplanar) systems operating at between 0.064 and 0.3 T (Blanco Sequeiros et al. 2002)

The improvement in access to the patient that is afforded by the open magnets is traded for decreased field strength and image quality. The main advantage of closed magnets, operating at high field strengths, is superior image quality relative to static magnetic field strengths and homogeneity. The disadvantages of this type of magnet design are the limited access to the patient and the relatively longer procedure times.

Factors such as lesion conspicuousness, needle passive image artifacts, and image contrast between the lesion and the instruments must be considered in a MR-guided procedure. The instrumentation-based image artifacts depend mainly on the following:

- Needle size.
- Orientation of the needle to the magnetic field.
- The magnetic field strength.
- The imaging sequence parameters used for the procedure.

The greater the angle of the needle to the magnetic field, the more conspicuous is the artifact size, with maximum visibility at 90°. The artifact becomes larger with increasing field strength. Gradient-echo sequences are more sensitive to local field inhomogeneities and intravoxel dephasing than spin-echo sequences are. Therefore, techniques such as T2-weighted fast spin-echo sequences produce smaller artifacts than those with gradient-echo scans. The physical basis of these phenomena has been well described in the literature (Ladd et al. 1996; Lewin et al. 1996). Beside visualization through the abovementioned artifacts ("passive visualization"), dedicated needles are available that contain a small transmitter and receiver coil ("active visualization") and require additional hardware and software components. While MR-guided interventions have been successfully performed with all field strengths from 0.2 to 1.5 T (Blanco Sequeiros et al. 2002, Rofsky et al. 1998, Salomonowitz, E. 2001), effective clinical application of MR-guided procedures generally requires consideration of these different factors and appropriate adaptation (see Chap. 3).

9.7.1 Indications

Indications for MR-guided biopsy in the abdomen include subdiaphragmatic liver lesions requiring a triangulated needle access. MR-guided biopsy may also be useful in selected cases of intraparenchymal liver lesions which cannot be visualized with ultrasound or CT. In the breast, interventional MR imaging has been established for tumor marking and percutaneous biopsy, especially to histologically confirm the diagnosis of malignancy preoperatively, and to visualize lesions smaller than 1 cm that cannot be detected with other imaging modalities (Heywang-Kobrunner et al. 2000). MR-guided bone biopsy is indicated in bone marrow lesions that are not detectable with CT (Blanco Sequeiros et al. 2002), and in children owing to lack of radiation exposure.

9.7.2 Material

MR-compatible accessories are available from several manufacturers. As with other cross-sectional imaging-guided modalities, such as CT and ultrasound, the correct needle choice depends on whether tissue is required for cytologic or histologic analysis. Fine-aspiration, side-cutting, and bone biopsy needles are

available in different combinations of diameter and length (Tables 9.2–9.4). To achieve minimal artifacts and no torque in the magnetic field, needles are composed of nonferromagnetic metals such as titanium, tantalum, and tungsten with aluminum or vanadium alloy.

The main disadvantage of these needles is their relative bluntness and softness compared with stainless steel needles. Thus, in the case of intact cortical bone or sclerotic bony lesions, the biopsy procedure may be technically difficult and time-consuming and the patient may experience some discomfort. MR-compatible bone drill systems are being developed to overcome this problem.

9.7.3 Technique

9.7.3.1 Abdomen

Imaging for abdominal MR-guided biopsy is performed under suspended respiration. Especially liver lesions can be visualized with a high contrast (Fig. 9.19). For lesion localization and tracking of the needle, T1-weighted gradient-echo sequences or fast single-shot T2-weighted spin-echo sequences are suitable. Preparation of the biopsy area, including sterile draping and skin disinfection, is performed analogous to that for CT-guided biopsy. First the needle entry point has to be defined. MR-compatible grids and the laser beam help to choose the suitable table position and needle angulation especially when a double-oblique access is necessary. The needle is then introduced under intermittent MR control, which currently takes up to 3 s of scan time. Stereotaxic guidance in combination with an open-configuration MR system has also been described (Silverman et al. 1995).

9.7.3.2 Bone

MR-guided bone biopsy requires strictly sterile conditions as established for CT guidance. Biopsies are commonly performed under local anesthesia, and exceptionally under general anesthesia (e.g., osteoid osteomas in children).

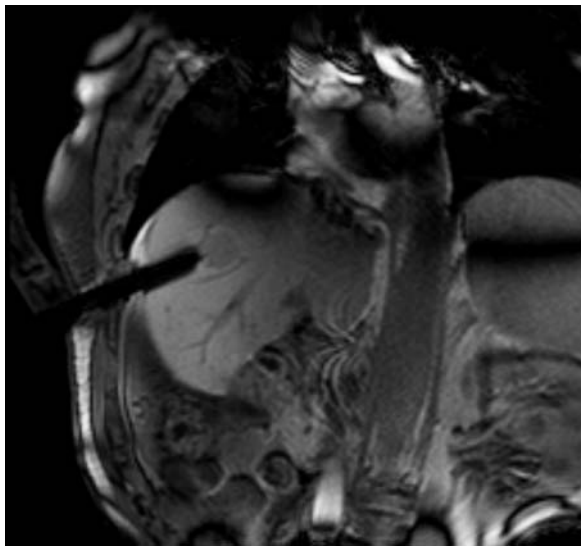

Fig. 9.19 Patient with a history of hepatocellular carcinoma who had undergone liver transplantation, showing a newly occurred liver lesion. Interventional magnetic resonance (paracoronal T1-weighted image) shows the tip of the 16G Tru-Cut biopsy needle next to the slightly hypointense liver lesion before sampling. Note the typical large needle artifact appearing to be a needle of larger diameter. Histopathologic analysis revealed recurrence of hepatocellular carcinoma within the transplant liver. (Image courtesy of Stephan Clasen, Department of Diagnostic Radiology, Eberhard Karls University, Tübingen, Germany)

9.7.4 Results

Several authors described successfully performing abdominal FNAB and core biopsies under MR guidance (Konig et al. 2003; Rofsky et al. 1998; Salomonowitz 2001; Schmidt et al. 1999; Silverman et al. 1995). In 60 patients, Schmidt et al. (1999) could not find a statistical difference regarding diagnostic yield and complication rates of liver biopsies performed under ultrasound (19G/21G coaxial FNAB set or 20G core biopsy; 61% diagnostic), CT (19G/21G coaxial FNAB set or 20G core biopsy; 67% diagnostic) or MR (18G/21G coaxial FNAB set; 61% diagnostic) guidance at 0.5 T.

Few studies on MR-guided biopsy of bone lesions have been performed (Adam et al. 1999; Alanen et al. 2004; Neuerburg et al. 1998). MR-guided trephine biopsy is described as a safe and accurate method comparable to CT, while the diagnostic accuracy of MR-guided FNAB can be low owing to sampling errors (Blanco Sequeiros et al. 2002).

9.7.5 Complications

Potential complications of MR-guided abdominal biopsies include adverse events such as bleeding, infection, and pneumothorax that are also commonly associated with procedures guided by ultrasound or CT/CTF. Side effects related to the magnetic field (e.g., implanted ferromagnetic clips, foreign bodies, pacemakers, etc.) should be ruled out before any MR-guided intervention.

Summary

In contrast to ultrasound and CT, MR imaging has been established as an imaging method for guiding percutaneous biopsies only in the last 15 years. Apart from scientific feasibility reports, with respect to economic efficiency, in most institutions the technique should be restricted to selected lesions that are difficult to visualize and access using alternative imaging techniques.

Key Points

- Needle artifacts proportional to needle diameter, field strength, and needle orientation within the magnetic field.
- T1-weighted gradient-echo sequences and fast single-shot T2-weighted spin-echo sequences for lesion localization and needle tracking.
- Passive visualization with nonferromagnetic MR-compatible biopsy needles is a common standard.
- Limited access to patient in closed magnets.

References

Adam G et al. (1999) Interventional MR imaging: percutaneous abdominal and skeletal biopsies and drainages of the abdomen. Eur Radiol 9(8):1471–1478

Alanen J et al. (2004) Cost comparison analysis of low-field (0.23 T) MRI- and CT-guided bone biopsies. Eur Radiol 14(1):123–128

Anderson JM et al. (2003) CT-guided lung biopsy: factors influencing diagnostic yield and complication rate. Clin Radiol 58(10):791–797

Arslan S et al. (2002) CT- guided transthoracic fine needle aspiration of pulmonary lesions: accuracy and complications in 294 patients. Med Sci Monit 8(7):CR493–497

Assaad MW et al. (2007) Diagnostic accuracy of image-guided percutaneous fine needle aspiration biopsy of the mediastinum. Diagn Cytopathol 35(11):705–709

Bickels J et al. (1999) Biopsy of musculoskeletal tumors. Current concepts. Clin Orthop Relat Res 368:212–219

Blanco Sequeiros R et al. (2002) MRI-guided trephine biopsy and fine-needle aspiration in the diagnosis of bone lesions in low-field (0.23 T) MRI system using optical instrument tracking. Eur Radiol 12(4):830–835

Brandt KR et al. (1993) CT- and US-guided biopsy of the pancreas. Radiology 187(1):99–104

Bret PM et al. (1988) Hepatocellular carcinoma: diagnosis by percutaneous fine needle biopsy. Gastrointest Radiol 13(3):253–255

Brierly RD et al. (2000) Evaluation of fine-needle aspiration cytology for renal masses. BJU Int 85(1):14–18

Cardella JF et al. (2003) Quality improvement guidelines for image-guided percutaneous biopsy in adults. J Vasc Interv Radiol 14(9 Pt 2):S227–S230

Carlson SK et al. (2001) Benefits and safety of CT fluoroscopy in interventional radiologic procedures. Radiology. 219(2):515–520

Charig MJ, Phillips AJ (2000) CT-guided cutting needle biopsy of lung lesions–safety and efficacy of an out-patient service. Clin Radiol 55(12):964–969

Cox JE et al. (1999) Transthoracic needle aspiration biopsy: variables that affect risk of pneumothorax. Radiology 212(1):165–168

Daly B, Templeton PA (1999) Real-time CT fluoroscopy: evolution of an interventional tool. Radiology 211(2):309–315

Dupuy DE et al. (1998) Accuracy of CT-guided needle biopsy of musculoskeletal neoplasms. AJR Am J Roentgenol 171(3):759–762

Elvin A et al. (1990) Biopsy of the pancreas with a biopsy gun. Radiology 176(3):677–679

Ferrucci JT Jr et al. (1980) Diagnosis of abdominal malignancy by radiologic fine-needle aspiration biopsy. AJR Am J Roentgenol 134(2):323–30

Fish GD et al. (1988) Postbiopsy pneumothorax: estimating the risk by chest radiography and pulmonary function tests. AJR Am J Roentgenol 150(1):71–74

Grant A, Neuberger J (1999) Guidelines on the use of liver biopsy in clinical practice. British Society of Gastroenterology. Gut 45(Suppl 4):IV1–IV11

Gupta S et al. (2002) Masses in or around the pancreatic head: CT-guided coaxial fine-needle aspiration biopsy with a posterior transcaval approach. Radiology 222(1):63–69

Haage P et al. (1999) CT-guided percutaneous biopsies for the classification of focal liver lesions: a comparison between 14 G and 18 G puncture biopsy needles. Rofo 171(1):44–48

Hau A et al. (2002) Accuracy of CT-guided biopsies in 359 patients with musculoskeletal lesions. Skeletal Radiol 31(6):349–353

Heywang-Kobrunner SH et al. (2000) Interventional MRI of the breast: lesion localisation and biopsy. Eur Radiol 10(1):36–45

Hopper KD et al. (1993) Automated biopsy devices: a blinded evaluation. Radiology 187(3):653–660

Irie T et al. (2001) Biopsy of lung nodules with use of I-I device under intermittent CT fluoroscopic guidance: preliminary clinical study. J Vasc Interv Radiol 12(2):215–219

Jelinek JS et al. (2002) Diagnosis of primary bone tumors with image-guided percutaneous biopsy: experience with 110 tumors. Radiology 223(3):731–737

Kariniemi J et al. (2005) MRI-guided abdominal biopsy in a 0.23-T open-configuration MRI system. Eur Radiol 15(6):1256–1262
Kazerooni EA et al. (1996) Risk of pneumothorax in CT-guided transthoracic needle aspiration biopsy of the lung. Radiology 198(2):371–375
Klein JS et al. (1996) Transthoracic needle biopsy with a coaxially placed 20-gauge automated cutting needle: results in 122 patients. Radiology 198(3):715–720
Konig CW et al. (2003) MR imaging-guided adrenal biopsy using an open low-field-strength scanner and MR fluoroscopy. AJR Am J Roentgenol 180(6):1567–1570
Ladd ME et al. (1996) Biopsy needle susceptibility artifacts. Magn Reson Med 36(4):646–651
Laurent F et al. (2000) CT-guided transthoracic needle biopsy of pulmonary nodules smaller than 20 mm: results with an automated 20-gauge coaxial cutting needle. Clin Radiol 55(4):281–287
Lechevallier E et al. (2000) Fine-needle percutaneous biopsy of renal masses with helical CT guidance. Radiology 216(2):506–510
Lee M (2004) Image-guided percutaneous biopsy. In: Kaufman J, Lee M (eds) Vascular and interventional radiology: the requisites. Mosby, Philadelphia, pp 469–488
Lewin JS et al. (1996) Needle localization in MR-guided biopsy and aspiration: effects of field strength, sequence design, and magnetic field orientation. AJR Am J Roentgenol 166(6):1337–1345
Li H et al. (1996) Diagnostic accuracy and safety of CT-guided percutaneous needle aspiration biopsy of the lung: comparison of small and large pulmonary nodules. AJR Am J Roentgenol 167(1):105–109
Llovet JM et al. (2001) Increased risk of tumor seeding after percutaneous radiofrequency ablation for single hepatocellular carcinoma. Hepatology 33(5):1124–1129
Lumachi F et al. (2001) Fine-needle aspiration cytology of adrenal masses in noncancer patients: clinicoradiologic and histologic correlations in functioning and nonfunctioning tumors. Cancer 93(5):323–329
Lumachi F et al. (2003) CT-scan, MRI and image-guided FNA cytology of incidental adrenal masses. Eur J Surg Oncol 29(8):689–692
Luning M et al. (1984) Analysis of the results of 96 CT-guided fine needle biopsies of liver masses. Rofo 141(3):267–275
Luning M et al. (1985) CT guided percutaneous fine-needle biopsy of the pancreas. Eur J Radiol 5(2):104–108
Memel DS et al. (1996) Efficacy of sonography as a guidance technique for biopsy of abdominal, pelvic, and retroperitoneal lymph nodes. AJR Am J Roentgenol 167(4):957–962
Mueller PR (1993) Pancreatic biopsy: striving for excellence. Radiology 187(1):15–16
Mueller PR et al. (1986) MR-guided aspiration biopsy: needle design and clinical trials. Radiology 161(3):605–609
Mueller PR et al. (1988) Severe acute pancreatitis after percutaneous biopsy of the pancreas. AJR Am J Roentgenol 151(3):493–494
Nahar Saikia U et al. (2002) Image-guided fine-needle aspiration cytology of deep-seated enlarged lymph nodes. Acta Radiol 43(2):230–234
Neuerburg J et al. (1998) A new MR- (and CT-) compatible bone biopsy system: first clinical results. Rofo 169(5):515–520
Pagani JJ (1983) Biopsy of focal hepatic lesions. Comparison of 18 and 22 gauge needles. Radiology 147(3):673–675
Piccinino F et al. (1986) Complications following percutaneous liver biopsy. A multicentre retrospective study on 68,276 biopsies. J Hepatol 2(2):165–173
Poe RH et al. (1984) Predicting risk of pneumothorax in needle biopsy of the lung. Chest 85(2):232–235
Pramesh CS et al. (2001) Core needle biopsy for bone tumours. Eur J Surg Oncol 27(7):668–671
Quon D et al. (1988) Pulmonary function testing in predicting complications from percutaneous lung biopsy. Can Assoc Radiol J 39(4):267–269
Renfrew DL et al. (1991) CT-guided percutaneous transpedicular biopsy of the spine. Radiology 180(2):574–576
Rofsky NM et al. (1998) MR-guided needle aspiration biopsies of hepatic masses using a closed bore magnet. J Comput Assist Tomogr 22(4):633–637
Salomonowitz E (2001) MR imaging-guided biopsy and therapeutic intervention in a closed-configuration magnet: single-center series of 361 punctures. AJR Am J Roentgenol 177(1):159–163
Salomonowitz EK et al. (2000) Simple and effective technique of guided biopsy in a closed MRI system. Abdom Imaging 25(6):638–642
Schmidt AJ et al. (1999) Diagnostic yield of MR-guided liver biopsies compared with CT- and US-guided liver biopsies. J Vasc Interv Radiol 10(10):1323–1329
Schweitzer ME et al. (1996) Percutaneous skeletal aspiration and core biopsy: complementary techniques. AJR Am J Roentgenol 166(2):415–418
Silverman SG et al. (1995) Interactive MR-guided biopsy in an open-configuration MR imaging system. Radiology 197(1):175–181
Silverman SG et al. (1999) CT fluoroscopy-guided abdominal interventions: techniques, results, and radiation exposure. Radiology 212(3):673–681
Smith EH (1991) Complications of percutaneous abdominal fine-needle biopsy. Review. Radiology 178(1):253–258
Sofocleous CT et al. (2004) CT-guided transvenous or transcaval needle biopsy of pancreatic and peripancreatic lesions. J Vasc Interv Radiol 15(10):1099–1104
Stattaus J, Kühl H, Hauth EA, Kalkmann J, Baba HA, Forsting M (2007) Liver biopsy under guidance of multislice computed tomography: comparison of 16G and 18G biopsy needles. Radiologe 47(5):430–438
Swischuk JL et al. (1998) Percutaneous transthoracic needle biopsy of the lung: review of 612 lesions. J Vasc Interv Radiol 9(2):347–352
Takamori R et al. (2000) Needle-tract implantation from hepatocellular cancer: is needle biopsy of the liver always necessary? Liver Transpl 6(1):67–72
Tanaka J, Sonomura T, Shioyama Y, Kutsukake Y, Tomita K, Ushimi T, Yokoyama Y, Abe K, Suzuki K (1996) "Oblique path" – the optimal needle path for computed tomographyguided biopsy of small subpleural lesions. Cardiovasc Intervent Radiol 19(5):332–334
Tomiyama N et al. (2000) CT-guided needle biopsy of small pulmonary nodules: value of respiratory gating. Radiology 217(3):907–910

Torzilli G et al. (1999) Accurate preoperative evaluation of liver mass lesions without fine-needle biopsy. Hepatology 30(4):889–893

Tsukada H et al. (2000) Diagnostic accuracy of CT-guided automated needle biopsy of lung nodules. AJR Am J Roentgenol 175(1):239–243

van Sonnenberg E, Casola G (1988) Interventional radiology 1988. Invest Radiol 23(2):75–92

van Sonnenberg E et al. (1988) Difficult thoracic lesions: CT-guided biopsy experience in 150 cases. Radiology 167(2):457–461

Wallace MJ et al. (2002) CT-guided percutaneous fine-needle aspiration biopsy of small (< or = 1-cm) pulmonary lesions. Radiology 225(3):823–828

Welch TJ et al. (1989) CT-guided biopsy: prospective analysis of 1,000 procedures. Radiology 171(2):493–496

Wildberger JE et al. (2003) Refinement of cytopathology of CT-guided fine needle aspiration biopsies with additional histologic examination of formalin-fixed blood-clots. Rofo 175(11):1532–1538

Wutke R et al. (2001) CT-guided percutaneous core biopsy: effective accuracy, diagnostic utility and effective costs. Rofo 173(11):1025–1033

Zangos S et al. (2003) MR-guided biopsies of undetermined liver lesions: technique and results. Rofo 175(5):688–694

Zwischenberger JB et al. (2002) Mediastinal transthoracic needle and core lymph node biopsy: should it replace mediastinoscopy? Chest 121(4):1165–1170

MR-Guided Breast Biopsy

10

Uta Preim

Contents

10.1 Introduction

Dynamic contrast-enhanced magnetic resonance (MR) imaging is currently the most sensitive imaging method for the detection of invasive breast carcinoma. Because of the limited specificity of dynamic contrast-enhanced MR imaging, minimally invasive breast biopsy is important to avoid unnecessary surgical procedures.

With the distribution of dedicated breast biopsy coils, MR-guided wire localization, MR-guided core-needle biopsies, and MR-guided vacuum-assisted biopsies have become increasingly popular. The value of MR-guided wire localization and biopsy is specifically high whenever a lesion is difficult to visualize by other methods. In addition, more and more patients present with findings from MR imaging not reproducible by other methods. Up to 40% of MR-visible lesions will have no detectable correlate even on targeted ultrasound, and an MR-guided intervention will be required (Kuhl 2007).

10.2 Indications

MR-guided breast biopsy is indicated in cases of suspected malignancy prior to surgery or neoadjuvant chemotherapy and in diagnostic workup of otherwise unclear findings and nonpalpable lesions if these lesions are not visible on ultrasound or mammography.

Patients have to provide informed consent prior to the procedure. Immediately before the diagnostic intervention, the radiologist should ensure that the lesion is still visible. A minimum breast thickness of 3 cm is required to perform MR-guided vacuum-assisted biopsy. In those patients for whom MR-guided vacuum-assisted biopsy is not possible, MR-guided wire localization may be performed alternatively. The timing of the biopsy should be adapted to the patient's menstrual cycle from day 7 to day 17. Hormone therapy must have been paused for 4–6 weeks. Coagulation parameters must be normal.

As for general MR examinations, pacemaker and other metallic implants are contraindications for an MR-guided intervention. Lesions smaller than 5 mm usually need not be biopsied because of their very low rate of malignancy (3%) (Liberman et al. 2005). If the lesion is located close to a breast implant the risk of a biopsy maybe increased and the indication should be validated carefully.

10.3 Material

Diagnostic MR mammographies are usually performed employing high-field MR-systems (1.5–3.0 T). For an MR-guided intervention, a breast biopsy coil with a dedicated biopsy compression device (grid-localizing system) is needed. A fiducial marker (T1 hyperintense marker – e.g., vitamin E, fish oil capsule, or gadolinium-impregnated marker) is helpful to determine the puncture entry site. For MR-guided core biopsies, usually 14G needles are used. Vacuum-assisted biopsies are performed with a 9G–11G vacuum-assisted MR-compatible biopsy system (vacuum-assisted biopsy device and probe; hand held, designed for MR biopsy). After vacuum-assisted biopsy, a titanium clip is placed into the cavity to mark it for later localization and surgical excision (Berg et al. 2006).

10.4 Technique

Interventions in a closed-bore MR scanner are usually performed after application of a contrast agent. After injection of gadolinium, a T1-weighted fat saturated sequence is performed. The biopsy should be performed quickly because lesion conspicuity usually diminishes with time after contrast injection. Furthermore, the faster the biopsy is accomplished, the less likely it is the patient will move. If the lesion is well depicted in nonenhanced images, it may even be punctured without administration of contrast agent.

There are several reasons why lesions may not be visualized at the time of biopsy. If compression is overly tight, vascular compression may prohibit appropriate contrast enhancement. Failed contrast injection and extravasation of contrast medium still have to be excluded. If the lesion cannot be depicted, a follow-up MR scan must be obtained.

Since interventions in the closed bore are performed outside the magnet, punctures and biopsies cannot be observed directly. Employing an open-magnet configuration, however, enables the use of fluoroscopic sequences and thereby online monitoring of the procedure.

For intervention in closed magnets, the breast is placed in a dedicated biopsy compression device featuring a grid-localizing system. Compression minimizes breast motion and breast thickness and ensures consistent lesion location (Berg et al. 2006).

The imaging protocol commonly includes a transversal T2-weighted fat-saturated sequence. A T1-weighted 3D gradient-echo sequence is continuously repeated before and four to six times after a rapid intravenous bolus injection of 0.1 mmol/kg body weight gadopentetate dimeglumine. Contrast-enhanced imaging continues until approximately 7 min after the contrast agent injection. The optimal temporal resolution is below 1 min per acquisition, so that the uptake and washout of the contrast agent, which in the most rapidly enhanced lesions typically occurs within 90–120 s after injection, can be measured accurately. The slice thickness should be 2 or 3 mm without an interslice gap. Subtraction techniques have proven to be very helpful to depict contrast-enhanced lesions (Rausch and Hendrick 2006).

To initiate the procedure in the closed bore, a fiducial marker is placed over the expected lesion site to also mark the intended entry point. Thereafter, the coordinates of the lesion are determined on the basis of the spatial relationship between lesion, fiducial marker, and grid lines. A mark is made on the skin overlying the lesion, and the skin is cleaned with alcohol and anesthetized with local anesthesia. A skin nick is made with a scalpel and an MR-compatible cannula is placed in the skin incision and advanced to the calculated depth. A transversal T1-weighted study (3-mm slice thickness) is performed to document the location of the tip of the cannula at the site of the lesion. Six to 12 samples are obtained with the vacuum-assisted biopsy device. Finally, a clip is placed at the biopsy site to mark its location for the surgeon (Berg et al. 2006).

Postbiopsy MR images should cover the entire breast. The radiologist needs to review the images to rule out postbiopsy changes and to evaluate the localizing clip and whether the target was sampled or even excised. Additional postbiopsy conventional mammograms (craniocaudal and 90° lateral) should document the clip position. To optimally support the pathologist, the report should include lesion size, location, morphology, and kinetics, gauge of the needle being used, clip placement, com-

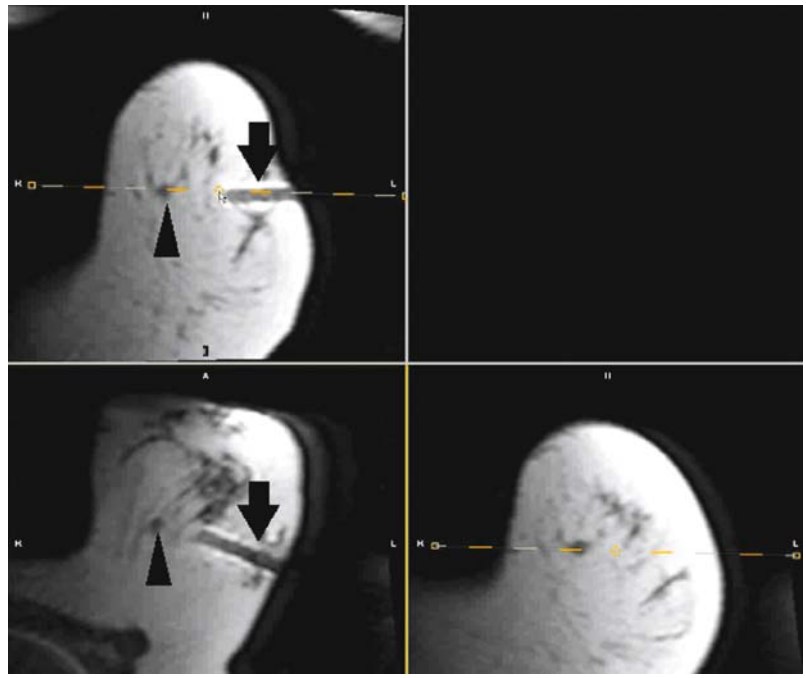

Fig. 10.1 Breast biopsy of a suspicious lesion (*arrowheads*) performed under magnetic resonance fluoroscopy in an open 1-T magnet. During fluoroscopy, visualization alternates between paracoronal (*upper left*) and axial orientation (*lower left*) to follow the biopsy needle (*arrows*) in real time

plications, and the postbiopsy mammogram (Berg et al. 2006).

Interventions in the open magnet can be performed inside the magnet and monitored online using MR fluoroscopy (Fig. 10.1). Since common real-time sequences do not allow simultaneous fat suppression, the biopsy has to be performed without the use of a contrast agent – most contrast-enhanced lesions will not be detectable in the bright fatty tissue in T1-weighted images without fat saturation. Therefore, after initial contrast-enhanced imaging the patient has to be removed from the MR device for some 90 min to await contrast agent washout. After washout of the contrast agent, the biopsy may be performed. Alternatively preprocedurally only nonenhanced images are obtained after a contrast-enhanced diagnostic scan several days prior to the procedure. Finger pointing is sufficient for the determination of the skin entry site. Afterwards, images in paratransversal and paracoronal planes are continuously obtained. These images need to include the puncture site and the lesion to visualize the advancing needle in real time. For this interactive technique, a monitor in the MR room is required. Real-time sequences need to be adapted to the needle chosen for puncture – images are usually best obtained with T1-weighted spin-echo sequences because of strong needle artifacts in gradient-echo sequences (Gehl and Frahm 1998) (see Chap. 3).

10.5 Results

Dynamic contrast-enhanced MR imaging of the breast has shown diagnostic sensitivity of 94–99% for invasive breast cancer, with specificity varying extensively among reporting groups (37–97%). If a lesion detected by dynamic contrast-enhanced MR imaging remains suspicious, biopsy is required to rule out malignancy (Tozaki et al. 2007).

Previous studies have reported technical success rates of 61–100% for MR-guided fine-needle aspiration, 33–100% for MR-guided core-needle biopsy, and 93–98% for MR-guided vacuum-assisted biopsy (Liberman et al. 2003). MR-guided hook-wire placement for localization of nonpalpable lesions visible only on MR images has become an easy, fast, and safe procedure. Some authors claim that MR-guided core-needle biopsy is not sufficiently accurate and, thus, cannot be recommended generally for the workup of MR-detected lesions (Fischer et al. 1998). Because of

the small size of the tissue cores, the histopathological diagnosis may be uncertain and, furthermore, the biopsy site cannot be identified – even in retrospect – if a surgical excision is required and no marker has been positioned previously.

Compared with MR-guided core-needle biopsy, MR-guided vacuum-assisted biopsy offers several important advantages:

- A larger tissue volume is acquired. This may be important for the histopathological diagnosis of small in situ malignancies or borderline lesions. Even very small lesions can be diagnosed with greater accuracy.
- Tissue shift by bleeding can usually be avoided, since continuous suction may evacuate blood volumes.
- Tissue shift during needle insertion also may be compensated, because a large area of tissue is removed.

Vacuum-assisted biopsy is faster, less invasive, and less expensive than surgery and it causes no breast deformity (Liberman et al. 2003). Finally, correct biopsy results can be verified by direct visualization of lesion removal on the postinterventional images (Perlet et al. 2006).

It should be mentioned, however, that punctures in a closed-bore MR-scanner suffer from a dead space of approximately 2 cm medially, close to the chest wall, since they commonly cannot be positioned deep enough in the breast coil to be reached by the biopsy needle.

The advantage of fluoroscopic puncture is its access to all areas in the breast. By interactive real-time visualization, the needle can be localized continuously. An essential problem is the determination of the lesion without contrast agent. Moreover, since the patient is removed from the magnet after diagnostic MR imaging until the contrast agent had been washed out, the position of the breast and the lesion may slightly differ.

Diagnosis of benign lesions after a successful MR-guided vacuum-assisted biopsy is very reliable (negative predictive value greater than 99%) and surgery can be avoided in these cases. If malignancy is proven, optimal planning of the oncosurgical approach is possible. However, when a malignant or borderline lesion is confirmed by MR-guided vacuum-assisted biopsy, excision of the cavity remains necessary, because residual microscopic malignancy cannot be excluded (Perlet et al. 2006). Correlation of imaging and histopathological findings is important: If the histological findings are not clearly compatible with those of imaging, immediate rebiopsy is recommended.

10.6 Complications

Bleeding during the intervention can terminate the procedure or can lead to impaired assessment of the biopsy. The lesion can be displaced by bleeding, and thus lead to inadequate biopsy acquisition and marker position. Hematoma usually resolves with compression and does not delay subsequent surgery. Further complications are infection or vasovagal reactions. Significant scarring has been denied by previous authors (Perlet et al. 2006).

Some patients suffer from neck pain from lying prone and are thus unable to complete the procedure. Because of strong patient motion, the biopsy may prove to be unsuccessful. Sometimes the intervention is complicated because needle artifacts obscure the lesion site (Schnall 2000). A problem of clip placement may be the migration along the track when the breast compression is released (Berg et al. 2006).

Summary

Careful patient selection for diagnostic MR mammography is crucial to limit the number of lesions that require biopsy and, thus, lead to unnecessary patient anxiety and avoidable procedural costs. Lesions that are only visible by MR imaging should undergo MR-guided vacuum-assisted biopsy. A benign diagnosis definitely avoids surgery. In the case of malignancy, optimized planning of the oncosurgical approach is possible. If MR-guided vacuum-assisted biopsy is not possible, MR-guided wire localization may be performed, followed by surgical excision. MR-guided core-needle biopsy has proven to be disadvantageous because of the small size of tissue cores. MR-depicted lesions smaller than 5 mm do not necessarily require biopsy because of a very low incidence of malignancy. However, if the lesion persists on the follow-up MR imaging and the patient desires definitive workup, a biopsy can be accomplished. Diagnostic biopsies can be performed in closed or open magnets. The most essential advantage of the open magnet is that the intervention can be performed under real-time fluoroscopy.

Key Points

- Indication: lesion detected or best visualized by MR imaging only
- Contraindications: pacemaker, metallic implants, impaired coagulation
- Thorough planning of the intervention: mammography, targeted ultrasound, preinterventional MR imaging
- Biopsy: if done in a closed bore it needs to be performed as quickly as possible because of washout of contrast medium and patient motion
- Clip placement after biopsy for surgical planning
- Postinterventional MR imaging of the entire breast
- Postinterventional mammography to document clip position
- Structured and overly accurate report for the pathologist
- Follow-up: MR-guided wire localization and surgical excision in the case of malignancy

References

Berg WA, Birdwell RL, Gombos EC, Wang SC, Parkinson BT, Raza S, Green GE, Kennedy A, Kettler MD (2006) Diagnostic imaging: breast, 1st edn. Amirsys, Salt Lake City

Fischer U, Kopka L, Grabbe, E (1998) Magnetic resonance guided localization and biopsy of suspicious breast lesions. Top Magn Reson Imaging 9:44–59

Gehl HB, Frahm C (1998) MR-gesteuerte Biopsien. Radiologe 38:194–199

Kuhl C (2007) The current status of breast MR imaging. Radiology 244(2):356–378

Liberman L, Morris EA, Dershaw DD, Thornton CM, Van Zee KJ, Tan LK (2003) Fast MRI-guided vacuum-assisted breast biopsy: initial experience. AJR Am J Roentgenol 181:1283–1293

Liberman L, Mason G, Morris EA et al. (2005) Does size matter? Positive predictive value of MRI-detected breast lesions as a function of lesion size. AJR Am J Roentgenol 186:426–430

Perlet C, Heywang-Kobrunner S, Heinig A, Sittek H, Casselman J, Anderson I, Taourel P (2006) Magnetic resonance-guided, vacuum-assisted breast biopsy: results from a European multicenter study of 538 lesions. Cancer 106:982–990

Rausch DR, Hendrick RE (2006) How to optimize clinical breast MR imaging practices and techniques on your 1.5-T system. Radiographics 26:1469–1484

Schnall MD (2000) MR-guided breast biopsy. In: Lufkin RB (ed) Interventional MRI. Mosby, St Louis, pp 315–319

Tozaki M, Yamashiro N, Fukuma E (2007) MR-guided vacuum-assisted breast biopsy using a non-titanium needle. Magn Reson Med Sci 6:259–264

Drainage

11

Roman Fischbach and Christian Hohl

Contents

11.1 Drainage in Abscess

Roman Fischbach

11.1.1 Introduction

Abscess formation is associated with significant morbidity and mortality, despite the availability of potent antibiotics. Undrained abscesses result in a mortality rate of 50–80% (Gervais and Dawson 2006). Therefore, early diagnosis and subsequent open surgical or percutaneous drainage are still the most important factors influencing successful abscess treatment. The main goal in drainage procedures is to decompress and drain as much pus as possible so that antibiotics will be (more) effective. The major benefit of the procedure, however, occurs at the time of intervention when the collection is evacuated (Mueller et al. 1984). This can lead to recovery of an unstable, critically ill patient within a matter of hours. Continued external drainage adds to the initial therapeutic effect.

Catheter drainage provides a rapid means of therapy with relatively simple devices and techniques and yields a high success rate with few complications. Percutaneous drainage either may be the only therapy necessary to effectively treat an abscess or will delay and downstage a necessary surgical procedure, decreasing surgery's risks (Aeder et al. 1983). Over the last 20 years, image-guided percutaneous abscess drainage has become accepted practice, replacing open surgical drainage in the vast majority of cases (van Sonnenberg et al. 2001). Especially in deep locations or complicated anatomic relations, introduction of cross-sectional imaging has facilitated diagnosis of abscess and access planning. Today, image-guided percutaneous aspiration and drainage is among the most frequent interventional procedures performed. Close follow-up of catheter drainage, adjunctive antibiotic therapy, controlled irrigation, and sometimes application of lytic agents to facilitate drainage of viscous fluid collections are necessary to ensure treatment success (Park et al. 1993). Follow-up imaging is important to document successful resolution of a fluid col-

Mahnken/Ricke (Eds.), *CT- and MR-Guided Interventions in Radiology*

lection. Minimal tube drainage alone does not necessarily equate with resolution of a fluid collection as the tube may be blocked, dislodged, or simply too small to drain the abscess content. Imaging remains crucial to identify an underlying cause for abscess development. If, for example, an enteric fistula is diagnosed, the fistula must heal before the drainage tube can be successfully removed.

11.1.2 Diagnosing Abscess

Prior to making a treatment decision the proper diagnosis of an abscess has to be established. This may by difficult especially in the postoperative patient in whom clinical symptoms of infection are common and oftentimes nonspecific. Ultrasound and computed tomography (CT) are commonly used to diagnose or rule out abscess formations, with CT being the preferred diagnostic method in most institutions. Ultrasound is readily available and is very reliable in diagnosing fluid collections. Still, extensive surgical wounds or dressings, obesity, and air-filled bowel may impair ultrasound but do not hamper CT. In addition, CT is ideal for image guidance in percutaneous drainage procedures or diagnostic needle aspiration. On the other hand, CT carries a significant radiation exposure, which has to be kept in mind when frequent follow-up imaging is necessary, as in patients suffering from enteric fistulae. Coronal or sagittal reformations from thin-slice CT sections are helpful in exactly describing the location of a fluid collection and neighboring structures. Delineating bowel anatomy in additional planes significantly helps differentiation of fluid-filled bowel loops from extraluminal fluid. In order to further improve the diagnostic quality of CT in questionable cases, delayed scans after additional oral or rectal contrast administration may help to distinguish bowel from extraluminal fluid collections especially in the pelvis. Delayed images after intravenous contrast administration help to differentiate a contrast-filled urinary bladder from fluid in the pouch of Douglas.

Strong signs of an abscess are a well-circumscribed fluid collection, thickened membranes or septations, gas bubbles, rim enhancement, and debris. Extraluminal air-fluid levels or air detected in an intrahepatic fluid collection renders an imaging diagnosis of an abscess very likely. Weaker signs are nonloculated or thin-walled nonenhanced collections that may have alternative explanations, such as peritoneal or pleural fluid. The differential diagnosis of potential abscess formations is substantial. Differential diagnosis of hepatic abscesses includes simple and complicated cysts, echinococcal cysts, hematoma, cystadenocarcinoma, and necrotic malignancies (Fig. 11.1). An abdominal fluid collection may include primary and secondary malignancy as well as benign processes such as hematoma, bilioma, pancreatic pseudocyst, or just distended bowel loops. The classic ultrasound appearance of an abscess as a well-circumscribed round anechoic lesion with posterior acoustic enhancement is found in less than 50% of abdominal abscesses. On the other hand, there are no imaging signs that exclude the infectious cause of an intraabdominal fluid accumulation. As specific signs are rare (less than 20% of hepatic abscesses reveal air inclusions) and the appearance of a fluid collection is quite variable depending on location, age, and composition, image interpretation remains a difficult task by either CT or ultrasound. In conclusion, any extraluminal fluid collection in the proper clinical setting is potentially an abscess and warrants further workup.

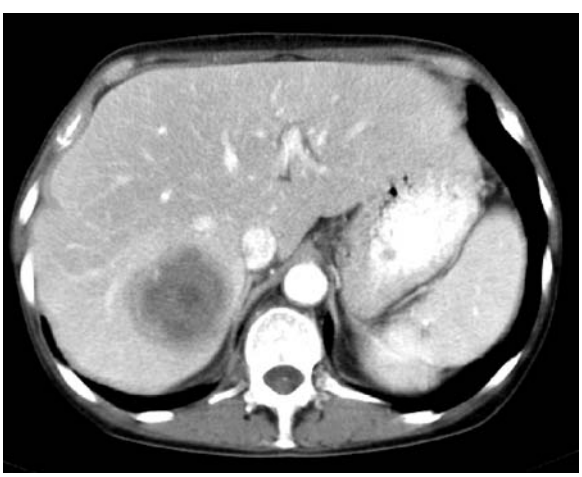

Fig. 11.1 Patient with fever. Computed tomography (CT) shows a hypodense mass in the right liver lobe. An abscess was included in the differential diagnosis, but needle aspiration revealed no fluid. Biopsy was performed and non-Hodgkin lymphoma was diagnosed

11.1.3 Indications and Contraindications

With any suspicious fluid collection a reliable diagnosis must be reached without significant delay. In the clinical setting, needle aspiration is the method of choice to clarify the nature of a fluid collection, as it can quickly confirm its infectious nature and will provide information on the viscosity or fluidity as well as the composition of a fluid collection (Fig. 11.2). This in turn will help to determine whether the abscess is amenable to catheter drainage and which type of catheter to choose (Mueller et al. 1984).

Thus, indications for percutaneous abscess drainage are straightforward, serving therapeutic and diagnostic purposes. Diagnostic information will be obtained from aspiration material. It should be preserved for microbiologic assessment to determine the microorganism causing the infection and for antibiotic testing. Small collections up to 3 cm in diameter may be successfully treated by aspiration and irrigation alone (Wroblicka and Kuligowska 1998).

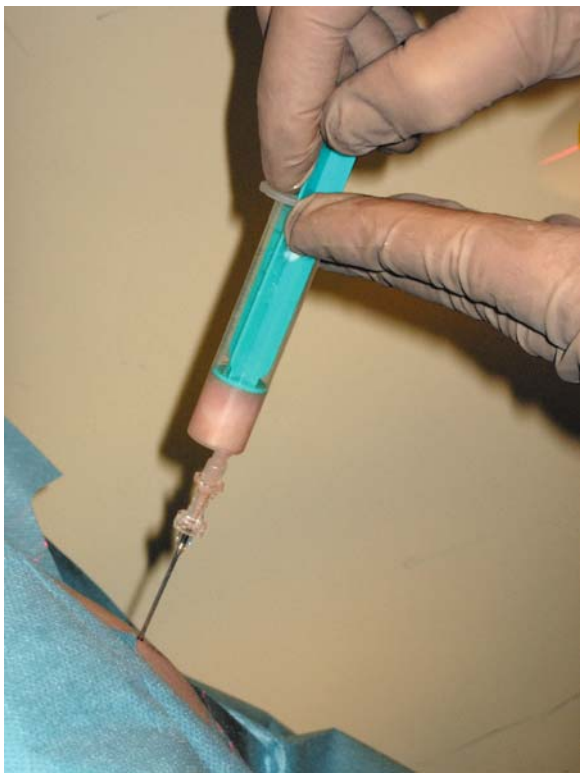

Fig. 11.2 CT-guided aspiration of a suspicious fluid collection. Abscess is confirmed as pus is aspirated

If a diagnosis of an abscess is made, the decision to proceed to drainage depends on:

- A safe access route
- Acceptable coagulation parameters
- Informed consent from patient or appropriate others

Absolute contraindications to percutaneous drainage are rare as treatment alternatives with smaller risk basically do not exist. Only in cases where no safe route for drainage can be determined, e.g., if a lesion is surrounded by bowel or if a high-flow enteric fistula is suspected, open surgical drainage may be preferred. Bleeding diatheses which cannot be corrected are another rare (relative) contraindication.

11.1.4 Material

All required materials have to be prepared prior to the intervention and should be readily available to ensure an uninterrupted procedure. The different procedure steps (access planning, needle aspiration, drainage) determine the material needed.

The access site is usually determined from axial CT images. To identify the skin entry site, a radiopaque marker attached to the patient's skin in the vicinity of the intended entry site is helpful. A simple wire or needle may serve as a marker; however, a grid made of an angiographic catheter (Fig. 11.3) or commercially available grids are easier to use, as the distance from a specific marker to the planned entry site is easier to gauge. A felt-tip marker to mark the skin site and a ruler to measure the distance between the marker and the entry site should be available. Alcohol spray or povidone iodine are used for skin disinfection.

The procedure tray should be large enough so that all materials needed can be placed on the tray and are within reach. The basic tray should contain sterile draping material, a long 21G needle for deep anesthesia infiltration, two 10-ml syringes, one for local anesthesia (1% mepavicain, lidocaine, or prilocaine) and another one for fluid aspiration, and a scalpel for skin incision (Fig. 11.4). A sterile microbiology vial for fluid aspirate should be prepared. In most cases an 18G, 15-cm trocar-type needle is used for diagnostic puncture and aspiration of fluid. The 18G needle is easy to control and to image and accepts a stan-

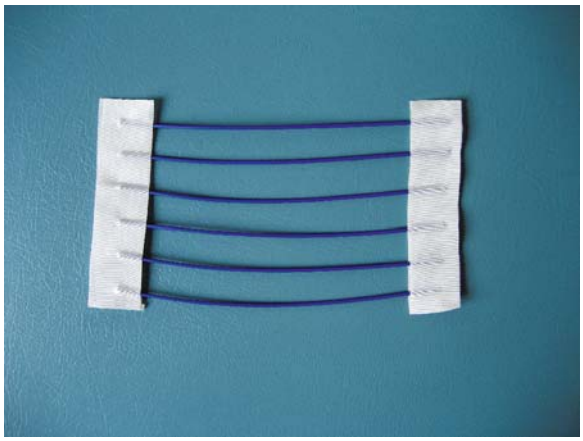

Fig. 11.3 Grid for marking the skin entry site made of angiographic catheter segments taped at the ends

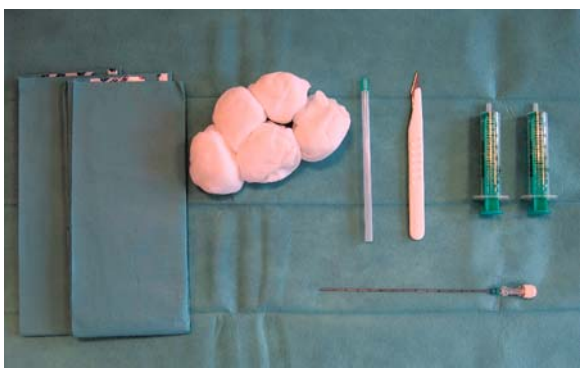

Fig. 11.4 Procedure tray for CT-guided puncture and aspiration. The initial tray has sterile draping material, a 21 G needle for local anesthesia, a scalpel for skin incision, an 18 G puncture needle, and two syringes for local anesthetics and aspiration

dard 0.035-in. guidewire for placement of drains using the Seldinger technique. A smaller needle may be preferred for a challenging localization to minimize puncture risk but at the expense of a significantly higher resistance to fluid flow. Therefore, a small needle carries the risk of false-negative aspirate as only clear supernatant may return through the needle. Furthermore, a 0.018-in. wire has to be followed by a coaxial dilator, which increases the necessary steps to complete the procedure and therefore carries higher cost. Moreover, a 0.018-in. guidewire is less stable than a heavy-duty wire and may dislocate when a coaxial dilator is introduced. In easily accessible abscesses a direct puncture using the trocar technique may be applied, omitting the need for a guidewire.

Other material needed should be at hand but should not be put on the procedure tray until the diagnosis of an abscess has been confirmed by aspiration. At that point an appropriate drainage katheter, a guidewire, a three-way stopcock, a drainage bag, skin fixation material, and wound dressing will be required.

11.1.4.1 Guidewire

For the Seldinger technique, supplies include a 0.035-in.-diameter, 90-cm extrastiff guidewire, a set of hydrophilic dilators (e.g., 8, 10, and 12 F) and a drainage catheter. A variety of guidewires are available for percutaneous abscess drainage with different properties and prices. Guidewires should be short to make their use convenient with short drainage catheters. The wire stiffness is crucial to guide the dilator and the catheter into the abscess; however, the wire tip needs to be floppy and several centimeters long to let the wire coil within the abscess and to prevent perforation of the abscess wall. Stainless steel is cheaper and stiffer than Nitinol but does not have Nitinol's kink resistance (Schroder 1993a, b).

11.1.4.2 Drainage Catheter

Commercial drainage catheters come in a wide variety of sizes and materials. Most catheters have a curved tip or pigtail configuration and come with a stiff inner metallic cannula and/or a more flexible plastic cannula. Many drainage catheters come with the option of being deployed as a trocar. In this case a stylet is placed inside the cannula.

As the drainage catheter is rather soft and flexible, dilation of the access tract is necessary before a tube is advanced into an abscess cavity. Dilators are well known from vascular procedures and most products now have a hydrophilic coating rendering them slippery when wet. Effective drainage is usually accomplished by 8- or 10-F catheters in small nonviscous collections. If the fluid can be easily aspirated by a 10-ml syringe through an 18 G needle, then the abscess fluidity will allow drainage with a single lumen 8- or 10-F catheter system (Gobien et al. 1985). The drainage catheters have multiple side holes and a curved tip (Fig. 11.5).

Larger tubes, such as 12–16-F drainage catheters are used when the contents are viscous or debris-laden. These larger catheters are usually available as double-lumen sump catheters. The sump catheter has a bigger lumen for drainage and a smaller lumen, which

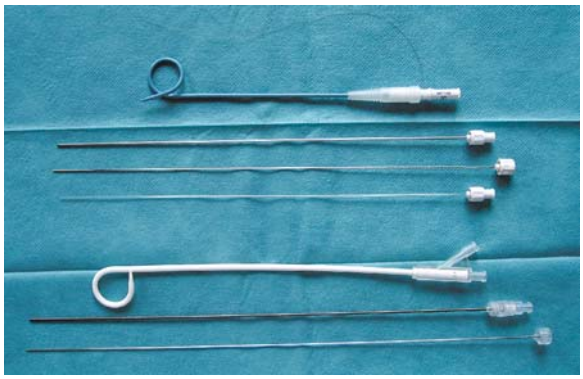

Fig. 11.5 An 8-F pigtail-shaped drainage catheter with an inner metallic cannula, an optional plastic cannula, and a trocar-type stylet in the *upper half* and a 12-F double-lumen sump catheter in the *lower half* (note the side port). The double-lumen catheter comes with an inner metallic cannula and a stylet

allows for circulation of room air into the abscess to avoid adherence of the abscess wall to the side holes of the catheter. Most double-lumen catheters come with an air filter that can be attached to the small lumen. The small lumen also serves for irrigation of the abscess. Sump drainage has a demonstrated higher efficiency than closed drainage and is the most common approach to infected fluids (van Sonnenberg et al. 2001). For complex abscesses containing necrotic tissue as in severe pancreatic necrosis or some empyemas, a catheter of 24–30 F might be necessary (van Sonnenberg et al. 1997). Initial catheter placement can almost always be performed using a 12-F system. In cases with complicated clinical course or debris detected on follow-up imaging, a small lumen catheter is easily exchanged for a larger lumen catheter later.

11.1.5 Technique

11.1.5.1 Patient Preparation

In order to ensure an efficient workflow, all possible scenarios need to be considered and should be planned for and discussed with the patient and the referring physicians prior to the diagnostic examination. A patient suspected of suffering from abscess may reveal normal unremarkable examination findings with no indication for percutaneous treatment, or may show an unspecific or suspicious fluid collection. In this case diagnostic needle aspiration or placement of a drainage catheter may follow the diagnostic study. Depending on the location and the composition of the fluid collection, the access route may be technically demanding and can carry specific risks. The patient therefore should be informed about the suspected diagnosis and about the possible necessity of a diagnostic needle aspiration or drainage as well as alternative treatment options.

Since obtaining informed consent with the patient on the CT table or even inside the examination room may not be accepted as legally correct in many countries, the informed consent statement should be signed before the examination begins. If the likelihood of infected fluid is low, the diagnostic scan can be completed first and the drainage is planned as a two-step procedure with separate discussion of potential risks of a drainage procedure. If intervention carries significant risks due to complexity of the abscess or intervening or adjacent vital structures, the patient should be informed accordingly and obtaining a detailed signed consent statement is advised. In these complex cases the clinical situation and the procedure as well as alternatives should be explained to the patient and need to be discussed with the referring clinicians.

Since percutaneous drainage is performed using standard aseptic technique and local anesthesia. The patient should have a well functioning intravenous access line and needs to be on antibiotics prior to the procedure. Intravenous broad-spectrum antibiotics covering multiple organisms should be initiated shortly prior to the procedure to address bacteremia resulting from catheter manipulation. If this is started not earlier than 1 h before the procedure it will not affect microbiological analysis. Postinterventionally, antibiotics are continued until a more appropriate agent is selected from the result of microbiological testing.

Usually, generous administration of local anesthesia is sufficient to perform the procedure without significant patient discomfort. One has to consider that the efficacy of local anesthetics is reduced in acidic milieu as it is present in infection. Particularly anesthesia of the abscess wall may not be possible with local anesthetics. In challenging access routes, sedation improves the safety of the procedure by reducing patient motion. However, there is a trade-off with patient cooperation. If sedation is necessary, adequate monitoring of the patient's vital signs (pulse oximetry, ECG) and specially trained personnel are required (see Chap. 5).

11.1.5.2 Abscess Drainage

Common locations for abscess formations are subphrenic, perihepatic, perisplenic, iliopsoas, abdominal wall, and pelvis. If a suspicious fluid collection is identified on a diagnostic CT examination, potential access routes have to be identified. The optimum access route is determined by the following:

- Shortest pathway
- Easiest angulation or localization
- Avoidance of intervening or adjacent structures
- Most convenient catheter location for the patient

Patient positioning largely depends on the location of the suspicious fluid collection and possible access routes. Superficial abscesses of the left or right liver lobes may be easily approached through a simple route in the axial plane on CT. Collections in the cranial part of the liver or spleen as well as subdiaphragmatic abscesses after liver or spleen surgery may be accessed using cranial angulation to avoid the pleural space. If cephalocranial angulation is necessary, gantry tilt might improve access planning (Maher et al. 2004). If gantry tilt is not possible, the triangulon method can be employed to plan needle angulation. Real-time ultrasound guidance may be superior to sequential CT in such cases. CT fluoroscopy is a helpful alternative imaging technique providing real-time images and therefore providing excellent guidance and monitoring of a puncture.

Multiplanar magnetic resonance (MR) imaging may be an alternative modality for image-guided drainage procedures (Buecker et al. 2001; Kariniemi et al. 2006). Using fast sequences and MR-compatible material, one can successfully complete percutaneous drainage using MR guidance. Still, MR guidance is rarely applied as patient access, patient monitoring in critically ill patients, and visualization of the puncture needle and guidewire are inferior to those in CT or fluoroscopy. Prolonged procedure times and limited access to MR systems further hamper widespread use of MR for percutaneous drainage procedures.

Bowel injury must be avoided owing to its high risk of peritonitis. Bowel transgression is of concern, particularly of the colon. The (small) bowel might be traversed when all alternatives have a less favorable risk–benefit ratio. One has to avoid aspiration of "low-probability" collections, such as hematoma through the colon.

If vital organs cannot be excluded from the access path, bleeding risk, especially in splenic puncture, has to be considered. A transpleural passage should be avoided especially in subphrenic abscess to prevent infectious spread to sterile pleural effusions. For a solid organ abscess (e.g., of the liver), the access route should traverse a small amount of normal organ parenchyma to reduce the risk of peritoneal spillage and bleeding (Men et al. 2002).

In pelvic or retroperitoneal abscesses as well as paraspinal collections the patient is placed in a prone or lateral position (Fig. 11.6). The prone position is more stable, but is less well tolerated by the patient as positioning of the patient's arms is difficult in the CT/MR gantry or breathing is impaired from chest compression or neck stiffness in elderly or ill patients. In our experience a lateral position facilitates comfortable positioning of the patient and improves access to the patient and is better tolerated than the prone position. The patient, however, can move more freely and anatomic landmarks may be obscured, making route planning more difficult. Once the access route has been planned, the patient is positioned accordingly. The abscess is located using a short spiral scan with a radiopaque marker or grid attached to the skin at the level of the lesion (Fig. 11.7). From the relation of the external marker to the underlying abscess formation, the exact skin entry site and the angulation of the access path are determined.

Using the laser light, one should chose the height of the CT table in a way that the desired entry site is in or below the center of the gantry. The distance from the skin marker to the entry site is assessed and marked on the skin with a felt-tip pen. Thereafter the patient can be moved out of the gantry for skin disinfection and appropriate draping. Then local anesthesia is applied. In difficult access routes, the small-caliber needle used for anesthesia can be left in place to check the entry point and angulation. Careful skin infiltration and infiltration of the entire access path should be performed. The peritoneum and pleura are very sensitive and sufficient local anesthesia improves patient compliance when dilating the puncture tract or advancing the drainage catheter.

In general there are two basic puncture techniques:

1. Seldinger technique (over the wire)
2. Trocar technique (direct puncture)

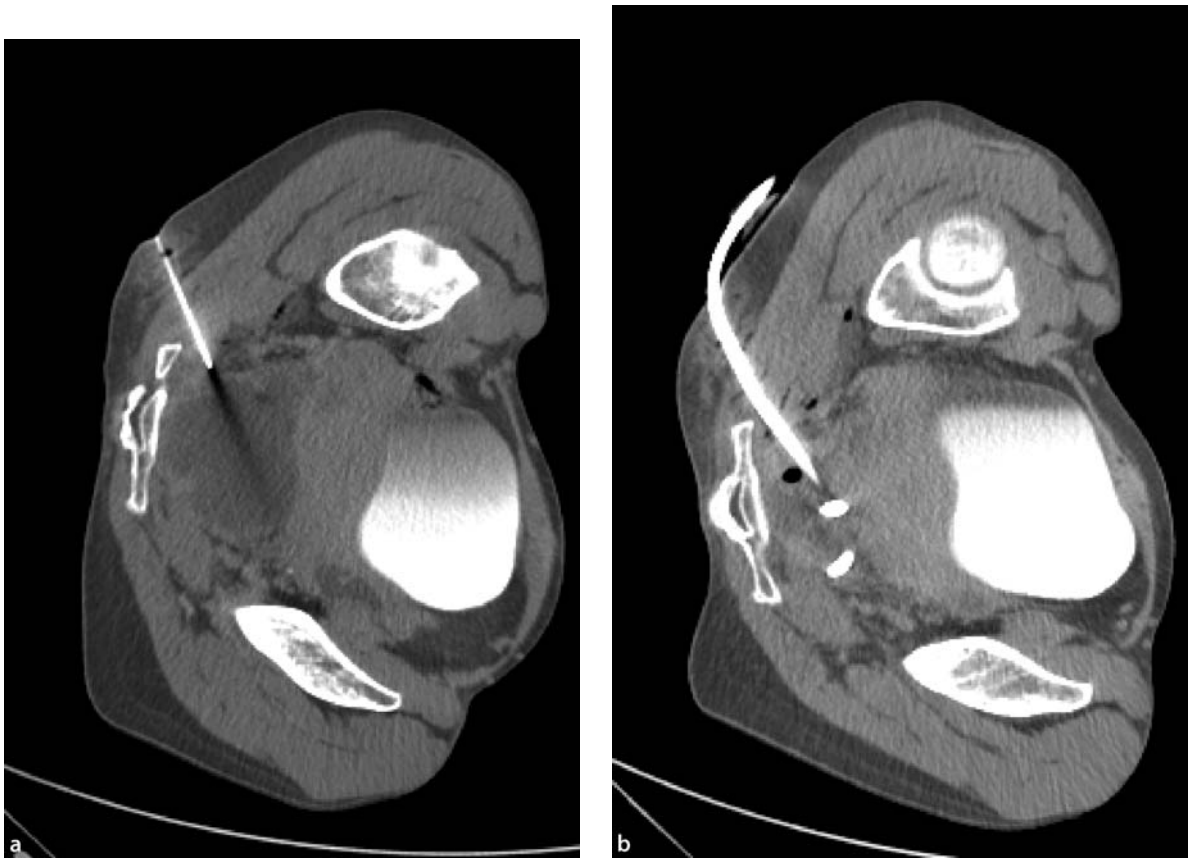

Fig. 11.6a,b Patient with recurrent abscess formation in the presacral and perirectal space suffering from Crohn's disease. The patient is positioned in a left lateral position and a transgluteal access is chosen. The needle is advanced into the fluid collection (**a**). Pus was confirmed and a 12-F sump catheter was introduced using the Seldinger technique (**b**). After evacuation, the abscess cavity has markedly decreased in size

If the Seldinger technique is used, an 18 G needle is advanced into the lesion. In deep locations, the puncture tract can be infiltrated with local anesthetics through the 18 G puncture needle as the needle is advanced. Needle advancement can be controlled by repetitive single scans or CT fluoroscopy. Especially in complex access routes CT fluoroscopy greatly improves puncture safety and speed as the advancement of the initial puncture needle can be monitored online (Daly et al. 1999). The abscess wall is usually felt as a tender resistance. The needle should be advanced with a short, firm motion into the collection. Once the intended puncture depth has been reached or passage through the abscess capsule is felt, diagnostic aspiration is performed. If fluid is purulent, catheter placement follows.

If a larger abscess or viscous fluid is present, a guidewire is advanced into the abscess through the needle. Care has to be taken to avoid perforation of the abscess wall. Usually a resistance is felt when advancing the guidewire and the wire starts to coil in the collection. If the position of the guidewire tip is uncertain, an axial control scan or a short scout view should be obtained. Once the guidewire has reached the desired position, it is critical not to lose guidewire access during the procedure. When access is lost, reentry may be difficult because of spontaneous decompression of the abscess or difficulties in imaging due to access tract manipulation especially in challenging anatomic situations.

Once the guidewire is secure, the puncture needle is carefully withdrawn, keeping the guidewire in place. Then, the puncture tract is dilated using hydrophilic coated dilators. Coated dilators greatly ease dilator passage compared with standard dilators with-

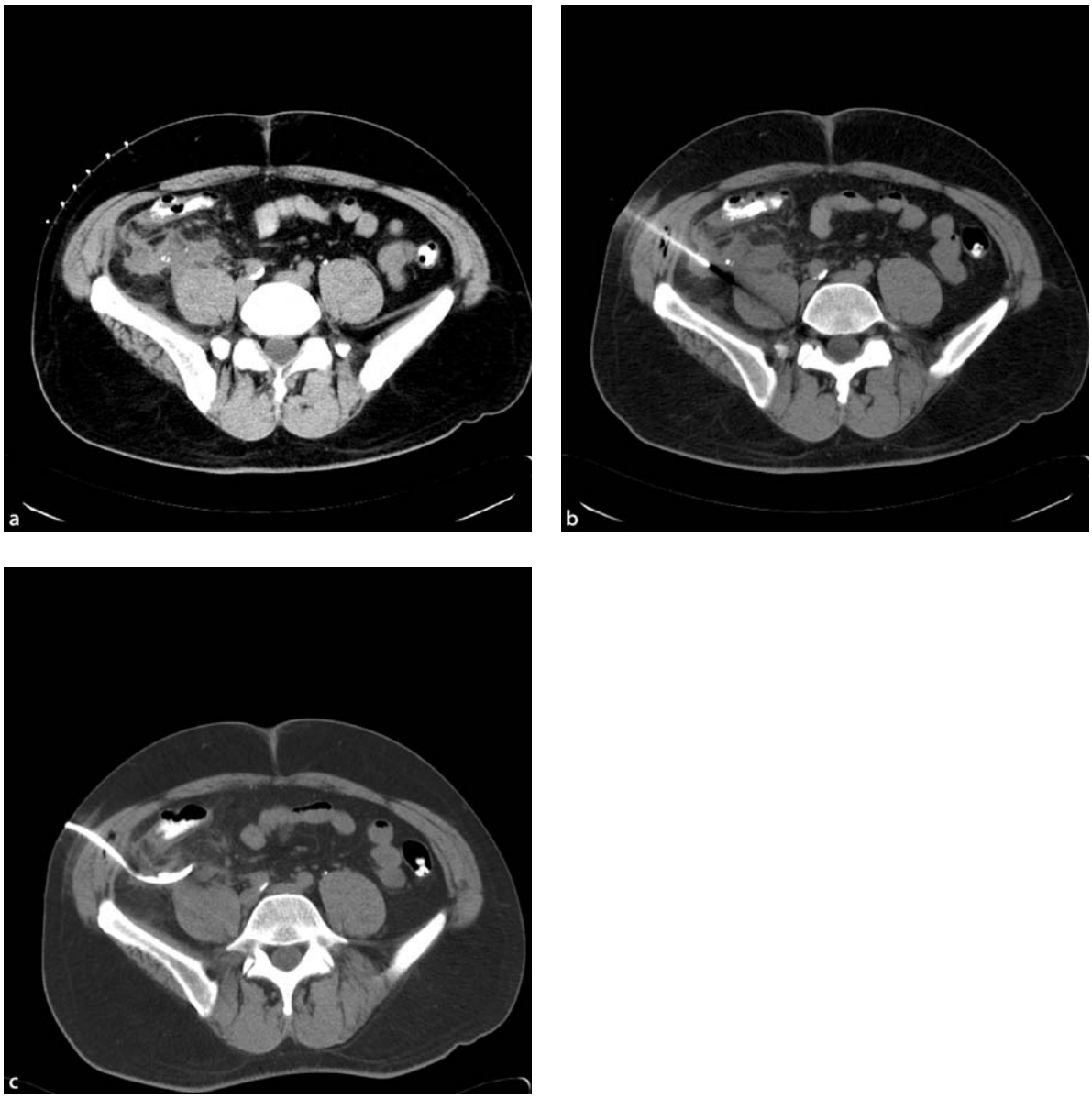

Fig. 11.7a–c Patient suffering from fever and groin pain after laparoscopic appendectomy. A fluid collection is identified in the cecal region. A radiopaque grid marker is positioned over the planned skin entry site (**a**). After local infiltration with an anesthetic, an 18 G needle is advanced (**b**). After aspiration of pus, a guidewire is introduced and a 10-F drainage catheter is positioned in the abscess cavity. The cavity is irrigated with saline and as much fluid as possible is evacuated (**c**)

out a coating. The effect is similar to that of a hydrophilic guidewire; therefore, the dilator should be moistened with saline to make it wet and slippery. Depending on the push resistance, it can be advisable to slightly overdilate the tract to the next dilator size to facilitate catheter passage. When encountering difficulties passing the dilator or drainage tube, one should make sure that the skin incision is large enough and that no strands of subcutaneous connective tissue have remained. If the skin tents up with gentle backward pull on the dilator or catheter, the incision should be enlarged.

When resistance to passing the dilator or catheter persists, the wire may kink under the skin. In these

cases it may be helpful to slightly withdraw the wire and advance the dilator over the kink and then slowly readvance the unit. The guidewire needs to be held straight. In bigger patients the procedure is facilitated by compressing the skin and holding the catheter close to the skin. If this fails, either a bigger dilator is needed or the catheter has to be exchanged for a smaller or more rigid system. A hydrophilic 5-F dilator can almost always be advanced. Once the dilator has reached the abscess, a kinked or soft guidewire can be exchanged for a stiffer wire. Therefore, it is crucial to continuously maintain guidewire access to the lesion.

Once the access tract has been secured and dilated, the drainage catheter is placed over the guidewire. In most cases a drainage catheter will be placed with an inner-stiffening cannula using an over-the-wire technique. When the metal cannula is used, the catheter–cannula combination is straightened and can be advanced as a unit into the fluid collection. It is helpful to measure the distance from the skin to the central abscess using the CT caliper to better estimate how far the catheter needs to be advanced. Once the catheter tip has reached the lesion, the inner-stiffening cannula is unlocked from the catheter. The catheter is then deployed like an intravenous catheter. The guidewire and inner cannula is held steady while the catheter is further advanced into the abscess. All catheter side holes need to be within the abscess cavity to prevent contamination of intervening spaces. Once the catheter is in place, the cannula can be removed.

Depending on the individual situation, the guidewire may remain in place when obtaining control images to check for the catheter position. If the catheter is documented well with the abscess, the guidewire is removed and fluid is evacuated.

Easily accessible abscesses may be drained with the trocar technique where a stylet is placed in the inner cannula. After the tip of the stylet and the inner cannula have reached the inside of the abscess, the stylet is removed and fluid is aspirated. If aspiration proves the correct catheter position, the catheter is advanced over the cannula, which is held in place until all side holes are inside the fluid collection. Thereafter the cannula is removed.

In order to drain as much pus as possible, the catheter should be flushed with 10–20 ml of saline. The fluid is aspirated and irrigation can be repeated several times to facilitate initial removal of debris and viscous fluids. If clear fluid returns, a CT scan should be obtained to document the size and residual filling of the abscess cavity. In abdominal or pelvic abscesses, opacification of the cavity with a solution of iodinated contrast material and saline (1:30) (Fig. 11.8) is performed to diagnose enteric fistula (Harisinghani et al. 2002) and to prove drainage of the entire fluid collection. This is particularly useful in septated abscess formations. Additional catheter manipulation or placement is based on these results.

Finally the catheter is fixed to the skin. Careful attention must be paid to securing the drainage catheter, as the most common postdrainage problem is catheter dislodgement. The classic approach in surgery is skin fixation of the drainage tube, which still is the most reliable fixation method. Various adhesive-type fixation devices are available, and can be used if skin suture has to be avoided or if short-term drainage is planned. If adhesive securing devices are used, two devices placed in tandem may prevent premature dislodgement.

11.1.5.3 Special Considerations

Spleen

Because of the vascularity of the spleen, coagulation parameters should be checked carefully and the catheter tract should traverse as little uninvolved spleen parenchyma as possible. In planning the access to a splenic abscess, structures such as colon, kidney, or pleura have to be avoided. Especially transpleural passage is of concern, as spread of the infection to an involved body compartment should be avoided. Therefore, access route planning should be done in deep inspiration to improve visualization of the pleural recess. The access route typically is steeply angulated in the caudocranial direction. CT fluoroscopy with close online control of the needle passage has greatly improved successful access to this difficult location. Multislice CT scanners with simultaneous display of four or more sections are very helpful to control angulations that cannot be followed by tilting the gantry. However, even if transpleural passage is discouraged, it may occur inadvertently (McNicholas et al. 1995).

Pancreas

Pancreatic abscesses are more difficult to treat than infected collections in pancreatitis. They are frequently septated, often associated with fistulas, and contain necrotic debris (Fig. 11.9). Combination of multiple

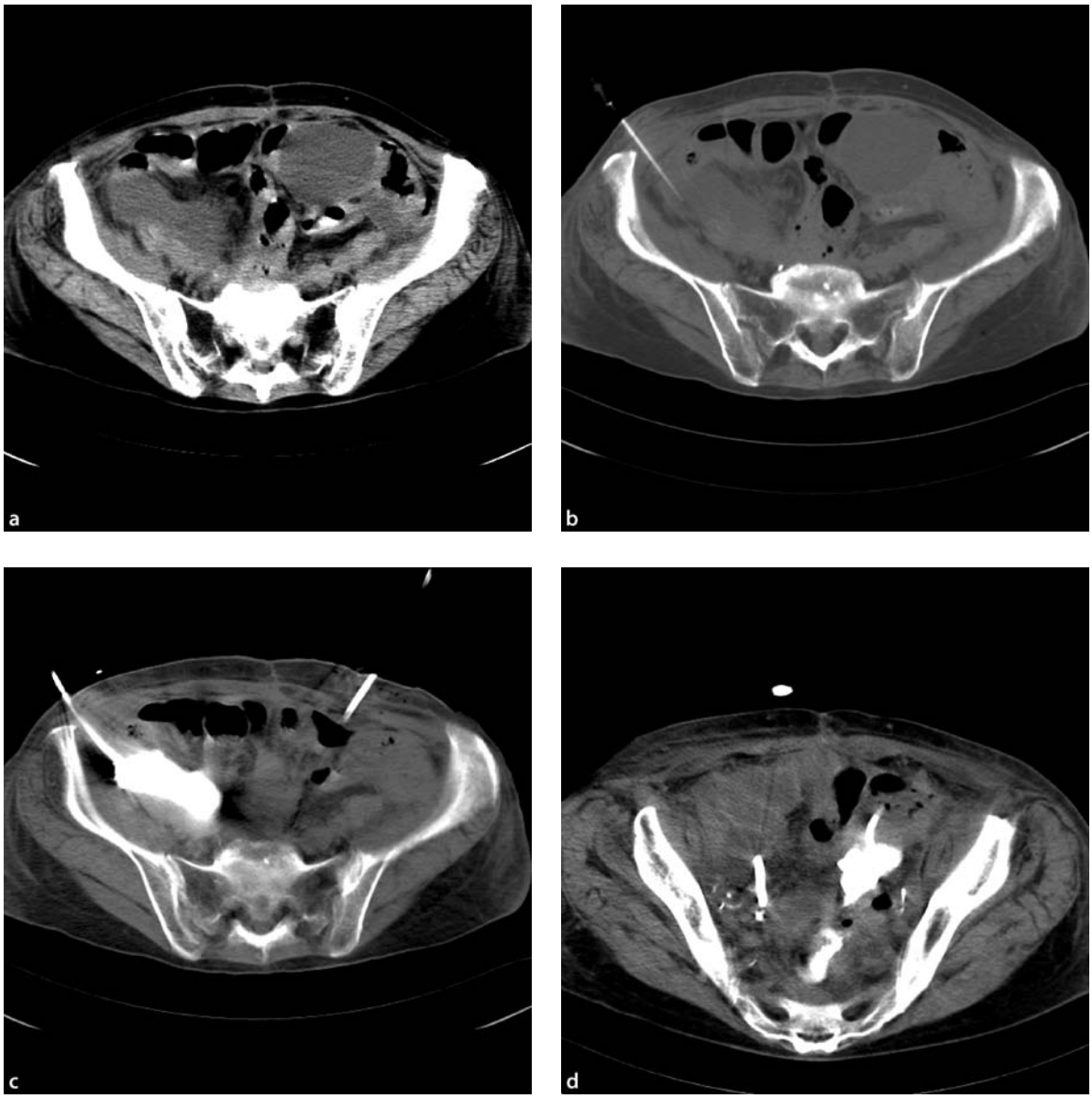

Fig. 11.8a–d Patient with multiple pelvic fluid collections after surgery for ovarian cancer (**a**). Needle aspiration revealed pus and a drainage catheter was placed in the right iliac abscess and the paramedian fluid collection (**b**). After evacuation and irrigation follow-up, imaging was performed after 2 days. The *right* cavity shows no communication with the intestine (**c**). When the left abscess cavity is filled, contrast is seen in the sigmoid and rectum, establishing the diagnosis of an enteric fistula (**d**)

drainage procedures with surgery may be necessary to successfully treat this type of abscess (Ferrucci and Mueller 2003). Drainage alone therefore is rarely the only method of therapy, but catheter drainage may improve the clinical situation of a patient to improve surgical outcome. Percutaneous treatment in pancreatitis has to consider the spread of pancreatic fluid into the lesser sac, pararenal space, and pericolic areas. Interventional treatment in infected pancreatic fluid collections requires aggressive therapy with large-lumen catheters to allow evacuation of viscous fluid and necrotic tissue. Close follow-up with imaging and clinical evaluation to identify complications or an unfavorable clinical course early is necessary.

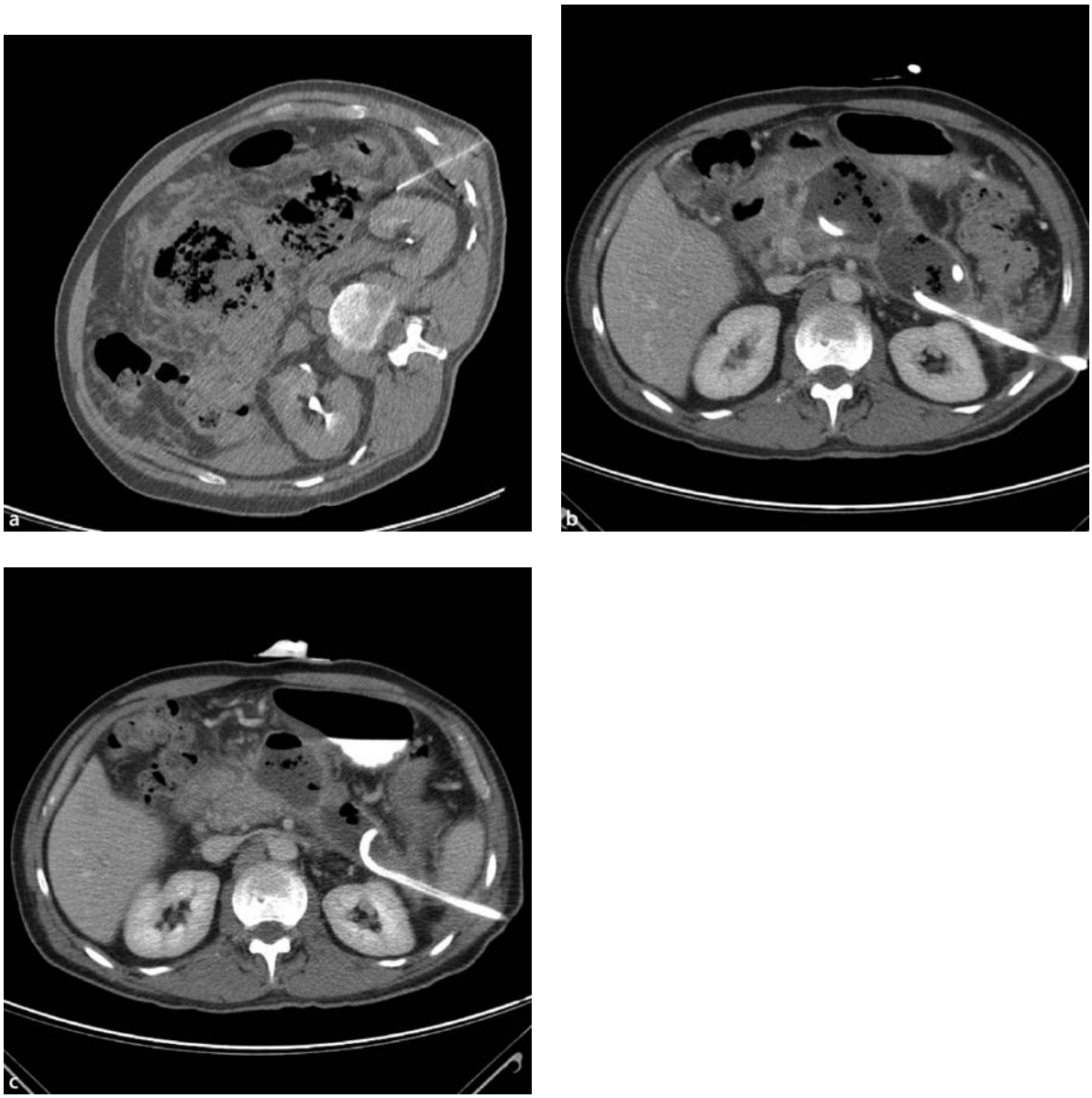

Fig. 11.9a–c Left lateral access to the pancreas in severe necrotizing pancreatitis. The puncture was performed with CT fluoroscopy guidance to access the pancreatic tail region, avoiding bowel injury by passing close to Gerota's fascia (**a**). A second drainage catheter was placed from a ventral access. The follow-up scan after 4 days with continuous irrigation and significant clinical improvement depicts the two catheters in place (**b**). The pancreatic bed is fluid-filled and contains air bubbles as well as necrotic tissue. Follow-up CT after 2 weeks with both catheters still in place shows a further decrease of the abscess cavity (**c**)

Psoas and Iliacus Muscle

Psoas abscess typically occurs secondary to disc infection or spondylodiscitis (Mückley et al. 2003). Other causes are retroperitoneal spread of diverticulitis or appendicitis or direct involvement from renal or pancreatic infections. Pain is frequently referred to the flank, hip, or knee, which makes clinical diagnosis difficult. With CT or MR, psoas enlargement and fluid accumulation in the muscle are easily depicted. In lumbar locations, drainage is performed from a posterior approach (Fig. 11.10). In pelvic spread an anterior

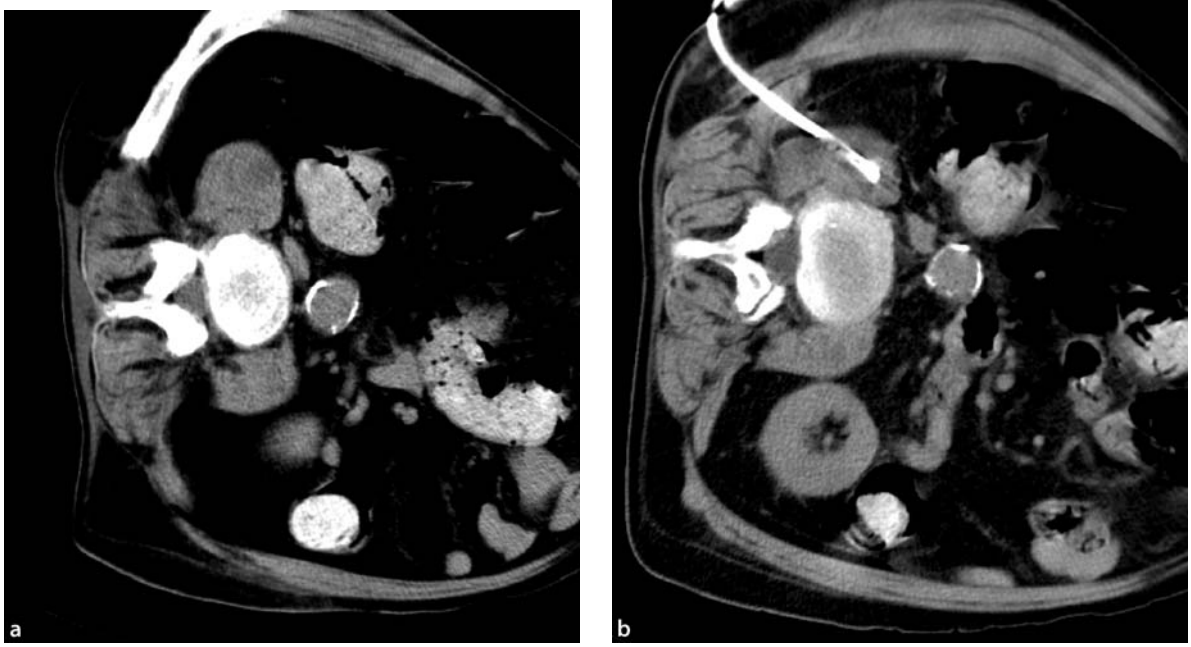

Fig. 11.10a,b Patient with right-sided psoas abscess. The psoas muscle is enlarged and a hypodense area representing the abscess formation is depicted (**a**). After puncture and aspiration, a sump catheter is placed within the abscess via a dorsal approach (**b**)

approach from the iliac rim into the iliacus or psoas avoiding the bowels is used.

Pelvis

Periappendiceal abscess may complicate acute appendicitis or appendectomy. CT with intravenous contrast administration can reliably stage complicated appendicitis and postappendectomy inflammation. CT-guided aspiration may still be beneficial for antibiotic sensitivity testing. Patients with larger, well-defined abscess responded well to percutaneous drainage. Drainage has to be maintained for several weeks to allow the fistula that is usually present to heal.

Crohn's disease is complicated by abscess formation in more than 20% of patients. MR imaging or CT is invaluable in early detection of abscess or fistula and in differentiation of abscess and phlegmon in these patients as clinical signs of infection and abscess formation may be masked by concurrent steroid therapy and diffuse complaints of the patient. In patients without enteric communication, percutaneous drainage is an effective treatment alternative to surgical drainage or may be used in conjunction with surgery. If enteric fistula is established, long-term drainage is often required to allow resolution of infection and closure of the enteric fistula (Casola et al. 1987; Sahai et al. 1997).

The transgluteal approach is chosen when a transabdominal route is not possible. This access safely avoids critical structures such as the sciatic nerve or gluteal arteries with CT guidance. The ideal access is through the sacrospinous ligament medially to avoid the neurovascular structures of the sciatic foramen. Pain is common owing to the close proximity of the sacral plexus and generous local anesthesia should be applied.

11.1.5.4 Postinterventional Care

Postinterventionally, 4–6 h of bed rest is recommended depending on the complexity of the procedure. Blood

pressure, pulse, and pain should be monitored shortly after the procedure, at 30 and 60 min and then at hourly intervals for at least 4 h after the procedure.

The catheter is repeatedly flushed with 10–20 ml of sterile normal saline at least three times a day. The quality and quantity of drainage is monitored along with signs of patient recovery. Clinical follow-up care may be augmented with CT, ultrasound, fluoroscopy, and plain film contrast studies if the infection is not resolving. In viscous or debris-laden fluids, continuous irrigation using 500–1000 ml of saline may help to clear the abscess.

White blood cell counts, fever, and pain have to be monitored. Normalization of white blood cell count and temperatures indicate improvement. Persistent fever or pain after 2 days indicates undrained pus and a repeat CT scan is warranted. Repeat imaging should be routinely performed after 3–4 days to assess drainage success and to rule out catheter dislodgement. This can be easily achieved using fluoroscopy. Depending on the case, treatment is complete within a matter of days to weeks. Simple abscess treatment is usually completed within 1–2 weeks. A complex abscess or enteric fistula may require weeks to months to heal. The drainage catheter should be kept in place until the abscess cavity begins to close and the drainage diminishes to a few milliliters per day of clear fluid. The patient has to be kept on antibiotic therapy as long as a drainage catheter is in place.

Successful percutaneous drainage depends upon the drainage device remaining in place as the greatest complication risk for all catheter placement procedures is catheter dislodgment. No ideal fixation device or technique is available and a catheter fixator can only be seen as a catheter position reminder. A patient rolling over in bed will overcome any catheter fixation system. Debilitated, confused, and uncooperative patients are at high risk of catheter dislodgement. Catheter dislodgment is reflected in a change in the length of the catheter visible outside the patient. Therefore, it is helpful for the nursing staff to have an adhesive marker attached to the catheter at the skin exit site to easily identify catheter dislodgement. When dislodgement is suspected, radiographs for comparison with the baseline study should be obtained. Catheter dislodgment may be noticed only when the catheter is leaking. Replacement catheters may be placed along the existing tract using an over-the-wire technique if catheter dislodgment is detected early.

11.1.6 Results

Comparison of percutaneous drainage and open surgical drainage in large published series revealed that the percutaneous approach is associated with a better overall outcome with fewer complications, more effective drainage, and shorter treatment duration (Johnson et al. 1981). Percutaneous drainage can frequently be performed using a short, direct approach and very little intervention-related trauma. Open midline incision can be avoided, therefore limiting the potential for spreading contamination. With percutaneous drainage a shorter hospital stay is anticipated, as general anesthesia is not necessary and patients can be discharged early with small catheters in place, which can be managed on an outpatient basis.

Many studies have documented the efficacy of catheter drainage in many anatomic locations. Success ranges from 80 to 90% in hepatic abscess. Even in septated abscesses catheter drainage is effective, as most locules will communicate. Mortality is reported to be 3–4% in solitary abscess, which is better than results from surgery, showing 9% mortality (Gerzof et al. 1985). In postsurgical patients anastomotic leak is a frequent complication occurring in 10–15% of patients. These postoperative complications are well addressed with percutaneous drainage and have a success rate close to 80% (Gervais et al. 2004).

In splenic abscess, drainage is the preferred over surgery with splenectomy, as percutaneous drainage preserves the spleen and reduces the risk of sepsis. Successful drainage in spleen abscess is reported in more than 70% of treatments. Factors impairing successful drainage are multiloculated abscess formations and phlegmonous infections (Quinn et al. 1986).

11.1.7 Complications

Complications of percutaneous puncture and drainage largely depend on the location of the collection, which determines the access route, and the underlying disease, which influences the clinical success of

a drainage procedure. The drainage route should avoid unnecessary contamination of uninvolved areas and thus should be short and simple. Spread of infection is possible as well as injury to organs, blood vessels, or intestine (Thomas et al. 2006). Specific complications related to access route include bowel perforation, fistula, spread of infection, pneumothorax, and catheter dislocation. As with all punctures local bleeding and discomfort are common. The most important complication is catheter dislodgement resulting in insufficient drainage or even spread of infection in the area of the puncture tract.

Summary

Percutaneous abscess drainage is a minimally invasive intervention performed under local anesthesia with success rates, morbidity, and mortality as good as or better than those of surgery. Complications are rare and mostly refer to pain and catheter dislodgement. In combination with surgery, the extent of subsequent surgery is reduced and one-stage procedures become possible. Owing to the minimally invasive nature and the availability of CT guidance, percutaneous drainage procedures have become an indispensable tool in successful management of the patient with infected fluid collections. Using CT fluoroscopy, one can reach almost any location safely, making percutaneous drainage the first choice. Even in recurrent abscess a repeated attempt using a percutaneous approach is warranted before open surgery is considered. Close follow-up of the patient with ongoing communication and consultation with the clinicians is necessary to ensure satisfactory outcome. Imaging follow-up is required to control or adjust catheter position, to prove resolution of abscess formation, or to make an early decision on whether to convert to surgery in unsuccessful cases.

Key Points

- Percutaneous abscess drainage has a better risk–success ratio than surgery.
- There are virtually no absolute contraindications to percutaneous abscess drainage.
- Needle aspiration is the best way to determine the nature of a fluid collection and to access its drainability.
- The catheter size needs to be selected on the basis of the fluid's viscosity.
- Proper catheter fixation is crucial as catheter dislodgement is the most important complication in percutaneous abscess drainage.
- Consequent irrigation and postinterventional care are vital for treatment success.

References

Aeder MI, Wellman JL, Haaga JR et al. (1983) Role of surgical and percutaneous drainage in the treatment of abdominal abscesses. Arch Surg 118:273–280

Buecker A, Neuerburg JM, Adam GB et al. (2001) MR-guided percutaneous drainage of abdominal fluid collections in combination with X-ray fluoroscopy: initial clinical experience. Eur Radiol 11:670–674

Casola G, van Sonnenberg E, Neff CC et al. (1987) Abscesses in Crohn disease: percutaneous drainage. Radiology 163:19–22

Daly B, Krebs TL, Wong-You-Cheong JJ et al. (1999) Percutaneous abdominal and pelvic interventional procedures using CT fluoroscopy guidance. AJR Am J Roentgenol 173:637–644

Ferrucci JT 3rd, Mueller PR (2003) Interventional approach to pancreatic fluid collections. Radiol Clin North Am 41:1217–1226, vii

Gervais D, Dawson S (2006) Percutaneous drainage of pelvic abscesses and fluid collections. In: Baum S, Pentecost M (eds) Abram's angiography: Interventional Radiology. Lippincott Williams Wilkins Philadelphia

Gervais DA, Ho CH, O'Neill MJ et al. (2004) Recurrent abdominal and pelvic abscesses: incidence, results of repeated percutaneous drainage, and underlying causes in 956 drainages. AJR Am J Roentgenol 182:463–466

Gerzof SG, Johnson WC, Robbins AH et al. (1985) Intrahepatic pyogenic abscesses: treatment by percutaneous drainage. Am J Surg 149:487–494

Gobien RP, Stanley JH, Schabel SI et al. (1985) The effect of drainage tube size on adequacy of percutaneous abscess drainage. Cardiovasc Intervent Radiol 8:100–102

Harisinghani MG, Gervais DA, Hahn PF et al. (2002) CT-guided transgluteal drainage of deep pelvic abscesses: indications, technique, procedure-related complications, and clinical outcome. Radiographics 22:1353–1367

Johnson WC, Gerzof SG, Robbins AH et al. (1981) Treatment of abdominal abscesses: comparative evaluation of operative drainage versus percutaneous catheter drainage guided by computed tomography or ultrasound. Ann Surg 194:510–520

Kariniemi J, Sequeiros RB, Ojala R et al. (2006) Feasibility of MR imaging-guided percutaneous drainage of pancreatic fluid collections. J Vasc Interv Radiol 17:1321–1326

Maher MM, Gervais DA, Kalra MK et al. (2004) The inaccessible or undrainable abscess: how to drain it. Radiographics 24:717–735

McNicholas MM, Mueller PR, Lee MJ et al. (1995) Percutaneous drainage of subphrenic fluid collections that occur after splenectomy: efficacy and safety of transpleural versus extrapleural approach. AJR Am J Roentgenol 165:355–359

Men S, Akhan O, Koroglu M (2002) Percutaneous drainage of abdominal abcess. Eur J Radiol 43:204–218

Mückley T, Schütz T, Kirschner M et al. (2003) Psoas abscess: the spine as a primary source of infection. Spine 28:E106–E113

Mueller PR, van Sonnenberg E, Ferrucci JT Jr (1984) Percutaneous drainage of 250 abdominal abscesses and fluid collections. Part II: Current procedural concepts. Radiology 151:343–347

Park JK, Kraus FC, Haaga JR (1993) Fluid flow during percutaneous drainage procedures: an in vitro study of the effects of fluid viscosity, catheter size, and adjunctive urokinase. AJR Am J Roentgenol 160:165–169
Quinn SF, van Sonnenberg E, Casola G et al. (1986) Interventional radiology in the spleen. Radiology 161:289–291
Sahai A, Belair M, Gianfelice D et al. (1997) Percutaneous drainage of intra-abdominal abscesses in Crohn's disease: short and long-term outcome. Am J Gastroenterol 92:275–278
Schroder J (1993a) The mechanical properties of guidewires. Part I: Stiffness and torsional strength. Cardiovasc Intervent Radiol 16:43–46
Schroder J (1993b) The mechanical properties of guidewires. Part II: Kinking resistance. Cardiovasc Intervent Radiol 16:47–48
Thomas J, Turner SR, Nelson RC et al. (2006) Postprocedure sepsis in imaging-guided percutaneous hepatic abscess drainage: how often does it occur? AJR Am J Roentgenol 186:1419–1422
van Sonnenberg E, Wittich GR, Chon KS et al. (1997) Percutaneous radiologic drainage of pancreatic abscesses. AJR Am J Roentgenol 168:979–984
van Sonnenberg E, Wittich GR, Goodacre BW et al. (2001) Percutaneous abscess drainage: update. World J Surg 25:362–369
Wroblicka JT, Kuligowska E (1998) One-step needle aspiration and lavage for the treatment of abdominal and pelvic abscesses. AJR Am J Roentgenol 170:1197–1203

11.2 Drainage in Pneumothorax
Christian Hohl

The use of small-caliber chest tubes to treat postinterventional pneumothorax was first described by Sargent and Turner (1970). They used a 9-F drainage catheter with a flutter valve as described by Heimlich (1968). Since then numerous reports have proved percutaneous radiological treatment to be a well-established and safe technique to handle postinterventional pneumothoraces.

11.2.1 Indications

Pneumothorax is the most common complication in CT-guided biopsy of pulmonary and pleural masses, with a frequency of 8.2–54.3% (Yamagami et al. 2005). It is more frequent in patients with emphysema or obstructive airway disease. Cox et al. (1999) noted that evidence of emphysema and smaller lung lesions (2 cm less) correlated with the incidence of pneumothorax after lung biopsy. Furthermore pneumothorax can occur in punctures for central vein catheters (subclavian or jugular vein) or biopsies of the upper abdomen. Thus, the ability to treat pneumothorax is as important as the ability to perform the primary intervention itself. Anybody participating in an intervention with the potential risk of pneumothorax must be familiar with the correct handling of chest tubes and the Heimlich valve.

If pneumothorax is recognized during a CT-guided intervention, there are three different therapeutic options:

1. Observation. In patients in which pneumothorax is only evident on the CT scan but who have no clinical symptoms such as dyspnea, tachypnea, or tachycardia, observation and control radiographs are a good option. If the pneumothorax is stable or decreasing under observation, no further action is necessary.
2. Aspiration. In patients with progressive pneumothorax on the control radiograph or in patients with mild symptoms, manual aspiration of air from the pleural space can help to stabilize the situation and reduce the need for subsequent chest tube placement.
3. Placement of pleural drainage (Fig. 11.11). When the pneumothorax recurs after aspiration, no second attempt should be made and chest tube placement is recommended immediately. Furthermore, Yamagami et al. (2005) recommend placing a chest tube if the aspirated volume is larger than 500 ml.

In all patients with severe complaints such as heavy dyspnea, symptoms of circulatory shock, or tension pneumothorax, instantaneous placement of a chest tube is essential. Also any patient with an iatrogenic pneumothorax on mechanical ventilation should strongly be considered for placement of a chest tube (Baumann and Noppen 2004).

11.2.2 Material

For thoracocentesis, which means the aspiration of air from the pleural space, no special equipment is needed. It can be performed with the use of a 14–18 G puncture needle, a connecting tube, a three-way stopcock, and a 50-ml syringe (Fig. 11.12).

For the placement of a chest tube with a Heimlich valve, prepacked sets are available (Fig. 11.13). To treat a postinterventional pneumothorax, a 9-F tube as described by Sargent and Turner (1970) is sufficient.

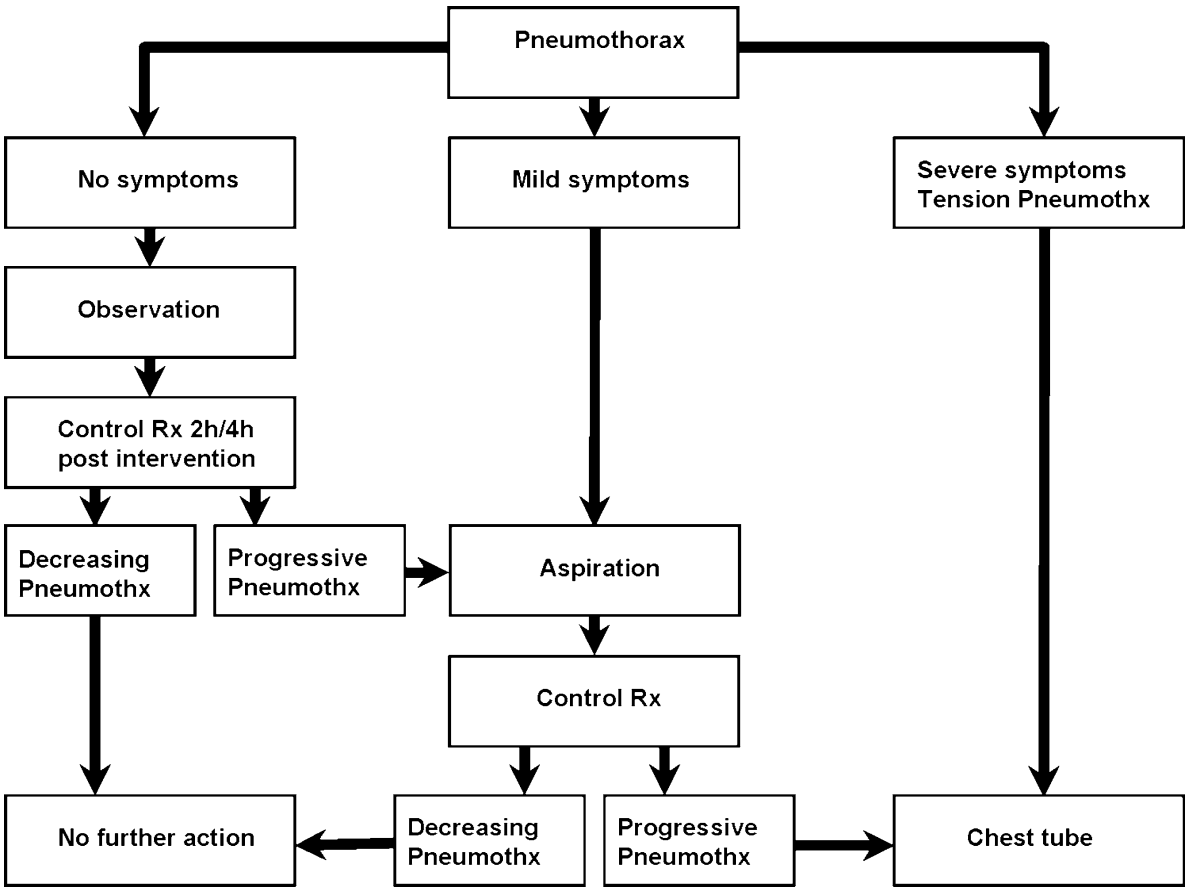

Fig. 11.11 Flow chart for the adequate procedure after postinterventional pneumothorax

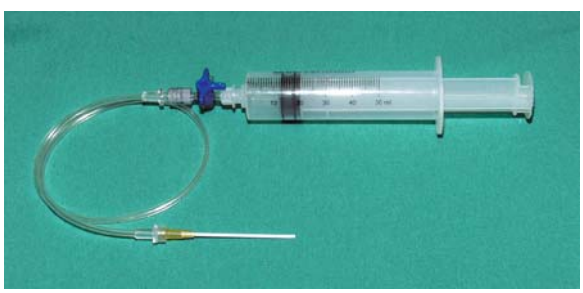

Fig. 11.12 Self-assembled set for thoracocentesis consisting of a 14 G puncture needle, a connecting tube, a three-way stopcock, and a 50-ml syringe

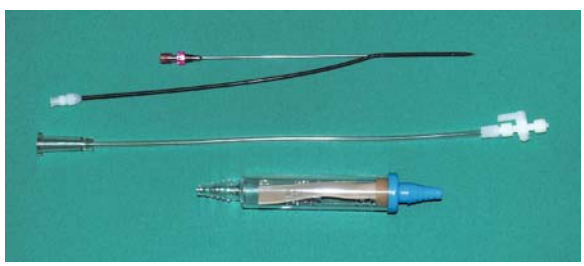

Fig. 11.13 Prepacked chest tube set (C-TPT-100, Cook Europe, Bjaeverskov, Denmark) consisting of an 18 G needle (20-cm length) with a premounted 9-F catheter (29-cm length) with four side holes near the tip, a connecting tube with a one-way stopcock, and a Heimlich valve

11.2.3 Technique

11.2.3.1 Aspiration

The aspiration of air from the pleural space can be performed in different locations; the appropriate site with the largest aspect of the pneumothorax is chosen from the CT scan. In most cases the second or the third intercostal space in the midclavicular line is a good choice in a patient in the supine position. A 14–18 G intravenous catheter is inserted (Fig. 11.14). Particular attention should be given to the puncture angle. With a slanted puncture in the craniocaudal direction, the

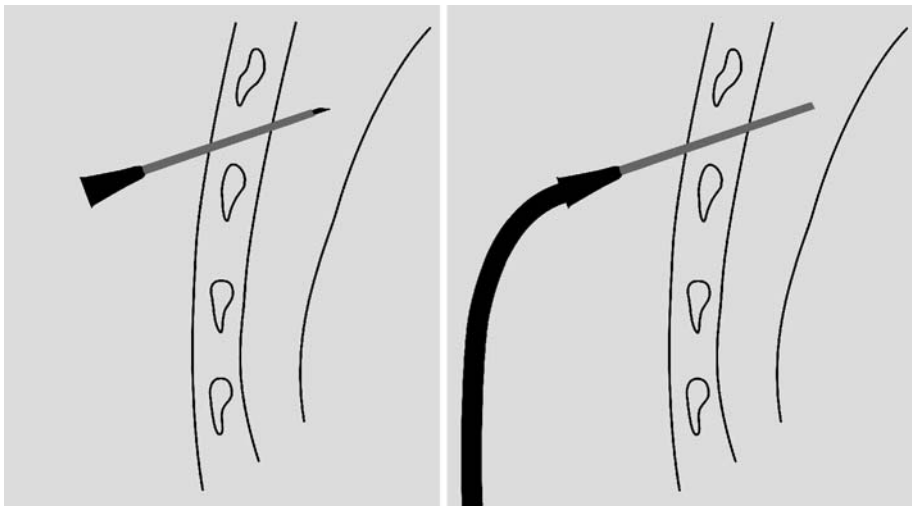

Fig. 11.14 Thoracocentesis with an intravenous catheter. The pleural space is punctured with a 14 G puncture needle until air can be aspirated (*left*). Then the stainless steel needle is removed and the Teflon catheter is pushed up against the thoracic wall. In this position the air in the pleural space can be aspirated with the syringe and removed via the three-way stopcock

puncture holes in the different layers of the thoracic wall are displaced a little from each other, which helps to prevent recurrent pneumothorax after catheter removal. To avoid the neurovascular bundle beneath the inferior aspect of the adjacent rib, the catheter should be placed close to the superior aspect of the rib. The catheter is advanced into the pleural space and the stylet is removed. The connection tube with the three-way stopcock is connected to the intravenous catheter and the air from the pneumothorax is drawn in the 50-ml syringe and expelled by alternately opening and closing the stopcock. Whenever resistance is encountered, the catheter is slightly withdrawn and aspiration is resumed. After complete or almost complete re-expansion of the lung has been documented on a control CT scan, the catheter is completely withdrawn. During catheter withdrawal, suction is maintained and the skin entry point should be manually compressed after catheter removal.

11.2.3.2 Chest Tube

For the insertion of a chest tube two different entry sites can be recommended: the fifth intercostal space in the anterior axillary line or the second intercostal space in the midclavicular line (Choi et al. 2007). After the entry site has been determined, the skin is prepared with antibacterial wash and draped in a sterile fashion. The catheter is preassembled, connecting the Heimlich valve and tube. It is important that the Heimlich valve is attached in the direction indicated by the arrow on the valve. Local anesthesia is injected liberally along the intended tube tract through skin, subcutaneous tissue, muscle, and fascia down to the parietal pleura. A small incision is made with a no. 11 blade at the entrance site, taking care to avoid the neurovascular bundle beneath the inferior aspect of the adjacent rib. Now the needle tip is inserted, with the catheter as its sheath, into the pleural cavity. Again it is advantageous to choose a slanted puncture angle to avoid an air leak after tube removal. The needle and the catheter are advanced with one hand, while the other hand maintains pressure upon the stylet within the needle. In patients with a large pneumothorax, when it is certain that the stylet and the catheter are well within the pleural cavity, the catheter is pushed forward by sliding it over the stylet into the pleural space (Fig. 11.15). If it is uncertain whether the needle and the catheter tip are well within the pleural space, a control scan is performed before the catheter is pushed forward. The catheter must be advanced so that all side holes are within the pleural space. While the catheter is being advanced, the needle is slowly withdrawn. The distal tip of the catheter should be positioned with the tip pointing towards the apex of the pleural space. When the catheter is in place and the needle has been completely withdrawn, the

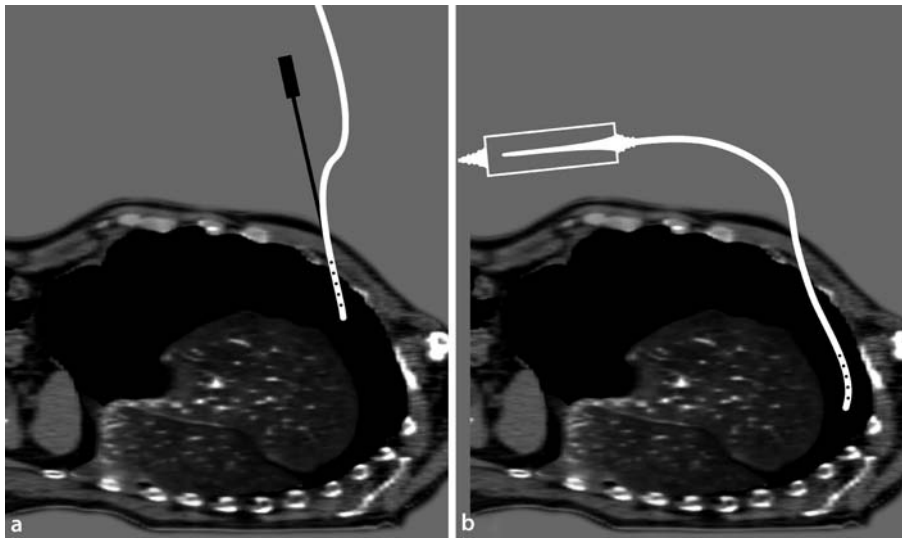

Fig. 11.15a,b Insertion of a 9-F catheter with the trocar technique. The pleural space is punctured with an 18 G stylet with the premounted 9-F catheter. When the catheter and the stylet are well within the pleural cavity, the catheter is pushed forward by sliding it over the stylet into the pleural space (**a**). The distal tip of the catheter should be positioned at the apex of the pleural space, whereas all side holes must be within the pleural space (**b**)

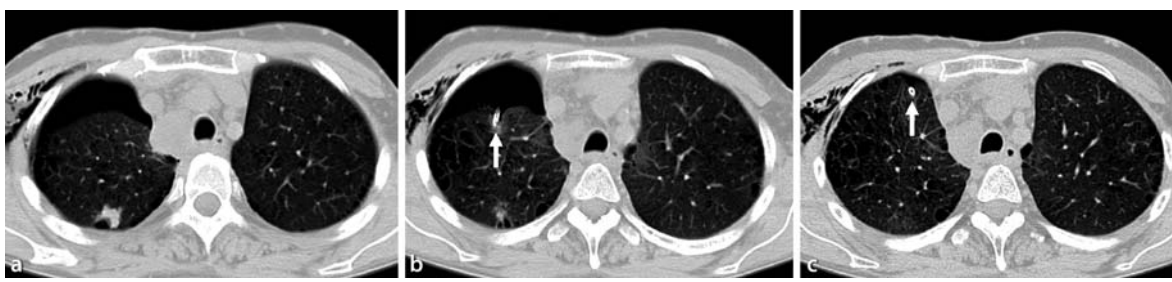

Fig. 11.16a–c A patient with severe emphysema and coin lesion in the right upper lobe developed pneumothorax after biopsy (**a**). Owing to dyspnoea, a catheter (*arrow*) with a Heimlich valve was inserted on the CT table (**b**). Five minutes after insertion of the catheter, the pneumothorax had completely resolved (**c**)

connection tube with the Heimlich valve is connected to the catheter and the stopcock is unblocked. To avoid displacement, the catheter is attached to the chest wall with skin suture and adhesive tape. A U-shaped suture around the skin entry point may be helpful. It can be pulled together during chest tube withdrawal and thereby help to avoid a recurrent pneumothorax due to a puncture site fistula.

In most patients the symptoms will improve within minutes after tube insertion (Fig. 11.16). In a few patients who do not improve noticeable, additional wall suction can be attached to the Heimlich valve.

Directly after placement of the drainage catheter a posteroanterior chest radiograph is obtained to confirm the catheter position and to examine for residual pneumothorax. The following morning and subsequently as indicated, chest X-rays should be obtained. If the lung remains expanded, the stopcock is turned off and a chest X-ray is obtained 4 h later. If the lung still remains expanded, the catheter can be removed (Conces et al. 1988). If pneumothorax recurs, the stopcock is opened again and the process is repeated at a later time.

Removal of the drainage catheter is performed in expiration under continuous suction on the catheter. After drainage with small-bore catheters (9 F), inflow of air into the pleural space can be avoided by short-term manual compression and adhesive bandage. After

removal of the catheter, a final chest X-ray is obtained to document the success.

11.2.4 Results

The success rate of chest tubes with a Heimlich valve in the treatment of pneumothoraces ranges between 87 and 95% (Conces et al. 1988). Typical reasons for malfunction of chest tubes with a Heimlich valve are kinking, malpositioning in a major fissure, inadvertent removal by the patient, or clogging of a tube or valve. Another very rare reason for malfunction of the catheter is an air leak that exceeds the catheter's ability to remove air. The mean duration of drainage with small-bore catheters with a Heimlich valve reported in the literature ranges between 1.6 and 5.1 days (Yamagami et al. 2005; Conces et al. 1988; Martin et al. 1996; Laronga et al. 2000; Niemi et al. 1999).

11.2.5 Complications

Unlike large-tube thoracostomy, no significant complications are observed with 9-F catheters with a Heimlich valve. Misplacement of catheters into lung parenchyma, liver, or spleen, as seen with surgical chest tubes, is nearly impossible under CT guidance. Hematoma of the chest wall can occur if the neurovascular bundle under the adjacent rib is punctured.

The presence of pleural fluid can result in clogging of the 9-F tube or the Heimlich valve. In the latter case, the problem can be solved by replacing the valve with a new one or by removing the valve and attaching the tube directly to suction (Conces et al.1988). If the catheter becomes clogged, placement of a second catheter may be required.

Summary

With use of the trocar technique, the use of a 9-F catheter is a safe and quick method to resolve postinterventional pneumothoraces. Following placement, little nursing care is required and patients with a Heimlich valve can even be treated as outpatients. When a patient is to be sent home with a catheter in place, one must ensure that the catheter is secured in such a fashion preventing it from being dislodged (Conces et al. 1988).

Key Points

- Successful management of pneumothorax depends on the correct indication (Fig. 11.11).
- The trocar technique described with a preassembled 9-F pneumothorax set and a flutter is a quick and safe method for treating postinterventional pneumothoraces.
- Sufficient catheter fixation is crucial to prevent catheter dislocation with subsequent treatment failure.

References

Baumann MH, Noppen M (2004) Pneumothorax. Respirology 9:157–164

Choi SH, Lee SW, Hong YS et al. (2007) Can spontaneous pneumothorax patients be treated by ambulatory care management? Eur J Cardiothorac Surg 31:491–495

Conces D, Jr, Tarver R, Gray W et al. (1988) Treatment of pneumothoraces utilizing small caliber chest tubes. Chest 94:55–57

Cox JE, Chiles C, McManus CM et al. (1999) Transthoracic Needle Aspiration Biopsy: Variables That Affect Risk of Pneumothorax. Radiology 212:165–168

Heimlich HJ (1968) Valve drainage of the pleural cavity. Dis Chest 53:282–287

Laronga C, Meric F, Truong MT et al. (2000) A treatment algorithm for pneumothoraces complicating central venous catheter insertion. Am J Surg 180:523–527

Martin T, Fontana G, Olak J et al. (1996) Use of pleural catheter for the management of simple pneumothorax. Chest 110:1169–1172

Niemi T, Hannukainen J, Aarnio P (1999) Use of the Heimlich valve for treating pneumothorax. Ann Chir Gynaecol 88:36–37

Sargent EN, Turner AF (1970) Emergency treatment of pneumothorax: A simple catheter technique for use in the radiology department. Am J Roentgenol 109:531–535

Yamagami T, Kato T, Iida S et al. (2005) Efficacy of Manual Aspiration Immediately after Complicated Pneumothorax in CT-guided Lung Biopsy. J Vasc Interv Radiol 16:477–483

11.3 Nephrostomy

Christian Hohl

11.3.1 Indications

Percutaneous nephrostomy (PCN) has been one of the most common interventional procedures since its first description in 1955 (Goodwin et al. 1955). A dilated collecting system is not a priori an indication for PCN,

the more so as the kidney function is not necessarily compromised by the obstruction and can remain normal for a length of time. In cases of superinfected obstruction, the parenchyma will quickly perish if PCN is not immediately performed. In most cases nephrostomy is performed as an elective procedure in patients with:

- Ureteric obstruction
- Obstructing tumors
- Urinary fistulas

Urgent drainage is needed in patients with:

- Infected postrenal obstruction
- Septicemia
- Uremia in which a rapid renal loss threatens the patient
- Infected postoperative urinomas

Further indications for PCN can be the access creation for endourologic interventions such as percutaneous nephrostolithotomy or antegrade ureteric dilatation or stent insertion (Matlaga et al. 2003). PCN is also performed prior to radiofrequency ablation of renal tumors to cool the renal pelvis and the calyces.

PCN is typically performed under ultrasound or fluoroscopic guidance, but sometimes CT or MR guidance can be advantageous. Especially in patients with an unfavorable anatomy (e.g., retrorenal colon) or a nondilated collecting system, it can sometimes be really difficult to find an appropriate access. In this chapter only the techniques of CT- and MR-guided nephrostomy are discussed; for detailed descriptions of fluoroscopic or ultrasound guidance please refer to the corresponding literature (Osman et al. 2005; Miller et al. 2007).

The minimal patient preparation includes besides the informed consent an up-to-date blood test (blood count, coagulation, renal function) and ultrasound of the kidneys. In elective interventions the International Normalized Ratio should be 2 or less and the platelet count should be above 80 000 mm^3. If the platelet count is less than this, platelet transfusion should be performed just before the intervention.

11.3.2 Material

In general, there are two different techniques to perform PCN: Seldinger technique and the one-step or trocar technique. For both techniques a variety of different prepacked sets, needles, and catheters are available. An exemplary prepacked nephrostomy set (Soft-Drain, Bard/Angiomed, Karlsruhe, Germany) for the Seldinger technique is shown in Fig. 11.17. Seldinger sets comprise, for example, a 17.5 G puncture needle, a 0.038-in. stiff guide wire with a floppy tip, and a 9-F drainage catheter in pigtail configuration. For selected patients the use of an atraumatic 22 G puncture needle and a 0.018-in. guidewire may be needed.

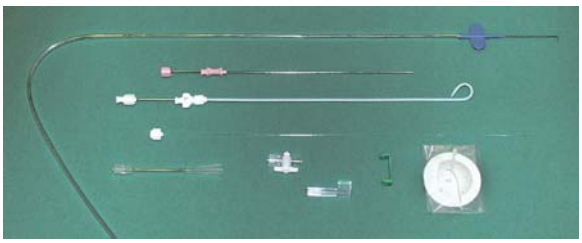

Fig. 11.17 Prepacked nephrostomy set for the Seldinger technique (Soft-Drain, Bard/Angiomed, Karlsruhe, Germany) containing a 17.5 G puncture needle (200 mm length), a 0.038-in. guidewire, and a 9-F drainage catheter (285 mm length) in pigtail configuration

For the trocar technique the drainage catheter is premounted on the puncture needle as shown in Fig. 11.18. Tubes of 8–10 F are usually sufficient for drainage of noninfected urine. Larger tubes (12–14 F) may be necessary for drainage of infected urine or to ensure appropriate urine flow in procedures complicated by gross hematuria. Additional required material includes sutures, drainage bags, connecting tubes, and drainage bag connectors.

11.3.3 Technique

Normally PCN can be performed under local anesthesia; only in children a deep sedation or general anesthesia is required. To prevent septicemia, single-shot antibiotic prophylaxis (e.g., 1500 mg cefuroxime) is recommended 1 h prior to the intervention (Lewis and Patel 2004).

PCN can be performed using two different techniques. The one-step or trocar technique is principally used in patients with a dilated collecting system and has the advantage that the renal parenchyma is only passed once and no guidewire maneuvers are necessary. The main drawback of the one-step technique is

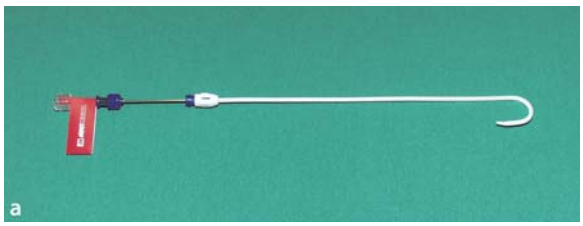

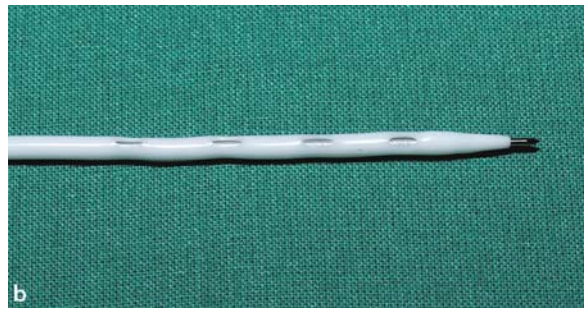

Fig. 11.18a,b Drainage catheter system for the trocar technique (Resolve, Merit Medical, South Jordan, UT, USA), composed of a 8.5-F J-tip catheter with hydrophilic coating, a metal stiffening cannula, and 0.038-in. trocar stylet (**a**). Before puncture the stiffening cannula and the stylet must be inserted completely into the catheter so that the J-tip is straightened (**b**). The catheter tip is tapered to provide a smooth transition. The four side holes are located at the inner circle of the J-tip to prevent sealing

that the kidney is punctured with a relatively chunky instrument with the risk of hemorrhage if the catheter is not positioned correctly at the first attempt. This can be problematic in patients with an undilated pelvicalyceal system.

The Seldinger technique, on the other hand, is more subtle and a little more complicated. In the Seldinger technique, the collecting system is punctured with a small puncture needle through which a guidewire is inserted and placed in the proximal ureter. Then the drainage catheter is placed in the renal pelvis over the guidewire.

For both techniques the patient positioning is pivotal for a successful intervention. The patient is positioned either in a prone or in a prone/oblique position on the examination table. It is important to obtain a position which is as comfortable as possible for the patient to ensure good compliance, especially if the intervention takes time.

A contrast-enhanced CT scan is not necessary to plan the intervention but especially in patients with an undilated collecting system a preceding intravenous injection of 20–40 ml iodinated contrast medium can be very helpful to identify the calices. If the intervention is performed under MR guidance, the collecting system can be depicted on T2-weighted images.

To minimize the risk of hemorrhage, puncture site selection should be performed with care. Brödel (1901) described the water shed between the anterior and the posterior vascularization of the kidney. This "avascular line" is located approximately 1–2 cm behind the lateral convex margin of the kidney. To avoid injury of interlobar arteries, which are situated in the renal columns between the renal papillae, the collecting system should be punctured through the papillae and the calyces. In this respect, a posterior calyx of the mid or lower pole should be chosen (Fig. 11.19). Puncture of upper-pole calyces is only necessary for nephrolithotomy. Direct puncture of the renal pelvis or anterior puncture should be avoided because of the risk of hemorrhage and extravasation due to lacking parenchymal cover.

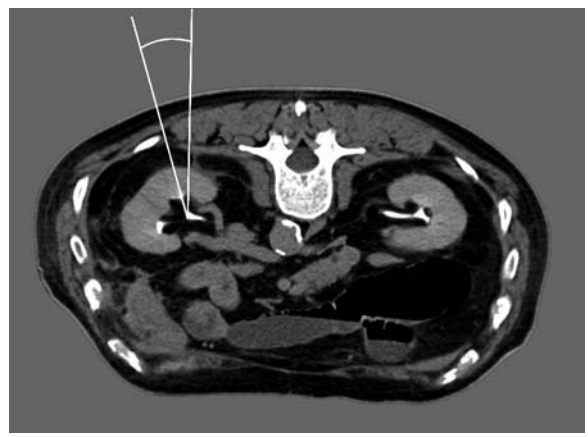

Fig. 11.19 Optimal approach for nephrostomy in nondilated collecting systems. The patient is positioned in a prone position. The posterior calyx of the lower pole is targeted via a posterolateral approach below the 12th rib

When the patient is positioned in a more or less comfortable position (prone or prone/oblique) on the table, the back and flank are sterilely cleansed and draped. Thereafter a planning scan is performed and an appropriate calyx has to be chosen. Once the tar-

get has been identified, the angle between the puncture path and the vertical center line is measured (Fig. 11.19). The needle entry point is marked with the usual technique with the help of the positioning laser and a planning grid. There are sophisticated instruments to guide the puncture needle along the exact path, but we prefer a straightforward method in which a colleague at the top of the table checks the correct angle with a simple goniometer. After infiltration of the skin and subcutaneous tissues with 1% lidocaine over the selected site, a skin incision appropriate for the anticipated nephrostomy tube size is made with a no. 11 blade, taking care to avoid the neurovascular bundle beneath the inferior aspect of the adjacent rib. Then respiration is suspended and the puncture needle is inserted. When the needle has been advanced a few centimeters, the correct path is checked by a single sequential control CT scan or a fast T2-weighted gradient-echo sequence. In this manner the needle is advanced step by step until the correct needle placement is documented and hopefully urine can be aspirated. There may be a sudden "give" when the calyx is entered. A urine sample is obtained on entry into the collecting system and sent for culture. The system should not be decompressed completely, as this makes subsequent manipulation more difficult.

In the one-step (trocar) technique, in patients with a dilated collecting system, the needle is advanced a little more until the tip is securely within the collecting system. Thereafter the stainless steel trocar is retained while the premounted drainage catheter is advanced with caution until all side holes are within the collecting system (Fig. 11.20).

In the Seldinger technique, a 0.038-in. guidewire is inserted over the puncture needle and should be advanced without resistance down the ureter. If it is difficult to find the way in the ureter, a 4-F multipurpose catheter can be helpful to negotiate the guidewire into the ureter. Once the guidewire is in position, the drainage catheter is inserted over the wire. If there is too much resistance when advancing the catheter, dilators can be inserted to widen the tract (Fig. 11.21). It may be necessary to overdilate a track by 1–2 F for tubes made of materials with high friction coefficients (e.g., silicone) or when there is significant perirenal scarring. Tubes coated with hydrophilic material are usually easily placed through tracks dilated to an identical French size. When the catheter is in place, a small amount of contrast is injected to document the correct position. Owing to the risk of septicemia, an infected system should never be overdistended. In difficult patients with a completely collapsed collecting system, the use of an atraumatic 22 G puncture needle and a 0.018-in. guidewire is recommended.

If the aspirated urine is clear or only slightly rosé, the drainage bag is collected. If the urine is dark red, a lavage with saline solution should be performed until it becomes rosé. If pus can be aspirated, the system should be decompressed without lavage. Finally the catheter should be secured in position by a suture and adhesive dressing to prevent dislocation with the need for subsequent reinterventions. A formal nephrostogram should be obtained not earlier than 24 h following tube placement.

Some CT scanners are equipped for CT fluoroscopy, which provides real-time reconstruction and display of CT images during interventional procedures. CT fluoroscopy guidance can increase target accuracy and reduce the intervention time (Silverman et al. 1999). When CT fluoroscopy is used, special attention has to be paid to radiation exposure as especially the interventionalist's hand is near the X-ray beam during the intervention. Therefore, the use of angular beam modulation, which turns off the X-ray beam in a 120° sector without impairing the image quality, is recommended during CT fluoroscopy guided nephrostomy (Hohl et al. 2008). During MR-guided nephrostomy, the same effect can be achieved with real-time imaging (Fritz and Pereira 2007).

11.3.4 Results

The technical success rate for PCN under fluoroscopic und ultrasound guidance varies between 95 and 98.5% (Gupta et al. 1997; Lang and Price 1983). With CT guidance the technical success rate can be improved up to 100% (Egilmez et al. 2007). CT guidance has its strength especially in difficult patients without dilation of the collecting system. The clinical impact of PCN as an emergency intervention can be demonstrated by the decrease of gram-negative septicemia from 40 to 8% (Lang and Price 1983).

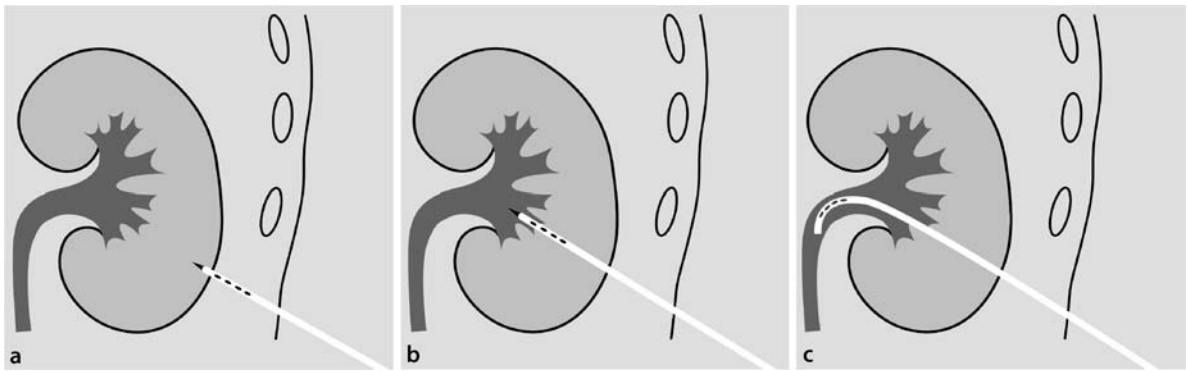

Fig. 11.20a–c Trocar technique for percutaneous nephrostomy. With a drainage catheter already mounted on a trocar stylet, the calyx is targeted (**a**). When the needle has entered the collecting system (**b**) and urine can be aspirated, the drainage catheter is advanced, while the stylet is kept in place (**c**)

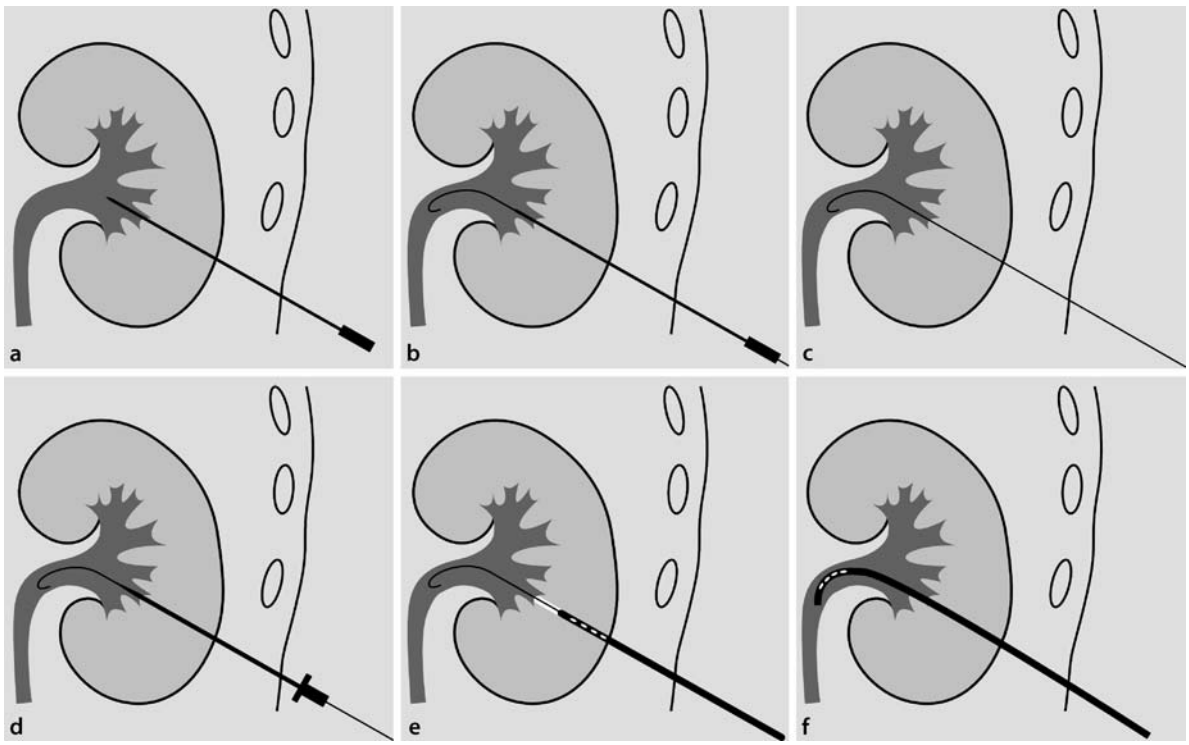

Fig. 11.21a–f Seldinger technique for percutaneous nephrostomy. A calyx is punctured with a 17.5 G needle (**a**). A 0.038-in. guidewire is inserted over the needle and placed with the tip in the proximal ureter (**b**). Then, the puncture needle is removed (**c**) and the tract is widened with a dilator if necessary (**d**). Finally, the drainage catheter is inserted (**e**) and the guidewire is retracted (**f**)

11.3.5 Complications

Major complications may be seen in 4–6% of patients who undergo fluoroscopy- or ultrasound-guided PCN procedure (Stables 1982; Zagoria and Dyer 1999). With use of CT as the guiding modality, the rate for major complications can be reduced to 0% (Egilmez et al. 2007; Thanos et al. 2006). Minor complications

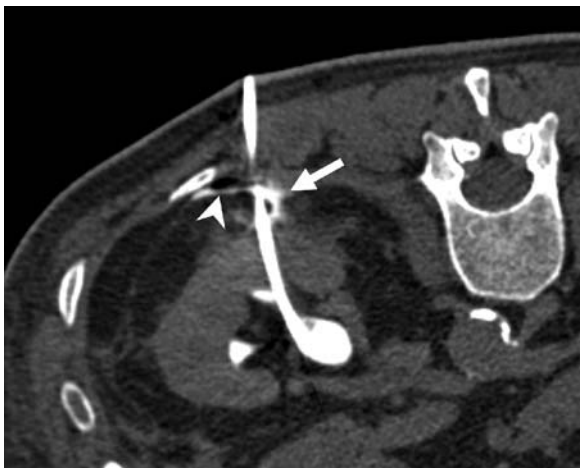

Fig. 11.22 Control CT scan after successful placement of the drainage catheter. Some contrast medium (*arrow*) and a little air (*arrowhead*) are visible in the perirenal fatty tissue. This extravasation along the drainage catheter is self-limiting and needs no further action as long as adequate drainage is provided

such as pain or transient macroscopic hematuria occur in 4.9–30.9% of patients, depending on the number of punctures (Egilmez et al. 2007; Thanos et al. 2006). The formation of clots in the renal pelvis is unproblematic owing to the endogenous thrombolytic activity of urokinase.

In most instances, significant bleeding noted at the time of nephrostomy can be controlled by tamponade of the track with a nephrostomy catheter for a small-bore track or with a balloon dilation catheter for large tracks. When this fails or when significant blood loss develops several days after nephrostomy tube placement or removal, angiographic evaluation for identification of a renal arteriovenous fistula, pseudoaneurysm, or vessel laceration is indicated (Dyer at al. 2002). If persistent bleeding from vascular injury is confirmed, it can be embolized during angiography in most cases. Surgical intervention is rarely necessary (Kessaris et al. 1995).

Sometimes a disruption of the renal pelvis with extravasation of contrast can be observed. If adequate drainage of the urinary system can be established, this extravasation will settle on its own. The same goes for extravasation of contrast along the drainage catheter (Fig. 11.22).

An inadvertent puncture of adjacent structures such as colon, liver, spleen, or lung is a typical complication of fluoroscopy or ultrasound guidance and can be avoided by CT guidance. If inadvertent puncture occurs nevertheless, no severe consequences should be expected if a small puncture needle is used.

Especially in patients with an infected urinary system, incrustation of the catheter can obstruct the lumen if the nephrostomy catheter stays in place too long; therefore, the catheter should be replaced approximately every 6 weeks if a long-term nephrostomy is indispensable.

Summary

PCN is a distinguished method for temporarily urine drainage. Furthermore, it enables minimally invasive alternatives for therapy of a number of urologic conditions. Also, primarily inoperable patients can be converted in an operable condition. CT-guided PCN has the lowest complication rate of all methods and is especially indicated in patients with an undilated collecting system or after unsuccessful drainage attempts under fluoroscopy or ultrasound guidance. MR-guided PCN is restricted to special cases such as allergic patients in which CT or ultrasound guidance is contraindicated or not possible.

Key Points

- Good patient selection and preparation are crucial for treatment success.
- An appropriate puncture site has to be selected (preferably a posterolateral calyx of the lower pole) to minimize the risk of hemorrhage.
- A massively dilated collecting system can be punctured using the trocar technique, whereas an undilated system should be approached using the Seldinger technique.
- Proper fixation of the catheter is needed to prevent dislocation with subsequent reinterventions.

References

Brödel M (1901) The intrinsic blood-vessels of the kidney and their significance in nephrotomy. Johns Hopkins Bull 12:10–13

Dyer RB, Regan JD, Kavanagh PV et al. (2002) Percutaneous nephrostomy with extensions of the technique: step by step. Radiographics 22:503–525

Egilmez H, Oztoprak I, Atalar M et al. (2007) The place of computed tomography as a guidance modality in percutaneous nephrostomy: analysis of a 10-year single-center experience. Acta Radiol 48:806–813

Fritz J, Pereira PL (2007) MR-gesteuerte Schmerztherapie: Prinzipien und klinische Applikationen. Rofo 179:914–924

Goodwin WE, Casey WC, Woolf W (1955) Percutaneous trocar (needle) nephrostomy in hydronephrosis. J Am Med Assoc 157:891–894

Gupta S, Gulati M, Uday Shankar K et al. (1997) Percutaneous nephrostomy with real-time sonographic guidance. Acta Radiol 38:454–457

Hohl C, Suess C, Wildberger JE et al. (2008) Dose reduction during CT fluoroscopy: phantom study of angular beam modulation. Radiology 246:519–525

Kessaris DN, Bellman GC, Pardalidis NP et al. (1995) Management of hemorrhage after percutaneous renal surgery. J Urol 153:604–608

Lang E, Price E (1983) Redefinitions of indications for percutaneous nephrostomy. Radiology 147:419-426

Lewis S, Patel U (2004) Major complications after percutaneous nephrostomy—lessons from a department audit. Clin Radiol 59:171–179

Matlaga BR, Shah OD, Zagoria RJ et al. (2003) Computerized tomography guided access for percutaneous nephrostolithotomy. J Urol 170:45–47

Miller NL, Matlaga BR, Lingeman JE (2007) Techniques for fluoroscopic percutaneous renal access. J Urol 178:15–23

Osman M, Wendt-Nordahl G, Heger K et al. (2005) Percutaneous nephrolithotomy with ultrasonography-guided renal access: experience from over 300 cases. BJU Int 96:875–878

Silverman SG, Tuncali K, Adams DF et al. (1999) CT fluoroscopy-guided abdominal interventions: techniques, results, and radiation exposure. Radiology 212:673–681

Stables DP (1982) Percutaneous nephrostomy: techniques, indications, and results. Urol Clin North Am 9:15–29

Thanos L, Mylona S, Stroumpouli E et al. (2006) Percutaneous CT-guided nephrostomy: a safe and quick alternative method in management of obstructive and nonobstructive uropathy. J Endourol 20:486–490

Zagoria RJ, Dyer RB (1999) Do's and don't's of percutaneous nephrostomy. Acad Radiol 6:370–377

Localization Techniques

12

Ulf Redlich

Contents

12.1 Indications

In diagnostic imaging, the detection of mostly singular, isolated tumors is a frequent problem since they often cannot be qualified. In risk populations such as smokers, 65% of patients present with noncalcified lung nodules, with less than 5% of lesions smaller than 1 cm being malignant. However, the incidence of malignancy increases dramatically above 1 cm lesion diameter (Diederich 2003). Even though lesion calcification helps to identify benign processes, lesion characterization by computed tomography (CT) or thorax radiography is unreliable. In unclear lesions with no previously known underlying malignancy, either follow-up imaging or percutaneous biopsy will usually be performed for further workup. In cases were either a primary lung cancer or limited metastatic disease is suspected, thoracic surgery will be considered. In recent years, thoracic surgery has adopted less- invasive approaches for confined lesions such as video-assisted thoracoscopic surgery (VATS). A problem often encountered during VATS is localizing the tumor, depending on its position relative to the lung surface. Pulmonary lesions located 5 mm or more from the visceral pleura with a diameter of 10 mm or less are hard to find during VATS and two thirds of these cases need to be converted to open surgery (Suzuki et al. 1999). In these cases, preoperative marker placement is extremely helpful and significantly improves the surgeon's technical success.

In 1991 wire marking was first described to mark small targets such as lymph nodes, neurofibromas, or foreign objects at various locations in the body (Finch 1991). Preoperative localization of musculoskeletal lesions, prolapsed discs, or even appendicoliths as an inflammatory focus in difficult-to-access peritoneal recesses has also been described (Morrison et al. 2001; Endres et al. 2005; Lossef 2005). To assist implantation of a transjugular intrahepatic portosystemic shunt, wire marking of the portal vein has also been used (Fontaine et al. 1997).

Preoperative localizations are most often done in lung and breast tumors. Mammography-, magnetic resonance (MR-), and CT-guided localization of breast lesions is performed routinely today. MR-assisted wire marking is a much more involved procedure, but is helpful specifically in the breast or, not frequently adopted, in the liver if a lesion is hard to identify with standard imaging procedures. In MR mammography, 10–39% of tumors detected are visible with MR only, making MR marking or guidance inevitable (Schneider et al 2002; LaTrenta et al. 2003; Heywang-Köbrunner et al. 2000).

Mahnken/Ricke (Eds.), *CT- and MR-Guided Interventions in Radiology*

12.2 Material

Localization material such as a wire marker is inserted via a cannulated puncture needle. The needle should be as thin as possible, but still well detectable by the imaging technique being used without applying to many artifacts to the image. For lung puncture, nothing larger than an 18 G needle should be used. The risk of pneumothorax or other, less common adverse events in lung puncture most likely is related to the diameter of the needle being inserted. The choice of materials for fluoroscopic or CT-assisted marking is simple; however, for MR-compatible materials, the range is wide and the optimal choice depends on several variables.

The marker material, from a variety of compositions, should ideally make the target region visible or palpable; however, some markers available are detectable only under fluoroscopy. Currently in use are wire systems (X, spiral, and hook), platinum coils, tantalum beads, methylene blue, lipiodol, barium suspension, or agar. Wire markers (Fig. 12.1) are composed of various materials (stainless steel, nitinol, etc.). The designs of the wires vary greatly (i.e., classic Kopans hook wire or the Miller corkscrew wire) and should be chosen according to the type of tissue to be marked. Dislocation in diligent tissue such as pulmonary parenchyma can, for example, best be avoided by using a four-leaf-clover design (Mullan et al. 1999).

Metal spirals or platinum coils, usually used for interventional occlusion of blood vessels, can also be used as marker material. The advantage is that after the marker has been placed no parts are left outside the body, therefore minimizing the risk of a pneumothorax or marker dislocation (Powell et al. 2004). However, just following a marker wire disappearing in a human body may ease the surgeon's job significantly.

Tantalum beads and contrast medium are visible under fluoroscopy only. During surgical removal of the target area it is thus necessary to use a C-arm for orientation. Liquid markers are injected via the cannulated puncture needle. A limitation is the diffusion of the material into the adjacent tissue and lymph drainage, making early surgery following marker placement necessary. An exception is barium, which usually remains stable in tissue. Fluoroscopy-assisted resection can be performed up to 1 week after injection (Kobayashi et al. 1997).

Agar is used only in pulmonary lesions. It provides a palpable area within the parenchyma, but requires an open surgical resection (Tsuchida et al. 1999).

12.3 Technique

The technique of localization of the target volume, for example, for potential tumors, follows a uniform process, regardless of which imaging modality is used:

- Lesion documentation (ultrasound, CT, MR imaging)
- Planning of the lowest-risk access
- Sedation
- Sterile covering, local anesthetic
- Localization intervention (e.g., by CT/MR fluoroscopy)
- Documentation of the proper marker location
- Ruling out complications (e.g., bleeding, pneumothorax)
- Prevention of dislocation of the marker (if necessary)
- Transportation of the patient to the operating room and resection

For wire marking, the access point should be planned – if possible – together with the surgeon. It is best to place the wire marker using the same access and course as the surgeon will use, then the preparation along the wire into the depth and finding the region to be removed is simple. The wire should ideally be placed through the tumor, but a deviation of up to 10 mm is generally considered tolerable.

If the peritoneal or pleural cavity has been crossed, the point of entry will be recognizable on the visceral side and will guide one to the target location even if the wire marker has been dislocated. A wire dislocation must be preserved by diligent fixation of the extracorporal wire part to the patient skin, e.g., by using sterile tape. In pulmonary nodules it is recommendable to cut the wire at skin level (Fig. 12.2). Metal spirals or platinum coils should be placed with one end at the tumor and the other end at the surface of the organ – the corresponding length has to be determined preinterventionally. To mark a pulmonary tumor before VATS, an 80-mm coil via a 22 G needle, for example, can be used. Because of possible marker dislocation, the injection of liquid marker material is of advantage when the targeted tissue is loosely structured, e.g., fatty tissue or preformed cavities. In order to keep the diffu-

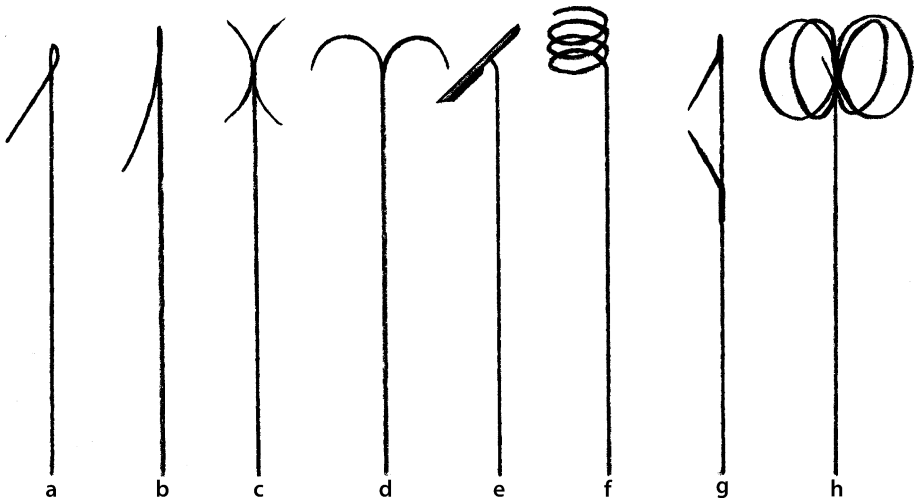

Fig. 12.1a–h Various designs of marker wires: **a** Kopans hook (breast, lung), **b** Hawkins II hook (breast), **c** X-hook (breast), **d** double hook (breast), **e** tumor loc (breast, lung), **f** Miller corkscrew (lung), **g** double hook (breast), **h** Mullan cloverleaf (lung)

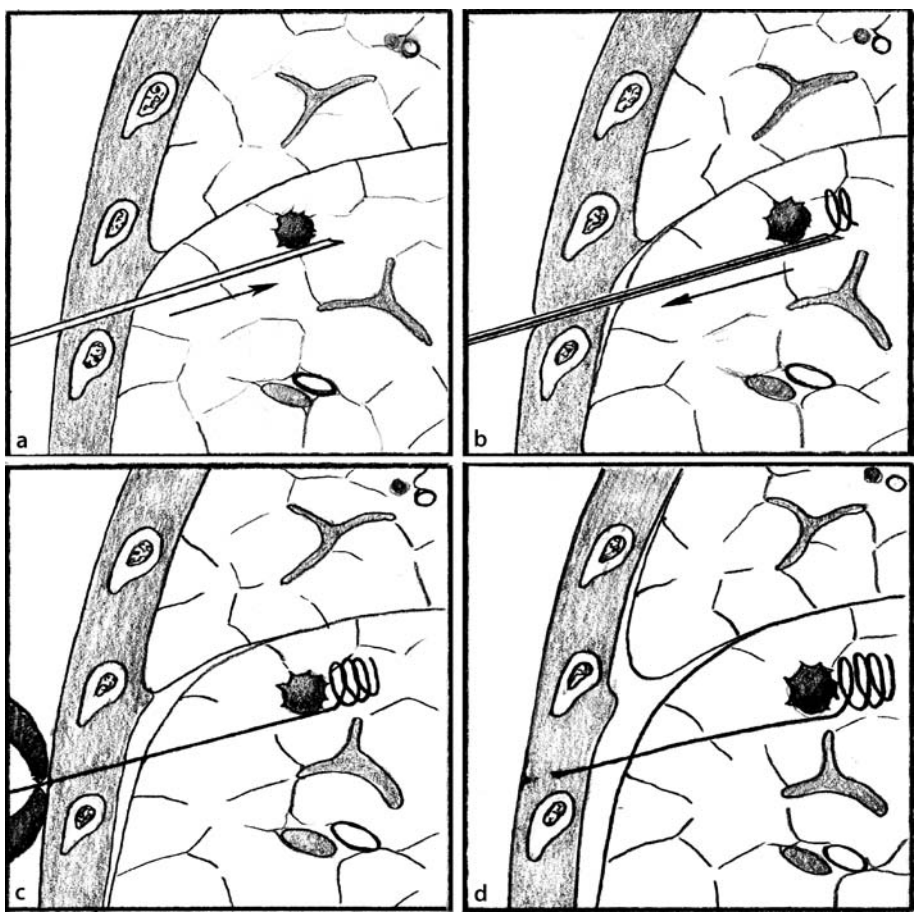

Fig. 12.2a–d Deposition of a marker wire near a pulmonary lesion

sion of the marker liquid to a minimum, surgery should be performed soon afterwards.

12.4 Results

The data available on CT- and MR-guided localization procedures are scarce and nonuniform. Localization of lung lesions with wire markers has technical success rates of up to 100% (Hänninnen et al. 2004; Kastl et al. 2006), most likely depending on the degree of experience of the interventionalist. Hence, such procedures, e.g., in the lung usually have a good acceptance rate once established, and they offer safe navigation with a short procedural time and very few complications. A 100% success rate has also been reported for needle localization of breast lesions (Kuhl 2002; Fischer et al. 1998).

The duration of the procedure depends on experience and the imaging modality which has been chosen. On average, a wire marking of a pulmonary nodule will add up to 7.5–25 min (Hänninnen et al. 2004; Kastl et al. 2006).

12.5 Complications

Wire dislocation mostly occurs when dealing with relatively soft tissue such as lung or breast. Between 2 and 5% of wire-marked breast tumors could not be removed because the wire had been displaced during surgery (Heywang-Köbrunner et al. 2000). In the case of dislocation of lung wire markers, pneumothorax is a frequent event (10–35%) (Shah et al. 1993; Poretti et al. 2002). However, since thoracoscopic surgery or open surgery is usually done soon after, usually no clinical consequences are faced. Serious complications are extremely rare and may include symptomatic bleeding or infections. A very rare complication in thoracic puncture is air embolism, which may potentially even require resuscitation of the patient (Horan et al. 2002).

Summary

Marking a surgical target prior to the operation is usually a simple procedure with a very low complication rate. It may provide faster and safer performance during subsequent minimally invasive or open surgery specifically in lung and breast lesions. In most regions of the human body, localization of tumors can be done quickly and with very little strain for the patient, and should therefore be considered more often.

Key Points

- Localization techniques can be applied to virtually all regions of the body.
- Wire markers offer perfect guidance for the surgeon and can be placed with minimal risk and discomfort for the patient.
- Specifically in lung and breast lesions, surgical results may improve significantly with a reduction in procedural time.

References

Diederich S (2003) Screening for early lung cancer with low-dose spiral computed tomography. Lancet 362:588–589

Endres S, Riegel T, Wilke A (2005) Präoperative Markierung thorakaler Bandscheibenvorfälle. Orthopädie 34:791–793

Finch IJ (1991) Preoperative CT-guided percutaneous localization of small masses with a Kopans needle. AJR Am J Röntgenol 157:179–180

Fischer U, Kopka L, Grabbe E (1998) Magnetic resonance guided localization and biopsy of suspicious breast lesions. Top Magn Reson Imaging 9:44–59

Fontaine AB, Verschyl A, Hoffer E et al. (1997) Use of CT-guided marking of the portal vein in creation of 150 transjugular intrahepatic portosystemic shunts. J Vasc Interv Radiol 8:1073–1077

Hänninen EL, Langrehr J, Raakow R et al. (2004) Computed tomography-guided pulmonary nodule localization before thoracoscopic resection. Acta Radiol 45:284–288

Heywang-Köbrunner SH, Heinig A, Pickuth D et al. (2000) Interventional MRI of the breast: lesion localization and biopsy. Eur Radiol 10:36–45

Horan TA, Pinheiro PM, Araujo LM et al. (2002) Massive gas embolism during pulmonary nodule hook wire localization. Ann Thorac Surg 73:1647–1649

Kastl S, Langwieler TE, Krupski-Berdien G et al. (2006) Percutaneous localization of pulmonary nodules prior to thoracoscopic surgery by CT-guided hook-wire. Anticancer Res 26:3123–3126

Kobayashi T, Kaneko M, KondoH et al. (1997) CT-guided bronchoscopic barium marking for resection of a fluoroscopically invisible peripheral pulmonary lesion. Jpn J Clin Oncol 27:204–205

Kuhl CK (2002) Interventional breast MRI: needle localisation and core biopsies. J Exp Clin Cancer Res 21(3 Suppl):65–68

LaTrenta LR, Menell JH, Morris EA et al. (2003) Breast lesions detected with MR imaging: utility and histopathologic importance of identification with US. Radiology 227:856–861

Lossef SV (2005) CT-guided Kopans hookwire placement for preoperative localization of an appendicolith. AJR Am J Roentgenol 185:81–83

Morrison WB, Sanders TG, Parsons TW et al. (2001) Preoperative CT-guided hookwire needle localization of musculoskeletal lesions. AJR Am J Roentgenol 176:1531–1533

Mullan BF, Stanford W, Barnhart W et al. (1999) Lung nodules: improved wire for CT-guided localization. Radiology 211:561–565

Poretti FP, Brunner E, Vorwerk D (2002) Einfache Lokalisation von intrapulmonalen Rundherden—CT-gesteuerte perkutane Hakenmarkierung. Rofo 174:202–207

Powell TI, Jangra D, Clifton JC et al. (2004) Peripheral lung nodules: fluoroscopically guided video-assisted thoracoscopic resection after computed tomography-guided localization using platinum microcoils. Ann Surg 240:481–489

Shah RM, Spirn PW, Salazar AM et al. (1993) Localization of peripheral pulmonary nodules for thoracoscopic excision: value of CT-guided wire placement. AJR Am J Roentgenol 161:279–283

Schneider JP, Schulz T, Rüger S et al. (2002) MRT-gestützte Markierung und Stanzbiopsie suspekter Mammaläsionen Möglichkeiten und Erfahrungen an einem vertikal offenen 0,5-T-System. Radiologe 42:33–41

Suzuki K, Nagai K, Yoshida J et al. (1999) Video-assisted thoracoscopic surgery for small indeterminate pulmonary nodules: indications for preoperative marking. Chest. 115:563–568

Tsuchida M, Yamato Y, Aoki T et al. (1999) CT-guided agar marking for localization of nonpalpable peripheral pulmonary lesions. Chest 116:139–143

Part III
Therapeutic Interventions

Interventional Oncology

13

Stephan Clasen, Philippe L. Pereira, Andreas Lubienski, Arnd-Oliver Schäfer, Andreas H. Mahnken, Thomas Helmberger, Thomas J. Vogl, Katrin Eichler, Thomas Lehnert, Martin G. Mack, Dirk Meister, Christian Rosenberg, Norbert Hosten, Markus Düx, Konrad Mohnike, Jens Ricke, Alexander Beck, and Susanne Hengst

Contents

13.1 Radiofrequency Ablation

13.1.1 Radiofrequency Ablation – Technical Basics

Stephan Clasen and Philippe L. Pereira

13.1.1.1 Introduction

Percutaneous thermal ablation therapy represents a local tumor treatment. Hyperthermal ablation procedures eradicate tumor tissue with heat in a circumscribed area. Applied techniques are radiofrequency (RF) ablation, laser interstitial thermotherapy, microwave ablation, and high-intensity focused ultrasound. Image guidance enables a minimally invasive application of thermal ablation therapy. Among these techniques, percutaneous RF ablation has attained widespread consideration. Image-guided local ablation therapy has gained importance predominantly in the therapy of primary and metastatic liver tumors (Solbiati et al. 2001; Livraghi et al. 2000). Beside the hepatic application, RF ablation is an established treatment for osteoid osteoma (Rosenthal et al. 2003). Furthermore, potential indications for image-guided RF ablation include primary and secondary pulmonary malignancies (Dupuy et al. 2000a), renal cell carcinoma (Gervais et al. 2003), and the treatment of symptomatic osseous and soft-tissue tumors (Goetz et al. 2004).

The application of heat for coagulation of vital tissue was mentioned in about 3000 B.C. in the Edwin Smith papyrus (Siperstein and Gitomirski 2000). In the Egyptian and Greek literature it is reported that the probes were heated by a flame. In the nineteenth century direct current became available and was used for cauterization to surgically control bleeding; thereby, the current induced a resistive heating within the tip of the surgical probes. The discovery of direct heating within living tissue by using a RF current was made by d'Arsonval in 1891. He described that an alternating current at high frequency (10 kHz) does not cause pain or muscular contractions, but causes elevation in temperature while passing through the living tissue (d'Arsonval 1891). This transformation of electric energy into thermal energy within living tissue represents the basis for RF ablation. In 1900, Riviere demonstrated that by increasing the density of the electric current with a small electrode, higher tissue temperatures with destructive effects are obtained (Siperstein and Gitomirski 2000). At the beginning of the nineteenth century, electrocauterization was characterized by a limited extent of thermally induced coagulation. In 1926, Cushing introduced RF energy to neurosurgery for ablation of intracranial tumors (Siperstein and Gitomirski 2000). In 1990, two independent groups of researchers introduced hepatic RF ablation (Rossi et al. 1990; McGahan et al. 1990). The clinical application of percutaneous RF ablation for the treatment of hepatic tumors was subsequently described by these two groups at the beginning of the 1990s. Since that time ongoing technical development of RF ablation has focused on the improvement of RF systems to induce predictable and larger zones of coagulation.

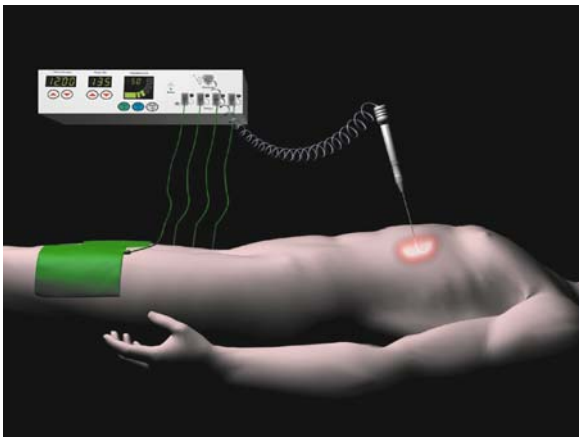

Fig. 13.1 The electric circuit of a monopolar radiofrequency (RF) system comprises the RF generator, cables, a needlelike "active" electrode placed within the target tissue, dispersive electrodes ("grounding pads") placed on the body surface, and the patient's body

13.1.1.2 Principle of RF Ablation

RF ablation is a local tumor treatment by inducing thermal injury within the target tissue. The principle of RF ablation is a transformation of electromagnetic energy into thermal energy. For that reason an alternating electric current that oscillates at a high frequency (200–1200 kHz) is applied (Rhim et al. 2001). Commercially available RF systems operate at a frequency in the range 375–480 kHz (Pereira et al. 2004; Clasen et al. 2006). High-frequency electric current causes the tissue ions to become agitated owing to the ions attempting to follow the changes in the direction of the alternating electric current (Rhim et al. 2001). The ion agitation causes frictional heat within the tissue. For a local tumor ablation, a focal induction of heat is essential to avoid thermal injury to critical anatomic structures in the surroundings of the target tissue. In monopolar RF systems, one electrical pole is placed inside the target tissue and the second electrical pole is placed on the body surface; in bipolar RF systems, both electrical poles are placed inside the target tissue. The most widely used RF devices are monopolar systems and the electric circuit comprises the RF generator, cables, a needlelike "active" electrode placed within the target tissue, dispersive electrodes ("grounding pads") placed on the body surface, and the patient's body (Rhim et al. 2001; Fig. 13.1). The tissue between the "active" electrode and the grounding pads acts as a resistor. Given the relatively high electrical resistance of tissue in comparison with that of the metal electrodes, there is a marked agitation of tissue ions (Rhim et al. 2001). Consequently, the tissue represents the source of heating and not a heated applicator placed in the target tissue. Due to the marked discrepancy between the surface area of the small needle electrode within the target tissue and the large dispersive electrode on the body surface, the density of the electric field is focused on the immediate surrounding of the

needle electrode; therefore, the heating is concentrated on the target tissue adjacent to the needle electrode. The use of multiple large grounding pads ensures an optimal dispersion of the electric current within the patient's body and minimizes the risk of unintended heating at a distance from the needle electrode. In addition, the grounding pads should be equidistant from the target tissue and should be oriented with the longest surface edge facing the needle electrode to avoid skin burns at the site of the grounding pads (Goldberg et al. 2000c). Modifications of the RF technique will be discussed in conjunction with the different RF systems.

13.1.1.3 Thermal Bioeffects

Interaction of Heat and Cell Function

Thermal effects depend on both the tissue temperature and the duration of heating. Cell homeostasis can be maintained if the normal body temperature is slightly increased in the region of up to 40 °C. An increased temperature in the range 42–45 °C results in the cells being more susceptible to damage (Seegenschmiedt et al. 1990). Exposure to 45 °C for several hours causes irreversible cellular damage (Rhim et al. 2001). A further increase in temperature to 50–55 °C reduces the duration necessary to irreversibly damage cells to 4–6 min (Rhim et al. 2001). With temperatures between 60 and 100 °C, nearly immediate thermal damage occurs, being characterized by irreversible protein denaturation, damage to cytosolic and mitochondrial enzymes, as well as destruction of the important protein structure of the DNA (Zervas and Kuwayama 1972; Goldberg et al. 2000a). Histopathologically, these high temperatures result in a coagulation necrosis. When the temperature is increased to more than 100–110 °C, tissue vaporizes and carbonizes. Vaporization and carbonization result in a marked increase of tissue resistance and subsequently in a reduced effectiveness of the RF energy applied; therefore, an increase in temperature to more than 100 °C should be avoided during RF ablation. Consequently, achievement and maintenance of a temperature in the range 60–100 °C within the entire target volume is considered optimal for RF ablation.

Interaction of RF Ablation and Tissue Characteristics

The physical parameters of tumor tissue and the surrounding tissue have a significant impact on the application of RF energy. Thermal and electrical conductivity influence the alternating electric current and the distribution of heat. The focus of generated heat by the alternating electric field is in the immediate surrounding of the noninsulated tip of the RF electrode. Since high thermal gradients occur during RF ablation, thermal conduction contributes significantly towards tissue heating in the periphery of the ablation zone (Schramm et al. 2006). High thermal conductivity may contribute to heat loss at the periphery of the ablation zone. On the other hand, increased thermal conductivity allows heat to diffuse more quickly and deeper into the tissue; consequently, increased thermal conductivity enables an increased input of energy and greater volumes of coagulation (Liu et al. 2005). Tissues with low thermal conductivity in the surrounding of the tumor tissue increase heating within the central tumor, particularly in long-lasting application of RF energy and in smaller tumors (Liu et al. 2006). For example, heating of hepatocellular carcinoma within a cirrhotic liver, having a low thermal conductivity, may be augmented (Liu et al. 2006). Electrical conductivity of the tumor and background tissue influences the electric field. Modulation of electrical conductivity in the surrounding of the RF electrode by injection of a conductive fluid such as saline is feasible. The effect of this modulation depends on generator capabilities, the type of fluid, as well as the volume and concentration of the injected fluid (Lobo et al. 2004; Bruners et al. 2007). Application of small amounts of saline in combination with a high concentration increases the efficiency of energy application by increasing the electrical conductivity in the surrounding of the RF electrode (Lobo et al. 2004). In contrast, there is an inverse relationship for the coagulation volume and the overall impedance of the electric circuit. A high impedance, corresponding to a low electrical conductivity, correlates to larger volumes of coagulation (Ahmed et al. 2004); therefore, a low electrical conductivity of the tissue surrounding the tumor may increase the effectiveness of RF ablation. For example, RF ablation in lung tissue is characterized by a low electrical conductivity of the normal lung parenchyma, leading to pronounced resistive heating at the interface of tumor tissue, having

a high electrical conductivity, and the lung tissue, having a low electrical conductivity (Ahmed et al. 2004). Therefore, beside the focus of heating adjacent to the RF electrode, there is a second focus of heating at the tumor periphery leading to larger volumes of coagulation. On the other hand, a low electrical conductivity at the tumor boundaries can restrict current flow into peripheral tissue; consequently, induction of a safety margin might be hindered (Ahmed et al. 2004).

Interaction of RF Ablation and Blood Flow

Convection by means of blood flow leads to removal of heat; therefore, vascularization of tumor tissue and the surrounding tissue does significantly determine the efficiency of the energy applied. Macroscopic vessels with a diameter of more than 1 mm lead to a so-called heat sink effect (Goldberg et al. 2005). In effect, the shape of coagulation is altered away from the blood vessel, and the overall volume of coagulation is reduced (Goldberg et al. 2005). This cooling effect of blood flow may protect macroscopic vessels from thermal injury and reduces the risk of bleeding and thrombosis. On the other hand, the probability of an incomplete ablation is increased owing to the possibility of persistent vital tumor cells adjacent to the vessels. The term "perfusion-mediated tissue cooling" encompasses the effects of larger heat sink vessels and the effects of capillary microperfusion (Goldberg et al. 1998a). Computer modeling has demonstrated that increased perfusion exponentially decreases the ablation zone and the time to achieve thermal equilibrium (Liu et al. 2007). For smaller tumors (2–3 cm), the tumor ablation is supposed to be mainly determined by the perfusion of the outer tissue. For larger tumors (4–5 cm), the inner tumor perfusion is supposed to be predominant (Liu et al. 2007). Owing to the significant impact of blood flow on the effectiveness of RF ablation, several strategies have been developed to overcome this limitation. Techniques are a pharmacologically decreased blood flow, temporary vascular balloon occlusion of specific vessels (for example, in hepatic RF ablation – hepatic artery, hepatic vein, portal vein), intraarterial embolization or chemoembolization, and a Pringle maneuver in the case of intraoperative hepatic RF ablation (Goldberg et al. 2005).

13.1.1.4 RF Systems

The initial RF systems were developed for neurosurgical and cardiac applications, such as the treatment of hyperactive neurological foci or aberrant cardiac conductive pathways (Gazelle et al. 2000); therefore, precise and small zones of coagulation were required. The use of conventional monopolar RF electrodes enabled a maximum diameter of induced coagulation no greater than 1.6 cm (Rhim et al. 2001). For the treatment of malignant tumors, larger zones of coagulation are required to enable complete coagulation of tumor tissue, including a safety margin. The numerous parameters influencing the volume of thermally induced coagulation necrosis were previously explained by Pennes (1948) using a complicated formula (Goldberg et al. 2000b; Liu et al. 2005):

$$\rho_t c_t \partial T(r,t)/\partial t = \nabla(k_t \nabla T) - c_b \rho_b m \rho_t (T - T_b) + Q_p(r,t) + Q_m(r,t)\,,$$

where ρ_t and ρ_b are the density of tissue and of blood (kg/m^3), c_t and c_b are the specific heat of tissue and of blood ($W\,s/kg\,^\circ C$), k_t is the thermal conductivity of tissue, m is the perfusion (blood flow rate per unit mass of tissue) ($m^3/kg\,s$), Q_p is the power absorbed per unit volume of tissue, and Q_m is the metabolic heating per unit volume of tissue (Goldberg et al. 2000b). In addition, one also has the electrostatic equation: $Q_p = j^2/\sigma$, where j is the current density and σ is the electrical conductivity (Liu et al. 2005).

This so-called bio-heat equation can be simplified by the formula extent of coagulation = applied energy × local tissue interactions − heat loss (Goldberg et al. 2000b). In accordance with the bio-heat equation, a strategy to extend the volume of coagulation is to increase the amount of energy applied. Therefore, investigators and manufacturers have made several technical developments to improve the RF systems to optimize the energy application. These strategies include:

- Internally cooled electrodes (Goldberg et al. 1998b)
- Perfusion electrodes (Schmidt et al. 2003)
- Multiprobe arrays such as clusters (Goldberg et al. 1995)
- Multitined expandable electrodes (de Baere et al. 2001)
- Bipolar and multipolar electrodes (Clasen et al. 2006)

Table 13.1 Technical data and characteristics of the most widely used radiofrequency (*RF*) systems

RF system	CC (Valleylab)	HiTT 106 (Integra)	Model 1500X (RITA)	RF 3000 (Boston Scientific)	CelonLab Power (Olympus)
Principle	Monopolar	Monopolar	Monopolar	Monopolar	Bi- and Multipolar
Maximum power output	200 W	60 W	250 W	200 W	250 W
Frequency	480 kHz	375 kHz	460 kHz	480 kHz	470 kHz
Applicator type	Internally cooled	Perfusion	Multitined expandable	Multitined expandable	Internally cooled
Applicator tip configuration	Straight	Straight	Christmas tree	Umbrella	Straight
Applicator shaft diameter	1.6 mm (single) 3 × 1.6 mm (cluster)	1.7 mm	2.2 mm	2.5 mm	1.8 mm (1–6 applicators)
Monitoring of ablation	Tissue impedance	Tissue impedance	Tissue impedance and temperature	Tissue impedance	Tissue resistance

- Modification of the algorithm of energy deposition (Goldberg et al. 1999)

In addition, the local tissue interaction may be modified by increasing the electrical conductivity within the target tissue, by improving the heat conduction into the tissue, or by increasing the vulnerability of the tumor tissue for thermal injury (Rhim et al. 2001). Moreover, the heat loss may be minimized by adjunct techniques to reduce perfusion-mediated tissue cooling (Rossi et al. 2000). The characteristics of different commercially available RF systems are summarized in Table 13.1.

Monopolar RF Systems

Monopolar RF systems apply the energy between an active electrode placed in the target tissue and one or more large dispersive electrodes (grounding pads) placed on the body surface. The alternating electric current is generated by an RF generator. The monopolar RF generators use a power output of 60 W (HiTT 106®, Integra, Plainsboro, NJ, USA), 200 W (RF 3000®, Boston Scientific, Mountain View, CA, USA, and CC®, Valleylab, Boulder, CO, USA), or 250 W (1500X®, RITA Medical Systems, Mountain View, CA, USA). The function of these RF generators is to generate a predefined alternating current and to control the amount of electric current applied to the tissue. The control of energy deposition is based on the tissue impedance (Integra, Boston Scientific, Valleylab), whereas the RITA systems additionally use the temperature at the electrode tip. The electrode design differs among the manufactures and has an important impact on the size and shape of the coagulation (Pereira et al. 2004).

Multitined Expandable Electrodes

The amount of energy applied can be increased by increasing the surface area of the noninsulated tip of the RF electrode placed within the target tissue (Goldberg et al. 1995; de Baere et al. 2001). Two manufacturers have designed multitined expandable electrodes. An array of multiple thin electrodes expands from a larger needle cannula. The array may have the configuration of an umbrella (Boston Scientific) or a Christmas tree (RITA Medical Systems). Usually the larger needle cannula is placed centrally within the target tissue and, thereafter, the smaller electrodes are expanded. Variable deployment lengths and diameters of the array are available. For larger arrays a stepwise deployment may be necessary.

Internally Cooled Electrodes

Internal cooling of the RF electrode is a strategy to increase energy application. Internal lumina enable a perfusion of the electrode shaft with saline or water. The fluid does contact with the tissue surrounding the RF electrode. By cooling the electrode tip during the application of RF energy, one can increase the generator output and prevent vaporization and carbonization adjacent to the RF electrode. Subsequently, internal cooling prevents or delays a deleterious increase in circuit impedance (Gazelle et al. 2000). To ensure

complete coagulation adjacent to the RF electrode, the internal cooling has to be switched off at the end of energy application. Application of an additional energy pulsing further increases the mean intensity of energy deposition (Goldberg et al. 2000b). When pulsing is used, periods of higher power output are rapidly alternated with periods of low power output (Goldberg et al. 1999). The periods of low power output enable preferential tissue cooling adjacent to the RF electrode without significantly decreasing heating deeper in the tissue (Goldberg et al. 2000b). The combination of pulsed energy application and internal cooling leads to a synergistic increase of induced coagulation (Goldberg et al. 2000b). Internally cooled electrodes are available as a straight single electrode and as a so-called cluster electrode with three straight electrodes combined in one applicator (Valleylab). The intention of these cluster electrodes is to increase the surface area of the RF electrode and, subsequently, to increase the energy deposition within the target tissue (Goldberg et al. 1995).

Perfusion Electrodes

This principle of perfusion electrodes is based on continuous infusion of fluid into the target tissue. The fluid is infused into the tissue through two to four micropores at the tip of the RF electrode (Integra, RITA). Usually normal or hypertonic saline is used to increase the electrical conductivity of the target tissue by application of ions. Other fluids, such as contrast ionic agents or ethanol, may be used alternatively (Bruners et al. 2007). Subsequently, the tissue resistance is reduced and the amount of energy applied can be increased. Perfusion electrodes enable the induction of large zones of coagulation (de Baere et al. 2001; Pereira et al. 2004). Disadvantages of a saline infusion may be an unpredictable distribution of fluid in the tissue (Gillams and Lees 2005) and the possibility of irregularly shaped zones of coagulation (Pereira et al. 2004).

Multiprobe Arrays

The combination of multiple monopolar RF electrodes can increase the volume of coagulation (Goldberg et al. 1995). The presence of multiple independent heat sources is supposed to lead to less heat dissipation (Haemmerich et al. 2001) and a synergistic effect of additive heat diffusion (Goldberg et al. 1995). A commercially available switching controller (Valleylab) enables rapid switching between three internally cooled single electrodes. If an impedance spike occurs during activation of one of these three electrodes, the application of energy is switched to the next electrode (Laeseke et al. 2006). This multiple electrode ablation induces larger volumes of coagulation compared with an internally cooled single or cluster electrode (Laeseke et al. 2006). In addition, the simultaneous production of separate zones of coagulation might be possible by switching the application of energy between different monopolar RF electrodes (Laeseke et al. 2005). For multiprobe arrays an accurate placement of all electrodes is necessary. This may lead to a prolonged electrode positioning compared with the application of one RF electrode.

Bipolar and Multipolar RF Systems

A different strategy compared with that for monopolar RF systems is to apply the RF energy exclusively in the target tissue by using bipolar or multipolar RF devices. In monopolar RF systems, the electric current passes through the whole tissue between the monopolar electrode and the grounding pads, and only a reduced amount of applied energy is used for RF ablation in the surrounding of the "active" electrode. The intention of bipolar and multipolar RF devices is to apply the RF energy exclusively within target tissue (Clasen et al. 2007). Therefore, in bipolar RF ablation the electric circuit is closed between two electrodes placed in proximity inside the target tissue and no grounding pads are required. A design with two electrodes located on different applicator shafts (McGahan et al. 1996) or on the same applicator shaft (Tacke et al. 2004; Clasen et al. 2007) is possible for bipolar RF ablation (Fig. 13.2). As opposed to the monopolar system, the tissue is heated around both poles of the electric circuit. In multipolar RF ablation more than two electrodes are placed within the target tissue and the electric field can be switched between every possible pair of electrodes. A commercially available RF generator (CelonLab Power, Celon, Berlin, Germany) providing a maximum power output of 250 W enables energy application in a bipolar and a multipolar mode. In the bipolar mode, RF energy is applied by an internally cooled applicator containing two noninsulated

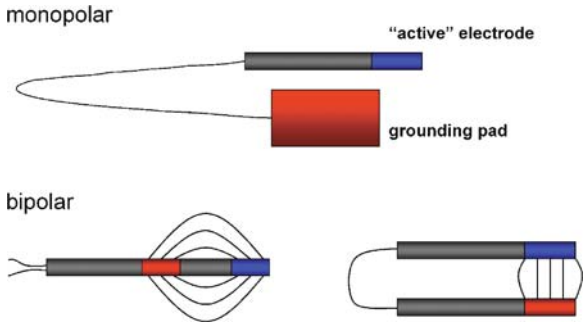

Fig. 13.2 The electric circuit in monopolar and bipolar RF ablation. In monopolar RF ablation, the electric circuit is closed between an "active" electrode placed within the target tissue and grounding pads placed on the body surface. In bipolar RF ablation, the electric circuit is closed between two electrodes placed within the target tissue, omitting the need for grounding pads. A design with two electrodes located on the same applicator shaft (*bottom left*) or on different applicator shafts (*bottom right*) is possible

electrodes separated by insulation. The electric field is orientated parallel to the bipolar applicator shaft. When more than one bipolar applicator is connected to the RF generator the electric current is automatically applied in a multipolar mode. In this multipolar mode every possible pair of electrodes is activated one after the other for a short period of time like a bipolar electrode, whereas the pairs of electrodes are not necessarily located on the same applicator shaft (Clasen et al. 2006). Therefore, the electric fields are orientated parallel to the bipolar applicators and cross the tissue within the applicators. Thus, when three bipolar applicators are used with six electrodes there are 15 possible combinations of electrode pairs. The tissue resistance between the electrodes is used to control bipolar and multipolar RF ablation.

Summary

Percutaneous RF ablation represents a technique for hyperthermal tumor ablation. Understanding the underlying mechanism and technical basics of RF ablation is essential to ensure safe and effective coagulation of the tumor tissue. The technical development of RF devices enables reproducible energy application and coagulation of tumor tissue. Several RF devices and protocols for energy application are available; however, clinical experience has shown that the standard protocols provided by the different manufacturers may have to be adapted to the individual situation because of the variable underlying tissue and tumor biology. Therefore, the interventional radiologist has to be familiar with the relationship between the parameters of RF ablation and the RF devices applied. Beside the technical aspects of RF ablation, the determination of appropriate indications for ablation therapy represents a key aspect for a reasonable and an effective clinical application of RF ablation. Considerations regarding the indication of RF ablation in relation to different tumor types and organ sites are discussed in subsequent sections.

Key Points

- RF ablation is influenced by multiple parameters, including tissue and tumor conductivity.
- The material has to be selected carefully for each ablation procedure.
- Additional measures such as fluid injection, preinterventional tumor embolization, or vessel occlusion may be used to modify the size and the shape of coagulation necrosis.

References

Ahmed M, Liu Z, Afzal KS et al. (2004) Radiofrequency ablation: effect of surrounding tissue composition on coagulation necrosis in a canine tumor model. Radiology 230:761–767

Bruners P, Hodenius M, Gunther RW et al. (2007) Flüssigkeitsmodulierte RF-Ablation: In-Vitro-Experimente Rofo 179:380–386

Clasen S, Schmidt D, Boss A et al. (2006) Multipolar radiofrequency ablation with internally cooled electrodes: experimental study in ex vivo bovine liver with mathematic modeling. Radiology 238:881–890

Clasen S, Schmidt D, Dietz K et al. (2007) Bipolar radiofrequency ablation using internally cooled electrodes in ex vivo bovine liver: prediction of coagulation volume from applied energy. Invest Radiol 42:29–36

d'Arsonval MA (1891) Action physiologique des courants alternatifs. C R Soc Biol 43:283–286

de Baere T, Denys A, Wood BJ et al. (2001) Radiofrequency liver ablation: experimental comparative study of water-cooled versus expandable systems. AJR Am J Roentgenol 176:187–192

Dupuy DE, Zagoria RJ, Akerley W et al. (2000) Percutaneous radiofrequency ablation of malignancies in the lung. AJR Am J Roentgenol 174:57–59

Gazelle GS, Goldberg SN, Solbiati L et al. (2000) Tumor ablation with radio-frequency energy. Radiology 217:633–646

Gervais DA, McGovern FJ, Arellano RS et al. (2003) Renal cell carcinoma: clinical experience and technical success with radio-frequency ablation of 42 tumors. Radiology 226: 417–424

Gillams AR, Lees WR (2005) CT mapping of the distribution of saline during radiofrequency ablation with perfusion electrodes. Cardiovasc Intervent Radiol 28:476–480

Goetz MP, Callstrom MR, Charboneau JW et al. (2004) Percutaneous image-guided radiofrequency ablation of painful metastases involving bone: a multicenter study. J Clin Oncol 22:300–306

Goldberg SN, Gazelle GS, Dawson SL et al. (1995) Tissue ablation with radiofrequency using multiprobe arrays. Acad Radiol 2:670–674

Goldberg SN, Hahn PF, Tanabe KK et al. (1998a) Percutaneous radiofrequency tissue ablation: Does perfusion-mediated tissue cooling limit coagulation necrosis? J Vasc Interv Radiol 9:101–111

Goldberg SN, Solbiati L, Hahn PF et al. (1998b) Large-volume tissue ablation with radio frequency by using a clustered, internally cooled electrode technique: laboratory and clinical experience in liver metastases. Radiology 209:371–379

Goldberg SN, Stein MC, Gazelle GS et al. (1999) Percutaneous radiofrequency tissue ablation: optimization of pulsed-radiofrequency technique to increase coagulation necrosis. J Vasc Interv Radiol 10:907–916

Goldberg SN, Gazelle GS, Compton CC et al. (2000a) Treatment of intrahepatic malignancy with radiofrequency ablation: radiologic-pathologic correlation. Cancer 88:2452–2463

Goldberg SN, Gazelle GS, Mueller PR (2000b) Thermal ablation therapy for focal malignancy: a unified approach to underlying principles, techniques, and diagnostic imaging guidance. AJR Am J Roentgenol 174:323–331

Goldberg SN, Solbiati L, Halpern EF et al. (2000c) Variables affecting proper system grounding for radiofrequency ablation in an animal model. J Vasc Interv Radiol 11:1069–1075

Goldberg SN, Grassi CJ, Cardella JF et al. (2005) Image-guided tumor ablation: standardization of terminology and reporting criteria. Radiology 235:728–739

Haemmerich D, Staelin ST, Tungjitkusolmun S et al. (2001) Hepatic bipolar radio-frequency ablation between separated multiprong electrodes. IEEE Trans Biomed Eng 48:1145–1152

Laeseke PF, Sampson LA, Haemmerich D et al. (2005) Multiple-electrode radiofrequency ablation: simultaneous production of separate zones of coagulation in an in vivo porcine liver model. J Vasc Interv Radiol 16:1727–1735

Laeseke PF, Sampson LA, Haemmerich D et al. (2006) Multiple-electrode radiofrequency ablation creates confluent areas of necrosis: in vivo porcine liver results. Radiology 241:116–124

Liu Z, Lobo SM, Humphries S et al. (2005) Radiofrequency tumor ablation: insight into improved efficacy using computer modeling. AJR Am J Roentgenol 184:1347–1352

Liu Z, Ahmed M, Weinstein Y et al. (2006) Characterization of the RF ablation-induced 'oven effect': the importance of background tissue thermal conductivity on tissue heating. Int J Hyperthermia 22:327–342

Liu Z, Ahmed M, Sabir A et al. (2007) Computer modeling of the effect of perfusion on heating patterns in radiofrequency tumor ablation. Int J Hyperthermia 23:49–58

Livraghi T, Goldberg SN, Lazzaroni S et al. (2000) Hepatocellular carcinoma: radio-frequency ablation of medium and large lesions. Radiology 214:761–768

Lobo SM, Afzal KS, Ahmed M et al. (2004) Radiofrequency ablation: modeling the enhanced temperature response to adjuvant NaCl pretreatment. Radiology 230:175–182

McGahan JP, Browning PD, Brock JM et al. (1990) Hepatic ablation using radiofrequency electrocautery. Invest Radiol 25:267–270

McGahan JP, Gu WZ, Brock JM et al. (1996) Hepatic ablation using bipolar radiofrequency electrocautery. Acad Radiol 3:418–422

Pennes HH (1948) Analysis of tissue and arterial blood temperatures in the resting human forearm. J Appl Physiol 1:93–122

Pereira PL, Trubenbach J, Schenk M et al. (2004) Radiofrequency ablation: in vivo comparison of four commercially available devices in pig livers. Radiology 232:482–490

Rhim H, Goldberg SN, Dodd GD 3rd et al. (2001) Essential techniques for successful radio-frequency thermal ablation of malignant hepatic tumors. Radiographics 21: 17–39

Rosenthal DI, Hornicek FJ, Torriani M et al. (2003) Osteoid osteoma: percutaneous treatment with radiofrequency energy. Radiology 229:171–175

Rossi S, Fornari F, Pathies C et al. (1990) Thermal lesions induced by 480 KHz localized current field in guinea pig and pig liver. Tumori 76:54–57

Rossi S, Garbagnati F, Lencioni R et al. (2000) Percutaneous radio-frequency thermal ablation of nonresectable hepatocellular carcinoma after occlusion of tumor blood supply. Radiology 217:119–126

Schmidt D, Trubenbach J, Brieger J et al. (2003) Automated saline-enhanced radiofrequency thermal ablation: initial results in ex vivo bovine livers. AJR Am J Roentgenol 180:163–165

Schramm W, Yang D, Haemmerich D (2006) Contribution of direct heating, thermal conduction and perfusion during radiofrequency and microwave ablation. Conf Proc IEEE Eng Med Biol Soc 1:5013–5016

Seegenschmiedt MH, Brady LW, Sauer R (1990) Interstitial thermoradiotherapy: review on technical and clinical aspects. Am J Clin Oncol 13:352–363

Siperstein AE, Gitomirski A (2000) History and technological aspects of radiofrequency thermalablation. Cancer J 6(Suppl 4):5293–5303

Solbiati L, Livraghi T, Goldberg SN et al. (2001) Percutaneous radio-frequency ablation of hepatic metastases from colorectal cancer: long-term results in 117 patients. Radiology 221:159–166

Tacke J, Mahnken A, Roggan A et al. (2004) Multipolar radiofrequency ablation: first clinical results. Rofo 176: 324–329

Zervas NT, Kuwayama A (1972) Pathological characteristics of experimental thermal lesions: Comparison of induction heating and radiofrequency electrocoagulation. J Neurosurg 37:418–422

13.1.2 RF Ablation of Liver Tumors

Andreas Lubienski

13.1.2.1 Indications

RF ablation of primary and secondary hepatic tumors has been used for more than 10 years. Continuous improvements of RF generators and probes have led to reproducible and satisfactory results. However, given the limitations of currently available RF systems in addition to oncological considerations, the size and the site of a liver tumor play a crucial role in the achievement of complete ablation (Kuvshinoff and Ota 2002). Therefore, based upon adequate assessment of the overall tumor situation, including a precise hepatic tumor staging, a dedicated oncology team (e.g., tumor board) has to balance advantages and disadvantages of a minimally invasive approach and has to incorporate the interventional therapy chosen into a comprehensive treatment concept. Especially for liver metastases, no recommendation for the general use of RF ablation exists worldwide, resulting in a broad spectrum of individual indications for RF ablation in the liver. Since RF ablation is not yet a generally accepted first- or second-line treatment, it has to be considered as a palliative intention-to-treat therapy option. Given the unique biology of metastatic neuroendocrine disease, surgical experience has shown that debulking of tumors can considerably improve patient survival and symptoms. However, there is no proven evidence of this concept in other tumor entities, even though one can argue that aggressive ablation of hepatic metastases with destruction of more than 90% of the tumor burden could result in a benefit (Atwell et al. 2005). Treatment strategies for hepatocellular carcinoma (HCC) also vary throughout the world, in particular owing to geographical differences in the incidence and presentation of the disease and the treatment options available. In contrast to secondary liver malignancies, several treatment guidelines for HCC have been published by the European Association for the Study of the Liver (Bruix et al. 2001), with the Barcelona Clinic Liver Cancer (BCLC) staging recommendation being the most accepted one (Table 13.2) (Sala et al. 2004; Mor et al. 1998). It links tumor stage with treatment strategy, and is aimed at incorporating an estimation of the prognosis and potential treatment advancements in a single unified proposal (Sala et al. 2004). According to these guidelines, RF ablation has substituted ethanol injection therapy and has a place in the treatment strategy of HCC, generally as a second choice when surgical techniques are precluded in patients with early-stage tumors; nevertheless, in some centers in Italy and Japan, RF ablation is even used as a first-line treatment option.

To destroy any given hepatic tumor completely the ablation volume should encompass the entire tumor burden with an additional safety margin of 5–10 mm according to the guidelines for liver surgery. The pathophysiological rationale for the safety margin is the high likelihood of scattered tumor cells (invisible to imaging) immediately around the tumor itself (visible by imaging). Tumors of 2-cm diameter present local metastases less than 10 mm distant from the primary tumor in about 10% of cases, and microscopic portal invasion in up to 25% of cases (Kojiro 2004). If only the visible tumor is ablated, local recurrence can easily emerge from the tumor cells remaining around the visible tumor. Since the available probe designs allow more or less spherical ablation volumes with a maximum diameter of about 4–5 cm in a single ablation session, tumors presenting with a diameter of 3–4 cm can be treated to achieve an adequate safety margin. A possible reason for failures in the treatment of larger tumors is the inability to determine the optimal number of ablations and the exact location of probe placement needed to completely destroy tumors larger than the size of a single ablation zone. To treat even larger tumors, multiple ablations need to be overlapped to build a composite thermal injury of sufficient size to kill the tumor and provide an adequate tumor-free margin (McGahan and Dodd 2001; Chen et al. 2004). Dodd et al. (2001) reported their results of computer analysis of the thermal injury sizes created by overlapping ablations and proposed six- and 14-ablation models for diameters of 4.25 and 6.3 cm, respectively. Their results demonstrated the importance of performing these types of calculations to develop tumor ablation strategies. These considerations are approved by the recent literature, in which local recurrence rates of primary and secondary liver tumors are reported to rise with tumor size after a single ablation, or several ablation sessions are needed to achieve complete ablation (Poon et al. 2002, 2004a,b; Lencioni et al. 2005; Lu et al. 2005; Choi et al. 2007a). According to these current data, the cut-off tumor diameter for a primary successful RF ablation in the liver

Table 13.2 Barcelona Clinic Liver Cancer: stage-dependant treatment of hepatocellular carcinoma (HCC)

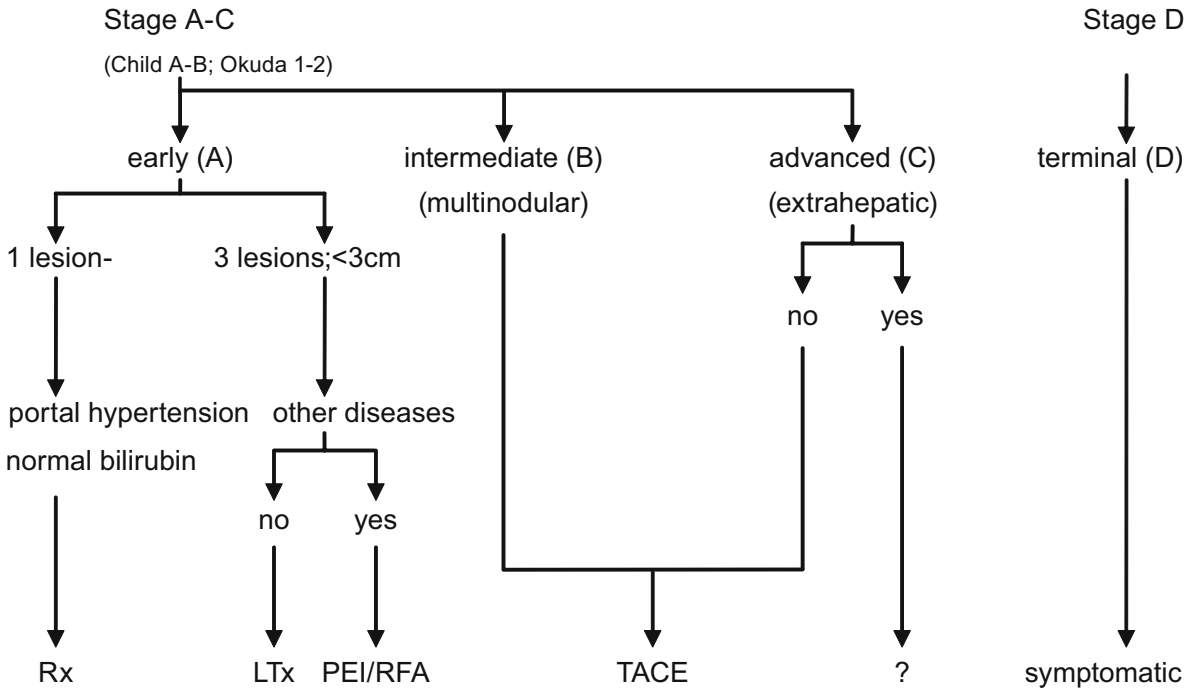

Rx – liver resection, LTx – liver transplantation, PEI – percutaneous ethanol injection, RFA – radiofrequency ablation, TACE – transarterial chemoembolization

Table 13.3 Inclusion and exclusion criteria for RF ablation in liver tumors

Prerequisites	Adequate assessment of the overall tumor situation
	Incorporation of RF ablation into a comprehensive treatment concept
	Balance of advantages and disadvantages of a minimally invasive therapy by an interdisciplinary oncology team
Indications	Exclusion of resectability
	Bilobar hepatic tumors
	Medical reasons
	Fewer than 4–5 tumors
	Tumor diameter $< 3.5-5$ cm
Contraindications	Progressive systemic disease
	More than 5 tumors
	Tumor diameter > 5 cm
	Colorectal metastases > 3.5 cm
	Portal vein thrombosis (single branch?)
	Septicemia, coagulopathy
	Tumor volume $> 50\%$ liver volume
Relative contraindications	Biliodigestive anastomosis
	Pacemaker
	Vicinity to critical structures

is about 3 cm using an RF system that is available at present – independent of the anatomical tumor site and histopathological tumor type.

Another independent predictor of a successful ablation is the so-called heat sink effect caused by heat dissipation when tumors are located adjacent to major vessels. Lu et al. (2003) showed that, in 105 tumors with a mean diameter of 2.4 cm treated with two different multitined and one clustered RF system (no difference regarding the RF system used or whether it was open or percutaneous access), tumors at least 3 mm from major vessels presented a primarily incomplete ablation or recurrence only in 7% of cases, while this was true in 48% of tumors that were located directly adjacent to major vessels. As a consequence, both these independent predictors of success – tumor

size and vascular proximity – have to be incorporated into an RF ablation treatment concept.

Although no general consensus concerning the indication of RF ablation in liver malignancies exists, basic inclusion and exclusion criteria as shown in Table 13.3 are recommended and should be taken into account when RF ablation in liver tumors is discussed.

13.1.2.2 Material

RF Generators

Several commercially available RF generators are FDA- and CE-approved and can be used in the clinical setting. These may be separated in monopolar, bipolar, und multipolar RF systems.

The monopolar RF generators work with a power ranging from 60 W (HiTT Elektrotom 106, Berchtold-Integra, Plainsboro, NJ, USA) to 200 W (RF 3000, Boston Scientific, Mountain View, CA, USA, and Cool Tip, Valleylab, Boulder, CO, USA) and 250 W (1500x, RITA Medical Systems, Mountain View, CA, USA). The different vendors pursue slightly different strategies in terms of generator control and therefore the ablation process. On the one hand ablation is controlled on the basis of tissue resistance (Berchtold-Integra, Boston Scientific, Valleylab) and on the other hand it is controlled on the basis of temperature (RITA) (see Sect. 13.1.1). Each device comes with a standard protocol for liver ablation which, from clinical experience, has to be adapted to each individual tumor. Thus, a successful tumor ablation depends on the experience of the interventionalist who has to decide on the ablation parameters, such as ablation length, probe, power output, and the number of applicator repositioning procedures required to treat the entire tumor, including a safety margin (Poon et al. 2004b). Recently a commercially available RF device (Celon Lab Power, Olympus-Celon, Teltow, Germany) providing a maximum power output of 250 W has enabled application of RF energy in bipolar and multipolar modes.

Monopolar Systems

Monopolar RF systems consist of an RF generator, large dispersive electrodes (grounding pads usually placed on the thighs of a patient), and a needle electrode. This setting turns the patient into a resistor within a closed-loop circuit. Thus, an alternating electric field is created within the tissue of the patient. The electrical energy is concentrated around the noninsulated tip of the needlelike electrode, resulting in marked agitation of the ions in the surrounding tissue (Ni et al. 2000; Goldberg and Gazelle 2001; Pereira et al. 2003).

Bipolar Systems

In contrast to monopolar systems, bipolar systems consist of two noninsulated electrodes (positive and negative) integrated into one applicator. Owing to the fact that the electrical circuit is closed between these two electrodes, grounding pads are not necessary. Tissue is heated either around the positive or the negative electrode, which in fact is different from monopolar systems. So far only one commercially available system can be used (Celon Lab Power, Olympus-Celon, Teltow, Germany). With this device, two electrodes are located on the same shaft of the applicator for bipolar RF ablation. The electric field is orientated parallel to the bipolar applicator shaft. Several of these bipolar probes can be placed clusterlike in situ, allowing multipolar ablation controlled by a specific switchbox. The combination of three bipolar probes leads to a more spherical ablation zone than with two bipolar arrays (Burdio et al. 2003; Tacke et al. 2004; Clasen et al. 2006, 2007).

RF Probes

Currently several different probe designs are available for clinical use. In principle, an RF electrode consists of an insulated metallic shaft and a noninsulated, active tip of variable length and/or design. The active tip is in contact with the target tissue to close the electric circuit including the RF generator, the probe, and the patient. As described already, the electrical energy provided by the RF generator is concentrated around the noninsulated tip of the probe, resulting in a certain ablation area which in fact is dependent on the design of the RF probe. To increase the ablation volume, several modifications to the probe design have been developed, e.g., extending the length of the antenna (cluster needle, umbrella-like/inverted-

umbrella-like design) or internal cooling of the probe to avoid premature carbonization around the needle tip followed by insulation and energy decay. At present, the available probes provide ablation volumes with more or less spherical diameters of between 2 and 5 cm. Although comparisons of different probe designs concerning efficacy have been made (Pereira et al. 2004b), it seems that a more important role regarding the proper use of a device might be how experienced the user is (Poon et al. 2004b; Lu et al. 2005). The rate of complete ablation significantly increased during the learning period in a prospective analysis regardless of the RF probe chosen (single or cluster electrode) (Poon et al. 2004b). Lu et al. (2005) confirmed these results, since in their work the most important factor influencing the primary success rate was tumor size, independent of electrode design (cluster vs. multitined).

13.1.2.3 Technique

Patient Preparation

Preprocedural evaluation should include adequate laboratory tests to rule out severe coagulopathy, acute inflammation, poor liver function (Child class B and C cirrhosis) and/or other severe comorbidities. A screening for viral hepatitis should follow. Baseline serum tumor markers – α-fetoptotein in patients with HCC and carcinoembryonic antigen in metastatic patients – are helpful for monitoring the therapeutic success during follow-up. For therapy planning, assessment of the tumor extent and of the tumor baseline for subsequent follow-up studies using contrast-enhanced dynamic computed tomography (CT) and magnetic resonance (MR) imaging still play the major role, while ultrasound is hampered by its reproducibility (Vilana et al. 2006). If there is a history of bone pain and/or the serum alkaline phosphatase is disproportionately elevated, a bone scan or whole-body MR imaging is necessary to rule out bone metastases (Nakanishi et al. 2005). Informed consent is necessary 24 h prior to the procedure at the latest.

RF ablation can usually be performed as a minimally invasive, percutaneous procedure under conscious sedation. General anesthesia is usually not required. For image guidance, ultrasound, CT, or MR imaging can be used (Lencioni et al. 2001). Since ultrasound is widely available and is a real-time, multiplanar technique which allows in many cases for easy in-plane and off-plane access to the target and visualization of the RF probe, it is reported to be the most often used guiding method for RF ablation (Solbiati et al. 2004a). However, depending on the given individual's anatomical and pathological characteristics, ultrasound is not able to tag the target or to follow the probe in all cases. Owing to the fact that during the ablation process the target is masked by a cloud of micro gas bubbles, it is difficult to identify the probe and the target during RF ablation and to assess the success of the ablation. Recent data suggest that contrast-enhanced ultrasound and new innovative hybrid systems merging the freedom of ultrasound guidance with the superior image information of CT or MR imaging may help to overcome the known ultrasound obstacles (Solbiati et al. 2004b; Nicolau et al. 2004). In contrast, CT guidance is mostly used by interventional radiologists (Fig. 13.3). It offers a significantly more "panoramic" view than ultrasound and especially when implemented with fluoroscopy it allows for optimal targeting of almost all hepatic tumors in all anatomical localizations. Major disadvantages are the lack of elbowroom within the scanner gantry, the exposure of the patient and the interventionalist to the radiation, and the use of a contrast agent for visualization of the target. In addition no significant changes in the treated tissue can be appreciated by CT in contrast to ultrasound. The full extent of the ablation can be identified only 12–18 h after RF ablation. Compared with ultrasound and CT, MR imaging offers the advantage to display heat-related intrinsic tissue alterations directly and on-line. In particular, MR-guided RF ablation is advantageous in locations unfavorable for CT guidance or in patients in whom iodized contrast media are contraindicated.

Procedure

To start the RF procedure for all guiding modalities the patient is usually placed in a supine position and an intravenous access line for sedation, analgesia, and emergent medication is established using an intravenous cannula placed in a cubital vein. Prophylactic antibiotics are usually not necessary. During the entire RF procedure the vital parameters of the patient are consequently monitored. After localization

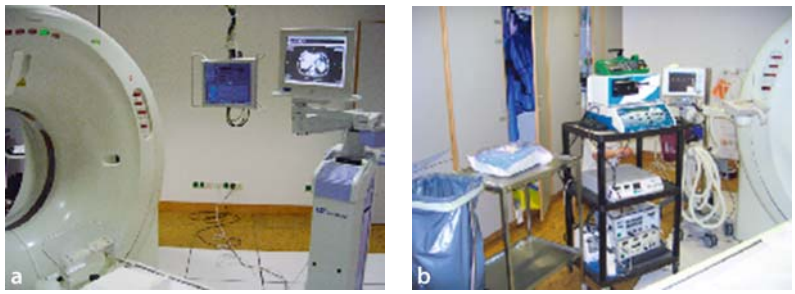

Fig. 13.3a,b Typical setting for RF ablation using computed tomography (CT) guidance. CT scanner with CT fluoroscopy and additional external guiding support (**a**). RF ablation rack with several commercially available RF systems, special equipment for CT-guided interventions (e.g., apron for X-ray protection), and monitoring devices for vital parameters (ECG, etc.) (**b**)

of the tumor using the preferred guidance method, the skin is prepped and draped. Then local anesthesia from the skin entry point of the needle down to the liver capsule is administered. For local anesthesia common local anesthetics such as mepivacaine, for sedation midazolam or fentanyl, and for analgesia piritramide can be used. Subsequently, the probe is placed within the tumor. Then the probe and in monopolar systems also the grounding pads have to be connected to the RF generator. Depending on the RF system used, the ablation process is started with different RF protocols. The control of the ablation itself is also device-dependent. Most RF systems use the relative increase of impedance as a parameter for controlling the ablation process, while increasing impedance regulates the delivered power down. At present only one system is equipped with multiple thermostats at the tips of the tines, thus offering on-line monitoring of the temperature. In general, to provide complete tissue necrosis the RF procedure takes 10–30 min per probe placement. Depending on the size of the tumor targeted, repositioning is required.

Postinterventional Follow-Up

Monitoring of therapy effectiveness is deemed to be a major issue in interventional tumor therapy. CT and MR imaging are, although widely used, of limited sensitivity, specificity, and accuracy when assessing the liver for residual tumor following RF ablation (Gillams and Lees 2000; Gillams 2001, 2003). This limitation relates to their predominantly morphologic character, which can only partly be compensated for by administration of contrast agents. The accuracy is limited by both spatial and contrast resolution to approximately 2–3 mm (depending on the imaging modality) (Gillams and Lees 2004). Postprocedural imaging findings are only a rough guide to the success of ablation therapy, since microscopic foci of residual disease, by definition, cannot be expected to be identified. Despite these facts, dynamic contrast-enhanced CT and MR imaging still play the major role in follow-up imaging after RF ablation (Fig. 13.4).

There are two types of imaging findings that can be identified after an ablation procedure: those related to zones of decreased or absent perfusion and those in which the signal intensity (MR imaging) or attenuation (CT) is altered (Dupuy and Goldberg 2001). Owing to the characteristics of some metastatic liver lesions (e.g., colorectal cancer), which are relatively hypovascular compared with the normal liver tissue, interpretation of follow-up scans is sometimes difficult since contrast enhancement of viable tumor foci may not be present or only minor. In addition, a periablational enhancement may be seen in early follow-up scans (Fig. 13.5). Especially in tumors with distinct contrast enhancement in preinterventional studies, rim enhancement after treatment might be confused with residual enhanced tumor tissue. Depending on the protocol used for contrast-enhanced imaging (injection rate and scanning delay), this transient finding can be seen immediately after ablation and can last for up to 6 months after ablation (Choi et al. 2001). It usually manifests itself as a penumbra, or a thin rim peripheral to the zone of ablation, that can typically measure up to 5 mm (in the immediate postinterventional phase), but most often measures 1–2 mm. It is characterized by a relatively concentric, symmetric, and uniform enhancement with smooth inner margins,

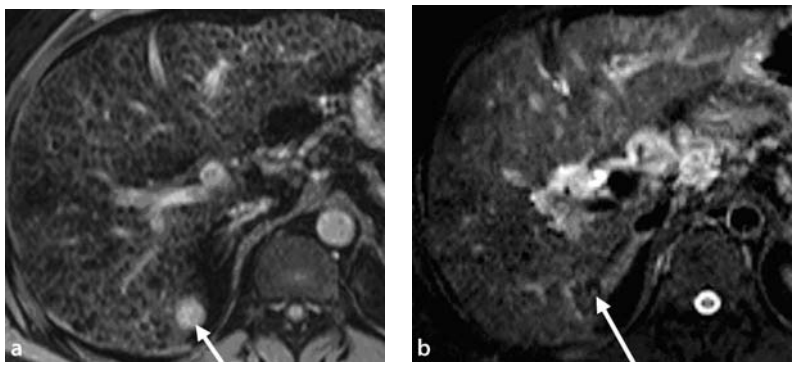

Fig. 13.4a,b T2-weighted magnetic resonance (MR) imaging using superparamagnetic iron oxide (SPIO) as a liver-specific contrast medium demonstrates clearly a hyperintense hepatocellular carcinoma (HCC) nodule in a subcapsular location in segment 6 (*arrow*) of the liver in a patient with underlying hepatitis C virus induced Child class A liver cirrhosis (**a**). Follow-up imaging 2 years after percutaneous RF ablation of the HCC: SPIO-MR imaging clearly shows complete ablation of the HCC with no evidence of viable tumor tissue in the former ablation area (**b**; *arrow*)

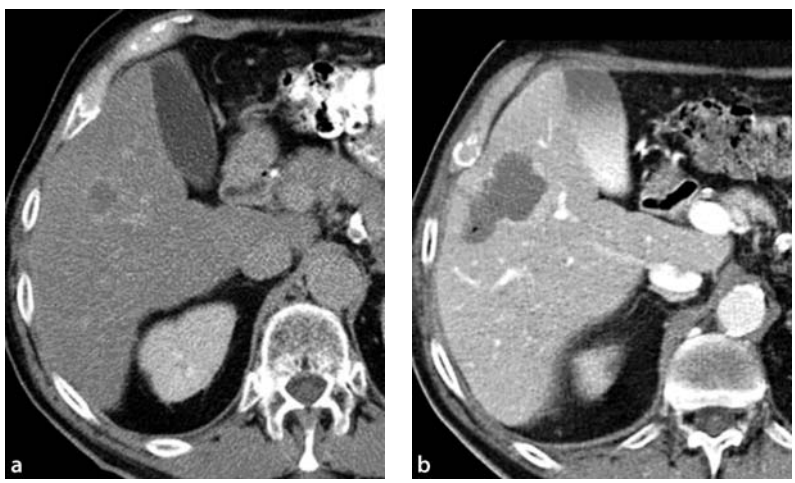

Fig. 13.5a,b CT scan prior to and 24 h after RF ablation of a recurrent unifocal liver metastasis of colorectal cancer. The contrast-enhanced portovenous CT scan delineates unifocal recurrent liver metastasis in segment 5 of the liver (**a**; *arrow*). **b** The contrast-enhanced portovenous CT scan 24 h after RF ablation shows a clear demarcation of the RF ablation zone (**b**; *short arrows*) including the probe track (*long arrow*) with a typical small hyperdense rim encompassing the former tumor nodule

which needs to be differentiated from irregular peripheral enhancement suspicious of recurrent or new tumor (Fig. 13.6). The finding is most readily appreciated on arterial phase CT scans, with persistent enhancement that is often seen on delayed MR images. Histopathologically, it represents a benign physiologic response to thermal injury (initially, reactive hyperemia; subsequently, fibrosis and giant cell reaction) (Goldberg et al. 2000). In contrast, irregular peripheral enhancement represents residual tumor at the treatment margin. It often appears in scattered, nodular, or eccentric patterns indicating incomplete local treatment (Figs. 13.6, 13.7). Given the delayed enhancement characteristics of many hypovascular tumors, this finding is often best appreciated in a side-by-side comparison of portal venous or delayed images (3 min or more after contrast material injection) with baseline images. Complete coagulation necrosis

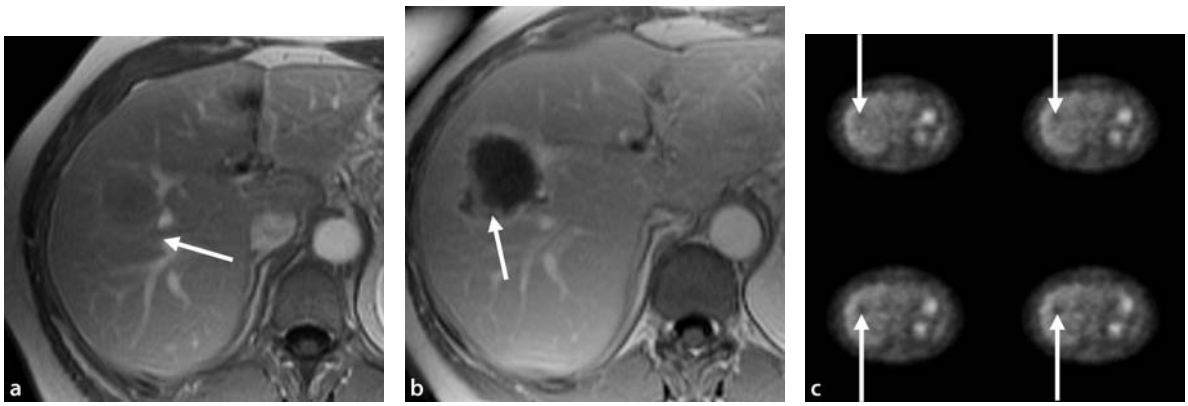

Fig. 13.6a–c CT scan prior to and 6 weeks after RF ablation and additional positron emission tomography (PET) scan of a recurrent unifocal liver metastasis of colorectal cancer. The contrast-enhanced portovenous CT scan delineates unifocal recurrent liver metastasis in segment 8 of the liver (**a**; *arrow*). The contrast-enhanced portovenous CT scan 6 weeks after RF ablation shows a clear demarcation of the RF ablation zone with some eccentric nodular irregularities at the posterolateral part of the ablation zone (**b**; *arrow*). The PET scan 8 weeks after RF ablation demonstrates no evidence of pathologic glucose metabolism within or around the ablation zone (*arrows*), representing complete RF ablation (**c**)

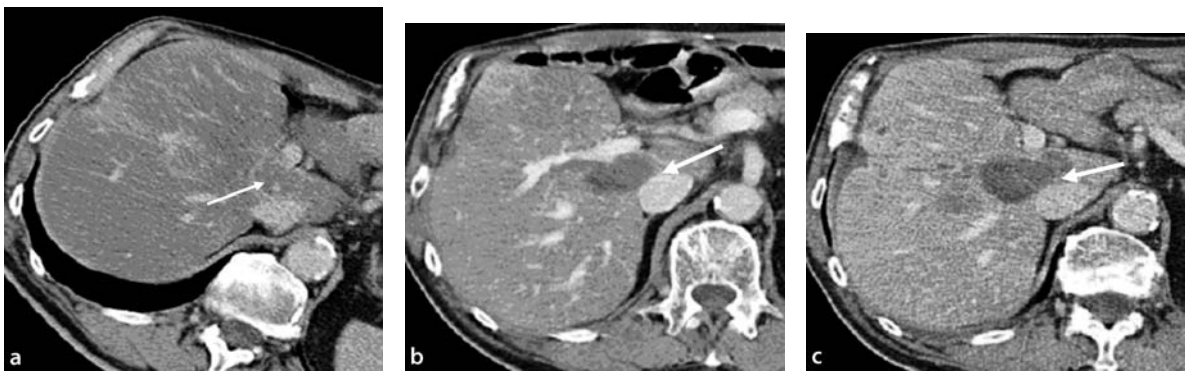

Fig. 13.7a–c CT scan prior to and 6 weeks after RF ablation and additional PET scan of a recurrent unifocal liver metastasis of colorectal cancer. The contrast-enhanced portovenous CT scan delineates unifocal recurrent liver metastasis in segment 8 of the liver (**a**; *arrow*). The contrast-enhanced portovenous CT scan 24 h after RF ablation shows a clear demarcation of the RF ablation zone (**b**; *arrow*). The contrast-enhanced portovenous CT scan 6 weeks after RF ablation shows a clear demarcation of the RF ablation zone with an eccentric nodular tumor recurrence at the peripheral part of the ablation zone in front of the inferior vena cava infiltrating segment 1 of the liver (**c**; *arrow*)

corresponds to hypoattenuating areas and fails to be enhanced after contrast injection. On MR imaging, the treated tumor is characterized by low signal intensity on T2-weighted images, whereas viable tumor is shown to be hyperintense on T2-weighted images (Sironi et al. 1999).

Biopsies of ablated areas in order to prove complete necrosis are generally unreliable and therefore not recommended (Solbiati et al. 2001). The ablation of appropriate margins (0.5–1.0 cm) beyond the borders of the tumor is necessary to achieve complete tumor destruction (Dodd et al. 2001). Therefore, an ablation zone that is not larger than the tumor before ablation should be followed up closely. Long-term follow-up imaging may show a gradual decrease in the volume of the ablation zone considered to represent only residual necrotic or fibrotic tissue that is present during the absorption process (Lim et al. 2001). It is important

to note that no or minimal involution does not imply treatment failure. Many other imaging findings, such as inflammatory stranding in the acute period after ablation, and more chronic findings, such as fibrosis, scarring, and architectural distortion that represent both host reaction to ablation and repair mechanisms will be seen.

When imaging and clinical findings at short-term follow-up are inconclusive and the suspected lesion is small, follow-up at 1–3-month intervals should be considered before performing an invasive diagnostic procedure such as percutaneous biopsy or repeated treatment (Lim and 2002). In most centers, follow-up scans are performed in 3-month intervals and are often combined with serum tumor markers such as carcinoembryonic antigen (Tacke 2003; Pereira et al. 2004a). Any increase in lesion size or irregularity or residual enhancement should be carefully interpreted in terms of residual tumor foci or recurrent metastases (Fig. 13.6). It is mandatory to look for evidence of both intrahepatic and extrahepatic tumor spread.

Initial results indicate that positron emission tomography (PET)/CT imaging may prove to be more accurate when evaluating the ablative zone for residual tumor than image analysis based on morphologic data alone. PET/CT may be expected to play a distinctive role in follow-up of patients undergoing RF ablation of liver lesions for the detection of residual tumor. The advantages of fused PET/CT data sets over PET alone and CT alone, respectively, are related to accurate localization of focally increased glucose metabolism in terms of therapeutic planning in an area of residual tumor, offering guidance for subsequent interventional procedures to these areas of viable tumor cells (Veit et al. 2006; Barker et al. 2005).

13.1.2.4 Results

The early clinical studies of RF ablation were performed to assess feasibility, aiming at safety, tolerability, and local therapeutic effect of the treatment. In recent years, RF ablation has evolved significantly concerning technical developments and procedure-related improvements and even in so-called difficult localization of hepatic tumors RF ablation can nowadays be performed safely and effectively (Figs. 13.8, 13.9). Therefore, the data collected in early studies may not be comparable with those of recent series. Although the findings of many studies on hepatic RF ablation as well as recommendations for the standardization and reporting criteria in RF ablation have been published, the analysis of clinical results of percutaneous RF ablation in liver tumors is still hampered by several problems (Goldberg et al. 2005). Many reports presented data which involve different tumor entities, including primary and metastatic liver tumors with different tumor sizes. Treatment was performed with different types of RF generators and probe designs and additional therapies such as resection, regional or systemic chemotherapy, and other local ablative techniques were used in combination with RF ablation. Finally, the studies had different end points and follow-up durations, as well as criteria for evaluating results.

Liver Metastases

So far no findings of randomized controlled trials evaluating RF ablation in the treatment of liver metastases have been published. In early clinical series Solbiati et al. (1997a) and Lencioni et al. (1998) performed RF ablation in patients with limited hepatic metastatic disease who were excluded from surgery. In the first series, 29 patients with 44 hepatic metastases ranging from 1.3 to 5.1 cm in diameter were treated. Each tumor was treated in one or two sessions, and technical success, defined as the lack of residual unablated tumor at CT or MR imaging obtained 7–14 days after completion of treatment, was achieved in 40 of 44 lesions. However, follow-up imaging studies confirmed complete necrosis of the entire metastasis in only 66% of the cases, whereas local tumor progression was observed in the remaining 34%. Only one complication, self-limited hemorrhage, was seen. One-year survival was 94%. In the study by Lencioni et al. (1998) 29 patients with 53 hepatic metastases ranging from 1.1 to 4.8 cm in diameter were enrolled. A total of 127 insertions were performed (mean, 2.4 insertions per lesion) during 84 treatment sessions (mean, 1.6 sessions per lesion) in the absence of complications. Complete tumor response, defined as the presence of a nonenhanced ablation zone larger than the treated tumor on posttreatment spiral CT, was seen in 41 (77%) of 53 lesions. After a mean follow-up period of 6.5 months (range, 3–9 months), local tumor progression was seen in 12% of cases. One-year survival was 93%.

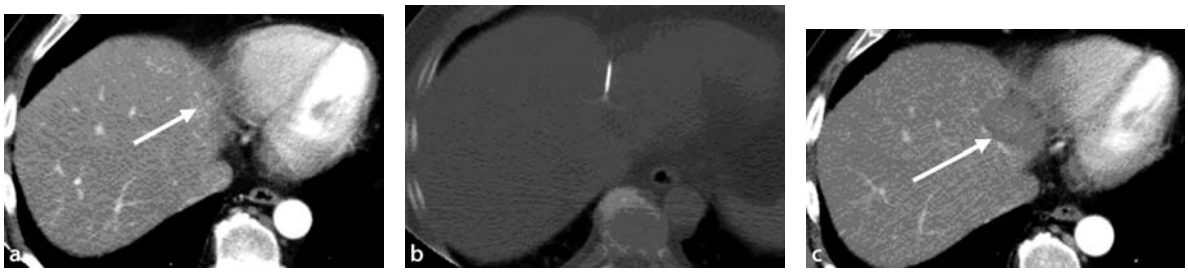

Fig. 13.8a–c Contrast-enhanced CT demonstrates a small recurrent metastasis in a subcapsular localization directly adjacent to the heart (**a**; *arrow*). CT-guided RF ablation was performed (**b**). The follow-up CT scan 24 h after RF ablation shows a clear demarcation of the ablation zone encompassing the tumor nodule (*arrow*) without collateral damage to the heart (**c**)

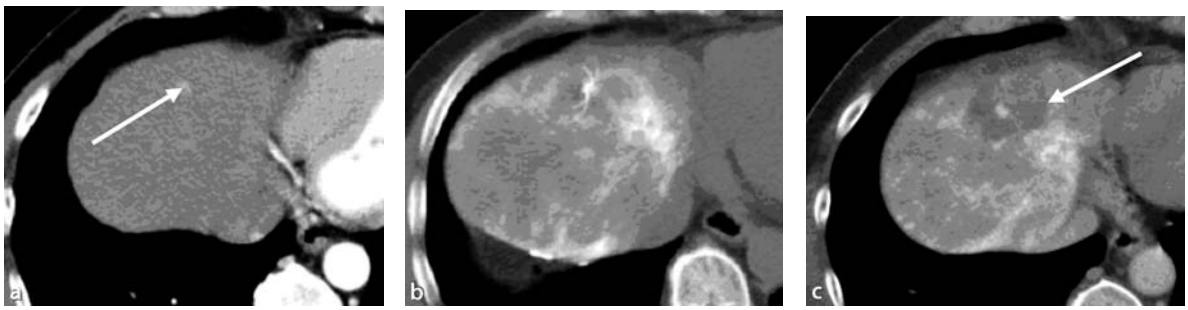

Fig. 13.9a–c Contrast-enhanced CT scan demonstrates a very small HCC nodule in the liver dome (*arrow*) in a patient after right hemihepatectomy (**a**). After transarterial "lipiodolization" the tumor could be targeted despite its small size very easily via a double-angulated route from a right intercostal approach. Note the RF probe being in place exactly at the center of the "lipiodol-marked" tumor (**b**; *arrow*). **c** The contrast-enhanced follow-up scan 24 h after RF ablation demonstrates a clear demarcation of the ablation zone entirely encompassing the tumor nodule (**c**)

A systematic review on the outcomes of RF ablation for unresectable hepatic metastases in 2002 revealed a dearth of long-term follow-up data. Seidenfeld et al. (2002) found only seven articles that provided data on disease-free or recurrence-free survival, rates of hepatic relapse, and median or percentage survival at 1–5 years after treatment. Five studies reported 86–94% survival at 1 year, but only one study reported survival at 2 years or longer (Solbiati et al. 1997b). In a recent study by Solbiati et al. (2001) the results from 109 patients with 172 metastatic lesions who underwent RF ablation under ultrasound guidance were analyzed. The median follow-up was 3 years and local tumor control was achieved in 70% of the lesions. Local recurrence – including residual tumor foci – occurred in 30% of the lesions and these were treated again by RF ablation, and the entire rate of local tumor control reached 78%. New metastases developed in 50.4% of the patients at a median time to recurrence of 12 months after RF ablation. The overall 2- and 3-year survival rates were 67 and 33% and the median survival was 30 months. This compares favorably with data reported by Gillams (2001) with a median survival of 34 months and a 3-year survival of 36%. Survival of 36% at 3 years for inoperable patients is similar to that for patients undergoing resection for operable metastatic disease, showing a 3-year survival of 42–44% (Jaeck et al. 1997; Jenkins et al. 1997). In another large series, 328 hepatic metastases in 76 patients were treated with RF ablation. At a mean follow-up of 15 months local recurrence was noted in 9% of patients (Bowles et al. 2001). Very recent data from the Tumor Radiofrequency Ablation Italian Network (TRAIN) study by Lencioni et al. (2004) demonstrated long-term data on colorectal and breast cancer metastases to the liver treated by RF ablation. In colorectal metastases, 423 patients were evaluated presenting unifocal liver metastases (mean size, 2.7 cm). The

overall survival after 1, 3, and 5 years was 86, 47, and 24%, respectively. Interestingly, the TRAIN study revealed very good 5-year survival of 56% in a subgroup of patients having one tumor nodule 2.5 cm or smaller. Patients with tumors bigger than 2.5 cm and multifocal tumors showed a significant decrease in the 5-year survival of 13 and 11%. The data of the 102 patients suffering from breast cancer metastases confirmed that in selected breast cancer patients where the metastases are unifocal with a mean diameter of 2.4 cm with no further extrahepatic spread RF ablation plays an interesting role in the treatment strategy, with overall survival rates after 1, 3, and 5 years being 95, 50, and 30% (Lencioni et al. 2004) (Table 13.4).

Recent studies analyzed the role of RF ablation with respect to surgical resection. Abdalla et al. (2004) evaluated the survival of 418 patients with colorectal metastases isolated to the liver who were treated with hepatic resection ($n = 190$), RF ablation plus resection ($n = 101$), RF ablation only ($n = 57$), or chemotherapy only ($n = 70$). Overall survival for patients treated with RF ablation plus resection or RF ablation only was significantly greater than for those who received chemotherapy only. However, overall survival was highest after resection: 4-year survival rates after resection, RF ablation plus resection, and RF ablation only were 65, 36, and 22%, respectively ($p < 0.0001$). However, RF ablation only had been used only in patients where surgery was not possible; thus, the results of this study are not comparable. In contrast, Oshowo et al. (2003) found no difference in survival outcome of patients with solitary colorectal liver metastases treated by surgery ($n = 20$) or by RF ablation ($n = 25$). In this study, the survival rate at 3 years was 55% for patients treated with surgery and 52% for those treated with RF ablation, suggesting that the survival after resection and RF ablation is the same. Elias et al. (2002) demonstrated that RF ablation instead of repeated resections for the treatment of liver tumor recurrence after partial hepatectomy has the potential to increase the percentage of curative local treatments for liver recurrence after hepatectomy from 17 to 26% and to decrease the proportion of repeated hepatectomies from 100 to 39%.

A completely different approach was taken by Livraghi et al. (2003a). They evaluated 88 patients with 134 colorectal liver metastases who were potential candidates for surgery concerning the potential role of performing RF ablation during the interval between diagnosis and resection as part of a "test-of-time" management approach. Among the 53 patients in whom complete tumor ablation was achieved after RF treatment, 98% were excluded from surgical resection: 44% because they remained free of disease, and 56% because they developed additional metastases leading to unresectability. No patient in whom RF treatment did not achieve complete tumor ablation became unresectable owing to the growth of the treated metastases.

Hepatocellular Carcinoma

Various minimally invasive interventions have been introduced and tested for the treatment of HCC over recent years. Among them, RF ablation has been the most widely assessed percutaneous therapy option after percutaneous ethanol injection (PEI) for local ablation of HCC (Gillams 2003, 2005; Goldberg and Ahmed 2002; Raut et al. 2005). Compared with PEI, which is recommended the treatment of choice in unresectable early stage HCC presenting with up to three tumors of 3 cm or less and underlying liver cirrhosis of Child class A and B according to the BCLC staging system (Llovet et al. 2003), RF ablation has proven more effective with fewer complications and therefore should replace PEI for those tumors (Table 13.5) (Lencioni et al. 2003; Lin et al. 2004, 2005; Shiina et al. 2005).

Treatment success, in terms of initial technical performance and long-term survival, is strongly influenced by tumor size and surrounding tissue. Lu et al. (2005) demonstrated complete tumor necrosis in 83% of tumors smaller than 3 cm and 88% of tumors in nonperivascular location. Poon et al. (2002) reported on studies where complete tumor necrosis could be achieved in a single treatment session in 80–90% of tumors smaller than 3–5 cm, whereas tumors exceeding 5 cm (mean diameter, 5.4 cm) seem to result in significantly less tumor necrosis (48%) after RF ablation as evaluated in 126 patients with medium and large HCC (Livraghi et al. 2000). To date the findings of seven randomized controlled trials evaluating the efficacy of RF ablation in HCC have been published (Table 13.5). Two studies recently reported the long-term outcome of RF ablation in HCC. In the first study, by Lencioni et al. (2005), RF ablation was used as first-line treatment for early stage HCC in 187 patients not eligible for surgery in an intention-to-treat prospec-

Table 13.4 Survival after RF ablation, selected references

Authors	No. of patients	Tumor	Survival (%)		
			1 year	3 years	5 years
Solbiati et al. (1997b)	29	CRC (22 patients)	94	–	–
Lencioni et al. (1998)	29	CRC (24 patients)	93	–	–
Gillams and Lees (2000)	69	CRC	90	34	22[a]
Solbiati et al. (2001)	109	CRC	–	33	–
Oshowo et al. (2003)	25	CRC	–	52	–
Abdalla et al. (2004)	57	CRC	–	–	22[a]
Gillams and Lees (2004)	167	CRC	–	–	30
Lencioni et al. (2004)	423	CRC	86	47	24
		CRC < 2.5 cm	–	–	56
		CRC > 2.5 cm	–	–	13
		CRC multifocal	–	–	11
	102	Breast cancer	95	50	30
	96	HCC ≤ 2 cm	99	88	65
		Child class A, unifocal	46[b]		
Livraghi et al. (2004)	210	Early HCC	90	83	43
	164	Late HCC	68	49	28
Tateishi et al. (2005)	319	HCC first-line	95	78	54
	345	Recurrent HCC	92	62	38
Chen et al. (2006)	205	HCC	90	60	
Choi et al. (2007b)	570	Early HCC	95	70	58
Choi et al. (2007a)	102	Recurrent HCC after resection ~ 2 cm	94	66	52
Takahashi et al. (2007)	171	Naïve HCC	99	91	77
Sorensen et al. (2007)	102	CRC	96	64	44

CRC – colorectal cancer metastases
[a] Four years
[b] Seven years

tive trial. Overall survival was 97% at 1 year, 67% at 3 years, and 41% at 5 years in 187 patients. Median survival was 49 months. Survival of patients treated with RF ablation was dependent on the Child class ($p = 0.0006$) and tumor multiplicity ($p = 0.0133$). Patients who had Child class A cirrhosis with solitary HCC ($n = 116$) had 1-, 3-, and 5-year survival rates of 100, 89, and 61%. Median survival was 65 months. The 1-, 3-, and 5-year recurrence rates were 14, 49, and 81% for the emergence of new tumors and 4, 10, and 10% for local tumor progression. In the second study, 319 patients received RF ablation as primary treatment and 345 patients received it for recurrent tumor after previous local treatment (Tateishi et al. 2005). In this particular study the cumulative survival rates at 3 and 5 years were 78 and 54% for primary treatment and 62 and 38% for recurrent tumor (Table 13.4).

The prognosis after RF ablation of HCC is significantly affected by the initial treatment response. Sala et al. (2004) reported 282 cirrhotic patients with early nonsurgical HCC who were treated with percutaneous RF ablation. Initial complete response was achieved in 192 patients and was independently related to the size of the main tumor and the tumor stage (2 cm or less, 96%; 2.1–3 cm, 78%; 3 cm or more, 56%; two to three nodules, 46%). Patients with Child class A cirrhosis with an initial complete response achieved 42% survival at 5 years and for tumors 2 cm of less the survival was 63%. These results were confirmed by two recent studies (Takahashi et al. 2007; Guglielmi et al. 2007). Takahashi et al. (2007) retrospectively analyzed 171 cirrhotic Child class A patients who received RF ablation for naïve HCC within the Milan criteria. Overall cumulative survival was 98.8, 91.1, and 76.8% at 1, 3, and 5 years. Cumulative survival in patients with no local recurrence was 96.6, 94.6, and 84.4% compared with 96.6, 74.8, and 42.1% in patients with local tumor recurrence.

A very recent study by Livraghi et al. (2008) questioned resection still being the treatment of choice in very early HCC and claimed a paradigm shift in the treatment of such patients. The authors evaluated 218

Table 13.5 Randomized trials including RF ablation for the treatment of HCC

Authors	Therapy	No. of patients	No. of tumors ≤ 2 cm/> 2 cm	Complete necrosis (%)	Survival (%) 1 year	2 years	3 years	Local recurrence (%)
Shibata et al. (2002)	RFA	36	23/32	96		NE		12[c]
	PMC	36	19/31	89		NE		24[c]
Lencioni et al. (2003)	RFA	52		91	100	98		4[d]
	PEI	50		82	96	88		38[d]
Lin et al. (2004)	RFA	52	47/110	96	90	82		18[c]
	PEI	52		88	85	61		45[c]
	High-dose PEI	53		92	88	63		33[c]
Akamatsu et al. (2004)	PTA	20 (14/6)	NE	NE	96	96	82	41[d]
	(PEI/RFA) TAE–PTA (PEI/RFA)	22 (12/10)	NE	NE	100	82	82	68[d]
Shiina et al. (2005)	RFA	118	102/130	100	97	91	74[b]	2[c]
	PEI	114		100	92	81	57[b]	11[c]
Lin et al. (2005)	RFA	62	111/76	96	93	81		14[c]
	PEI	62		88	88	66		34[c]
	PAI	63		92	90	67		31[c]
Shibata et al. (2006)	RFA (internally cooled probe)	38	41[a]	95	100	94	94	20[c]
	RFA (umbrella probe)	36	42[a]	93	94	92	77	22[c]

PAI – percutaneous acetic acid injection, *PTA* – percutaneous tumor ablation, *PMC* – percutaneous microwave coagulation, *TAE* – transarterial embolization NE not evaluated

[a] Three centimeters or less

[b] Four years

[c] Two years

[d] Two-year local recurrence free survival

patients with single HCC of 2 cm or less (very early or T1 stage) concerning the rate of sustained, local, complete response, the rate of treatment-related complications, and secondary 5-year survival in the 100 patients whose tumors had been considered potentially operable. After a median follow-up of 31 months, sustained complete response was observed in 216 patients (97.2%), with a perioperative mortality of 0%, a major complication rate of 1.8% and a 5-year survival rate of 68.5%. On the basis of these results they concluded that percutaneous RF ablation in very early HCC is less invasive and associated with lower complications than resection ensuring similar local control and survival and therefore should be considered the treatment of choice in single HCC of 2 cm or less, even when surgical resection is possible.

13.1.2.5 Complications

The overall complication rate for RF ablation seems low in comparison with that of other more or less minimally invasive procedures. Nevertheless a significant number of major complications (2.4%) were recently reported by an Italian multicenter trial including 3,554 lesions in 2,320 patients (Livraghi et al. 2003b). The latter was confirmed by Rhim et al. (Rhim et al. 2003, 2004), who presented a survey of 11 Korean institutions, including 1,663 lesions in 1,139 patients, with the rate of major complications being 2.43%. Mortality was 0.3 and 0.09%, respectively, which is similar to the findings of a meta-analysis by Mulier et al. (2002), who recently reviewed a total of 3,670 patients after RF ablation with a mortality rate of 0.5%. The authors could also demonstrate the lowest total complication rate of 7.2% for percutaneous RF ablation, compared with laparoscopic (9.5%), intraoperative (9.5%), and combined procedures with resection and open RF ablation (31.8%).

The total minor complication rate including common side effects ranges between 4.6 and 36% (Mulier et al. 2002; Livraghi et al. 2003b; Rhim et al. 2003, 2004). This wide range depends on the fact that minor complications according to the Society of Inter-

ventional Radiology guidelines are usually not listed in the published data, so the true (whenever clinically not relevant) minor complication rate is difficult to assess. Common side effects in RF ablation are pain in the area of the puncture site, peritoneal irritation, nausea, vomiting, moderate fever, tiredness, and headache. The so-called postablation syndrome including fever, nausea, vomiting, and tiredness can last for up to several weeks and can be found in up to two thirds of patients. Symptomatic supportive care is sufficient in such cases.

Complications may occur immediately or with a delay after RF ablation, and may be related to the puncture, the entire procedure, or the patient's disease and individual situation (de Baere et al. 2003). Immediate complications can be due to vascular, nonvascular, and metabolic reasons, whereas delayed complications usually derive from complex metabolic reactions, infections, biliary obstruction, and tumor seeding.

Concerning vascular complications, there are several factors which influence the risk of bleeding: the patient's coagulation status, tumor type and site, surrounding tissue properties, the way to the target, and interpositioned anatomical structures. To avoid bleeding especially from the access route in coagulopathies special measures have to be taken to correct coagulation abnormalities by additional infusion of platelets or fresh frozen plasma and stopping anticoagulative regimens if justifiable.

Vascular complications such as arterial bleeding (Fig. 13.10), pseudoaneurysm, arteriovenous/arterioportovenous fistulae, and hepatic and portal vein thrombosis, with subsequent hepatic infarction in extremely rare cases (Fig. 13.11), may occur from mechanical injuries caused by the RF probe traversing a vessel or from sustained ablation. Real-time imaging such as ultrasound or CT fluoroscopy during the procedure might help to minimize the rate of such complications. Nevertheless self-limiting hemorrhagic diapedesis usually representing hemorrhage due to thermal damage to the capillary bed of the tumor can be appreciated during the ablation process. In cases of intraprocedural bleeding and significant, ongoing pain a baseline follow-up study has to be performed within the first 3 h after the ablation. In cases of vascular injuries, early angiography with interventional standby is mandatory (Fig. 13.10). To avoid needle track bleeding it is recommended to perform "hot" probe repositioning and removal ("track ablation"). Therefore, regarding the present literature, bleeding in total is a rare, in most cases self-limiting, complication with an overall frequency of no more than 2%. Mulier et al. (2002) recently found in a total of 3,670 patients after RF ablation intraperitoneal bleeding in 0.8%, subcapsular hematoma in 0.6%, and hepatic vascular damage in 0.4%.

Nonvascular complications include infection, tumor seeding, and nontarget thermal damage. Predisposing factors such as an underlying inflammatory focus, a compromised immune system, or a bilioenteric anastomosis usually promote infectious complications. Although infectious complications in total seem to be rare (about 1.5%), de Baere et al. (2003) found a significantly higher incidence of liver abscesses in patients with a bilioenteric anastomosis. Patients who underwent a Whipple procedure, for example, were jeopardized by colonization of the biliary tract by ascending infections and consecutive abscess formation within the ablation volume. Any persistent or recurrent fever in the 2–3 weeks after RF ablation should increase awareness concerning an infectious complication such as abscess formation. In fact, such patients can be treated interventionally by placing a drainage under image guidance. Additionally, there seems to be an increased risk for infection also in patients who previously underwent lipiodol embolization for HCC.

Neoplastic seeding along the needle tract usually occurs 3–12 months after RF ablation and is due to the carrying of tumor cells on the probe itself. It accounted for 0.3% in the analysis of Mulier et al. (2002), whereas a rate of 12.5% was found in the study population of Llovet et al. (2001). De Baere et al. (2003) reported seeding also to be rare with 0.5%. The reason for this significant difference was most likely due to the technique with no track ablation applied. In a very recent multicenter study including 1,314 patients with 2,542 HCC nodules by Livraghi et al. (2005) neoplastic seeding was identified in 12 patients (0.9%); the rates were comparable at the three centers (0.9, 0.7, and 1.4%). Only previous biopsy was significantly associated with tumor seeding ($p = 0.004$). Although the authors included only HCC, it seems that the seeding rate reported by Llovet et al. (2001) was definitely not representative concerning implantation metastases. Jaskolka et al. (2005) found three statistically significant risk factors for needle tract seeding

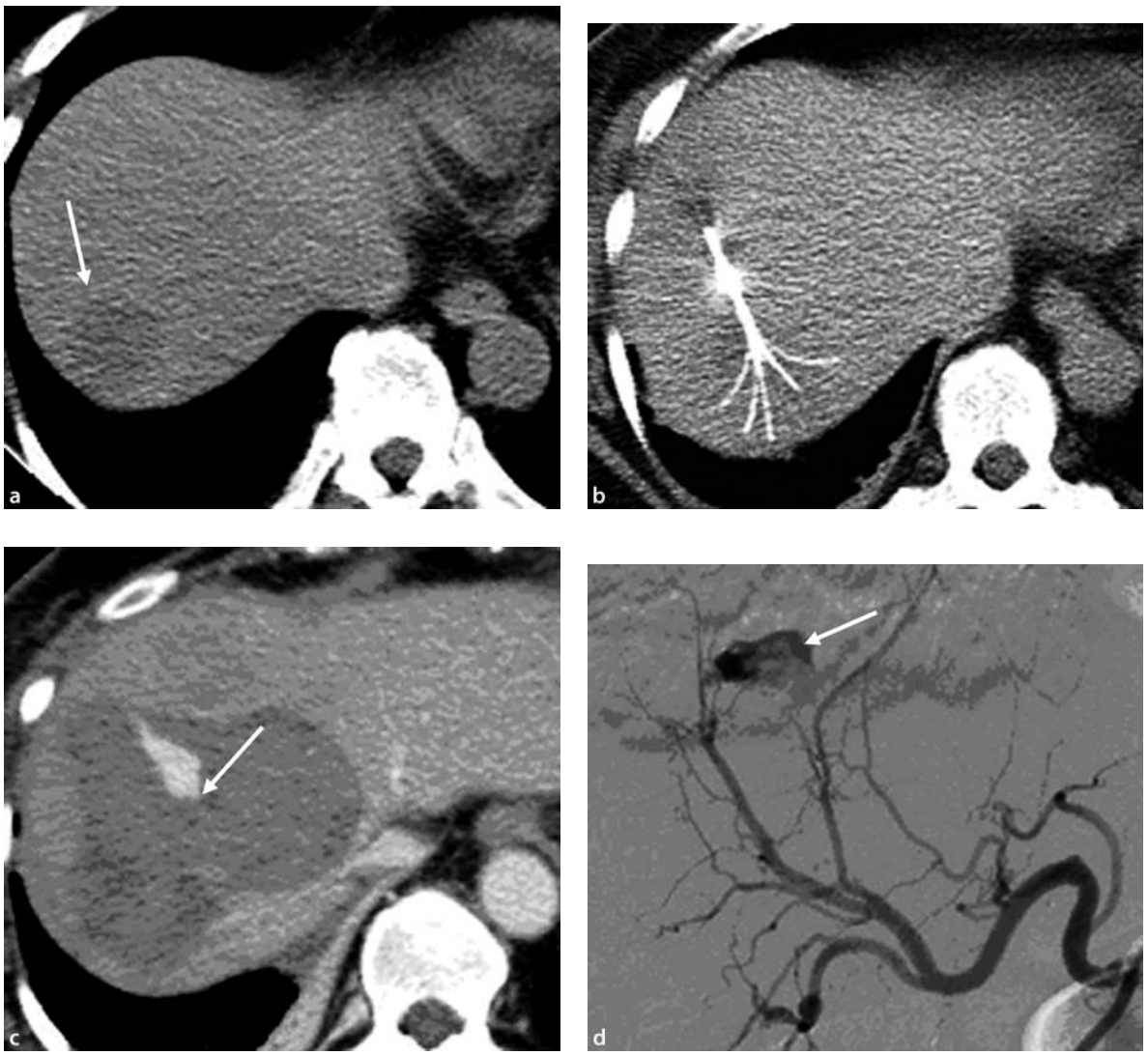

Fig. 13.10a–d CT demonstrates a hypodense focal lesion in liver segment 7 (*arrow*) representing the breast cancer liver metastasis (**a**). CT-guided RF ablation was performed. CT shows the RF probe at the posterior rim of the tumor (**b**). The contrast-enhanced CT scan showed active arterial bleeding (*arrow*) with a consecutive huge intrahepatic hematoma (**c**). The subsequently obtained selective diagnostic angiogram demonstrates a laceration of the segment 8 artery with pathologic extravasation of contrast medium (**d**; *arrow*)

in 200 patients treated 298 times with RF ablation for different hepatic tumors: treatment of a subcapsular lesion (odds ratio, 11.57; $p = 0.007$), multiple treatment sessions (odds ratio, 2.0; $p = 0.037$), and multiple electrode placements (odds ratio, 1.4; $p = 0.006$). The risk can be almost eliminated if the RF probe is properly positioned on the first pass and does not cross the tumor primarily, otherwise tumor cells can be pushed out of the tumor at its periphery. A sufficient safety margin around the tumor and removing the probe by additional ablation of the needle tract will further lower the risk of tumor cell spread (Fig. 13.5).

Complications related to the thermal ablation itself include unintentional thermal harm to nontargeted areas, including burns at the dispersive electrodes and interference with metallic implants such as pacemaker wires and cardioverter defibrillators. Therefore, exact selection and consecutive placement of the dispersive electrodes is crucial to minimize the risk for pad skin burns. There is an increased risk of pad burns which

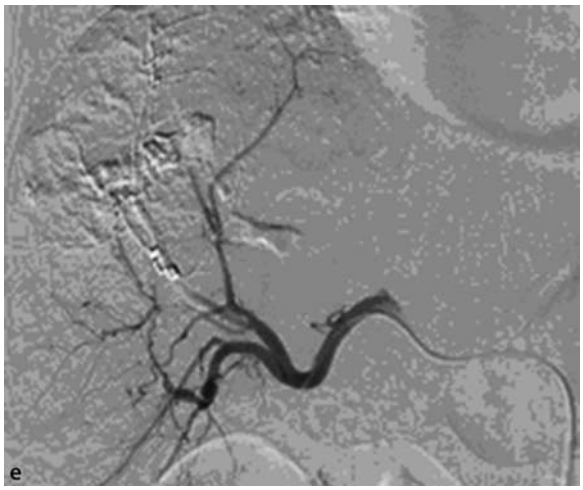

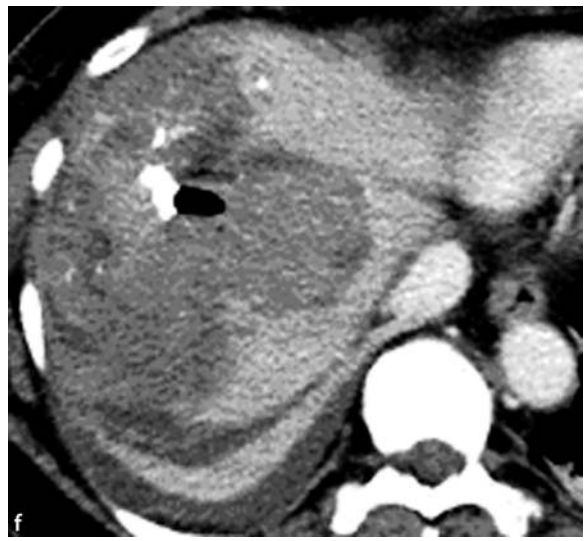

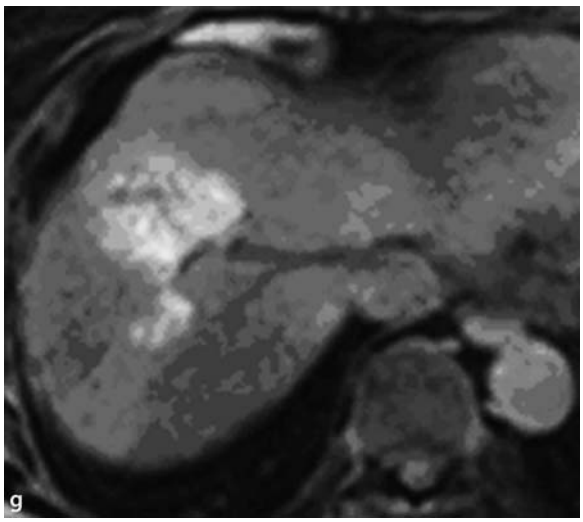

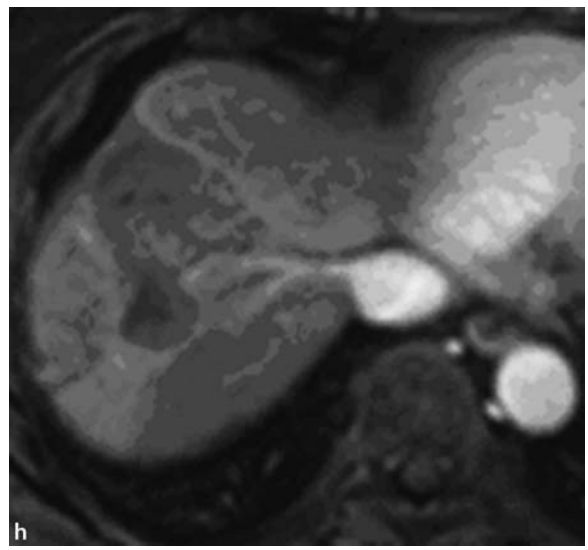

Fig. 13.10e–h The vessel was selectively embolized with coils and a histoacryl–lipiodol mixture. The control angiogram shows no evidence of further active arterial bleeding (**e**). The corresponding contrast-enhanced CT scan after bleeding embolization shows the hematoma without evidence of an active bleeding site (**f**). Follow-up MR imaging (native and contrast-enhanced T1-weighted images) 8 months after embolization showed a marked decrease of the intrahepatic hematoma and no viable tumor (**g**,**h**)

closely correlates with the amount of energy delivered if the grounding pads are too small or not equidistant from the active electrode in monopolar systems. In consequence, more or larger grounding pads should be used if more power is applied. If the contact of the dispersive electrodes with the skin surface is not sufficient (e.g., by sweat or hairs under the pad), the RF power is not dispersed efficiently and "spots" of high current flow may be generated, resulting in burns. Defects in the electrode's insulation or metallic coaxial introducers, which may act as secondary antenna by induction, can also create burns at the skin entry site.

To prevent unintentional burns to anatomical structures within the vicinity of the targeted ablation area a thorough planning of the access route and final probe placement may help to avoid damage of such structures, e.g., the gallbladder, bile ducts (Fig. 13.12), or the renal calices. In clinical reality, vascular heat sink effects, the peritoneal surfaces, and the motility/mobility of some organs such as stomach and large

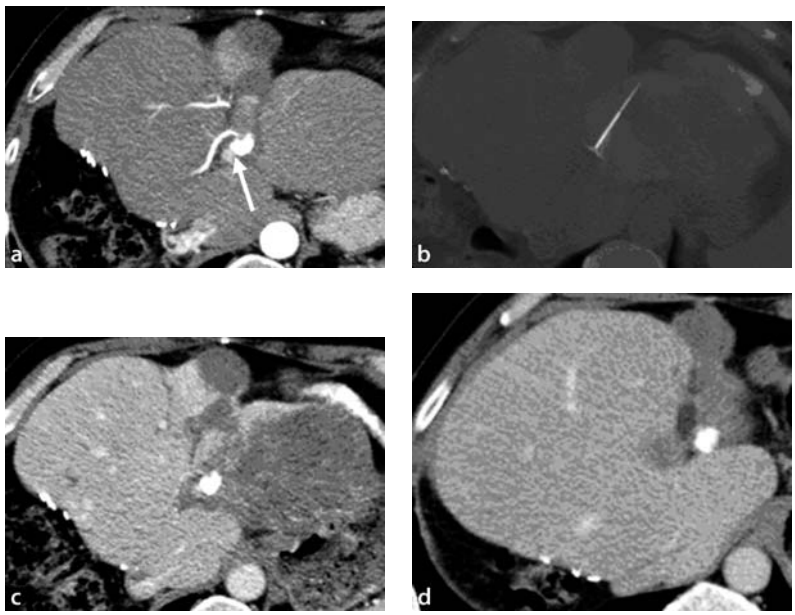

Fig. 13.11a–d Hepatic infarction of liver segments 2 and 3 after RF ablation for a recurrent HCC nodule adjacent to the falciform ligament. CT demonstrating a recurrent HCC nodule in liver segment 3 adjacent to the falciforme ligament after transarterial chemoembolization with nodular contrast enhancement during arterial-phase scan (**a**; *arrow*). Note the formerly treated HCC still displays some lipiodol uptake. CT with the RF probe exactly within the recurrent HCC nodule (**b**). **c** Twenty-four hours after the procedure, CT reveals a complete necrosis of liver segments 2 and 3 (**c**). Eighteen months after RF ablation, CT demonstrates nearly complete shrinkage of liver segments 2 and 3 with no evidence of tumor recurrence (**d**)

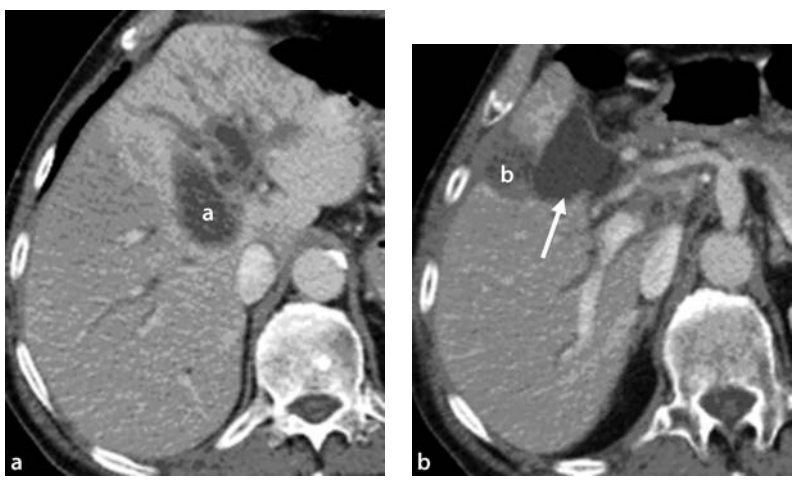

Fig. 13.12a,b Biliary leakage with consecutive biloma and cholestasis of the right hepatic lobe and bile duct necrosis of the left main duct with consecutive massive cholestasis of the left liver lobe after laparoscopic RF ablation in a patient with multifocal colorectal liver metastases. The contrast-enhanced CT scan 3 weeks after laparoscopic RF ablation demonstrates cholestasis of the left and the right liver lobe (**a**) accompanied by a biloma (**b**; *arrow*) adjacent to two RF ablation zones (**a** and **b**)

bowel may also have some protective properties. Nevertheless, there are some reports documenting the fatal outcome of secondary thermal damage to the stomach or bowel (Choi et al. 2001; Meloni et al. 2002; Livraghi et al. 2003b; Rhim et al. 2003). Particularly after previous surgery, where intra-abdominal adhesions may fix the stomach or bowel to the surface of the liver surface, there is an increased risk

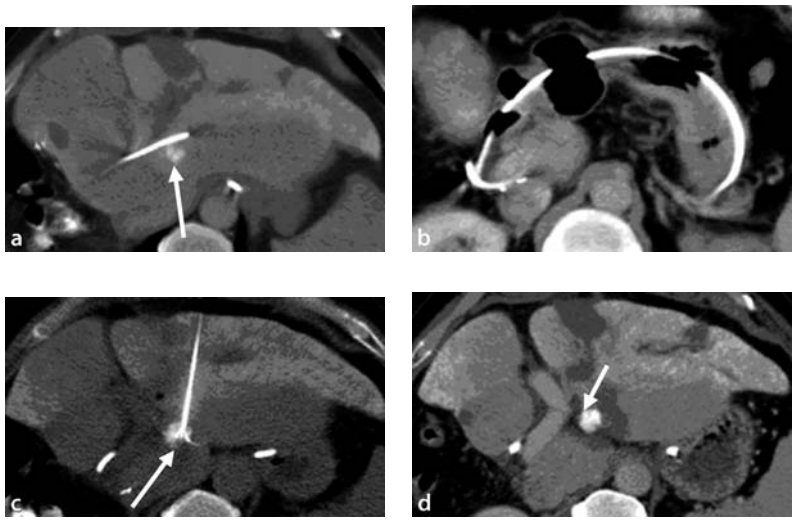

Fig. 13.13a–d CT shows a recurrent HCC nodule in liver segment 3 after transarterial chemoembolization (**a**; *arrow*). Note the nasobiliary tube adjacent to the tumor. The CT scan demonstrating the endoscopically placed nasobiliary tube that was used for continuous cooling of the adjacent bile ducts (**b**). The CT scan with the RF probe already placed at the center of the tumor (**c**; *arrow*). **d** Twenty-four hours after RF ablation the ablation zone entirely encompasses the tumor nodule without any collateral damage (**d**; *arrow*)

of thermal damage to these organs. Dislodgement by air insufflation or glucose injection will protect these structures at risk. Additionally, cooling of adjacent structures such as bile ducts via interventionally placed tubes may also prevent secondary thermal damage (Fig. 13.13). Therefore, collateral damage to vital structures can be generally avoided if organ-specific anatomical peculiarities are considered.

There is clear evidence that the patient's condition during the procedure can be affected by changes of the metabolic status of the patient such as changes in blood pressure, heart rhythm, hormonal reactions, or sensations of pain. So-called metabolic complications are mainly dependent on the underlying or accompanying disease; therefore, it is mandatory to know the patient's medical condition prior to RF ablation to address any necessary additional medication ahead of a potential complication.

Summary

The liver is frequently affected by metastases of different tumor entities. Surgical resection provides the greatest potential for cure in patients with secondary liver tumors; however, surgery can be offered only to a small number of patients (5–20%). In selected patients image-guided minimally invasive treatment such as percutaneous RF ablation takes the role as a palliative treatment option with a potential curative intention especially in patients who are technically and/or medically not eligible for surgery. According to the BCLC guidelines, RF ablation has a clear indication in patients not eligible for surgery and suffering from early stage HCC with one to three nodules of 3 cm or less. In selected patients with very early HCC it seems that RF ablation might be the treatment of choice despite operability. The effective and reproducible tumor destruction of RF ablation is accompanied by an acceptable mortality and morbidity. Although usually "unfavorable" patients in a highly palliative situation are treated with RF ablation, local tumor control by RF ablation is often as good as or even better than systemic chemotherapy. Combination of RF ablation with other treatments is an area of ongoing active research. It is highly desirable to implement local ablative therapies such as RF ablation in the treatment algorithm for nonresectable liver tumors not only as third-line but also as second- or first-line treatment in early HCC probably, in metastatic disease, in combination with systemic chemotherapy. RF ablation should always be embedded in a multidisciplinary treatment strategy tailored to the individual patient and to the features of the disease ("customized therapy"). Patient selection is very crucial for successful treatment with RF ablation. It should be based upon tumor site and size, prox-

imity of large vessels, bleeding risk, respiratory motion, probe pathway, and last but not least the physician's experience. The technique is operator-dependent with a steep learning curve. Until the role of RF ablation within a multimodal treatment strategy for liver tumors is completely defined, RF ablation should be restricted to centers with highly experienced interventionalists incorporated into an interdisciplinary oncology team.

Because follow-up imaging is very crucial in determining therapy success, imaging of ablation should also be performed by physicians experienced with RF ablation. To further assess the role of RF ablation in tumor patients multicenter trials, more long-term follow-up data, further refinements in technique and procedure-related features, and studies of combined treatments, including all therapies available for liver tumors, must be evaluated with respect to the current therapeutical reference standard to date.

Key Points

Crucial points for successful image-guided, percutaneous RF ablation include:

- Tumor size 3–3.5 cm or less (prevention of local recurrence by avoiding multiple probe positioning).
- Tumor tissue (vascularity; preinterventional embolization?).
- Surrounding tissue properties (e.g., vascularity).
- Thorough planning of the access route to prevent complications.
- "Hot" probe repositioning and removal to prevent tumor seeding and bleeding.
- Intention of "complete" tumor ablation is a significant prognostic factor
- Close follow-up ("postablation is preablation").
- Close cooperation with surgeons and oncologists is needed as tumor treatment is always a multidisciplinary issue.

References

Abdalla EK, Vauthey JN, Ellis LM, Ellis V et al. (2004) Recurrence and outcomes following hepatic resection, radiofrequency ablation, and combined resection/ablation for colorectal liver metastases. Ann Surg 239:818–825; discussion 825–827

Akamatsu M, Yoshida H, Obi S et al. (2004) Evaluation of transcatheter arterial embolization prior to percutaneous tumor ablation in patients with hepatocellular carcinoma:a randomized controlled trial. Liver International 24:625–630

Atwell TD, Charboneau JW, Que FG, Rubin J et al. (2005) Treatment of Neuroendocrine Cancer Metastatic to the Liver: The Role of Ablative Techniques. Cardiovasc Intervent Radiol 28:409–421

Barker DW, Zagoria RJ, Morton KA, Kavanagh PV, Shen P (2005) Evaluation of liver metastases after radiofrequency ablation: utility of 18F-FDG PET and PET/CT. Am J Roentgenol 184:1096–102

Bowles BJ, Machi J, Limm WM et al. (2001) Safety and efficacy of radiofrequency thermal ablation in advanced liver tumors. Arch Surg 136:864–869

Bruix J, Sherman M, Llovet JM et al. (2001) Clinical management of hepatocellular carcinoma. Conclusions of the Barcelona-2000 EASL Conference. J Hepatol 35:421–430

Burdio F, Guemes A, Burdio JM et al. (2003) Bipolar saline-enhanced electrode for radiofrequency ablation: results of experimental study of in vivo porcine liver. Radiology 229:447–456

Chen MH, Yang W, Yan K et al. (2004) Large liver tumors: protocol for radiofrequency ablation and its clinical application in 110 patients – mathematic model, overlapping mode, and electrode placement process. Radiology 232:260–271

Chen MH, Wei Y, Yan K et al. (2006) Treatment strategy tooptimize radiofrequency ablation for liver malignancies. J Vasc Interv Radiol 17:671–683

Choi H, Loyer EM, DuBrow RA et al. (2001) Radio-frequency ablation of liver tumors: assessment of therapeutic response and complications. Radiographics 21:S41–S54

Choi D, Lim HK, Rhim H et al. (2007a) Percutaneous radiofrequency ablation for recurrent hepatocellular carcinoma after hepatectomy: long-term results and prognostic factors. Ann Surg Oncol 14:2319–2329

Choi D, Lim HK, Rhim H et al. (2007b) Percutaneous radiofrequency ablation for early stage hepatocellular carcinoma as a first line treatment:long-term results and prognostic factors in a large single-institution series. Eur Radiol 17:684–692

Clasen S, Schmidt D, Boss A et al. (2006) Multipolar radiofrequency ablation with internally cooled electrodes: experimental study in ex vivo bovine liver with mathematic modeling, Radiology 238:881–890

Clasen S, Schmidt D, Dietz K et al. (2007) Bipolar radiofrequency ablation using internally cooled electrodes in ex vivo bovine liver: prediction of coagulation volume from applied energy. Invest Radiol 42:29–36

de Baere T, Risse O, Kuoch V et al. (2003) Adverse events during radiofrequency treatment of 582 hepatic tumors. Am J Roentgenol 181:695–700

Dodd GD, 3rd, Frank MS, Aribandi M, Chopra S et al. (2001) Radiofrequency thermal ablation: computer analysis of the size of the thermal injury created by overlapping ablations. Am J Roentgenol 177:777–782

Dupuy DE, Goldberg SN (2001) Image-guided radiofrequency tumor ablation: challenges and opportunities – part II. J Vasc Interv Radiol 12:1135–1148

Elias D, De Baere T, Smayra T et al. (2002) Percutaneous radiofrequency thermoablation as an alternative to surgery for treatment of liver tumour recurrence after hepatectomy. Br J Surg 89:752–756

Gillams A (2001) Thermal ablation of liver metastases. Abdominal Imaging 26:361–368

Gillams AR, Lees WR. (2000) Survival after percutaneous, image-guided, thermal ablation of hepatic metastases from colorectal cancer. Dis Colon Rectum 43:656–661

Gillams AR (2003) Radiofrequency ablation in the management of liver tumours. Eur J Surg Oncol 29:9–16

Gillams AR, Lees WR (2004) Radio-frequency ablation of colorectal liver metastases in 167 patients. Eur Radiol 14: 2261–2267

Gillams AR (2005) The use of radiofrequency in cancer. Br J Cancer 92:1825–1829

Goldberg SN, Ahmed M (2002) Minimally invasive image-guided therapies for hepatocellular carcinoma. J Clin Gastroenterol 35:S115–S129

Goldberg SN, Gazelle GS, Compton CC et al. (2000) Treatment of intrahepatic malignancy with radiofrequency ablation: radiologic-pathologic correlation. Cancer 88: 2452–2463

Goldberg SN, Gazelle GS (2001) Radiofrequency tissue ablation: physical principles and techniques for increasing coagulation necrosis. Hepatogastroenterology 48:359–367

Goldberg SN, Grassi CJ, Cardella JF et al. (2005) Image-guided tumor ablation: standardization of terminology and reporting criteria. Radiology 235:728–739

Guglielmi A, Ruzzenente A, Sandri M et al. (2007) Radiofrequency ablation for hepatocellular carcinoma in cirrhotic patients: prognostic factors for survival. J Gastrointest Surg 11:143–149

Jaeck D, Bachellier PGM, Boudjema K et al. (1997) Long-term survival following resection of colorectal hepatic metastases. Association Francaise de Chirurgie. Br J Surg 84: 977–980

Jaskolka JD, Asch MR, Kachura JR et al. (2005) Needle tract seeding after radiofrequency ablation of hepatic tumors. J Vasc Interv Radiol 16:485–491

Jenkins LT, Millikan KW, Bines SD et al. (1997) Hepatic resection for metastatic colorectal cancer. Am Surg 63:605–610

Kojiro M (2004) Focus on dysplastic nodules and early hepatocellular carcinoma: an eastern point of view. Liver Transpl 10:S3–S8

Kuvshinoff BW, Ota DM (2002) Radiofrequency ablation of liver tumors: influence of technique and tumor size. Sugery 132:605–611; discussion 611–612

Lencioni R, Goletti O, Armillotta N et al. (1998) Radiofrequency thermal ablation of liver metastases with a cooled-tip electrode needle: results of a pilot clinical trial. Eur Radiol 8:1205–1211

Lencioni R, Cioni D, Bartolozzi C (2001) Percutaneous radiofrequency thermal ablation of liver malignancies: techniques, indications, imaging findings, and clinical results. Abdom Imaging 26:345–360

Lencioni RA, Allgaier HP, Cioni D et al. (2003) Small hepatocellular carcinoma in cirrhosis: randomized comparison of radio-frequency thermalablation versus percutaneous ethanol injection. Radiology 228:235–240

Lencioni R, Crocetti L, Cioni D et al. (2004) Percutaneous radiofrequency ablation of hepatic colorectal metastases: technique, indications, results, and new promises. Invest Radiol 39:689–697

Lencioni R, Cioni D, Crocetti L et al. (2005) Early-stage hepatocellular carcinoma in patients with cirrhosis: long-term results of percutaneous image-guided radiofrequency ablation. Radiology 234:961–967

Lim HK, Choi D, Lee WJ et al. (2001) Hepatocellular carcinoma treated with percutaneous radio-frequency ablation: evaluation with follow-up multiphase helical CT. Radiology 221:447–454

Lim HK, Han JK (2002) Hepatocellular carcinoma: evaluation of therapeutic response to interventional procedures. Abdom Imaging 27:168–179

Lin SM, Lin CJ, Lin CC et al. (2004) Radiofrequency ablation improves prognosis compared with ethanol injection for hepatocellular carcinoma ≤ 4 cm. Gastroenterology 127: 1714–1723

Lin SM, Lin CJ, Lin CC et al. (2005) Randomised controlled trial comparing percutaneous radiofrequency thermal ablation, percutaneous ethanol injection, and percutaneous acetic acid injection to treat hepatocellular carcinoma of 3 cm or less. Gut 54:1151–1156

Livraghi T, Goldberg SN, Lazzaroni S et al. (2000) Hepatocellular carcinoma: radio-frequency ablation of medium and large lesions. Radiology 214:761–768

Livraghi T, Solbiati L, Meloni F et al. (2003a) Percutaneous radiofrequency ablation of liver metastases in potential candidates for resection: the "test-of-time approach". Cancer 97:3027–3035

Livraghi T, Solbiati L, Meloni MF et al. (2003b) Treatment of focal liver tumors with percutaneous radio-frequency ablation: complications encountered in a multicenter study. Radiology 226:441–451

Livraghi T, Meloni F, Morabito A, Vettori C (2004) Multimodal image-guided tailored therapy of early and intermediate hepatocellular carcinoma: long-term survival in the experience of a single radiologic referral center. Liver Transpl 10 (Suppl 1):S98–S106

Livraghi T, Lazzaroni S, Meloni F et al. (2005) Risk of tumour seeding after percutaneous radiofrequency ablation for hepatocellular carcinoma. Br J Surg 92:856–858

Livraghi T, Meloni F, Di Stasi M et al. (2008) Sustained complete response and complication rates after radiofrequency ablation of very early hepatocellular carcinoma in cirrhosis: is resection still the treatment of choice? Hepatology 47:82–89

Llovet JM, Burroughs A, Bruix J (2003) Hepatocellular carcinoma. Lancet 362:1907–1917

Llovet JM, Vilana R, Bru C et al. (2001). Increased risk of tumor seeding after percutaneous radiofrequency ablation for single hepatocellular carcinoma. Hepatology 33:1124–1129

Lu DS, Raman SS, Limanond P et al. (2003) Influence of large peritumoral vessels on outcome of radiofrequency ablation of liver tumors. J Vasc Interv Radiol 14:1267–1274

Lu DS, Yu NC, Raman SS et al. (2005) Radiofrequency ablation of hepatocellular carcinoma: treatment success as defined by histologic examination of the explanted liver. Radiology 234:954–960

McGahan JP, Dodd III GD (2001) Radiofrequency ablation of the liver: current status. Am J Roentgenol 176:3–16

Meloni MF, Goldberg SN, Moser V et al. (2002) Colonic perforation and abscess following radiofrequency ablation treatment of hepatoma. Eur J Ultrasound 15:73–76

Mor E, Kaspa RT, Sheiner P, Schwartz M (1998) Treatment of hepatocellular carcinoma associated with cirrhosis in the era of liver transplantation. Ann Intern Med 129:643–653

Mulier S, Mulier P, Ni Y et al. (2002) Complications of radiofrequency coagulation of liver tumours. Br J Surg 89: 1206–1222

Nakanishi K, Kobayashi M, Takahashi S et al. (2005) Whole body MRI for detecting metastatic bone tumor: comparison with bone scintigrams. Magn Reson Med Sci 4:11–17

Ni Y, Miao Y, Mulier S et al. (2000) A novel cooled-wet electrode for radiofrequency ablation. Eur Radiol 10:852–854
Nicolau C, Català V, Vilana R et al. (2004) Evaluation of hepatocellular carcinoma using SonoVue, a second generation ultrasound contrast agent: correlation with cellular differentiation. Eur Radiol 14:1092–1099
Oshowo A, Gillams A, Harrison E et al. (2003) Comparison of resection and radiofrequency ablation for treatment of solitary colorectal liver metastases. Br J Surg 90:1240–1243
Pereira PL, Clasen S, Boss A et al. (2004a) Radiofrequency ablation of liver metastases. Radiologe 44:347–357
Pereira PL, Truebenbach J, Schenk M et al. (2004b) Radiofrequency ablation: in vivo comparison of four commercially available devices in pig livers. Radiology 232:482–490
Pereira PL, Truebenbach J, Schmidt D (2003) Radiofrequency ablation: basic principles, techniques and challenges Rofo 175:20–27
Poon RT, Fan ST, Tsang FH et al. (2002) Locoregional therapies for hepatocellular carcinoma: a critical review from the surgeon's perspective. Ann Surg 235:466–486
Poon RT, Ng KK, Lam CM et al. (2004a) Effectiveness of radiofrequency ablation for hepatocellular carcinomas larger than 3 cm in diameter. Arch Surg 139:281–287
Poon RT, Ng KK, Lam CM et al. (2004b) Learning curve for radiofrequency ablation of liver tumors: prospective analysis of initial 100 patients in a tertiary institution. Ann Surg 239:441–449
Raut CP, Izzo F, Marra P et al. (2005) Significant long-term survival after radiofrequency ablation for hepatocellular carcinoma in patients with cirrhosis. Ann Surg Oncol 12:616–628
Rhim H, Yoon KH, Lee JM et al. (2003) Major complications after radio-frequency thermal ablation of hepatic tumors: spectrum of imaging findings. Radiographics 23:123–134; discussion 134–136
Rhim H, Dodd GD 3rd, Chintapalli KN et al. (2004) Radiofrequency thermal ablation of abdominal tumors: lessons learned from complications. Radiographics 24:41–52
Sala M, Llovet JM, Vilana R et al. (2004) Initial response to percutaneous ablation predicts survival in patients with hepatocellular carcinoma. Hepatology 40:1352–1360
Seidenfeld J, Korn A, Aronson N (2002) Radiofrequency ablation of unresectable liver metastases. J Am Coll Surg 195:378–386
Shibata T, Iimuro Y, Yamamoto Y et al. (2002) Small hepatocellular carcinoma: comparison of radio-frequency ablation and percutaneous microwave coagulation therapy. Radiology 223:331–337
Shibata T, Shibata T, Metani Y et al. (2006) Radiofrequency ablation for small hepatocellular carcinoma: prospective comparison of internally cooled electrode and expandable electrode. Radiology 238:346–353
Shiina S, Teratani T, Obi S et al. (2005) A randomized controlled trial of radiofrequency ablation with ethanol injection for small hepatocellular carcinoma. Gastroenterology 129: 122–130
Sironi S, Livraghi T, Meloni F et al. (1999) Small hepatocellular carcinoma treated with percutaneous RF ablation: MR imaging follow-up. Am J Roentgenol 173:1225–1229
Sorensen SM, Mortensen FV, Nielsen DT (2007) Radiofrequency ablation of colorectal liver metastases: long-term survival. Acta Radiol 48:253–258
Solbiati L, Goldberg SN, Ierace T et al. (1997a) Hepatic metastases: percutaneous radio-frequency ablation with cooled-tip electrodes. Radiology 205:367–373
Solbiati L, Ierace T, Goldberg SN et al. (1997b) Percutaneous US-guided radio-frequency tissue ablation of liver metastases: treatment and follow-up in 16 patients. Radiology 202:195–203
Solbiati L, Ierace T, Tonolini M et al. (2001) Radiofrequency thermal ablation of hepatic metastases. Eur J Ultrasound 13:149–158
Solbiati L, Tonolini M, Cova L (2004a) Monitoring RF ablation. Eur Radiol 14 Suppl 8:P34–P42
Solbiati L, Ierace T, Tonolini M, Cova L (2004b) Guidance and monitoring of radiofrequency liver tumor ablation with contrast-enhanced ultrasound. Eur J Radiol 51:S19–S23
Tacke J (2003) Percutaneous radiofrequency ablation – clinical indications and results. Rofo 175:156–168
Tacke J, Mahnken A, Roggan A et al. (2004) Multipolar radiofrequency ablation: first clinical results. Rofo 176: 324–329
Takahashi S, Kudo M, Chung H et al. (2007) Initial treatment response is essential to improve survival in patients with hepatocellular carcinoma who underwent curative radiofrequency ablation therapy. Oncology 72 (Suppl 1): 98–103
Tateishi R, Shiina S, Teratani T et al. (2005) Percutaneous radiofrequency ablation for hepatocellular carcinoma. Cancer 103:1201–1209
Veit P, Antoch G, Stergar H et al. (2006) Detection of residual tumor after radiofrequency ablation of liver metastasis with dual-modality PET/CT: initial results. Eur Radiol 16: 80–87
Vilana R, Bianchi L, Varela M et al. (2006) Is microbubble-enhanced ultrasonography sufficient for assessment of response to percutaneous treatment in patients with early hepatocellular carcinoma? Eur Radiol 16:2454–2462

13.1.3 RF Ablation of Lung Tumors

Arnd-Oliver Schäfer

13.1.3.1 Introduction

Lung cancer is among the most commonly occurring malignancies worldwide. Non-small-cell lung cancer (NSCLC) comprises approximately 80% of primary malignant tumors of the lung. Surgical resection is the treatment of choice for early-stage NSCLC. Patients with NSCLC are frequently poor surgical candidates owing to coexistent chronic obstructive bronchopneumopathy or other underlying diseases. Unfortunately, NSCLC tends to recur even after successful resection. Survival rates after surgical treatment range from 63 to 67% in stage IA, 46 to 57% in stage IB, 52 to 55% in stage IIA, 33 to 39% in stage IIB, and

19 to 23% in stage IIIA (Mountain 1997; Van Rens et al. 2000). Conventional treatment of inoperable or unresectable patients with systemic chemotherapy and external-beam radiation therapy has not been satisfactory in terms of survival outcomes. The median survivals have been reported to be less than 1 year after chemotherapy alone (7.1–9.9 months) or radiation therapy alone (9.7–10.3 months). Despite combined use of both treatments, the survival rates have not been greatly improved (10.4–13.8 months) (Akeboshi et al. 2004).

In addition, lung parenchyma is the second most frequent site of metastatic spread from various malignancies, for example, in patients with colorectal carcinoma. And although lung resection can achieve a 5-year survival rate of 20–40% (Yan et al. 2007), it is limited to only a small proportion of patients. Furthermore, surgery is often precluded by the number and the location of metastatic lesions. The high risk of recurrence in patients with metastatic disease and the need to remove healthy lung calls for alternative therapeutic procedures. Attention has therefore been focused on interventional treatment options such RF ablation, which achieves tumor destruction in patients with unresectable primary or secondary lung malignancies. Although RF ablation cannot realistically be expected to reach the same degree of tumor eradication as complete lobar resection, patients may experience survival benefit and relief of symptoms. RF ablation can also be used as an adjunct to chemotherapy and radiation therapy.

13.1.3.2 Indications

Considering the current literature, there are two groups of patients who have to be considered suitable candidates for lung RF ablation: patients suffering from stage IA or IB NSCLC and patients with pulmonary metastases from colorectal carcinoma who were considered to be inoperable as a result of the number of tumors and the distribution of tumor spread or poor performance status, especially concomitant cardiovascular disease and chronic lung disease.

Therefore, the indications for lung RF ablation are either for definitive tumor therapy (NSCLC) or palliation (metastases). The rationales for palliative therapy are tumor reduction prior to systemic chemotherapy, and relief of symptoms such as chest pain, dyspnea, hemoptysis, and cough.

Inclusion criteria for lung RF ablation are as follows:

- Patient age 18 years or more.
- Patients who were considered nonsurgical candidates.
- Refusal of surgery.
- Stage I NSCLC.
- Target tumor not exceeding 5 cm in greatest diameter, preferably 3.5 cm or less.
- Lesions farther than 1 cm from heart, major blood vessels, or airways.
- No invasion of the hilum or mediastinum.
- Number of lesions between one and five per hemithorax.
- Complete resection of the primary tumor in the case of lung metastasis.
- Extrapulmonary metastases are acceptable if they do not increase in size during systemic chemotherapy.
- In patients with no history of cancer outside the lung, malignancy of the target lesion has to be proven by histologic analysis.
- In patients with a history of cancer and lung metastases, an increase in the size of the target lesion of at least 25% has to be observed on preinterventional imaging.

Exclusion criteria for lung RF ablation comprise:

- Lesions adjacent to major pulmonary vessels, the heart, and major bronchi
- Bleeding diatheses not responding to medical therapy with an International Normalized Ratio greater than 1.5 and/or a platelet count of 100×10^9 g/l or less
- Significantly compromised lung function, with an expiratory volume in 1 s of less than 0.8–1 l
- Active infection
- Concomitant disease with restricted life expectancy of less than 6 months

The final decision for RF ablation, particularly the exclusion from surgery, should be determined by a multidisciplinary team (tumor board) including thoracic surgeons, radiation therapists, oncologists, and interventional radiologists. Written informed consent has to be obtained from the patient.

13.1.3.3 Materials and Techniques

Preinterventional Patient Management

All patients should undergo extensive preinterventional investigations including routine physical examination, spirometry, cardiovascular assessment, and an imaging-based tumor staging including abdominal and chest CT 2–4 weeks prior to RF ablation. Staging may be completed by a bone scan. To exclude mediastinal lymph node involvement, PET is recommended. Baseline chest CT plays the key role in diagnostic workup of RF ablation candidates since it determines the number, size, and exact location of the target lesions and provides the terms of reference for all postinterventional follow-up imaging studies. Blood tests focus on the exclusion of renal function impairment and coagulopathy.

Antiplatelet and anticoagulation medications have to be discontinued at least 2 prior to the intervention. Routine antibiotic treatment is not required, although some centers prophylactically administer antibiotics, especially in patients with underlying lung disease as well as in elderly or immunocompromised patients with subsequently increased risk of infection. In those cases, a second-generation cephalosporine can be administered intravenously for 2 days starting on the day of the procedure. It should be continued orally for 1 week.

Anesthesiology Care

To date, no consensus has been reached on the optimal anesthesiology care for lung RF ablation. Patients who are considered candidates for the procedure normally have a medium to high risk of undergoing anesthesia, while local anesthesia does not provide adequate pain relief for thermal ablation. To keep the hospitalization short, RF ablation is most frequently performed with the patient in conscious sedation. The combination of a hypnotic drug and a short-half-life analgesic drug enables mild sedation and allows for bearing of pain induced by the ablation procedure and the often uncomfortable position and for cooperation with the operator. Typically recommended agents are fentanyl and midazolam hydrochloride (see Chap. 5). Conscious sedation requires continuous electrocardiography and pulse oximetry with blood pressure monitoring throughout the entire ablation process. Only a few centers propose epidural block or general anesthesia.

The puncture of the target lesion is performed with the patient under local anesthesia, while sedation is started immediately before the current is turned on. Keeping this order is helpful, as the patients may cooperate and not hold their breath under sedation as needed for a safe puncture of a lung lesion.

RF Ablation Procedure

Percutaneous lung RF ablation is routinely performed under CT guidance, ideally with the use of CT fluoroscopy following standard rules for CT-guided lung biopsy.

First the patient is placed in the appropriate position: supine, prone, or lateral decubitus according to the location of the target lesion. A radiopaque grid is fixed on the patient's skin and this is followed by a nonenhanced CT scan of the anticipated region with 3–5-mm section thickness. The shortest path that thoroughly avoids bullae, interlobar fissures, vessels, and bronchi is chosen. Thereafter the skin entry point is marked with a permanent ink marker. Depending on whether a monopolar or a (bipolar) multipolar RF ablation system is used, none or up to four grounding pads are applied to the patient's opposite chest wall, abdomen, back, or shaved thighs. Standard surgical prepping and draping is mandatory. The skin at the needle entry point is cleaned with a 10% solution of providone iodine. Subsequently, 10–30 ml of a local anesthetic such as lidocaine (1–2%) is instilled using a 22G needle. Local anesthesia should include the skin and the deep subcutaneous tissue and should reach down to the pleura. To facilitate insertion of the RF probe, a small incision of the skin is performed.

Following accurate preparation, the needle electrode is advanced to the lesion. Needle advancement requires careful planning since minor degrees of malalignment can cause the tip of the needle to miss the target, particularly in small deep parenchymal lesions. Special attention must be paid to verify the correct placement of the active part of the electrode with respect to the tumor. Usually it should be placed centrally inside the tumor. If expandable electrodes are used, the prongs should exceed beyond the tumor margin. Care has to be taken to avoid placement of

tines into vessels or bronchi. Needle electrodes should exceed the opposite tumor margin by only a few millimeters. Multiple or cluster electrodes may be used to increase the ablation volume. Owing to multiple passages of the pleura, this approach increases the risk of pneumothorax and should therefore be avoided whenever possible. To prove the correct position of the RF probe, it is strongly recommended to assess the relationship between the needle electrode and the target lesion by assessing axial slices as well as multiplanar reformations.

Once the needle electrode has been correctly positioned and connected to the RF generator, the ablation cycle is initiated. During the ablation, either impedance or temperature or both are continuously monitored and recorded (see Sect. 13.1.1). Treatment algorithms are based on incremental power delivery. The different steps of the procedure should follow the protocols provided by the manufacturers. If expandable RF probes are used, the tines should be withdrawn after one treatment cycle and the electrode rotated through 90°. Subsequently, the tines should be redeployed and the ablation repeated. Thereby the presence of viable tumor cells beyond the initial area of ablation is minimized (Gillams and Lees 2008). Generally lung ablation requires less energy than hepatic or renal RF ablation, because the tumor is insulated by the surrounding air, resulting in heat being trapped inside the lesion.

For lesions that exceed a diameter of 3 cm, overlapping ablations have to be performed to ensure complete ablation. To minimize the risk of pneumothorax, the position of the electrode within the tumor is changed by withdrawing it into superficial lung tissue along its major axis, changing its angle, and then reinserting the probe into the target without an additional passage of the pleura. When technically feasible, the ablation zone should encompass the tumor by at least 1 cm. After the ablation has been completed, the needle electrodes are retracted and the device is removed. Track ablation is routinely performed with cautery of the access tract on the way out after completion of lesion ablation.

A control CT scan is obtained within 30 min after completion of the procedure. The total duration of the RF procedure varies widely owing to lesion geometry, lesion size, and the RF system used. Ablation times may range from 7 to 100 min (Suh et al. 2003; Lee et al. 2004).

Postinterventional Patient Management

Following lung RF ablation, the patients should be instructed to stay in bed for 4 h. Chest radiographs are obtained within the first 4 h after the procedure and before discharge to exclude pneumothorax. The hospital observation period can be limited to 24 h in the majority of cases. Patients with a small (less than 30%), asymptomatic pneumothorax are observed in hospital without any specific therapy. In symptomatic patients or large pneumothorax, needle aspiration or a chest tube may be needed (see Sect. 11.2). To evacuate small intraprocedural pneumothoraces, needle aspiration can be used, as well as pigtail catheter insertion.

Postinterventional Imaging Assessment

There has been a lively discussion about the value of different imaging modalities during follow-up. Thin-slice pre- and postcontrast multidetector CT is currently the most commonly used imaging modality for follow-up after pulmonary RF ablation, although PET scanning is suggested by some authors to be superior to CT for the detection of residual or recurrent tumors (Akeboshi et al. 2004; Dupuy et al. 2006; Kang et al. 2004). Others are of the opinion that high-quality CT scans interpreted by an experienced radiologist will be more sensitive to subtle recurrence (Bojarski et al. 2005; Jin et al. 2004; Rossi et al. 2006; Suh et al. 2003).

Postinterventional contrast-enhanced CT scans are acquired on the day following the procedure to detect delayed complications. After that, the patients should be reviewed at 1, 3, and 6 months following RF ablation, and every 6 months thereafter with dual-phase chest CT.

Lesion size is measured and reported as the largest bidimensional diameters. Nonenhanced CT scans are obtained before, during, and immediately after RF ablation. Follow-up CT examinations have to be compared with preinterventional CT imaging. Decisive findings include:

- Presence and extent of ground-glass opacification
- Patterns of contrast enhancement of the lesion
- Attenuation of the lesion on noncontrast scans
- Peripheral rim enhancement
- Complications

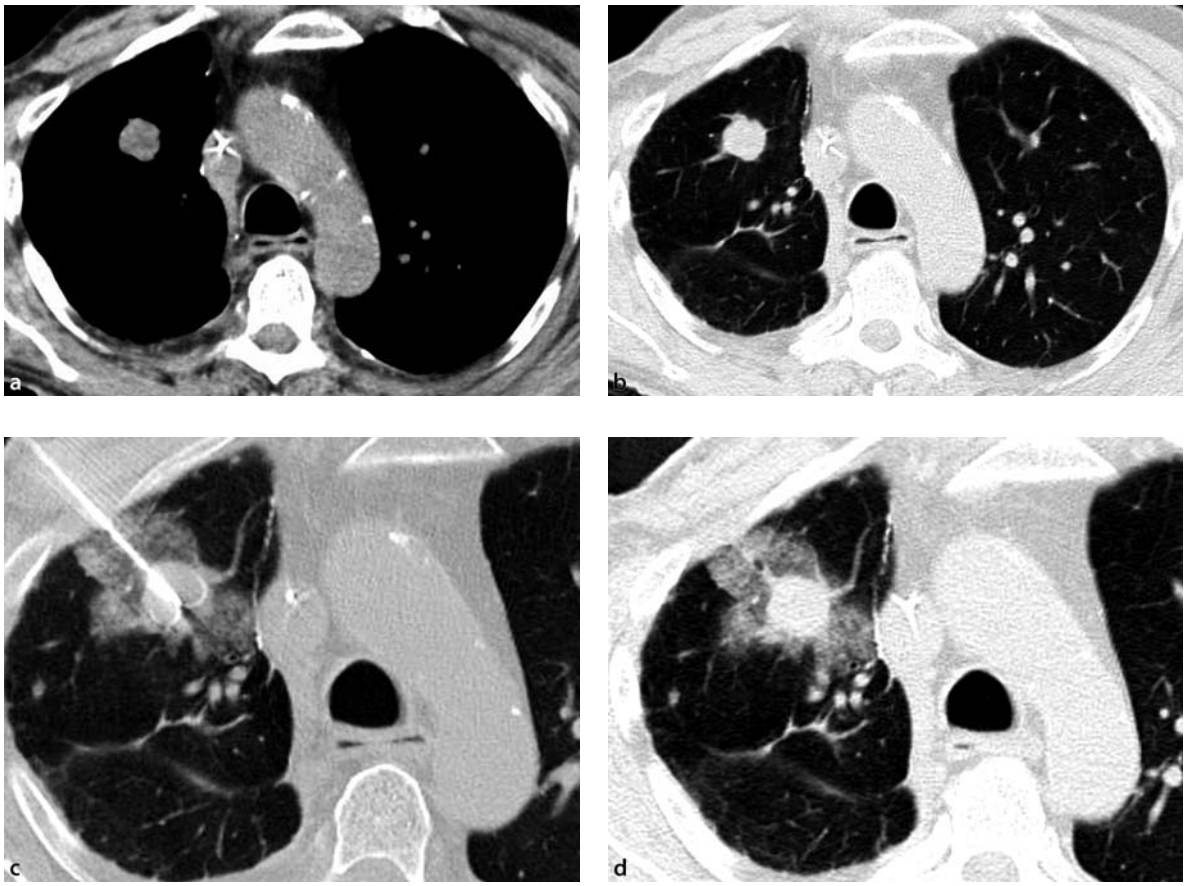

Fig. 13.14a–d CT-guided RF ablation of a colorectal pulmonary metastasis of the right upper lobe (**a**,**b**). During insertion of the needle electrode, self-limiting, parenchymal hemorrhage occurred (**c**). The CT scan immediately after RF ablation displays enlargement of the treated metastasis surrounded by ground-glass opacity of the lung parenchyma in the vicinity of the lesion indicating successful treatment (**d**)

Immediately after RF ablation, nonenhanced CT scans show a decreased attenuation of the tumor and ground-glass opacification enveloping the treated zone. The thickness and pattern of ground-glass opacity is one of the most reliable predictors of treatment success (Fig. 13.14). Ground-glass opacifications should extend more than 5 mm beyond the margins of the treated tumor. They likely represent localized edema and hemorrhage. If the tumor is only incompletely surrounded by ground-glass opacifications immediately after the procedure, the intervention should be continued.

On initial contrast-enhanced CT, a well-demarcated nonenhanced zone is visible. Tumor necrosis is considered complete if the nonenhanced area at the treatment site has a diameter greater than or equal to that of the treated tumor. All contrast-enhancement profiles within the ablation zone should remain lower than those prior to the procedure. Any portion of the treated lesion that is enhanced by more than 15 HU when compared with the initial postinterventional images after contrast material administration is highly suspicious of local tumor recurrence. Within 6 months after ablation a circumferential rim of enhancement no larger than 5 mm around the ablation zone is considered to be reactive.

Local tumor progression is defined as tumor growth from the zone of ablation, whereas local treatment success is defined as involution of the ablation zone over time. However, owing to intratumoral hemorrhage the treated lesion may increase in size, but will start shrinking after a few months (Fig. 13.15). If the size of the ablation zone does not decrease by at least

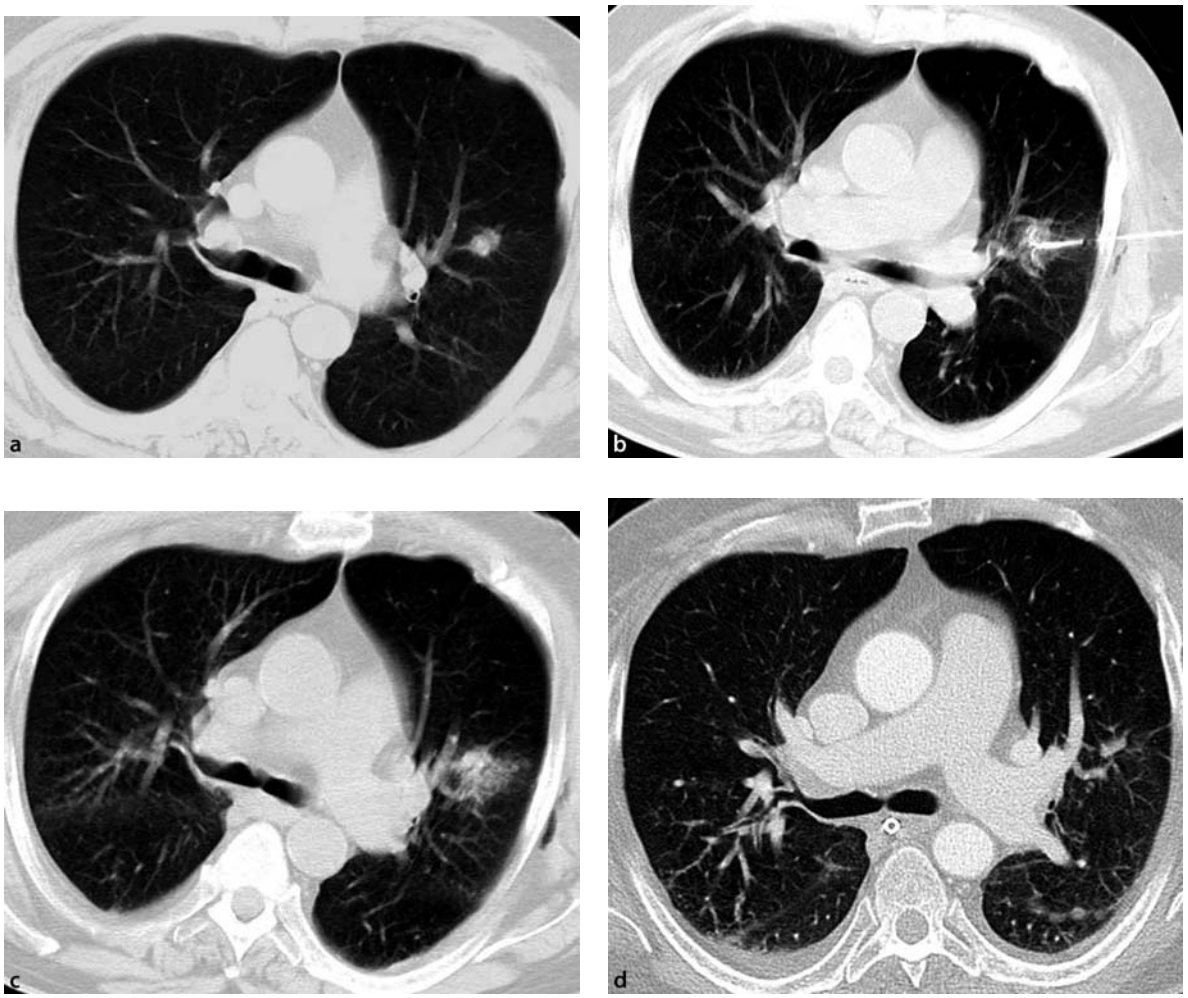

Fig. 13.15a–d CT-guided RF ablation procedure of an early-stage non-small-cell lung cancer (NSCLC) in the left upper lobe adjacent to a major pulmonary artery (**a**). Enfolded jackhooks of an expandable needle electrode within the tumor (**b**). The control scan reveals ground-glass opacification encompassing the treated tumor nodule (**c**). Follow-up CT after 6 months demonstrates considerable shrinkage of the coagulation necrosis indicative of successful tumor treatment (**d**)

25% between 6 and 9 months after ablation, PET is recommended to assess metabolic activity. Two characteristic types of local recurrence are described following RF ablation of the lung. The most common type is seen as enlargement of parts of the ablation zone with or without contrast enhancement. A different type of local relapse is represented by the development of tumor nodules adjacent to the ablation zone.

As neither change in tumor shape and size nor enhancement pattern unequivocally predicts complete ablation, CT-guided biopsy and histologic analysis in combination with the CT findings may be used for follow-up (Belfiore et al. 2004). Indeed, biopsy of the ablation zone has been recommended, but sampling error is inevitable as only parts of the treated tumor can be targeted. Thus, the combination of tumor morphology and contrast enhancement seems to be the most practical approach for predicting incomplete treatment and local tumor recurrence.

13.1.3.4 Results

In early clinical experience with lung RF ablation, patients were treated within a framework of feasibility studies to investigate safety, tolerability, and local ther-

apeutic effects of the procedure. The first percutaneous RF ablation of a lung tumor was reported by Dupuy et al. (2000). However, regardless of the great amount of data on the clinical and radiological response of RF ablation in lung tumors published so far, its efficacy in the mid and long term still remains poorly understood. Rationales for the existence of residual tumor may be intrinsic heat-resistant properties of a tumor, residual vascular flow, or reperfusion of the ablation zone.

Technical Success and Local Tumor Control

RF ablation was used in a study of 31 patients with 54 tumors and the initial therapeutic response has been evaluated with both ^{18}F-fluorodeoxyglucose PET and contrast-enhanced CT (Akeboshi et al. 2004). Complete necrosis could be achieved in 32 of the 54 treated nodules. A significant difference in the rate of complete tumor necrosis was found for tumors 3 cm or less and tumors more than 3 cm in diameter (69% vs 39%). Tumor type did not influence complete necrosis rates.

Recently, a recurrence rate of 100% for tumors exceeding 3.5 cm was reported (Gillams and Lees 2008). Therefore, either more than one ablation procedure or additional therapy can be expected when ablating tumors larger than 3.5 cm. The authors concluded that the optimal ablation is achieved in peripheral, less than 3.5-cm diameter tumors which are not in direct contact with vessels larger than 3 mm. Another interesting finding refers to viable tumor cells beyond the periphery of the ablation zone resulting in tumor recurrence. The cause of this special nodular pattern of recurrence is still unknown and may be based on satellites that were not recognized at the time of initial treatment or cells carried into the parenchyma by the expanding tines of the RF electrode (Fig. 13.16).

In a study conducted on 26 patients with 27 NSCLC and four patients with five lung metastases, complete tumor necrosis could be established in 12 of 32 lesions (38%) and partial necrosis in 20 of 32 (62%) confirmed by contrast-enhanced CT during follow-up (Lee et al. 2004). The mean survival time in patients with complete necrosis was 19.7 months, in contrast to 8.7 months for those patients in which only partial necrosis was obtained by RF ablation. Additionally, the results of the study demonstrate excellent palliation of mild hemoptysis (80%) but a less satisfactory palliation of chest pain (36%), and cough (25%).

Twenty-one RF-ablated lung lesions were evaluated with helical CT during follow-up by comparing two groups of patients (complete ablation vs partial necrosis) (Jin et al. 2004). Immediately obtained CT scans of the ablated lesions revealed an increase in mean diameters. In the complete-ablation group, the diameters of the treated lesions decreased at 3, 6, 9, 12, and 15 months compared with the diameters measured on the immediate postinterventional CT. In contrast, lesion diameters in the partial-necrosis group increased gradually on follow-up CT scans at 9 and 11 months after initial shrinkage.

Patient Survival

RF ablation has provided good results for local tumor control in the short-term follow-up; however, reliable data confirming its efficacy in the mid- and long-term clinical course are scarce. De Baère et al. (2006) treated 97 lung tumors with RF ablation. The authors found 18-month overall survival rates of 76% for primary tumors and of 71% for metastases. The 18-month lung disease-free survival rates were 44% for primary tumors and 32% for metastases.

In another study of 153 patients with 189 consecutive lesions, 602 RF ablations were accomplished in 183 sessions (Simon et al. 2007). Technical success was achieved in 159 (98.1%) of 162 tumors ablated for local control. Observed residual tumor enhancement immediately after RF ablation was attributed to the close proximity to major pulmonary arteries or veins 3 mm or more in diameter and the subsequent subcytotoxic temperatures recorded at the end of ablation. The Kaplan–Meier median time to death for all patients with stage I NSCLC was 29 months, with estimated 1-, 2-, 3-, 4-, and 5-year survival rates of 78, 57, 36, 27, and 27%, respectively. For patients with colorectal metastases, the estimated 1-, 2-, 3-, 4-, and 5-year survival rates were 87, 78, 57, 57, and 57%, respectively. Local tumor progression rates over time turned out to be significantly lower in patients with smaller index tumors (smaller than 3 vs larger than 3 cm). The calculated Kaplan–Meier median time to progression for tumors 3 cm or smaller was 45 months, with estimated 1-, 2-, 3-, 4-, and 5-year progression-free rates of 83, 64, 57, 47, and 47%, respectively, while the median

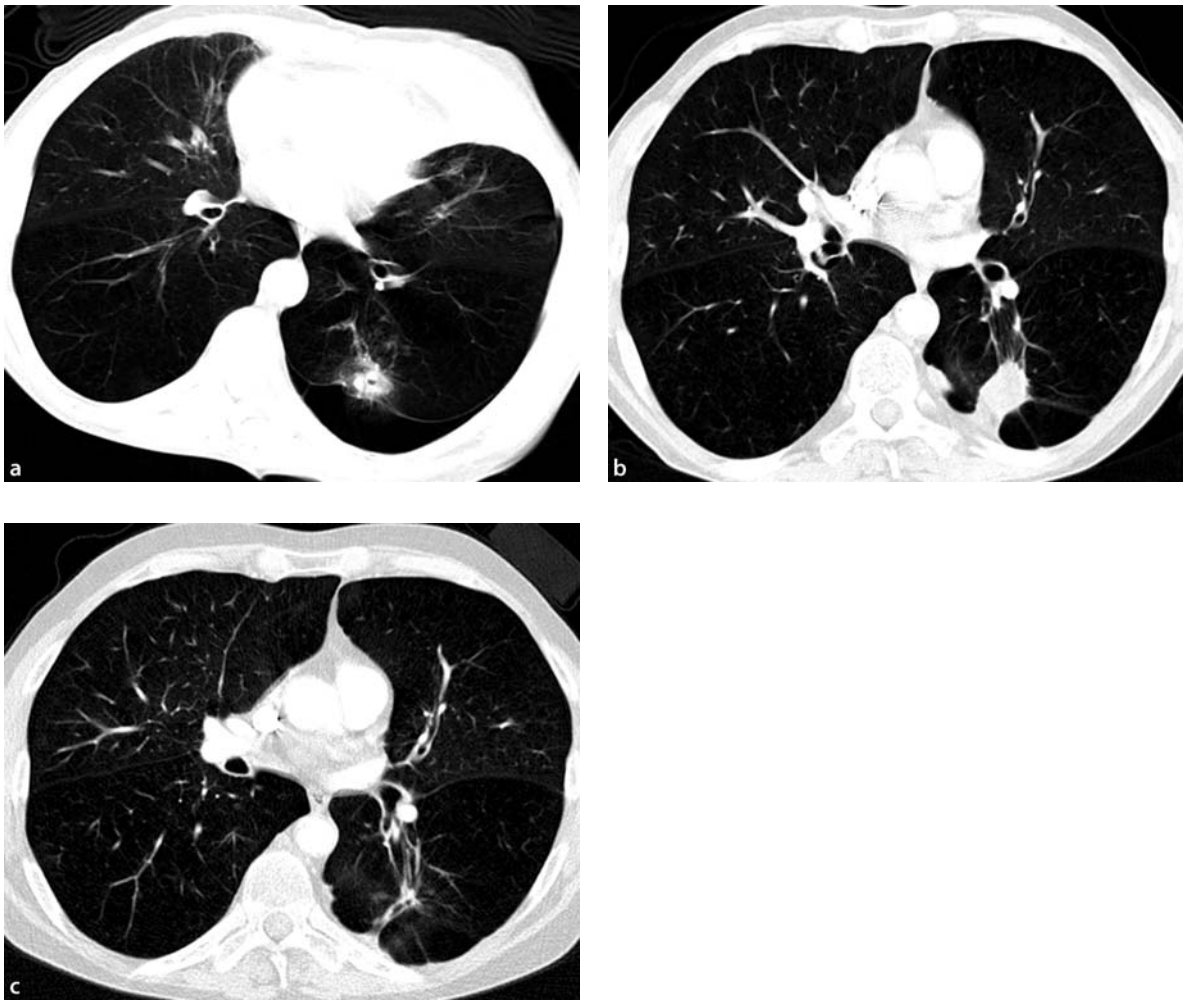

Fig. 13.16a–c Small intraprocedural pneumothorax occurred during percutaneous RF ablation of an early-stage NSCLC of the left lower lobe (**a**). Note the underlying lung emphysema. On the follow-up CT scan after 3 months the treated tumor increased in size, exhibiting pleural contact in the region of the needle entry (**b**). The CT scan 6 months after the procedure reveals shrinkage of the ablation zone with scar formation (**c**)

time to progression for tumors larger than 3 cm was 12 months, with estimated 1-, 2-, 3-, 4-, and 5-year progression-free rates of 45, 25, 25, 25, and 25%, respectively.

Yamakado et al. (2007) reported an intrapulmonary total recurrence rate of 47% after RF ablation within a mean follow-up of 19 months. Not surprisingly, the local tumor progression rate was 11% in patients with tumors 3 cm or smaller and 50% in those with tumors larger than 3 cm. Of the 33 patients with pulmonary recurrence, 19 patients underwent repeat lung RF ablation. The 1-, 2-, and 3-year survival rates were 84, 62, and 46%, respectively. The median survival time was 31 months. Tumor size and extrapulmonary metastases represented significant independent factors affecting prognosis in the study.

Furthermore, a follow-up study of RF ablation for pulmonary colorectal metastases demonstrated a median survival of 32 months with 1-, 2-, and 3-year survival rates of 75, 63, and 45%, respectively (Yan et al. 2007). The size of the largest pulmonary metastasis, proximity of metastases to major pulmonary vessels, pre-lung-RF-ablation carcinoembryonic antigen level, and post-lung-RF-ablation carcinoembry-

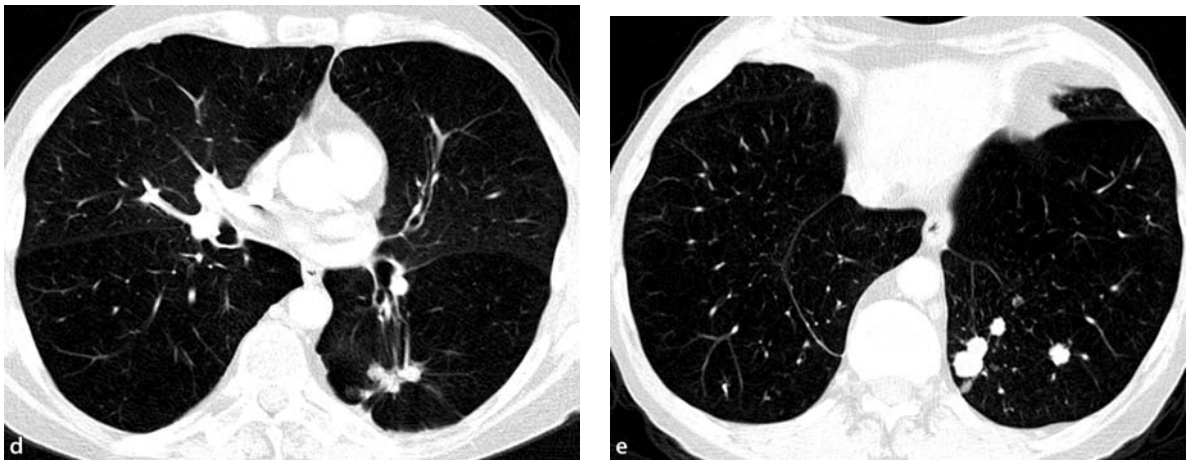

Fig. 13.16d,e (continued) On the CT scan 12 months following RF ablation, local recurrence is visible arising from both the ablation zone and the surrounding lung parenchyma, where a number of newly diagnosed satellites can be detected (**d**,**e**)

onic antigen level were found to significantly influence survival.

13.1.3.5 Complications

Mortality

So far, no intraprocedural deaths have been reported for lung RF ablation. However, in a large series the overall 30-day mortality rate was 3.9% (six of 153 patients), with four deaths (2.6%) being believed to be procedure-related (Simon et al. 2007). In another study, a procedure-related mortality rate of 0.9% was reported (Sano et al. 2007).

Morbidity

From the preliminary experiences, lung RF ablation seems to be associated with an acceptable rate of adverse events that can be divided into three groups according to the criteria of the Society of Interventional Radiology Technology Assessment Committee and the International Working Group on Image-Guided Tumor Ablation (Goldberg et al. 2005):

1. Major complications
2. Minor complications
3. Side effects

A major complication is defined as an event that leads to substantial morbidity and disability, increased level of care, or results in hospital admission or substantially lengthened hospital stay. This includes any case in which a blood transfusion or interventional drainage procedure is required. All other complications are considered minor. Side effects were considered undesired consequences of the procedure that, although occurring frequently, rarely result in substantial morbidity.

Reported overall morbidity rates vary widely in the range from 15.2 to 64.9% (Ambrogi et al. 2006; Fernando et al. 2005; Sano et al. 2007). Mostly minor complications were reported; however, Sano et al. (2007) noted a major complication rate of 17.1%. Pneumothorax is one of the most common complications of lung RF ablation, occurring in 30–51.2% of procedures (Steinke et al. 2004; Sano et al. 2007). It may be associated with central location of the tumor, obstructive airway disease, emphysema, and multiple electrode insertions. Aspiration may be needed in up to 9% of cases and chest tube placement in 11.8% of cases (Sano et al. 2007). The number of ablated lung lesions and the duration of the ablation procedure are two important risk factors closely associated with overall morbidity, pneumothorax, and chest drain requirement.

The majority of patients treated with RF ablation experience mild to moderate pain during the procedure. Asymptomatic pleural effusion and development of postablation syndrome consisting of mild fever and fatigue for several days are other common side effects after lung ablation. Acute hemorrhage can occur

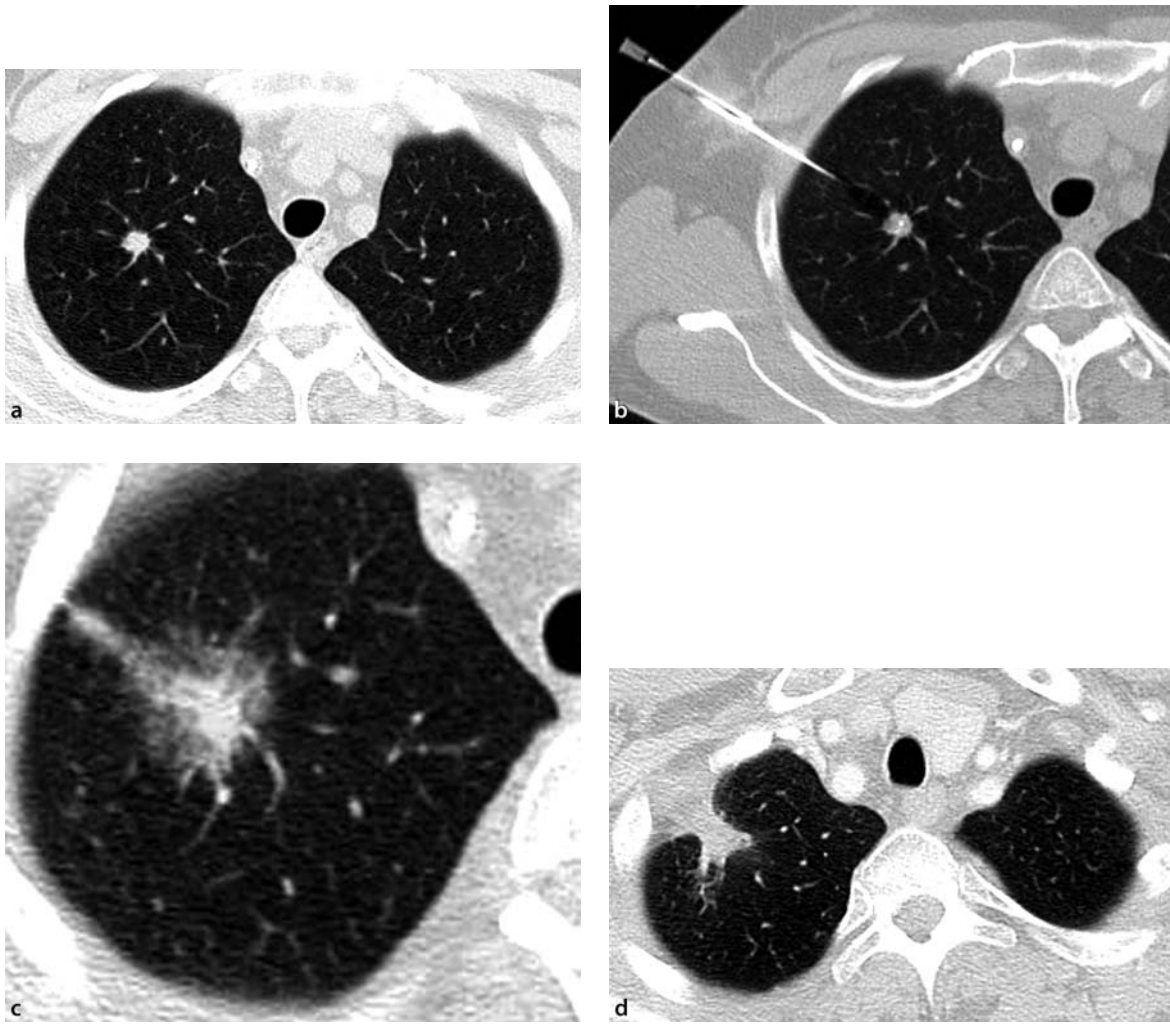

Fig. 13.17a–d RF ablation of a small NSCLC in the right upper lobe (**a**). Needle electrode placement using a tandem technique with a second needle for guiding the RF probe resulting in a central position of the enfolded tines (**b**). Postablation needle track hemorrhage and typical ground-glass opacification indicating a successful procedure (**c**). The control scan after 3 months shows enlargement of the treated tumor and thickening of the pleura in the region of the former needle entry site (**d**)

following probe insertion, which is demonstrated on control CT scans as sudden opacification surrounding the electrode. As it is self-limiting in the vast majority of cases, it rarely requires additional treatment. Cavitation can also be observed as a result of the RF ablation. In most cases cavitation resolves spontaneously within 3 months after the procedure. Sometimes it may persist for up to 1 year. Only a few patients develop infection at the site of cavitation requiring hospitalization and antibiotic treatment. Malignant seeding along the needle tract is another extremely rare complication. The track ablation procedure at the end of procedure should render this serious adverse event unlikely.

In summary, major procedure-related complications include:

- Pneumothorax requiring chest tube placement
- Pleural effusion requiring intercostal drainage
- Massive hemorrhage
- Pneumonia
- Lung abscess
- Empyema
- Bronchopleural fistula
- Acute respiratory distress syndrome

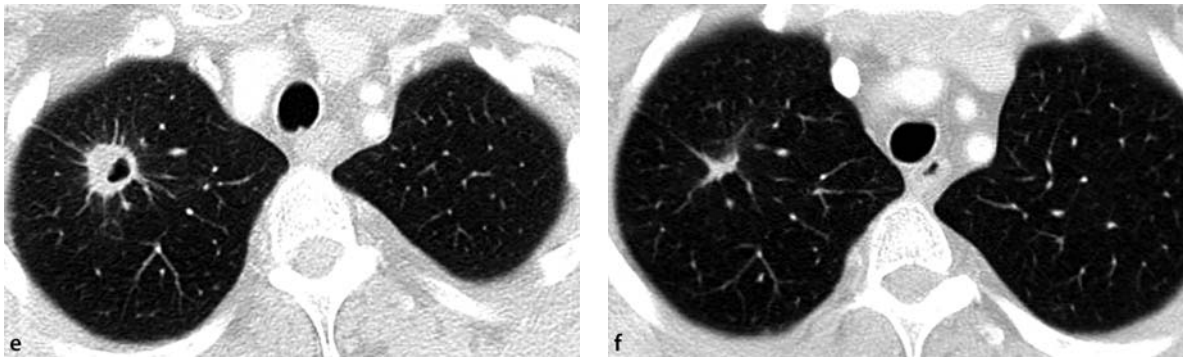

Fig. 13.17e,f (continued) On follow-up CT after 6 months, central cavitation can be differentiated (**e**). Follow-up CT 2 years after the ablation procedure reveals scar formation with no signs of local recurrence (**f**)

Minor complications following lung RF ablation comprise:

- Intraparenchymal, self-limiting hemorrhage
- Hemosputum lasting 1–2 weeks after ablation
- Nausea and/or vomiting
- Subcutaneous emphysema
- Dyspnea
- Cough
- Skin burn
- Atelectasis
- Subileus
- Myalgia

Summary

CT-guided percutaneous lung RF ablation is a promising minimally invasive technique for the treatment of nonoperable early-stage NSCLC and pulmonary metastases. So far, it is difficult to determine the true clinical efficacy of RF ablation, especially since the reported follow-up periods tend to be short and some recurrences may remain undetected. However, all recent clinical trials have reported a good local response, and an acceptable rate of complications. Nevertheless, its role in the treatment of lung malignancies is promising and the clinical acceptance is evolving.

Lung ablation can be used as an adjuvant therapy to systemic anticancer treatment, including chemotherapy or radiation therapy, to decrease the tumor cell volume with reasonably low morbidity and mortality in the otherwise severely ill patient. Furthermore, it could be a powerful alternative to surgical treatment or chemotherapy, particularly in selected patients with tumors smaller than 3 cm in diameter who have combined medical illnesses or limited functional lung reserve (Fig. 13.17). Since lung tumors cause debilitating symptoms such as cough, hemoptysis, and pain, percutaneous lung RF ablation may also have a role in improving the quality of life even in this patient group with a palliative intent.

Key Points

- Select patients carefully, taking into account selection factors such as expected survival, size, number, and location of pulmonary lesions.
- The final decision to perform RF ablation is made in an interdisciplinary consensus with the referring physicians and the individual patient.
- Adequate local anesthesia of the puncture site and an appropriate dose of intravenous sedation are imperative to minimize the irritation to the pleura and to facilitate the procedure.
- Whenever possible, treat lesions of one hemithorax in a single session; at the beginning select patients with a maximum of two lesions per hemithorax and a diameter of 3 cm or less.
- Avoid multiple needle insertions.
- Control the RF ablation process by using repeated CT scans.
- Close patient monitoring during the course of the intervention is mandatory.
- Management of major complications is a cornerstone of the procedure.
- Record and report all adverse events precisely.
- Propose a structured clinical and imaging follow-up protocol, including dual-phase CT scans in the close postprocedural period, after 4 weeks, 3 and 6 months, and in intervals of 3–6 months thereafter.

References

Akeboshi M, Yamakado K, Nakatsuka A et al. (2004) Percutaneous radiofrequency ablation of lung neoplasms: initial therapeutic response. J Vasc Interv Radiol 15:463–470

Ambrogi MC, Lucchi M, Dini P et al. (2006) Percutaneous radiofrequency of lung tumors: results in the mid-term. Eur J Cardiothorac Surg 30:177–183

Belfiore G, Moggio G, Tedeschi E et al. (2004) CT-guided radiofrequency ablation: a potential complementary therapy for patients with unresectable primary lung cancer – a preliminary report of 33 patients. Am J Roentgenol 183: 1003–1011

Bojarski JD, Dupuy DE, Mayo-Smith WW (2005) CT imaging findings of pulmonary neoplasms after treatment with radiofrequency ablation: results in 32 tumors. Am J Roentgenol 185:466–471

De Baère T, Palussière J, Aupérin A et al. (2006) Midterm local efficacy and survival after radiofrequency ablation of lung tumors with minimum follow-up of 1 year: prospective evaluation. Radiology 240:587–596

Dupuy DE, DiPetrillo T, Gandhi S et al. (2006) Radiofrequency ablation followed by conventional radiotherapy for medically inoperable stage I non-small cell lung cancer. Chest 129:738–745

Dupuy DE, Zagoria RJ, Akerley W et al. (2000) Percutaneous radiofrequency ablation of malignancies in the lung. Am J Roentgenol 175:1263–1266

Fernando HC, De Hoyos A, Landreneau RJ et al. (2005) Radiofrequency ablation for the treatment of non-small cell lung cancer in marginal surgical candidates. J Thorac Cardiovasc Surg 129:639–644

Gillams AR, Lees WR (2008) Radiofrequency ablation of lung metastases: factors influencing success. Eur Radiol 16: 672–677

Goldberg SN, Grassi CJ, Cardella JF et al. (2005) Image-guided tumor ablation: standardization of terminology and reporting criteria. Radiology 235:728–739

Jin GY, Lee JM, Lee YC et al. (2004) Primary and secondary lung malignancies treated with percutaneous radiofrequency ablation: evaluation with follow-up helical CT. Am J Roentgenol 183:1013–1020

Kang S, Luo R, Liao W et al. (2004) Single group study to evaluate the feasibility and complications of radiofrequency ablation and usefulness of post treatment positron emission tomography in lung tumours. World J Surg Oncol 2:30

Lee JM, Jin GY, Goldberg SN et al. (2004) Percutaneous radiofrequency ablation for inoperable non-small cell lung cancer and metastases: preliminary report. Radiology 230:125–134

Mountain CF (1997) Revisions in the international system for staging lung cancer. Chest 111:1710–1717

Rossi S, Dore R, Cascina A et al. (2006) Percutaneous computed tomography-guided radiofrequency thermal ablation of small unresectable lung tumours. Eur Respir J 27: 556–563

Sano Y, Kanazawa S, Gobara H et al. (2007) Feasibility of percutaneous radiofrequency ablation for intrathoracic malignancies: a large single-center experience. Cancer 109: 1397–1405

Simon CJ, Dupuy DE, DiPetrillo TA et al. (2007) Pulmonary radiofrequency ablation: long-term safety and efficacy in 153 patients. Radiology 243:268–275

Steinke K, King J, Glenn D et al. (2003) Pulmonary hemorrhage during percutaneous radiofrequency ablation: a more frequent complication than assumed? Interact Cardiovasc Thorac Surg 2:462–465

Suh RD, Wallace AB, Sheehan RE et al. (2003) Unresectable pulmonary malignancies: CT-guided percutaneous radiofrequency ablation – preliminary results. Radiology 229: 821–829

Van Rens M, de la Riviere AB, Elbers HJR et al. (2000) Prognostic assessment of 2,361 patients who underwent pulmonary resection for non-small cell lung cancer, stage I, II, and IIIA. Chest 117:374–379

Van Sonnenberg E, Shankar S, Morrison PR et al. (2005) Radiofrequency ablation of thoracic lesions: part 2, initial clinical experience – technical and multidisciplinary considerations in 30 patients. Am J Roentgenol 184:381–390

Yamakado K, Hase S, Matsuoka T et al. (2007) Radiofrequency ablation for the treatment of unresectable lung metastases in patients with colorectal cancer: a multicenter study in Japan. J Vasc Interv Radiol 18:393–398

Yan TD, King J, Ebrahimi A et al. (2007) Hepatectomy and lung radiofrequency ablation for hepatic and subsequent pulmonary metastases from colorectal carcinoma. J Surg Oncol 96:367–373

Further Reading

Kelekis AD, Thanos L, Mylona S et al. (2006) Percutaneous radiofrequency ablation of lung tumors with expandable needle electrodes: current status. Eur Radiol 16:2471–2482

Lencioni R, Crocetti L, Cioni R et al. (2004) Radiofrequency ablation of lung malignancies: where do we stand? Cardiovasc Intervent Radiol 27:581–590

Morrison PR, vanSonnenberg E, Shankar S et al. (2005) Radiofrequency ablation of thoracic lesions: part 1, experiments in the normal porcine thorax. Am J Roentgenol 184:375–380

Nguyen CL, Scott WJ, Young NA et al. (2005) Radiofrequency ablation of primary lung cancer: results from an ablate and resect pilot study. Chest 128:3507–3511

Okuma T, Matsuoka T, Yamamoto A et al. (2007) Factors contributing to cavitation after CT-guided percutaneous radiofrequency ablation of lung tumors. J Vasc Interv Radiol 18:399–404

Steinke K, Sewell PE, Dupuy D et al. (2004) Pulmonary radiofrequency ablation – an international study survey. Anticancer Res 24:339–343

Tominaga J, Miyachi H, Takase K et al. (2005) Time-related changes in computed tomographic appearance and pathologic findings after radiofrequency ablation of the rabbit lung: preliminary experimental study. J Vasc Interv Radiol 16:1719–1726

Yamakado K, Akeboshi M, Nakatsuka A et al. (2005) Tumor seeding following lung radiofrequency ablation: a case report. Cardiovasc Intervent Radiol 28:530–532

Yan TD, King J, Sjarif A et al. (2006a) Percutaneous radiofrequency ablation of pulmonary metastases from colorectal carcinoma: prognostic determinants for survival. Ann Surg Oncol 13:1529–1537

Yan TD, King J, Sjarif A et al. (2006b) Learning curve for percutaneous radiofrequency ablation of pulmonary metastases from colorectal carcinoma: a prospective study of 70 consecutive cases. Ann Surg Oncol 13:1588–1595

13.1.4 Renal RF Ablation

Andreas H. Mahnken

13.1.4.1 Introduction

In 2007 the American Cancer Society (2007) estimated 51,190 new cases of cancer of the kidney and the renal pelvis, accounting for 12,890 deaths. Besides sporadic tumor occurrence, several hereditary syndromes are associated with an increased risk of renal cell carcinoma (RCC), of which von Hippel–Lindau disease is the most recognized, with up to 45% of affected patients developing one or more RCCs during their lifetime (Herring et al. 2001). Historically RCC was detected by flank pain and hematuria, but with introduction of cross-sectional imaging techniques such as ultrasound and CT renal tumors are increasingly detected at earlier asymptomatic stages (Pantuck et al. 2001). Nowadays about two thirds of all RCCs are discovered incidentally (Homma et al. 1995). Tumor stage and histological tumor type are the most relevant prognostic factors. As small tumors (4 cm or smaller) rarely metastasize, there is a rationale for local therapy of small RCCs. This knowledge was used when nephron-sparing surgical techniques such as partial nephrectomy via an open or laparoscopic approach were established in clinical routine (Uzzo and Novick 2001). The 10-year tumor-free survival rates are greater than 85%, equaling the result of open surgical nephrectomy (Fergany et al. 2000). These findings paved the way for the introduction of new therapeutic concepts, including minimally invasive, energy-based treatment options, of which RF ablation has evolved as the most commonly used technique.

13.1.4.2 Indications

First of all, even before considering RF ablation as a treatment option in suspected RCC, a recent (not older than 2 weeks) contrast-enhanced cross-sectional imaging study (CT or MR) needs to be performed. Thoracic and abdominal imaging is needed to perform preinterventional staging, because the number of lesions, the tumor size and location, and extrarenal tumor manifestations may influence the choice of treatment.

From a technical point of view RF ablation may be performed open surgically, laparoscopically, or percutaneously. From animal experiments the results of the different approaches towards the kidney are known to be comparable (Crowley et al. 2000). If the percutaneous approach is used, RF ablation does not necessarily require general anesthesia. Eventually it can be applied on an outpatient basis. It is technically feasible to treat multiple tumors in both kidneys. In exophytic tumors 3 cm or smaller, complete tumor ablation is consistently achieved, while larger tumors may require repeated treatment (Gervais et al. 2005). Generally RF ablation preserves larger amounts of healthy renal parenchyma than surgery. Centrally located tumors are associated with a higher risk of incomplete ablation and thermal damage to the urinary system than exophytic tumors.

From a clinical perspective the treatment strategy has to be adapted to the individual patient. The overall clinical situation, including age and life expectancy, physical and laboratory parameters, as well as patient compliance, needs to be considered. So far radical nephrectomy is the gold standard for treatment of RCC against which all other forms of treatment have to be measured. A direct comparison with this standard of reference has not yet been performed and only limited long-term follow-up data are available on renal RF ablation (McDougal et al. 2005). Consequently the indication for renal RF ablation is an individual therapeutic decision that limits renal RF ablation to selected patients. An interdisciplinary consensus between urologists, the oncologist, and the interventional radiologist is essential to provide the optimal therapy to the patient and to select the right patients for RF ablation.

Considering the above mentioned basics, RF ablation has to be considered as a treatment option for patients with contraindications for surgery, predominantly patients with comorbid conditions or those who refuse open surgery (Table 13.6). RF ablation is particularly suited for elderly patients with risks for anesthesia. In patients with impaired renal function, solitary kidney, von Hippel–Lindau disease or multiple

Table 13.6 Indications and contraindications for renal RF ablation, with the ideal candidate being a patient an exophytic tumor with a diameter of 5 cm or less. Extended indications and relative contraindications are given in *parentheses*

Indication	Contraindication
Exophytic tumor $\leq$ 5 cm[a]	Sepsis
Unfit for surgery	Vascular invasion
Solitary kidney	Coagulopathy
Multiple renal tumors	
von Hippel–Lindau disease	
(Refractory hematuria)	(Life expectancy $<$ 1 year or $>$ 10 years)
(Tumor debulking)	(Severe debilitation)
(Extrarenal tumor manifestation)	(Central tumor location)
(Bosniak III and IV lesions)	

[a] Larger or more centrally located tumors may be suited for ablation, depending on the expertise of the interventional radiologist

tumors, it is a viable alternative to nephron-sparing surgery. In these patients thermal ablation helps to avoid dialysis. Potential palliative indications include the treatment of refractory hematuria (Neeman et al. 2005) or tumor debulking prior to immunotherapy in patients with an advanced stage of disease or local tumor recurrence after nephrectomy. RF ablation should be considered the method of choice for local tumor treatment in patients with extrarenal metastases. Owing to its minimally invasive character it can also be considered a therapeutic option in patients suffering from Bosniak III and IV lesions, which have to be considered potentially malignant (Bosniak 1986).

In strictly selected patients RF ablation may be thought of as an innovative, experimental therapeutic option. Successful RF ablation has been reported from of a Wilms tumor refractory to chemotherapy in a multimorbid child with a solitary kidney (Brown et al. 2005).

Besides treating tumors of the renal parenchyma, this technique might be also applied to transitional cell carcinomas (Schultze et al. 2003). However, transitional cell carcinoma may grow inside the urothelium unnoticed by current imaging techniques and may metastasize early. In these patients RF ablation is restricted to a salvage option.

To achieve local tumor control it is mandatory to completely coagulate the entire lesion. In centrally located tumors thermal damaging of the calices and renal pelvis is feared; therefore, these tumors are considered a relative contraindication, while exophytic tumors are ideal candidates for RF ablation (Gervais et al. 2003) (Fig. 13.18). The decision to treat central lesions depends on the interventionalist's expertise and the availability of protective measures (see later). With adequate precautions even centrally located renal tumors can be treated successfully.

Currently sepsis, uncorrectable coagulopathies and the presence of a tumor thrombus in the renal vein are rated as absolute contraindications to renal RF ablation. Some centers limit treatment with curative intent to patients with greater than 1 year life expectancy (McDougal et al. 2005). As RCCs normally grow slowly with an increase in tumor diameter of 0.2–1.2 cm/year, a wait-and-see strategy may be justified in patients with a life expectancy of less than 1 year (Sowery and Siemens 2004). In the reverse case, patients without comorbid conditions and with life expectancies longer than 5–10 years are often excluded from RF ablation.

13.1.4.3 Material

Probe and Generator

For renal RF ablation monopolar as well as bipolar ablation systems may be used (see Sect. 13.1.1). No RF system has specifically been designed for renal application. Needle electrodes as well as hooked or umbrella-shaped arrays are suited for renal tumor ablation as long as the shape of the active needle tip fits the shape and the size of the tumor. Besides these general thoughts, there are some particular considerations for selecting the appropriate RF device for renal ablation:

1. To completely destroy the tumor, heat must exceed the tumor margin into healthy renal parenchyma. This concern greatly affects the choice of the applicator
    a. When an expandable device is chosen, the size of the RF probe should exactly fit or better slightly exceed (3 mm or less in each direction) the circumference of the tumor. If no adequate probe is available, the probe has to be repositioned during the intervention.
    b. If a needle electrode – or in bigger tumors a needle array – has been chosen, the length

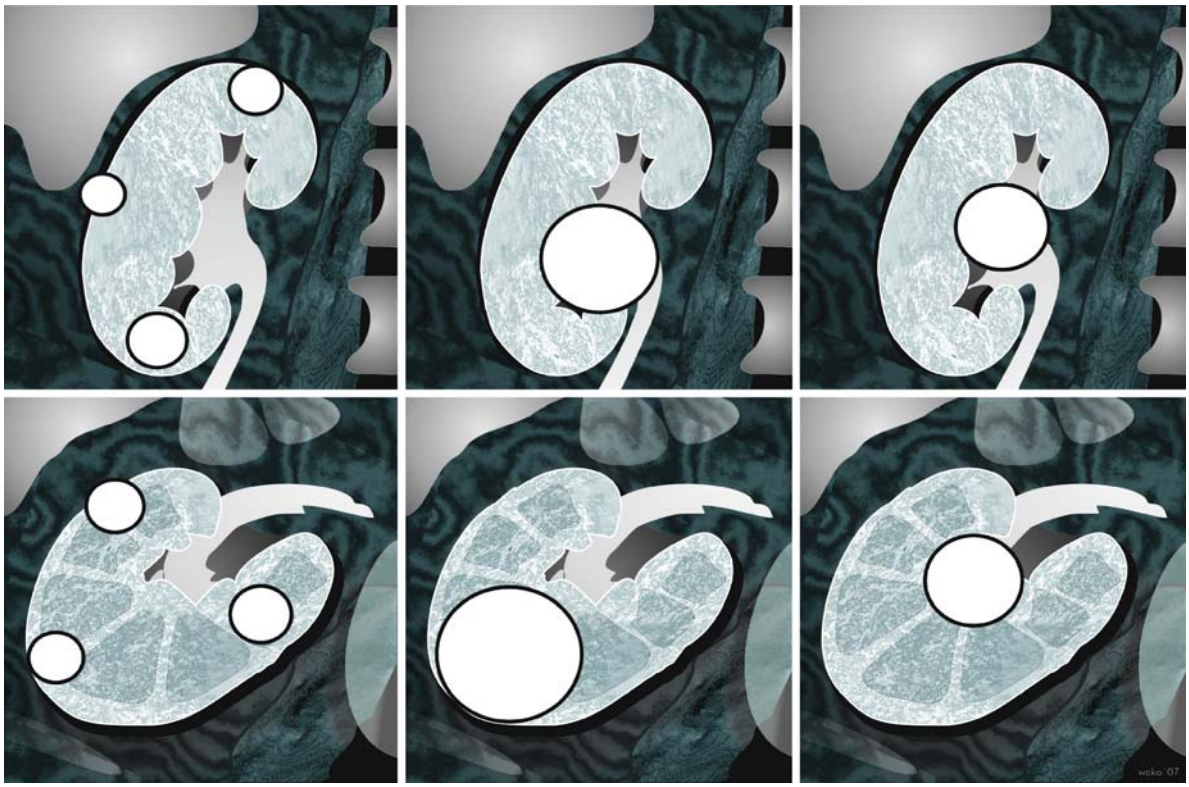

Fig. 13.18 Exophytic and cortical tumours (*left column*) are ideal candidates for percutaneous renal RF ablation. Parenchymal tumor location with contact to the renal hilum (*middle column*) might be considered for RF ablation. Central tumor location (*right column*) is generally considered a contraindication for RF ablation

of the needle (array) should exceed the diameter of the tumor by approximately 3 mm. If this is not achievable, repeated ablations using the pull-back technique are recommended.

2. If a biopsy is to be obtained during the same intervention, the use of a coaxial ablation device is recommended to avoid tumor seeding.

Further Mandatory Equipment

For all ablation procedures sterile drape and disinfectant (e.g., povidone iodine) need to be available for preparation of a sterile working place. To avoid unintentional traction on the RF probe additional sterile tape should be on hand for fixation of the cables.

Fine needles (20G–22G) should be available, as they are sometimes needed for bowel displacement by injecting a fluid or air. For this purpose either up to 1.5 l of 5% glucose (for fluid injection) or a sterile air filter with a Luer–Lock connection (for air insufflation) needs to be on hand.

If centrally located tumors are treated, a nephrostomy kit (see Sect. 11.3) may be required, to provide external–external cooling via a double-lumen nephrostomy catheter or external–internal cooling via a single-lumen nephrostomy catheter.

13.1.4.4 Technique

Preparation

Renal RF ablation can be performed either with intravenous analgosedation or under general anesthesia. The latter ensures optimal patient compliance and comfort. A single-shot preinterventional antibiotic prophylaxis is recommended using a cephalosporin (e.g., 1.5 g cefuroxim) if:

- Nephrostomy is performed for the intervention.
- Repositioning maneuvers have to be performed.
- Additional injection of air or fluid is needed for bowel displacement.
- The procedure is expected to take longer than 2 h.

For renal RF ablation the patient needs to be positioned comfortably in the prone or lateral position. The optimal patient position is derived from preinterventional imaging. It is mandatory to achieve a comfortable position, particularly if analgosedation is used. The use of dedicated positioning and fixation devices is strongly recommended to firstly guarantee the same position during the entire procedure and secondly to avoid damage to the skin. If needed, body fixation devices such as a vacuum mattress, bandages, or soft tape are helpful. Thereafter, imaging for planning the access route can be performed.

Procedure

If expandable probes are used, a small incision following the tension lines of the skin is made after analgesia. For sharpened needle-shaped probes a direct puncture technique is preferable. Ideally the lesion is punctured centrally with the ablation device covering the entire lesion at once. To achieve this target, the RF probe is advanced just before the lesion. After the positions of the probe and the tumor have been controlled, the needle is inserted into the center of the tumor. As the renal capsule presents elastic resistance to the probe, it is helpful to rapidly advance the probe to pass the renal capsule. Repeated passages of the renal capsule should be avoided to reduce the risk of bleeding and local tumor seeding. Needle electrodes are advanced through the lesion, so that the tip of the probe passes the lesion by approximately 3 mm. Expandable probes are positioned to extend their tines exactly to the tumor margin, better about 1–3 mm beyond the tumor margin (Fig. 13.19). This technique preserves most of the healthy renal parenchyma, as it results in a scanty safety margin. Nevertheless, this approach is sufficient to ensure local tumor control, because renal tumors do not show an infiltrative growth pattern.

If the tumor geometry and the expected shape and/or size of the ablation zone do not match perfectly, overlapping ablations may be needed. Depending on the deviation between the expected volume of necrosis and tumor size and shape, repositioning the RF probe may involve a simple pull-back maneuver to cover the length of the tumor along the puncture path, or it may require withdrawal from the lesion and reinsertion at a different angle. As lesion size and shape depend on the selected RF system as well as on the parameters used for ablation, detailed knowledge of the specific characteristics of the RF system used is helpful to ensure complete and reliable ablation. For renal ablation the same energy settings as for hepatic ablation can be used.

At the end of the procedure the needle is removed. To avoid bleeding and tumor seeding along the puncture track, so-called track ablation is performed. For this purpose the needle is slowly retracted while a reduced amount of energy in the range 10–25 W is applied. If internally cooled electrodes are used, the cooling has to be ceased by switching off the pump. If an expandable probe is used, the tines need to be pulled back and it has to be ensured that there is an uninsulated part at the tip of the probe after the prongs have been retracted, otherwise track ablation will be insufficient. Energy deposition has to be ended as soon as the active tip of the probe enters the subcutaneous fat.

Special Considerations

With approximately 4 ml/min/g, the kidneys are much better perfused than liver (hepatic artery 0.3 ml/min/g, portal vein 0.7 ml/min/g) or muscle (0.04 ml/min/g) (Klinke and Silbernagel 2003). Moreover, renal tumors are typically hypervascularized, resulting in an even higher intratumoral perfusion. Increased perfusion requires one either to apply more energy over a longer time or to accept smaller volumes of necrosis. This is the basis for the marked efficacy of local blood flow modulation in renal RF ablation. Selective transarterial tumor embolization with microparticles (300–700 µm) or microcoils prior to RF ablation reduces the blood flow in the embolized tissue and therefore results in more a homogeneous heat distribution (Fig. 13.20). Alternatively, lipiodol may be used for preablative embolization. It does not only embolize the tumor, it also marks the lesion for CT guidance. As a noteworthy limitation, lipiodol masks contrast enhancement during CT follow-up. In these patients MR imaging is better suited for postinterventional imaging. Ablation of previously embolized tumors requires much less energy to achieve the same size of necrosis, when compared with normally

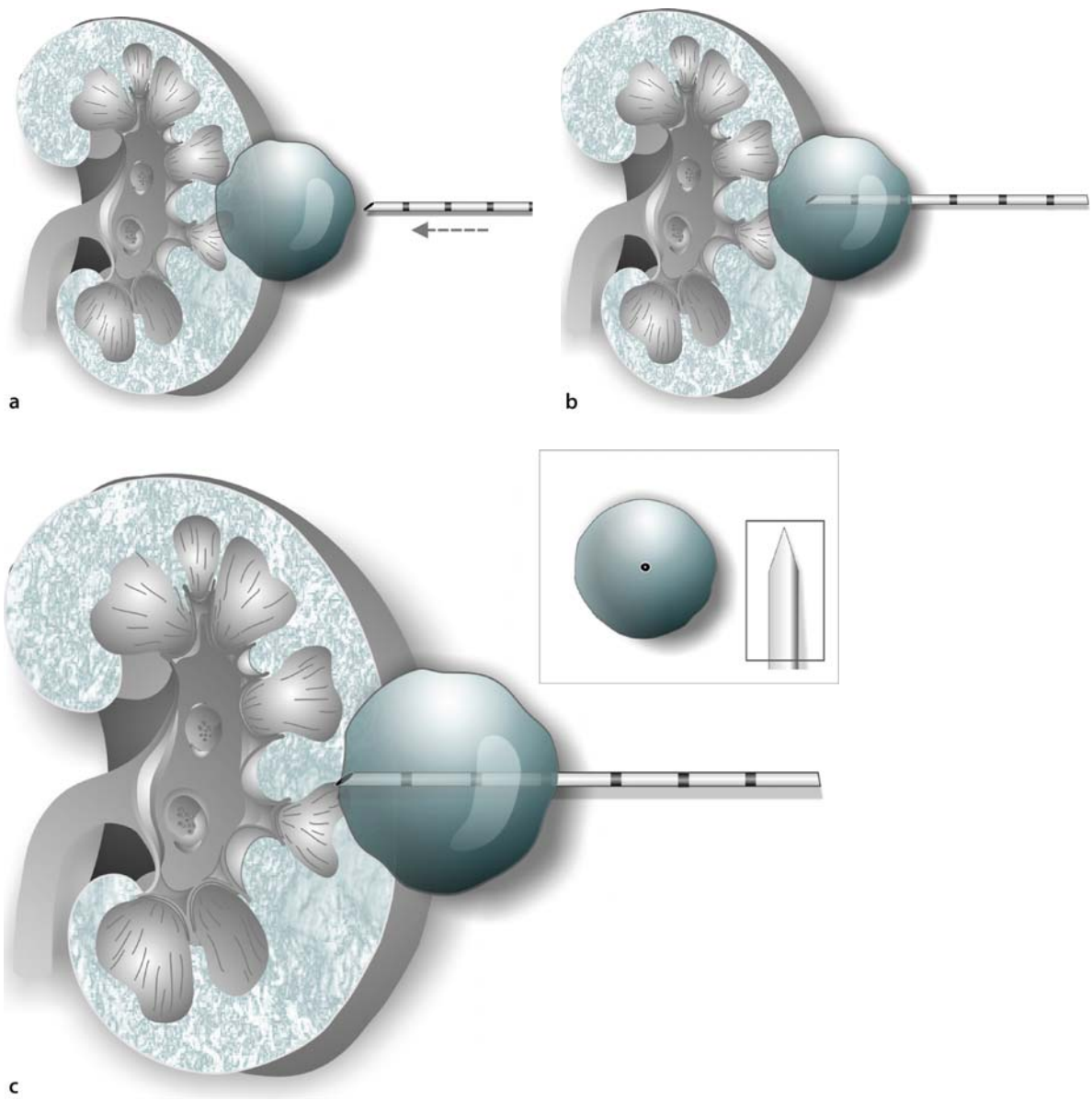

Fig. 13.19a–c For renal RF ablation the RF probe is advanced just before the lesion (**a**). After the positions of the probe and the tumor have been controlled, the needle is rapidly inserted into the center of the tumor (**b**). If a needle probe is used, the tip of the needle is advanced through the lesion (**c**)

perfused tissue. Furthermore, embolization adds a therapeutic effect on its own. Consequently, preablative embolization of hypervascularized renal tumors with a diameter of more than 3 cm is recommended (Mahnken et al. 2005).

If the tumor is located directly beside a major artery with a diameter of 0.5 mm or more or close to the renal vein, the so-called heat sink effect will occur, where heat is removed from the ablation area by using the blood vessels as a heat exchanger. This effect is particularly strong in the renal hilum. Instead of a local heating of the tumor, it may result in a systemic hyperthermia and even more importantly may leave viable tumor cells close to the vessel wall, where the temperature fails to rise above 60 °C, which is needed to guarantee coagulation necrosis. This effect is ad-

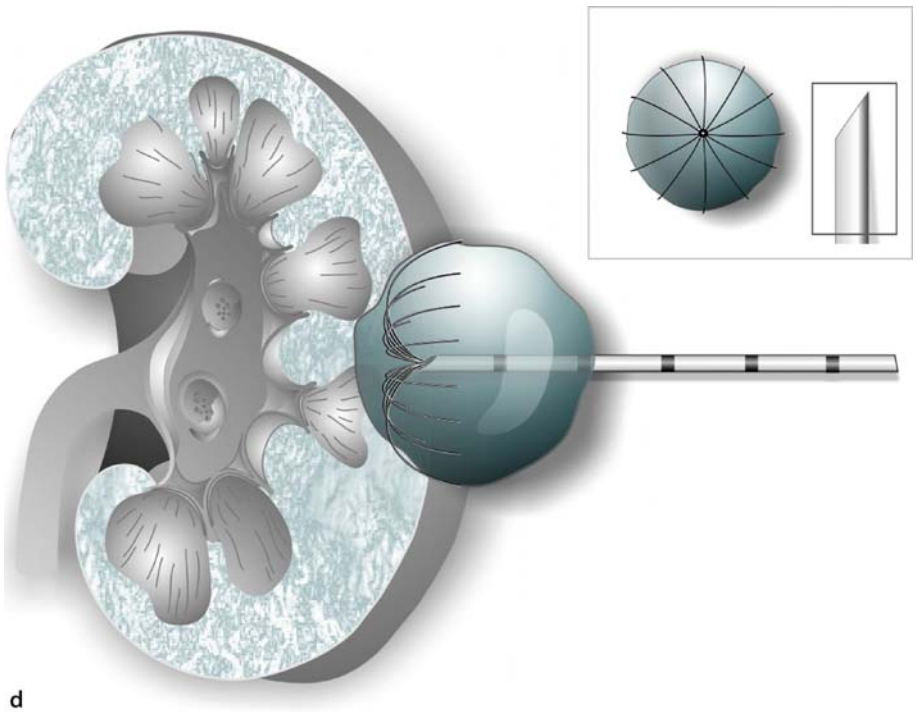

Fig. 13.19d (continued) If an expandable RF probe is used, the probe is expanded so that the tines of the probe extend 1–3 mm beyond the tumor margin (**d**)

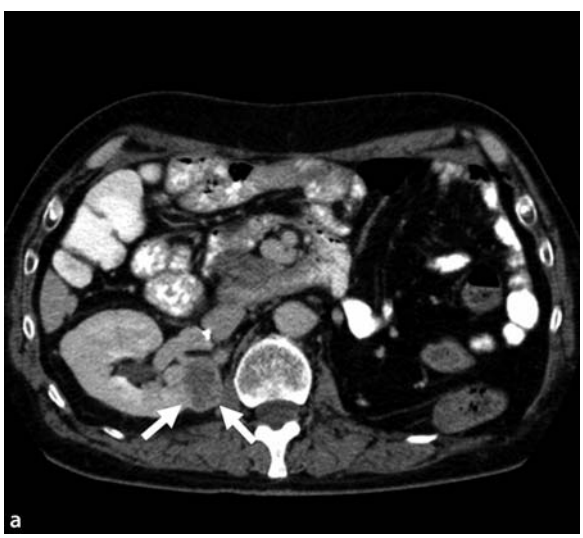

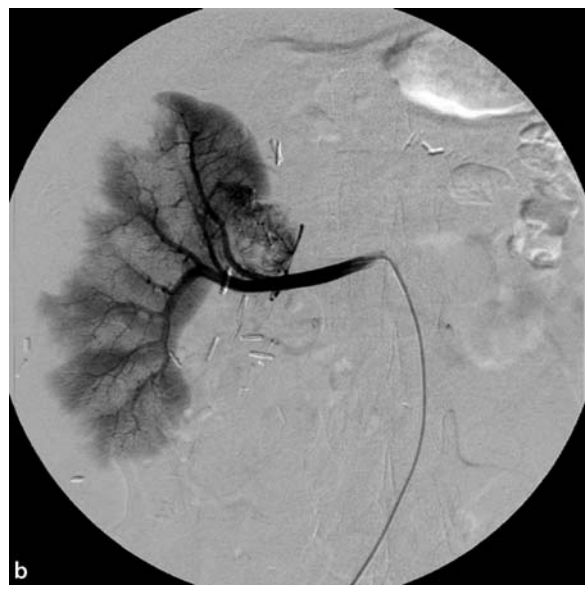

Fig. 13.20a,b A 64-year-old patient with recurrent renal cell carcinoma in the right kidney (*arrows*) after previous nephrectomy on the left (**a**). With a diameter of 3.5 cm preinterventional angiography (**b**) and subsequent embolization of the hypervascularized tumor were performed to achieve a more homogeneous heat distribution

dressed either by preinterventional transarterial tumor embolization or by placing the probe directly beside the vessel.

In central lesions there is an increased risk of damaging the collecting system. This may result in hematuria with or without obstructive coagulation, de-

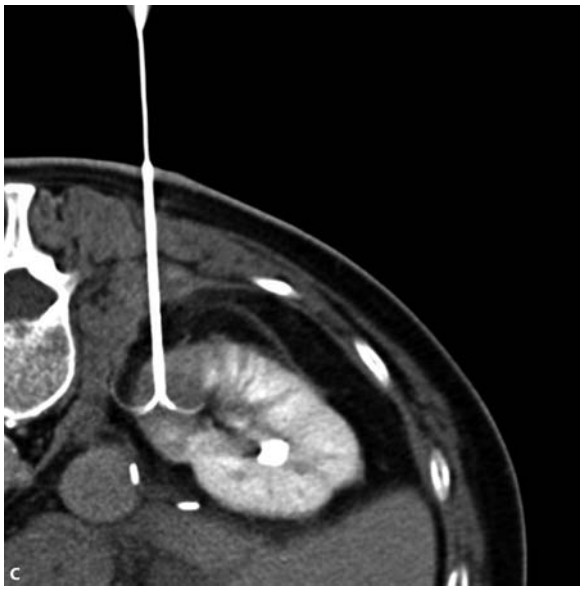

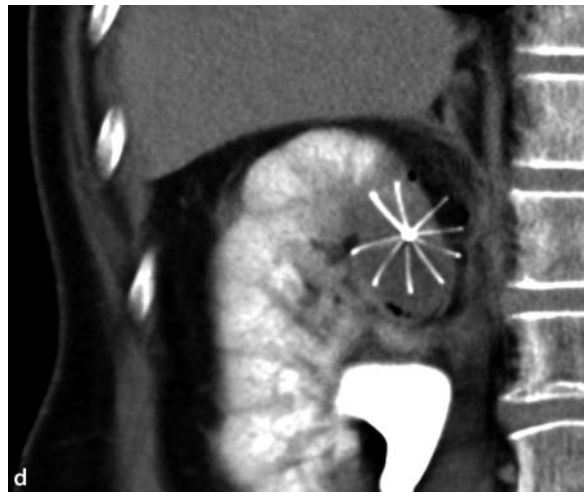

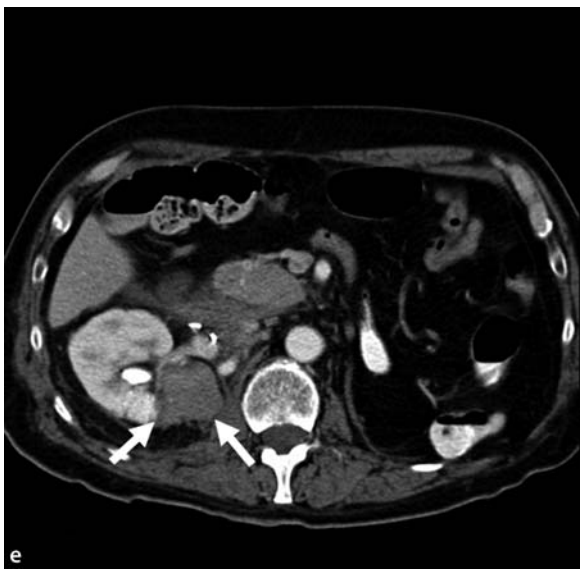

Fig. 13.20c–e (continued) The day after the embolization procedure RF ablation was performed with an expandable, umbrella-shaped LeVeen probe (**c**). The probe was placed inside the tumor with the tines exceeding the tumor margin (**d**). To avoid damage to the renal pelvis a slightly eccentric probe position was chosen. With application of the pull-back technique, the tumor was completely ablated, resulting in a homogeneous coagulation necrosis (**e**; *arrows*)

velopment of strictures, or perforation. The latter may result in external fistulas. In these patients the heat sink effect can be used to protect the collecting system from thermal damage by either external–external cooling via a double-lumen nephrostomy catheter or external–internal cooling using a single-lumen nephrostomy catheter with or without additional drainage via a transureteral catheter. Normally infusion of saline at room temperature is sufficient to avoid thermal damage. If only small amounts of fluid can be injected into the collecting system, the use of cooled saline should be considered (Margulis et al. 2005).

As imaging-based differentiation of renal tumors (benign vs. malignant, classification of RCC) – particularly in tumors 4 cm or smaller – remains difficult, a biopsy should be obtained prior to ablation. The re-

sults of the biopsy will affect subsequent patient management, particularly if biopsy proves the lesion to be nonmalignant. Biopsy should be performed in combination with RF ablation using a coaxial needle system. This approach firstly secures the tract during the biopsy procedure and seals the access route by so-called tract ablation at the end of the procedure, and thereby tumor seeding along the puncture tract can be avoided. The sole use of the track ablation technique after a renal biopsy may not be sufficient, as the paths of the biopsy needle and of the ablation device may differ if separate needles are used.

To avoid thermal damage to neighboring structures, particularly to the colon, pararenal injection of fluid or gas might be useful to displace endangered organs. It is recommended to use an isolating substance. From various experiments glucose and air are known to be suited best for this purpose. If air is used, it should be filtered prior to insufflation. The gas or fluid is injected via 18G–20G fine needles with end holes. The different distribution volumes of fluids and gas need to be considered when planning to displace neighboring structures. In some patients it might be necessary to use multiple needles and large amounts of fluids, exceeding 1 l. This technique, however, may be limited by adhesions after previous surgery. In very rare cases, optimal access to the tumor can also include induction of an iatrogenic pneumothorax.

13.1.4.5 Results

Imaging Findings

For the assessment of technical success and further imaging surveillance, contrast-enhanced CT or MR imaging is recommended. After successful RF ablation of renal tumors, a wedge-shaped defect with a lack of contrast enhancement, shrinkage, and occasional retraction from normal parenchyma by fat infiltration are seen on cross-sectional imaging (Matsumoto et al. 2004). Typical MR imaging characteristics in successfully treated lesions include a hypointense lesion surrounded by a bright rim on T2-weighted images. On T1-weighted images these lesions appear hyperintense. After administration of contrast material, a thin rim enhancement may be seen (Merkle et al. 2005). Consequently, nonenhanced as well as contrast-enhanced imaging studies are needed to reliably assess treatment success. If no viable tumor is demonstrated, subsequent scans are recommended at 3 months, 6 months, and every year. If there is residual tumor on postinterventional imaging, repeated RF ablation is needed.

Histology

From histopathologically controlled animal studies, the zone of RF ablation is known as a sharply delineated area (Hsu et al. 2000). Immediately after the procedure microscopy reveals increased cytoplasmic eosinophilia, loss of cell border integrity, blurring of nuclear chromatin, and interstitial hemorrhage. Typical coagulative necrosis develops by day 3. Until then the tumor may appear viable on simple hematoxylin–eosin staining. Thus, dedicated staining techniques, e.g., for NADHase or apoptosis, are needed to avoid misjudging the histological finding as happened in early studies on renal RF ablation (Rendon et al. 2002). From day 3 to day 14, inflammatory and fibroblastic changes separate ablated renal tissue from the adjacent healthy renal parenchyma. This process is followed by necrosis without features of renal parenchyma. From the center to the periphery four different zones can be distinguished from histologic analysis: complete necrosis, inflammatory infiltrate, hemorrhage, and fibrosis and regeneration (Crowley et al. 2000).

Therapy Outcome

The first successful clinical case of renal RF ablation was reported in 1997 (Zlotta et al. 1997). In 2003 the findings of the first relevant series with 34 patients (42 RCC; 1.1–8.9 cm) with a mean follow-up period of 13.2 months were published (Gervais et al. 2003). Most important, this study firstly identified relevant factors for success of the ablation procedure. While parenchymal and central tumors recur more frequently if the diameter exceeds 3 cm, exophytic tumors can be treated effectively, even if they are bigger than 3 cm in diameter. The effectiveness of RF treatment was proven by a histologically controlled case series with tumor resection secondary to laparoscopic RF ablation in five of 17 RCCs (Jacomides et al. 2003). The latter is supported by initial 4-year results without tumor recurrence (McDougal et al. 2005). The short-term effectiveness of renal RF ablation has been shown by several studies (Table 13.7).

Table 13.7 Results of percutaneous renal RF ablation. Only case series including 50 or more tumors were included in this summary

Authors	Technique	No. of patients/ no. of tumors	Mean size (cm)	Local Tumor control (%)[a]	Follow-up (months)
Matsumoto et al. (2005)	Percutaneous CT, laparoscopic	91/109	2.4	100	–
Gervais et al. (2005)	Percutaneous CT/US	85/100	3.2	89	28
Varkarakis et al. (2005)	Percutaneous CT	46/56	2.2	93.5	27.5
Breen et al. (2007)	Percutaneous CT/US	97/105	3.2	90.5	16.7
All/mean		319/370	2.8	93.3	24.1

US – ultrasound, *CT* – computed tomography
[a] Including reinterventions

13.1.4.6 Complications

The most common complication is self limiting hematuria. More severe complications include bleeding, hematoma, urinoma, renal infarction, ureteral obstruction, cutaneous fistulas, skin burns, and nerve damage (Rhim et al. 2004). Tumor seeding along the puncture tract was reported, but can be avoided by using a proper ablation technique (Mayo-Smith et al. 2003). Animal experiments indicate that central tumors are more prone to major complications than exophytic tumors (Lee et al. 2003). In total, complications occur in about 7% of patients. Most of these complications can be treated conservatively.

Summary

Experimental as well as clinical studies have proved percutaneous renal RF ablation to be an accurate and safe alternative to open or laparoscopic surgery in the treatment of small renal tumors. It is well tolerated in patients with percutaneously accessible lesions. Moreover, it is known to be less costly than open or laparoscopic partial nephrectomy (Lotan et al. 2005). It has the potential to replace surgery as first-line therapy in small RCCs, but the long-term outcome of this technique remains to be determined.

Key Points

- Preinterventional patient evaluation including a physical examination (renal function, coagulation, platelet count, comorbidity) combined with a thorough imaging workup is the basis for correct patient selection.
- Availability of adequate material for the intervention has to be ensured to be prepared for unexpected periinterventional developments.
- Hypervascular tumors with a diameter of 3 cm or more should be embolized prior to ablation. In all patients a biopsy should be obtained.
- To ensure long-term success, stringent postinterventional imaging surveillance is mandatory.

References

American Cancer Society (2007) Cancer Facts & Figures 2007. American Cancer Society, Atlanta

Bosniak MA (1986) The current radiological approach to renal cysts. Radiology 158:1–10.

Breen DJ, Rutherford EE, Stedman B et al. (2007) Management of renal tumors by image-guided radiofrequency ablation: experience in 105 tumors. Cardiovasc Intervent Radiol 30:936–942

Brown SD, Vansonnenberg E, Morrison PR et al. (2005) CT-guided radiofrequency ablation of pediatric Wilms tumor in a solitary kidney. Pediatr Radiol 35:923–928

Crowley JD, Shelton J, Iverson AJ et al. (2000) Laparoscopic and computed tomography-guided percutaneous radiofrequency ablation of renal tissue: acute and chronic effects in an animal model. Urology 57:976–980

Fergany AF, Hafez KS, Novick AC (2000) Long-term results of nephron-sparing surgery for localized renal cell carcinoma: 10-year follow up. J Urol 163:442–445

Gervais DA, McGovern FJ, Arellano RS et al. (2003) Renal cell carcinoma: clinical experience and technical success with radio-frequency ablation of 42 tumors. Radiology 226: 417–424

Gervais DA, McGovern FJ, Arellano RS et al. (2005) Radiofrequency ablation of renal cell carcinoma: part 1, Indications, results, and role in patient management over a 6-year period and ablation of 100 tumors. AJR Am J Roentgenol 185:64–71

Herring JC, Enquist EG, Chernoff A et al. (2001) Parenchymal sparing surgery in patients with hereditary renal cell carcinoma: 10–year experience. J Urol 165:777–781

Homma Y, Kawabe K, Kitamura T et al. (1995) Increased incidental detection and reduced mortality in renal cancer - recent retrospective analysis at eight institutions. Int J Urol 2:77–80

Hsu TH, Fidler ME, Gill IS (2000) Radiofrequency ablation of the kidney: acute and chronic histology in porcine model. Urology 56:872–875
Jacomides L, Ogan K, Watumull L et al. (2003) Laparoscopic application of radio frequency energy enables in situ renal tumor ablation and partial nephrectomy. J Urol 169:49–53
Klinke R, Silbernagel S (2003) Lehrbuch der Physiologie. Stuttgart, Thieme
Lee JM, Kim SW, Chung GH et al. (2003) Open radio-frequency thermal ablation of renal VX2 tumors in a rabbit model using a cooled-tip electrode: feasibility, safety, and effectiveness. Eur Radiol 13:1324–1332
Lotan Y Cadeddu JA (2005) A cost comparison of nephron-sparing surgical techniques for renal tumour. BJU Int 95:1039–1042
Mahnken A, Rohde D, Brkovic D et al. (2005) Percutaneous radiofrequency ablation of renal cell carcinoma: preliminary results. Acta Radiol 46:208–214
Margulis V, Matsumoto ED, Taylor G et al. (2005) Retrograde renal cooling during Radiofrequency ablation to protect from renal collecting system injury J Urol 174:350–352
Matsumoto ED, Johnson DB, Ogan K et al. (2005) Short-term efficacy of temperature-based radiofrequency ablation of small renal tumors. Urology 65:877–881
Matsumoto ED, Watumull L, Johnson DB et al. (2004) The radiographic evolution of radio frequency ablated renal tumors. J Urol 172:45–48
Mayo-Smith WW, Dupuy DE, Parikh PM et al. (2003) Imaging-guided percutaneous radiofrequency ablation of solid renal masses: techniques and outcomes of 38 treatment sessions in 32 consecutive patients. AJR Am J Roentgenol 180: 1503–1508
McDougal WS, Gervais DA, McGovern FJ et al. (2005) Long-term follow-up of patients with renal cell carcinoma treated with radiofrequency ablation with curative intent. J Urol 174:61–63
Merkle EM, Nour SG, Lewin JS (2005) MR imaging follow-up after percutaneous Radiofrequency ablation of renal cell carcinoma: findings in 18 patients during first 6 months. Radiology 235:1065–1071
Neeman Z, Sarin S, Coleman J, Fojo T et al. (2005) Radiofrequency ablation for tumor-related massive hematuria. J Vasc Interv Radiol 16:417–421
Pantuck AJ, Zisman A, Belldegrun AS (2001) The changing natural history of renal cell carcinoma. J Urol 166:297–301
Rendon RA, Kachura JR, Sweet JM et al. (2002) The uncertainty of radiofrequency treatment of renal cell carcinoma: findings at immediate and delayed nephrectomy. J Urol 167: 1587–1592
Rhim H, Dodd GD, Chintapalli KN et al. (2004) Radiofrequency thermal ablation of abdominal tumors: lessons learned from complications. Radiographics 24:41–52
Schultze D, Morris CS, Bhave AD et al. (2003) Radiofrequency ablation of renal transitional cell carcinoma with protective cold saline infusion. J Vasc Interv Radiol 14:489–492
Sowery RD, Siemens DR (2004) Growth characteristics of renal cortical tumors in patients managed by watchful waiting. Can J Urol 11:2407–2410
Uzzo RG, Novick AC (2001) Nephron sparing surgery for renal tumors: indications techniques and outcomes. J Urol 166: 6–18
Varkarakis IM, Allaf ME, Inagaki T et al. (2005) Percutaneous Radiofrequency ablation of renal masses: results at a 2-year mean follow up J Urol 174:456–460
Zlotta AR, Wildschutz T, Raviv G et al. (1997) Radiofrequency interstitial tumor ablation (RITA) is a possible new modality for treatment of renal cancer: ex vivo and in vivo experience. J Endourol 11:251–258

13.1.5 RF Ablation – Miscellaneous

Thomas Helmberger

13.1.5.1 Introduction

RF ablation of hepatic, renal, and pulmonary malignancies as well as of benign bone tumors, particularly osteoid osteoma, is already widely accepted as a very effective therapeutical option, given the specific inclusion and exclusion criteria as outlined in the previous chapters (Lindner et al. 2001). Based on the rather longstanding experience in these areas in many centers, RF ablation came into operation also for other tumor entities. These entities encompass tumors of the bones, and various and soft tissues. Even though osseous, lymphatic, and soft-tissue tumors are unfortunately very common (secondary ones much more so than primary ones), valid, study-proven data on RF ablation of these tumor types are still rather limited. Nevertheless, there has been rapid growth in the number of publications over the last few years, with most of the publications being anecdotal case reports or case collections. The reason for that is mainly related to the pathological characteristics of the tumors, whereas a specific tumor manifestation of an in general more widespread tumor disease needs a local treatment. Therefore, RF ablation treatment in many of the tumors of the bones and soft tissue follows the concept of local, symptomatic therapy, which defines the major difference from the therapeutical concepts for the tumor entities discussed above.

13.1.5.2 Indications

In general, local ablative tumor therapy as RF ablation follows the rule of treatment of a locally limited disease where the intended lesion to be treated is the leading, survival- or life-quality-determining manifestation of the specific disease. Up to now there

is no proof that in hepatic, pulmonary, or renal tumors debulking in terms of partial or incomplete ablation may affect the patients' outcome effectively. Whether these procedures might positively influence subsequent chemotherapies or radiation therapies also remains doubtful. In consequence, local ablation of these tumor entities should strictly be subject to indications where the tumor extent anticipates complete tumor eradication with a very high likelihood.

In contrast, the indications of local ablative therapy in bone and soft-tissue tumors are not yet well defined and are based on personal experience in many centers (Table 13.8). In most cases, pain palliation or decompression of space-occupying masses will be the predominant therapeutic goal (Simon and Dupuy 2006). Only in osteoid osteomas minimally invasive thermal ablation is considered as the most effective therapy and is widely accepted as a method of primary treatment (Ghanem 2006; Rosenthal 2006; see Sect. 15.1).

In general, the contraindications for RF ablation of miscellaneous tumors are the same as for RF ablation of, for instance, hepatic tumors:

- Acute infection
- Coagulopathy
- Tumor size
- Number of lesions not suitable for ablation by the RF systems available (Coldwell and Sewell 2005; Simon and Dupuy 2006)

13.1.5.3 Material and Technique

The RF generators and probes used for thermal ablation in bone and soft-tissue tumors are generally not different from those used for other tumor entities, and are discussed extensively in Sect. 13.1.1. Nevertheless, some "adjustments" might be necessary to take specific pathoanatomical conditions into consideration. The potentially close vicinity of damageable structures in the case of spinal or intra-abdominal lesions demands special attention to anatomical conditions and the choice of the appropriate RF probe. For instance, in osteoid osteomas with a small nidus a single needle probe with a short active tip might be much more appropriate and applicable than a multitined expandable probe. Regarding the anatomical localization of the tumor, close proximity to neurovascular structures – which is often the reason for the clinical symptoms – may prohibit local thermal therapy. Otherwise, severe, permanent damage might occur to these structures. In these lesions injections of a cooling fluid or an insulating gas such as carbon dioxide via a second needle may prevent adverse events and warrant a safe and successful ablation procedure. Moreover, often less energy is needed to achieve a sufficient result in terms of pain control or decompression of a space-occupying mass.

For probe placement imaging guidance by ultrasound, CT, or MR tomography is necessary. Adequate guidance is mandatory to provide proper probe placement into the target and to avoid collateral damage along the pathway to the target. For RF ablation of osseous and nearby lesions, CT will be the imaging method of choice, while ultrasound might be suitable and easy to use in superficial soft-tissue tumors, e.g., breast lesions, and MR imaging will be reserved to dedicated equipment and dedicated tumor locations that can only be displayed by MR imaging.

13.1.5.4 Results

Malignant Bone Tumors

Bone metastases are very frequent and can be found in 70–90% of all patients with an underlying malignant disease, predominantly in patients with breast, lung, kidney, and prostate cancer. Owing to the distribution of the red bone marrow, the most common localization of bone metastases is the spine, followed by pelvis, femur, skull, and other long bones. More than 50% of all patients will develop severe pain during their remaining life time caused by osteolyses affecting soft tissue and periostal nerve endings. Ongoing osteolytic destruction will destabilize the bone, causing occult micro and macro fractures. Standard therapies in those patients include surgery, chemotherapy, radiation therapy, and adjuvant administration of analgesics. An increasing number of patients are encountering a rather wide variety of sequential therapies, where tumors might lose their sensitivity for chemotherapy, will have already been irradiated and where an additional radiation therapy would exceed the maximum suitable radiation dose, and where supportive analgesic therapy is no longer tolerable because of increasing side effects. Nevertheless, these "prolonged" therapies will result in "prolonged" survival times in many cases, whereas intensified supportive care is often necessary. Especially with regard to supportive care, local ablative therapies such as RF

Table 13.8 Indications and contraindications of RF ablation in bone and soft-tissue tumors

Potential indications	Benign bone tumor[a]	Malignant bone tumor	Lymph node	Soft tissue
Tumor treatment	Definitive	Symptomatic	Symptomatic	Symptomatic
Pain relief	Very effective	Effective	NA	Effective
Contraindications	Impending fracture			
	Direct contact of tumor with neurovascular and other structures susceptible to thermal damage			
	Impending secondary burns due to metallic internal fixations			
	Acute infection			
	Coagulopathy			
	Lesion size too large for local treatment			

NA – not applicable
[a] Osteoid osteoma, osteoblastoma (Afshin Gangi, University Hospital Strasbourg, France, personal communication)

Table 13.9 Primary and secondary success rate of RF ablation in malignant bone tumors in comparison with various ablation therapies in terms of pain relief

Authors	No. of patients/ no. of procedures	Method	Primary success (%)	Long-term success (%)	Complications	Follow-up (months)
Weill et al. (1996)	37/52	OP	94	73	Neurologic ($n = 3$)	13
Alvarez et al. (2003)	21	OP + R (15), surgery (3)	81	–	Neuritis ($n = 1$)	5.6 (1–18)
Fourney et al. (2003)	56/97	OP/KP	84	–	0	4.5 (1–19.7)
Goetz et al. (2004)	43	RFA	95	–	Burns ($n = 1$), transient incontinence ($n = 1$), fracture ($n = 1$)	16
Jagas et al. (2005)	21/21	OP + R	100		0	1–8
Jang and Lee (2005)	28/72	OP + R	89	–	0	1–9
Kelekis et al. (2005)	14/23	OP	92	–	Leakage ($n = 1$)	9 (1–24)
Mont'Alverne et al. (2005)	12/12 (axis)	OP	80	–	Neurologic ($n = 2$)	6.9
Toyota et al. (2005)	17/23	RFA + OP	100	82.4	Hematoma ($n = 1$)	1–30
Callstrom et al. (2006)	14/22	Cryo	67	86	0	3–24
Calmels et al. (2007)	52/59	OP	86	92	Neurologic ($n = 4$), hematothorax ($n = 1$), pulmonary embolism ($n = 2$)	17
Hoffmann et al. (2008)	22/28	RFA + OP	90.9	100	0	7.7 (3–15)
Total	337/428		88.2	86.7	17/428 (4.0%)	8.5 (1–30)

OP – osteoplasty, *KP* – kyphoplasty, *Cryo* – cryoplasty, *RFA* – RF ablation, *R* – radiation therapy

and laser ablation as well as osteoplasty with local cement injection (Hoffmann et al. 2008) will support the concept for palliation in pain of soft-tissue and osseous tumors (Goetz et al. 2004; Gangi et al. 2005; Callstrom et al. 2006). The pathophysiological process causing the pain relief by RF ablation is not yet completely understood. Most likely, periostal nociceptors might be destroyed by the direct impact of heat. Nevertheless, the success rate of RF ablation of 67–100% of immediate postprocedural pain relief seems to be equivalent to that of the other therapies and combination methods mentioned above (Table 13.9).

It is still being debated whether the combination therapy of thermal ablation together with, e.g., cementoplasty is superior to a single therapy (Fig. 13.21). Furthermore, there are a few cases of painful bone tumors with a dense stroma that hinders a cement injection. In these cases, thermal ablation may soften the tumor stroma, allowing subsequent cement instillation (Hoffmann et al. 2008).

Breast Tumors

In industrialized countries, breast cancer is a major health problem. More than a quarter of all cancer occurring in women will be breast cancer, and 40% of all patients will be younger than 60 years. Even

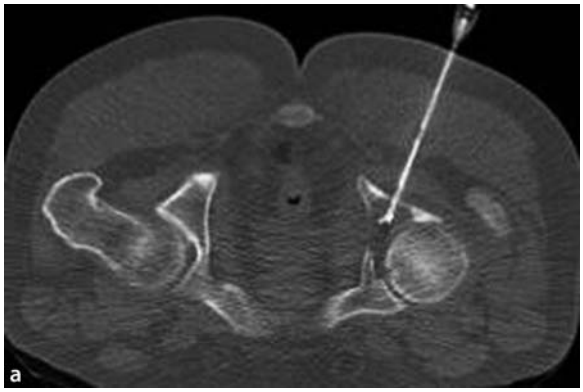

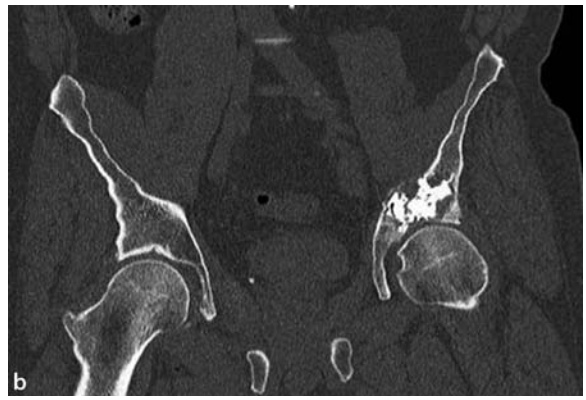

Fig. 13.21a,b This osteolytic metastasis of a follicular thyroid cancer in the weight-bearing parts of the left acetabulum was first treated by RF ablation with a multitined probe (**a**) followed by percutaneous cement injection for stabilization (**b**). Significant pain relief could be achieved; nevertheless, the patient died 4 months later owing to rapid progress of the underlying disease

if breast-conserving therapy with or without postoperative radiotherapy and chemotherapy – depending on the stage of the disease – is considered the therapy of first choice, the advent of screening programs and the increasing number of small tumors detected (less than 2 cm) also enforces the trend to more minimally invasive therapies. Consequently, the concepts of local thermal ablation therapy can be also translated into the field of minimally invasive therapy of breast tumors. Currently, RF ablation of breast cancer is still work-in-progress; nevertheless, just recently this field has evolved rapidly and the first, though limited, data are available (Noguchi et al. 2006; Earashi et al. 2007; Khatri et al. 2007; Oura et al. 2007; Susini et al. 2007; van der Ploeg et al. 2007). After the first intraoperative attempts to treat larger tumors up to 7 cm in diameter (Jeffrey et al. 1999), recent studies have incorporated smaller tumors up to 3 cm (Izzo et al. 2001; Singletary et al. 2002; Hayashi et al. 2003; Fornage et al. 2004; Roberts et al. 2006), and complete coagulation necroses could be achieved between 80 and 100% despite many methodological differences. In a very recent study 52 patients with a mean tumor diameter of 1.3 cm (0.5–2.0 cm) underwent RF ablation and adjuvant chemotherapy and/or endocrine therapy and radiotherapy (50 Gy) with no recurrence after 15 months (6–30 months). The cosmetic aspect after RF ablation was considered excellent in 43 patients (83%), good in six (12%), and fair in three (6%). One patient experienced skin burn at the entry site of the RF ablation probe (Oura et al. 2007).

So far, RF ablation seems to be a very promising new tool for minimally invasive therapy for small breast carcinomas. Intensive further investigation is needed to identify the best candidates and best comprehensive concepts for this therapy (van der Ploeg et al. 2007).

Other Tumors

In most malignancies metastatic spread to the lymphatic system or to soft tissue by more or less direct invasion is common. Since such a tumor manifestation represents a systemic tumor burden, commonly local ablative therapy has no influence on the patient's outcome. Nevertheless, secondary symptoms such as pain and compression may require medical intervention. On the basis of only anecdotal reports on RF ablation in lymph node metastases (Hiraki et al. 2005; Hanazaki et al. 2006) or secondary (metastatic) and primary soft-tissue tumors such as liposarcoma or rhabdomyosarcoma (Ahrar 2004; Jakobs et al. 2004; Locklin et al. 2004; Nashida et al. 2007; Keil et al. 2008), it seems that RF ablation can play a role in adjuvant palliative treatment – in most cases without intention to cure but to preserve quality of life (Fig. 13.22).

13.1.5.5 Complications

The overall complication rate of RF ablation in bone and soft-tissue tumors is not different from that of

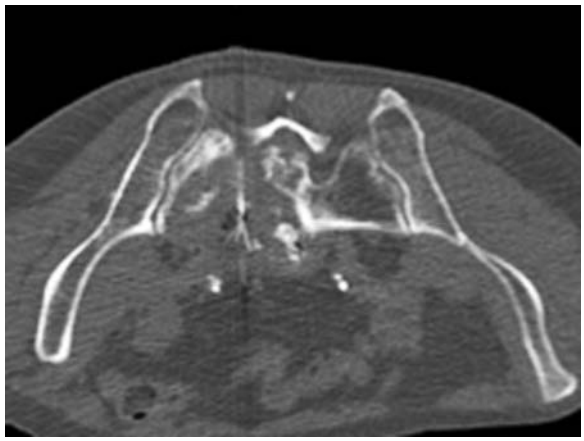

Fig. 13.22 In this local recurrence of a colorectal carcinoma with a large osteolytic bone metastasis of the sacral bone with an extensive soft-tissue component, RF ablation using a multitined RF probe could achieve significant pain relief for 6 months till the patient died from massive multiorgan metastasis of the underlying malignancy

RF ablation in other anatomical areas and tumor entities. According to the Society of Interventional Radiology classification, the reported complication rates are below 4%, without reports on major complications (Table 13.9). Adverse events may be puncture-related such as hemorrhage at the entry site or technical-procedure-related such as skin burns, and neurological symptoms due to secondary thermal damage to nontarget ablation (e.g., close vicinity to nerve or joint structures), and are usually self-limiting.

Incomplete treatment with residual or recurrent tumor tissue particularly in bone tumors is accepted with acquiescence since clinically pain is the leading symptom triggering the indication for therapy (Cioni et al. 2004; Marchal et al. 2006; Gangi et al. 2007; Thanos et al. 2008).

Summary

Even though the present data base is somewhat limited and lacks large studies, RF ablation of bone and soft-tissue tumors is already producing evidence of its high efficacy in pain treatment and consequently in improving the quality of life in patients with primary and secondary bone tumors and with space-occupying soft-tissue masses. In osteoid osteoma the results of RF ablation with a very high success rate, a very low complication rate, and – socioeconomically also important – a very short recovery time represent the standard of care. In other tumor entities, such as in bone metastases, breast carcinomas, and other so far rare cases of locally symptomatic soft-tissue tumors, local thermal ablation could prove its efficacy mainly in terms of pain relief as well. Therefore, it can be anticipated that RF ablation will play an even further growing valuable role also in the adjuvant, minimally invasive therapy of bone and soft-tissue tumors.

Key Points

- RF ablation in bone and soft-tissue tumors is a powerful minimally invasive tool to control lesion-related symptoms such as pain and may also prove to be efficient in local tumor control.
- Although there have been no large-scale studies on RF ablation in malignant bone tumors or non-organ-related soft-tissue tumors, RF ablation should be considered a valuable treatment option in nonsurgical candidates.

References

Ahrar K (2004) The role and limitations of radiofrequency ablation in treatment of bone and soft tissue tumors. Curr Oncol Rep 6:315–320

Alvarez L, Perez-Higueras A, Quinones D et al. (2003) Vertebroplasty in the treatment of vertebral tumors: postprocedural outcome and quality of life. Eur Spine J 12:356–360

Callstrom MR, Charboneau JW, Goetz MP et al. (2006) Image-guided ablation of painful metastatic bone tumors: a new and effective approach to a difficult problem. Skeletal Radiol 35:1–15

Calmels V, Vallee JN, Rose M et al. (2007) Osteoblastic and mixed spinal metastases: evaluation of the analgesic efficacy of percutaneous vertebroplasty. AJNR Am J Neuroradiol 28:570–574

Cioni R, Armillotta N et al. (2004) CT-guided radiofrequency ablation of osteoid osteoma: long-term results. Eur Radiol 14:1203–8

Coldwell DM, Sewell PE (2005) The expanding role of interventional radiology in the supportive care of the oncology patient: from diagnosis to therapy. Semin Oncol 32:169–173

Earashi M, Noguchi M, Motoyoshi A et al. (2007) Radiofrequency ablation therapy for small breast cancer followed by immediate surgical resection or delayed mammotome excision. Breast Cancer 14:39–47

Fornage BD, Sneige N, Ross MI et al. (2004) Small (< or = 2-cm) breast cancer treated with US-guided radiofrequency ablation: feasibility study. Radiology 231:215–224

Fourney DR, Schomer DF, Nader R et al. (2003) Percutaneous vertebroplasty and kyphoplasty for painful vertebral body fractures in cancer patients. J Neurosurg 98(1 Suppl):21–30

Gangi A, Alizadeh H et al. (2007) Osteoid osteoma: percutaneous laser ablation and follow-up in 114 patients. Radiology 242:293–301

Gangi A, Basile A, Buy X et al. (2005) Radiofrequency and laser ablation of spinal lesions. Semin Ultrasound CT MR 26: 89–97
Ghanem I (2006) The management of osteoid osteoma: updates and controversies. Curr Opin Pediatr 18:36–41
Goetz MP, Callstrom MR, Charboneau JW et al. (2004) Percutaneous image-guided radiofrequency ablation of painful metastases involving bone: a multicenter study. J Clin Oncol 22:300–306
Hanazaki M, Taga N, Nakatsuka H et al. (2006) Anesthetic management of radiofrequency ablation of mediastinal metastatic lymph nodes adjacent to the trachea. Anesth Analg 103:1041–1042
Hayashi AH, Silver SF, van der Westhuizen NG et al. (2003) Treatment of invasive breast carcinoma with ultrasound-guided radiofrequency ablation. Am J Surg 185:429–435
Hiraki T, Yasui K, Mimura H et al. (2005) Radiofrequency ablation of metastatic mediastinal lymph nodes during cooling and temperature monitoring of the tracheal mucosa to prevent thermal tracheal damage: initial experience. Radiology 237:1068–1074
Hoffmann RT, Jakobs TF, Trumm C et al. (2008) Radiofrequency ablation in combination with osteoplasty for the treatment of bone malignancies. J Vasc Interv Radiol 19:419–425
Izzo F, Thomas R, Delrio P et al. (2001) Radiofrequency ablation in patients with primary breast carcinoma: a pilot study in 26 patients. Cancer 92:2036–2044
Jagas M, Patrzyk R, Zwolinski J et al. (2005) Vertebroplasty with methacrylate bone cement and radiotherapy in the treatment of spinal metastases with epidural spinal cord compression. Preliminary report. Ortop Traumatol Rehabil 7:491–498
Jakobs TF, Hoffmann RT, Vick C et al. (2004) RFA des Knochens und der Weichteile. Radiologe 44:370–375
Jang JS, Lee SH (2005) Efficacy of percutaneous vertebroplasty combined with radiotherapy in osteolytic metastatic spinal tumors. J Neurosurg Spine 2:243–248
Jeffrey SS, Birdwell RL, Ikeda DM et al. (1999) Radiofrequency ablation of breast cancer: first report of an emerging technology. Arch Surg 134:1064–1068
Keil S, Bruners P, Brehmer B, Mahnken AH (2008) Percutaneous radiofrequency ablation for treatment of recurrent retroperitoneal liposarcoma. Cardiovasc Intervent Radiol 31(Suppl 2):S213–S216
Kelekis A, Lovblad KO, Mehdizade A et al. (2005) Pelvic osteoplasty in osteolytic metastases: technical approach under fluoroscopic guidance and early clinical results. J Vasc Interv Radiol 16:81–88
Khatri VP, McGahan JP, Ramsamooj R et al. (2007) A phase II trial of image-guided radiofrequency ablation of small invasive breast carcinomas: use of saline-cooled tip electrode. Ann Surg Oncol 14:1644–1652
Lindner NJ, Ozaki T, Roedl R et al. (2001) Percutaneous radiofrequency ablation in osteoid osteoma. J Bone Joint Surg Br 83:391–396
Locklin JK, Mannes A, Berger A et al. (2004) Palliation of soft tissue cancer pain with radiofrequency ablation. J Support Oncol 2:439–445
Marchal F, Brunaud L, Bazin C et al. (2006) Radiofrequency ablation in palliative supportive care: early clinical experience. Oncol Rep 15:495–499
Mont'Alverne F, Vallee JN, Cormier E et al. (2005) Percutaneous vertebroplasty for metastatic involvement of the axis. AJNR Am J Neuroradiol 26:1641–1645
Nashida Y, Yamakado K, Kumamoto T et al. (2007) Radiofrequency ablation used for the treatment of frequently recurrent rhabdomyosarcoma in the masticator space in a 10-year-old girl. J Pediatr Hematol Oncol 29:640–642
Noguchi M, Earashi M, Fujii H et al. (2006) Radiofrequency ablation of small breast cancer followed by surgical resection. J Surg Oncol 93:120–128
Oura S, Tamaki T, Hirai I et al. (2007) Radiofrequency ablation therapy in patients with breast cancers two centimeters or less in size. Breast Cancer 14:48–54
Roberts J, Morden L, MacMath S et al. (2006) The quality of life of elderly women who underwent radiofrequency ablation to treat breast cancer. Qual Health Res 16:762–772
Rosenthal DI (2006) Radiofrequency treatment. Orthop Clin North Am 37:475–484
Simon CJ, Dupuy DE (2006) Percutaneous minimally invasive therapies in the treatment of bone tumors: thermal ablation. Semin Musculoskelet Radiol 10:137–144
Singletary SE, Fornage BD, Sneige N et al. (2002) Radiofrequency ablation of early-stage invasive breast tumors: an overview. Cancer J 8:177–180
Susini T, Nori J, Olivieri S et al. (2007) Radiofrequency ablation for minimally invasive treatment of breast carcinoma. A pilot study in elderly inoperable patients. Gynecol Oncol 104:304–310
Thanos L, Mylona S, Galani P et al. (2008) Radiofrequency ablation of osseous metastases for the palliation of pain. Skeletal Radiol 37:189–194
Toyota N, Naito A, Kakizawa H et al. (2005) Radiofrequency ablation therapy combined with cementoplasty for painful bone metastases: initial experience. Cardiovasc Intervent Radiol 28:578–583
van der Ploeg IM, van Esser S, van den Bosch MA et al. (2007) Radiofrequency ablation for breast cancer: a review of the literature. Eur J Surg Oncol 33:673–677
Weill A, Chiras J, Simon JM et al. (1996) Spinal metastases: indications for and results of percutaneous injection of acrylic surgical cement. Radiology 199:241–247

13.2 Laser-Induced Thermography

13.2.1 Temperature Mapping for MR-Guided LITT

Thomas J. Vogl, Katrin Eichler, Thomas Lehnert, Martin Mack, and Dirk Meister

13.2.1.1 Introduction

Laser-induced thermotherapy (LITT) is a minimal invasive locoregional procedure for treating metastases

and tumors in the liver and other solid organs (Vogl et al. 2002, 2003; Yoon and Tanabe 1999). In abdominal organs it is commonly performed under magnetic resonance (MR)-guidance -monitoring. LITT provides a photothermal tumor destruction technique, permitting solid tumor configuration inside parenchymatous organs to be destroyed. The expansion of the tissue-destroying effect is dependent on the choice of radiation capacity and radiation time. This means that the parameters must be preselected in such a way that, if possible, all tumor cells are exposed to the coagulative effect. Besides, there must also be a safety margin of at least 5–10 mm in width. Therefore techniques for monitoring the intervention were sought to optimize MR-guided LITT, among them MR-thermometry.

13.2.1.2 Materials

Laser coagulation is accomplished using an Nd-YAG laser light with a wavelength of 1 064 nm (MidLAas 5060, MediLas 5100, Dornier Germering, Germany), delivered through optic fibers terminated by a specially developed diffuser. In the beginning a diffuser tip with a glass dome of 0.9 mm in diameter was used, which was mounted at the end of a 10 m long silica fiber (400 µm in diameter). Since the year 2000, a flexible diffuser tip has been used with a diameter of 1.0 nm, which makes the laser applications much easier due to the fact that the risk of damage to the diffuser tip has dropped to almost zero. The active length of the diffuser tip ranges between 20 and 40 mm in length. The laser power is adjusted to 12 Watts per cm active length of the laser applicator.

The laser application kit (SOMATEX, Berlin, Germany) consists of a cannulation needle, a sheath system, and a protective catheter, which prevents direct contact of the laser applicator with the treated tissue and allows cooling of the tip of the laser applicator. The closed end of the protective catheter enables complete removal of the applicator even in the unlikely event of damage to the fiber during treatment. This simplifies the procedure and makes it safer for the patient.

The laser itself is installed outside the MR examination room, and the light is transmitted through a 10 m long optical fiber. All patients are examined using an MR imaging protocol including gradient-echo (GE) T1-weighted plain and contrast-enhanced Gd-DTPA 0.1 mmol/kg body weight. T2- and T1-weighted images are performed for localizing the target lesion and planning the interventional procedure.

13.2.1.3 Image Guidance

After informing the patients about potential complications, advantages, and disadvantages of LITT, consent is obtained. The metastases are localized on ultrasound or computed tomography and the injection site is infiltrated with 20 ml of 1% lidocaine. Under CT guidance the laser application system is inserted using the Seldinger technique.

After positioning the patient on the MR table, the laser catheter is inserted into the protective catheter. MR imaging is widely used for treatment planning, for positioning the applicators and for monitoring the progress of the treatment (Vogl et al. 1996; Eichler et al. 2001). For improving the clinical success of the treatment, it is desirable to monitor on-line the thermal changes in the tissue. If only one residual tumor cell remains, the probability of recurrent carcinomas is high. With the help of MR thermometry the area of the coagulative effect can be estimated, leading to a complete ablation of the tumor while preventing surrounding structures from unnecessary damage.

MR thermometry is the only completely non-invasive method for measuring temperature changes inside the body that has been developed so far (Germain et al. 2002). MR sequences are performed every 30 s to assess the progress in heating the lesion and the surrounding tissue. Heating is revealed as signal loss in the T1-weighted gradient-echo images as a result of the heat-induced increase of the T1 relaxation time. Depending on the geometry, intensity of the signal loss, and speed of the heat distribution, the position of the laser fibers, the laser power and the cooling rate are readjusted. Treatment is stopped after total coagulation of the lesion, and a safety margin from 5 to 15 mm surrounding the lesion can be visualized in MR images.

After switching the laser off, T1-weighted contrast-enhanced FLASH-2D images are obtained for verifying the induced necrosis. After the procedure the puncture channel is sealed with fibrin glue. Follow-up examinations using plain and contrast-enhanced sequences are performed after 24 to 48 h, and every three months thereafter. Quantitative and qualitative parameters, including size, morphology, signal behavior, and contrast enhancement are evaluated for deciding

whether treatment can be considered successful, or whether subsequent treatment sessions are required.

Laser-induced effects are evaluated by comparing images of lesions and surrounding liver parenchyma obtained before and after laser treatment with each other, and with those obtained at follow up examinations. Tumor volume and volume of coagulative necrosis are calculated using three-dimensional MR images and measurements of the maximum diameter in three planes.

After a successful LITT procedure the volume of the induced coagulative necrosis 24 h after LITT treatment exceeds the volume of the initial tumor significantly. During follow-up examinations the volume of the induced necrosis is getting smaller again due to resorption and shrinking of the lesion. In the three-month follow-up the volume of the coagulative necrosis is already about half of the initial volume of the necrosis, but still larger than the initial tumor volume.

Evaluation of the MR thermometry data during MR-guided LITT demonstrates that metastatic tissue is very sensitive to heat, showing earlier and more widespread temperature distribution of the delivered thermal energy than does surrounding liver parenchyma. Online MR-thermometric changes correlate exactly with the findings of contrast-enhanced T1-weighted sequences obtained after therapy. Plain and contrast MR imaging is performed in all cases for verifying the obtained necrosis.

13.2.1.4 Temperature Mapping

In order to do justice to the coagulation of three-dimensional tumor geometry, it must be possible to heat an approximately spherical volume of tissue at the same time. For this reason application systems of defined space radiation have been developed, the distal ends of which are prepared in such a way that the result is an even circumference of radiation. The laser light is transmitted to the tumor through optical fibers. The tips of the fibers scatter the light resulting in a half-ellipsoidal coagulation zone. With a water-cooled power laser application system, the volume of coagulative necrosis can be increased compared to non-cooled devices, while preventing carbonization at the tip of the laser applicator. When using these power applicators the applied laser power can reach 30 Watts.

Different MR parameters can be used for deriving temperatures: the temperature dependence of the spin-lattice T1-relaxation time, changes of the proton resonance frequency (PRF), and the diffusion coefficient (D) are most common. As the diffusion coefficient strongly depends on geometric issues (e.g. boundary layers like membranes) and motion it was not used for estimating temperatures in the reported data.

T1 Thermometry

The spin-lattice relaxation time T1 has shown an approximately linear relationship with temperature. However, the strength of the effect depends strongly on the type of tissue. The temperature dependency of T1 varies from 0.8% per °C to 2% per °C (Cline et al. 1994). Therefore, individual calibration experiments are necessary for a reliable temperature measurement. The temperature is mostly derived through pixelwise determination of T1 values. A widespread method for T1 calculation is applying a sequence of inversion recovery acquisitions with different inversion times. However, the accurate determination of T1 is time-consuming. During LITT temperatures rise beyond 80 °C within minutes or even seconds, too fast for conventional T1 estimations. A feasible thermometry should be able to monitor almost real-time, at least within a few seconds. A shortcut for T1 temperature measurement is to use directly the magnitude values of T1-weighted images. It has been shown previously that magnitude attenuations of T1-weighted sequences are considerably linear within the desired range of temperature. Again, temperatures can only be measured by referring to a baseline image at the temperature T_0:

$$T = T_0 + b\Delta S_N\,, \tag{1}$$

where $\Delta S_N = S_0 - S_N$ is the magnitude signal difference of the baseline image and the actual image.

PRF Thermometry

Measuring temperature with the PRF method implies application of phase images and calculating the phase differences between the applications. This leads to changes in the resonance frequency, as variations in frequency cause changes in the phase. The resonance frequency of water protons depends linearly on

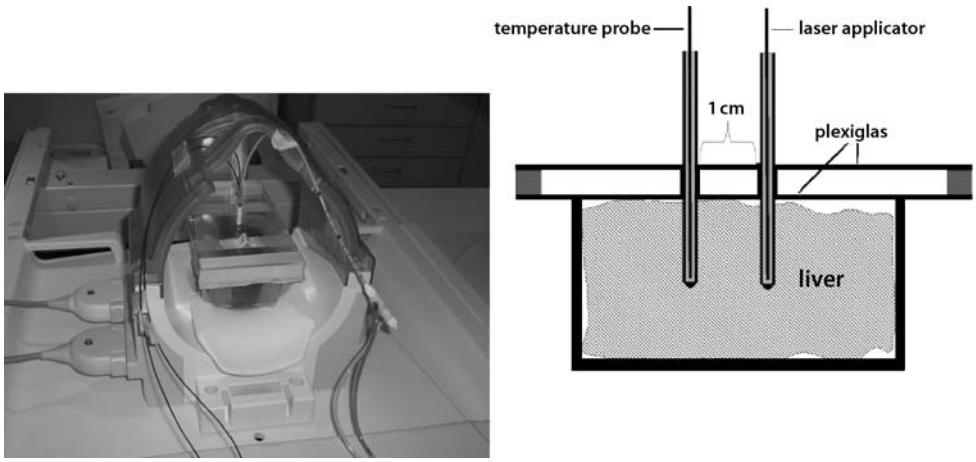

Fig. 13.23 Measurement setup in the head coil and positioning of the fibers

the temperature over a wide temperature range with a coefficient α of approximately -0.01 ppm (MacFall et al. 1995; De Poorter et al. 1995; Clegg 1995). There is almost no variation of the temperature coefficient regarding different tissue types.

With the differences in phase $\Delta\varphi$ the difference of temperature ΔT to a reference temperature can be calculated as

$$\Delta T = \frac{\Delta\varphi}{\gamma \cdot B_0 \cdot \alpha \cdot T_{\mathrm{E}}}, \qquad (2)$$

where $\gamma/2\pi = 42.58\,\mathrm{MHz\,T^{-1}}$ is the gyro magnetic factor, B_0 is the magnetic field strength and T_E is the echo time (Bohris et al. 1999; Wlodarcyk et al. 1999).

Table 13.10 Parameters of the T1 sequences. For all sequences slice was 8 mm and matrix was 128×128. At MR Open FOV was 300×300, at MR Sonata it was 200×200

	GRE	TRUFI	SRTF	IRTF
MR Open				
TR [ms]	23	10.46	1030	758
TE [ms]	9	5.23	7.73	7.73
TI [ms]			380	380
Flip angle [°]	26	63	90	90
Number of acquisitions	2	4	1	1
Acquisition time [s]	5.9	5.4	6.2	4.5
MR Sonata				
TR [ms]	18	4.3	600	600
TE [ms]	6	2.15	1.81	1.81
TI [ms]			300	300
Flip angle [°]	26	63	20	20
Number of acquisitions	1	3	3	3
Acquisition time [s]	2.3	1.7	1.8	1.8

Temperature Mapping

MR thermometry was carried out during LITT experiments on agarose gel and lobes of pig liver. The gel consisted of 1.5% agarose, 0.2% carbon black for better absorption of laser light, 0.2% natrium nitrite for conservation and 1 mmol/l Gd-DTPA for contrast enhancement.

The porcine liver was stored for 4 h at room temperature for temperature equalization.

Two MR scanners were used: an open 0.2-T Scanner (MR Concerto, Siemens, Erlangen, Germany) and a 1.5-T whole body scanner (MR Sonata, Siemens, Erlangen, Germany). Five measurements were performed for each phantom and scanner.

The laser applicators were inserted in double-tube protective 9F catheters (SOMATEX Medical Technologies GmbH, Teltow) with the water-cooling. This application system was inserted in the phantom and fixed with an adjusting device. Sensors of an optical thermometer (Luxtron 790, Luxtron Corporation, Santa Clara, CA, USA) were also inserted in catheters and attached in a distance of 1 cm to the applicator for temperature control (Fig. 13.23).

The temperature resolution of the optical thermometer is 0.1 °C; accuracy is denoted as 1 °C. The laser system (MY 30, Martin Medizin-Technik Tuttlingen, Germany) was placed outside of the scanner room to reduce electromagnetic distortions in the MR images.

Scout sequences were applied to find a slice where laser applicator and temperature probe were both

Table 13.11 Parameter of PRF sequences, matrix 128 × 128

	PRF-GRE Siemens (MR Sonata)	PRF-TFL Siemens (MR Sonata)	PRF-GRE (MR Sonata)	PRF-TRUFI (MR Sonata)	PRF-GRE (MR Open)
TR [ms]	40	2000	40	8.5	40
TE [ms]	10	5	20	1.57, 2.91, 4.25, 5.59, 6.93	30
Flip angle [°]	25	8	25	90	25
Number of acquisitions	1	1	1	1	1
Acquisition time [s]	5.1	2.0	5.1	1.09	5.1
FOV	200 × 200	200 × 200	200 × 200	200 × 200	300 × 300

visible. Thereafter four different sequences were used for T1 thermometry: gradient echo (GRE), TrueFISP (TRUFI), Saturation Recovery Turbo-FLASH (SRTF) and Inversion Recovery Turbo-FLASH (IRTF) sequences (Table 13.10). At the MR Sonata, PRF was also measured with four different sequences: two fast-spoiled GRE sequences, a Turbo FLASH and a multiecho TRUFI sequence (Table 13.11).

Temperature estimation with the T1 method was performed in two phases: first determination of the tissue-dependent temperature coefficient, and then, based on this coefficient, temperature calculation. For the calibration measurements, probes of liver and agarose were heated up to 60 °C and then cooled down. At each temperature, lowering of 4 °C an MR image was acquired and the according fluoroptic temperature was measured. With these data and Eq. 1, the temperature coefficient was calculated as the slope of a linear fit. During the heating experiments the temperature was determined with this coefficient and the same relation.

Results of the Temperature Measurements

Temperature rise resulted in a decrease of signal intensity on T1-weighted images (Fig. 13.24). The calculated MR temperature was plotted on the temperature that was measured with the fluoroptic thermometer, and a linear regression was performed. Tables 13.12, 13.13 and 13.14 show the mean values of six experiments. The absolute difference ΔT [°C] of the calculated temperature and the fiberoptic temperature was considered as the main quality indicator for thermometry and was defined as the temperature accuracy.

At the liver, protein denaturation causes strong non-linear dependencies of the MR parameters above 60 °C, and temperature calculation gets less accurate. Nevertheless, this temperature range is very important for thermal ablation of tumors. The deviation inside a ROI proceeds strongly with temperature for the PRF sequences. This shows up through rising error bars in the figures. Regarding the other sequences, temperature is distributed more evenly in a ROI.

The agarose experiments revealed similar temperature accuracies of 3–5 °C.

When dealing with liver, the PRF sequences performed much better than the T1 with accuracies of 5–12 °C (T1 sequences: 14–17 °C). In terms of accuracy, the different T1 sequences were all very similar to each other.

Table 13.12 T1 temperature coefficients calculated from six calibration measurements

	R^2	m [%/°C]	σ_m [%/°C]
MR Sonata Agarose			
T_1-FLASH	0.99	0.89	0.07
T_1-TRUFI	0.67	0.37	0.29
T_1-SRTF	0.99	1.24	0.13
T_1-IRTF	0.99	1.40	0.25
Porcine liver			
T_1-FLASH	0.98	0.88	0.31
T_1-TRUFI	0.98	0.86	0.17
T_1-SRTF	0.99	1.00	0.14
T_1-IRTF	0.98	1.21	0.15
MR open Agarose			
T_1-FLASH	0.97	0.55	0.04
T_1-TRUFI	0.39	0.17	0.22
T_1-SRTF	0.97	0.60	0.05
T_1-IRTF	0.98	0.92	0.16
Porcine liver			
T_1-FLASH	0.98	0.52	0.11
T_1-TRUFI	0.98	0.55	0.07
T_1-SRTF	0.99	0.73	0.18
T_1-IRTF	0.98	0.92	0.22

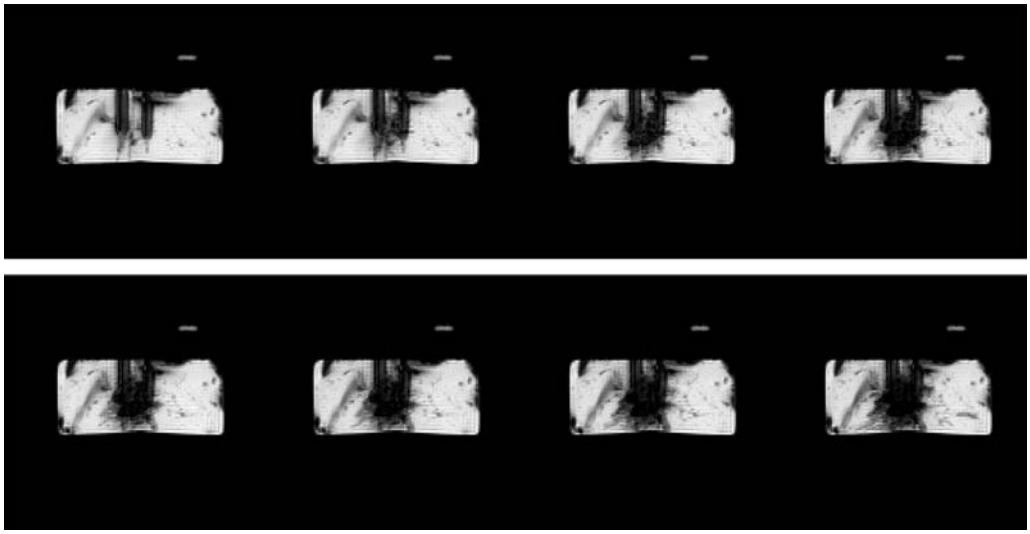

Fig. 13.24 Signal loss in a series of T1-weighted magnitude images at different temperatures. Temperature rises *from upper left to lower right*: 37.3, 47, 53.3, 60.2, 64.3, 68.5, 73.2, and 80.4 (T1-weighted FLASH, TR 18 ms, TE 6 ms and flip angle 26°)

Table 13.13 Accuracy of temperature measurement at agarose gel and porcine liver for the 1.5-T scanner. Coefficient of determination R^2, slope of the linear fit a, mean temperature difference of estimated and fluoroptic temperature $\overline{\Delta T}$

	R^2	a	$\overline{\Delta T}$ [°C]
Agarose			
T_1-FLASH	0.977	0.77	5.75
T_1-TRUFI	0.413	0.47	18.81
T_1-SRTF	0.978	0.71	5.41
T_1-IRTF	0.981	0.75	4.42
PRF-FLASH, Siemens	0.995	0.88	5.12
PRF-TFL, Siemens	0.990	1.01	4.71
PRF-FLASH	0.960	0.97	5.06
PRF- TRUFI	0.997	1.05	4.85
Porcine liver			
T_1-FLASH	0.874	0.55	14.31
T_1-TRUFI	0.938	0.47	17.78
T_1-SRTF	0.973	0.52	14.18
T_1-IRTF	0.985	0.52	14.98
PRF-FLASH, Siemens	0.977	0.98	5.09
PRF-TFL, Siemens	0.977	0.91	7.50
PRF-FLASH	0.946	0.79	9.28
PRF-TRUFI	0.914	0.85	12.04

Table 13.14 Accuracy of temperature measurement at agarose gel and porcine liver for the 0.2-T (b) scanner. Coefficient of determination R^2, slope of the linear fit a, mean temperature difference of estimated and fluoroptic temperature $\overline{\Delta T}$

	R^2	a	$\overline{\Delta T}$ [°C]
Agarose			
T_1-FLASH	0.945	0.71	4.81
T_1-TRUFI	0.314	0.75	50.27
T_1-SRTF	0.954	0.99	8.07
T_1-IRTF	0.975	0.76	3.89
PRF-FLASH	0.939	0.82	3.28
Porcine liver			
T_1-FLASH	0.959	0.84	7.03
T_1-TRUFI	0.966	0.85	8.32
T_1-SRTF	0.985	0.89	6.40
T_1-IRTF	0.977	0.69	11.03
PRF-FLASH	0.659	0.42	13.70

Summary

MR-thermometry offers the possibility of on-line monitoring the temperature distribution during thermal therapies (Vogl et al. 2005). On-line temperature control could be a basis for adjusting therapy parameters and serve as an indicator for endpoints of the treatment. With this, MR-thermometry can help to prevent surrounding structures from unnecessary damage (Mensel et al. 2005). Complete ablation of the tumors is important as residual tumor cells post LITT can lead to a rapid regrowth of the tumor. MR-thermometry could help to ensure a security zone (Maataoui et al. 2005).

There are some requirements for using MR thermometry for LITT. Temperature monitoring has to be fast and the time delay should be small enough that

there is no major proceeding of the necrosis zone between measurements. In addition spatial resolution has to be high enough for analysis of anatomic structures.

Currently there are still some limitations to this technology. A typical problem are temperature gradients within the region of interest causing inaccurate temperature estimates. However, the linearity of most sequences lead to the assumption that temperature can be measured precisely with MR imaging. MR thermometry can help to improve MR-guided LITT. The most important temperature range between 60 °C and 90 °C can be reliably monitored with a temporal resolution of 1–5 s. With the help of MR thermometry, tumors can be safely coagulated, including a security zone. Damage to important surrounding structures can be limited.

Key Points

T1-weighted SRTF and FLASH sequences perform best MR-thermometry at low-field scanners. High-field MR-thermometry reveals best results for the PRF method with FLASH and TFL sequences.

References

Bohris C, Schreiber WG, Jenne J et al. (1999) Quantitative MR temperature monitoring of high-intensity focused ultrasound therapy. Magn Reson Imaging 17:603–610

Clegg ST, Das SK, Zhang Y et al. (1995) Verification of a hyperthermia model method using MR thermometry. Int J Hyperthermia 11:409–424

Cline HE, Hynynen K, Hardy CJ et al. (1994) MR temperature mapping of focused ultrasound surgery. Magn Reson Med 31:628–636

De Poorter J, De Wagter C, De Deene Y et al. (1995) Noninvasive MRI thermometry with a proton resonance frequency (PRF) method: In vivo results in human muscle Magn Reson Med 33:74–81

Eichler K, Mack MG, Straub R et al. (2001) Oligonoduläres hepatozelluläres Karzinom (HCC): MR-gesteuerte laserinduzierte Thermotherapie. Radiologe 41:915–922

Germain D, Vahala E, Ehnholm GJ et al. (2002) MR temperature measurement in liver tissue at 0.23T with a steady-state free precession sequence. Mag Reson Med 47:940–947

Maataoui A, Qian J, Mack MG et al. (2005) Laserinduzierte interstitielle Thermotherapie (LITT) von Lebermetastasen unterschiedlicher Größe im Kleintiermodell. Rofo 177: 405–410

MacFall J, Prescott DM, Fullar E et al. (1995) Temperature dependence of canine brain tissue diffusion coefficient measured in vivo with magnetic resonance echo-planar imaging. Int J Hyperthermia 11:73–86

Mensel B, Weigel C, Heidecke CC et al. (2005) Laserinduzierte Thermotherapie (LITT) von Lebertumoren in zentraler Lokalisation: Ergebnisse und Komplikationen. Rofo 177:1267–1275

Vogl TJ, Weinhold N, Müller P et al. (1996) MR-gesteuerte laserinduzierte Thermotherapie (LITT) von Lebermetastasen: Klinische Erfahrung. Röntgenpraxis 49:161–168

Vogl TJ, Straub R, Eichler K et al. (2002) Malignant liver tumors treated with MR imaging-guided laser-induced thermotherapy: experience with complications in 899 patients (2,520 lesions). Radiology 225:367–377

Vogl TJ, Mack MG, Balzer J et al. (2003) Liver metastases: neoadjuvant downsizing with transarterial chemoembolization before laser-induced thermotherapy. Radiology 229:457–464

Vogl TJ, Eichler K, Zangos S et al. (2005) Interstital laser therapy of liver lesions. Med Laser Appl 20:115–118

Wlodarcyk W, Boroschewski R, Hentshel M et al. (1999) Comparison of four magnetic resonance methods for mapping small temperature change. Phys Med Biol 44:607–624

Yoon SS, Tanabe KK (1999) Surgical treatment and other regional treatments for colorectal cancer liver metastases. Oncologist 4:197–208

13.2.2 Laser Ablation – Liver and Beyond

Martin G. Mack, Katrin Eichler, and Thomas J. Vogl

13.2.2.1 Introduction

Interstitial laser-induced thermotherapy (LITT) is a minimally invasive technique suitable for local tumor destruction within solid organs, using optical fibers to deliver high-energy laser radiation to the target lesion (Mack et al. 2004; Vogl et al. 1997a, 2004a). Due to light absorption, temperatures of up to 120 °C are reached within the tumor, leading to substantial coagulation necrosis. Magnetic resonance (MR) imaging is used both for placement of the laser applicator in the tumor and for monitoring progress of thermocoagulation. The thermosensitivity of certain MR sequences is the key to real-time monitoring, allowing accurate estimation of the actual extent of thermal damage (Castren Persons et al. 1992; Jolesz et al. 1988; Le Bihan et al. 1989).

Thus, laser can destroy a tumor by direct heating, while greatly limiting damage to surrounding structures. Experimental work has shown that a well defined area of coagulative necrosis is obtained around the fiber tip, with minimal damage to surrounding structures. Pilot clinical studies have demonstrated

that this technique is practical for the palliation of hepatic tumors (Amin et al. 1993; Masters et al. 1992; Matsumoto et al. 1992). The success of LITT depends on delivering the optical fibres to the target area, real time monitoring of the effects of the treatment and subsequent evaluation of the extent of thermal damage (Vogl et al. 1996). The key to achieving these objectives is the imaging methods used.

MR-guided laser-induced thermotherapy offers a number of potential treatment benefits. First, MR imaging provides excellent topographic accuracy due to its excellent soft-tissue contrast and high spatial resolution. Second, the temperature sensitivity of specially designed MR sequences can be used to monitor the temperature elevation in the tumor and surrounding normal tissues (Meister et al. 2007). This enables the exact visualization of the growing coagulative necrosis. On-line MR imaging during LITT is helpful for avoiding local complications due to laser treatment. Third, recovery times, lengths of hospital stay, and the risk of infection and other complications can be reduced when compared with palliative open surgery. Finally, successful implementation of such minimal invasive procedures has the potential to significantly reduce costs in comparison to surgical procedures. A further, indirect advantage is the psychological effect due to avoidance of cosmetic deformities that can result from major reconstructive surgery.

To generate an MR image a radiofrequency pulse is used. If there is any RF-source in the MR room there is always interference between the radiofrequencies from the RF-generator and the radiofrequencies from the MR scanner resulting in a complete destruction of the MR image. Even with MR-compatible RF-probe it is necessary to disconnect the probes for every MR scan which is quite uncomfortable. Another advantage of the laser is that multiple laser applicators can be used in completely different parts of the liver simultaneously, because the different laser applicators don't interact. Therefore two or three metastases can be ablated simultaneously with the laser, permitting short overall intervention times. This may be done under local anesthesia on an outpatient basis.

MR-guided minimally invasive LITT has become a well-established procedure for local treatment of liver metastases and primary liver tumors in some European centers. Several studies using this technique have shown that local minimally invasive destruction of liver tumors improves the survival rate of patients with liver metastases (Mack et al. 2004; Vogl et al. 2004b). For recurrent extrahepatic tumors the value of minimally invasive treatment modalities has not yet been demonstrated. Initial clinical data obtained from laser therapy of lung cancer (Vogl et al. 2004a) and head and neck tumors (Mack and Vogl 2004) suggest that there are indications for minimal treatment of tumors in other regions of the body.

13.2.2.2 Indications

The primary therapy goal is defined as the local tumor control in patients with limited hepatic malignant tumor involvement. The majority of patients suffer from liver metastases of colorectal cancer. Generally accepted indications for LITT of liver tumors are:

- The maximum diameter of the lesion should not exceed 5 cm.
- The maximum number of lesions should be 5.
- Patients with tumor recurrence after surgery, radiation or chemotherapy.
- New metastases after liver resection.
- No response to chemotherapy.
- Metastases in both liver lobes.
- Lesions in high-risk locations, e.g. near the bile duct.
- LITT as a replacement for other oncological therapy in case of patient refusal.

More than five lesions or patients with extrahepatic disease (e.g. lung or bone metastases) can be treated under certain circumstances based on an individual decision.

Contraindications for MR-guided LITT are as follows:

- Extensive extrahepatic tumor spread
- Contraindications for MRI (pace-maker)
- Ascites
- Apparent infections
- Diffuse and multiple patterns of metastasis
- Insufficient coagulation parameter

Written informed consent has to be obtained from the patient, including the information of the patients about possible complications and side effects as well as alternative treatment options at least 24 h before the treatment.

Before LITT a plain and contrast enhanced MR imaging of the liver or the region of interest is

performed. The imaging protocol included a T2-weighted breath-hold TSE sequence in transverse slice orientation, a HASTE sequence, and a T1-weighted unenhanced and contrast-enhanced gradient (GRE) sequence in transverse and sagittal slice orientation followed by a dynamic evaluation during contrast administration. After contrast administration the T1-weighted GRE sequences are repeated.

LITT can be also performed without MR-guidance using ultrasound (US) or CT-guidance. MR monitoring, particularly MR temperature mapping, allows an exact guidance of the treatment and avoids over- or undertreatment potentially resulting in better local tumor control.

The following indications for extrahepatic LITT can be claimed. However, all treatment decisions of extrahepatic tumors have to be made on an individual basis, preferable within an interdisciplinary tumor board. The discussion should focus on therapeutic alternatives and on the individual situation of the patient:

1. LITT of lung metastases and lung tumors
2. LITT of soft tissue tumors
   - Residual tumors
     - Head and neck region
     - Upper abdomen
     - Retroperitoneum
   - Lymph node metastases
     - Head and neck region
   - Upper abdomen
     - Retroperitoneum
3. Rare indications
   - Kidney tumors
   - Prostate tumors
   - …

13.2.2.3 Material

Laser System

Laser coagulation is accomplished using a Neodymium-YAG laser light with a wavelength of 1 064 nm (MediLas 5060, MediLas 5100, Dornier Germering, Germany) (Fig. 13.25), delivered through optic fibers terminated by a flexible diffuser tip with a diameter of 1.0 mm. The flexible tip reduces the risk of damage to

Fig. 13.25 A Nd:YAG laser with a maximum output power of 100 W. Note the roller pump which is included for the irrigated laser application system. The laser is equipped with a light guide protection system (LPS) which switches the laser off immediately in the case of any damage to the laser fiber

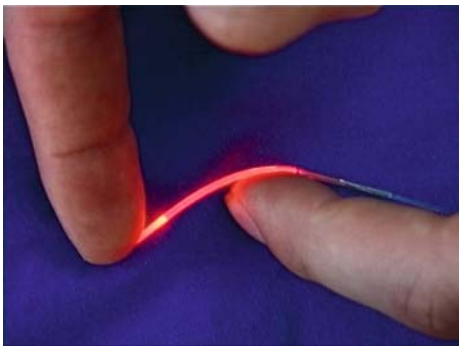

Fig. 13.26 A laser applicator with a flexible diffuser tip and an active length of 3 cm

the diffuser tip to almost zero (Fig. 13.26). The diffuser tip is mounted at the end of a 10 m long silica fiber (diameter 400 µm). The active length of the diffusor tip ranges from 20 to 40 mm. The laser power is adjusted to 10–12 W per cm active length of the laser applicator. The effective laser power at the diffuser tip should be verified with a power meter. The laser system is equipped with a roller pump, which allows internal cooling of the protective catheter.

Laser Application Set

The power laser application system (Fig. 13.27) (SOMATEX, Teltow, Germany) for MR-guided minimally

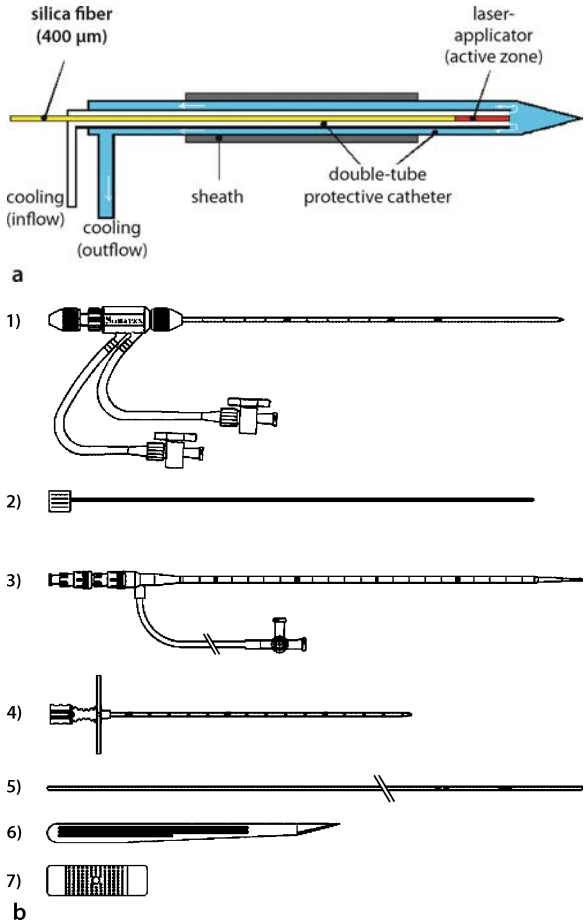

Fig. 13.27 **a** Illustration of the internally cooled power laser system. **b** Schematic drawing of all components of the laser application system. *1* Protective catheter; *2* Mandrin for protective catheter; *3* Sheath with dilator; *4* Puncture needle; *5* Guide wire; *6* Scalpel; *7* Fixation plaster

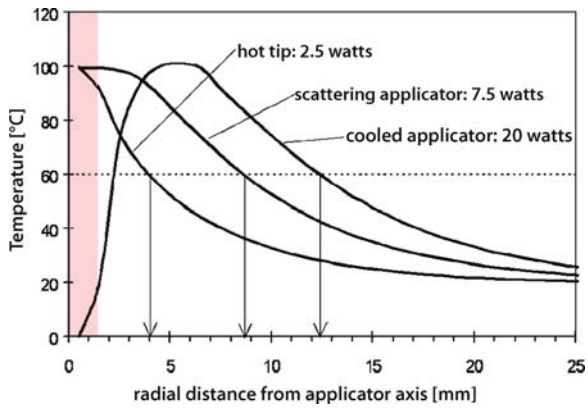

Fig. 13.28 The influence of internal cooling of the laser application system. The cooling allows ablation with higher power settings and results in larger ablation volumes

invasive percutaneous laser-induced thermotherapy of soft tissue tumors consists of an MR-compatible cannulation needle (length 20 cm, diameter 1.3 mm) with a tetragonally beveled tip and stylet; guide-wire (length 100 cm); 9-French sheath with stylet; and a 7-French double-tube thermostable (up to 400 °C) protective catheter (length 40 cm) also with a stylet which enables internal cooling with saline solution and prevents direct contact of the laser applicator with the treated tissues (Vogl et al. 1997b). Cooling of the surface of the laser applicator modifies the radial temperature distribution so that the maximum temperature shifts into deeper tissue layers (Fig. 13.28). This was evaluated by computer simulations calculating the temperature distribution of different types of applicators in pig liver by defining the input power to achieve a maximum tissue temperature of 100 °C. The temperature distribution at the cooled applicator is a combined effect of deep optical penetration of Neodymium-YAG laser and cooling of the applicator surface. Hence the cooled applicator can be used at higher laser powers than non-cooled systems without exceeding critical temperatures. The protective catheter is flexible, transparent for near infrared radiation and made of Teflon. Marks on the sheath and the protective catheter allow exact positioning of the sheath and the protective catheter in the patient. The protective catheter has a sharpened tip, which – in combination with an adapted mandrin – allows repositioning of the system.

The system is fully compatible with MR imaging systems. Magnetite markers on the laser-applicator allow an easier visualizing and positioning procedure.

The laser itself is installed outside of the examination unit; the light is transmitted via a 10 m long optical fiber. The complete clinical set-up used for LITT is shown in Fig. 13.29a. Up to two laser fibers can be connected to one laser system via a beam splitter (Fig. 13.29b).

13.2.2.4 Technique

The success of LITT depends on delivering the optical fibers to the target area, real time monitoring of the effects of the treatment and subsequent evaluation of the extent of thermal damage. The key to achieve these objectives is the imaging methods used.

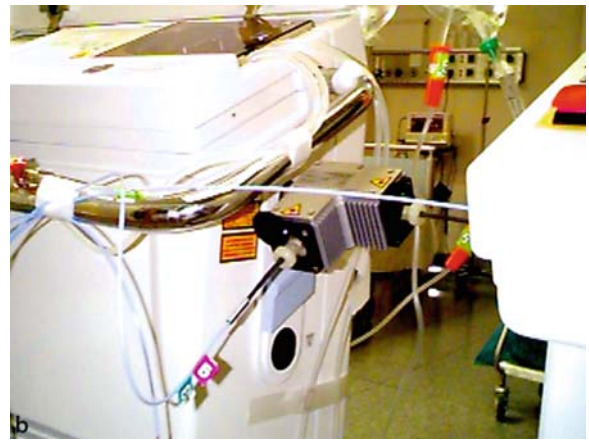

Fig. 13.29 **a** The setup of five laser systems (Dornier MediLas 5100) in the control room for simultaneous treatment of multiple lesions. To each of the five laser systems up to two laser fibers can be connected via a beam splitter (see also **b**). **b** A beam splitter, connected to the laser, which allows the simultaneous use of two laser fibers at one laser system

The metastasis is localized on computed tomographic scans and the access to the lesion is planned. The entrance and destination points are marked at the skin, followed by a skin disinfection and sterile covering (Fig. 13.30). After that, the injection site is infiltrated with 10–40 ml of 1% Scandicain. The laser application system is inserted under CT guidance using the Seldinger technique. Initially a puncture needle (18G) is advanced to the tumor. The position of the tip of the needle is verified by a CT scan. Afterwards the mandrin of the needle is removed and a guide wire inserted until the end of the needle. In the following step, the needle is removed and the guidewire held in place. After that, the sheath with the mandrin is advanced over the guide wire with the tip of the sheath to the end of the guide wire. Afterwards the mandrin of the sheath is removed and the protective catheter placed through the sheath. The tip of the protective catheter should be advanced until the distal end of the sheath system. Afterwards the sheath is pulled back 5 cm while the protective catheter is held in place. This allows the laser light to penetrate through the protective catheter into the tissue without hitting the sheath system, which is not transparent to laser light. Reference markers on all devices help to position the system in the right way. After that the sheath is fixed at the skin with a special plaster.

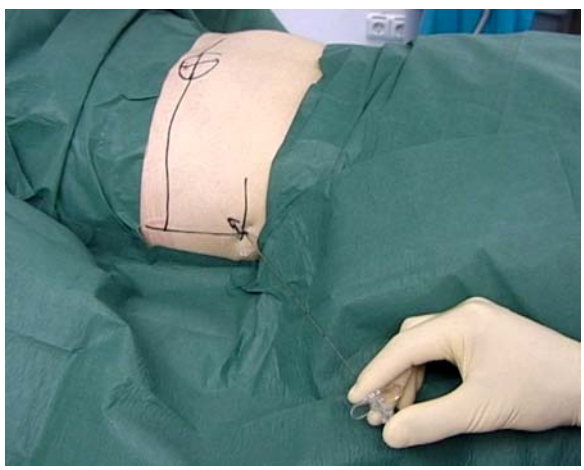

Fig. 13.30 The access planning to a lesion in segment 7. Skin entrance and location of the target are marked with a waterproof pen

Depending on the size of the lesion up to five laser applicators are used simultaneously. Based on the fact that a safety margin of about 5–10 mm at least should be always ablated, surrounding the lesion, the following rough rule can be used to calculate the number of laser applicators which should be inserted. Per centimeter metastases, one laser applicator should be used (Fig. 13.31). Based on the size of the lesion and the active length of the laser applicator, it can be necessary to use the pull back technique in addition either alone or in combination with multiple applicators (Fig. 13.32a–c). The pull-back technique is used to enlarge the coagulation necrosis in the longitudinal axis and is always used, if the active length of the laser ap-

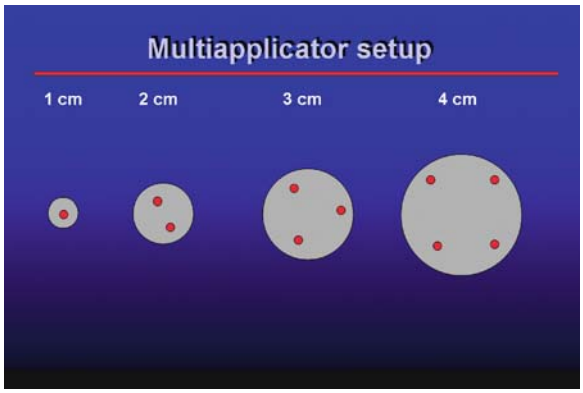

Fig. 13.31 The principal use of the multiapplicator technique. Depending on the size of the lesion, one or more laser application systems should be inserted to get a complete ablation of the lesion and a reliable safety margin

plicator is shorter than the required length of the coagulation area. In these cases we start with an ablation at the distal end of the lesion or even behind the lesion. If then the MR thermometry shows complete ablation in this area, we pull back the laser fiber within the protective catheter between 1 and 2.5 cm and continue the ablation in the proximal part of the lesion.

The LITT treatment itself should be performed under MR-monitoring. For this purpose we use a 0.5-Tesla scanner (Privilig, Escint, Israel) and T1-weighted GRE sequences (TR/TE = 140/12, flip angle = 80°, matrix 128 × 256, 5 slices, slice thickness 8 mm, interslice gap 30%, acquisition time 15 s) in axial slice orientation and parallel to the laser applicators. These two sequences are repeated every 1 min. However, every other MR unit can be used for peri-interventional monitoring. From our experience we recommend the use of T1-weighted gradient echo sequences for thermal monitoring. These sequences are very robust and generally result in acceptable images even in case of moving or pulsating artifacts. With increasing tissue temperature there is an increase in T1 relaxation time of the tissue, which results in a decrease of signal intensity. There is an almost linear correlation between decreasing signal intensity and increasing tissue temperature in the temperature range, which is relevant for LITT treatment (Fig. 13.33).

The entire LITT treatment can be performed using local anesthesia and intravenously injected analgesics (e.g. Pethidin 10–80 mg and/or Piritramid 5–15 mg) and sedation (2–10 mg Midazolam). Local anesthesia can be achieved with 10–40 ml of 1% Scandicain (see Chap. 1).

After the procedure, the needle track is closed with fibrin glue. For this procedure the sheaths are pushed

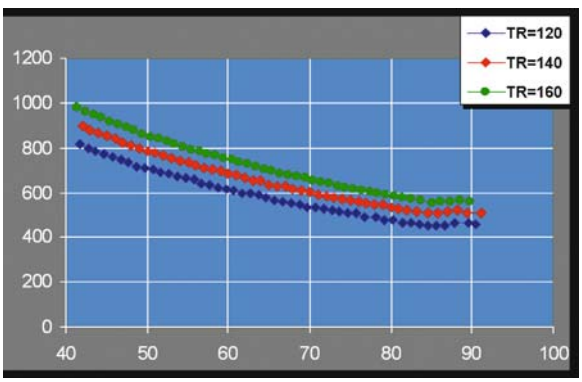

Fig. 13.33 Relationship between signal intensity and temperature using T1-weighted gradient echo sequences with variable TR

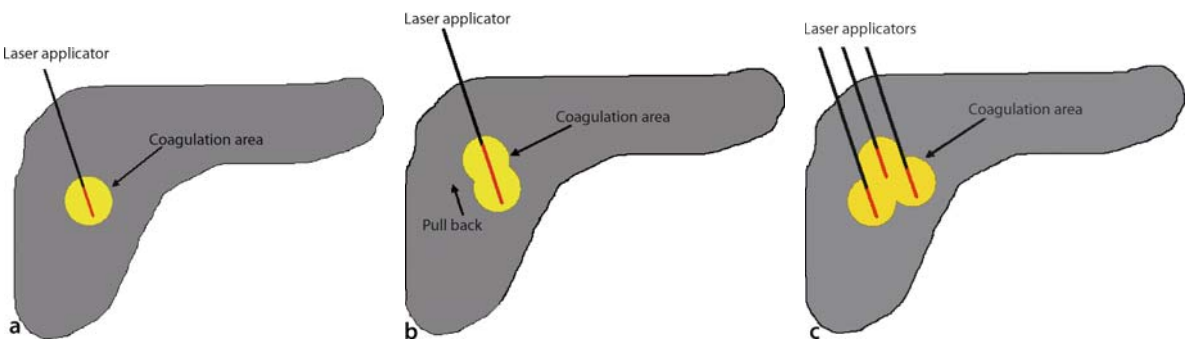

Fig. 13.32 **a** Demonstration of a single applicator with a single ablation zone. **b** Demonstration of a single applicator in combination with a pull back technique. This technique permits increasing the volume of ablation along the needle path. **c** Demonstration of the multiapplicator technique. Overlapping ablation with multiple laser probes allows to treat large liver lesions up to a diameter of 5 cm

forward to the end of the protective catheter and the protective catheter will be removed. After that a two lumen catheter is inserted through the sheath system (Fig. 13.34a) and the fibrin glue is connected (Fig. 13.34b). The double lumen catheter results in mixing of the two components of the fibrin glue at the distal end. Afterwards the complete system is removed slowly under continuous injection of fibrin glue (Fig. 13.34c). After complete removal of the system only a small skin lesion is visible (Fig. 13.34d), which should be covered with a small plaster.

The first follow-up MR imaging study should be performed on the day after the procedure in order to verify the obtained coagulation area (Figs. 13.35–13.37). Further follow-up studies are recommended every 3 months after the intervention.

13.2.2.5 Results

Most experience is with colorectal and breast cancer metastases to the liver. A large-scale, 14-year study has found that laser ablation with MR-guidance is very effective in the treatment of liver tumors. In the meantime we ablated a total of 4887 liver lesions in a total of 1833 patients. The two largest patient groups are patients suffering from colorectal liver metastases and breast cancer liver metastases.

Colorectal Liver Metastases

In our institution, MR-guided LITT was performed in 980 patients with 2874 liver metastases of colorec-

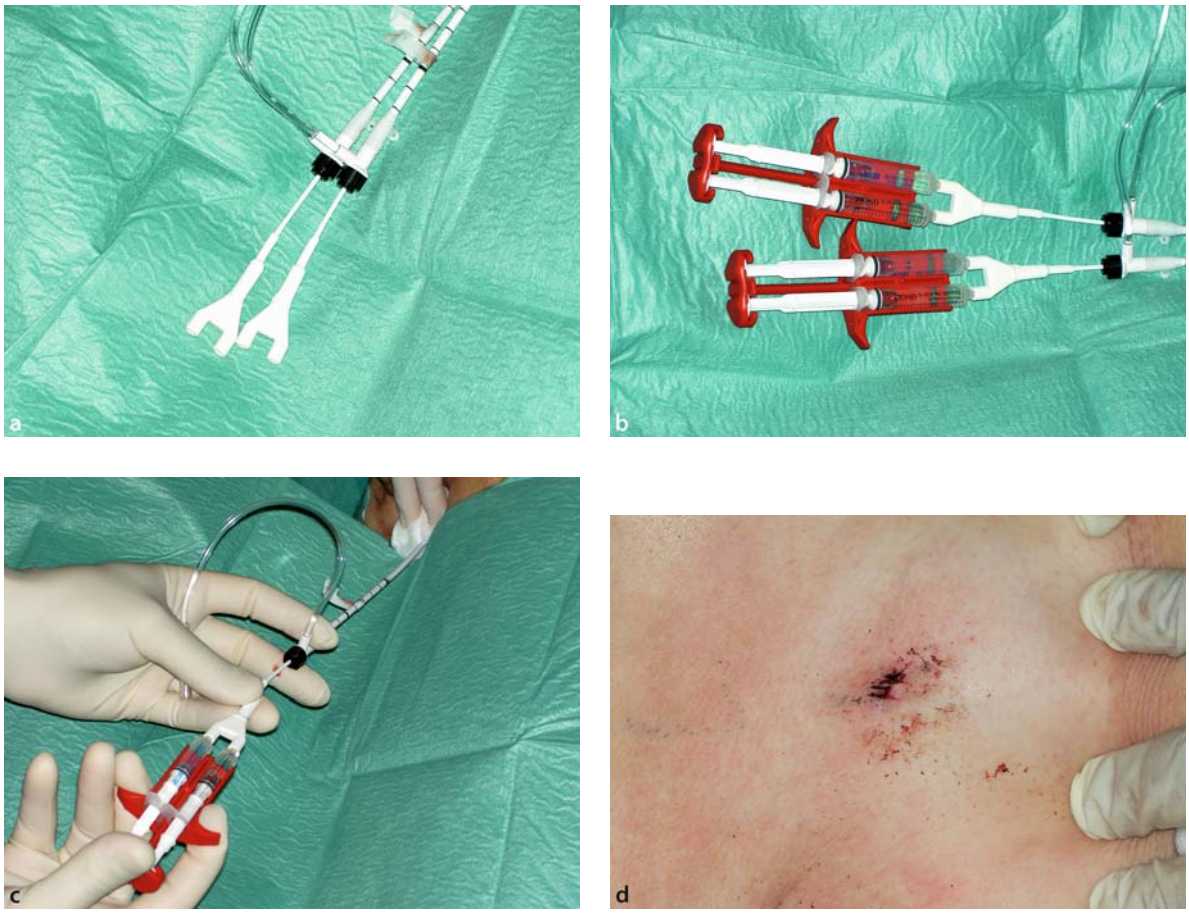

Fig. 13.34 **a** Two double lumen catheters were inserted into the sheaths. **b** The fibrin glue is connected to the double lumen catheter. **c** The continuous removal of the complete system under injection of fibrin glue. **d** After complete removal of the system only a small wound is visible, which should be covered with a small plaster

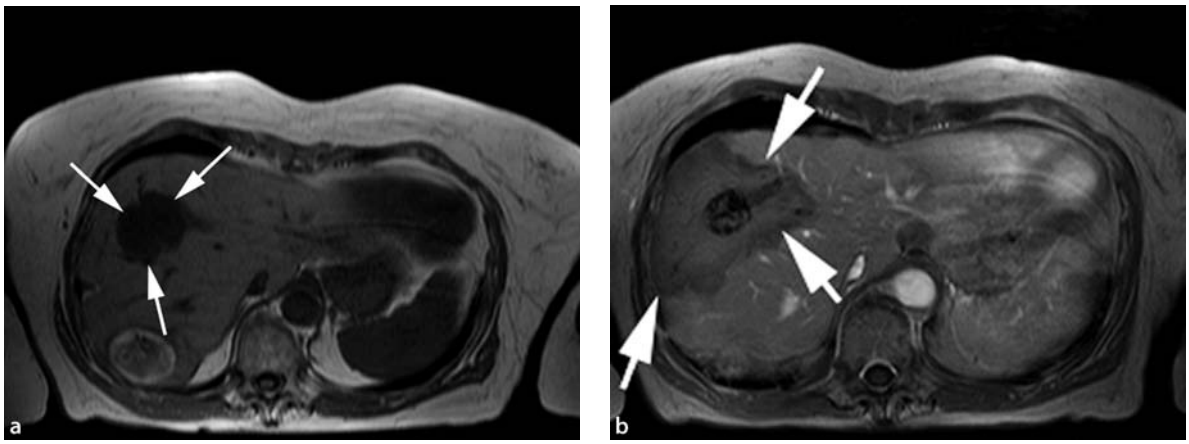

Fig. 13.35 **a** T1-weighted plain image showing a liver metastasis (*arrows*) with a diameter of 4.9 cm. **b** Contrast enhanced MR image 24 h after LITT showing the obtained coagulation area (*arrows*), significantly exceeding the initial tumor volume

tal cancer between 1993 and 2007. Of the patients, 31.1% had recurrent metastases after surgery, 37.8% metastases in both liver lobes, 14.8% refused surgical resection, 3.5% had contraindications for surgery and 12.8% had metastases at difficult localization for surgery. In all, 734 patients were treated in curative intention and 246 patients were treated in palliative intention.

The mean survival rate (SR) for all patients with curative intention, starting the calculation at the date of diagnosis of the metastases which were treated with LITT, was 3.6 years (95% confidence interval (CI): 3.4–3.9 years). In the palliative group, mean survival was 2.7 years (95% CI: 2.4–3.0 years). Patients who refused surgical resection of resectable liver metastases ($n = 135$) had a mean survival of 4.3 years.

Prognostic factors are the primary lymph node status, the number of initial metastases, synchronous metastases vs metachronous, the complete ablation of all visible metastases, the indication for LITT, the size of the treated metastases and the time between the primary metastases and the development of the first liver metastases.

Breast Cancer Liver Metastases

In patients suffering from breast cancer liver metastases LITT is also an effective treatment option. Between 1993 and 2007 we treated 965 metastases in 421 patients. The influence of prognostic factors as number of treated metastases, presence of bone metastases and the hormone receptor status were evaluated. Of the patients, 73.4% were treated in curative intention (≤ 5 metastases, no extrahepatic disease except controlled bone metastases) and 26.6% were treated in palliative intention (> 5 metastases and/or extrahepatic disease).

The mean overall SR was 4.6 years (95% CI: 4.2–5.0 years, 1-year-SR 95%, 2-year-SR 77%, 3-year-SR 58%, 5-year-SR 35%) after diagnosis of treated metastases. In the curative patient-group the mean SR was 5.0 years (95% CI: 4.5–5.4 years) and significantly superior to the palliative group with a mean survival of 3.2 years (95% CI: 2.7–3.7 years).

Hepatocellular Carcinoma (HCC)

A total of 156 lesions were treated in 99 patients. The mean survival was 4.3 years (95% CI: 3.6–4.9 years, 1-year-SR 95%, 2-year-SR 72%, 3-year-SR 54%, 5-year SR 32%).

Extrahepatic LITT

There is little data on extrahepatic LITT. The following tumors were treated: paravertebral recurrence of hypernephroma (Fig. 13.38), recurrence of uterus carcinoma, recurrence of chondrosarcoma of the pubic bone, presacral recurrence of rectal carcinoma and

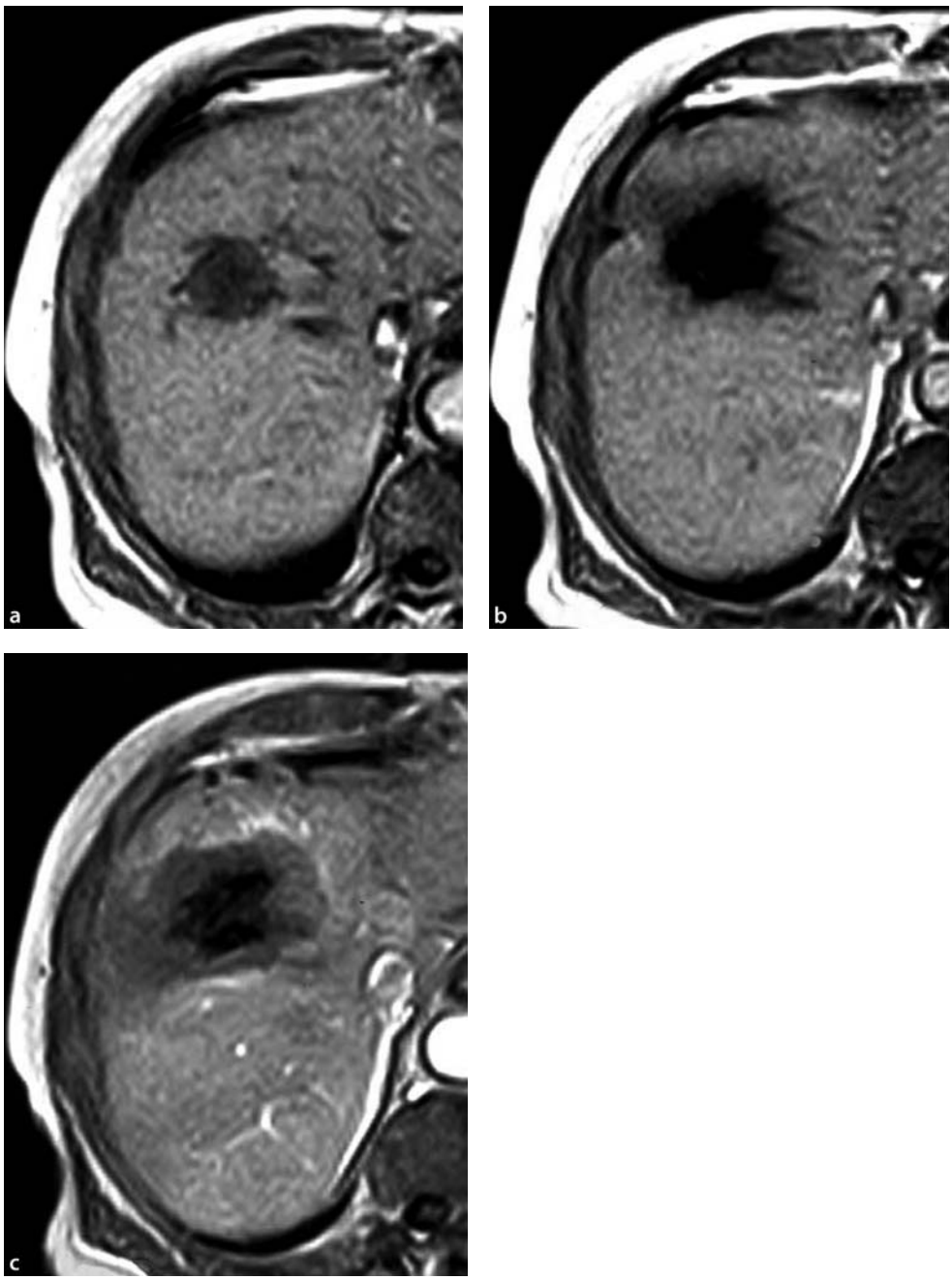

Fig. 13.36 **a** FLASH 2D image showing the metastases in segment 8 before starting laser ablation. **b** FLASH 2D image showing the decrease of signal intensity 18 min after starting laser ablation. **c** Contrast enhanced FLASH 2D image immediately after stopping laser ablation showing coagulation area, which exactly corresponds with the area of decreased signal intensity during ablation (compare **b**)

anal cancer, metastases in the abdominal wall, and lymph node metastases of colorectal carcinoma close to the aorta or inferior vena cava. The maximum diameter of the lymph node metastases was 3.5 cm. Other indications for LITT were malignant kidney tumors and recurrent tumors in the head and neck region. LITT of lung tumor is described in detail in Sect. 13.2.3.

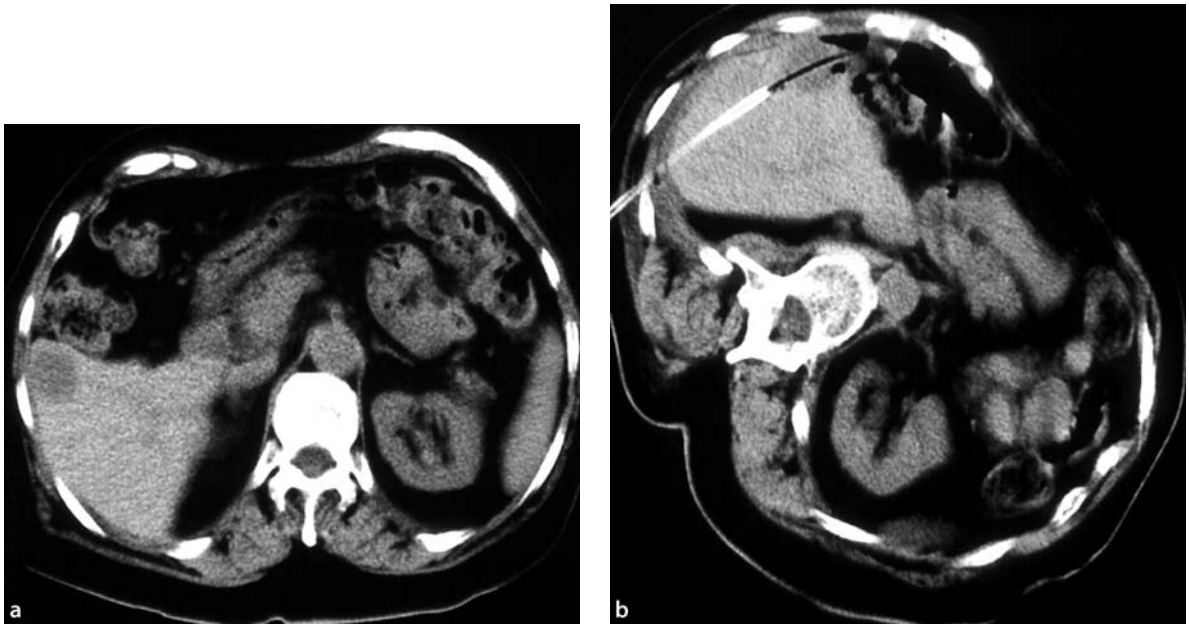

Fig. 13.37 **a** CT image showing a metastasis at the anterior border of the liver. **b** CT image showing a positioned laser applicator

Especially in the head and neck area, which contains a multitude of small, complexly arranged anatomic structures; intimate knowledge of normal spatial relationships and variations is necessary to plan and implement appropriate therapy. Lesions often lie near vital structures, complicating diagnostic and therapeutic procedures. Improved visualization during such procedures can therefore provide the physician with critical information, permitting innovative procedures. For the treatment of tumors of the nasopharynx and parapharyngeal space a subzygomatic approach is used (Fig. 13.39). Tumors of the maxillary sinus are directly punctured from anterior or lateral, lesion of the neck and the floor of the mouth are punctured using either an anterior or lateral approach.

13.2.2.6 Complications

Typical complications of LITT include pleural effusion and subcapsular hematoma. Common side effects are short term fever and fatigue as well as local pain in the case where the lesions were close to the capsule. Most of these complications are minor and do not cause hospitalization.

In our experience the most common side effect of LITT treatment is reactive pleural effusion. In detail typical complications are as follows:

- Pleural effusion (9.2%) requiring puncture in 1.0%
- Small, self limiting subcapsular hematoma (4.3%)
- Intrahepatic abscess (1.1%)
- Intrahepatic bleeding (0.6%) requiring treatment in 0.1%
- Intraabdominal bleeding (0.2%) requiring treatment in 0.1%
- Pleural empyema (0.1%)
- Local infection (0.1%)
- Injury to the bile duct (0.1%)

Four patients (0.2% on a patient basis, 0.1% on a treatment session basis) died within 30 days. Interestingly, patients who were treated for pancreatic metastases have a higher risk of developing a liver abscess, which was observed in 12.5% compared to 0.6% in the other patients.

Summary

Up to 70% of patients with colorectal cancer – which is among the most common cancers – eventually develop liver metastases. In 30% to 40% of those patients with metastases their metastases are confined to the liver

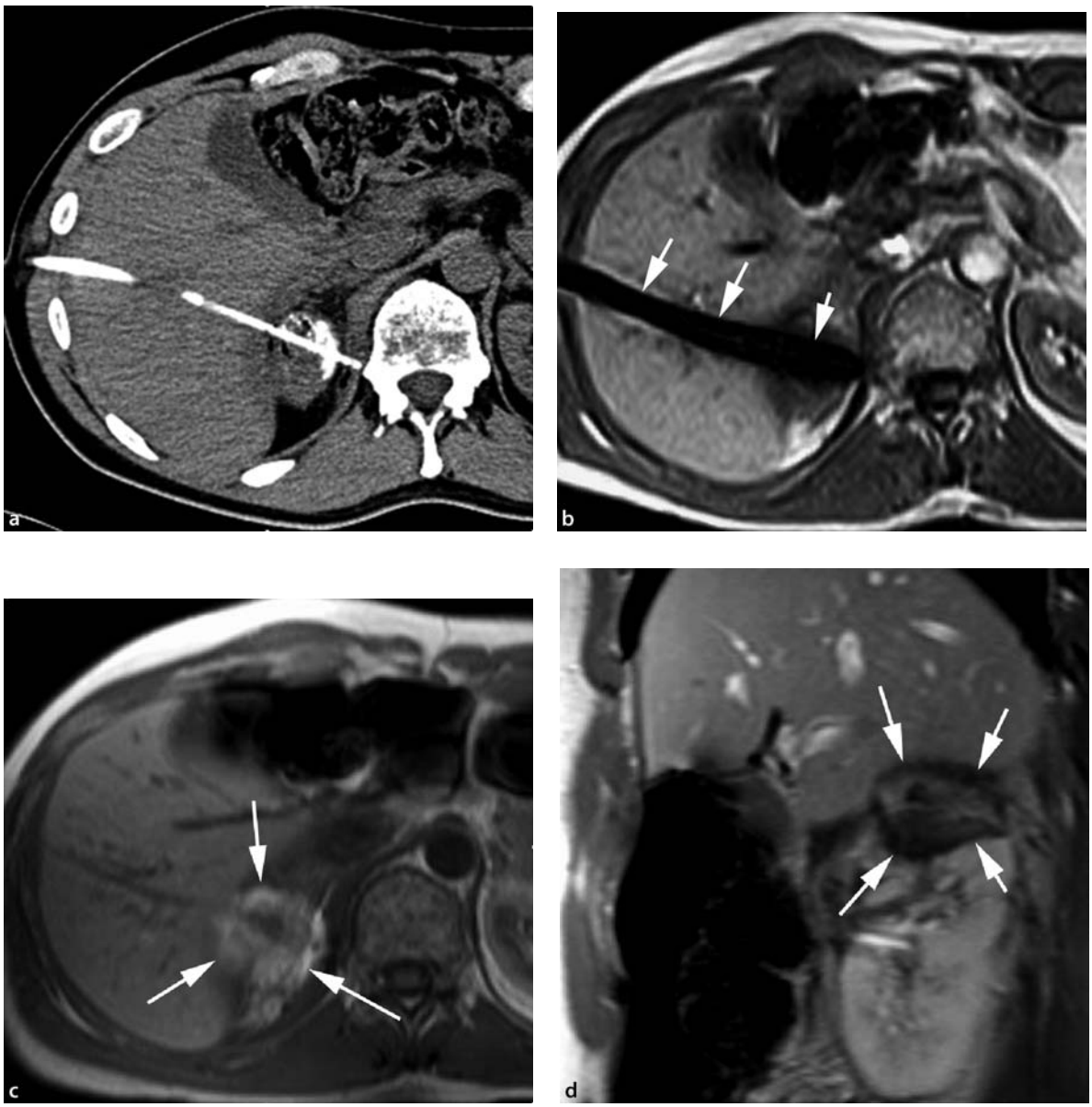

Fig. 13.38a–d **a** CT-guided transhepatic placement of a laser application system in an embolized kidney carcinoma. **b** Gradient echo image showing the susceptibility artifact of the laser application system due to the inserted magnetite marker (*arrows*) in order to verify the positioning on MR imaging. **c** Non-enhanced FLASH 2D image 24 h after ablation showing the induced coagulation area. Note the typical hyperintense signal of the coagulation area due to hemorrhagic diffusion into the coagulation area. **d** Contrast enhanced FLASH 2D image (0.1 mmol Gd/kg b.w.) 24 h after ablation showing the induced coagulation area (*arrows*)

at the time of diagnosis (Harned et al. 1994; Hughes et al. 1988; Nordlinger et al. 1996; Scheele et al. 1991, 1996).

Until recently, the traditional treatment for primary or metastatic liver tumors has been surgical resection. However, only 25% of those with liver metastases are candidates for surgery because of the size, distribution or accessibility of their tumors. Also, the morbidity rate for surgery is high. Therapeutic alternatives are also needed because the incidence of new liver metastases

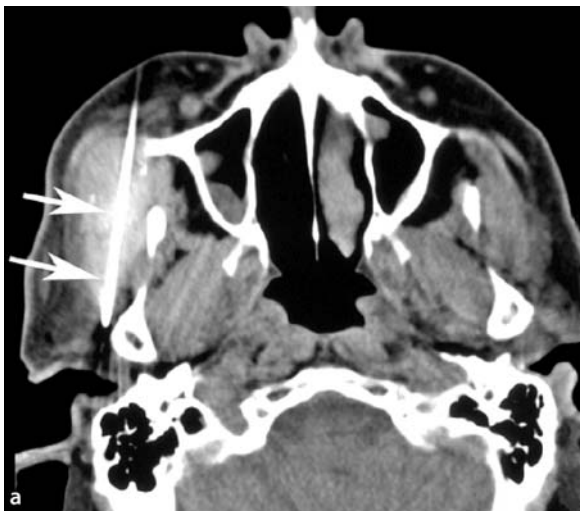

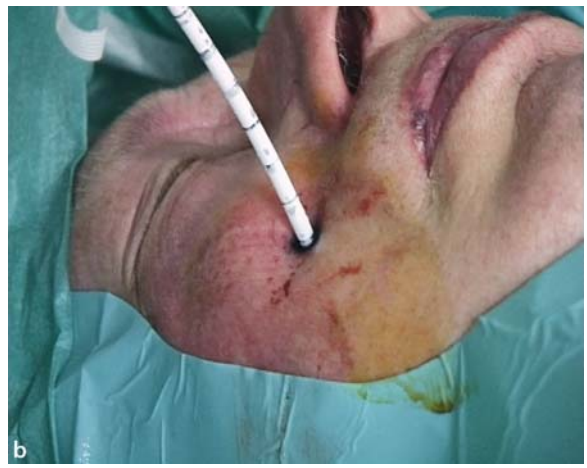

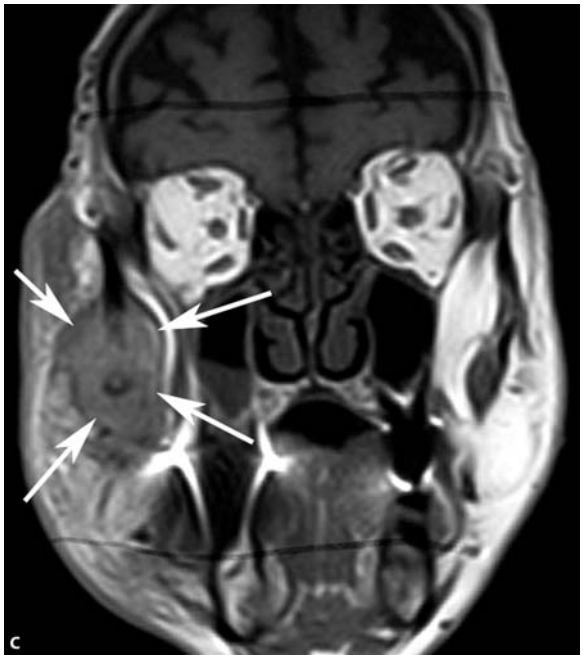

Fig. 13.39a–c Metastases of a hepatocellular carcinoma in the masticator space. **a** CT-guided puncture of the lesion. Note the positioning of the needle (*arrows*). **b** Clinical image showing the laser application system in situ using a subzygomatic approach. **c** This contrast enhanced T1-weighted sequence after LITT (12 min, 22.8 W) shows a significant amount of necrosis (*arrows*)

following successful resection of metastases is high – at 60% to 80%. Many studies have shown that large liver resections stimulate many growth factors, including growths of micro-metastases, which are potentially somewhere else in the liver. This is probably the reason why many patients are already developing new metastases in the first year after surgical resection. There also are indicators that the stimulation of the growth factors after surgical resection is not only stimulating the development of new metastases within the liver, but also outside of the liver, such as in the lung or lymph nodes. Chemotherapy is still widely used to treat liver metas-

tases. However, the survival is still limited and many patients are suffering from relevant side effects (Gallagher et al. 2007; Mehta et al. 2007; Mentha et al. 2007; Min et al. 2007; Tan et al. 2007; Ychou et al. 2008; Zorzi et al. 2007).

Therefore, we believe that minimal invasive tumor ablation using the LITT technique is resulting in improved survival and should be routinely used in an adapted oncologic concept including surgery, chemotherapy and ablation.

Key Points

- Select your patients carefully.
- Discuss all therapeutic alternatives with the patients.
- Do an optimal treatment planning, including high resolution cross-sectional imaging and access planning.
- Know the possible complications and stick to the thesis that the best way to avoid complications is, to know the potential complications.
- Integrate the patients into a well adapted oncologic concept.
- Follow up your patients regularly.

References

Amin Z, Bown SG, Lees WR (1993) Local treatment of colorectal liver metastases: a comparison of interstitial laser photocoagulation (ILP) and percutaneous alcohol injection (PAI). Clin Radiol 48:166–171

Castren Persons M, Lipasti J, Puolakkainen P et al. (1992) Laser-induced hyperthermia: comparison of two different methods. Lasers Surg Med 12:665–668

Gallagher DJ, Capanu M, Raggio G et al. (2007) Hepatic arterial infusion plus systemic irinotecan in patients with unresectable hepatic metastases from colorectal cancer previously treated with systemic oxaliplatin: a retrospective analysis. Ann Oncol 18:1995–1999

Harned RK, Chezmar JL, Nelson RC (1994) Recurrent tumor after resection of hepatic metastases from colorectal carcinoma: location and time of discovery as determined by CT. AJR Am J Roentgenol 163:93–97

Hughes KS, Rosenstein RB, Songhorabodi S et al. (1988) Resection of the liver for colorectal carcinoma metastases. A multi-institutional study of long-term survivors. Dis Colon Rectum 31:1–4

Jolesz FA, Bleier AR, Jakab P et al. (1988) MR imaging of laser-tissue interactions. Radiology 168:249–253

Le Bihan D, Delannoy J, Levin RL (1989) Temperature mapping with MR imaging of molecular diffusion: application to hyperthermia. Radiology 171:853–857

Mack M, Vogl T (2004) MR-guided ablation of head and neck tumors. Neuroimaging Clin N Am 14:853–859

Mack M, Straub R, Eichler K et al. (2004) Breast cancer metastases in liver: laser-induced interstitial thermotherapy–local tumor control rate and survival data. Radiology 233:400–409

Masters A, Steger AC, Lees WR et al. (1992) Interstitial laser hyperthermia: a new approach for treating liver metastases. Br J Cancer 66:518–522

Matsumoto R, Selig AM, Colucci VM et al. (1992) Interstitial Nd:YAG laser ablation in normal rabbit liver: trial to maximize the size of laser-induced lesions. Lasers Surg Med 12:650–658

Mehta NN, Ravikumar R, Coldham CA et al. (2007) Effect of preoperative chemotherapy on liver resection for colorectal liver metastases. Eur J Surg Oncol 33(Suppl 2):S76–83

Meister D, Hubner F, Mack M et al. (2007) MR-Thermometrie bei 1,5 Tesla zur thermischen Ablation mittels laserinduzierter Thermotherapie. Rofo 179:497–505

Mentha G, Majno P, Terraz S et al. (2007) Treatment strategies for the management of advanced colorectal liver metastases detected synchronously with the primary tumour. Eur J Surg Oncol 33(Suppl 2):S76–83

Min BS, Kim NK, Ahn JB et al. (2007) Cetuximab in combination with 5-fluorouracil, leucovorin and irinotecan as a neoadjuvant chemotherapy in patients with initially unresectable colorectal liver metastases. Onkologie 30:637–643

Nordlinger B, Guiguet M, Vaillant JC et al. (1996) Surgical resection of colorectal carcinoma metastases to the liver. A prognostic scoring system to improve case selection, based on 1568 patients. Association Francaise de Chirurgie. Cancer 77:1254–1262

Scheele J, Stangl R, Altendorf-Hofmann A et al. (1991) Indicators of prognosis after hepatic resection for colorectal secondaries. Surgery 110:13–29

Scheele J, Altendorf-Hofmann A, Stangl R et al. (1996) Surgical resection of colorectal liver metastases: gold standard for solitary and completely resectable lesions. Swiss Surg Suppl 4:4–17

Tan MC, Linehan DC, Hawkins WG et al. (2007) Chemotherapy-induced normalization of FDG uptake by colorectal liver metastases does not usually indicate complete pathologic response. J Gastrointest Surg 11:1112–1119

Vogl TJ, Mack MG, Scholz WR et al. (1996) MR imaging guided laser-induced thermotherapy. Min Invas Ther Allied Technol 5:243–248

Vogl TJ, Mack MG, Hirsch HH et al. (1997a) In-vitro evaluation of MR-thermometry for laser-induced thermotherapy. Rofo 167:638–644

Vogl TJ, Mack MG, Staub R et al. (1997b) Internallly cooled laser applicator system for MR-guided laser induced thermotherapy. Radiology 205(P):177

Vogl TJ, Fieguth H, Eichler K et al. (2004a) Laserinduzierte Thermotherapie von Lungenmetastasen und primären Lungentumoren Radiologe 44:693–699

Vogl TJ, Straub R, Eichler K et al. (2004b) Colorectal carcinoma metastases in liver: laser-induced interstitial thermotherapy–local tumor control rate and survival data. Radiology 230:450–458

Ychou M, Viret F, Kramar A et al. (2008) Tritherapy with fluorouracil/leucovorin, irinotecan and oxaliplatin (FOLFIRINOX): a phase II study in colorectal cancer patients with non-resectable liver metastases. Cancer Chemother Pharmacol 62(2):195–201

Zorzi D, Laurent A, Pawlik TM et al. (2007) Chemotherapy-associated hepatotoxicity and surgery for colorectal liver metastases. Br J Surg 94:274–286

13.2.3 Laser Ablation – Lung

Christian Rosenberg
and Norbert Hosten

13.2.3.1 Introduction

Imaging-guided percutaneous laser ablation (LA), also known as laser induced thermal therapy (LITT), is a local treatment option for primary and secondary malignant lung tumors, primarily in patients not amenable to surgical resection.

Local treatment of distant tumor metastases as part of a multimodal cancer therapy has been reported to deliver a proven survival advantage for selective patients, as known from the surgical patient collective (Goya et al. 1989; McCormack et al. 1992; Martini et al. 1995; Shirouzu et al. 1995; Okumura et al. 1996; Baron et al. 1998; Pastorino et al. 1998; Friedel et al. 1999; Inoue et al. 2000; Pages Navarrete et al. 2000; Davidson et al. 2001; Hendriks et al. 2001; Rena et al. 2002; Vogelsang et al. 2004). Despite recent successes in developing systemic therapy regimens and new drugs, surgical resection is the only known curative therapy option in stage IV colorectal carcinoma patients with pulmonary metastases as sole residual disease (Pfannschmidt et al. 2002; Watanabe et al. 2003). However, a huge number of patients with metastatic disease confined to the lungs are not amenable to surgery for different reasons (Penna and Nordlinger 2002). Non-small cell lung cancer (NSCLC) is one of the most common cancer diseases worldwide. Only 20% of the patients with primary diagnosis of NSCLC are suitable for potentially curative resection, usually the treatment of choice for localized cancers (Simon et al. 2007). The possibility of reoperation in case of recurrent tumor, metastatic or primary, is limited due to the repeat loss of parenchyma. Other local therapies are less tissue-consumptive and with less morbidity have become more important during the last few years. Video-assisted thoracoscopic surgery (VATS) accounts for respectable therapy results. However, it comprises technical limitations due to a high dependance on tumor localization (Landreneau 1996; McCormack et al. 1996). In this context, minimally invasive procedures, such as percutaneous thermal ablation, have gained influence. Selective heating of tumor tissue to temperatures of over 60 °C leads to irreversible protein denaturation and cell death. Both laser- and radiofrequency-induced thermal ablation have comparable parenchymal impact and side effects. Nevertheless, lung-specific conduction characteristics for laser light are proposed to improve therapeutic success and control (Knappe and Mols 2004).

13.2.3.2 Indications

In our own experience after six years of performing laser ablation in lungs, several criteria as stated below have been found to be crucial for treatment eligibilty.

Inclusion Criteria

1. Histologic proof of malignancy of the lung tumor or newly found lung nodule in a patient suffering from a previously treated primary tumor known to metastasize to the lung.
2. Interdisciplinary stating of inoperability.
3. Patient rejects surgery/radiation therapy (best discussed in an institutional tumor board).
4. At the time of presentation the patient has received adequate therapy of his primary tumor. Depending on tumor entity and staging these will be either surgical resection, chemotherapy and/or radiotherapy.
5. In case of metastatic disease the patient has been staged “R0” concerning his primary tumor at time of presentation. If the patient suffers from primary NSCLC it is critical to exclude metastatic disease to mediastinal lymph nodes.

Exclusion Criteria

1. Constitutional or medically induced coagulopathies:

- Platelet count $< 50.000/mm^3$
- PTT > 50 s
- Quick value $< 50\%$.

2. A Karnowsky index below 60% or a body weight of more than 30% below ideal weight are considered contraindications.
3. A tumor size beyond 4 cm both for primary cancer and metastatic disease, a tumor count of more than 10 for both lungs, infiltration of the pleura or central necrosis with drainage into bronchi are considered relative contraindications. Such constellations demand case-specific decisions. Diagnosis of lung emphysema was not an exclusion criterion.

A technically complete therapy may include several ablational procedures. It comprises an adequate therapeutical impact per tumor and treatment of all known tumor correlate. Therapy goals may therefore be either 'technically complete' or 'cytoreductive', the latter aiming at symptom palliation or systemic therapy support. The therapy goal should be initially determined and communicated to both patient and referring physician.

13.2.3.3 Material

Different laser generating systems are designed for specific medical use. For interstitial ablation the neodymium yttrium aluminum garnet (Nd:YAG) laser with a near infrared wavelenght of 1 064 nm is best suited. The specific wavelength utilizes deeper light penetration into tissue (Roggan et al. 1997). In our own setting we use three Nd:YAG laser generators, fitted with facultative two- and four-time beam splitters providing a variety of setting designs if it comes to simultaneous use of multiple fibers.

A variety of commercially available applicator systems is being used for LA. All systems safely provide transmission of light through an optical fiber and into the target zone, energy transformation into heat and fiber cooling to prevent carbonization. Whereas an established 9 French system with a closed cooling circuit is widely used in hepatic tumor ablation (Vogl et al. 2000), only one system has been designed especially for the use in lungs (Monocath, Trumpf Medizinsysteme, Umkirch, Germany) (Hosten et al. 2003). It consists of the optical laser fiber with a flexible diffusor tip and a surrounding 5.5 French teflon tube (Fig. 13.40). The major advantage is its comparably small diameter, mostly due to invention of a one-way open cooling solution. Cooling of the heat-releasing fiber tip is provided by continuous instillation of cooling saline (sterile isotone sodium chloride, 40 mL/h, regular perfusor) through a capillary gap between tube and fiber in an open system. A Y-shaped connection piece comprises an axial adjustment capability, haemostatic valve and connection of the cooling line. Minimal residual fluid will evaporate into surrounding lung parenchyma at the terminal tube opening. For applicator placement a sharpend titanium mandrin carries the flexible tube and is later replaced by the laser fiber. Different lengths of diffusor tips (1, 2, 2.5 or 3 cm) are available, as well as different applicator lengths of 12, 14, 16 and 18 cm.

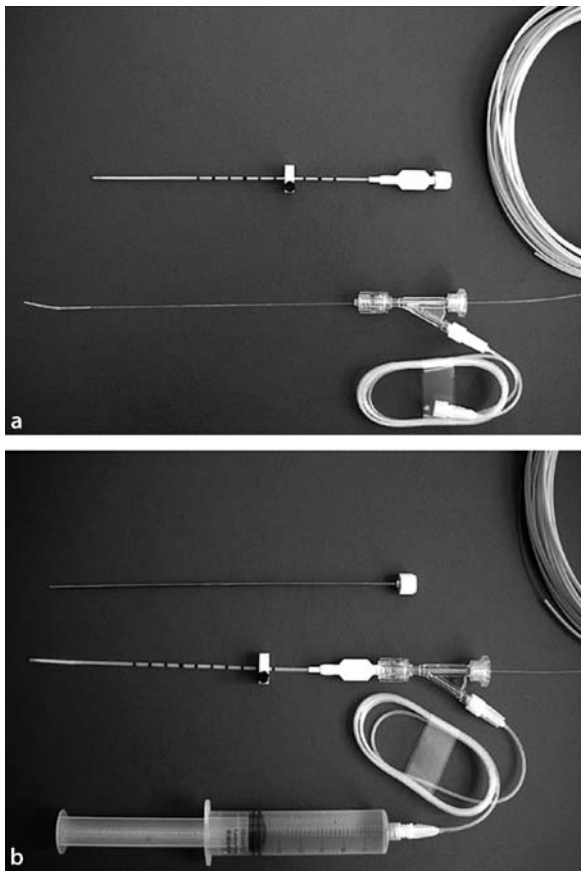

Fig. 13.40a,b Applicator: Miniaturized applicator system consisting of 5.5 F teflon tube with titanium mandrin (**a**). In the second picture the mandrin is removed and replaced by the laser fiber with a 3-cm flexible diffusor tip (**b**)

CT fluoroscopy is the preferred imaging technique for imaging guidance and therapy monitoring. Sterile draping is performed analogously to any surgical procedure. Material and skills for implementation of a thoracic drainage must be in place to treat periprocedural pneumothoraces (see Sect. 11.2). Instrumentation for synchronous air aspiration from the pleural space through a small lumen cannula should be prepared. Capabilities to monitor oxygen saturation and heart rate and to apply oxygen are demanded. Skills and instrumentation to intubate the patient immediately should be within range.

13.2.3.4 Technique

Pre-interventional Work-up

Preinterventional imaging involves a contrast-enhanced computed tomography (CT) scan of the chest with a standardized intravenous contrast injection protocol (tube voltage 120 kVp, 5 mm slice thickness with overlapping increment, tube current 80–120 mA, 27–35 g iodine, injected with a flow rate of 0.9–1.3 mg iodine/s, injection delay 25 s). If the patient underwent CT within one month prior to presentation, a plain spiral CT at the day of the intervention is usually sufficient for procedure planning.

Pre-procedural measures include:

- Patient anamnesis
- Clinical examination
- Spirometry
- Blood sampling (small blood count, coagulation parameters, serum creatinine, TSH)

Informed consent has to be obtained at least 24 h before each procedure. It is critical and has to be achieved in analogy to any elective surgical procedure. At that state the patient has signed a written document stating that he or she is informed about treatment options and risks and willing to undergo the treatment. He or she has explicitly been informed about laser ablation being a local treatment in contrast to a systemic cancer therapy.

Procedure

At the day of ablation, patients are transferred to the CT suite. The lung ablational procedure is performed in the CT suite with the patient positioned on the CT table during the entire procedure. The easiest approach to the target lesion determines the patient position, which is supine in most cases, prone or lateral to access, e.g. dorsal or pericardial tumors. Dedicated technical or nursing radiology staff performs sterile draping and assists the procedure.

Cooperation of the conscious patient, who is supposed to follow breathing commands, will be appreciated in most cases, even though it is not critical. The patient receives local anesthesia (e.g. Lidocaine 1%) at the puncture site, infiltrating subcutis, costal periosteum and parietal pleura. Accessing the thoracic space, intercostal and internal thoracic arteries have to be avoided. The patient is asked to suppress coughing in case it is triggered passing the pleural space. A wide enough angle to the pleura, fast puncture and a minimum of pleural penetrations are most important to prevent pneumothorax. The duplicated visceral pleura of the interlobar spaces has to be taken into account when planning the procedural approach. A translobar access should be avoided whenever possible.

CT fluoroscopy with 5 mm slice thickness, 120 kV and approximately 60 mA s is the preferred imaging technique. The patient is conscious and under intravenous analgosedation, e.g. 10 mg Haloperidole and 100 mg Pethidine slowly infused together with 20 mg of Metoclopramide in 500 mL sodium chloride (see Chap. 5). Oximetry, breathing frequency and electrocardiography are measured continuously throughout the procedure.

Ablation parameters, including count and type of applicators, number and length of treatments are to be determined according to tumor size, location and primary treatment goal. Lung metastases are treated using single or multiple applicators synchronously (Fig. 13.41). In general, tumors larger than 2 cm are treated with at least two applicators in parallel or crossed position. In case of metastases that are too small to be speared, two applicators are used to flank the nodule on both sides. Performing with a single applicator, it is positioned in the middle of the target metastasis, piercing both opposite tumor margins. In most cases 3-cm active tips will be used; only small nodules located close to vulnerable structures, such as pericardium or pleura, sometimes indicate the use of shorter tips (1, 2 or 2.5 cm). The pre-procedural measurement of the puncture depth determines the choice of applicator length (12, 14, 16 or 18 cm). Using multiple applicators simultaneously,

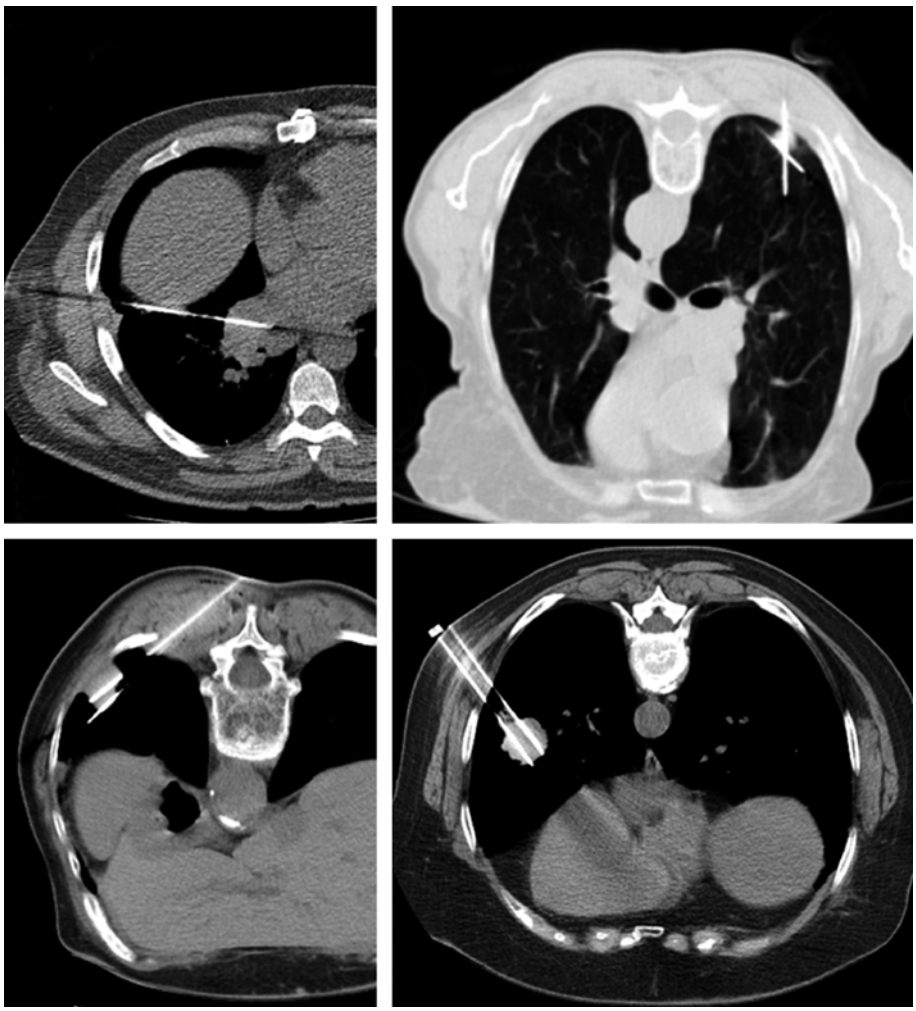

Fig. 13.41 Four different lung metastases being punctured for laser ablative therapy in single or multiple applicator technique. Depending on tumor size and location (pericardial, peripheral and subpleural) different puncture techniques are used

overlapping impact zones are calculated. For procedure planning an ellipsoid zone of sufficient impact with the length of the active tip, that is used, and a maximum width of 2.5 cm is estimated. Overlapping of at least 0.5 cm is mandatory. Depending on tumor size, tumor shape or number of metastases, repeated treatment may be needed to achieve local tumor control. Duration of therapy, meaning continuous application of laser light, and maximum energy, are standardized according to earlier ex-vivo and in-vivo experiments (Hosten et al. 2003; Knappe and Mols 2004). In these experiments the extent of therapy impact had been saturated after 15 min and a maximum energy of 14 W. In our own treatment regimen we elevate the Watt count stepwise (2 W/min) and maintain the maximum energy of 14 W for at least 15 min.

Once all applicators are in place, the titanium mandrins are removed one by one and immediately replaced by the prepared laser fibers. CT fluoroscopy in repeated sequences is used to monitor therapeutic effects within the impact zone (intratumoral lytic changes and a hemorrhagic external rim) and to exclude progressive pneumothoraces, parenchymal bleeding or atypical distribution of cooling fluid.

After the therapy is completed, fibers and tubes are removed. Performing laser ablation in the lungs puncture tract coagulation is not necessary. A final regional fluoroscopic CT scan is done to document absence of pneumothorax and bleeding. Small and locally defined

air inclusions within the pleural space can be tolerated if not progressive. If a pneumothorax develops on table, during or after the procedure, a small-lumen cannula can be applied at the highest point of the widened pleural space to extract air manually and simultaneously without disturbing the setting. If larger or unstable pneumothoraces are detected, drain implementation and connection to a suction machine is mandatory, preferably done still on table (see Sect. 11.2). Most patients can immediately be transferred to the standard care unit and regularly dismissed the day after, after two nights in case of drainage, respectively. All patients receive a control chest radiograph 2–4 h after the procedure in order to rule out delayed or progressive pneumothorax. Postprocedural oral analgetics (e.g. 3 × 40 novaminsulfonium drops) should be given depending on the patients' symptoms (see Chap. 5).

Follow-Up

Follow-up imaging is performed using a spiral CT scanner with single or multi-row helical technique. Non-enhanced and contrast-enhanced images of the entire chest are acquired. For the contrast enhanced CT scan the same scan protocol as for pre-interventional imaging is used. A contrast-enhanced CT, acquired the first postprocedural day, is used for definitive treatment evaluation. A coagulative zone – demarcated either by a thin hyperemic line, diffuse hyperdensity or as a cavitary defect – fully covering the index tumor and comprising a safety margin (aimed at 5 mm) of altered regular tissue in all three dimensions on the one hand, absence of contrast enhancement within the treated tumor on the other hand is read as a technical ablative success. In a few cases of non-reactive (as far as imaging is concerned) and primarily or secondarily very dense index tumors a complete lack of earlier shown contrast enhancement is the only therapy-related alteration and read as technically successfully ablated. Immediately after therapy tumors may slightly increase in size due to necrosis and interstitial fluid uptake. Other tumors, mainly small-sized, will significantly decrease in size and leave an amorphous residuum of fat- or air-isodense signal. If the first day control exam shows residual vital tumor, due to insufficient extent of the ablative zone or due to intratumoral contrast enhancement, a re-intervention within the actual hospital stay is the treatment of choice.

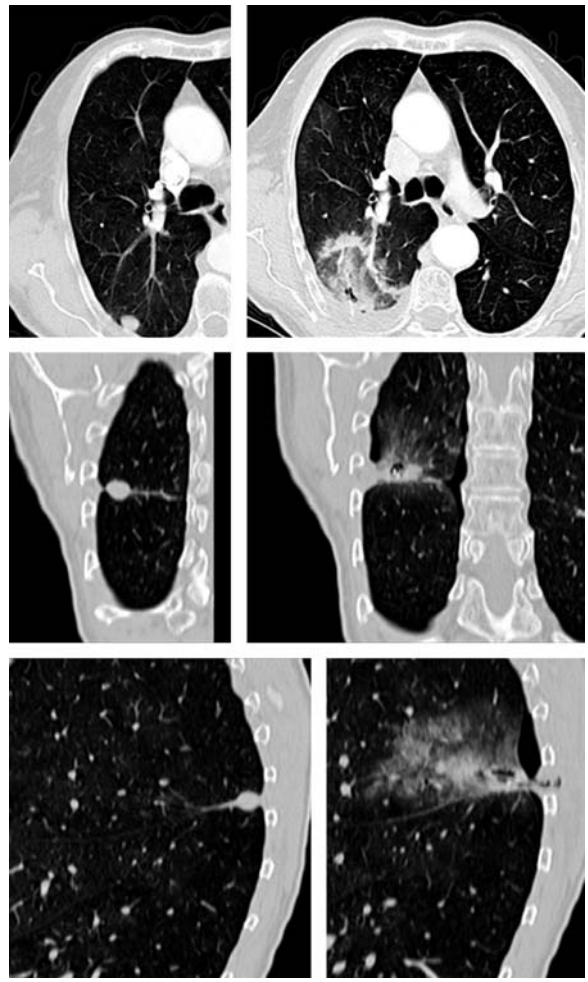

Fig. 13.42 The same right upper lobe (segment 3) peripheral metastasis before and after therapy in three different planes. CT thin-slice reconstruction helps to correlate tumor and ablative zone for therapy evaluation. Notice the small air-isodense body in the center of the ablative zone, consistent with the coagulated residual target lesion

Follow-up CT exams are performed within 6 weeks after the procedure, then 3, 6, 9 and 12 months after the ablation and all 6 months thereafter. Patients receive contrast enhancement if not contraindicated. Newly found contrast enhancement within the treated tumor or residuum, respectively, or within the ablative zone, if at least 3 months from the date of procedure, are read as recurrent tumor. Also progression in size – of the residuum in toto or marginal and eccentric – compared with the initial postablative exam is read as recurrent tumor growth if not inflammatory. Typically the diagnosis of recurrent or residual tumor initiates

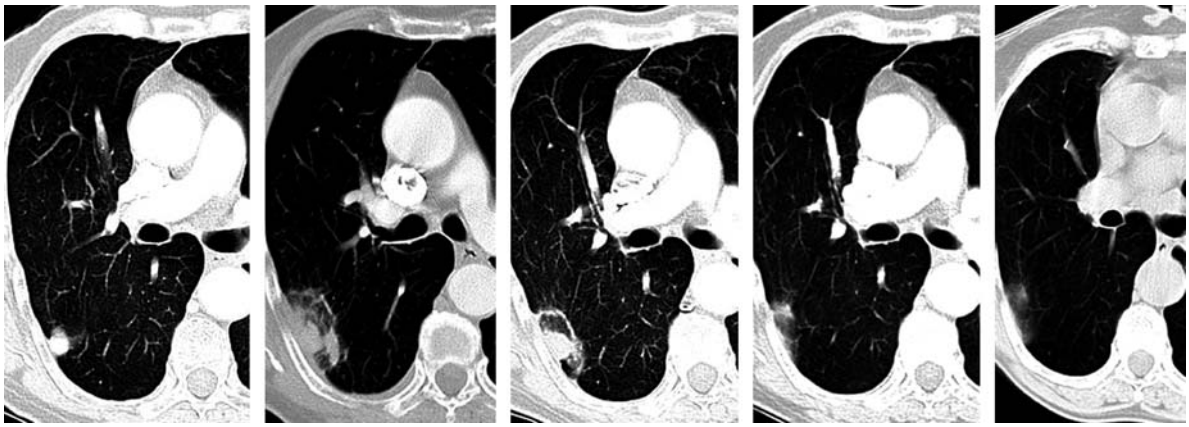

Fig. 13.43 An 83-year-old female patient with subpleural metastasis of a renal cell carcinoma in the right lower lobe segment 6. Scans are taken before, immediately after laser ablation, four weeks, three and six months thereafter. The coagulative zone is nicely demarcated and retracts over weeks. The latest scan shows a residual scar

a re-ablation. In consultation with the patient and referring physician, achievement of local tumor control, the patient's overall condition and state of disease are re-evaluated.

The vast majority of treated tumors show a peritumoral diffuse hyperdensity consistent with reactive edema after heat injury. Regularly a thin hyperdense line, representing hyperemic tissue, demarcates the zone of coagulative impact (Figs. 13.42 and 13.43). In a minority of cases therapy will cause cavitation.

Retraction and significant size reduction can be seen after 12 weeks at the earliest. Scar formation as residual finding will be observed in about half of the cases. For all tumors in common, postprocedural absence of contrast enhancement within the treated tumors is critical (Weigel et al. 2006).

Tumor tissue reaction – imaging-wise – can be diverse and depends on tumor entity and pretreatment. A hypervascular metastasis of a renal cell carcinoma without pretreatment may disappear soon after ablative therapy, leaving a flurry scar, whereas metastases of a hepatocellular carcinoma in another case, representing a stable disease after radiation therapy, may show no correlate for therapy success but loss of contrast enhancement.

13.2.3.5 Results

In our institution, 135 interventional procedures have been performed in 69 patients with an overall tumor count of 113. In seven cases, two seperate lung tumors were targeted in the same session, and consecutive total count of targets was 142. Of these 142 targets, 29 were treated repetitively. Two sessions to complete treatment of a single tumor were necessary in seven cases, and in two other cases three sessions were needed. Initial technical success – according to the criteria described in Sect. 13.2.3.1 – was achieved in 88/113 (78%) tumors.

Per-lesion based tumor progression rate after therapy was 31% (35/113) for all 113 treated metastases. Local recurrence after initially complete therapy was diagnosed in 25 of 88 (28%) tumors. Tumor recurrence was seen as late as 25 months after initial procedure (1.1–24.5 months, median 6.7 months). The overall recurrence-free interval was median 4.6 months (0.0–52.9 months). If the tumor size was greater than 4.0 cm, the tumor progression rate was 43% (6/14) for these lesions; in tumors smaller than 1.5 cm it was 19% (7/36) with progression-free intervals of median 1.2 months (0.0–52.9 months) and 4.6 months (0.0–52.5 months), respectively.

The Kaplan–Meier median time to death for all 69 treated patients was 23.4 months (95% confidence interval, 16.4–29.9 months) months with 1-, 2-, 3-, 4- and 5-year survival rates of 68, 49, 31, 31 and 19%. Of these patients, 36 did not receive technically complete therapy of their initially diagnosed disease; therefore they were primarily or secondarily treated with cytoreductive intent. For these patients the median survival was 15.6 months (95% CI 2.5–21.9 months) with 1-, 2-, and 3-year survival rates of 55, 38, 13%. For

Table 13.15 Therapy outcome and survival rates for hyperthermal lung ablation as reported by different authors

Year	Authors	Modality	Entity	Patients/lesions	1-year survival (%)	3-year survival (%)	5-year survival (%)
2006	Yan et al.	RFA	Colorectal metastases	55/–	85	46	–
2007	Simon et al.	RFA	NSCLC	75/–	78	36	27
2007	Yamakado et al.	RFA	Colorectal metastases	71/–	84	46	–
2007	Own data	LA	Diverse metastases	69/113	68	31	19
			Technically complete	33	82	46	27

NSCLC – Non Small Cell Lung Cancer
RFA – Radiofrequency Ablation
LA – Laser Ablation

33 patients, who were technically completly treated, median time to death was 32.9 months (95% confidence interval (CI) 17.8–47.0 months) with 1-, 2-, 3-, 4- and 5-year survival rates of 82, 61, 46, 46 and 27%. Difference in the curves of full vs cytoreductive therapy was statistically significant ($p = 0.007$). Median time to death in the subgroups renal cell carcinoma ($n = 10$) and colorectal carcinoma metastasis ($n = 20$) were 24.3 and 33.6 months, respectively.

The rate of local tumor recurrence in a per-patient based calculation was 28% for all treated patients. Later progressive pulmonary disease was seen in 26/69 (38%) cases, the latest after 24.5 months (0.5–24.5 months, median 2.8 months). Patients who received full treatment of their initial disease showed later pulmonary progression in only 30% (10/33) of the cases. Extrapulmonary metastasis occurred in 34/69 (49%) patients, after 0.5–52.9 months (median 4.5 months). In the Kaplan–Meier analysis the median recurrence-free interval was 7.8 months (95% CI 0.0–9.0 months) for patients who received technically complete treatment. Recurrence-free intervals of median 10.9 months (95% CI 3.9–11.8 months) for colorectal metastasis patients were the longest within the treated patient collective. The Morris group from Sydney reported local recurrence in 38% and systemic progression in 66% of their 55 patients having undergone radiofrequency ablation of colorectal metastatic disease. It achieved a progression-free interval of median 15 months. Both the Dupuy group from Providence and the Osaka group presented variing recurrence times of 12–45 months and 11–50 months, respectively, depending on target sizes with tumors larger than 3 cm showing worse outcomes. Both groups used radiofrequency-induced thermal ablation to treat primary NSCLC or colorectal metastases in an inhomogeneous patient population in the first case and solely colorectal metastases in the second case.

Table 13.16 Complications in 135 procedures (own data)

Complication	Rate (%)
Minor complications	
Pneumothorax	39 (52/135)
Asymptomatic	33 (45/135)
Chest tube	7 (9/135)
Effusion	20 (27/135)
Parenchymal bleeding	13 (18/135)
Hemoptysis	7 (9/135)
Pain	4 (6/135)
Nausea/dysregulation	4 (6/135)
Soft tissue emphysema	4 (5/135)
Dyspnea	3 (4/135)
Infection	3 (4/135)
Pneumonia	2 (3/135)
Empyema	1 (1/135)
Major complications	4 (5/135)
Prolonged stay without ICU	2 (3/135)
ICU	1 (2/135)

ICU – Intensive Care Unit

Further outcome data on thermal ablation in the lung is summarized in Table 13.15.

13.2.3.6 Complications

Major and minor complications should always be differentiated in accordance with the guidelines of the Society Interventional Radiology (SIR), with major complications inducing an unexpected demand of treatment or a prolonged hospitalization period (Omary et al. 2003).

In a per-procedure based calculation, minor complications occurred in 60% of all 135 procedures

Table 13.17 Procedure-related complications for different local lung ablation techniques as reported by different authors

Year	Authors	Modality	Pneumothorax	Chest tube	Hemoptysis	Infection
2004	Steinke et al.	RFA	43%	7%	9%	n.a.
2004	Yamakado et al.	RFA	17%	20%	n.a.	1% severe 20% mild
2005	VanSonnenberg et al.	RFA	22%	3%	11%	n.a.
2006	Weigel et al.	LA	40%	7%	9%	1%
2007	Simon et al.	RFA	18.6%	9.8%	2.7%	2.2%

RFA – Radiofrequency Ablation
LA – Laser Ablation

that were performed in our institution (Table 13.15). Five cases of major complications led to delayed dismissal, unexpected escalation of treatment measures or readmission. Three of these patients were transferred to the intensive care unit for overnight monitoring after coincidence of parenchymal bleeding and dyspnoe. All of them were retransferred to the standard care unit the day after. Another patient was hospitalized for 7 days from initial admission because of postprocedural prolonged circulatory dysregulation. In one case late onset pneumonia lead to readmission 6 weeks after therapy with the diagnosis of empyema. The patient received abscess drainage and demanded intensive care treatment for two nights. There were no therapy-related deaths. Pneumothorax appeared in 39% (52/135) of the cases, with the need of periprocedural drainage in 9/135 (7%) cases. Parenchymal bleeding (13%, 18/135) was always self-limited and led to temporary hemoptysis in 9/135 (7%) cases. Small reactive effusion in 27/135 (20%) cases never required drainage (Table 13.16). Simon et al. (2007) reported 4 procedure-related deaths after radiofrequency-induced thermal ablation in 153 patients. Compared with other groups performing percutaneous thermal ablation, the necessity of chest tube application to treat pneumothorax was very low in our patient population. Other authors report indications for tube drainage in up to 22% of the procedures. Variable data on incidence of pneumothorax (between 17% and 43%) should mainly be due to different measuring criteria (Grieco et al. 2006; Yan et al. 2006; Simon et al. 2007; Yamakado et al. 2007). Data on procedure-related complications after different local ablative therapies is summarized in Table 13.17.

Summary

Percutaneous laser ablation in the lung is an effective and safe procedure. Our results show 1-, 2-. 3-, 4- and 5-year survivals of 82, 61, 46, 46 and 27% for patients after definite ablative therapy of their pulmonary metastatic disease. These data correlate not only with recently published survival rates after radiofrequency ablation of pulmonary malignancies (Grieco et al. 2006; Yan et al. 2006; Simon et al. 2007; Yamakado et al. 2007) but also with findings in surgical patients who underwent local resection to treat their lung metastases (McCormack et al. 1992; Landreneau 1996; Baron et al. 1998; Friedel et al. 1999; Inoue et al. 2000; Pfannschmidt et al. 2002) (Table 13.15),

Our own results showed no significant increase in incidence of periprocedural complications compared with daily routine diagnostic lung biopsies (Weigel et al. 2004). Mortality is negligible compared with thoracotomy. However, we are aware of reported cases of central embolism in patients who underwent radiofrequency ablation of pulmonary metastases (Yamamoto et al. 2004; Ghaye et al. 2006; Hiraki et al. 2007). Aberrant currents or uncontrolled heat proliferation in contrast to radiofrequency-based ablational concepts have never been a challenge in laser-induced thermal therapy.

In conclusion, laser ablative therapy of primary and secondary malignant tumors in the lung is a promising option in multimodal cancer therapy. Procedure safety and efficacy have been proven. First clinical outcome data strongly support the therapy's potential to improve survival and recurrence-free intervals.

Key Points

- A modern cancer therapy comprises a multimodal treatment which is preferably determined in an interdisciplinary tumorboard.

- The primary therapy goal, either "complete treatment of all tumor correlate" or "cytoreduction" should be determined initially when evaluating a patient – preferably not as a secondary result of therapy failure.
- Setting patient eligibility criteria is crucial.
- Take your time for procedure planning.
- Have your patient feel comfortable.
- Pneumothorax can always be controlled without therapy break-off.

References

Baron O, Hamy A, Micaud JL et al. (1998) Surgical treatment of pulmonary metastasis of colorectal cancer. Prognostic survival factors. Presse Med 27:885–888 [in French]

Davidson RS, Nwogu CE, Brentjens MJ et al. (2001) The surgical management of pulmonary metastasis: current concepts. Surg Oncol 10:35–42

Friedel G, Pastorino U, Buyse M et al. (1999) Resection of lung metastases: long-term results and prognostic analysis based on 5206 cases – the international registry of lung metastases. Zentralbl Chir 124:96–103 [in German]

Ghaye B, Bruyere PJ, Dondelinger RF (2006) Nonfatal systemic air embolism during percutaneous radiofrequency ablation of a pulmonary metastasis. AJR Am J Roentgenol 187:W327–328

Goya T, Miyazawa N, Kondo H et al. (1989) Surgical resection of pulmonary metastases from colorectal cancer. 10-year follow-up. Cancer 64:1418–1421

Grieco CA, Simon CJ, Mayo-Smith WW et al. (2006) Percutaneous image-guided thermal ablation and radiation therapy: outcomes of combined treatment for 41 patients with inoperable stage i/ii non-small-cell lung cancer. J Vasc Interv Radiol 17:1117–1124

Hendriks JM, Romijn S, van Putte B et al. (2001) Long-term results of surgical resection of lung metastases. Acta Chir Belg 101:267–272

Hiraki T, Fujiwara H, Sakurai J et al. (2007) Nonfatal systemic air embolism complicating percutaneous ct-guided transthoracic needle biopsy: four cases from a single institution. Chest 132:684–690

Hosten N, Stier A, Weigel C et al. (2003) Laser-induced thermotherapy (litt) of lung metastases: Description of a miniaturized applicator, optimization, and initial treatment of patients. Rofo 175(3):393–400 [in German]

Inoue M, Kotake Y, Nakagawa K et al. (2000) Surgery for pulmonary metastases from colorectal carcinoma. Ann Thorac Surg 70:380–383

Knappe V, Mols A (2004) Laser therapy of the lung: biophysical background. Radiologe 44:677–683 [in German]

Landreneau RJ (1996) Vats anatomic lung resections. The Hong Kong experience. Chest 109:1–2

Martini N, Bains MS, Burt ME et al. (1995) Incidence of local recurrence and second primary tumors in resected stage i lung cancer. J Thorac Cardiovasc Surg 109:120–129

McCormack PM, Burt ME, Bains MS et al. (1992) Lung resection for colorectal metastases. 10-year results. Arch Surg 127:1403–1406

McCormack PM, Bains MS, Begg CB et al. (1996) Role of video-assisted thoracic surgery in the treatment of pulmonary metastases: results of a prospective trial. Ann Thorac Surg 62:213–217

Okumura S, Kondo H, Tsuboi M et al. (1996) Pulmonary resection for metastatic colorectal cancer: experiences with 159 patients. J Thorac Cardiovasc Surg 112:867–874

Omary RA, Bettmann MA, Cardella JF et al. (2003) Quality improvement guidelines for the reporting and archiving of interventional radiology procedures. J Vasc Interv Radiol 14:S293–295

Pages Navarrete C, Ruiz Zafra J, Simon Adiego C et al. (2000) Surgical treatment of pulmonary metastasis: survival study. Arch Bronconeumol 36:569–573 [in Spanish]

Pastorino U, McCormack PM, Ginsberg RJ (1998) A new staging proposal for pulmonary metastases. The results of analysis of 5206 cases of resected pulmonary metastases. Chest Surg Clin N Am 8:197–202

Penna C, Nordlinger B (2002) Colorectal metastasis (liver and lung). Surg Clin North Am 82:1075–1090

Pfannschmidt J, Hoffmann H, Muley T et al. (2002) Prognostic factors for survival after pulmonary resection of metastatic renal cell carcinoma. Ann Thorac Surg 74:1653–1657

Rena O, Casadio C, Viano F et al. (2002) Pulmonary resection for metastases from colorectal cancer: factors influencing prognosis. Twenty-year experience. Eur J Cardiothorac Surg 21:906–912

Roggan A, Mesecke-von Rheinbaben I, Knappe V et al. (1997) Applicator development and irradiation planning in laser-induced thermotherapy (litt). Biomed Tech (Berl) 42(Suppl):332–333 [in German]

Shirouzu K, Isomoto H, Hayashi A et al. (1995) Surgical treatment for patients with pulmonary metastases after resection of primary colorectal carcinoma. Cancer 76:393–398

Simon CJ, Dupuy DE, DiPetrillo TA et al. (2007) Pulmonary radiofrequency ablation: long-term safety and efficacy in 153 patients. Radiology 243:268–275

Steinke K, Sewell PE, Dupuy D et al. (2004) Pulmonary radiofrequency ablation–an international study survey. Anticancer Res 24:339–343

VanSonnenberg E, Shankar S, Morrison RR et al. (2005) Radiofrequency ablation of thoracic lesions: Part 2, initial clinical experience – technical and multidisciplinary considerations in 30 patients. AJR Am J Roentgenol 184: 381–390

Vogelsang H, Haas S, Hierholzer C et al. (2004) Factors influencing survival after resection of pulmonary metastases from colorectal cancer. Br J Surg 91:1066–1071

Vogl TJ, Mack M, Straub R et al. (2000) Percutaneous interstitial thermotherapy of malignant liver tumors. Rofo 172: 12–22 [in German]

Watanabe I, Arai T, Ono M et al. (2003) Prognostic factors in resection of pulmonary metastasis from colorectal cancer. Br J Surg 90:1436–1440

Weigel C, Kirsch M, Mensel B et al. (2004) Percutaneous laser-induced thermotherapy of lung metastases: experience gained during 4 years. Radiologe 44:700–707 [in German]

Weigel C, Rosenberg C, Langner S et al. (2006) Laser ablation of lung metastases: results according to diameter and location. Eur Radiol 16:1769–1778
Yamakado K, Nakatsuka A, Akeboshi M et al. (2004) Combination therapy with radiofrequency ablation and transcatheter chemoembolization for the treatment of hepatocellular carcinoma: short-term recurrences and survival. Oncol Rep 11:105–109
Yamakado K, Hase S, Matsuoka T et al. (2007) Radiofrequency ablation for the treatment of unresectable lung metastases in patients with colorectal cancer: a multicenter study in Japan. J Vasc Interv Radiol 18:393–398
Yamamoto A, Matsuoka T, Toyoshima M et al. (2004) Assessment of cerebral microembolism during percutaneous radiofrequency ablation of lung tumors using diffusion-weighted imaging. AJR Am J Roentgenol 183:1785–1789
Yan TD, King J, Sjarif A et al. (2006) Percutaneous radiofrequency ablation of pulmonary metastases from colorectal carcinoma: prognostic determinants for survival. Ann Surg Oncol 13:1529–1537

13.3 Percutaneous Ethanol Injection

Markus Düx

13.3.1 Introduction

Percutaneous ethanol injection (PEI) represents one of the most commonly performed techniques of local tumor ablation world-wide. Since it was performed first in 1983, PEI has been increasingly used for treating hepatocellular carcinoma (HCC). Nowadays, thermal ablation techniques tend to gradually replace PEI which is therefore no longer a first line treatment of HCC. However, besides its unchallenged low cost profile, PEI may still offer distinct advantages over other regional therapies in some situations (Lin et al. 2004, 2005).

Absolute alcohol works in two ways. First, it leads to coagulation necrosis at a cellular level as it diffuses into the neoplastic cells causing immediate dehydration of the cytoplasm. Cellular necrosis finally results in a fibrous reaction. The second mechanism induces necrosis of endothelial cells and platelet aggregation with subsequent thrombosis of the small vessels. The thromboembolic effect of absolute alcohol leads to ischemia of the neoplastic tissue (Festi et al. 1990). Percutaneous acetic acid injection may be an alternative to ethanol injection also causing dehydration of the cytoplasm, endothelial necrosis as well as thrombosis of the small vessels (Tsai et al. 2008).

HCC in cirrhotic liver is best suited to be treated by PEI because in this case the tumor tissue is softer than the surrounding cirrhotic tissue of the liver. As a result, alcohol selectively diffuses within the HCC. Moreover, HCC with a size of 2 cm and more shows arterial hypervascularization that ensures a uniform distribution of alcohol within the rich network of the neoplastic sinusoids (Livraghi 1999).

On one hand, the combination of liver cirrhosis and arterial hypervascularization of HCC results in a tremendous local effect of alcohol to the tumor tissue as it is not able to disrupt the intratumoral septa and the surrounding tumor capsule. On the other hand, increasing size of HCC reduces the antitumoral effect of PEI because it does not reach all parts of the tumor and may not destroy all neoplastic cells (Llovet and Sala 2005). In addition, tumors that are not surrounded by cirrhotic liver tissue are not a target of PEI because diffusion of the alcohol is not limited to the tumor and a sufficient antitumoral effect cannot be achieved. Thus, PEI is a technique that is linked together with the treatment of HCC and only some rare oncologic indications other than HCC.

13.3.2 Indications

Patient selection is very crucial for successful local treatment of HCC. It should be based upon tumor localization, size, proximity to large vessels, bleeding risk, respiratory motion, pathway of probe, and last but not least physician's experience. The most important question is whether the tumor is accessible under image guidance without putting the patient at increased risk for bleeding complications, injury of bileducts or bowel loops. Thermal ablation of HCC nodules may often be difficult or impossible due to one of the reasons mentioned before. In those cases, PEI is a welcome alternative to perform local tumor ablation as there is hardly any reason not to be able to reach a tumor nodule with a fine-needle.

The best candidates for PEI are those with Child A cirrhosis (Tables 13.18 and 13.19) and small tumors ($\leq$ 3 cm). The cancer should be confined to the liver and the number of hepatic tumors to be treated by PEI should not exceed four to five lesions. In addition, the patient should be classified unresectable because of the distribution of disease or due to the

Table 13.18 Calculation of the Child–Pugh Score uses five parameters, each scored 1–3, with 3 indicating most severe derangement

Measure	1 point	2 points	3 points	Units
Bilirubin (total)	< 34 (< 2)	34–50 (2–3)	> 50 (> 3)	µmol/l (mg/dl)
Serum albumin	> 35	28–35	< 28	g/l
INR	< 1.7	1.71–2.20	> 2.20	–
Ascites	None	Suppressed with medication	Refractory	–
Hepatic encephalopathy	None	Grade I–II (or suppressed with medication)	Grade III–IV (or refractory)	–

Table 13.19 By adding the scores from Table 13.18, chronic liver disease can be classified in Child–Pugh stage A to C, indicating the patients prognosis

Points	Class	1-year survival	2-year survival
5–6	A	100%	85%
7–9	B	81%	57%
10–15	C	45%	35%

severity of underlying cirrhosis (Ebara et al. 2005). HCC $\leq$ 3 cm treated by PEI are expected to achieve complete responses (Lin et al. 2004; Livraghi et al. 1999). Treatment of patients with larger tumors (3–5 cm) or advanced liver failure (Child B) has to be decided on a patient's individual basis. According to the Barcelona Clinic Liver cancer staging classification (Table 13.20), patients classified as stage A, who do not fulfill the criteria for tumor resection or liver transplantation, qualify best for percutaneous ablation (Bruix et al. 2001).

Limitations for PEI are rare including:

- Systemic tumor progression
- Severe coagulopathy (Quick < 35%, platelets < 40.000/ml)
- Child C cirrhosis with refractory ascites
- Limited life expectancy (Ebara et al. 2005, Lencioni et al 2003)

In order to reduce the risk for recurrent tumor and to enhance overall survival, combined treatment options including PEI have been evaluated for HCC. It has been demonstrated that transluminal arterial chemoembolization (TACE) combined with alcohol injection has the potential to prolong survival compared to TACE alone in small HCC (Koda et al. 2001) and even in nodules with a mean size of 8 cm (Lubienski et al. 2004). Thus, stage B and C patients according to the Barcelona Clinic Liver cancer staging classification may also profit from PEI as far as they are candidates for TACE.

There are some rare oncologic indications for PEI other than HCC. It may be an effective treatment in benign nodular thyroid disease used for sclerotherapy of solid non-toxic and autonomously functioning nodules as well as cystic nodules of the thyroid gland (Chu et al. 2003). Other indications for PEI are tumors of the kidney or parathyroid as well as adrenocortical adenoma (Wang et al. 2003).

According to a recent report (Tsai et al. 2008), alcohol injection may be replaced by percutaneous acetic acid injection especially in HCC resulting in fewer treatment sessions and providing better survival of patients. Basically, indications as well as technical considerations are the same for PEI and acetic acid injection.

13.3.3 Material and Technique

13.3.3.1 Preprocedural Tests

Preprocedural evaluation should include adequate laboratory tests to rule out severe coagulopathy, acute inflammation, poor liver function (Child B and C cirrhosis) and/or other severe comorbidities. A screening for viral hepatitis is mandatory and baseline serum tumor markers – alpha-fetoprotein (AFP) in patients with HCC – are helpful to monitor the therapeutic success during follow-up.

Assessment of the tumor extent and staging for metastatic disease are the baseline for subsequent follow-up studies. To decide on size, location and number of liver lesions, contrast-enhanced computed tomography (CT) and magnetic resonance (MR) imaging play a major role, while ultrasound (US) is hampered by its reproducibility (Vilana et al. 2006). As

Table 13.20 Barcelona Clinic Liver cancer staging classification (BCLC): stage-dependant treatment of HCC (Rx – liver resection; LTx – liver transplantation)

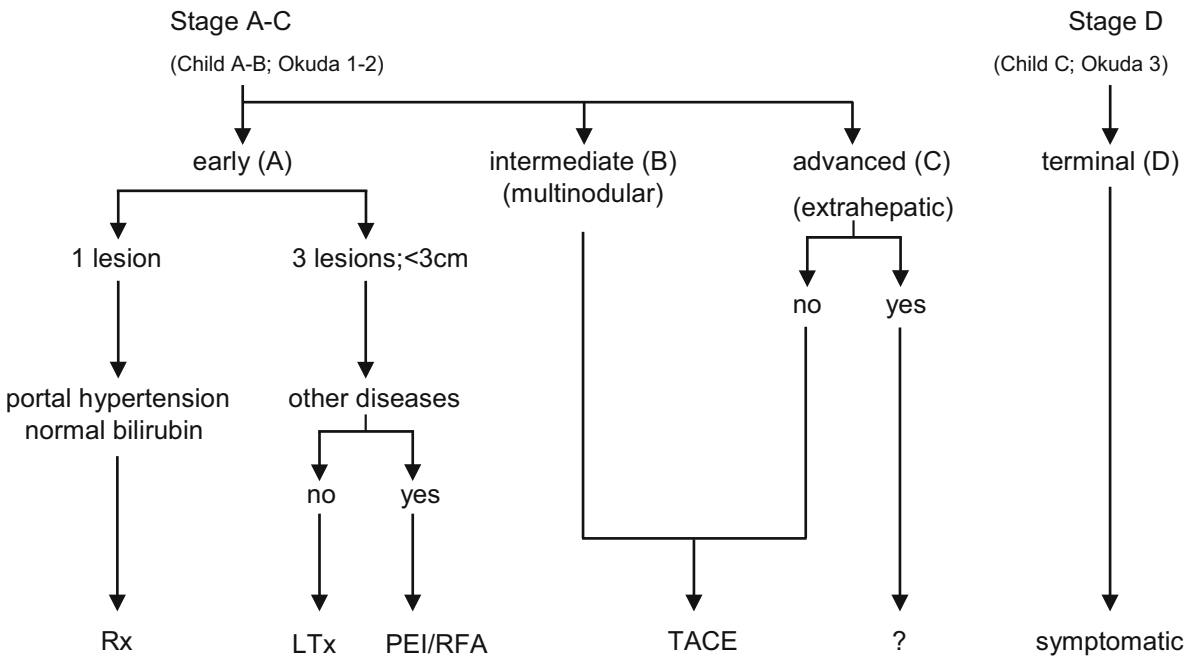

HCC is characterized by arterial hypervascularization, any imaging test needs to be obtained during the arterial phase of contrast enhancement followed by image acquisitions during the portal and venous phase of liver perfusion. Thus, multiphase liver imaging is necessary to allow an appropriate diagnosis of HCC, the number and size of tumor nodules and their location to correctly plan local ablation treatments. If there is a history of bone pain and/or the serum alkaline phosphatase is disproportionately elevated a bone scan or whole body MR imaging is necessary to rule out bone metastases (Nakanishi et al. 2005). Informed consent has to be obtained 24 h prior to the procedure by the latest.

13.3.3.2 Imaging Considerations

PEI is most commonly performed under US guidance (see Sect. 13.3.3.3). When a single session approach is used, CT is a regularly used technique for performing and monitoring the procedure. MR imaging can also be used to perform PEI (Adam et al. 1997; Kim et al. 2005). Due to its physicochemical properties, alcohol injection/diffusion can be reliably visualized by MR imaging. In particular, MR-guided PEI is being advantageous in locations unfavorable for CT guidance or in patients in whom iodized contrast media are contraindicated. At MR imaging it is suggested to use an inversion-recovery spin-echo sequence using an inversion time of 250 ms and an echo time of 150 ms in combination with water saturation pulses which effectively suppresses the tissue water signal from human liver while obtaining a high signal from the alcohol (Alexander et al. 1996).

13.3.3.3 Ablation Technique

Puncture and Injection Technique

PEI does not differ much from fine-needle aspiration biopsy. An intravenous access line for sedation and analgesia is established using an intravenous cannula placed in a cubital vein. There is no need for prophylactic antibiotics. The patient's skin is prepped and draped. Then local anesthesia from the skin entry point of the needle down to the liver capsule is administered. For local anesthesia, common local anesthetics such as mepivacain, for sedation midazolam or fen-

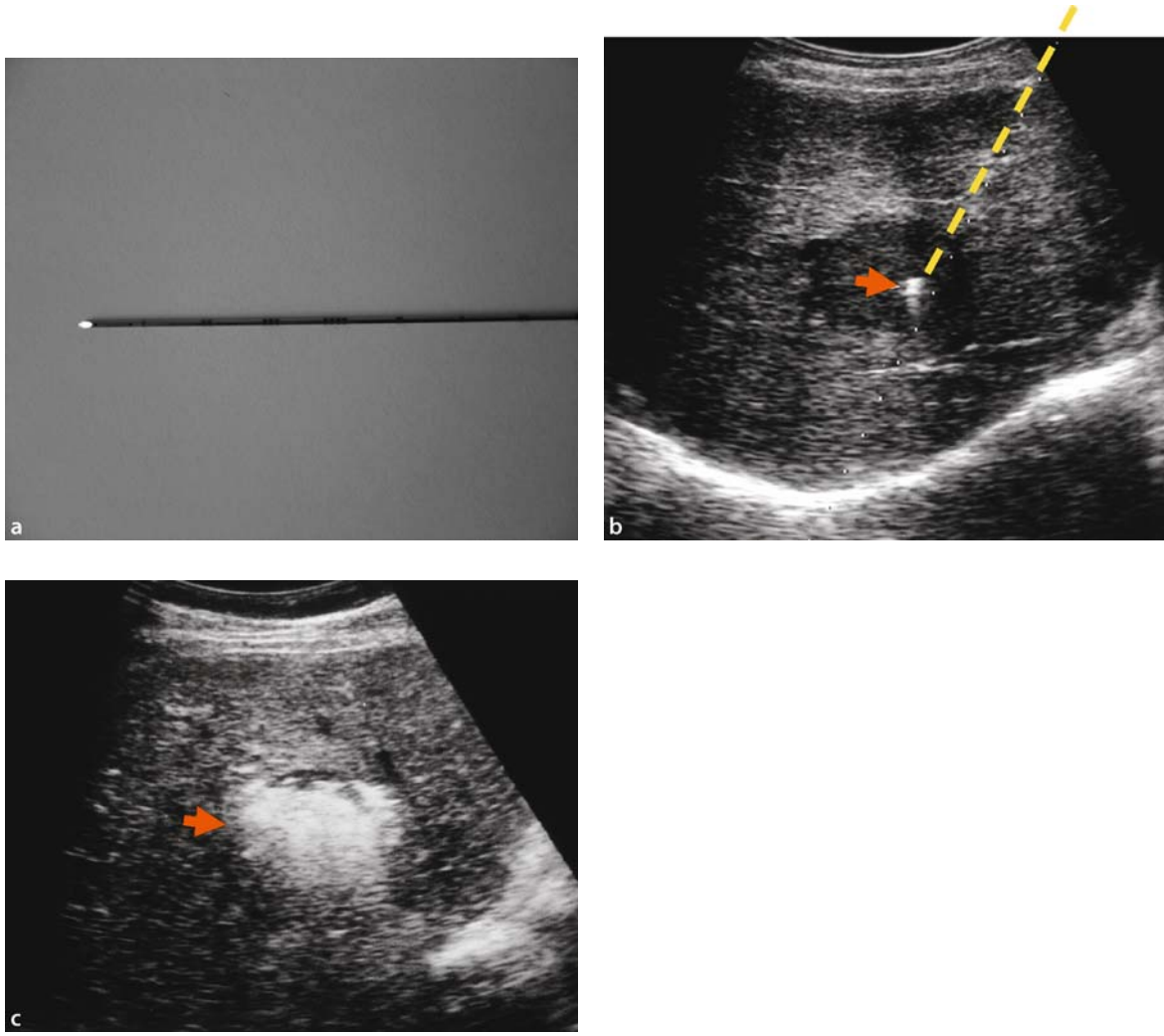

Fig. 13.44 **a** PEI needle: fine-needle with a conical tip, that is closed and releases the alcohol by sideholes. **b** Encapsulated HCC that has been punctured by ultrasound guidance (*yellow line*). The bright echo within the tumor nodule indicates the needle tip (*arrow*). **c** During the course of alcohol injection a dense echogenic cloud (*arrow*) forms with distal acoustic shadowing that makes it difficult to evaluate whether the alcohol has diffused through the entire tumor or not

tanyl and for analgesia piritramid can be used. Subsequently, the tumor is punctured, using a fine-needle (20- to 22-gauge) with a length of 10–20 cm. There are fine-needles that are dedicated to the PEI procedure, whose tips are closed, conical and equipped with several sideholes that release the alcohol (Livraghi 1998). Those needles are preferred because they offer a more homogeneous release of alcohol into the tumor tissue. The needle is passed to the distal margin of the tumor and absolute alcohol is injected slowly while rotating the needle. Ethanol usually spreads within a radius of 1–3 cm around the tip of the needle to the periphery of the tumor (Livraghi 1998). Alternatively, a normal fine needle may be used instead of the needle with the closed conical tip and sideholes. In this case, the alcohol is injected via the endhole without rotating the needle. It is gradually withdrawn towards the proximal edge of the tumor and injection is stopped when the alcohol saturation of the tumor is considered to be total.

For monitoring alcohol distribution within the tumor, either CT or US may be used. On US, which

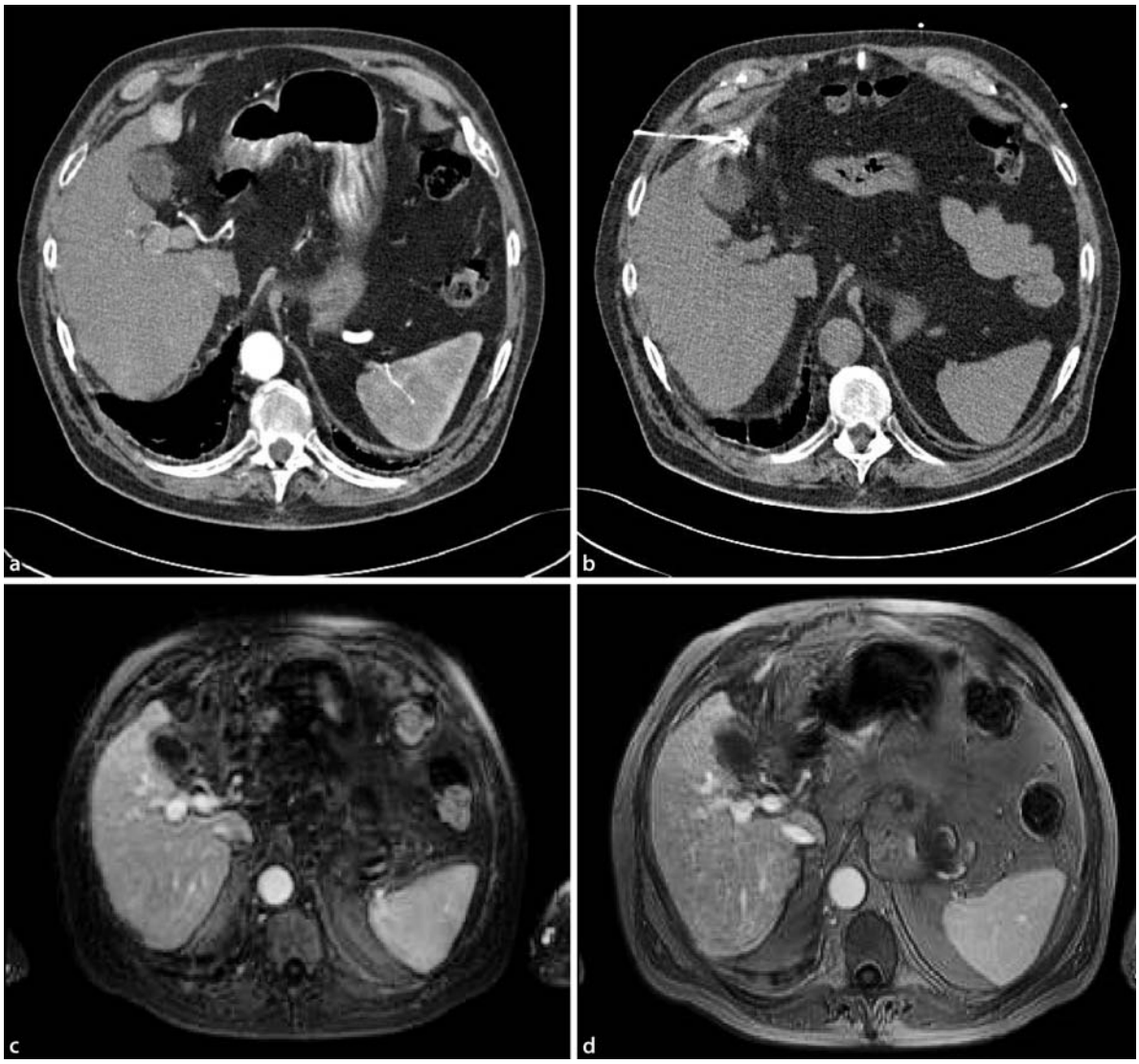

Fig. 13.45 **a** A small HCC is depicted hyperdense on CT during the arterial phase. **b** A PEI needle is positioned within the center of the tumor and contrast material was injected through the needle to estimate the distribution of the alcohol. MR imaging control 24 h later indicates complete necrosis of the tumor without uptake of contrast media during the arterial (**c**) and portal (**d**) venous phase

is well suited for real time imaging of the procedure, the entire tumor appears hyperechoic when it is completely filled with alcohol (Fig. 13.44). For CT monitoring of the alcohol distribution it can be mixed with a little iodinated contrast material (Fig. 13.45). Alternatively the alcohol appears as hypodense area after injection (Fig. 13.46). If alcohol is observed to flow into a blood vessel, bile duct, or leaks outside the tumor into the liver, the needle is repositioned. Depending on the size and shape of the tumor repositioning of the needle is mandatory to not only treat the center but also the edges of the tumor. This prevents tumor tissue to survive in parts isolated by a tumor capsule or intratumorous septae.

After completing the injection, the needle is left in place for 1–2 min to allow the alcohol to diffuse into the tumor and away from the needle tract. Then the

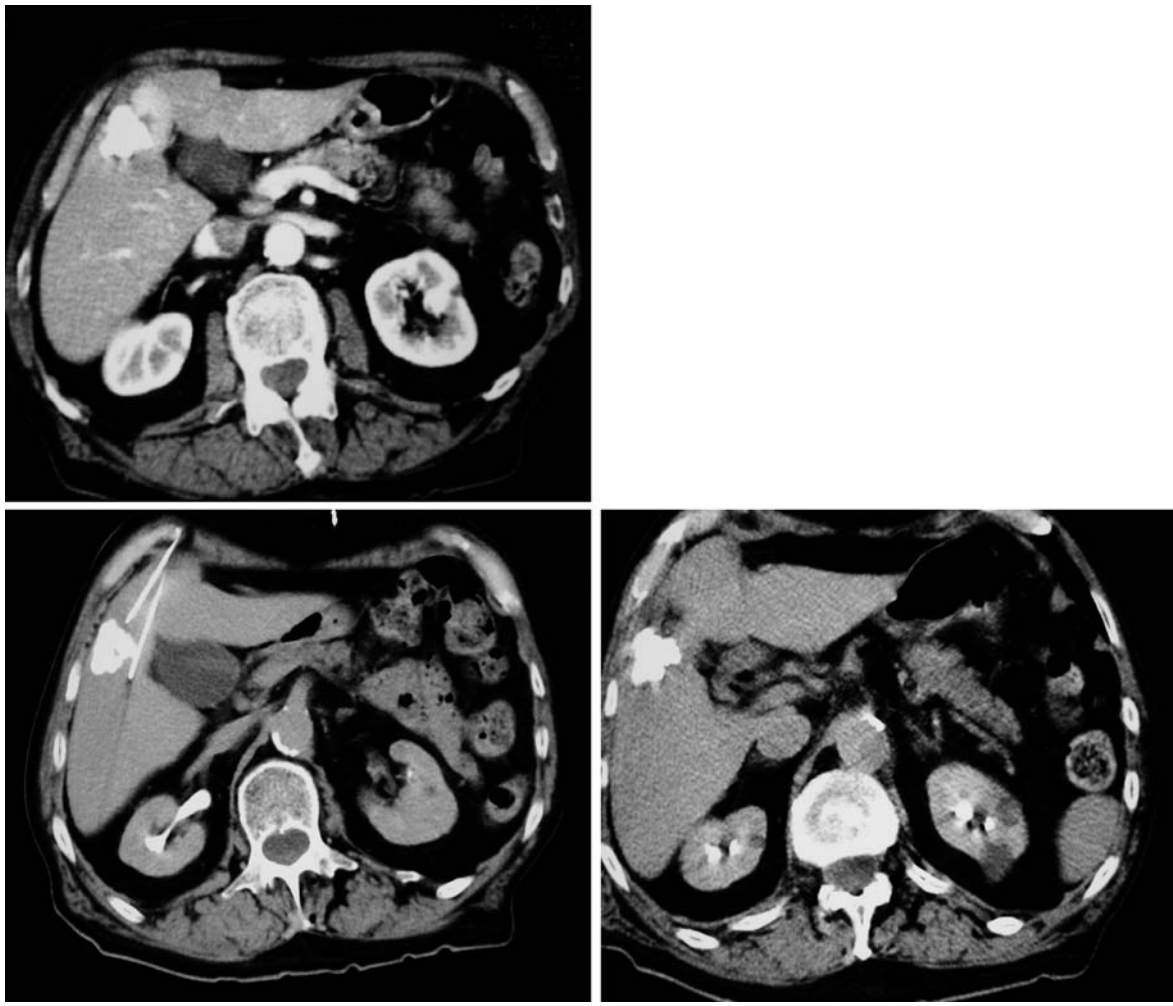

Fig. 13.46 HCC of 5.5 cm in diameter that had been submitted to repeated TACE before. Homogeneous uptake of lipiodol that shows no metabolism over time indicates inactive tumor tissue. However, the CT scan also shows viable tumor next to the lipiodol deposition that therefore selectively was treated by PEI due to its neighborhood to the gall bladder. The control scan shows the distribution of the alcohol that is depicted hypodense at CT

needle is aspirated firmly during withdrawal to minimize leakage since alcohol reflux may cause pain.

Multisession Approach

Most PEI procedures are performed under the US-guidance, allowing one to control not only the puncture itself but also the release of the alcohol into the tumor tissue. Real-time visualization of the alcohol diffusion may be accomplished since microbubbles contained in the injected alcohol are markedly echogenic just after injection. However, in the late course of alcohol injection, a dense echogenic cloud forms with distal acoustic shadowing that makes it difficult to evaluate whether the alcohol has diffused through the entire tumor or not (Fig. 13.44). US guided PEI is an outpatient procedure and the injected volume per session/per tumor varies between 2 and 10 ml. The toxic dose of ethanol is 0.8–1.0 cm^3/kg with a recommended maximum volume of 30–40 ml per session. Tumors smaller than 2 cm are treated by 3–4 sessions, tumors of 2–3.5 cm by 8–12 sessions (Lee et al. 1995). Usually two to four treatment sessions per week

are performed using this US-guided multisession approach (Adam et al. 1997). The end-point of the treatment is the arterial devascularization of the tumor depicted by color-coded duplex sonography.

Single-Session Approach

Multisession treatment of HCC needs the patient to come in regularly to receive PEI. Alternatively, a single-session procedure offers the advantage that the "treatment logistics" are more acceptable for the patient (Fig. 13.45). However, depending on the tumor size, an appropriate volume of absolute alcohol is required to kill the tumor entirely. It is reported to use volumes of 40 ml up to more than 200 ml per session (Livraghi et al. 1998). In order to prevent serious side effects of a single-session treatment, the total volume of alcohol applied to the tumor should not exceed 70 ml. Injection volume may be calculated from the radius of the tumor, using the formula for the volume of a sphere, $4/3\pi \times (\text{radius} + 0.5\,\text{cm})^3$. Here, 0.5 cm is added to the radius to obtain a margin. That means a total volume of 32 ml is necessary to cover a tumor of 3 cm in diameter ($V = 4/3\pi$ (1.5 cm + 0.5 cm)). According to the formula a tumor 4 cm in size should be treated with 65 ml of alcohol and a tumor of 5 cm in diameter needs 113 ml of alcohol to devascularize it entirely. However, it is well accepted to treat HCC $\leq$ 3 cm in diameter by percutaneous tumor ablation only.

To avoid pain sensations to the patient, single-session procedures are usually performed under general anesthesia that results in better control of the procedure. In order to cover sufficiently the entire tumor volume with alcohol, CT guidance is preferred as it may be necessary to position a second, third, fourth or even fifth needle within the tumor (Fig. 13.46). The total amount of alcohol is divided into portions and is injected slowly via the different needles into the tumor. During the injection each needle is gently pulled back within the tumor in order to treat the edges and the center of the tumor equally. The treatment is ended when the entire tumor appears hypodense, or if mixed with contrast material, hyperdense on CT or the calculated total amount of alcohol is injected (Livraghi et al. 1995) (Fig. 13.46).

Single-session treatment offers the advantage that bigger tumors can be treated much faster and more fully, which may well be documented by a CT/MRI scan 24 h postprocedurally (Fig. 13.46). In the case of incomplete ablation, a second treatment session should be scheduled instead of increasing the total amount of alcohol.

Combined Treatment Approaches

By solely using PEI, complete necrosis can be achieved in 70–92% of cases of tumors $\leq$ 3 cm (Ikeda et al. 2001; Lin et al. 2004; Livraghi et al. 1999). Efficacy of PEI decreases with increasing tumor size. Therefore combined approaches were sought. HCC $>$ 3 cm in size should be treated by TACE first and then in a second step by percutaneous ablation. TACE significantly reduces arterial inflow into the tumor and breaks down intratumoral septae. Persistent/recurrent ischemia by repeated TACE improves the effect of PEI as the alcohol may diffuse more easily within the tumor and, on the other hand, its wash-out is minimized due to the reduced arterial in- and outflow. As a consequence, additional PEI may be performed with reduced amounts of alcohol to reach entire devascularization of the tumor. Combined procedures to treat HCC $>$ 3 cm always start with repeated TACE. CT helps to judge the uptake of lipiodol into the tumor as well as its metabolism. Areas of the tumor that show a persistent uptake of lipiodol are supposed to be inactive for the moment as the tumor is not capable to metabolize it (Fig. 13.46). Thus, single-session PEI may be steered according to the uptake of lipiodol and the results obtained by multiphase contrast enhanced CT or MR imaging of the liver. CT imaging enables, on the one hand, positioning of the needles into all parts of the tumor in order to cover it completely with alcohol. On the other hand, the total amount of alcohol injected into the tumor is divided into portions aiming predominantly at the viable areas of the tumor (Fig. 13.46). As a result, parts of the tumor with persistent uptake of lipiodol receive less alcohol compared to those that show a marked contrast enhancement at CT/MR imaging. As mentioned before, single-session treatment should not exceed 70 ml of absolute alcohol. Due to repeated TACE prior to the PEI procedure in HCC $>$ 3 cm, it is recommended to consider the maximum diameter of the tumor to calculate the total amount of alcohol. Although this is only subject to

personal experiences, a tumor of 3 cm, 4 cm, 5 cm, 6 cm and 7 cm in diameter may sufficiently be treated by 30 ml, 40 ml, 50 ml, 60 ml and 70 ml of alcohol, respectively.

13.3.4 Results

PEI is efficient in the treatment of HCC and may achieve a complete tumor necrosis in more than 80% of tumors smaller than 3 cm in diameter. However, response rates decrease with growing size of HCC and tumor necrosis is obtained in only 50% of tumors measuring 3–5 cm in diameter (Lencioni and Crocetti 2005; Livraghi et al. 1995). Histopathology reveals complete coagulation necrosis after PEI in 70% of tumors smaller than 3 cm in diameter and no damage to healthy tissue surrounding the tumor. The 5-year survival of patients with an HCC < 3 cm treated by PEI ranges between 48% and 78% (Arii et al. 2000; Ebara et al. 2005; Lencioni et al. 1997; Livraghi et al. 1995, 2004; Omata et al. 2004; Sakamoto and Hirohashi 1998). Recent long term data with 20 years of follow-up show that Child A patients with a solitary tumor smaller than or equal to 2 cm in diameter have better long-term outcomes compared to patients with a 2–3-cm HCC (Ebara et al. 2005). They not only have the best overall survival, but also show significantly less tumor recurrences that usually develop from the treated nodule. Those results are confirmed by a recent study by Sala et al. (2005). Independent predictors of survival are:

- Initial complete response
- Child–Pugh score
- Number or size of nodules
- Base-line alpha-fetoprotein levels

The major limitation of PEI is the high local recurrence rate that may reach 33% in tumors smaller than 3 cm and 43% in tumors exceeding 3 cm (Khan et al. 2000; Koda et al. 2000).

When considering PEI as a treatment option in HCC, one has to keep in mind that radiofrequency (RF) ablation is superior to PEI with 80% vs 90% of complete response rates in tumors ≤ 3 cm. This has been achieved in a substantially lower number of treatment sessions (Livraghi et al. 1999). A similar study in 119 patients with solitary HCC less than 3 cm in diameter treated either by RF ablation or PEI shows complete tumor responses in 100% and 94% of patients, respectively (Ikeda et al. 2001). RF ablation needed 1.5 vs 4 treatment sessions in the PEI group. Lencioni et al. (2003) performed a prospective randomized analysis of RF ablation vs PEI in small HCC and reports an overall 1- and 2-year survival of 100% and 98% compared to 96% and 88% which has not been statistically significant. However, the 1- and 2-year local recurrence-free survival has been significantly higher using thermal ablation (98% and 96% vs 83% and 62%). Currently, there are three other randomized controlled trials comparing RF ablation vs PEI in early-stage HCC that confirm the superiority of RF ablation vs PEI treatment (Lin et al. 2004, 2005; Shiina et al. 2005). Lin et al. (2004, 2005) report survival advantages of RF ablation in a subgroup of tumors larger than 2 cm compared to either percutaneous ethanol or acetic acid injection. As a result RF treatment is confirmed as an independent prognostic factor for local recurrence-free survival by multivariate analysis (Lencioni et al. 2003).

Percutaneous acetic acid injection seems to be advantageous compared to ethanol injection, too (Tsai et al. 2008). According to recent data, the local recurrence rate and new tumor recurrence rate are reported to be similar between alcohol and acetic acid injection. However, acetic acid injection resulted in a significantly better survival and multivariate analysis revealed acetic acid to be the significant factor associated with overall survival. In addition, the treatment sessions required to achieve complete tumor necrosis were significantly fewer using acetic acid. Although RF ablation as well as acetic acid injection tend to be superior to alcohol with respect to local tumor control and patient survival, PEI is a safe and well established technique for local tumor ablation. Worldwide it has been successfully used for decades and because of its low-cost and availability PEI will remain a treatment option of HCC in the near future.

Most recent data suggest PEI to be an important modulator of tissue properties prior or directly during RF ablation. Tissue modulation with alcohol lowers the boiling point of the tissue resulting in reduced ablation times. According to Kurokohchi et al. (2005), injection of alcohol prior to RF ablation may equally enhance the volume of coagulated necrosis in three dimensions regardless of types of RFA instruments. It has been demonstrated that the volumes of coagulated necrosis were significantly larger in the group

of patients treated by PEI and RF ablation compared to HCC patients treated by RF ablation alone. The amount of total energy required was comparable between both groups and it was concluded that the energy needed for coagulation per unit volume is significantly lower in case of a combined treatment by PEI and RF ablation. Furthermore, the volume of coagulated necrosis showed a stronger correlation with the amount of alcohol injected than the total energy requirements, respectively. Obviously, less energy is required when combining PEI and RF ablation to induce ablation areas similar to those that may be obtained by RF ablation alone. In addition, antitumoral effects of PEI may lower recurrence rates when combined with RF ablation (Kurokohci et al. 2005).

It has been demonstrated that TACE combined with alcohol injection has the potential to prolong survival compared to TACE alone in small HCC (Koda et al. 2001) and even in nodules with a mean size of 8 cm (Lubienski et al 2004). A retrospective evaluation of patients suffering from large HCC with a medium size of 8.6 cm $\pm$ 4.5 cm and multifocal disease in 46% of cases compared efficacy of TACE alone and TACE combined with PEI (Lubienski et al. 2004). It reported an overall 1-, 2- and 3-year survival of 21%, 4% and 4% compared to 55%, 39% and 22% which has been statistically significant. There are several other studies (Cheng et al. 2008; Georgiades et al. 2008; Guan and Liu 2006; Kurokohchi et al. 2006) that forecast a better outcome of HCC patients if treated by a combination of arterial devascularization and percutaneous ablation such as PEI or RFA. Thus, quality of life, survival without local recurrence as well as long-term survival are significantly improved by a combination therapy in HCC $\geq$ 3 cm.

13.3.5 Complications

Care has to be taken to avoid direct injection of ethanol into the hepatic veins, because a sudden and high concentration of ethanol in terms of a bolus may lead to prolonged hypoxemia with cardiopulmonary arrest (Livraghi 1998). Livraghi et al. (1998) reported a significant higher rate of mortality (0.1% vs 4.6%) while performing single-session treatment under general anesthesia. However, alcohol volumes of more than 200 ml had been used that should strictly be avoided.

A major concern of percutaneous tumor ablation is seeding along the needle tract. Because injected alcohol damages cancer cells immediately (Shiina et al. 1991), seeding of cancer cells is unlikely to occur. Nevertheless, it has been reported in $< 0.01-0.6\%$ of patients (di Stasi et al. 1997; Livraghi et al. 1995). Altogether, PEI results in low complication rates (morbidity 1.7%) and a negligible rate of treatment related deaths (mortality 0.1%).

Summary

In most centers PEI has an accepted role in the treatment strategy of small HCC. When surgical techniques are precluded in patients with early-stage tumors, PEI is generally regarded as a second choice treatment (Llovet et al. 2003). In those patients RFA is the first choice treatment since complete tumor necrosis that may be achieved in small tumors is significantly higher using thermal ablation techniques. Combined treatments using TACE and PEI have the potential to prolong survival compared to TACE alone in small HCC. Even stage B and C patients, according to the Barcelona Clinic Liver cancer staging classification, may profit from additional PEI as far as they are candidates for TACE. The final role of PEI in combination with RFA is not established so far since there is no sufficient study evidence.

Key Points

- PEI is a cheap, easy and safe procedure in the treatment of HCC.
- PEI may only be used in cirrhotic livers and has no effect in non-cirrhotic patients suffering from HCC.
- Single session treatment appears advantageous when compared with multisession treatment.
- PEI is generally regarded as a second choice treatment of HCC compared to RF ablation.
- Small HCC may be treated by RF ablation or PEI alone.
- Combined therapies including TACE and RF ablation or PEI markedly increase efficacy of treatment of HCC $\geq$ 3 cm.
- Combining PEI and RF ablation may lower recurrence rates; however, the final role of this combination is not definitely established due to the lack of study evidence.

References

Adam G, Neuerburg J, Bucker A et al. (1997) Interventional magnetic resonance. Initial clinical experience with a 1.5-tesla magnetic resonance system combined with c-arm fluoroscopy. Invest Radiol 32:191–197

Alexander AL, Barrette TR, Unger EC (1996) Magnetic resonance guidance of percutaneous ethanol injection in liver. Acad Radiol 3:18–25

Arii S, Yamaoka Y, Futugawa S et al. (2000) Results of surgical and nonsurgical treatment for small-sized hepatocellular carcinomas: a retrospective and nationwide survey in Japan. Hepatology 32:1224–1229

Bruix J, Sherman M, Llovet JM et al. (2001) For the EASL Panel of Experts on HCC. Clinical management of hepatocellular carcinoma. Conclusions of the Barcelona-2000 EASL Conference. J Hepatol 35:421–430

Cheng BQ, Jia CQ, Liu CT et al. (2008) Chemoembolization combined with radiofrequency ablation for patients with hepatocellular carcinoma larger than 3 cm: a randomized controlled trial. JAMA 299:1669–1677

Chu CH, Chuang MJ, Wang MC et al. (2003) Sclerotherapy of thyroid cystic nodules. J Formos Med Assoc 102:625–630

Di Stasi M, Buscarini L, Livraghi T et al. (1997) Percutaneous ethanol injection in the treatment of hepatocellular carcinoma. A multicenter survey of evaluation practices and complication rates. Scand J Gastroenterol 32:1168–1173

Ebara M, Okabe S, Kita K et al. (2005) Percutaneous ethanol injection for small hepatocellular carcinoma: therapeutic efficacy based on 20-year observation. J Hepatol 43:458–464

Festi D, Monti F, Casanova S et al. (1990) Morphological and biochemical effects of intrahepatic alcohol injection in the rabbit. J Gastroenterol Hepatol 5:402–406

Georgiades CS, Hong K, Geschwind JF (2008) Radiofrequency ablation and chemoembolization for hepatocellular carcinoma. Cancer J 14:117–122

Guan YS, Liu Y (2006) Interventional treatments for hepatocellular carcinoma. Hepatobiliary Pancreat Dis Int 5:495–500

Ikeda M, Okada S, Ueno H et al. (2001) Radiofrequency ablation and percutaneous ethanol injection in patients with small hepatocellular carcinoma: a comparative study. Jpn J Clin Oncol 31:322–326

Khan KN, Yatsuhashi H, Yamasaki K et al. (2000) Prospective analysis of risk factors for early intrahepatic recurrence of hepatocellular carcinoma following ethanol injection. J Hepatol 32:269–278

Kim YJ, Raman SS, Yu NC et al. (2005) MR-guided percutaneous ethanol injection for hepatocellular carcinoma in a 0.2T open MR system. J Magn Reson Imaging 22:566–571

Koda M, Murawaki Y, Mitsuda A et al. (2000) Predictive factors for intrahepatic recurrence after percutaneous ethanol injection therapy for small hepatocellular carcinoma. Cancer 88:529–537

Koda M, Murawaki Y, Mitsuda A et al. (2001) Combination therapy with transcatheter arterial chemoembolization and percutaneous ethanol injection compared with percutaneous ethanol injection alone for patients with small hepatocellular carcinoma: a randomized control study. Cancer 92:1516–1524

Kurokohchi K, Watanabe S, Masaki T et al. (2005) Comparison between combination therapy of percutaneous ethanol injection and radiofrequency ablation and radiofrequency ablation alone for patients with hepatocellular carcinoma. World J Gastroenterol 11:1426–1432

Kurokohchi K, Hosomi N, Yoshitake A et al. (2006) Successful treatment of large-size advanced hepatocellular carcinoma by transarterial chemoembolization followed by the combination therapy of percutaneous ethanol-lipiodol injection and radiofrequency ablation. Oncol Rep 16:1067–1070

Lee MJ, Mueller PR, Dawson SL et al. (1995) Percutaneous ethanol injection for the treatment of hepatic tumors: indications, mechanism of action, technique, and efficacy. AJR Am J Roentgenol 164: 215–220

Lencioni R, Crocetti L (2005) A critical appraisal of the literature on local ablative therapies for hepatocellular carcinoma. Clin Liver Dis 9:301–314

Lencioni R, Pinto F, Armillotta N et al. (1997) Long-term results of percutaneous ethanol injection therapy for hepatocellular carcinoma in cirrhosis: a European experience. Eur Radiol 7:514–519

Lencioni RA, Allgaier HP, Cioni D et al. (2003) Small hepatocellular carcinoma in cirrhosis: randomized comparison of radiofrequency thermal ablation versus percutaneous ethanol injection. Radiology 228:235–240

Lin SM, Lin CJ, Lin CC et al. (2004) Radiofrequency ablation improves prognosis compared with ethanol injection for hepatocellular carcinoma $\leq$ 4 cm. Gastroenterology 127: 1714–1723

Lin SM, Lin CJ, Lin CC et al. (2005) Randomised controlled trial comparing percutaneous radiofrequency thermal ablation, percutaneous ethanol injection, and percutaneous acetic acid injection to treat hepatocellular carcinoma of 3 cm or less. GUT 54:1151–1156

Livraghi T (1998) Percutaneous ethanol injection in the treatment of hepatocellular carcinoma in cirrhosis. Hepato-Gastroenterology 45:1248–1253

Livraghi T, Giorgio A, Marin G et al. (1995) Hepatocellular carcinoma and cirrhosis in 746 patients: long-term results of percutaneous ethanol injection. Radiology 197:101–108

Livraghi T, Benedini V, Lazzaroni S et al. (1998) Long term results of single session percutaneous ethanol injection in patients with large hepatocellular carcinoma. Cancer 83: 48–57

Livraghi T, Goldberg SN, Lazzaroni S et al. (1999) Small hepatocellular carcinoma: treatment with radio-frequency ablation versus ethanol injection. Radiology 210:655–661

Livraghi T, Meloni F, Morabito A et al. (2004) Multimodal image-guided tailored therapy of early and intermediate hepatocellular carcinoma: long-term survival in the experience of a single radiologic referral center. Liver Transpl 10: 98–106

Llovet JM, Sala M (2005) Non-surgical therapies of hepatocellular carcinoma. Eur J Gastroenterol Hepatol 17:505–513

Llovet JM, Burroughs A, Bruix J (2003) Hepatocellular carcinoma. Lancet 362:1907–1917

Lubienski A, Bitsch RG, Schemmer P et al. (2004) Langzeitergebnisse der interventionellen Therapie von großen, inoperablen hepatozellulären Karzinomen (HCC): signifikanter Überlebensvorteil von transarterieller Chemoembolisation (TACE) und perkutaner Ethanolinjektion (PEI) gegenüber der TACE-Monotherapie. Fortschr Röntgenstr 176: 1794–802 [German]

Nakanishi K, Kobayashi M, Takahashi S et al. (2005) Whole body MRI for detecting metastatic bone tumor: comparison with bone scintigrams. Magn Reson Med Sci 4:11–17

Omata M, Tateishi R, Yoshida H et al. (2004) Treatment of hepatocellular carcinoma by percutaneous tumor ablation meth-

ods: ethanol injection therapy and radiofrequency ablation. Gastroenterology 127:159–166
Sakamoto M, Hirohashi S (1998) Natural history and prognosis of adenomatous hyperplasia and early hepatocellular carcinoma: multi-institutional analysis of 53 nodules followed up for more than 6 months and 141 patients with single early hepatocellular carcinoma treated by surgical resection or percutaneous ethanol injection. Jpn J Clin Oncol 28: 604–608
Sala M, Llovet JM, Vilana R et al. (2005) Barcelona Clinic Liver Cancer Group. Initial response to percutaneous ablation predicts survival in patients with hepatocellular carcinoma. Hepatology 40:1352–1360
Shiina S, Tagawa K, Unuma T et al. (1991) Percutaneous ethanol injection therapy for hepatocellular carcinoma: a histopathologic study. Cancer 68:1524–1530
Shiina S, Teratani T, Obi S, Sato S et al. (2005) A randomized controlled trial of radiofrequency ablation with ethanol injection for small hepatocellular carcinoma. Gastroenterology 129:122–130
Tsai WL, Cheng JS, Lai KH et al. (2008) Review article: percutaneous acetic acid injection versus percutaneous ethanol injection for small hepatocellular carcinoma – a long-term follow-up study. Aliment Pharmacol Ther 2008 Apr 4 [Epub ahead of print]
Vilana R, Bianchi L, Varela M et al. (2006) Is microbubble-enhanced ultrasonography sufficient for assessment of response to percutaneous treatment in patients with early hepatocellular carcinoma? Eur Radiol 16:2454–2462
Wang P, Zuo C, Qian Z et al. (2003) Computerized tomography guided percutaneous ethanol injection for the treatment of hyperfunctioning pheochromocytoma. J Urol 170: 1132–1134

13.4 CT-Guided HDR Brachytherapy

Konrad Mohnike and Jens Ricke

13.4.1 Indications

Indications for computed tomography (CT)-guided brachytherapy comprise of unresectable liver and extrahepatic malignancies, unlimited by size or location near risk structures such as liver hilum, gall bladder or large vessels which frequently limit the use of thermal techniques such as radiofrequency or laser ablation.

The majority of indications targets large liver metastases of colorectal or other primary cancers as well as hepatocellular carcinoma (HCC) or cholangiocarcinoma. Patients should not be eligible for surgical resection with curative intent, and local ablation must be part of a multimodal therapeutic management. In most patients with metastatic disease, local ablation serves to enable a pause of chemotherapy, or as a salvage approach if systemic therapies are not well tolerated. In any case, systemic therapy should be stopped two weeks before the procedure and should not started earlier than one week after the intervention to avoid cumulative toxic effects, e.g. from radiosensitising agents. Almost any tumor location outside the central nervous system has been described to be eligible for brachytherapy. Outside the liver, specifically lung tumors at difficult locations close to the lung hilum, but also tumors with pleural or mediastinal infiltration dominate the list of indications (Amthauer et al. 2006; Bergk et al. 2005; Ricke et al. 2004a; Wieners et al. 2006).

Eligibility criteria include a preserved hemostasis, but diminished liver function is a relative contraindication only because it may be the leading prognostic factor, and local tumor ablation may not help to improve the patient's prognosis. Interventions in patients with high bilirubin levels > 3 mg/dl or liver cirrhosis Child–Pugh B or even C have been performed successfully in selected cases.

13.4.2 Material and Technique

Beside the typical material used for cross-sectional image-guided procedures like sterile drapings, povidone-iodine or scalpel for skin incision, some dedicated material needs to be on hand:

- 18G puncture needle of various length
- 6F-introducer sheath (25 cm length)
- Stiff angiographic guide-wire
- Brachytheraphy catheters
- Gelfoam

The placement of the applicators usually is performed using CT-fluoroscopy. As the common 16G brachytherapy catheters have a closed tip, a sheath needs to be used for application in the tumor volume. The sheath itself may be a regular 6F vascular sheath of appropriate length (commonly up to 25 cm). A hydrophilic coating has proven to minimize patient discomfort when the sheath is pushed through the liver capsule. For sheath placement, an 18G puncture needle is placed in the according position, and exchanged against the sheath over a very stiff angiographic guide wire. If the guide wire has a soft tip it should be used with the stiff end going in first.

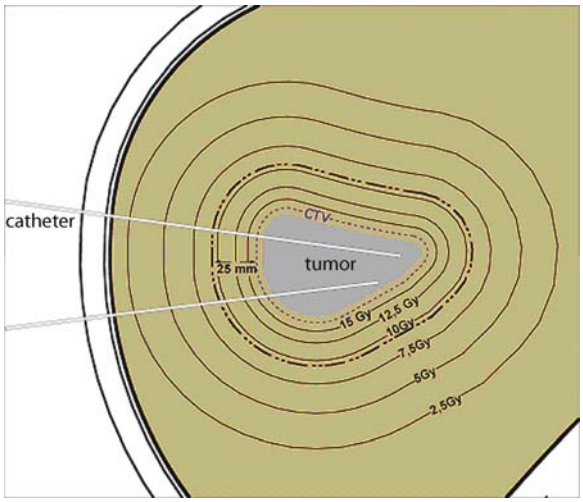

Fig. 13.47 Isodose distribution in CT-guided HDR-brachytherapy of a liver lesion. Radiographic tumor volume (*grey*), clinical target volume (tumor volume and safety margin, *dotted line*) and dose distribution around the tumor (courtesy of M. Seidensticker). Note the steep dose gradient outside the clinical target volume

For treatment planning purposes, a spiral CT of the liver enhanced by i.v. application of iodinated contrast media is acquired after catheter placement in breath-hold technique and transferred to the treatment planning unit. Electronic data handling with DICOM data transferred directly from CT or magnetic resonance (MR) into the treatment planning system is helpful.

Definition of the catheter positions and tumor boundaries in the 3D-CT dataset is performed using a dedicated software system which in most cases will be integrated in the afterloading unit (Figs. 13.47 and 13.48). The high-dose-rate (HDR) afterloading system employs a ^{192}Iridium source of 10 Ci. The source diameter is usually < 1 mm. Dwell positions are located every 5 mm.

In the majority of patients, a reference dose between 15 and 25 Gy is prescribed, which is by definition identical with the minimum dose enclosing the lesion, and applied as a single dose. Even though no appropriate comparison is available, colorectal metastases will most likely need higher doses than breast cancer or hepatocellular carcinoma to achieve long term local tumor control (see Sect. 13.4.3).

CT guidance for catheter placement has some drawbacks. In liver intervention, numerous lesions will be masked on non-enhanced imaging. During the intervention, non-enhanced fluoroscopy can be used to determine the target, often visually correlated with anatomic landmarks and corrected using previous MR imaging examinations. As a result, it may sometimes be necessary to reposition or add catheters after acquisition of the contrast-enhanced CT dataset. Furthermore, tumor volume is systematically underestimated in contrast-enhanced CT compared to MR imaging (Pech et al. 2008). For this reason, MR-guidance using open MR systems may in future become state of the art specifically for liver tumor ablation.

To prevent bleeding, Gelfoam embolization should be performed during step-by-step removal of the sheath.

13.4.3 Dose Considerations

CT-guided brachytherapy in some ways opposes the mainstream in radiotherapy today. The key issue in traditional electron beam percutaneous irradiation is to deliver a dose from an external source with optimal homogeneity in the target volume. In interstitial brachytherapy, things are very different, and its inherent character is that the dose is delivered with substantial heterogeneity, since the radiation source is located at several widely distributed positions inside the tumor volume. It is quite obvious that a very dense catheter distribution will increase the degree of homogeneity – however, the primary goal of catheter positioning for therapy is not the dose homogeneity inside the tumor, but the minimal (and hopefully lethal) dose delivered in the clinical target volume (CTV, tumor plus safety margin) as well as the dose gradient outside the CTV. The dose gradient outside the CTV is decisive to spare adjacent risk organs as well as healthy tissue (e.g., functional liver parenchyma). As a rule of thumb, 1 catheter per 1–2 cm tumor diameter is used by our group, and preplanning of the catheter positions by a medical physicist previous to the intervention may prove helpful specifically in very large tumor volumes or if risk organs are close. However, the inherent advantage of the overall technique remains the ability to vary radiation time at each given dwell position following diligent calculations of the optimal dosimetry after the catheters have been positioned in the tumor. Out of experience, even for senior interventionalists, the final catheter positions will be somewhat different from any preplan.

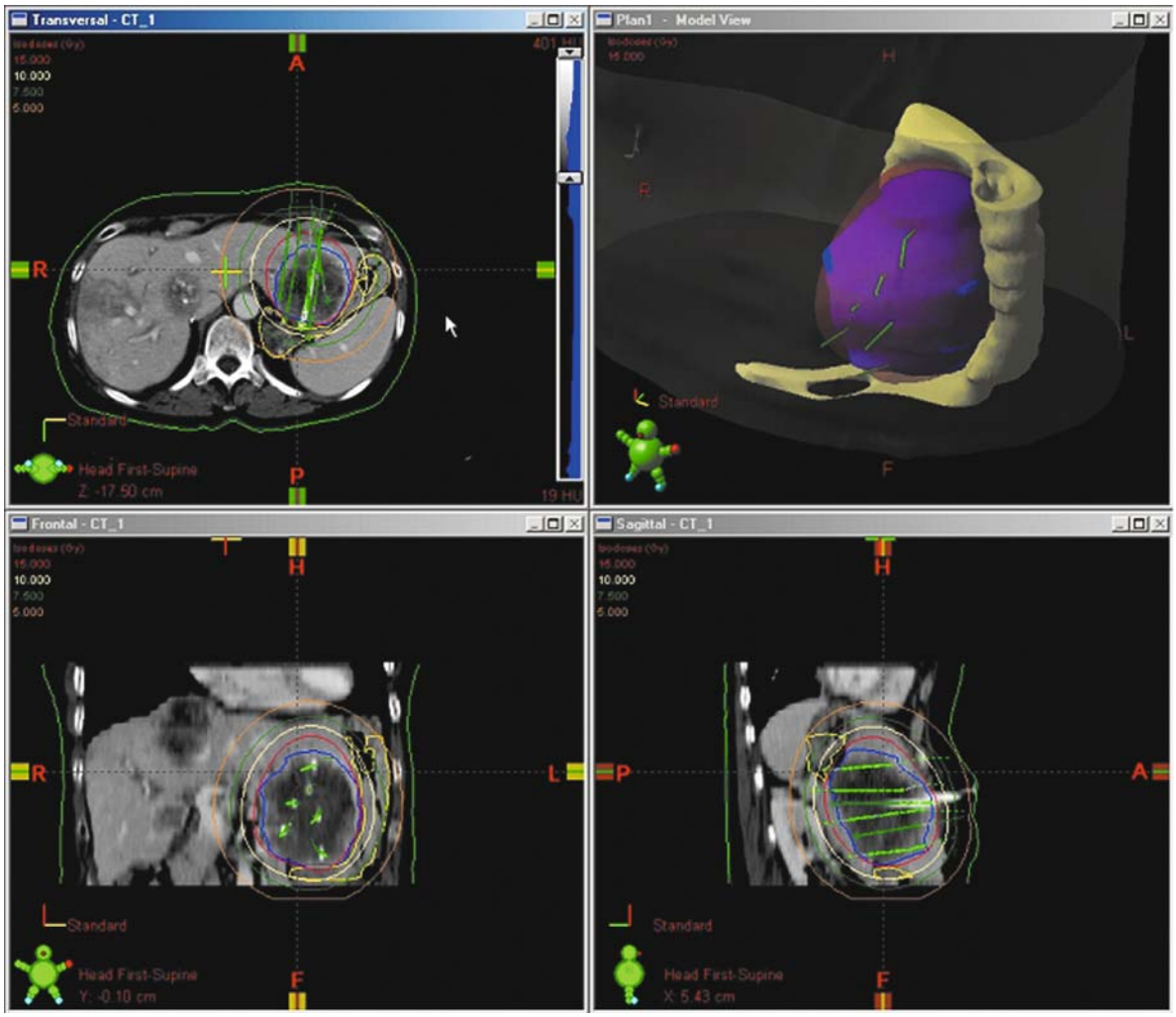

Fig. 13.48 Liver metastasis of colorectal carcinoma after application of six brachytherapy catheters. Isodose distribution as calculated by BrachyVision® (Varian, Palo Alto, CA, USA). The two other lesions visible had been treated in previous sessions

No maximum dose constraints are given inside the tumor volume, but the total irradiation time has to be carefully considered. Iridium sources decay and have to be exchanged in regular intervals. A correction factor is applied to ensure that the dose prescribed is delivered irrespective of the source's age. However, if source exchange is undertaken only every 8 or even every 12 weeks, radiation time may be prolonged by a factor greater than 2. No threshold radiation time can be given but it is obvious that prolonged radiation bares the risk of increased rates of adverse events, starting with general symptoms of radiation toxicity such as nausea and vomiting up to 48 h after treatment. In our own patients radiation time typically ranges between 20 and 40 min. However, we regard 60 min as the preferred maximum irradiation time that should be given, and we have not encountered unexpected toxicity in more than 1000 applications. However, directly after extraction of the catheters, severe and uncontrolled postprocedural shivering may molest the patient in some cases, usually without accompanying fevers but sometimes associated with a vasovagal reaction. We hypothesize that this event is not related to the total radiation time, but induced by extraction of the brachytherapy catheters triggering endotoxine release from lytic tumor cells into tumor blood vessels.

If a total irradiation time of 60 min is expected to be exceeded either due to a high iridium source

factor or due to a very large tumor volume to be treated, the intervention may be divided into two or even three steps. In tumors or tumor conglomerates exceeding 8 cm diameter it may be recommended to perform two interventions. In a first session, one half of the tumor may be treated; preplanning of the catheter positions during the second session for the other half of the tumor is suggested to minimize radiation overlap.

The minimal single fraction dose covering the CTV, which is necessary to achieve long-term local tumor control, varies considerably between tumor biologies. In addition, tumor volume influences the dose necessary – the higher the cell count, the higher the applied radiation dose should be. Randomized data is available for colorectal or breast cancer metastases as well as HCC (Ricke et al. 2008; Mohnike et al. 2008). HCC as well as breast cancer metastases may be treated with 15 Gy minimal dose inside the CTV, and local control rates after 12 months between 80% and 90% can be expected for tumors with a median size of 4–5 cm. In colorectal cancer, minimal doses inside the CTV unfortunately need to be considerably higher, and local control rates of $>$ 80% after 12 months are limited to tumors covered by 20 Gy at minimum. However, applying a minimal dose 20 Gy may often not be possible in large or multiple large tumor volumes since radiation time or overall patient distress due to potentially multiple treatments may be excessive. Lower doses such as 15 Gy may be applied in these patients in palliative intent, counting on the fact that cytoreduction will nevertheless be extensive and local control will still be around 70% after 12 months in these patients. It is worth mentioning that, at least in the liver, repeated treatments in case of local tumor progression may be performed without a significant increase of toxicity. In an own, yet unpublished, series of 30 patients with liver tumors receiving 2–4 treatment repetitions at the same or nearby locations, no adverse events were recorded.

Since we established CT-guided brachytherapy as an application specifically in liver and lung tumors, we have almost always applied brachytherapy as a single fraction. In some patients, leaving the catheters inside the tumor for two or even three days for repeated irradiation with lower single doses may be an interesting option which has not been systematically followed yet. We have applied this approach in abdominal locations in selected patients with excellent results (e.g. lymphoma or symptomatic peritoneal carcinomatosis from rectal cancer). In these patients, adjacent gut prohibited dose delivery in a single fraction; thus dose might be delivered in three fractions of 5–8 Gy each within two days.

Data on dose tolerance of risk organs may be derived from experiences after percutaneous irradiation or intraoperative brachytherapy. Since percutaneous irradiation usually is applied in multiple fractions, according doses for HDR single fraction brachytherapy must be calculated by applying the $\alpha\beta$-model. Organs at risk for liver intervention include bile duct, gall bladder, spinal cord, stomach, duodenum or colon. From intraoperative brachytherapy it is known that bile duct or gall bladder maybe exposed to 20 Gy without acute or late toxicity, an experience we share with our own patients, where we applied a threshold of 20 Gy per max. 1 ml tissue surface without evident acute or late failures such as bile duct strictures. Applying 15 Gy per max. 1 ml gastric surface will induce a 5% risk of symptomatic stomach ulceration (Streitparth et al. 2006). Stomach protection (e.g. proton pump inhibitors) should be prescribed in all patients where a significant organ exposure cannot be avoided (such as when treating metastases of the left liver lobe).

13.4.4 Results

CT-guided brachytherapy is generally very well tolerated, and analgosedation during the intervention is sufficient in almost all patients.

As for most ablation techniques, data available focuses on technical aspects and local tumor control in phase II studies, even though prospective randomized data is now available for brachytherapy of liver metastases from colorectal carcinoma. Local tumor control after brachytherapy of liver metastases or HCC is similar to thermal techniques, with control rates between 70% and 90% after 12 months. However, in contrast to thermal ablation, size does not necessarily hamper local control when brachytherapy is employed, and local control specifically for large HCC may be $>$ 90%. This is even more remarkable since thermal

ablation of HCC is often limited by high tumor perfusion leading to adverse cooling effects and early local recurrence. In addition, repeated treatments in case of local failure are usually well tolerated specifically in the liver. Even though no reliable data is available, repeated brachytherapy of the identical tumor location in the lung must probably be handled with more caution due to the risk of local bronchial necrosis.

A phase III trial was performed in patients with surgically unresectable liver malignancies of colorectal cancer. All patients displayed failure of second-line chemotherapy or absolute or relative contraindications to chemotherapy (comorbidity, age, general condition). CT-guided brachytherapy was applied repeatedly if technically applicable in case of any tumor progression. In this study, repeated tumor ablation proved to be the dominant prognostic factor, dominating also salvage chemotherapies when applicable (Ricke et al. 2008). No upper size limit for the metastases was applied. Mean local recurrence free survival for all lesions was 34 months (median not reached), and local tumor control demonstrated a strong dose dependency.

In a prospective study of 83 patients presenting 140 lesions of HCC, a matched pair analysis was performed indicating a significant survival benefit of patients compared to best supportive care. Patients presented with a median diameter of 5.1 cm of the largest lesion and a comparatively high proportion of Child B stages of 20%. Median survival achieved was 17 months after the intervention and 36 months after first diagnosis, and survival was strongly associated with the Clip-score (Mohnike et al. 2008).

13.4.5 Complications

Typical side-effects comprise moderate gastric and intestinal toxicity, prevented effectively by peri-interventional antiemetic drugs. These general symptoms of radiation exposure are usually limited to the day of treatment. Subfebrile temperatures up to 1 week after the intervention are frequently observed, as are moderate leucocytosis, and elevated C-reactive protein as well as moderately elevated liver enzymes.

Local bleeding is the most common complication. Diligent Gelfoam embolization during sheath removal is extremely helpful to lower the bleeding risk of patients, and close post interventional monitoring specifically of patients with underlying cirrhosis is mandatory. However, the rate of major bleeding complications requiring blood transfusion or embolization still is $< 5\%$ even in the high risk group. It has to be noted though that specifically in HCC patients additional major complications such as symptomatic pleural effusion or other conditions prolonging the hospital stay make up for a 10% rate of major complications. Complications are associated with the high degree of comorbidity in cirrhotic patients and include transient diminished liver function treated symptomatically post intervention. Close collaboration with hepatologists is extremely valuable in these patients. We have never observed acute encephalopathy due to liver function failure after treatment. Clinically relevant radiation induced liver disease (RILD) has yet not been observed due to the limited irradiation volumes even in cases of advanced cirrhosis. Liver abscesses are another important, but rare complications with less than 0.5%, and bleeding complications are usually limited to cirrhotic patients specifically when portal vein thrombosis is present.

Summary

The inherent advantage of brachytherapy as compared to thermal ablation is the lack of a technical size limit of the target as well as the fact that it may be applied adjacent to risk structures due to its precise dose planning and distribution. Even though CT-guided brachytherapy is more complex than for example radiofrequency (RF)-ablation, its value lies in the broad range of indications it provides. Even very large tumor conglomerates may be treated in multiple steps at a very low risk of adverse events and with only minimal discomfort for the patient. Compared to percutaneous irradiation, again the lack of a size limit is advantageous, as well as the fact that the method is motion independent, which gives it superiority specifically in moving targets such as liver or lung tumors (Pech et al. 2008; Ricke et al. 2004a,b,c, 2005a,b; Streitparth et al. 2006; Wieners et al. 2006).

Key Points

- Local tumor ablation by CT-guided brachytherapy is valuable and may well improve prognosis if patients are selected appropriately.

- Successful application of local ablation depends on careful planning of the individual oncological concept of each patient.
- Brachytherapy bears no technical size limit of the target; it delivers a reliable prediction of the dose distribution unaffected by patient motion, and it may be applied almost anywhere in the body.

References

Amthauer H, Denecke T, Hildebrandt B et al. (2006) Evaluation of patients with liver metastases from colorectal cancer for locally ablative treatment with laser induced thermotherapy – impact of PET with F-18-fluorodeoxyglucose on therapeutic decisions. Nuklearmedizin 45:177–184

Bergk A, Wieners G, Weich V et al. (2005) CT-guided brachytherapy of hepatocellular carcinoma in liver cirrhosis – a novel therapeutic approach. J Hepatol 42:89 [Abstract]

Mohnike K, Pech M, Seidensticker M et al. (2008) A matched pair analysis comparing local ablation of HCC by CT-guided HDR brachytherapy with best supportive care. Submitted

Pech M, Mohnike K, Wieners G et al. (2008) Radiotherapy of liver metastases – comparison of target volumes and dose-volume histograms employing CT- or MRI-based treatment planning. Strahlenther Onkol 184:256–261

Ricke J, Wust P, Wieners G et al. (2004a) Liver malignancies: CT-guided interstitial brachytherapy in patients with unfavorable lesions for thermal ablation. J Vasc Interv Radiol 15:1279–1286

Ricke J, Wust P, Stohlmann A et al. (2004b) CT-guided interstitial brachytherapy of liver malignancies alone or in combination with thermal ablation: phase I–II results of a novel technique. Int J Radiat Oncol Biol Phys 58:1496–1505

Ricke J, Wust P, Stohlmann A et al. (2004c) CT-gesteuerte Brachytherapie. Eine neue perkutane Technik zur interstitiellen Ablation von Lebermetastasen. Strahlenther Onkol 2004;180:274–280 [German]

Ricke J, Seidensticker M, Ludemann L et al. (2005a) In vivo assessment of the tolerance dose of small liver volumes after single-fraction HDR irradiation. Int J Radiat Oncol Biol Phys 62:776–784

Ricke J, Wust P, Wieners G et al. (2005b) CT-guided interstitial single-fraction brachytherapy of lung tumors: phase I results of a novel technique. Chest 127:2237–2242

Ricke J, Mohnike K, Pech M et al. (2008) Local response and impact on survival after local ablation of liver malignancies from colorectal carcinoma by CT-guided HDR-brachytherapy. Submitted

Streitparth F, Pech M, Bohmig M et al. (2006) In vivo assessment of the gastric mucosal tolerance dose after single fraction, small volume irradiation of liver malignancies by computed tomography-guided, high-dose-rate brachytherapy. Int J Radiat Oncol Biol Phys 65:1479–1486

Wieners G, Pech M, Rudzinska M et al. (2006) CT-guided interstitial brachytherapy in the local treatment of extrahepatic, extrapulmonary secondary malignancies. Eur Radiol 16:2586–2593

13.5 High Intensity Focused Ultrasound

13.5.1 Technical Basics of MR-Guided Focused Ultrasound Surgery

Alexander Beck and Susanne Hengst

13.5.1.1 Introduction

The abbreviation HIFUS stands for "High intensity focused ultrasound" and is a totally non-invasive thermoablation method. Usually it is combined with imaging equipment to control the ultrasound beam. The method of choice for imaging is Magnetic Resonance (MR) imaging because it can give both good imaging for targeting and real time thermometry to control thermoablation during ultrasound (US) application (McDannold et al. 2006). HIFUS combined with real time imaging and thermometry by MR imaging has become the method of choice and the technical aspects of this technique will be described in the following chapter. Combination of HIFUS with real time MR imaging is usually abbreviated MRgFUS, which stands for Magnetic Resonance guided focused ultrasound surgery and gives a pretty good short description of this technique.

Probably the first descriptions of US waves for thermal ablation of tissues date back to the first half of the last century and are made by Wood and Loomis (1927) and Lynn et al. (1942). Due to lack of adequate imaging equipment the technique was not widely used and started to become of more clinical relevance with introduction of MR imaging into regular practice. Several authors describe the application of MRgFUS in humans – clinical indications now include several organ systems like brain (Jääskeläinen 2003; Fry and Fry 1960), breast (Gombos et al. 2006), uterus – especially leiomyomas (Hengst et al. 2004), bone (Catane et al. 2007), liver (Hengst et al. 2004; Kopelman et al. 2006) or prostate (Murat et al. 2007).

Limitations for MRgFUS are organ systems that cannot be reached by US waves, especially systems that are anatomically behind structures of high acoustic impedance (for example lung) or patients that are not suitable for MR imaging (for example those with metal implants or cardiac pacemakers). In some cases like brain interventions, additional invasive measures

may be necessary such as skull trepanation to enable access (Jääskeläinen 2003; Fry and Fry 1960).

13.5.1.2 Material

In order to perform MRgFUS treatment an US application unit and a MR-System are needed. In our practice we use a treatment unit (Exablate 2000, Insightec, Haifa, Israel) that is integrated in a regular MR-Scanner table for patient positioning (Signa, General Electric Medical Systems, Milwaukee, USA). Several other vendors provide very similar systems. Each different system is usually integrated into a dedicated MR system and can only be used with that specific hard- and software.

The treatment unit is integrated into the regular patient MR-table. In a central position of this table, the US applicator is placed with a sliding positioning system. The whole system is enclosed in an $83 \times 34 \times 11$ cm basin filled with degassed water and covered by a membrane made of polyvinylchloride. In order to enable acoustic coupling with the patient on top of the membrane a gel-pad and additional degassed water is applied for each treatment – it is essential to perform this preparation carefully to avoid enclosing air bubbles as this might locally increase acoustic impedance and can be a reason for treatment failure or complications like serious skin burns (Hengst et al. 2004).

The ultrasound applicator can be moved in a longitudinal und horizontal axis. It can also be tilted up to 20° in two directions. In combination with a phased array transducer the focus depth of each US application, in the following referred to as a "sonication", can be chosen in the range 5–22 cm. The focus spot size can be switched from small sizes beginning at $2 \times 2 \times 4$ mm up to $10 \times 10 \times 30$ mm or $6 \times 6 \times 45$ mm if larger volumes shall be treated. The maximum energy of the transducer is 1 300 Watts, applied at frequencies of 1–1.5 MHz. This setting in our experience is sufficient to reach temperatures $> 60\,^{\circ}$C needed for treatment within even large sonication spots over an application time of 16–30 s for each spot (Gombos et al. 2006; Hengst et al. 2004; Hindley et al. 2004).

Sufficient temperatures are reached if the proteins within the volume of the sonication spot are denaturized – as a usual parameter, an equivalent time of 240 min exposure at 43 °C is quoted to be sufficient for denaturation (Meshorer et al. 1983; Damianou and Hynynen 1994). The equivalent time $t43$ is estimated by the formula of Sapareto and Dewey (1984). $t43$ is calculated by:

$$t43 = \sum_{t=0}^{t=\text{final}} R^{(43-T)} \Delta t \,,$$

where $t43$ equals the thermal equivalent dose at 43 °C, T is the mean temperature during time Δt, and R is a constant that equals 0.50 above 43 °C and 0.25 below 43 °C. The temperature profiles gathered from MR-thermometry for each voxel are interpolated linearly with a time-step of $\Delta t = 0.1$ second (Sapareto and Dewey 1984; Nathan et al. 2000). Other authors postulate that even shorter $t43$ times are sufficient to denaturize proteins completely if a minimum temperature is reached. Nathan et al. (2000) showed that in a rabbit model a $t43$ of 31.2 equivalent minutes and a minimum temperature of 50.4 °C induce enough thermal stress for protein destruction. In common MRgFUS systems the values of $t43$ are automatically calculated, color coded and displayed for each sonication. This information is mandatory to evaluate the efficacy and progress of each treatment. Real-time imaging of temperature changes within the target volume is necessary to monitor treatment progress and to avoid thermal damage of non-target tissues. On their way to their target, ultrasound waves have to pass through different tissue types. Specific absorption, dispersion and reflection based on different acoustic impedance of tissue reflect differences in speed of sound in different tissue types (i.e. muscle 1 590 m/s, water 1 526 m/s or fat 1 468 m/s). These differences may account for changes of spot position and varying focus characteristics (Hengst et al. 2004; Damianou and Hynynen 1994; Mahoney et al. 2001). Target volume temperature is also influenced by the absorption rate within the target volume and by external cooling effects such as tissue perfusion. These conditions may differ at each individual sonication.

Real time MR-thermometry (Fig. 13.49) may be performed accurately by employing changes of the proton-resonance-frequency (PRF) (Mulkern et al. 1998). The shift in proton-resonance-frequency is nearly linear within the temperature range (40–90 °C) needed for MRgFUS treatments (Wlodarczyk et al. 1999). PRF changes are calculated as changes in phase divided by $2 \times \pi$ multiplied by echo time. Subtraction images based on acquisitions before and during

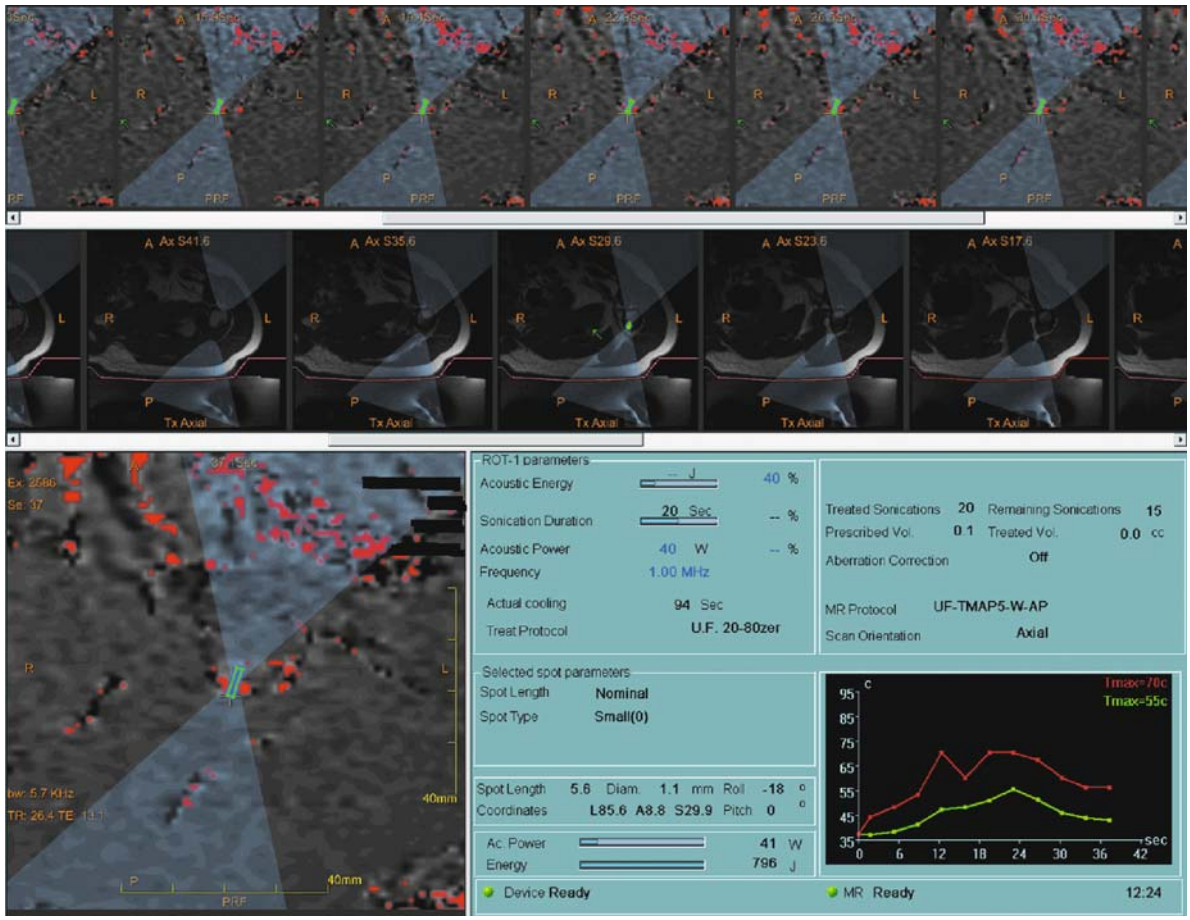

Fig. 13.49 User interface of the MRgFUS system during treatment. The location of one sonication spot is displayed as well as the MR-thermometry over time. In this example, the according temperature has been reached depositing 40 Watts over 20 s duration of the sonication

sonications allow a relatively reliable measurement of temperature changes in and around the target (Hengst et al. 2004; Damianou and Hynynen 1994; Nathan et al. 2000). Post-interventional imaging is commonly based on MR imaging, providing detailed information on treatment success (Fig. 13.50).

13.5.1.3 Complications

Complications are rare and in most cases easy to manage (Hengst et al. 2004). General complications refer to the inevitable use of MR imaging including the application of MR contrast agents. Specific risks of MRgFUS include:

1. Heat development outside the according target occurs in the path of the beam due to acoustic impedance changes: Predominant organ at risk is skin in case of scars, hair, gels or air bubbles at the entry point of the beam. If the patient is awake skin heating will lead to pain and the energy deposition can be adjusted. However, skin burns are very limited in size as a function of the small sonication spots.
2. In abdominal MRgFUS, a rare complication is thermal injury to the bowel. To avoid such an event sonication must not be performed through bowel.
3. The "back-beam" may reach other structures, which are apparently not in the path of the beam. This may include nerves roots along the sacral bone. However, energy deposited through the back-beam most likely is not high enough to provoke serious injuries.

Fig. 13.50 Post treatment T2-weighted image, bone metastasis of the humerus. Note the edema of the lesion in the upper humerus as well as the adjacent tissue (*arrowhead*)

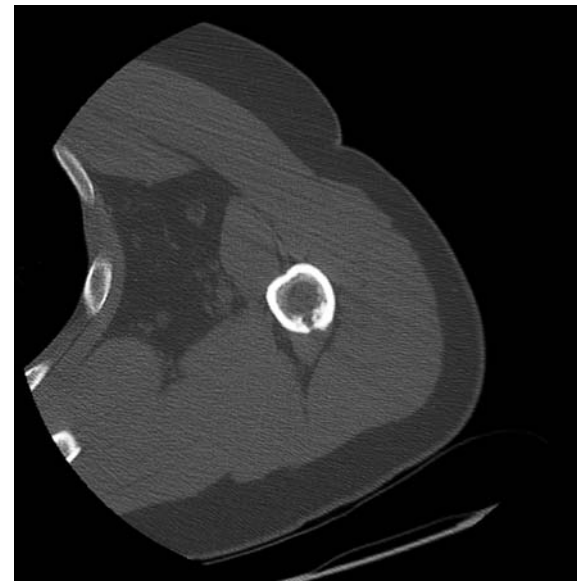

Fig. 13.51 Preinterventional CT of a bone metastasis of the humerus from a cholangiocellular carcinoma (same patient as in Fig. 13.50). Free access from the posterior aspect without nerves or vessels within the expected ultrasound beam path

Summary

MRgFUS is a non-invasive and safe intervention. It offers a unique and non-invasive method for tissue ablation. In combination with MR imaging it is also free from radiation. Unfortunately, access to target volume is a limiting factor.

Key Points

- Accessibility of target-tissue volume is the key to successful MRgFUS treatment (Fig. 13.51).
- Most careful treatment planning will ensure a safe and efficient intervention.
- Temperature mapping allows detailed treatment monitoring.
- If any doubt persists with respect to safety of the beam path, other methods should be considered.

References

Catane R, Beck A, Inbar Y et al. (2007) MR-guided focused ultrasound surgery (MRgFUS) for the palliation of pain in patients with bone metastases – preliminary clinical experience. Ann Oncol 18:163–167

Damianou C, Hynynen K (1994) The effect of various physical parameters on the size and shape of necrosed tissue volume during ultrasound surgery. J Acoust Soc Am 95:1641–1649

Fry WJ, Fry FJ (1960) Fundamental neurological research and human neurosurgery using intense ultrasound. Trans Med Electron ME-7:166–181

Gombos EC, Kacher DF, Furusawa H et al. (2006) Breast focused ultrasound surgery with magnetic resonance guidance. Top Magn Reson Imaging 17:181–188

Hengst SA, Ehrenstein T, Herzog H et al. (2004) Magnetresonanztomographiegesteuerter fokussierter Ultraschall (MRgFUS) in der Tumortherapie – eine neuartige nichtinvasive Therapieoption. Radiologe 44:339–346 [German]

Hindley J, Gedroyc WM, Regan L et al. (2004) MRI guidance of focused ultrasound therapy of uterine fibroids: early results. AJR Am J Roentgenol 183:1713–1719

Jääskeläinen J (2003) Non-invasive transcranial high intensity focused ultrasound (HIFUS) under MRI thermometry and guidance in the treatment of brain lesions. Acta Neurochir Suppl 88:57–60

Kopelman D, Inbar Y, Hanannel A et al. (2006) Magnetic resonance-guided focused ultrasound surgery (MRgFUS): ablation of liver tissue in a porcine model. Eur J Radiol 59:157–162

Lynn JG, Zwemer RL, Chick AJ et al. (1942) A new method for the generation and use of focused ultrasound in experimental biology. J Gen Physiol 26:179–193

Mahoney K, Fjield T, Mcdannold N et al. (2001) Comparison of modelled and observed in vivo temperature elevations induced by focused ultrasound: implications for treatment planning. Phys Med Biol 46:1785–1798

McDannold N, Tempany CM, Fennessy FM et al. (2006) Uterine leiomyomas: MR imaging-based thermometry and thermal dosimetry during focused ultrasound thermal ablation. Radiology 240:263–272

Meshorer A, Prionas SD, Fajardo LF et al. (1983) The effects of hyperthermia on normal mesenchymal tissues. Application of a histologic grading system. Arch Pathol Lab Med 107:328–334
Mulkern RV, Panych LP, McDannold NJ et al. (1998) Tissue temperature monitoring with multiple gradient-echo imaging sequences. J Magn Reson Imaging 8:493–502
Murat FJ, Poissonnier L, Pasticier G et al. (2007) High-intensity focused ultrasound (HIFU) for prostate cancer. Cancer Control 14:244–249
Nathan J, McDannold BS, Randy L et al. (2000) Usefulness of MR imaging-derived thermometry and dosimetry in determining the threshold for tissue damage induced by thermal surgery in rabbits. Radiology 216:517–523
Sapareto SA, Dewey WC (1984) Thermal dose determination in cancer therapy. Int J Radiat Oncol Biol Phys 10:787–800
Wlodarczyk W, Hentschel M, Wust P et al. (1999) Comparison of four magnetic resonance methods for mapping small temperature changes. Phys Med Biol 44:607–624
Wood RW, Loomis AL (1927) The physical and biological effects of high-frequency sound waves of great intensity. London Edinburgh Dublin Phil Mag J Sci 4:417–436

13.5.2 Clinical Application of MR-Guided Focused Ultrasound Surgery

Susanne Hengst and Alexander Beck

13.5.2.1 Introduction

Nowadays most invasive modalities are evaluated not only by their ability to cure but by their side effect profile including the cosmetic, physic and psychological outcome. High intensity focused ultrasound (HIFUS) is an important step on the way to non-invasive surgery. In fact, ultrasound (US) was first researched due to its therapeutic possibilities before starting its successful use in diagnostics. Today, specifically the combination of magnetic resonance (MR) guidance and MR thermometry with focused ultrasound therapy offers most promising perspective for non-invasive surgery.

13.5.2.2 Indications

Uterine Fibroids

Perhaps the most common application of MR-guided focused ultrasound surgery (MRgFUS) today is thermoablation of uterine fibroids. More than 5000 patients have been treated to date with this method worldwide. Uterine fibroids are the most common benign tumors of the inner female genitals. Up to 25% of all woman suffer from fibroid related symptoms such as hypermenorrhoea, dysmenorrhoea and bulk related symptoms (Stewart 2001). A patient asking for organ-preserving therapy is a suitable candidate for MRgFUS if the following criteria are met:

- The patient suffers from fibroid related symptoms.
- Five or less fibroids with each single fibroid smaller than 8 cm are to be treated. In fibroids larger than 8 cm (approximately up to 12 cm) a pre-treatment with GnRH-Analoga is suggested.
- The patient should have no scars, tattoos or skin abnormalities of the abdominal wall within the treatment area.
- The woman must be able to tolerate the procedure in prone position for up to 3 h.
- All fibroids have to be accessible with no risk structures in the expected beam path. This excludes fibroids with intestine loops wedged between the tumor and the abdominal wall and targets closer than 4 cm to the sacral bone.

Pedunculated fibroids should not be treated with MRgFUS. Although no standard recommendations concerning fibroid location and fibroid morphology exist, some authors recommend the treatment of low and medium signal intensity fibroids only, as may be determined on T2 weighted images (Funaki et al. 2007a).

Patients diagnosed with uterine fibroids who desire future pregnancy present a therapeutic dilemma. Considering the prevalence of uterine fibroids, many women conceive and experience an uneventful pregnancy despite having uterine fibroids. On the other hand, uterine fibroids are associated with secondary infertility and several complications during the course of pregnancy, with lower birth weight, premature birth, placenta abnormalities or severe pain related to fibroid infarction. However, the currently available surgical standard treatment options increase the complication rate during consecutive pregnancies due to traumatisation of the uterus. Embolization suffers from the need for radiation exposure. Thus, MRgFUS might be a good alternative for these patients.

Musculoskeletal

Bones absorb US particularly well. Primary indication for bone lesion treatment is pain management. In contrast to the point shape focus used for soft tissues,

a wide beam approach is the method of choice for the treatment of bone lesions. In combination with low energy sonications this method allows a fast, yet effective heating of the bone and metastases, with a proposed denervation leading to symptom relief. Preliminary results of a multicenter trial with 13 patients suffering from painful bone metastases show a significant reduction in pain intensity and a reduction of pain medication in the weeks following treatment. However, extensive research still has to be performed to evaluate the long term effectiveness and side effect profile for this intervention (Catane et al. 2007).

Prostate

Madersbach et al. (1993) first published phase II results of the treatment of benign prostate hyperplasia with high intensity focused ultrasound based also on US for treatment guidance. Since then the use of HIFUS has become more widespread in urology, including clinical trials for such a treatment option in prostate cancer. Most commonly, endorectal probes are used. However, the clinical use of this technique is limited due to difficulties in real time thermometry and in the definition of the target by ultrasound. MR-based systems with endorectal applicators are as yet not available. Significant improvements of treatment outcomes can be expected.

Breast

First studies demonstrating the safety and effectiveness of MRgFUS for benign and malignant tumors of the breast were published in 2001 and 2003. (Hynynen et al. 2001; Gianfelice et al. 2003a,b,c). Whereas treatment with MRgFUS is planned with plain T2-weighted or T1-weighted images, patients with breast carcinoma benefit greatly from contrast-enhanced imaging for treatment planning. Furusawa et al. (2007) treated 21 patients for primary breast cancer. Follow up was performed by MR imaging. After a median follow up period of 14 months (ranging from 6 to 26 months), one case of local recurrence was observed.

Liver

Focused ultrasound has proven to be effective for the treatment of hepatic lesions in early studies (Wu et al. 2004; Visioli et al. 1999; Rowland et al. 1997). For this research, mostly US guidance or no optical guidance have been employed. Even worse, the interventionalist had no feedback regarding the target temperature. The combination of MR guidance and HIFUS most likely increases efficacy by providing excellent visibility of the target and real time feedback by thermomapping. First animal studies have already been published. Some 15 pig livers were treated with MRgFUS. Complete destruction of the lesions was demonstrated by histopathology (Kopelman and Papa 2007; Kopelman et al. 2006). Jolesz published favorable results for the treatment of hepatocellular carcinoma in two patients (Jolesz et al. 2004). Several obstacles have to be overcome though before MRgFUS may be established as a reasonable alternative for the treatment of liver lesions. With applicators available to date, the majority of the liver volume cannot be reached because of the limited acoustic windows between the ribs. To minimize movement of the target during ablation, this procedure has still to be performed in intermittent apnoea under general anaesthesia. Extensive research is to be done to overcome these problems.

13.5.2.3 Technique

Patient Preparation (Uterine Fibroids)

MRgFUS for uterine fibroids is commonly performed on an outpatient basis. To ensure a constant position of the uterus a Foley catheter is inserted. The patient is positioned prone with her pelvis above a gel pad. The aim of a careful positioning maneuver is an air free coupling between the transducer and the target volume (Fig. 13.52). For this purpose the transducer unit may be placed within a water bath of degassed water. The skin has to be shaved, and no additional gels should be applied to the skin. It is also essential to exclude scars as they have higher acoustic impedance. Patient motion has to be reduced to a minimum to ease targeting and real-time-thermometry during the intervention. A stable i.v. access and continuous monitoring of vital signs are mandatory. MRgFUS is commonly performed under minimal analgosedation. The use 1–5 mg of midazolam i.v. and up to 15 mg of piritramid i.v. is usually sufficient for this purpose. The use of general anesthesia is normally not needed. Moreover, it contradicts the non-invasiveness

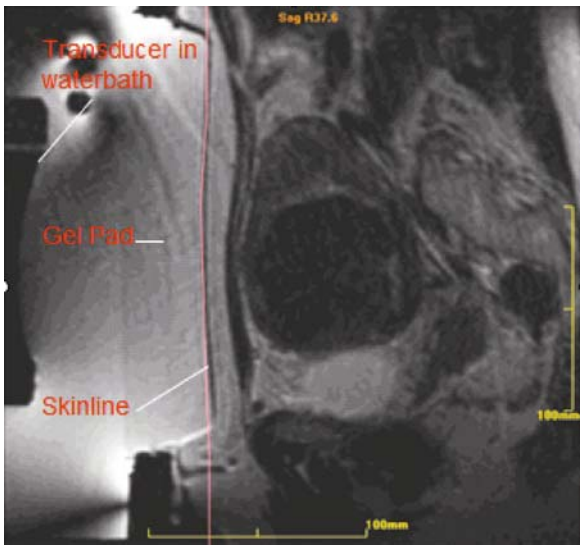

Fig. 13.52 Positioning for MRgFUS of uterine fibroids

of the method, complicates patient positioning, is expensive and – most important – may mask symptoms of complications such as emerging pain from skin burns.

Procedure (Uterine Fibroids)

For treatment planning purposes, T2-weighted images are obtained in three different planes. In a 3D planning module the target area and treatment protocol (diameter and length of spots, grid density, acoustic energy, wave frequency, sonication and cooling duration) are defined. Landmarks and heat sensitive structures at risk such as bowel or the pubic bone are marked on the treatment planning images. The system calculates the sonications needed to treat the target volume identified in the planning MR images. Sonications that are close to or pass through sensitive structures are marked and can be edited by changing the angulation of the transducer in two planes to modify the direction of the beam path. As soon as geometrical planning is complete a first low dose test-sonication is performed. After verification of the target spots with initial low energy sonications the fibroid is ablated in up to 100 single sonications. The MRgFUS system enslaves the MR scanner during this period and real time thermometry is obtained. The operator can manually adjust the power level for each sonication to optimize the target temperature and minimize the patient pain and discomfort level. Depending on the volume of the treated area, treatment time can be very variable – sonication time is about 20–30 s per spot, between each spot an individually calculated "cooling time" of up to 90 s is needed to prevent peripheral tissue damage from heat still within the beam path. Different techniques like an interleaved sonication with reduced cooling time or a wide beam approach for bone treatment can shorten intervention time significantly. During this whole process the patient is able to stop a sonication at each time point with a "panic button". To ensure treatment success, the interventionalist should always aim for the highest volume that may be ablated safely. The treatment ends with T2-weighted and contrast enhanced T1-weighted sequences to document treatment outcome.

13.5.2.4 Results

MRgFUS has proven to be a safe and effective method for symptomatic uterine fibroids. A recent study by Rabinovici et al. (2007) shows a significant or partial symptom relief in 69% of the treated patients after 12 months. Stewart et al. (2006) determine the amount of symptom relief on the uterine-fibroid symptom severity score (UF-SSS) by 39%. In this study with 109 patients, 71% reached the target symptom relief of 10 points on the UF-SSS. Recent studies show favorable outcomes regarding the volume loss of the fibroids and better symptom relief for patients with larger ablated volumes. A minimum of 20% non-perfused volume is the proposed threshold for symptomatic improvement (Stewart et al. 2007).

In patients with childbearing potential there are currently extensive research activities investigating the possibility and safety of pregnancies following MRgFUS treatment. Latest reports indicate that safe pregnancies and vaginal deliveries are possible after treatment of uterine fibroids or adenomyosis with MRgFUS (Rabinovici et al. 2006; Hanstede et al. 2007).

13.5.2.5 Complications

All current studies show that MRgFUS may be applied safely for treatment of uterine fibroids (Stewart et al. 2003; Fennessy and Tempany 2005; Funaki et al. 2007b). Known adverse events result mostly

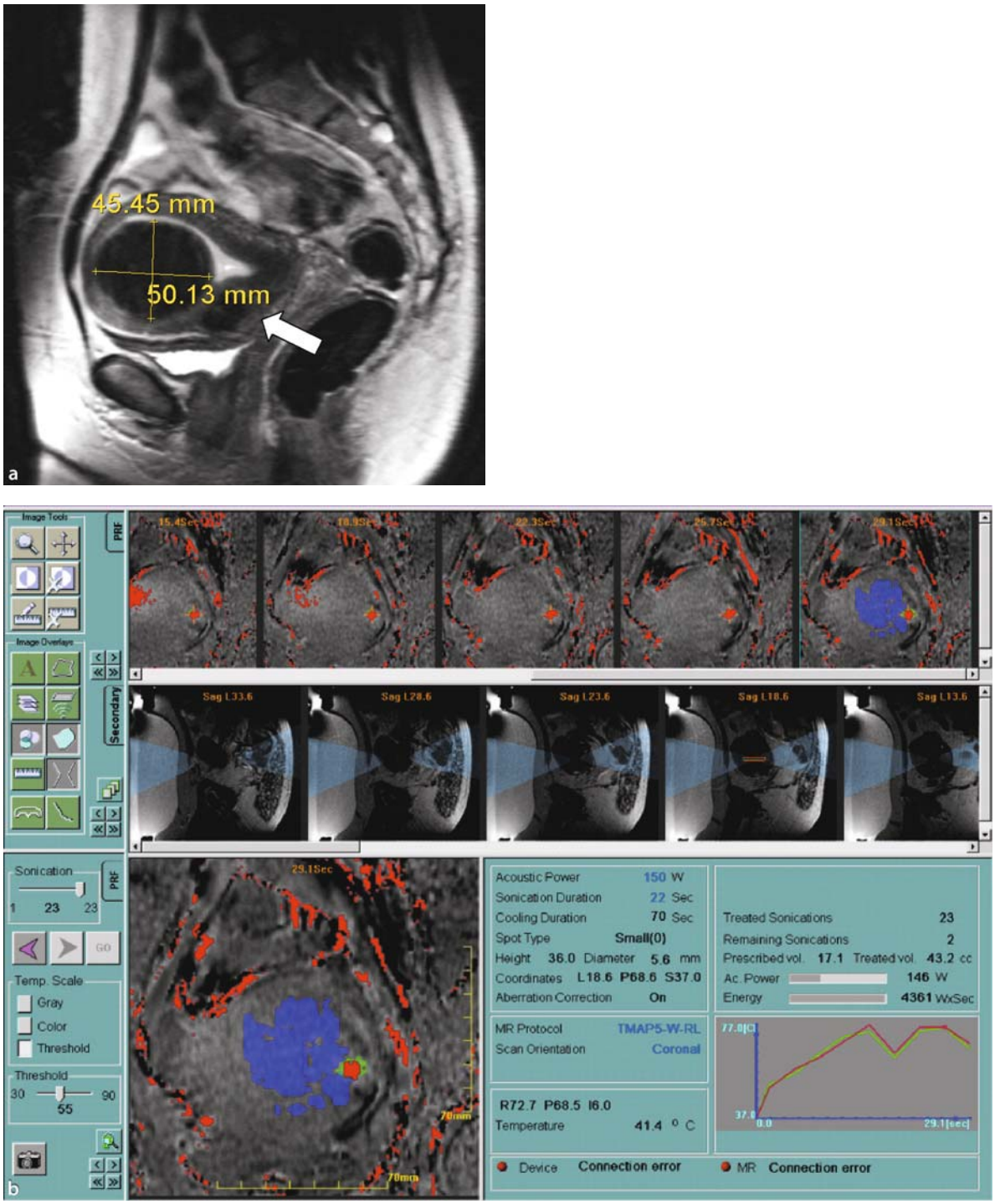

Fig. 13.53 **a** Pre-treatment T2-weighted sagittal image shows a large submucous fibroid of the uterus. In addition, a small intramural fibroid can be seen (*white arrow*). **b** Thermomapping during MRgFUS. *Blue areas* indicate the volume that has already been treated. The *yellow and green dots* show the ongoing sonication. The *curve on the right side* indicates the temperature in the target area

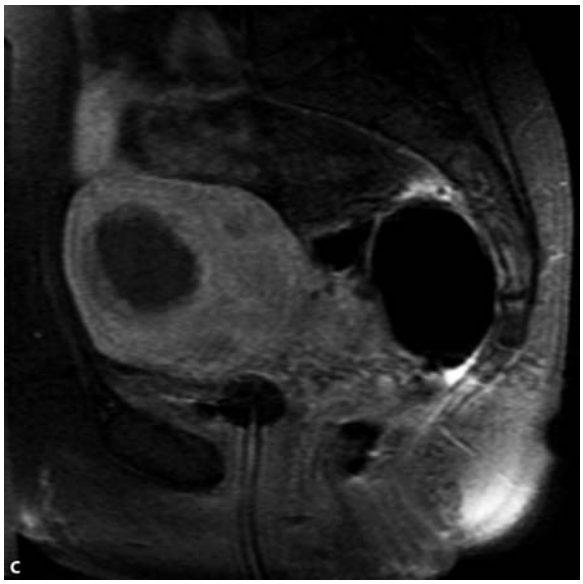

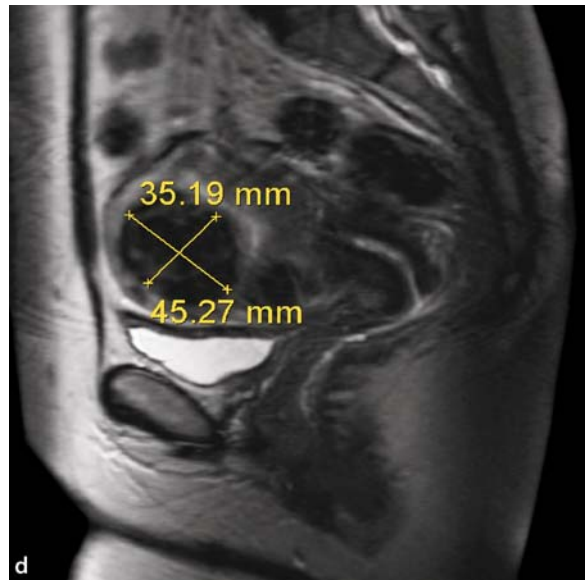

Fig. 13.53 (continued) **c** Immediately post treatment, contrast-enhanced T1-weighted images are obtained to demonstrate the extent of the non-perfused volume in the fibroid. **d** T2-weighted image 6 months post MRgFUS reveals a relevant decrease of lesion volume

from adverse heat refocusing outside the actual target area. Seldom does the patients experience grade 1 or grade 2 skin burns. Grade 3 skin burns are very rarely encountered. These serious burns usually result from pre-existing skin abnormalities such as scars. Cases of damage to the intestine have been reported as a rare complication. Additionally, heat absorption in the sacral bone may provoke temporary symptoms of lumbosacral nerve irritation as radiating pain or dysaesthesia. No case of permanent nerve damage has been reported to date. However, minor discomfort and pain or increased menstrual bleeding in the first weeks following treatment are reported quite frequently.

Summary

MRgFUS is a new non-invasive thermoablative procedure. In several centers it has already become a routine procedure for uterine fibroids. The indication, however, has to weighed against routine techniques like surgery and embolization. Moreover, long term results still need to be assessed. Indications for MRgFUS are likely to expand dramatically following modifications and improvements of current technologies.

Key Points

- MRgFUS is a totally non-invasive therapy.
- It can be used for treating patients with symptomatic fibroids as well as in case of childbearing wish
- For the treatment of uterine fibroids it is a routine procedure in dedicated centers; other indications have currently to be considered experimental.

References

Catane R, Beck A, Inbar Y et al. (2007) MR-guided focused ultrasound surgery (MRgFUS) for the palliation of pain in patients with bone metastases – preliminary clinical experience. Ann Oncol 18:163–167

Fennessy FM, Tempany CM (2005) MRI-guided focused ultrasound surgery of uterine leiomyomas. Acad Radiol 12: 1158–1166

Fennessy FM, Tempany CM, McDannold NJ et al. (2007) Uterine leiomyomas: MR imaging-guided focused ultrasound surgery – results of different treatment protocols. Radiology 243:885–893

Funaki K, Sawada K, Maeda F et al. (2007a) Subjective effect of magnetic resonance-guided focused ultrasound surgery for uterine fibroids. J Obstet Gynaecol Res 33:834–839

Funaki K, Fukunishi H, Funaki T et al. (2007b) Mid-term outcome of magnetic resonance-guided focused ultrasound

surgery for uterine myomas: from six to twelve months after volume reduction. J Minim Invasive Gynecol 14:616–621

Furusawa H, Namba K, Nakahara H et al. (2007) The evolving non-surgical ablation of breast cancer: MR guided focused ultrasound (MRgFUS). Breast Cancer 14:55–58

Gianfelice D, Khiat A, Amara M et al. (2003a) MR imaging-guided focused ultrasound surgery of breast cancer: correlation of dynamic contrast-enhanced MRI with histopathologic findings. Breast Cancer Res Treat 82:93–101

Gianfelice D, Khiat A, Amara M et al. (2003b) MR imaging-guided focused US ablation of breast cancer: histopathologic assessment of effectiveness – initial experience. Radiology 227:849–855

Gianfelice D, Khiat A, Boulanger Y et al. (2003c) Feasibility of magnetic resonance imaging-guided focused ultrasound surgery as an adjunct to tamoxifen therapy in high-risk surgical patients with breast carcinoma. J Vasc Interv Radiol 14:1275–1282

Hanstede MM, Tempany CM, Stewart EA (2007) Focused ultrasound surgery of intramural leiomyomas may facilitate fertility: a case report. Fertil Steril 88:497 e495-497

Hynynen K, Pomeroy O, Smith DN et al. (2001) MR imaging-guided focused ultrasound surgery of fibroadenomas in the breast: a feasibility study. Radiology 219:176–185

Jolesz FA, Hynynen K, McDannold N et al. (2004) Noninvasive thermal ablation of hepatocellular carcinoma by using magnetic resonance imaging-guided focused ultrasound. Gastroenterology 127:S242–247

Kopelman D, Papa M. (2007) Magnetic resonance-guided focused ultrasound surgery for the noninvasive curative ablation of tumors and palliative treatments: a review. Ann Surg Oncol 14:1540–1550

Kopelman D, Inbar Y, Hanannel A et al. (2006) Magnetic resonance-guided focused ultrasound surgery (MRgFUS): ablation of liver tissue in a porcine model. Eur J Radiol 59:157–162

Madersbacher S, Kratzik C, Szabo N et al. (1993) Tissue ablation in benign prostatic hyperplasia with high-intensity focused ultrasound. Eur Urol 23(Suppl 1):39–43

Rabinovici J, Inbar Y, Revel A et al. (2007) Clinical improvement and shrinkage of uterine fibroids after thermal ablation by magnetic resonance-guided focused ultrasound surgery. Ultrasound Obstet Gynecol 30:771–777

Rabinovici J, Inbar Y, Eylon SC et al. (2006) Pregnancy and live birth after focused ultrasound surgery for symptomatic focal adenomyosis: a case report. Hum Reprod 21:1255–1259

Rowland IJ, Rivens I, Chen L et al. (1997) MRI study of hepatic tumours following high intensity focused ultrasound surgery. Br J Radiol 70:144–153

Stewart EA (2001) Uterine fibroids. Lancet 357:293–298

Stewart EA, Gedroyc WM, Tempany CM et al. (2003) Focused ultrasound treatment of uterine fibroid tumors: safety and feasibility of a noninvasive thermoablative technique. Am J Obstet Gynecol 189:48–54

Stewart EA, Rabinovici J, Tempany CM et al. (2006) Clinical outcomes of focused ultrasound surgery for the treatment of uterine fibroids. Fertil Steril 85:22–29

Stewart EA, Gostout B, Rabinovici J et al. (2007) Sustained relief of leiomyoma symptoms by using focused ultrasound surgery. Obstet Gynecol 110:279–287

Visioli AG, Rivens IH, ter Haar GR et al. (1999) Preliminary results of a phase I dose escalation clinical trial using focused ultrasound in the treatment of localised tumours. Eur J Ultrasound 9:11–18

Wu F, Wang ZB, Chen WZ et al. (2004) Extracorporeal high intensity focused ultrasound ablation in the treatment of patients with large hepatocellular carcinoma. Ann Surg Oncol 11:1061–1069

Interventional Pain Management

14

Jan Hoeltje, Roland Bruening, Bruno Kastler, Reto Bale, Gerlig Widmann, Bernd Turowski, Gero Wieners and Oliver Beuing

Contents

14.1 Neurolysis of the Facet Joint

Jan Hoeltje and Roland Bruening

14.1.1 Introduction

Chronic back pain is a widespread disease. (Manchikanti et al. 2004; Neuhauser et al. 2005; Schwarzer et al. 1995). Due to the anatomy of the intervertebral joints and the increasing static load towards the lumbar spine, the lumbar facet syndrome is definitely more frequently observed than the cervical or thoracic one (Masharawi et al. 2004; Yoganandan et al. 2003). In many cases, the origin of pain may not be attributed to a focus, e.g. disc damage, neither by the clinical examination nor by the imaging methods.

A sufficiently reliable clinical definition of pain as caused by facet joint arthrosis is not possible (Helbig and Lee 1988; Jackson et al. 1988; Laslett et al. 2004, 2006; Lilius et al. 1990; Manchikanti et al. 2000; Revel et al. 1998; Schwarzer et al. 1994b, 1995). It may become manifest as unilateral or bilateral, exclusively lumbar or cervical pain whereby irradiation into the legs or arms does not exclude the spectrum of facet pain.

The preferred imaging modality of choice in most centres is the CT-guided approach, as it is the most exact procedure and allows reliable positioning of the probe and exact documentation of it. Alternatively, conventional two-dimensional fluoroscopy can be used (Gofeld et al. 2007).

Clinically, an increased sensitivity to pressure is found above the concerned facet joint. In some cases, certain movements may increase pain. In contrast to disc prolapses, lumbar pain is not intensified by increasing intraabdominal pressure by such as coughing. Cases of painful facet joint arthrosis are found increasingly in persons older than 65 years. Another criterion is the absence of pain in rotation in extension or in flexion and absence of pain when straightening up from flexion. In a prone position and when walking, pain often decreases. There are controversial positions whether the pain does not occur in hyperextension or is even increased by this situation (Hildebrandt 2001; Revel et al. 1998; Schwarzer et al. 1994b).

There are different techniques available for temporary or permanent facet joint neurolysis. The sole use of anaesthetics, e.g. 1% xylocaine, is recommended for diagnostic reasons because of its very fast onset of only few minutes, very little side effects and reversibility. Crystalloid long acting steroids such as triamcinolone are most commonly used to achieve a longer lasting therapeutic effect. The injection of ethanol or phenol for permanent neurolysis of the medial branch is described by some authors; none of these is based on a controlled study; because of this very sparse evidence we do not deal with that particular technique in this chapter. More common in neurolysis of the medial branch is radiofrequency ablation. An alternative approach for neurolysis is kryotherapy.

Anatomically, the facet joints are supplied by the dorsal spinal root through the ramus medianus (Fig. 14.1). The inferior part of the joint receives fibres of the same level (L 2/3 by L 3), the superior part from the root placed above it (Bogduk et al. 1982; Cohen and Raja 2007; Suseki et al. 1997).

Due to this anatomy it is possible to inject directly in the capsule of the facet joint. For RF ablation the probe should be placed near by the capsule to affect all innervating fibers or to perform a neurolysis of the medial branch transverse process spinosus and facet joint in two levels, i.e. if it is not possible to inject into the joint cavity (Kaplan et al. 1998; Marks et al. 1992; van Kleef et al. 1999).

To guarantee a precise intra-artricular injection or the correct placement of the RF-probe at the medial branch, a CT or MR must be performed. With conventional fluoroscopy or “blind” injection it is only possible to locate the needle tip approximately near your aim in the three-dimensional body. Moreover, monitoring of the distribution of injected liquids is much more precise with CT or MR (Meleka et al. 2005; Murtagh 1988).

14.1.2 Indications

Facet joint neurolysis is indicated in patients with chronic back pain that arises from the facet joints as described above. However, it is not always possible to differentiate exclusively clinically and by morphological imaging the facet joint pain as unique focus or at least as an important one for the genesis of pain. In these cases, temporary facet joint neurolysis has to be performed above all for diagnostic purposes and for this reason, at one (or two levels) only. Periarticular infiltration with local anaesthetics on a large area has to be avoided. At the beginning of such a diagnostic infiltration, pain should have been occurring for 2–4 weeks and before commencement of the infiltration, and treatment with, e.g. non-steroidal antirheumatics should have been previously performed and should have proven ineffective.

There are no absolute contraindications to facet joint neurolysis. Prior to the intervention, coagulation disorders or known intolerance to the substances used should be excluded. Infectious cutaneous lesions along the access route have to be treated previously. In case of a planned cortisone injection, diabetes has to be considered as a relative contraindication, particularly for diagnostic infiltrations.

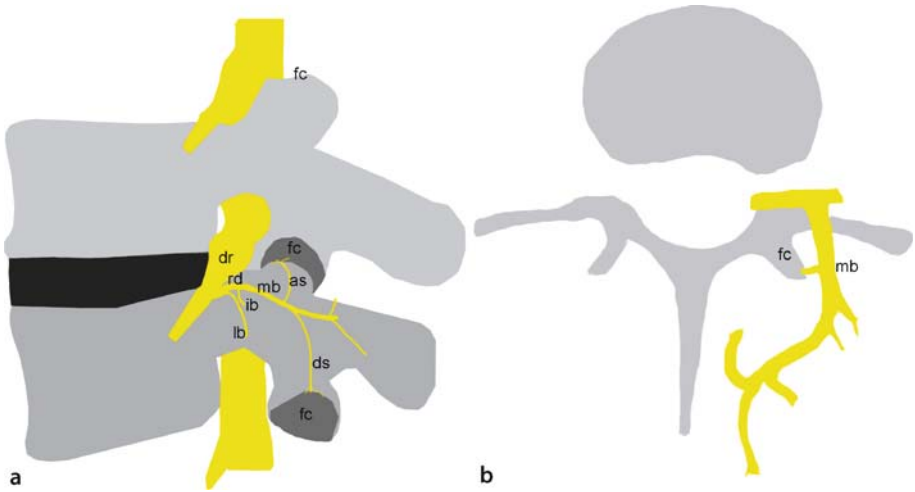

Fig. 14.1a,b Schematic image of the facet joint innervation. **a** Sagittal view. **b** Axial view: The ramus dorsalis (rd) arise from dorsal root (dr) and branching into lateral (lb), intermediate (ib) and medial branch (mb), from medial branch arises an ascending branch (as) to the level above and a descending branch (ds) to the nerve root level

The patient should be informed, despite the general risks, about risks of haemorrhage, infection (Okada et al. 2005; Park et al. 2007) and drug intolerance. Possible treatment failure as well as conservative and operative treatment alternatives should be listed.

14.1.3 Material

For diagnostic injection the following material are needed:

- 22–26 G needle with 7–15 cm length with atraumatic cut if possible, possibly with short guiding needle, endhole or sidehole depends on personal preferences
- 10 ml local anaesthetic (e.g. 1% xylocaine) (10-ml syringe)
- 2 ml of a 1 : 1 mixture of contrast medium and saline (2-ml syringe)
- Sterile table
- Sterile draping, sterile gloves, sterile gowns, skin disinfection

For therapeutic procedure also:

- 40 mg (1 ml) triamcinolone (2-ml syringe) or RF-probe

14.1.4 Technique

CT- or MR-guided intratricular injection of the facet joint or neurolysis of the medial branch can be performed as follows:

- Level identification on the basis of a lateral scout image.
- Performance of an axial scan for planning of the access route in order to reach the joint cavity as far as possible (Fig. 14.2). For medial branch neurolysis aim at the junction between the processus articularis superior and the processus transverses superior, for L5 the Ala sacralis instead.
- Skin markers such as barium paste, radiopaque, gadolinium filled or metal marker grids may be used.
- Skin disinfection and sterile draping.
- Puncture with the infiltration needle according to the planning until a slightly elastic or osseous resistance is registered. Local anaesthesia may be used.
- Performance of a control tomography, possibly correction of the needle position.
- If the patient reports to experience his known pain by provocation with the needle point, this confirms the needle position additionally. Optional injection of a very small quantity of contrast medium (ca. 0.3–0.5 ml), in case of pain, cessation of injection and ask for the pain irradiation area and whether this pain is identical with the known one. Per-

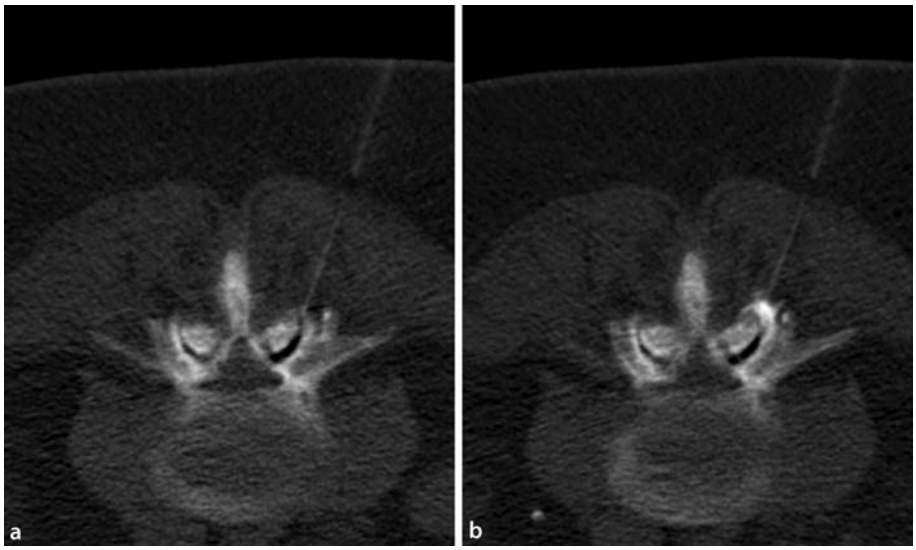

Fig. 14.2a,b CT-guided fact joint neurolysis. For injection therapy a 25 G needle was placed in the arthrotic facet joint (**a**). After injection of approximately 0.1 ml of a contrast medium/NaCl mixture, CT shows a homogenous intraarticular distribution of the contrast medium (**b**)

formance of a control tomography. If the contrast medium distributes in the joint cavity, needle position is correct.

- Injection of 0.5 ml 1% xylocaine for a diagnostic purpose. In case of a therapeutic injection possibly 0.5 ml (20 mg) triamcinolone can be injected afterwards.
- Injection of no more than a total of 1.5 ml of fluid for there is danger of rupture of the joint capsule.
- In case of a diagnostic infiltration, withdrawal of the needle. For diagnostic injections it is crucial to avoid periarticular infiltration on a large extent as this will limit the diagnostic significance of the procedure.
- In case of a therapeutic procedure, slow withdrawal of the needle under aspiration and infiltration of the facet surrounding with local anaesthetic.
- In case of RF-ablation of the facet joint the nerves are ablated outside the capsule. To achieve an optimal contact between RF-probe and the nerve, the probe is inserted with a 15° caudo-cranial angulation directly beneath the joint. For RF ablation a 90–120 s heating ($\geq$ 90 °C) per position is sufficient.

If the patient has tolerated this procedure well, subjective pain relief is key following application of analgesics. A few minutes after the end of intervention, the patient should report a clear relief or absence of pain. Since, in a lot of patients, spondylarthrosis is not the only painful degenerative change and after subsidence of this kind of pain another one, e.g. coxarthrotic pain, will dominate, such a patient has to be asked sometimes explicitly for changes of the treated pain syndrome in order to evaluate the result. According to the galenic properties of the local anaesthetic, pain relief may prolong only a few hours and the beginning of the action of cortisone may delay up to 12 h. It is not unusual that the pain will occur again during the following days. A longer period of pain absence will be achieved after at least a twofold repetition of the infiltration with a one week interval each time.

14.1.5 Results

The therapeutic value of facet joint neurolysis is still in discussion (Aguirre et al. 2005; Cohen et al. 2008; Kaplan et al. 1998; Levin 2007; Lilius et al. 1990; Manchikanti et al. 2004; Marks et al. 1992; Nelemans et al. 2001; Schwarzer et al. 1994a). In 2007, a randomized, double-blind study was published

comparing long-term success of facet blockages with and without cortisone (Manchikanti et al. 2007). Although the number of patients involved was relatively small with 30 per study arm, a long-term success of the infiltrations could be shown for an average of four infiltrations per year. A superiority of infiltration with an addition of cortisone was not found so that evidence to use a cortisone mix is lacking. However, these results will have been confirmed by a larger study. A clear pain reduction lasting over some weeks is to be assumed in most of the patients. A multicenter study including 262 patients performed RF-ablation, after six month 54% of patients report a pain relief of 50% or greater and 66% perceived a positive global effect (Cohen et al. 2008) another trial reported about 68.4% with good to excellent outcome.

Because other measurements such as physiotherapy have not been evaluated systematically together with a facet infiltration, their combined benefit remains unclear. Possibly, if these approaches were used in an optimized manner, opiates as well as their side effects may be avoided in some cases (Cohen et al. 2008).

14.1.6 Complications

In all, complications are rarely reported with only few case reports. In controlled studies no complications were reported. Paraspinal abscesses (Park et al. 2007) and cases of facet joint arthritis after infiltration are sporadically described in the literature; a transmission towards the epidural space or with resulting meningitis (Alcock et al. 2003; Gaul et al. 2005; Okada et al. 2005) was detected and estimated in less than $1^0/_{00}$. In case of a suspected abscess, an MR scan and, after possible confirmation, relieving surgery should be performed. The danger of a paraspinal abscess thus has to be considered as extremely low under a sterile procedure. The different descriptions of cases of abscess extension towards the epidural space, however, underline the necessity of observing absolute sterile conditions also in the case of a low needle diameter.

Summary

Some authors contest the facet syndrome as an own entity. However, its involvement in chronic back pain has to be taken as a basis (Helbig and Lee 1988; Hildebrandt 2001; Jackson et al. 1988; Laslett et al. 2006; Revel et al. 1998; Schwarzer et al. 1994b). A clinically pathognomonic symptom may not be found but evidence is that many patients experienced repeatedly absence or relief of pain after two local anaesthetics with different action time had been injected in an interval. To guarantee a reliable diagnostic procedure, protagonists of this point of view require a blockage with different anaesthetics twice in order to exclude false-positive Infiltrations (Dreyfuss et al. 2003; Schwarzer et al. 1994a). Remarkably, only sparse evidence exists on the use of facet joint infiltration in relation to the outcome of a subsequent surgical intervention, e.g. arthrodesis (Cohen and Hurley 2007; Esses and Moro 1993).

Key Points

- Percutaneous image-guided facet joint neurolysis is a safe procedure with an extremely low complication rate.
- In many cases, diagnostic facet infiltration is the only procedure to clarify whether the facet joints are involved in the genesis of back pain.
- In most of the cases, a quick relieve of pain is achieved and may last several months.
- If needed facet joint neurolysis can be repeated several times.
- Repeated injections usually increase the length of the asymptomatic interval.

References

Aguirre DA, Bermudez S, Diaz OM (2005) Spinal CT-guided interventional procedures for management of chronic back pain. J Vasc Interv Radiol 16(5):689–697

Alcock E, Regaard A, Browne J (2003) Facet joint injection: a rare form cause of epidural abscess formation. Pain 103(1/2):209–210

Bogduk N, Wilson AS, Tynan W (1982) The human lumbar dorsal rami. J Anat 134(2):383–397

Cohen SP, Hurley RW (2007) The ability of diagnostic spinal injections to predict surgical outcomes. Anesth Analg 105(6):1756–1775

Cohen SP, Raja SN (2007) Pathogenesis, diagnosis, and treatment of lumbar zygapophysial (facet) joint pain. Anesthesiology 106(3):591–614
Cohen SP, Stojanovic MP, Crooks M et al. (2008) Lumbar zygapophysial (facet) joint radiofrequency denervation success as a function of pain relief during diagnostic medial branch blocks: a multicenter analysis. Spine J 8(3):498–504
Dreyfuss PH, Dreyer SJ, Vaccaro (2003) Lumbar zygapophysial (facet) joint injections. Spine J 3 (3, Suppl 1):50–59
Esses SI, Moro JK(1993) The value of facet joint blocks in patient selection for lumbar fusion. Spine 18(2):185–190
Gaul C, Neundorfer B, Winterholler e(2005) Iatrogenic (para-) spinal abscesses and meningitis following injection therapy for low back pain. Pain 116(3):407–410
Gofeld M, Jitendra J, Faclier G (2007) Radiofrequency denervation of the lumbar zygapophysial joints: 10-year prospective clinical audit. Pain Physician 10(2):291–300
Helbig T, Lee CK (1988) The lumbar facet syndrome. Spine 13(1):61–64
Hildebrandt J (2001) Relevance of nerve blocks in treating and diagnosing low back pain – is the quality decisive? Schmerz 15(6):474–483
Jackson RP, Jacobs RR, Montesano PX (1988) 1988 Volvo award in clinical sciences. Facet joint injection in low-back pain. A prospective statistical study. Spine 13(9):966–971
Kaplan M, Dreyfuss P, Halbrook B et al. (1998) The ability of lumbar medial branch blocks to anesthetize the zygapophysial joint. A physiologic challenge. Spine 23(17):1847–1852
Laslett M, Oberg B, Aprill CN et al. (2004) Zygapophysial joint blocks in chronic low back pain: a test of Revel's model as a screening test. BMC Musculoskelet Disord 5:43
Laslett M, McDonald B, Aprill et al. (2006) Clinical predictors of screening lumbar zygapophyseal joint blocks: development of clinical prediction rules. Spine J 6(4):370–379
Levin KH (2007) Nonsurgical interventions for spine pain. Neurol Clin 25(2):495–505
Lilius G, Harilainen A, Laasonen EM et al. (1990) Chronic unilateral low-back pain. Predictors of outcome of facet joint injections. Spine 15(8):780–782
Manchikanti L, Pampati V, Fellows B et al. (2000) The inability of the clinical picture to characterize pain from facet joints. Pain Physician 3(2):158–166
Manchikanti L, Boswell MV, Singh V et al. (2004) Prevalence of facet joint pain in chronic spinal pain of cervical, thoracic, and lumbar regions. BMC Musculoskelet Disord 5:15
Manchikanti L, Manchikanti KN, Manchukonda R et al. (2007) Evaluation of lumbar facet joint nerve blocks in the management of chronic low back pain: preliminary report of a randomized, double-blind controlled trial: clinical trial NCT00355914. Pain Physician 10(3):425–440
Marks MJ, Pauly JR, Gross SD, et al. (1992) Nicotine binding and nicotinic receptor subunit RNA after chronic nicotine treatment. J Neurosci 12(7):2765–2784
Masharawi Y, Rothschild B, Dar G et al. (2004) Facet orientation in the thoracolumbar spine: three-dimensional anatomic and biomechanical analysis. Spine 29(16):1755–1763
Meleka S, Patra A, Minkoff E et al. (2005) Value of CT fluoroscopy for lumbar facet blocks. AJNR Am J Neuroradiol 26(5):1001–1003
Murtagh FR (1988) Computed tomography and fluoroscopy guided anesthesia and steroid injection in facet syndrome. Spine 13(6):686–689
Nelemans PJ, deBie RA, deVet HC et al. (2001) Injection therapy for subacute and chronic benign low back pain. Spine 26(5):501–515
Neuhauser H, Ellert U, Ziese T (2005) Chronic back pain in the general population in Germany 2002/2003: prevalence and highly affected population groups. Gesundheitswesen 67(10):685–693 [German]
Okada F, Takayama H, Doita M et al. (2005) Lumbar facet joint infection associated with epidural and paraspinal abscess: a case report with review of the literature. J Spinal Disord Tech 18(5):458–461
Park MS, Moon SH, Hahn SB et al. (2007) Paraspinal abscess communicated with epidural abscess after extra-articular facet joint injection. Yonsei Med J 48(4):711–714
Revel M, Poiraudeau S, Auleley GR et al. (1998) Capacity of the clinical picture to characterize low back pain relieved by facet joint anesthesia. Proposed criteria to identify patients with painful facet joints Spine 23(18):1972–1976; discussion 1977
Schwarzer AC, Aprill CN, Derby R et al. (1994a) The false-positive rate of uncontrolled diagnostic blocks of the lumbar zygapophysial joints. Pain 58(2):195–200
Schwarzer AC, Aprill CN, Derby R et al. (1994b) Clinical features of patients with pain stemming from the lumbar zygapophysial joints. Is the lumbar facet syndrome a clinical entity? Spine 19(10):1132–1137
Schwarzer AC, Wang SC, Bogduk N et al. (1995) Prevalence and clinical features of lumbar zygapophysial joint pain: a study in an Australian population with chronic low back pain. Ann Rheum Dis 54(2):100–106
Suseki K, Takahashi Y, Takahashi K et al. (1997) Innervation of the lumbar facet joints. Origins and functions. Spine 22(5):477–485
van Kleef M, Barendse GA, Kessels A et al. (1999) Randomized trial of radiofrequency lumbar facet denervation for chronic low back pain. Spine 24(18):1937–1942
Yoganandan N, Knowles SA, Maiman DJ et al. (2003) Anatomic study of the morphology of human cervical facet joint. Spine 28(20):2317–2323

14.2 Image-Guided Nerve Blocs and Infiltrations in Pain Management

Bruno Kastler

14.2.1 Introduction

Cross-sectional imaging namely computed tomography (CT) and magnetic resonance (MR) imaging offer an excellent and safe means of guiding procedures by displaying a very good contrast between soft tissues,

bone and vessels. CT guidance in contrast to fluoroscopic guidance allows safe needle progression and precise positioning at targets which reduces complications and optimizes procedure results (Kastler et al. 1999). We will demonstrate step by step our routinely used technique under cross-sectional imaging-guidance (patient positioning, gantry tilting, saline injection, needle steering, etc.). Examples at different anatomic sites are presented which can be used either in addition to or as an alternative to other conventional methods in pain management (Kastler 2007). To perform cross sectional imaging-guided interventional procedures one must first have a good understanding of the anatomical relationship of the target and the surrounding structures which determine the possible safe percutaneous pathways.

14.2.2 Materials and Techniques – General Considerations

14.2.2.1 Radiofrequency Ablation

Radiofrequency (RF) ablation of nerves involves the placement of an insulated electrode-needle with an uninsulated small tip precisely targeted beneath or into nervous tissue. Heat is generated by the interaction between tissue and high frequency current (see Sect. 13.1.1). In order to control thermal lesion size a constant electrode tip temperature of $\geq 90\,^{\circ}\mathrm{C}$ has to be maintained for 1–2 min. Tissue charring and boiling should be avoided in RF for pain management. Ideally small needle electrodes (20 Gauge) with active tip length in the range of 3 to 5 mm are available for pain treatment. When compared with other techniques, RF ablation offers numerous advantages for interventional pain management:

- Adequate control of lesion size.
- Control of needle placement by electrical stimulation with testing of possible pain reduction.
- Selective sensory lesion (with no motor damage).
- Lower incidence of complications.
- Ability to repeat treatment safely if the neural pathway regenerates.

However, it requires an initial investment (RF generator), and RF electrodes are more costly than simple spinal needles needed for injection therapy. Moreover, RF ablation is also more time consuming.

14.2.2.2 Alcohol Ablation

Percutaneous injection of alcohol (95%) or phenol (6%) can be used to perform neurolysis in analogy to its use as a destructive agent in tumor therapy.

For interventional pain management with alcohol the correct position of the needle tip at target is determined by a test injection of diluted contrast media with local anesthetics (Kastler et al. 1999), which allows one to anticipate possible diffusion of the alcohol and also to perform a block test.

In the estimation of the diffusion of alcohol it needs to be noted that alcohol is simultaneously hydrosoluble and liposoluble. The diffusion of absolute alcohol is thus not completely controllable and not strictly consistent with the diffusion of the preliminarily injected anesthetic-contrast mixture, which is hydrosoluble only.

To realize an adequate neurolytic effect an intramural alcohol concentration of 66% to 75% is required. The calculation for the concentration follows a simple rule: the injected total quantity of absolute (96%) alcohol (A), which follows the injection of lidocaine-contrast mixture (X) must be at least twice – or better three times – the quantity of X ($A = 2 \times X$ or $A = 3 \times X$). With the injection of highly concentrated alcohol, smaller total ablation volumes can be achieved, when compared with the anesthetic effect of the test injection.

Alcohol must be instilled slowly and aspiration is performed before injection to avoid accidental intravascular injection. Rare complications can be minimized by injecting small volumes of alcohol and by correctly positioning the needle tip. After injection, alcohol can be seen as a hypodense area diluting the contrast media. Appropriate local anesthesia is needed to reduce the painful alcohol instillation. Before the needle is removed, it is flushed with a small amount of saline or anesthetic. An important advantage of alcohol ablation is its low cost and the longer lasting effects when compared with RF ablation. Relevant drawbacks include the possible spread on distant motor nerves.

14.2.2.3 Steroid Infiltration

The injection of steroids can be used in local pain management because of its analgesic and antiinflammatory

effects. The procedure equals alcohol injection therapy, but unlike alcohol injection steroid injection per se is not painful.

Short acting steroids are used for spinal epidural or periganglionic foraminal infiltration because of steroid-induced arachnoiditis risk. Prednisolone (1 ml/5 ml volume which is equivalent to 25/125 mg of prednisone) is typically used for this indication. For peripheral infiltration long-acting glucocorticoids should be used (e.g. cortivasol 1.5 ml which is equivalent to 75 mg prednisone).

14.2.2.4 Patient Preparation

All interventional procedures should be preceded by a consultant a few days prior to the procedure (at least 24 h). Obtaining a detailed patient history is necessary to rule out contra-indications to the procedure. It also helps to establish patient's confidence through individual, clear and simple explanation of the course of the procedure. The patient is informed on the possible rare complications of the procedure and given consent should be obtained depending on federal and national country regulations.

Prior to the intervention a review of the patient's complete blood count and blood chemistry by the interventionalist is necessary. Special attention is given to the hemostasis parameters including thromboplastin time, partial thromboplastin time and platelet count in order to rule out bleeding disorders. Contraindications for percutaneous procedures are represented by a platelet count lower than 100 000 /mm^3, a thromboplastin time below 60% and an international normalized ratio ≥ 2. To ensure sufficient renal function, blood creatinin is assessed. In the case of known hypersensitivity, anti-allergic premedication may be appropriate. It is important that the patient does not eat for a minimum of 4 h prior to the intervention. In our experience a preliminary empathic conversation makes an important contribution to an optimal cooperation of the patient. Particularly anxious patients require prescription of anxiolytic medication prior to the procedure.

14.2.2.5 Intervention Room Preparation

Prior to each intervention, cleaning and disinfection of all surfaces such as the CT-scan table and gantry, as well as the room floor, is routinely performed. The mobile stainless steel instrument table is covered with sterile sheets. The following items should be available:

- Syringes (5-ml, 10-ml and 20-ml).
- Hypodermic needle for local anesthesia.
- Saline solution, anesthetics and different volumes of ionized contrast medium. In addition to clear labeling it is advised to use a fixed arrangement in order to avoid confusion.
- Sterile pads.
- A set of sterile sheet for interventional purposes.
- Flexible or rigid 20 Gauge therapy needles (22 Gauge for neurolysis).
- Absolute (dehydrated) alcohol, steroids, etc. (depending on the procedure).

14.2.2.6 Image Guidance: How I Do It

For procedure planning, images of recent examinations can be used. To increase the precision of navigation we prefer to acquire an additional set of contrast enhanced cross-sectional images of the anatomical area of interest at the beginning of the intervention.

In detail the procedure runs as follows (Kastler et al. 1999 – Kastler B 2007):

1. The patient is placed in a supine or prone position depending on the entry point.
2. Contiguous axial CT sections with 3–5 mm slice thickness covering the entire region of interest are obtained.
3. A safe pathway is chosen, carefully avoiding inadvertent puncture of vessels or hollow organs. Injection of contrast material may be needed to identify vessels.
4. The optimal skin entry point is determined and marked on the skin with a waterproof felt-tip pen.
5. The, the skin scrubbed and sterilized and the patient is draped in a sterile fashion. Local anesthesia is instilled at the skin entry point.
6. The hypodermic needle used for local anesthesia should first be left in place and used to visualize the actual skin entry point on CT, and to estimate and verify relevant information regarding the optimal puncture angle, the direction and the distance to the target of the therapy needle.
7. The therapy needle is slowly moved forward towards the target. This can either be done step by step under image guidance or continuously using

CT-fluoroscopy. On CT images the needle direction can be estimated from its hypodense shadow. This phenomenon is due to hardening of the X-ray beam. Correct positioning of the needle tip on the target can be verified by injecting contrast media. When using RF the stimulation mode of the generator may be switched on. Reaction of the targeted nerve proves correct needle placement.

A control CT scan at the end of the procedure ensures the absence of complications. Most pain management procedures can easily be performed under CT-guidance on an outpatient basis. Local anesthesia is normally sufficient for intervention related pain.

14.2.3 Materials and Techniques – Detailed Considerations

14.2.3.1 Pterygopalatine Ganglion Neurolysis

Indication

Neurolysis or blockade of the pterygopalatine ganglion (PPG) is an efficient method in the management of pain in patients suffering from (Devoghel 1981):

- Cluster headaches
- Atypical facial pain
- Trigeminal neuralgia
- PPG neuritis
- Postherpetic neuralgia
- Severe intractable cancer-related pain

Anatomy

The pterygopalatine fossa (Hardebo and Elner 1987; de Kersaint-Gilly et al. 1991) is located directly posterior to the maxillary sinus (Fig. 14.3). It houses the internal maxillary artery, the pterygopalatine ganglion and the maxillary nerve. In general, the arterial component of the fossa lies anteriorly and the neural component, posteriorly.

Image Guidance for Alcoholization and RF Procedure (Clair et al. 1998; Kastler B 2007)

The patient is placed in a supine position on the CT table with his head turned opposite to the side of puncture. Injection of a bolus of contrast media is required to visualize the course of the internal maxillary artery. Axial CT sections with a slice thickness of 3–5 mm are acquired from the upper part of the zygomatic arch to the lower part of the maxillary bone. The pterygopalatine fossa is seen dorsal to the maxillary sinus and anterior to the lateral pterygopalatine plate. The PPG is located at the level of the sphenopalatine foramen.

The skin entry point is located just above zygomatic arch. A safe pathway is chosen in order to avoid damage to the internal maxillary artery (Fig. 14.3). The needle is slowly advanced forward using step by step CT guidance until the needle tip is safely placed within the pterygopalatine fossa.

The correct position of the needle tip (disposable 22.5 Gauge – 12.70-cm spinal needle (BD) at target is determined by an injection of 0.5 ml local anesthetic diluted (10%) with contrast media (Fig. 14.3). Before the injection the mounted syringe is maintained in aspiration (under vacuum) for 5 s in order to detect blood (vascular puncture). Neurolysis is performed with 1 ml of absolute alcohol which should be instilled slowly. Alternatively, RF ablation may be used. The procedure is carried out on an outpatient basis and the patient is kept under observation for 1 h.

Complications

Complications are rare. Control CT imaging at the end of the procedure ensures the absence of complications, particularly hematoma. It also shows the distribution of the neurolytic agent. Some patients experience epistaxis following this procedure. They should not be discharged until this condition has fully disappeared. The number of complications can be minimized by keeping the volume of injected alcohol within 1 ml and by correctly positioning the needle tip.

14.2.3.2 Arnold's Nerve Infiltration

Indication

Neurolysis or blockade of the nerve of Arnold is an efficient method in the management of Arnold's neuralgia. The symptoms have been well described. The typically unilateral (rarely bilateral) pain mostly starts in the suboccipital region and radiates over the posterior scalp to the top of the head. Retro-orbital pain may

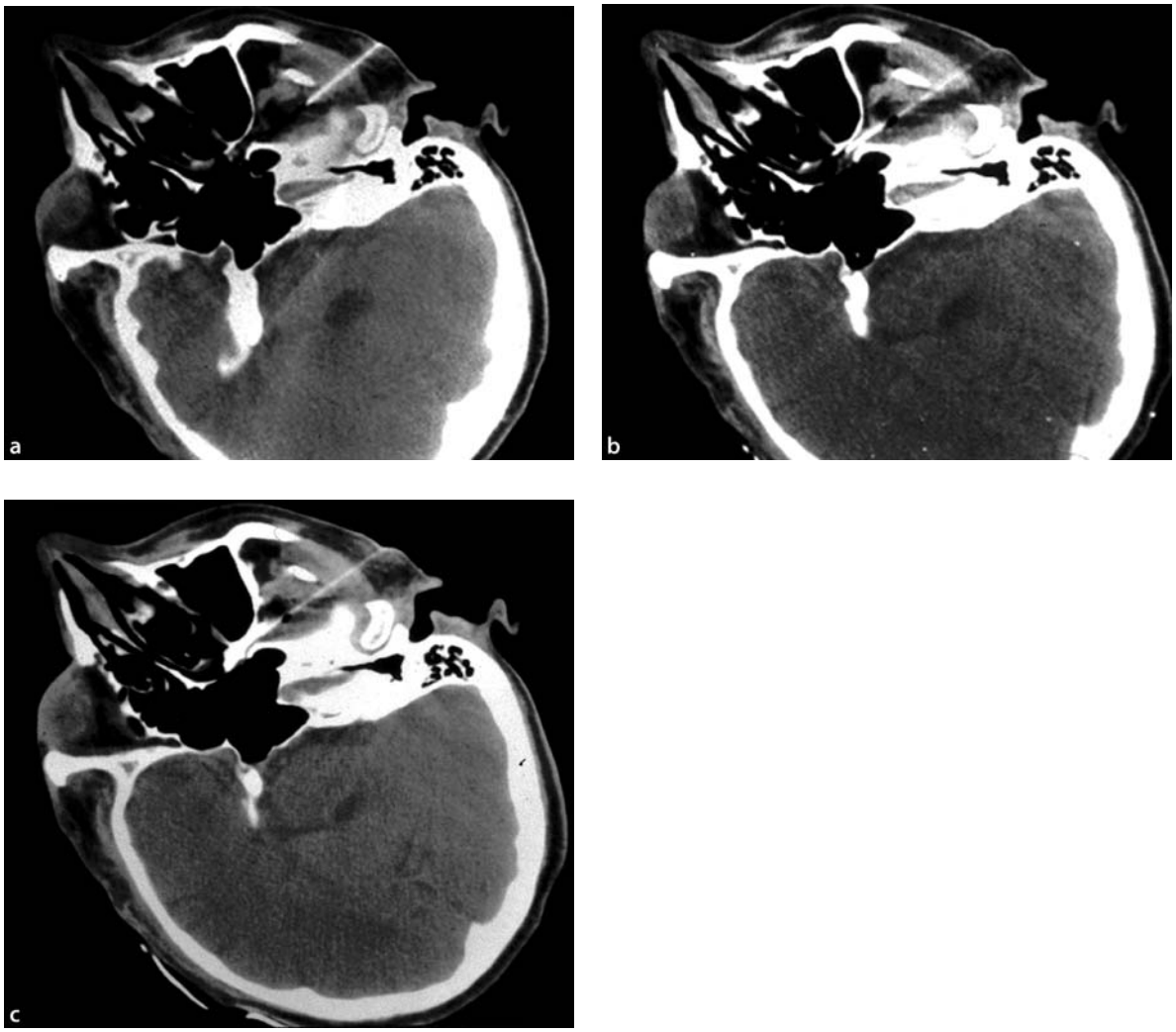

Fig. 14.3a–c Pterygopalatine ganglion neurolysis: The needle is placed under step-by-step CT guidance (**a**,**b**) and contrast media with a local anesthetic is injected to assure correct needle tip position on the target (**c**). Finally 1 ml of absolute alcohol is slowly instilled

be present in severe attacks. Two forms have been described: a paroxysmal form and a continuous form.

Anatomy (Bogduk 1980)

The greater occipital nerve (GON) or nerve of Arnold corresponds to the posterior branch (sensory) of the second cervical nerve. It originates between the posterior arch of the atlas (C1) and the lamina of the axis (C2). The GON has a complex winding comprising a series of segments and angles. This complex course exposes the nerve to possible compression and/or stretching, particularly during movement of the head (Vital et al. 1989). Two zones where the nerve is anatomically vulnerable and where infiltrations can be of benefit can be outlined (Bogduk 1981; Bovim et al. 1992; Bovim and Sand 1992; Kastler B 2007):

- Proximally at its origin ("or", "first site") and at its first bend ("b1", "second site") where the GON curves around the inferior oblique capitis muscle.
- Distally at its emergence at the narrow and rigid aperture when perforating the tendinous area of the trapezius muscle ("em", "third site"; (pain trigger zone).

Image Guidance for Infiltration Procedure (Kastler B 2007)

Infiltration of the GON at its origin ("or", "first site"). The approach is posterior or posterolateral and the patient is placed in a comfortable prone position with a pillow under his or her chest. The patient's head is turned opposite to the puncture site for a unilateral infiltration (Fig. 14.4) and face down on a padded surgical ring for a bilateral infiltration (Fig. 14.5). After bolus contrast injection, an initial series of axial 3–5-mm slices covering the occipital bone to C3 is obtained in order to visualize vascular structures, particularly the vertebral artery, and to ensure that it lies outside the chosen pathway).

The target "or" is at an intermediate level between the two arches, slightly below the posterior margin of the posterior arch of C1, directly behind the C1–C2 joint capsule (Fig. 14.4). Before the injection the mounted syringe is maintained in aspiration (under vacuum) for 5 s in order to detect blood (vascular puncture) or cerebrospinal fluid (dural effraction). First a mixture of 1 ml of saline and contrast medium (90%/10%) is injected. If the needle tip is safely positioned (outside of vascular structures and the foramen magnum) the spread of saline-contrast mixture molds the dura mater (and ideally the spinal C2 ganglion). Thereafter the steroid is administered: slow depot steroid instillation of prednisolone 2 ml (50 mg prednisone equivalent).

If a radiofrequency generator is available, initially a test is performed in the stimulation mode at the C1 ganglion level; the patient should feel a tingling effect in the territory of the GON. Subsequently thermal ablation can be performed.

Infiltration of the GON at the second proximal site ("b1"). We advocate when retrieving the needle (or, alternatively, when aiming at the target), that a second infiltration be given behind the inferior oblique capitis muscle around which the GON describes its first bend (Fig. 14.4). The needle tip visualized by the tip artifact should be located in the fatty compartment between the dorsal aspect of the inferior oblique capitis muscle and the deep aspect of the semispinalis capitis muscle. The infiltration starts with a block comprising a 3-ml mixture of short and long acting anesthetics (lidocaine 1/3 and ropivacaine 2/3) and contrast media (10%). The proper diffusion of this hyperdense mixture between the two muscles confirms that the needle tip is safely positioned (Fig. 14.5). The injection of prednisolone (2 ml; 50 mg prednisone equivalent) or cortivazol (1 ml; 50 mg prednisone equivalent) can then safely be performed.

Infiltration of the GON at its emergence ("em", "third site"). The infiltration is usually conducted using bony and palpable landmarks. The infiltration can also be performed under CT guidance by finding the occipital artery on the slice where the occipital artery becomes subcutaneous (accompanying the GON), usually close to the superior nuchal line (pain trigger zone).

Complications

At the origin of the nerve, the most frequent complication is the inadvertent puncture of the vertebral artery. This is avoided by CT guidance, which is far more precise than fluoroscopic guidance (Bogduk 1981; Bovim et al. 1992). The same applies for piercing the dura matter or infiltration of the neck muscle on the pathway. Pain at the puncture site, transitory torticollis, nausea, and dizziness are rare adverse reactions.

14.2.3.3 Stellate Ganglion Neurolysis

Indications

Neurolysis or stellate ganglion block is an efficient and accepted method in the diagnosis and treatment of acute and chronic sympathetically maintained pain syndrome of the upper limb, thoracic viscera, and head and neck (Forouzanfar et al. 2000; Kastler et al. 2001). Indications including:

- Algodystrophy or reflex sympathetic dystrophy syndrome, currently referred to as type I complex regional pain syndrome (CRPS). It is a combination of a non-systematic pain syndrome, tenderness and swelling, changes in cutaneous blood flow, abnormal sweating, and stiff joints. CRPS, although benign, is highly invalidating because it resists specific medication.
- Causalgia or type II chronic regional pain syndrome.
- Post-herpetic neuralgia (see Sect. 14.3).

It is also an effective treatment option in cases of severe intractable cancer-related pain arising from regional neoplasms invading the stellate ganglion (Pancoast and cervical tumors) (Gangi et al. 1996).

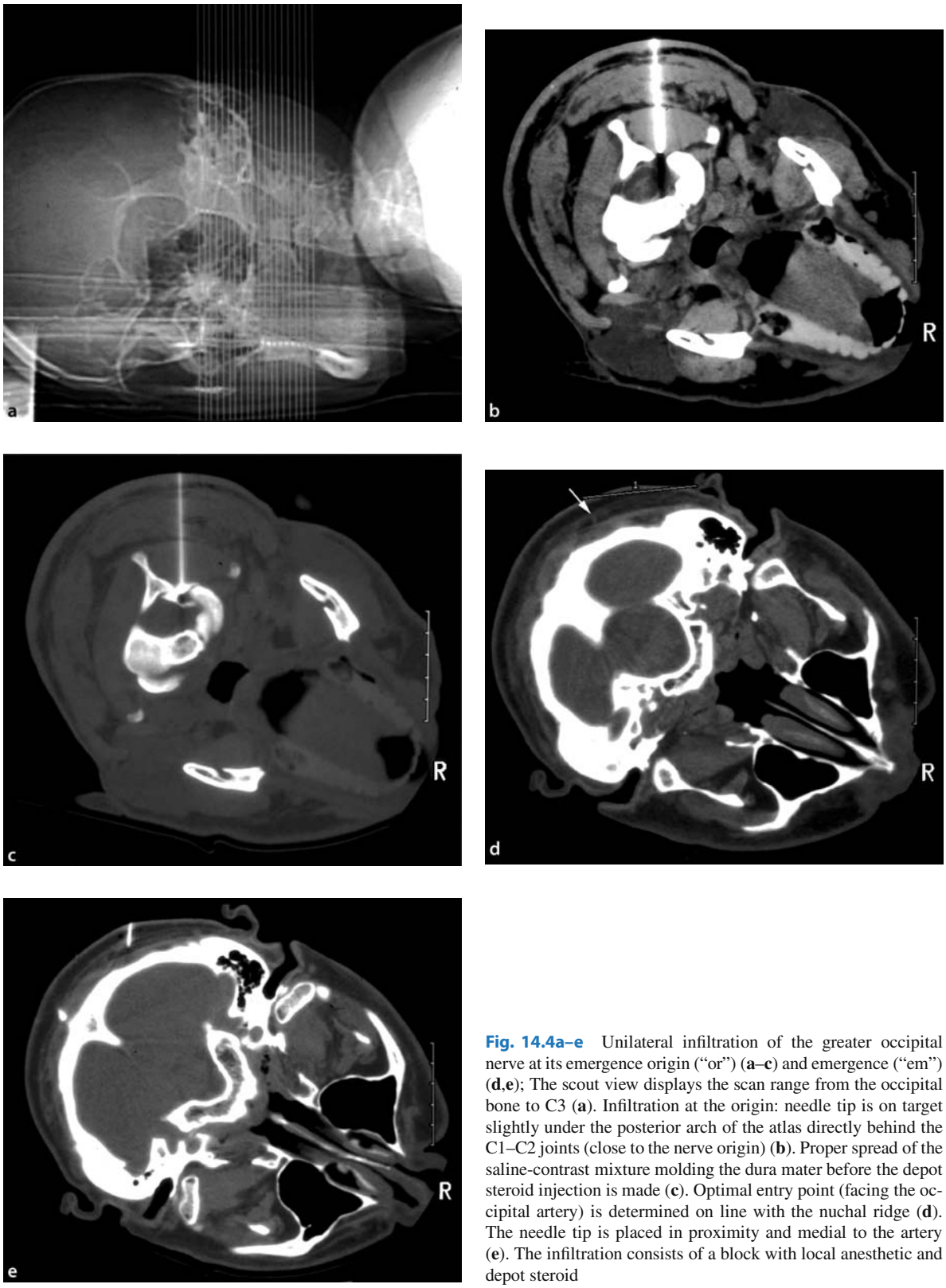

Fig. 14.4a–e Unilateral infiltration of the greater occipital nerve at its emergence origin ("or") (**a**–**c**) and emergence ("em") (**d**,**e**); The scout view displays the scan range from the occipital bone to C3 (**a**). Infiltration at the origin: needle tip is on target slightly under the posterior arch of the atlas directly behind the C1–C2 joints (close to the nerve origin) (**b**). Proper spread of the saline-contrast mixture molding the dura mater before the depot steroid injection is made (**c**). Optimal entry point (facing the occipital artery) is determined on line with the nuchal ridge (**d**). The needle tip is placed in proximity and medial to the artery (**e**). The infiltration consists of a block with local anesthetic and depot steroid

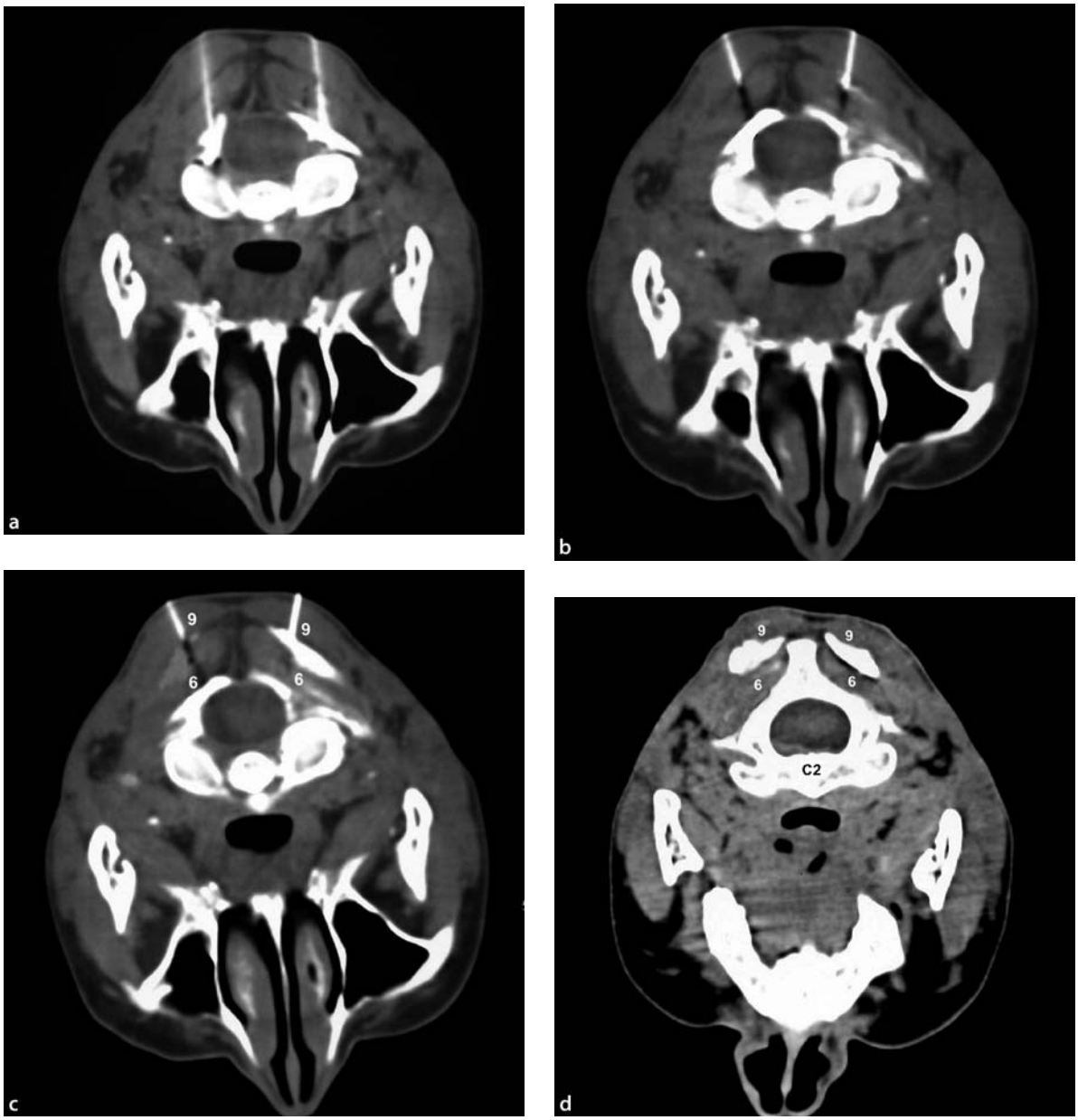

Fig. 14.5a–d Bilateral infiltration of the greater occipital nerve at its origin ("or") and on the second proximal site, first bend ("b1"): Left needle and right needle are on target slightly under the posterior arch of the atlas directly behind the C1–C2 joints (close to the nerve origin). Proper spread of saline-contrast mixture molding the dura matter before the depot steroid injection is made (**a**). A second infiltration is performed by pulling back on the needles to arrive at the first bend (around the inferior oblique capitis muscle) with the needle tips being placed in the fatty compartment between the dorsal aspect of the inferior oblique capitis muscle (6) and the deep aspect of the semispinalis capitis muscle (9) (**b**). The proper spread of this hyperdense mixture between the two muscles (especially towards the "b1" bend) can be verified on control CT slices (**c**,**d**). The depot steroid injection is performed at "b1 target"

Anatomy

The stellate ganglion is a rather large oval-shaped structure. It typically measures 2.5 cm × 1 cm × 0.5 cm. It is formed by the fusion of the inferior cervical and first thoracic sympathetic ganglia and is oriented along the axis of the spine. It is located anterior to the neck of the first rib, the transverse process of the seventh cervical vertebra and posterior to the vertebral artery at the origin from the subclavian artery (Hogan and Erickson 1992; Hogan et al. 1992).

Image Guidance for Alcoholization and RF Procedure (Kastler B 2007)

The patient is placed in a supine position on the CT table with his head turned opposite the side of puncture and his arms at his sides. Axial CT contiguous slices of ≤ 5 mm in thickness are obtained from the superior aspect of the sixth cervical vertebra through the superior level of the second thoracic vertebra as determined from the scout view. The stellate ganglion lies immediately in front of the transverse process of the seventh cervical vertebra and the neck of the first rib. It is targeted on these slice levels. A bolus injection of contrast media is given to display possible intervening vascular structures, particularly the vertebral artery. An anterolateral pathway is chosen. Inadvertent puncture of the external and internal jugular veins as well as the carotid and vertebral arteries need to be avoided meticulously. The needle is slowly moved forward using either sequential or real-time fluoroscopic CT images until its tip is correctly positioned within the target (Kastler et al 2001; Scott et al. 1993).

The ablation may be done by RF neurolysis (Fig. 14.6) or by the injection of ethanol (Fig. 14.7). For RF neurolysis the 20 gauge RF electrode is used. The thermal lesion is created at a temperature of 6080 °C which has to be maintained for 60–120 s. This procedure can be repeated up to three times moving the cannula forward and backward 1 mm each time. The level of the seventh vertebra and the neck of the first rib both should be targeted for RF ablation. As described above, RF thermal neurolysis creates a discreet lesion which provides good pain relief, but which does not interrupt the entire ganglion function and does not tend to produce a Horner's syndrome.

For alcohol ablation the correct position of the needle tip at target (seventh cervical vertebra) is determined by an injection of 1 ml contrast medium 10% diluted in a mixture of lidocaine 1/3 and ropivacaine 2/3. Before the injection the mounted syringe is maintained in aspiration (under vacuum) for 5 s in order to detect blood (vascular puncture). The injected volume should be kept below 1 ml. The procedure is carried out on an outpatient basis and the patient is kept under observation for 1 h.

Complications

A CT control covering the third cervical to second thoracic vertebra at the end of the procedure ensures the absence of complications. Using RF ablation complications are less common when compared with alcohol ablation. Alcohol neurolysis usually produces a Horner's syndrome and should be limited to patients with a low life expectancy (intractable cancer-related pain). Alcohol may diffuse to surrounding motor nerves: the C8 and T1 roots of the brachial plexus are particularly exposed as they are located posterior to the stellate ganglion.

14.2.3.4 Celiac Plexus Neurolysis

Indications

Neurolysis of the celiac plexus (Buy et al. 1982) is an efficient method to treat pain secondary to malignancies of the retroperitoneum and the upper abdomen or secondary to pancreatitis.

Anatomy

The greater, lesser and least splanchnic nerves provide the major preganglionic contribution to the celiac plexus. The celiac plexus is located anterior to the crus of the diaphragm and extends in front of and around the aorta. The ganglia usually lie approximately at the level of the first lumbar vertebra, at the level of the celiac arterial trunk (Ward et al. 1979).

Image Guidance and Alcoholization Procedure (Kastler B 2007)

The posterior transcrural approach with two needles and a trans-aortic approach are our techniques of

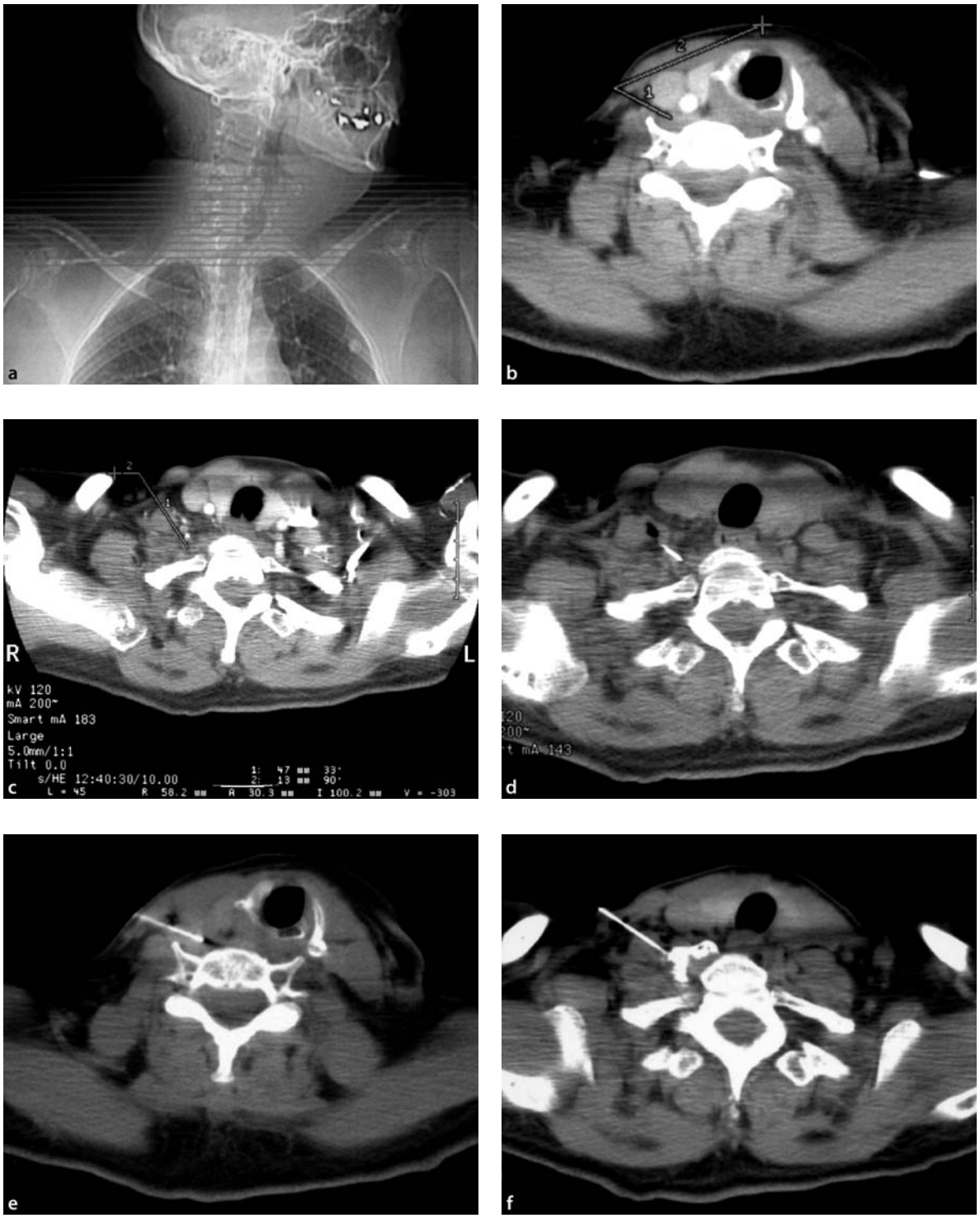

Fig. 14.6a–f Radiofrequency (RF) neurolysis of the stellate ganglion: 49-year-old man suffering CRPS type 1 syndrome after wrist trauma. Scan range is displayed on scout view (**a**). Entry points and trans-scalenic pathway are displayed at C7 and T1 levels (**b**,**c**). RF needle tips on targets at C7 and T1 levels (**d**,**e**). After RF thermolysis additional blockade with local anesthetics was performed at the end of the procedure. Control CT scan shows the contrast-anesthetic mixture diffusing around the needle tip (**f**). Clinically a good long term result was obtained after the procedure

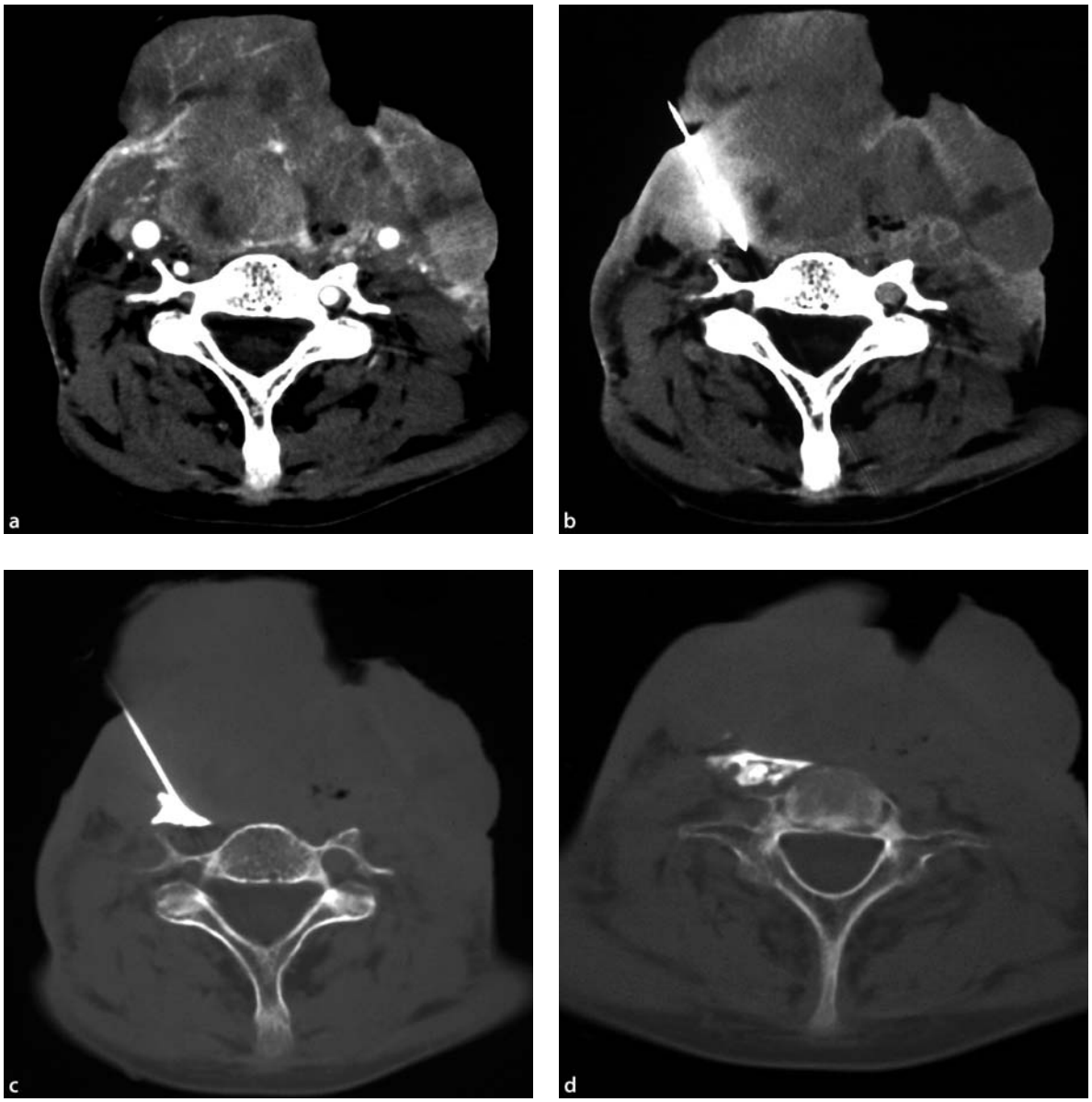

Fig. 14.7a–d Alcohol neurolysis of the stellate ganglion: 45-year-old male patient with locally advanced throat cancer suffering severe intractable cervical pain. Image after bolus contrast injection (**a**). Excellent pain relief was observed immediately following ethanol neurolysis. This effect lasted until the patient died five months later. An anterolateral approach at the posterolateral aspect of the mass at the level of C7 was chosen to avoid the hypervascularized tumor (**b**). Correct positioning of the needle tip at target is attested by the diffusion of a local anesthetic diluted with contrast medium showing good diffusion around and particularly behind the vertebral artery (**c**). Injection of 1 ml of absolute alcohol appearing as hypodensities within the contrast medium (**d**)

choice (Ischia et al. 1983, 1992; Kastler B 2007). Therefore the patient is placed in the prone position with a pillow placed under the abdomen. Axial CT sections of ≤ 5 mm in thickness with injection of contrast media are obtained from the level of the eleventh thoracic vertebra to the second lumbar vertebra. The target level is chosen between the celiac arterial trunk and superior mesenteric artery. The 20–22 gauge needles

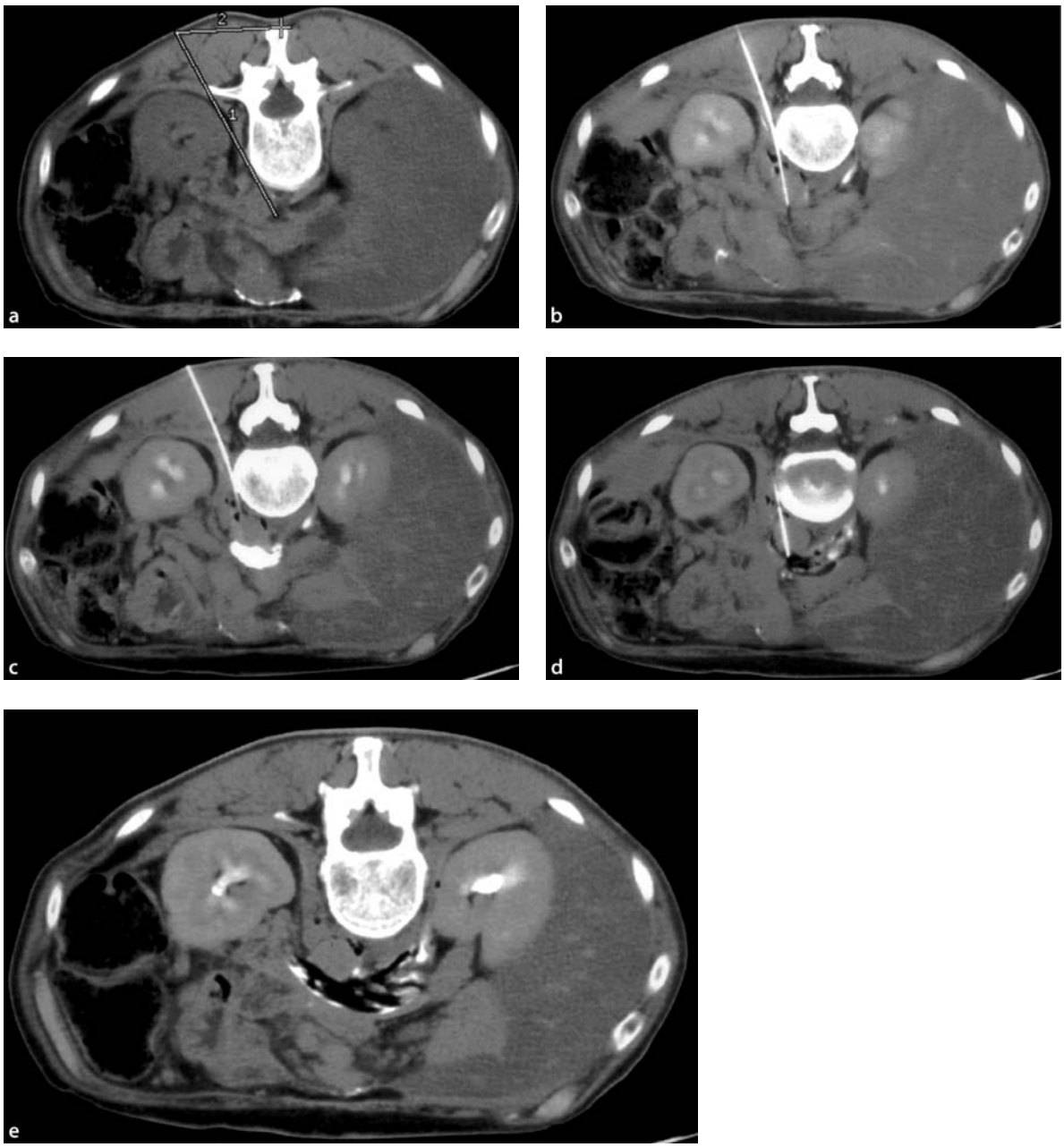

Fig. 14.8a–e Celiac plexus neurolysis: direct access using transaortic passage. Trajectory (*line*) for transaortic celiac neurolysis (**a**). Transaortic passage of the needle to the celiac site (**b**). After injection of a lidocaine/contrast mixture there is a good symmetrical diffusion anterior to the aorta (**c**). Control after injection of 5 ml absolute alcohol seen as hypodensity within the contrast agent (**d**). Control scan after end of injection of 15 ml of absolute alcohol shows an excellent alcohol diffusion in the celiac region (**e**)

are advanced under repeated sequential or fluoroscopic real time CT guidance until their tips are positioned at the splanchnic nerves anterior and lateral to the first lumbar vertebral body. The left needle crosses the aorta to the region of the celiac ganglia. Adequate positioning is attested by a test injection of contrast

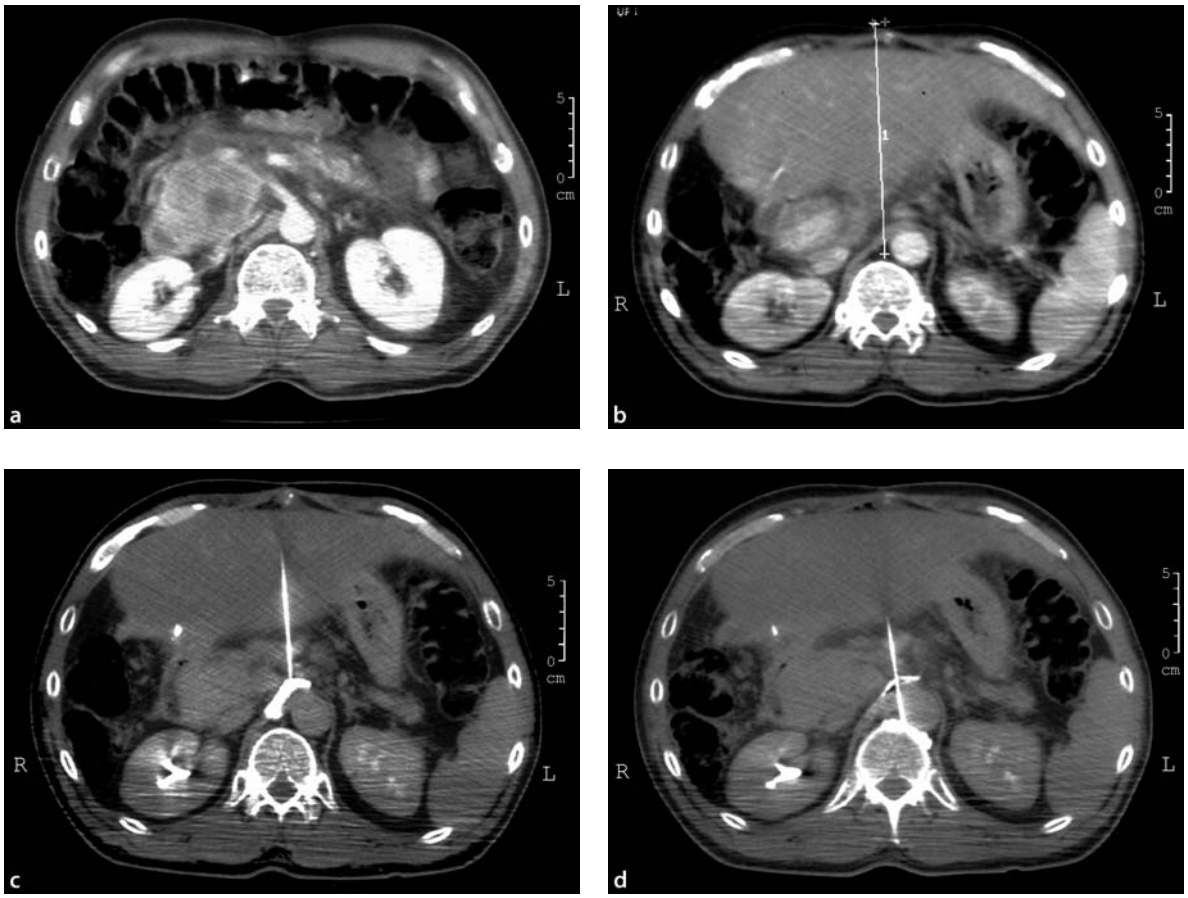

Fig. 14.9a–d Splanchnic and celiac neurolysis via an anterior approach: cancer of the pancreas (**a**). Trajectory indicated (*line*) for celiac and splanchnic neurolysis (**b**). Celiac neurolysis is performed (**c**), followed by splanchnic neurolysis via an approach lateral to the aorta (**d**). A transaortic approach is also possible for the splanchnic neurolysis

medium 10% diluted in a mixture of lidocaine 1/3 and ropivacaine 2/3 (3 ml celiac, 1 ml splanchnic). Before the injection the mounted syringe is maintained in aspiration (under vacuum) for 5 s in order to detect blood (vascular puncture). The contrast media should be seen in the pre-aortic area and surrounding the aorta and celiac trunk (Fig. 14.8). Finally a 10–15 ml volume of absolute alcohol is instilled slowly (Haaga et al 1984; Lee et al. 1993).

A transaortic path is excluded in aortic aneurysm, voluminous calcified parietal plaque, or mural thrombus and should be avoided with patients suffering from chronic respiratory insufficiency.

Alternatively, a posterior approach may be used using two needles with a lateral aortic approach. The material however rarely spreads as it should bilaterally in front of the aorta and/or on the right for the contralateral injection; the inferior vena cava or another obstacle often hinders the needle's trajectory.

The anterior approach to the celiac plexus involves the passage of a fine needle through the liver, stomach, and pancreas (Fig. 14.9). It is most useful in patients who are unable to lie prone. An anterior approach should be avoided when there is significant gastric stasis with distension.

Complications

Complications include local pain, and orthostatic hypotension. Thus, the patient is observed for hemodynamic changes because of profound sympathetic blockade. Pleural effusion has been described (Fujita and Takaori 1987). Post-block diarrhea occurs in approximately 50% of patients (Gafanovich et al.

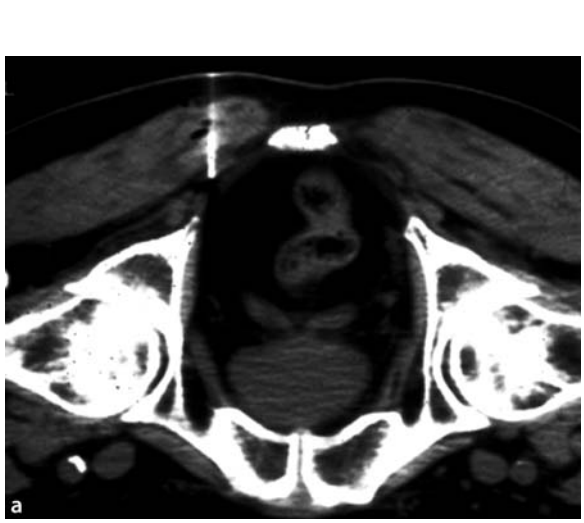

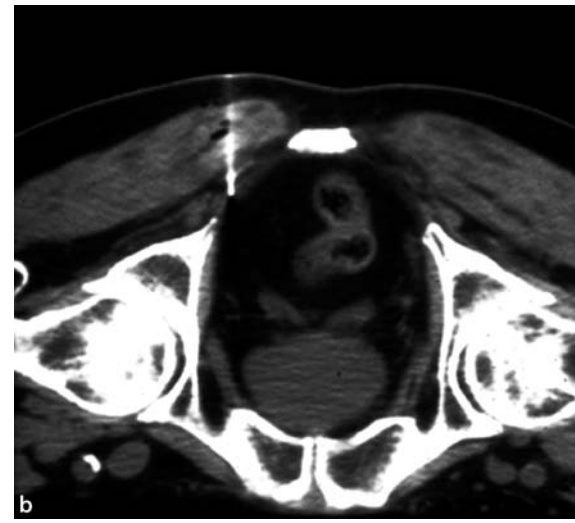

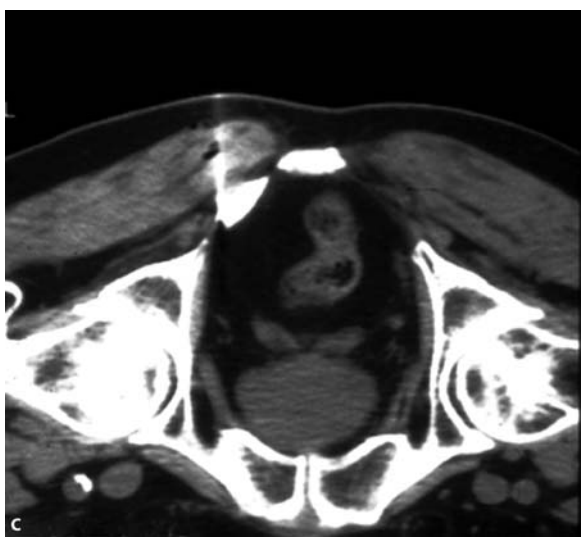

Fig. 14.10a–c Pudendal nerve infiltration first site: sequential CT monitoring the needle tip progressing on the right to the ischial spine between the sacrospinous and sacrotuberal ligaments (**a**,**b**). Here the added contrast media to the local anesthetics (not mandatory) diffuses between the sacrospinous and sacrotuberal ligaments (**c**; first site). The depot steroid injection can be performed

1988). The latter in fact often alleviates the frequent cases of chronic constipation in these patients under opiates.

14.2.3.5 Pudendal Nerve Infiltration

Indications

Pudendal neuralgia is rare and very painful and invalidating (Amarenco et al. 1988). Infiltration (Corréas et al. 1990) has been found helpful in managing the pain and to predict efficacy of surgical decompression.

Anatomy

The pudendal nerve is formed from the fusion of the 2nd, 3rd and 4th sacral nerves which merge posterior to the ischiatic spine. Anatomical studies suggest that there are two possible conflicting sites:

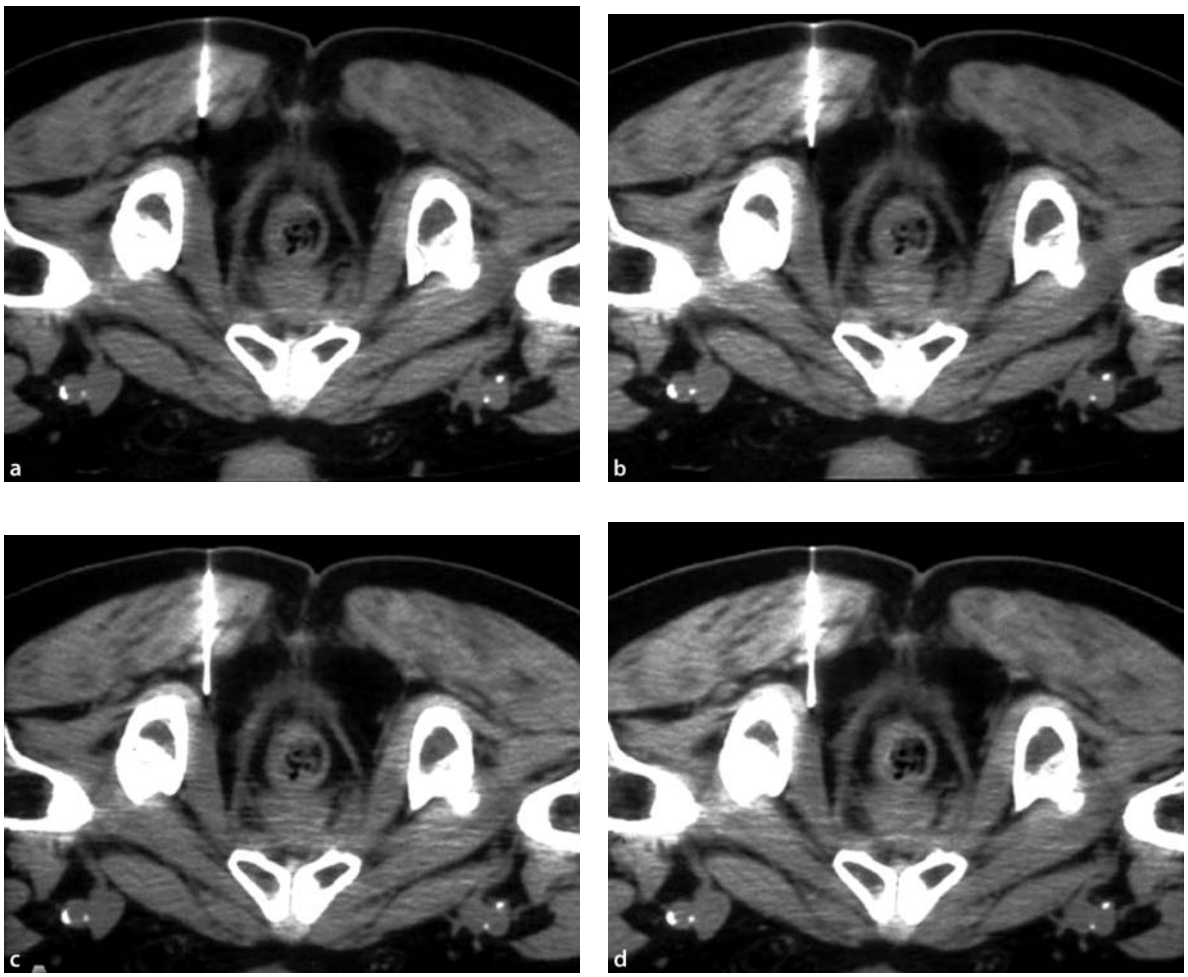

Fig. 14.11a–d Pudendal nerve infiltration second site: CT shows the progress of the needle tip on the right to Alcock's canal (**a**–**c**) abutting the pudendal nerve (C; second site)

1. entrapment of the pudendal nerve during its course at the ischial spine as the nerve can be entrapped under the sacrospinous ligament and/or
2. the Alcock's canal a non-stretchable aponeurotic tunnel.

Image Guidance and Infiltration Procedure (Clair C 1998; Kastler B 2007)

The patient is placed in a prone position. Axial slices of ≤ 5 mm thickness are obtained covering the region of the obturator foramen. Both possible conflict sites are targeted (Figs. 14.10 and 14.11). Optimal skin entry points are determined choosing a grossly vertical course. The needles are slowly advanced transglutally under imaging guidance. Following the anesthetic block test the patient should note a decrease in his pain. Before the injection the mounted syringe is maintained in aspiration (under vacuum) for 5 s in order to detect blood (vascular puncture). Thereafter the infiltration is performed with 1 ml of long-release-glucocorticoid (e.g. cortivazol 3.75 mg) which should be slowly instilled at both levels. After the infiltration the solution is seen within the pudendal canal along the internal obturator muscle and between the sacrotuberal and sacrospinal ligaments.

A CT control at the end of the procedure ensures the absence of complications, namely hematoma. The procedure is carried out on an outpatient basis and the patient is kept under observation for 1 h. Controlateral

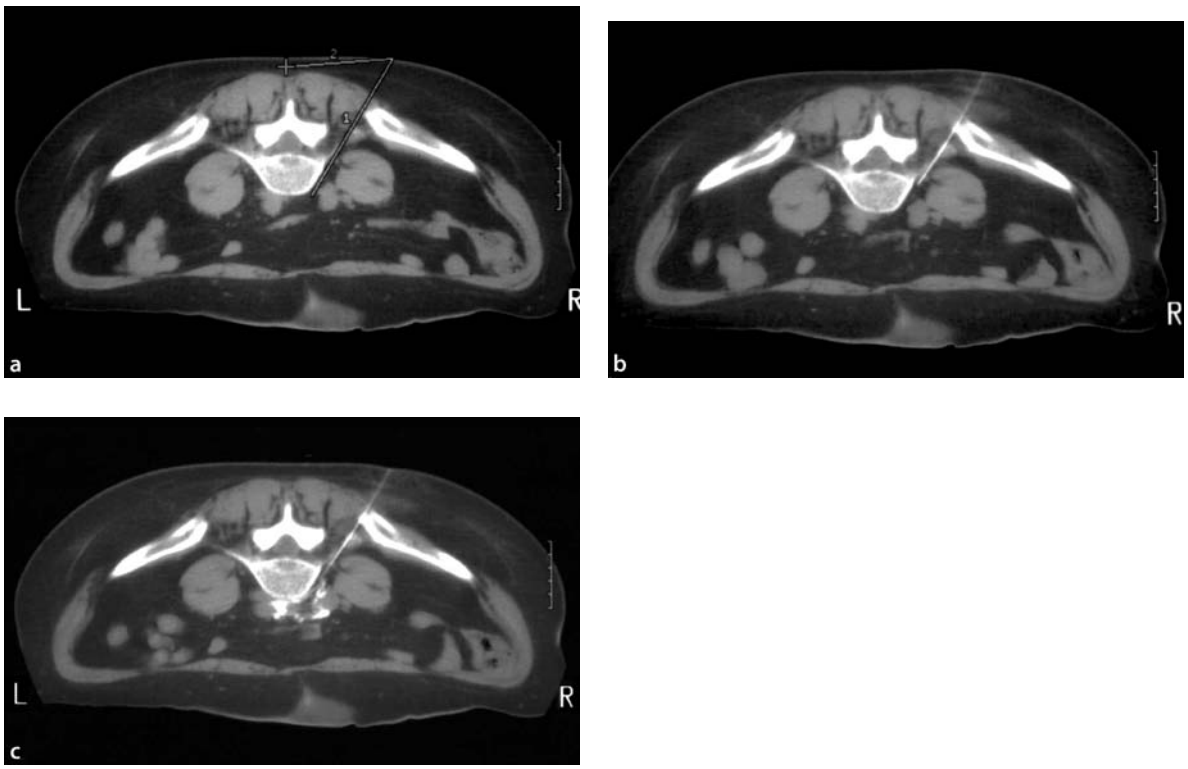

Fig. 14.12a–c Neurolysis of the interiliac plexus (presacral nerves): locating the trajectory with the patient in prone position (**a**). Progressive introduction of the needle behind the iliac vessels at the L5–S1 level (**b**). Injection of a contrast-anesthetic mixture (5 ml) followed by a slow-release corticoid (**c**)

treatment (if justified) can be carried out around two weeks afterwards.

14.2.3.6 Interiliac Sympathetic Plexus and Ganglion Impar Neurolysis

Indications

These techniques are generally recommended in the case of pelvic pain caused by a tumoral invasion of colorecteal or gynaecological cancers and also of radiation rectitis. The treatment of chronic pain related to endometriosis can also benefit from this procedure (Wechsler et al. 1996).

Anatomy

The interiliac plexus (corresponding to the presacral nerve) is located in an anterolateral position at L5–S1 beneath the aortic bifurcation between the common iliac arteries. It extends into the pelvis and divides into two streams, which integrate the hypogastric plexus. A section of the presacral nerve causes hypoesthesia of the pelvic organs, vasomotor changes in women and ejaculatory problems in men.

The ganglion impar, also know as the Walther ganglion corresponds to anastomosis of the caudal tip of the laterovertebral chains. It is medially located at the anterior side of the coccyx.

Image Guidance for Alcoholization and RF Procedure (Kastler B 2007)

In the case of the presacral nerve, a postero-lateral approach is taken, the patient positioned in a procubitus position (Fig. 14.12). The tip of a 22 Gauge needle is positioned in front of L5-S1, dorsal to the iliac vessels. An anesthetic block test (e.g.

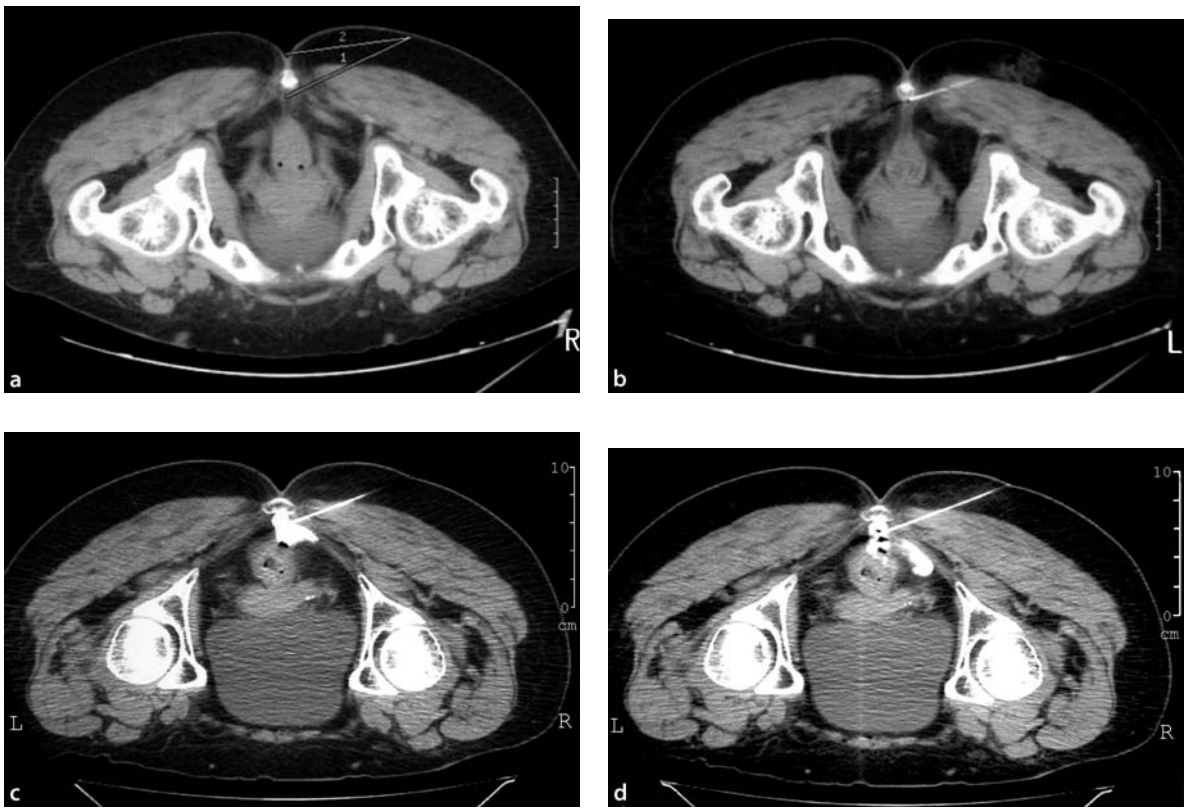

Fig. 14.13a–d Neurolysis of the ganglion impar in a patient suffering from acute coccygodynia. Locating the trajectory (**a**). Positioning the needle in front of the coccyx (**b**). An anesthetic block with an additional slow-release corticoid resulted in pain relief for three weeks. A second session with injection of a contrast-anesthetic mixture was performed (**c**). Radiofrequency ablation was performed resulting in definitive pain relief. Note the formation of bubbles due to vaporization (**d**)

5 ml ropivacain 0.25) is performed, as is contrast medium to ascertain diffusion between the vessels, followed by an injection of delayed corticoid. Before the injection the mounted syringe is maintained in aspiration (under vacuum) for 5 s in order to detect blood (vascular puncture). If a more definitive neurolysis is recommended, 3–5 ml of absolute alcohol are injected slowly. Full neurolysis generally requires several sessions carried out every three weeks.

In the case of neurolysis of the ganglion impar, the approach is lateral and the tip of the needle is positioned in front and median to the coccyx, behind the rectum (Fig. 14.13). In the case of coccygodynia, the infiltration of anaesthetics and corticoids in the pericoccygeal can be completed by RF neurolysis of the ganglion impar (unpaired).

Summary

CT guided procedure can be used either in addition to or as an alternative to the conventional methods of pain therapy. They are usually performed on an outpatient basis. CT-guidance allows step by step control of the procedure and is much safer and reliable than fluoroscopy guidance. Radiologist should become skilled in this field of interventional radiology aimed at pain therapy.

Key Points

- There are image-guided procedures for pain management for many otherwise untreatable pain syndromes including cancer pain, cluster headache, atypical facial pain, pudendal pain or Arnold's neuralgia.
- Interventional pain management is safe and effective.
- Detailed knowledge of anatomy is mandatory for the interventionalist.

References

Amarenco G, Lanoe Y, Ghnassia RT et al. (1988) Syndrome du canal d'Alcock et névralgies périnéales. Rev Neurol (Paris) 144: 523–526 [French]

Bogduk N (1980) The anatomy of occipital neuralgia. Clin Exp Neurol 17:167–184

Bogduk N (1981) Local anesthetic blocks of the second cervical ganglion: a technique with application in occipital headache. Cephalgia 1:41–50

Bovim G, Sand T (1992) Cervicogenic headache, migraine without aura and tension-type headache. Diagnostic blockade of greater occipital and supra-orbital nerves. Pain 51:43–48

Bovim G, Fredriksen T, Stolt-Nielsen A et al. (1992) Neurolysis of the greater occipital nerve in cervicogenic headache. A follow up study. Headache 32:175–179

Buy JN, Moss AA, Singler RC (1982) CT guided celiac plexus and splanchnic nerve neurolysis. J Comput Assist Tomogr 6:315–319

Clair C, Kastler B, Aubry R et al. (1998) Neurolyse du ganglion sphénopalatin sous contrôle TDM. Radiologie J CEPUR 18:405–411 [French]

Devoghel JC (1981) Cluster headache and sphenopalatine block. Acta Anaesthesiol Belg 32:101–107

Corréas JM, Belin X, Amarenco G et al. (1990) Infiltration scano-guidée dans le syndrome du canal d'Alcock chronique. Rev Im Med 2:547–549 [French]

de Kersaint-Gilly A, Sonier CB, Legent F et al. (1991) Radioanatomie de la fosse infratemporale. Région ptérygo-maxillaire. Ann Otolaryngol Chir Cervicofac 108:77–81 [French]

Forouzanfar T, Van Kleef M, Weber WEJ (2000) Radiofrequency lesions of the stellate ganglion in chronic pain syndromes. Clin J Pain 16:164–168

Fujita Y, Takaori M (1987) Pleural effusion after CT guided alcohol celiac plexus block. Anesth Analg 66:911–912

Gafanovich I, Shir Y, Tsvang E et al. (1988) Chronic diarrhoea induced by celiac plexus block. J Clin Gastroenterol 26:300–302

Gangi A, Dietemann JL, Schultz A et al. (1996) Interventional radiologic procedures with CT guidance in cancer pain management. Radiographics 16:1289–1306

Haaga JR, Kori SH, Eastwood DW et al. (1984) Improved technique for CT-guided celiac ganglia block. AJR Am J Roentgenol 142:1201–1204

Hardebo JE, Elner A (1987) Nerves and vessels in the pterygopalatine fossa and symptoms of cluster headache. Headache 27:528–532

Hogan QH, Erickson SJ (1992) MR imaging of the stellate ganglion: normal appearance. AJR Am J Roentgenol 158:655–659

Hogan QH, Erickson SJ, Abram SE (1992) Computerized tomography (CT) guided stellate ganglion blockade. Anesthesiology 77:596–599

Ischia S, Luzzani A, Ischia A et al. (1983) A new approach to neurolytic block of the celiac plexus: the transaortic technique. Pain 16:333–341

Ischia S, Ischia A, Polati E et al. (1992) Three posterior percutaneous celiac plexus block techniques. A prospective, randomized study in 61 patients with pancreatic cancer pain. Anesthesiology 76:534–540

Kastler B (2007) Interventional radiology in pain management. Springer, Berlin Heidleberg New York

Kastler B, Couvreur M, Clair C et al. (1999) Tomodensitométrie interventionnelle: suivez le guide. Feuillets de Radiologie 39:421–432 [French]

Kastler B, Narboux Y, Clair C (2001) Neurolyse par radiofréquence du ganglion stellaire. À propos d'un cas traité et suivi sur trois ans. J Radiol 82:76–78 [French]

Lee MJ, Mueller PR, Van Sonnenberg E (1993) CT-guided celiac ganglion block with alcohol. AJR Am J Roentgenol 161:633–636

Scott J, Erickson SJ, Quinn H et al. (1993) CT guided injection of the stellate ganglion: description of technique and efficacy of sympathetic blockade. Radiology 188:707–709

Vital JM, Grenier F, Dautheribes M et al. (1989) An anatomic and dynamic study of the greater occipital nerve (n. of Arnold). Applications to the treatment of Arnold's neuralgia. Surg Radiol Anat 11:205–210

Ward EM, Rorle DK, Nauss LA et al. (1979) The celiac ganglia in man: normal anatomic variations. Anesth Analg 68:461–465

Wechsler RJ, Maurer PM, Halpern EJ et al. (1996) Superior hypogastric plexus bloc for chronic pain in the presence of endometriosis: CT technique and results. Radiology 105:103–105

14.3 Thoracic and Lumbar Sympathicolysis

Jan Hoeltje, Bruno Kastler and Roland Bruening

14.3.1 Introduction

The sympathetic trunk is an extension of the cervical sympathetic chain. It is made up of nervous filaments with ganglion relays located on either side of the vertebra. As a doubled nerval network with segmental paired ganglia it mimics a ladder-like appearance. In the chest these paired ganglia are bilateral, situated latero-ventrally to the vertebral body in front of the capitulum of the rib. The second thoracic ganglion lies at the second rib neck (the first thoracic ganglion is fused with the eighth cervical nerve root forming the stellate ganglion); ganglia T3 to T6 lie at the rib heads and T7 to T10 ganglia are located at the costovertebral joints (in front of the costovertebral ligaments); T1 and T12 are more anterior in a lateral position in relation to the vertebra. In the lumbar region the ganglia are located more anterior than the sympathetic thoracic sym-

pathetic chain. On the left side they are located dorsolaterally of the aorta, on the right side behind the inferior vena cava. In the upper abdomen some fibers form the sympathetic ganglia branches to the celiac plexus (see Sect. 14.2). Laterally the lumbar sympathetic ganglia are bordered by the Iliopsoas muscle, in which the lumbar plexus branches. The skin branches of the extremities are nearly completely innervated by the parasympathetic trunk. The sympathetic trunk also influences the regulation of the tonus of the peripheral arteries and thus to the perfusion of the limbs. It is also part of the regulation of peripheral hidrosis and plays a role in chronic pain syndromes.

Its anatomical location leading from the cervical ganglia to the thoracic paravertebral and finally to the lumbar prevertebral space it is easily assessable for percutaneous CT or MR controlled treatment.

14.3.2 Indications and Contraindications

Jaboulay (1899) described the first surgical sympathectomy for pain therapy in peripheral arterial occlusive disease. Currently the most common indication for sympathicolysis is treatment of chronic limb ischemia in otherwise untreatable peripheral arterial occlusive disease (PAOD) with a PAOD grade III or IV according to Fontaine (Lee et al. 1983; Rosen et al. 1983; Duda et al. 1994; Heindel et al. 1998; Feinglass et al. 1999; Finkenzeller et al. 2001; Huttner et al. 2002; Pieri et al. 2005; Schmid et al. 2006). In other words, sympaticolysis is considered an indication, if the patients are strongly affected, if their chronic pain syndrome exists for years and the available therapies had failed or have had only a short-term effect.

Clinical severe limb ischemia caused by Raynaud's disease (Janoff et al. 1985; Di Lorenzo et al. 1998; Thune et al. 2006; Maga et al. 2007), or thromboangiitis obliterans (M. Buerger) may also be an indication for sympaticolysis (Lau and Cheng 1997; Arkkila 2006).

Further indications for image guided sympathicolysis include:

- Distal arthritis
- Distal arterial embolism
- Frostbite
- Post-traumatic dystrophy and causalgia (sympathetically maintained pain syndrome)
- Neoplasm of paravertebral gutters with vertebral invasion
- Phantom limb
- Palmar or axillary hyperhydrosis

In suspected sympathetically maintained pain syndrome (SMP) a detailed history of the patient, cross sectional imaging and laboratory examinations are mandatory to exclude other causes of pain.

There are no absolute contraindications to sympathicolysis; however, a sufficient thrombocytic platelet count ($> 80\,000/\text{mm}^2$) and absence of antiplatelet medication or coagulation disorders should be ensured. Prior to the intervention known intolerance to the substances used should be excluded. Infectious cutaneous lesions along the access route have to be treated previously.

14.3.3 Material

- 20–22 G trocar with mandrin with a length of 10–25 cm depending on puncture site and patient constitution.
- 10 ml local anesthetic (e.g. prilocaine 2%).
- 96% ethanol.
- Iodinated contrast medium.
- Physiologic saline solution.
- Sterile bowl.
- 10-ml syringe (A luer lock syringe is recommended particularly in combination with alcohol. It is easier to guide than a standard syringe and improves safety during injection).
- 2×5-ml syringe.
- Short extension line.
- Sterile table.
- Sterile draping, sterile gloves, sterile gowns, skin disinfection.

14.3.4 Technique

Prior to any percutaneous sympathectomy, an intravenous access line should be applied. If bilateral treatment is intended, the more affected side should be treated first and after successful therapy, the contralateral treatment should be performed after an interval of at least 24 h.

14.3.4.1 Thoracic Sympathicolysis

In our experience, the approach in prone position with the needle advanced from behind is preferable (Fig. 14.14). In principle, an approach from ventral can also be employed for both thoracic and abdominal sites, but will not be described in detail here. The intervention is performed as follows:

- Patient in comfortable prone position or, if impossible, transversal position.
- CT or MR scan from thoracic vertebral body 2–4, if possible in the arterial contrast phase with a slice thickness of approximately 3 mm.
- Planning of the access route from dorsolateral as the sympathetic trunk is situated ventrolaterally to the vertebral body in front of the capitulum of the rib.
- The level of the intervention depends on the indication: palmar hyperhidrosis = T4, axillary hyperhidrosis = T2/3, ischemic pain = T2/3, tumor-associated pain or SMP according to the pain location). Alternatively a two level therapy at T2 and T3 may be performed to improve success rate.
- Thorough skin surface disinfection and coverage with a sterile draping.
- Careful needle advancement to the target point under cross-sectional imaging control with either repeated sequential images or under CT or MR-fluoroscopy in order to follow the needle position and to avoid critical structures.
- If the puncture is hampered by a close relationship to the pleura, the pleura may be displaced laterally by a saline depot of 20 ml or more if needed.

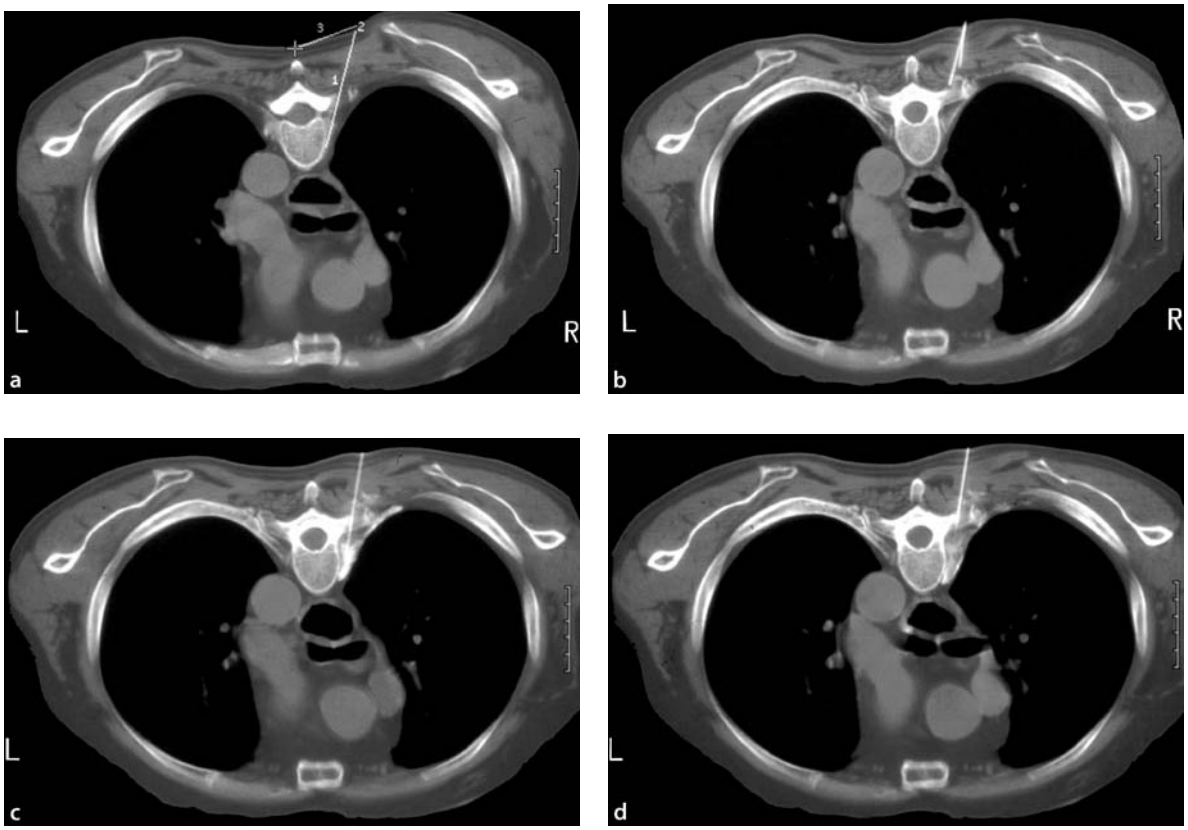

Fig. 14.14a–d Patient with thrombosis of the right subclavian artery following a stent emplacement. Sympathicolysis is planned at the level T3 (**a**) The space between pleura and the lateral aspect of the vertebral body is almost nonexistent, too narrow for an adequate pathway. Guidance by the anesthesia needle left in position (**b**). Widening of the channel by injection of physiological saline and contrast, thus pushing away the pleuropulmonary parenchyma (**c**). Injection of absolute alcohol, resulting in a dilution of the contrast medium by the hypodense alcohol (**d**)

- After correct needle placement ventral to the capitulum of the rib the extension line is fixed to the cannula. After aspiration to exclude intravascular needle position it is irrigated with a contrast/prilocaine solution.
- Subsequently of 2 ml of a 1:4 contrast medium/prilocaine solution and a control scan are performed.
- The position of the needle is correct when the sympathetic ganglion is irrigated and no clinical symptoms of Horner's syndrome or other neurological disorder occur and there is no intraspinal contrast distribution.
- Mixing of 9 ml ethanol, 4.5 ml prilocain and 1.5 ml contrast medium (6 : 3 : 1) in the bowl to be drawn up in the 10-ml syringe.
- Slow injection of a total of 2–3 ml ethanol solution. Injection is stopped in case of pain.
- Irrigation of the cannula with a very small amount of saline and withdrawal.
- Control scan according to the initial one to document the diffusion of the contrast medium and to exclude a pneumothorax.

Patients unwilling to run the risk of Horner's syndrome or surgery are treated by RF. The very localized character of thermal lesion ablation removes the risk of this complication. For RF ablation a disposable RF probe without interbal cooling is used in order restrict the ablation volume. First a stimulation mode test is carried out. The patient should describe a posterior thoracic pain. There must be no intercostal fasciculation. Thereafter one ml of local anesthetics is injected followed by 80 °C thermolysis for 90 s. The needle is inserted 2 mm further and a second thermolysis carried out.

Independent if alcohol or RF ablation are used for the procedure; the patient should experience heat in the upper limb treated in particular of the hand. Effectivity of the procedure can be objectivized by comparing the temperature of both hands.

14.3.4.2 Lumbar Sympathicolysis

- Patient in comfortable prone position.
- Imaging from lumbar vertebra 1 to lumbar vertebra 5. If CT is used imaging might be performed during the urographic contrast phase in order to delineate the ureter clearly.
- Planning of the access route. The sympathetic trunk takes its course dorsal to the aorta and the inferior caval vein. The target ganglia are located at the level L3 and L4. Injection may be performed at a single or at two levels simultaneously, with the latter improving treatment success. The L2 level should be left out because of the potential of intestinal motility disorders. The cutaneous entry point and trajectory are determined to ensure that the kidney, transverse process, colon, vertebral body and intervertebral disk are avoided.
- Careful advancement of the puncture needle with repeated control scans if needed or use of CT-/MR-fluoroscopy.
- When the needle point is in correct position, in front of the psoas and dorsal to the aorta or inferior vena cava, an extension line irrigated with contrast medium/prilocaine solution is fixed to the needle. After aspiration about 3 ml of a 1:4 contrast medium/prilocaine solution are injected and a control scan is performed.
- The needle position is correct when the contrast medium spreads semicircularly around the dorsal aspect of the inferior caval vein and/or the aorta, excepting the ureter.
- Mixing of 9 ml ethanol, 4.5 ml prilocaine and 1.5 ml contrast medium (6:3:1) to be drawn up in the 10-ml syringe.
- Slow injection of up to 15 ml ethanol solution under repeated imaging control. Injection needs to be interrupted in case of significant diffusion towards the ureter, rear at the level of the second lumbar vertebra, because of the origin of the inguinofemoral nerves. Between L1 to L3 the femoral and obturator nerves originate while L4–L5 is important because of the sciatic nerve origin. Injection needs also to be stopped in case of pain.
- Final control scan according for documentation of the spreading (Fig. 14.15).

For RF ablation the same needle position as for ethanol injection may be used. After needle placement a stimulation mode test is carried out; the patient should describe a posterior lumbar pain. Thereafter local anesthesia is applied, followed by 80 °C thermolysis for 90 s. The needle is inserted 2 mm further and a second thermolysis carried out.

Independently of the puncture site, all patients should be supervised for at least 4–6 h postinterventionally for pulse and blood pressure. Taking into con-

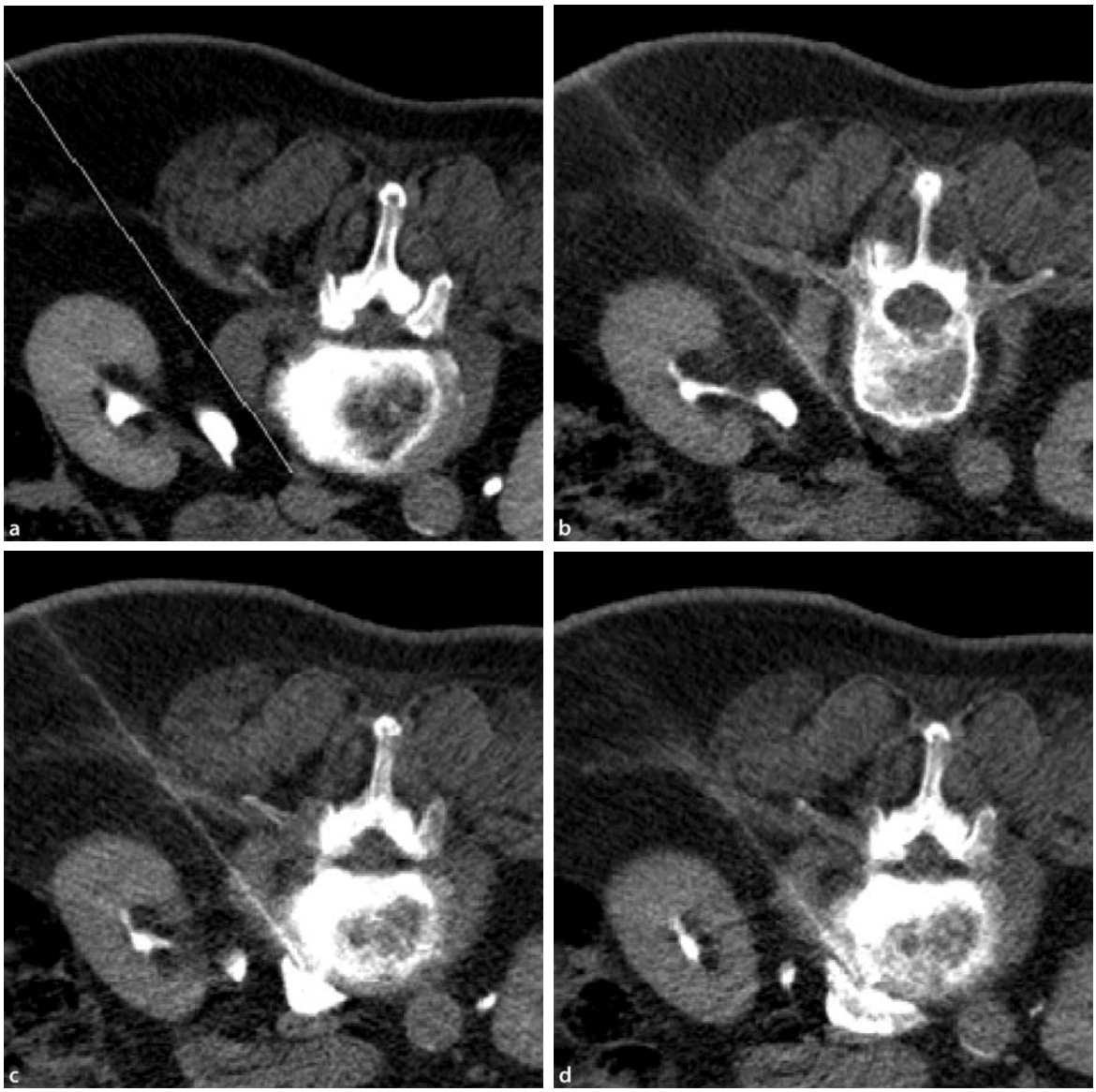

Fig. 14.15 A 79-year-old female patient suffering from PAOD grade IV with moist gangrene of the right foot and PAOD III on the left side. On the level of lumbar vertebra 3, the sympathetic trunk is situated ventral of the vertebral body. In this patient it was reached best from the right side. After planning of the access route (**a**) the needle was advanced step by step and the final needle position documented on CT (**b**). After a test injection of local anesthetics mixed with contrast media, CT scan shows regular contrast distribution preserving the ureter (**c**). Finally, CT control after ethanol injection shows the same contrast distribution without spread to critical structures (**d**). The patient reported a sensation of heat on discharge after 4 h and pain relief at the control consultation two weeks later. The gangrene had become dry meanwhile, so the clinical staging improved from Fontaine Stage IV to IIb

sideration a possible orthostatic pressure drop, monitoring is advised and the patient should get up slowly at first under supervision.

In pain therapy, repeated blockages with local anesthetics are often sufficient so that a definitive destruction with alcohol of nerve fibres may be avoided.

14.3.5 Results

In case of ischemic pain in PAOD, pain relief or healing of an open wound has to be considered as treatment success. Clinically, regaining of a heat sensation in the dependent vascular areas is observed first. Typically, after one to three month improvement is seen in 39–79% of cases (Duda et al. 1994; Huttner et al. 2002). In PAOD, long-term improvement of the Fontaine grade or avoidance of amputation is described in up to over 35% (Lee et al. 1983; Schild et al. 1984; Di Lorenzo et al. 1998, Huttner et al. 2002).

In case of other states of pain, Zoster's neuralgia, SMP or tumor-associated pain, the aim of therapy is achieved when the patient reports absence or marked relief of pain. There are only few small studies and case on this problem indicating a sometimes only temporary pain relieve in SMP of 44% and in Zoster's neuralgia ($n = 3$) of 100%. (Furlan et al. 2001; Price et al. 1998; Vranken et al. 2002).

If thoracic or lumbar sympathicolysis was performed for treatment of hyperhidrosis, therapy may be considered successful if hyperhidrosis is reduced to a tolerable degree. The latter will be reached in more than 98% with long term success in more than 80% of patients (Adler et al. 1990; Romano et al. 2002).

14.3.6 Complications

Complications are rare, but there are several side effects of interventional sympathicolysis. Deep abdominal or genital (N. genitofemoralis) pain is not uncommon during the injection. It usually ends when the injection is terminated. Orthostatic dysregulation, which typically normalizes within 24 h, may be observed. Bed rest and a blood pressure monitoring are recommended to prevent complications. In most cases, accidental vessel puncture does not cause relevant hemorrhage because of the very small needle diameters.

Compensatory sweating (Baumgartner and Toh 2003; Katara et al. 2007; Montessi et al. 2007) should be mentioned, particularly if hyperhidrosis is the indication for treatment. Furthermore, temporary or persisting hypoesthesia in the corresponding skin region may develop subsequently to a sympathicolysis. The patient has to be informed about the side effects referring to the substances used and the possibly resulting allergy.

For the thoracic level, the danger of a pneumothorax has to be mentioned. A possible but unlikely danger of infection may cause pleuritis or, at the lumbar level, peritonitis. If a thoracic sympathicolysis has to be performed, Horner's syndrome may also occur. If T1 is affected, up to 20% complete or incomplete Horner's syndrome may be observed. A theoretical complication results from accidental intrathecal intrapinal injection.

Lumbar sympathicolysis involves the risk of renal puncture and an intestinal perforation. The most relevant problem, however, is a possible stricture or necrosis of the ureter with consecutive hydronephrosis. In case of affection of the ureter, renal function needs to be monitored and sonographic evaluation of the affected kidney is needed two weeks after the intervention. In case of renal engorgement, insertion of a DJ catheter has to be discussed with a urologist. Bilateral lumbar treatment at the L2 level may cause disorders of voiding the bladder, as well as disorders of the intestinal motility and of ejaculation.

Summary

The benefit of sympathectomy introduced 100 years ago by Jaboulay (1899) for the treatment of PAOD in connection with ischemic pain is still given in patients with finally unresponsive angioplastic treatment. Surgical sympathectomy is often and successfully used for this indication. In comparison, the radiological interventional procedure offers several advantages including the minimal invasive approach, the option of an outpatient treatment, lack of anesthesia and a low complication rate (Adler et al. 1990; Schneider et al. 1996; Chen et al. 2001; Baumgartner and Toh 2003; Moya et al. 2006; Katara et al. 2007; Montessi et al. 2007) In case of symptom recurrence, several repetitions of a sympathicolysis are possible.

One has to bear in mind that all procedures described above represent ultima ratio decisions and that the patients concerned often have suffered a long history of chronic disease and consider this kind of therapy as final option. Thus, indication should be liberal. As landmark structures neighboring the sympathetic trunk such as the pleura, the superior or inferior vena cava, aorta or ureter are best visualized using cross sectional imaging; this technique is very safe and conventional fluoroscopy controlled sympathicolysis should not be used any more.

Key Points

- Sympathicolysis is a safe procedure with a low complication rate.
- Sympathicolysis is very successful in over 70% of cases of hyperhidrosis and in up to 80% of ischemic pain treatment.
- In ischemia induced pain treatment after failure of transarterial or surgical treatment, this procedure may still provide an improvement in the quality of life in many cases and helps to delay or avoid amputations.
- For treatment of the SMP and neuralgia, blockages without destruction of the nerves are often sufficient.

References

Adler OB, Engel A, Rosenberger A et al. (1990) Palmar hyperhidrosis CT guided chemical percutaneous thoracic sympathectomy. Rofo 153:400–403

Arkkila PE (2006) Thromboangiitis obliterans (Buerger's disease). Orphanet J Rare Dis 1:14

Baumgartner FJ, Toh Y (2003) Severe hyperhidrosis: clinical features and current thoracoscopic surgical management. Ann Thorac Surg 76:1878–1883

Chen HJ, Liang CL, Lu K (2001) Associated change in plantar temperature and sweating after transthoracic endoscopic T2-3 sympathectomy for palmar hyperhidrosis. J Neurosurg 95(Suppl 1):58–63

Di Lorenzo N, Sica GS, Sileri P et al. (1998) Thoracoscopic sympathectomy for vasospastic diseases. Jsls 2:249–253

Duda SH, Huppert PE, Heinzelmann B et al. (1994) CT-gestützte perkutane lumbale Sympathikolyse bei peripherer Verschlusskrankheit. Rofo 160:132–136 [German]

Feinglass J, Brown JL, LoSasso A et al. (1999) Rates of lower-extremity amputation and arterial reconstruction in the United States, 1979 to 1996. Am J Public Health 89:1222–1227

Finkenzeller T, Techert J, Lenhart J et al. (2001) CT-gesteuerte thorakale Sympathikolyse zur Behandlung der peripheren arteriellen Verschlusskrankheit und thorakaler Schmerzen in 6 Fällen. Rofo 173:920–923 [German]

Furlan AD, Ping-Wing L, Mailis A (2001) Chemical sympathectomy for neuropathic pain: does it work? Case report and systematic literature review. Clin J Pain 17:327–336

Heindel W, Ernst S, Manshausen G et al. (1998) CT-guided lumbar sympathectomy: results and analysis of factors influencing the outcome. Cardiovasc Intervent Radiol 21:319–323

Huttner S, Huttner M, Neher M et al. (2002) CT-gesteuerte Sympathikolyse bei peripherer arterieller Verschlusskrankheit – Indikationen, Patientenauswahl, Langzeitergebnisse. Rofo 174:480–484 [German]

Jaboulay M (1899) Le traitment de quelques troubles trophiques du pied et dela jambe par la dénudation de l'àterie fémorale et la distension des nerfs vasculaires. Lyon Méd 91:467–468 [French]

Janoff KA, Phinney ES, Porter JM (1985) Lumbar sympathectomy for lower extremity vasospasm. Am J Surg 150:147–152

Katara AN, Domino JP, Cheah WK et al. (2007) Comparing T2 and T2-T3 ablation in thoracoscopic sympathectomy for palmar hyperhidrosis: a randomized control trial. Surg Endosc 21:1768–1771

Lau H, Cheng SW (1997) Buerger's disease in Hong Kong: a review of 89 cases. Aust N Z J Surg 67:264–269

Lee BY, Madden JL, Thoden WR et al. (1983) Lumbar sympathectomy for toe gangrene: long-term follow-up. Am J Surg 145:398–401

Maga P, Kuzdzal J, Nizankowski R et al. (2007) Long-term effects of thoracic sympathectomy on microcirculation in the hands of patients with primary Raynaud disease. J Thorac Cardiovasc Surg 133:1428–1433

Montessi J, de Almeida EP, Viera JP et al. (2007) Video-assisted thoracic sympathectomy in the treatment of primary hyperhidrosis: a retrospective study of 521 cases comparing different levels of ablation. J Bras Pneumol 33:248–254

Moya J, Ramos R, Morera R et al. (2006) Thoracic sympathicolysis for primary hyperhidrosis: a review of 918 procedures. Surg Endosc 20:598–602

Pieri S, Agresti P, Ialongo P et al. (2005) Lumbar sympathectomy under CT guidance: therapeutic option in critical limb ischaemia. Radiol Med (Torino) 109:430–437

Price DD, Long S, Wilsey B et al. (1998) Analysis of peak magnitude and duration of analgesia produced by local anesthetics injected into sympathetic ganglia of complex regional pain syndrome patients. Clin J Pain 14:216–226

Romano M, Giojelli A, Mainenti PP et al. (2002) Upper thoracic sympathetic chain neurolysis under CT guidance. A two year follow-up in patients with palmar and axillary hyperhidrosis. Radiol Med (Torino) 104:421–425

Rosen RJ, Miller DL, Imparato AM et al. (1983) Percutaneous phenol sympathectomy in advanced vascular disease. AJR Am J Roentgenol 141:597–600

Schild H, Grönniger J, Günther R et al. (1984) Transabdominelle CT-gesteuerte Sympathektomie. Rofo 141:504–508 [German]

Schmid MR, Kissling RO, Curt A et al. (2006) Sympathetic skin response: monitoring of CT-guided lumbar sympathetic blocks. Radiology 241:595–602

Schneider B, Richter GM, Roeren T et al. (1996) CT-gesteuerte Neurolysen. Stand der Technik und aktuelle Ergebnisse. Radiologe 36:692–699 [German]

Thune TH, Ladegaard L, Licht PB (2006) Thoracoscopic sympathectomy for Raynaud's phenomenon–a long term follow-up study. Eur J Vasc Endovasc Surg 32:198–202

Vranken JH, Zuurmond WW, van Kemenade FJ et al. (2002) Neurohistopathologic findings after a neurolytic celiac plexus block with alcohol in patients with pancreatic cancer pain. Acta Anaesthesiol Scand 46:827–830

14.4 Trigeminal Ablation

Reto Bale and Gerlig Widmann

14.4.1 Introduction

Trigeminal neuralgia (TN), or tic douloureux, is a syndrome characterized by paroxysms of lancinating, shock like pain in the distribution of the trigeminal nerve. It usually begins as a relapsing disease with pain-free intervals that may last months or years. These intervals decrease and eventually disappear. Pain attacks are being triggered by touching the skin, intraoral mucosa or the tongue or they occur spontaneously. Many patients have difficulties maintaining facial hygiene, talking and eating. TN is either idiopathic (primary) or due to structural lesions including multiple sclerosis, tumor or aneurysm (secondary). It is more common in females, in the right side of the face and in people older than 40 years. If major pain lasts for a period of seconds or minutes, atypical trigeminal neuralgia is diagnosed. Atypical symptoms are a negative predictor of outcome.

Although many patients respond to drugs (e.g. carbamazepine, baclofen, gabapentin, phenytoin, clonazepam), about 50% of the patients require invasive treatment because they cannot tolerate the medications or their symptoms are intractable (Katusic et al. 1991).

14.4.2 Indications

Ablative techniques include neurectomy of peripheral trigeminal nerve branches, radiofrequency (RF) thermocoagulation, injection of glycerol into the trigeminal cistern (glycerol rhizolysis – GR), trigeminal ganglion balloon microcompression (BC) or stereotactic radiosurgery (SRS), causing controlled injury to the trigeminal nerve, ganglion or root (Barker et al. 1996). More invasive approaches intend to relieve compression of the nerve at some point along its course. The most popular surgical procedure is the posterior fossa exploration for microvascular decompression (MVD). However, open surgical techniques are associated with a small but significant morbidity (keratitis, hemiparesis, hemorrhage, . . .) and mortality (1–2%).

Based on a literature review and analysis of patients, Taha and Tew (1996) recommend RF thermocoagulation as the method of choice for the first treatment of TN. This review included patients who underwent RF thermocoagulation (6205 patients), GR (1217 patients), BC (759 patients), MVD (1417 patients) and partial trigeminal rhizotomy (250 patients). RF thermocoagulation and MVD had the highest rate of initial pain relief and the lowest rate of pain recurrence. MVD showed the lowest rate of technical success and the highest rate of permanent cranial nerve deficit, intracranial hemorrhage or infarction and perioperative morbidity and mortality. However, MVD had the lowest rates of facial numbness, dysaesthesia, corneal dysaesthesia and keratitis. Based on their own results and the review of the literature, Taha and Tew recommend RF rhizotomy as the procedure of choice for TN patients undergoing first treatment. MVD is recommended in patients who have pain in the first ophthalmic trigeminal division and in patients who desire no sensory deficit.

14.4.3 Material

Beside the routine material like sterile draping, disinfectant, local anesthesia, syringes and scalpels, a dedicated ablation device is needed. For RF thermocoagulation a RF probe with a thermocouple sensor is strongly recommended in order to produce a precise lesion at the electrode tip by monitoring the temperature (e.g. Neurotherm RF generator NT 1000; Precision Medical Engineering, Inc., MA, USA). For navigated ablation of the Gasserian ganglion a dedicated head holder (e.g. Vogele-Bale-Hohner (VBH) head holder; Medical Intelligence GmbH, Schwabmuenchen, Germany) and a three-dimensional surgical navigation system are needed.

14.4.4 Technique

14.4.4.1 Pre-interventional Diagnostics

Before therapy the patient has to be evaluated with a comprehensive interview, history, and physical examination of the cranial nerves. According to Scrivani et al. (1999) the clinical diagnosis of TN should be based on the following findings:

- Paroxysmal, lancinating, electric-like pain
- Tactile trigger areas
- Unilateral symptoms
- No neurosensory deficit

In addition, magnetic resonance (MR) imaging of the brain and brainstem has to be performed in order to exclude tumor, vascular abnormality or demyelization.

14.4.4.2 Patient Preparation

The patient is positioned supine with the head lying on a radiolucent headrest. Continuous assessment of blood oxygen saturation and cardiac function is demanded. A nasal tube for oxygen administration may be helpful while the patient is covered by sterile drapes. Percutaneous RF thermocoagulation of the Gasserian ganglion is typically performed under intravenous sedation (puncture), and short general anesthesia (ablation) (see Chap. 5). The dose of anesthetic medication is gradually increased to provide a considerable level of anesthesia so that patients experience no or minimal pain. Anesthesia is administered at a level that gives comfort to both the patient and the interventionalist during the electrical test procedure, for the ablation procedure a short general anesthesia is performed.

During penetration of the foramen ovale vagal reflex may lead to bradycardia, which may be treated with atropine. Complete general anesthesia should only be used in selected cases since the electrical test procedure is an important part of the intervention.

14.4.4.3 Puncture Technique

The RF thermocoagulation needle may be placed under fluoroscopic-, computed tomography (CT)- (Liu 2005) or three-dimensionally navigated image guidance (Bale et al. 2000; Hajioff et al. 2000; Xu et al. 2006b; Yang et al. 2007).

Conventional Approach

The conventional fluoroscopy guided approach has been extensively described by Gauci et al. (2004). In brief, fluoroscopy should be used in order to visualize the foramen ovale in an orthogonal view. Therefore the X-ray beam has to make an angle of 45° to an imaginary vertical line stretching from the lower margin of the orbit to the external ear channel and about 40° between the sagittal and vertical planes. The foramen ovale can be clearly visualized medial to the upper parts of the mandible.

The skin entrance point is about one inch lateral to the angle of the mouth at the level of the upper 6th tooth. To reach the maxillary and mandibular division of the trigeminal nerve the foramen ovale should be entered in the middle of the foramen ovale. If just the 3rd branch has to be reached, the entrance point is only half an inch lateral to the angle of the mouth. The direction of the needle in the lateral view is the middle point of the zygomatic arch and in the antero-posterior plane the infraorbital foramen (Fig. 14.16).

Local anesthesia may be applied at the skin entrance point. The needle is advanced to the foramen ovale under tunnel vision. Just before the foramen ovale is entered a lateral view is obtained in order to advance the tip of the needle just above the bony skull base (the needle tip should be advanced about 1.5 cm further than the entrance into the foramen ovale). The cranial projection of the needle trajectory should lead directly into the angle formed by the clivus in the anterior and the petrous temporal bone in the posterior aspect. Cerebrospinal fluid should flow out as the trigeminal cistern is entered indicating correct placement.

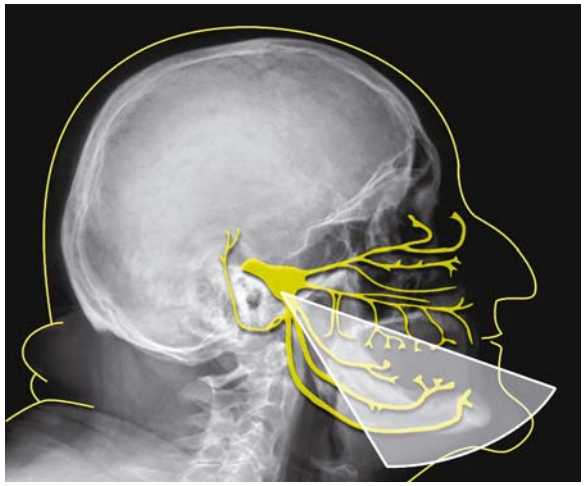

Fig. 14.16 Schematic draw of the puncture direction for reaching the third branch of the trigeminal nerve via the oval foramen

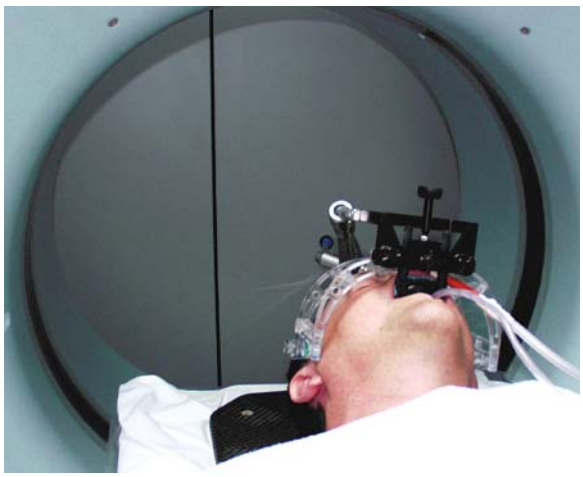

Fig. 14.17 Fixation of patient in VBH head holder with SIP reference frame

Navigated CT-Guided Approach

The navigated CT-guided Innsbruck approach is based on the VBH head holder and a three-dimensional surgical navigation system. The head holder consists of the VBH vacuum mouthpiece, an adjustable, locking, adaptable mechanical arm and a base plate (40 cm × 30 cm, with multiple fixing areas to hold the mechanical arms) with head rest. The VBH mouthpiece is based on an individualized dental mould that is held against the upper palate by negative pressure (Bale et al. 1997a,b, 2000, 2006). Correct repositioning and precise fit on the patient is verified by successful generation of a negative pressure of 0.5–0.6 atm. The mechanical arm is connected to the two anterior extensions of the VBH mouthpiece for rigid immobilization of the patient's head at the base plate.

For image-to-patient registration, which is the essential step for navigated interventions (see Chap. 7), an external U-shaped Plexiglas frame equipped with 11 spherical CT markers (glass, diameter 5.8 mm), broadly distributed around the region of interest, is mounted to the mouthpiece (Fig. 14.17).

CT imaging with no more than 2 mm slice thickness is performed in the interventional CT unit. Thereafter planning of the puncture path is performed on the navigation software. It includes trajectory planning as visualized on the two-dimensional and three-dimensional reconstructions of the patient's CT-data. By using the longitudinal and orthogonal cuts along the planned path potential penetration of the oral mucosa and damage of vital structures can be prevented (Fig. 14.18). For registration, the CT markers on the registration frame are replaced by registration markers that have a cone-shaped bur-hole in their geometric centre. Thereby the tip of the navigation systems probe can be precisely placed. After non-sterile registration and verification of registration accuracy, the interventional field is wrapped and prepared for the procedure.

The targeting device (e.g. Atlas™, Medtronic Inc., Louisville, KY, USA) is used for navigated adjustment of the planned trajectory. A coaxial needle is advanced through the aiming device to the calculated center of the foramen ovale. Finally a low dose CT scan is performed for verification of precise needle positioning (Fig. 14.19).

14.4.4.4 RF Thermocoagulation

After verification of precise needle position, the electrocoagulation needle is advanced through the coaxial guiding needle. For determination of the individual trigeminal branch, neurophysiologic testing should be performed which requires the cooperation of the patient throughout the procedure. To get the patient to cooperate and respond, the VBH mouthpiece can be removed and disconnected from the head holder.

Thereafter, controlled thermocoagulation is performed which includes a first series of 60–90 s (73°), and, in case of involvement of the maxillary and the mandibular branch, followed by a second series of 60 s (73°) after retraction of the needle of about 3–4 mms. During the coagulation procedure the patients are usually anesthetized.

14.4.5 Results

In a systematic review of ablative neurosurgical techniques for the treatment of trigeminal neuralgia, Lopez et al. (Lopez 2004) showed that RF thermocoagulation showed the highest rate of complete pain relief. RF thermocoagulation may safely be repeated if the pain recurs (Kanpolat et al. 2001). Satisfactory results and good long-term pain control can be obtained in

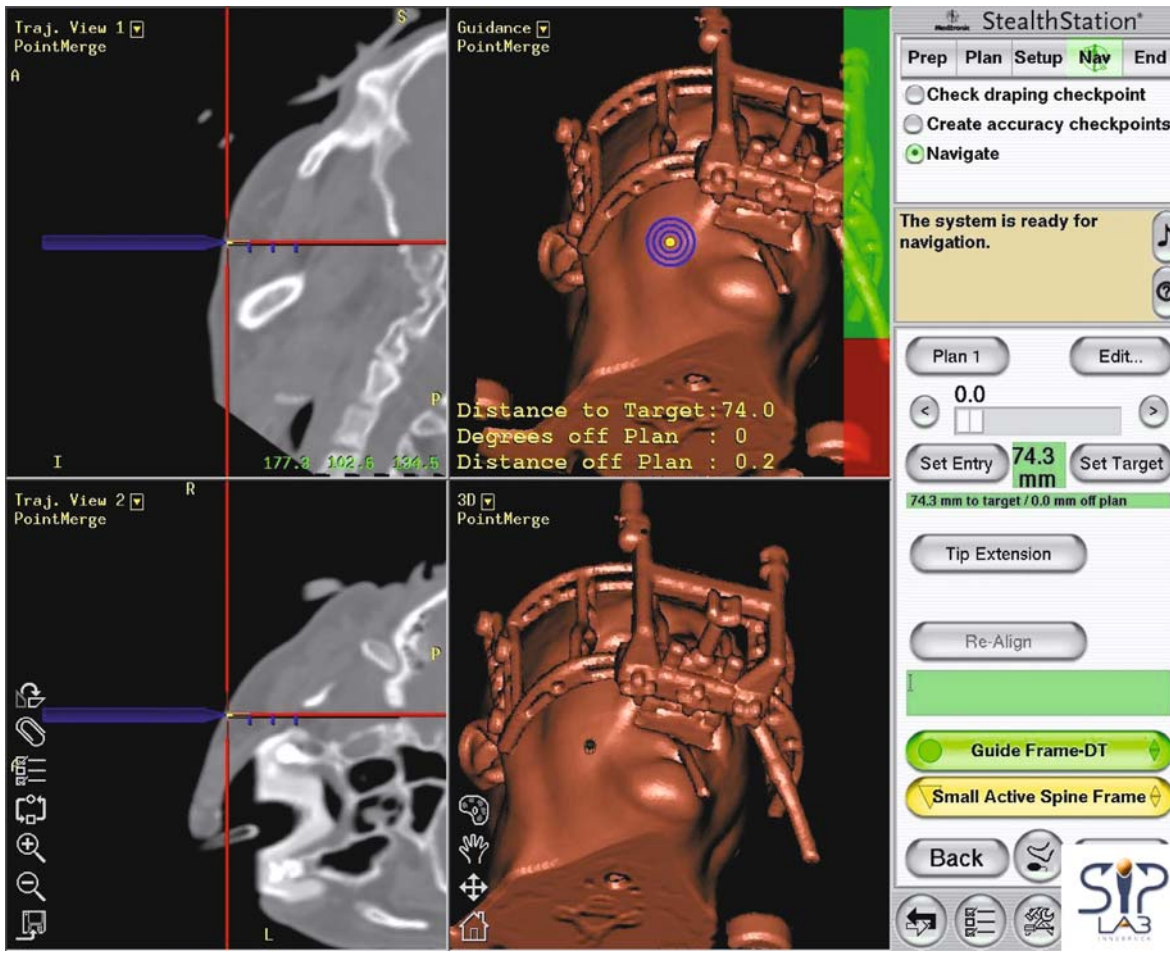

Fig. 14.18 Pathplanning on 2D- and 3D- reconstructed CT data. The *blue line* indicates the trajectory through the foramen ovale

patients having TN due to Multiple Sclerosis with percutaneous controlled RF thermocoagulation (Kanpolat et al. 2000). Initial pain relief is about 98%, but pain recurrence occurs in 20% in nine years and in 15% in five years.

14.4.6 Complications

Correct puncture of the foramen ovale is a crucial step and the incidence of complications due to incorrect puncture ranges from 5% to 7% (Xu et al. 2006a).

Typical adverse effects and complication include:

- Postoperative trigeminal nerve sensory loss (98%)
- Permanent trigeminal nerve sensory loss (30%)
- Masticatory weakness (12%)
- Corneal numbness (10%)
- Major dysesthesia (4%)
- Anesthesia dolorosa (2%)
- Keratitis (1%)

Rare complications (less than 1%) include mortality (Egan et al. 2001b), meningitis (Sweet 1986), temporal lobe hemorrhage, seizure, stroke, cranial nerve deficit, carotid-cavernous fistula, monocular blindness (Egan et al. 2001a), brain stem injury (Berk and Honey 2004), diplopia, and rhinorrhea. However, these severe but rare complications are mostly due to severe puncture failure or hygiene deficiency. Introduction of navigated cross-sectional imaging guided intervention techniques will help to reduce the number of puncture related complications.

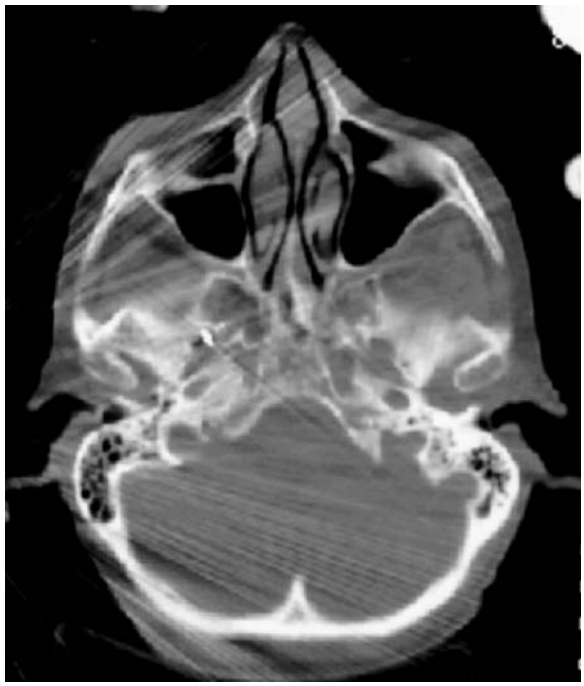

Fig. 14.19 Axial control-CT showing the needle in the right foramen ovale

Summary

When compared to conventional two-dimensional image guidance (fluoroscopy), navigated, cross-sectional image guided interventions require additional procedures including system set-up, instrument calibration, registration, verification of accuracy, intraoperative application and dismantling of the navigation system. Familiarity with these systems is important for routine and fast use. For the application of most navigation systems an additional person (technician) is helpful and the costs for the purchase of the guidance system and the additional costs for the man power are often hardly affordable for small hospitals. However, this technology will enhance patient security and puncture success independent from the interventionalist's experience (including complete forensic documentation) with acceptable duration and effort for routine clinical application and may be beneficial to all patients in whom trigeminal nerve ablation is recommended.

Key Points

- Before therapy the patient has to be evaluated with a comprehensive interview, history, and physical examination of the cranial nerves.
- Tumor, vascular abnormality or demyelination has to be excluded and a clear diagnosis of trigeminal neuralgia has to be verified.
- Correct puncture of the foramen ovale is a crucial step of percutaneous RF thermocoagulation and the needle position has to be controlled by CT scan before the ablation procedure.
- Navigated CT-guided approaches may provide significant benefit compared to non-guided approaches through cross-sectional imaging, virtual interventional planning and intra-operative three-dimensional guidance, which helps in improving puncture accuracy and reduction of complication rate.

References

Bale RJ, Vogele M, Freysinger W et al. (1997a) Minimally invasive head holder to improve the performance of frameless stereotactic surgery. Laryngoscope 107:373–377

Bale RJ, Vogele M, Martin A et al. (1997b) VBH head holder to improve frameless stereotactic brachytherapy of cranial tumors. Comput Aided Surg 2:286–291

Bale RJ, Freysinger W, Gunkel AR et al. (2000) Head and neck tumors: fractionated frameless stereotactic interstitial brachytherapy-initial experience. Radiology 214:591–595

Bale RJ, Laimer I, Martin A et al. (2006) Frameless stereotactic cannulation of the foramen ovale for ablative treatment of trigeminal neuralgia. Neurosurgery 59:ONS394-ONS401

Barker FG, Jannetta PJ, Bissonette DJ et al. (1996) The long-term outcome of microvascular decompression for trigeminal neuralgia. N Engl J Med 334:1077–1083

Berk C, Honey CR (2004) Brain stem injury after radiofrequency trigeminal rhizotomy. Acta Neurochir (Wien) 146:635–636

Egan RA, Pless M, Shults WT (2001a) Monocular blindness as a complication of trigeminal radiofrequency rhizotomy. Am J Ophthalmol 131:237–240

Egan RA, Pless M, Shults WT (2001b) Monocular blindness as a complication of trigeminal radiofrequency rhizotomy. Am J Ophthalmol 131:237–240

Gauci C, Trigeminal Ganglion RF (2004) In: Gauci C (ed) Manual of RF techniques. Flivo Press SA, Switzerland

Hajioff D, Dorward NL, Wadley JP et al. (2000) Precise cannulation of the foramen ovale in trigeminal neuralgia complicating osteogenesis imperfecta with basilar invagination: technical case report. Neurosurgery 46:1005–1008

Kanpolat Y, Berk C, Savas A et al. (2000) Percutaneous controlled radiofrequency rhizotomy in the management of patients with trigeminal neuralgia due to multiple sclerosis. Acta Neurochir (Wien) 142:685–689

Kanpolat Y, Savas A, Bekar A et al. (2001) Percutaneous controlled radiofrequency trigeminal rhizotomy for the treatment of idiopathic trigeminal neuralgia: 25-year experience with 1,600 patients. Neurosurgery 48:524–532

Katusic S, Williams DB, Beard CM et al. (1991) Incidence and clinical features of glossopharyngeal neuralgia, Rochester, Minnesota, 1945–1984. Neuroepidemiology 10:266–275
Liu M, Wu CY, Liu YG et al. (2005) Three-dimensional computed tomography-guided radiofrequency trigeminal rhizotomy for treatment of idiopathic trigeminal neuralgia. Chin Med Sci J 20:206–209
Lopez BC, Hamlyn PJ, Zakrzewska JM (2004) Systematic review of ablative neurosurgical techniques for the treatment of trigeminal neuralgia. Neurosurgery 54:973–982
Scrivani SJ, Keith DA, Mathews ES et al. (1999) Percutaneous stereotactic differential radiofrequency thermal rhizotomy for the treatment of trigeminal neuralgia. J Oral Maxillofac Surg 57:104–111
Sweet WG (1986) The treatment of trigeminal neuralgia (tic douloureux). N Engl J Med 315:174–177
Taha JM, Tew JM Jr (1996) Comparison of surgical treatments for trigeminal neuralgia: reevaluation of radiofrequency rhizotomy. Neurosurgery 38:865–871
Xu SJ, Zhang WH, Chen T et al. (2006a) Neuronavigator-guided percutaneous radiofrequency thermocoagulation in the treatment of intractable trigeminal neuralgia. Chin Med J (Engl) 119:1528–1535
Xu SJ, Zhang WH, Chen T et al. (2006b) Neuronavigator-guided percutaneous radiofrequency thermocoagulation in the treatment of intractable trigeminal neuralgia. Chin Med J (Engl) 119:1528–1535
Yang Y, Shao Y, Wang H et al. (2007) Neuronavigation-assisted percutaneous radiofrequency thermocoagulation therapy in trigeminal neuralgia. Clin J Pain 23:159–164

14.5 Epidural Injection Therapy

Bernd Turowski

14.5.1 Introduction

Epidural therapy implies positioning of a therapeutic agent in the epidural space close to the spinal dura. This region becomes accessible for therapy as dura mater and periost are not fixed together in the spinal canal as they are intracranially. Instead more or less fat is interposed between the bone and the spinal dura.

Image guidance comprises techniques like fluoroscopy, ultrasound (US), computed tomography (CT) or magnetic resonance (MR) imaging. Fluoroscopy only displays bony structures while soft tissue is not shown. Thus puncture planning has to be done by deducing this information from anatomical knowledge. Individual variation and particularly pathological changes may lead to inaccurate distribution of any therapeutic agent. The same holds true if the access route is oriented at anatomical landmarks without image guiding. US is limited by acoustical shadows due to bony structures. MR-guidance requires much effort including MR compatible instruments. In addition, small gantry-opening hampers access to the site of puncture. However, cross-sectional imaging guidance has some relevant advantages:

- The injection can be accomplished close to the dura mater avoiding transdural puncture.
- The distribution of the injected substance can be monitored. Injection can be stopped as soon the desired distribution is reached.
- The injection can be stopped in time if the injected agent causes compression of the dural sac.

Based on these considerations, CT-guidance appears to be the most effective technique for spinal epidural injection-techniques and is described in the following. The technique of epidural injection will be demonstrated on the example of the therapy of a cerebrospinal fluid leakage (Ishikawa et al. 2007). Moreover, the presented technical skills may be an instrument for epidural placement of any therapeutic agent.

14.5.2 Indications

Typical indications for epidural injection therapy include:

- Cerebrospinal fluid leakage
- Spontaneous intracranial hypotension (SIH)

The most important (relative) contraindications to epidural injection therapy are:

- Infection
- Immunosuppression
- Allergy to contrast media

Cerebrospinal fluid leakage may be acquired due to trauma (Huntoon and Watson 2007; Takagi et al. 2007) or diagnostic puncture. But recently more and more publications address the clinical symptoms of spontaneous intracranial hypotension (SIH) in relationship to a spinal fluid leakage (Schaltenbrand 1938; Schwedt and Dodick 2007).

The pathophysiological mechanism of clinical symptoms is based on reduced cerebrospinal fluid (CSF)-volume (Gideon et al 1994; Mokri and Low 2003; Thomke et al. 1999). Reduction of CSF-volume results in a downwards-movement of the brain. Due to constancy of intracranial volume defined by the skull (Monroe-Kellie-Doctrin), volume compensation is necessary.

The cardinal clinical symptom of SIH is orthostatic headache, which is characterized by aggravation within 15 to 30 min after rising from recumbency. Within 30 min after lying down, orthostatic headache disappears. Intracranial low pressure with venous volume compensation may even result in subdural hygroma or subdural hematoma. Downward placement of the brain mechanically irritates cranial nerves. This may result in symptomatic affection of cranial nerves. In descending frequency the clinical symptoms are paresis of cranial nerves VI, IV, III (diplopic images), II (impaired vision), V, VII, VIII (tinnitus, vertigo), IX (dysphagia). Nausea, neck pain, neck rigidity, nystagmus, ataxia and psychosyndrom may be observed, too. Rarely disturbance of the venous drainage (Chen et al. 1999) and venous thrombosis have been described (Savoiardo et al. 2006, 2007). Clinical course of the disease may be chronic or recurrent with symptom free intervals.

14.5.3 Preprocedural Imaging

In a patient presenting with typical symptoms of low CSF-pressure, cranial MR imaging with contrast will be performed. Imaging should include coronal slices, which can easily depict meningeal contrast enhancement and subdural hygroma or hematoma. Spinal MR imaging with heavily T2-weighted axial images with fat-suppression may help to find pathologic epidural fluid collections (Tsai et al. 2007). Alternatively, scintigraphy may be performed. If CSF-leakage is confirmed, the localisation of the leakage by CT-myelography is important.

14.5.3.1 MR Imaging

Based on the typical clinical symptoms, the proof of *menigeal contrast enhancement* on MR images is evidentiary for leakage of CSF as long as there was no precedent lumbar puncture.

Other imaging sings of low CSF pressure may be:

- Subdural hygroma or hematoma
- Narrowed ventricles, interpeduncular fossa, chiasmatic cistern
- Flattening of the pons
- Enlargement of intracranial veins
- Enlargement of epidural venous plexus
- Lowered cerebellar tonsils
- Venous congestion may mimic hypophyseal enlargement
- Detection of epidural fluid signal extending in paraspinal tissue

Direct localisation of the leakage itself is difficult.

14.5.3.2 Scintigraphy

Scintigraphy after direct injection of a radionuclide into the cerebrospinal fluid is a highly sensitive method for proving the existence of a leakage. The complete neuro-axis can be displayed in a single examination. Sensitivity results from temporal sampling so that even small leaks may be found directly or indirectly by early renal excretion (Lay 2002). Due to limited spatial resolution, the direct localisation of the leakage is difficult.

14.5.3.3 CT-Myelography

CT-myelography is sensitive for any leakage of contrast-enhanced CSF. High spatial resolution of CT mostly allows direct visualization of leakage. Technically perfect subarachnoid contrast application is the

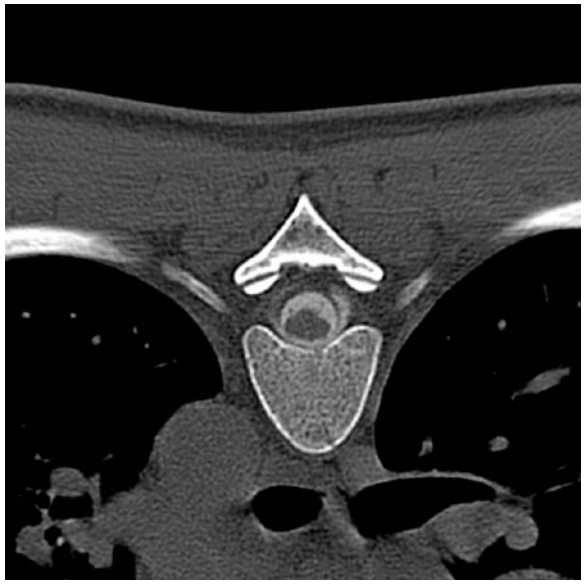

Fig. 14.20 Epidural extravasation of contrast material surrounding the contrast filled dural-sack is proven by CT-myelography

key requirement for the success of CT-myelography. Puncture of the CSF-space should be performed as distal as possible to the assumed location of leakage in order to avoid interference with iatrogenic epidural contrast. For leakages in the level of the upper spinal canal a lumbar contrast-application is recommended; for lower leakages a cervical puncture is reasonable. Concerning cervical contrast application lateral puncture in the C1/C2-level instead of suboccipital puncture should be considered.

A first CT-scan of the suspected region will be obtained with the patient positioned supine 30 min after injection of about 20 ml of a dedicated myelographic contrast medium. If no epidural contrast is be seen, a second CT scan will be performed about 1 h later, with the patient positioned prone (Fig. 14.20).

14.5.4 Material

- Spinal needle (20 G)
- 20-ml syringe with Luer-Lock adapter
- 16–18 G peripheral venous access for taking fresh whole blood
- Dedicated contrast agent for myelography (e.g. Iotrolan)
- Sterile compresses
- Plaster
- Sterile draping
- Local anesthesia for skin infiltration

14.5.5 Technique

Prior to the intervention, informed consent needs to be obtained. Discussion of therapeutic options must include information about the spontaneous course of the disease with approximately 80% of symptoms resolving within 6 to 12 months. Only in a small subgroup will there not be spontaneous healing within an acceptable period of time.

To avoid movement of the patient between localisation of the site of injection and blood-injection, a stable and comfortable positioning of the patient is important. Thereafter, thorough skin disinfection and sterile draping is performed. The use of sterile gloves is mandatory for hygiene. Under sterile conditions and CT-guidance the spinal-needle will be positioned either using a step-by-step method or alternatively CT-fluoroscopy. In order to avoid puncture of the dural sack, a trajectory tangentially to the dural sack is planned (Fig. 14.21). As soon as the target area has been reached, control aspiration may exclude subarachnoid or intravascular position of the needle tip. To confirm epidural position of the needle 1 ml air or alternatively contrast material should be injected (Fig. 14.22).

If epidural distribution of air or contrast is proven without a doubt, about 15–20 ml whole blood will be sampled from a cubital vein. The blood is mixed with 1 ml of myelographic contrast agent contrast (e.g. Iotrolan) in order to be able to monitor the propagation of blood during injection. The speed of injection depends on individual conditions. One should avoid producing a locally space occupying hematoma which may affect the cervical myelon. Slow injection allows the blood to spread around the dural-sack and cranially as well as caudally. This may exclude local compression effects. Iatrogenic myelon compression by locally trapped blood must be avoided. The epidural blood-patch typically distributes from the level of injection usually about three vertebral body heights cranially and caudally. Complete peridural cover normally only occurs close to the level of injection (Fig. 14.23).

After injection of 7–20 ml blood (depending on localization of the injection: less volume for cervical in-

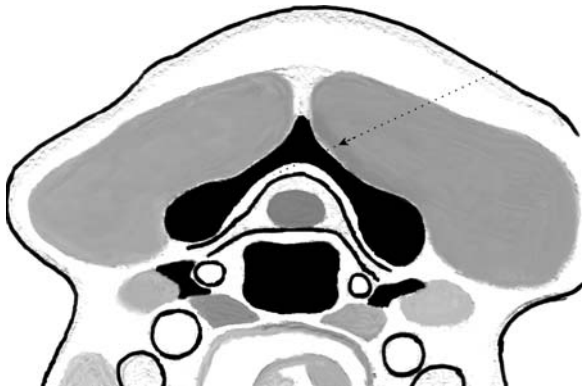

Fig. 14.21 Schematic display of the access for epidural injection. In order to avoid contact to the nerve roots the dorsal circumference of the dural sack should be the targeted with the tip of the needle. A latero-dorsal approach allows careful advancement. For unhindered access to the epidural space the roofing tile-like construction the spinal processes has to be taken into account. Thus a caudo-cranial orientation of the needle is needed

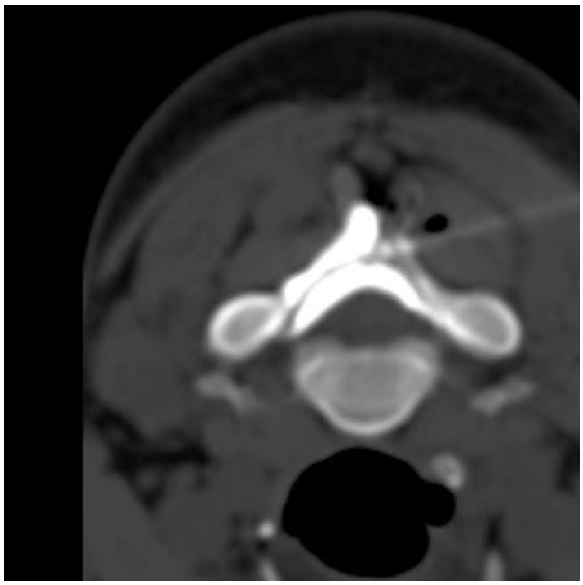

Fig. 14.22 CT-control of the needle position in the epidural space with epidural distribution of contrast

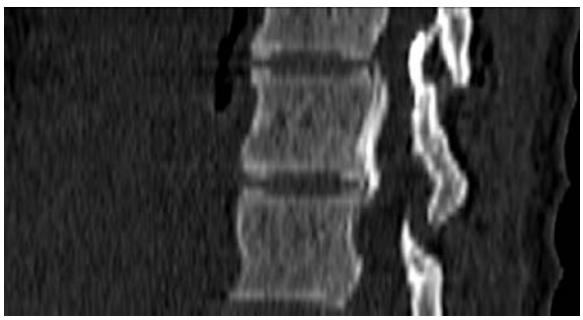

Fig. 14.23 CT-myelography shows epi- and peridural localization of the contrasted blood-patch after thoracic treatment. The blood-patch extends over one vertebral body height corresponding to the site of the leakage

jections – more volume in lumbar injections) a range of four vertebral bodies above and below the level of injection is examined to show longitudinal and peridural dissemination of the blood-patch.

In order to avoid displacement of the blood-patch following gravity, rest in bed is recommended for 6–8 h after the injection.

14.5.6 Results

According to our experience in 50–60% of all patients presenting with the clinical symptoms of orthostatic headache, the CSF-leakage could be proven with imaging. In chronic whiplash disorder in which the pathophysiology may be comparable to intracranial hypotension one week after blood-patch therapy as well as in a six months follow up, Ishikawa et al. (2007) observed a significant percentage of patients with decreased symptoms compared to that before therapy. Headache as leading symptom in 100% of patients could be found only in 17% of all patients after therapy. Visual impairment could be resolved in two thirds, nausea in 50%.

In some cases only repeated epidural blood-patch therapy is successful, but in many cases only one well directed injection is sufficient. Symptoms should disappear within 72 h after successful therapy.

14.5.7 Complications

Due to short diffusion distances, epidurally injected substances may affect spinal nerves and even the myelon. Therefore all interventions close to the structures of the central nervous system may have an effect on neural function.

If performed by an experienced interventionalist the technique is safe. Typical complications and their management include (see Table 14.1).

Summary

In case of CSF leakage, pharmacological therapy with caffeine may help in some cases. Surgical occlusion of the leakage is an invasive option. In contrast, local application of blood is a very effective method to treat CSF-leakage with peridural adhesions producing the designated result. Taking into account risks and complications, indication should be clearly defined. Therapy should be performed by an experienced interventionalist.

Key Points

- The correct indication is the key for a successful intervention, as only patients with CSF-leakage will benefit from an epidural blood-patch.
- Extensive experiences in image-guided interventions is recommended.
- Careful positioning and control of correct needle placement is the key for successful treatment without complications.

Table 14.1

Infection	The risk will be minimized by sterile work and good skin disinfection (at the site of injection as well as at site of blood-sampling)
Puncture of the dura mater	In case of accidental puncture of the duramater the needle should be repositioned. Injection of a small amount of myelographic contrast agent may proof correct extradural position of the tip of the needle and exclude intradural injection
Puncture of the myelon	In the best case hazard puncture of the myelon has no further consequences if there is no injection. However, a puncture may result in bleedings. Intramedullary injection of any fluid may be disastrous and lead to paraplegia
Injection of into the subarachnoid space	Accidental injection of blood into the subarachnoid space may cause a space occupying lesion that requires surgery. It may lead also to headaches and to subarachnoidal adhesions

References

Chen CC, Luo CL, Wang SJ et al. (1999) Colour doppler imaging for diagnosis of intracranial hypotension. Lancet 354:826–829

Gideon P, Thomsen C, Stahlberg F et al. (1994) Cerebrospinal fluid production and dynamics in normal aging: a MRI phase-mapping study. Acta Neurol Scand 89:362–366

Huntoon MA, Watson JC (2007) Intracranial hypotension following motor vehicle accident: an overlooked cause of post-traumatic head and neck pain? Pain Pract 7:47–52

Ishikawa S, Yokoyama M, Mizobuchi S et al. (2007) Epidural blood patch therapy for chronic whiplash-associated disorder. Anesth Analg 105:809–814

Lay CM (2002) Low cerebrospinal fluid pressure headache. Curr Treat Options Neurol 4:357–363

Mokri B, Low PA (2003) Orthostatic headaches without CSF leak in postural tachycardia syndrome. Neurology 61:980–982

Savoiardo M, Armenise S, Spagnolo P et al. (2006) Dural sinus thrombosis in spontaneous intracranial hypotension: Hypotheses on possible mechanisms. J Neurol 253:1197–1202

Savoiardo M, Minati L, Farina L et al. (2007) Spontaneous intracranial hypotension with deep brain swelling. Brain 130:1884–1893

Schaltenbrand G (1938) Neuere Anschauungen zur Pathophysiologie der Liquorzirkulation. Zentralbl Neurochir 290–299

Schwedt TJ, Dodick DW (2007) Spontaneous intracranial hypotension. Curr Pain Headache Rep 11:56–61

Takagi K, Bolke E, Peiper M et al. (2007) Chronic headache after cranio-cervical trauma – hypothetical pathomechanism based upon neuroanatomical considerations. Eur J Med Res 12:249–254

Thomke F, Bredel-Geissler A, Mika-Gruttner A et al. (1999) [Spontaneous intracranial hypotension syndrome. Clinical, neuroradiological and cerebrospinal fluid findings]. Nervenarzt 70:909–915 [German]

Tsai PH, Fuh JL, Lirng JF et al. (2007) Heavily T2-weighted MR myelography in patients with spontaneous intracranial hypotension: a case-control study. Cephalalgia 27:929–934

14.6 CT-Guided Periradicular Therapy (PRT)

Gero Wieners

14.6.1 Indications

Radicular or pseudoradicular pain is one of the most common painful spinal disorders. Most patients suffer from acute or chronic disc herniation, degenerative spinal disease or postoperative epidural fibrosis. Next to paresthesia, pain is the leading symptom. Primary aim of therapy is pain control. Selective nerve root block by injecting lidocaine was first described by Macnab (1971). Several randomized studies on the effect of local application of corticosteroids have been performed since then (Narozny et al. 2001; Blankenbaker et al. 2005). In summary, best improvement of symptoms was gained by injecting a combination of local anesthetics and corticosteroids compared to an injection of just local anesthetics. The simple explanation for the benefit from corticosteroids is the fact that the nucleus pulposus tissue has inflammatory properties, leading to an intraneural edema, which is a very important factor in the pathogenesis of sciatic pain (Olmarker et al. 1995). The application of corticosteroids around the nerve root and epidural space reduces local edema and inflammation by reducing the release of inflammatoric enzymes such as phospholipase A2 in the degenerated and herniated disc (Nygaard et al. 1997; Blankenbaker et al. 2005).

Computed tomography (CT)-guided periradicular therapy was introduced in 1989 (Groenemeyer and

Seibel 1989). Periradicular therapy (PRT) was usually performed by orthopaedic or neurosurgeons in a free-hand technique or under fluoroscopic guidance. In recent years, CT-guided periradicular therapy performed by interventional radiologists gained acceptance due to the accuracy of needle positioning right next to the nerve root under CT-image control. In addition, drug distribution around the nerve can be optimally controlled by adding a small amount of contrast agent (Silbergleit et al. 2001; Link et al. 1998). Studies of CT-guided periradicular pain therapy have shown very good short term success with long term duration in some cases (Zennaro et al. 1998; Lee et al. 2005; Riew et al. 2006).

14.6.1.1 Material

Materials needed for PRT include:

- Fenestrated sterile draping.
- Local anesthetics (5 ml xylocitin 1%).
- Compresses.
- Spinal needle 20 or 22 G of about 10 or 15 cm depending on patient and target localization. For cervical intervention a 22 G spinal needle is usually appropriate.
- Drugs (may be varied according to individual preferences):
  - 1 ml bupivacaine 0.5% plus 0.3 ml nonionic contrast agent in a 2-ml syringe.
  - 1 ml triamcinolonacetonide (40 mg) in a 2-ml syringe.
- Adhesive plaster.

14.6.2 Technique

14.6.2.1 Preparation

The most important aspect in successful PRT is the accuracy of neurological preinterventional evaluation. A precise correlation of the dermatoma and the nerve root to be targeted needs to be established. In this context CT- or MR-images are helpful in defining the appropriate level for PRT. In addition, these images may exclude further pathologies. Informed consent has to be obtained prior to the intervention.

14.6.2.2 Intervention

A PRT cycle is normally best performed in three interventions with an interval of three weeks between each intervention. All procedures are best performed under CT or MR guidance. For lumbar PRT the patient is placed head first in prone position on the CT or MR table with cushioning between table and pelvis. This improves the dorsal access to the nerve root and also patient comfort. For cervical PRT the patient is placed in a supine position.

Under CT guidance, a lateral topogram has to be acquired to identify the right disc level and neuroforamen. Single CT slices serve to adjust the image plane to the according neuroforamen and nerve root. Slice thickness may be 5 mm or more. The point of needle insertion should be marked on the skin, usually lumbar about 3–4 cm lateral of the midline and cervical on the dorso-lateral neck. The skin should be disinfected and covered with a fenestrated sterile sheet.

An axial slice guides the needle from the insertion point to the nerve root ganglion. The spinal needle should be advanced stepwise in the axial plane until access to the neuforamen close to the processus transversus is gained. For reaching the S1 nerve root, the spinal needle has to be advanced through the dorsal neuroforamen of the Os sacrum (foramen sacrale dorsale).

The needle tip should be close to the nerve root, but direct contact should be avoided. In this position retrograde distribution of the drug along the inserted needle is prevented by the cribriforme fascia and, most often, contrast will distribute along the axis of the nerve root and reach the epidural space.

Application of 0.5 ml of non-ionic contrast agent and bupivacain should be controlled under fluoroscopy to confirm washout of the contrast agent from the area around the nerve (Fig. 14.24). After the correct distribution has been documented the syringe is changed against another syringe containing 1 ml triamcinolonacetonide (40 mg). The corticosteroid is injected slowly, again followed by an exchange of the syringe to inject the remaining bupivacain. Doses from 1 ml triamcinolonacetonide (40 mg) and 1 ml bupivacaine up to 6 ml of this steroid-anaesthetic combination have been described in the literature (Lee et al. 2005). However, most authors recommend an amount of just 1 ml triamcinolonacetonide (40 mg) and 1 ml bupivacaine.

For PRT of cervical nerve roots the tip of the needle should be placed ventral to the vertebral transverse process (Fig. 14.25). The safest approach is puncture from the dorsolateral neck directly to the transverse process and after contact to the bone stepwise progression into the final position. This approach provides greatest safety to avoid contact to the vertebral artery.

The mean duration of this procedure is less than 20 min. It is generally performed as an outpatient treatment. Surveillance of the patient is usually limited to 30 min after treatment.

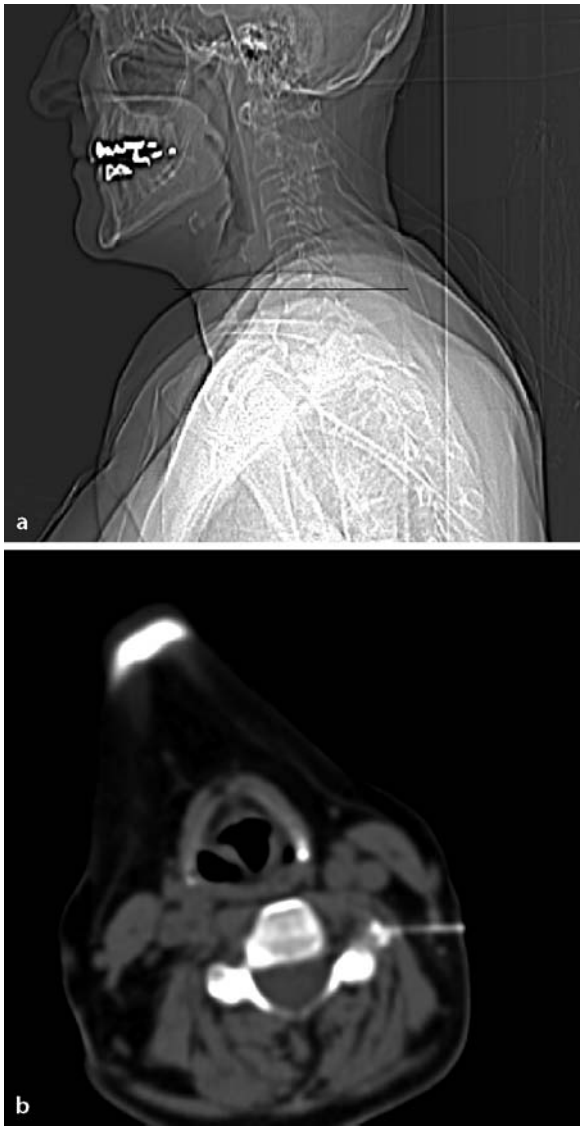

Fig. 14.24a,b CT-guided periradicular therapy of the cervical spine. After CT-guided periradicular needle placement (**a**) a steroid mixed with contrast medium was injected (**b**)

Sometimes the correlation between dermatoma and nerve root is not clearly defined (Boos and Lander 1996). In this case a stepwise therapy concept should be recommended. This means that it is better to treat

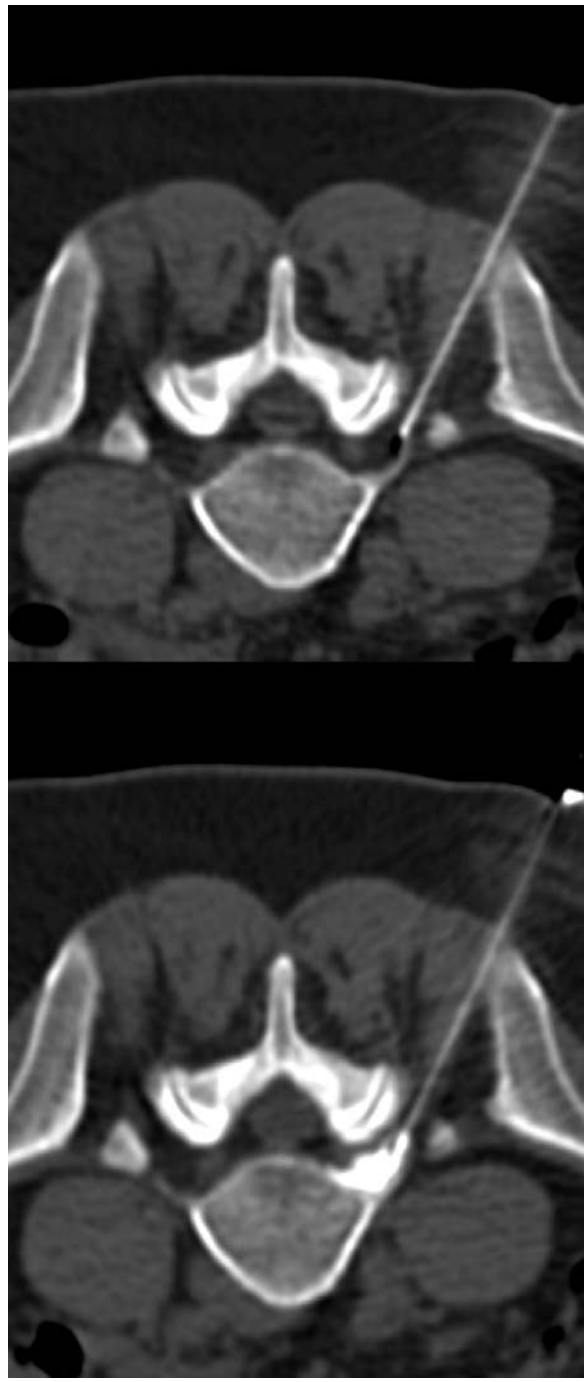

Fig. 14.25 CT-guided periradicular therapy of the lumbar spine

just the nerve root causing most severe symptoms at the first date of treatment. If there is only a response in the treated dermatoma and there is still pain or paresthesia, a combined therapy should be performed 3 weeks later on the same nerve root and following that on the nerve root above or below. This treatment should be repeated twice with an interval of three weeks to complete a cycle of therapy.

After one cycle of treatment an interval of six months at minimum is recommended. In exceptional cases, the interval can be reduced. However, adverse effects of systemic corticosteroid distribution have to be considered.

14.6.3 Results

Cervical and lumbar nerve root blocks have become more popular for treating patients with radiculopathy. CT or MR guided periradicular therapy is the safest and most accurate way for the application of drugs around spinal nerve roots. Of the patients, 60–80% benefit significantly from the first treatment. However, a cycle of three injections should be completed to gain full and long lasting therapeutic effects (Lee et al. 2005; Riew et al. 2006; Narozny et al. 2001). Recent studies have shown excellent long term results for patients who refused surgical intervention, but who were considered to be candidates for surgical intervention because of symptoms and failure of non-operative treatment (Peul et al. 2007; Riew et al. 2006). Five year results of the study from Riew et al. (2006) were similar to the results of patients who underwent surgery, without the substantial risks of surgical interventions. The authors recommend CT-guided PRT of the nerve root as a first step prior to operative intervention in patients with radiculopathy due to a herniated nucleus pulposus or spinal stenosis. Surgery on patients presenting a radiculopathy with or without minor sensory/motor deficit is only required if pain cannot be controlled by non-operative means (Saal and Saal 1989). This allows an effective reduction of costs, which would be necessary for surgical intervention (Karppinen et al. 2001).

Schmidt et al. (2006) evaluated dose exposure with a low dose protocol during periradicular treatment under CT-fluoroscopy guidance. The effective dose was 0.22 mSv and 0.43 mSv for 4 and 10 CT-scans, respectively. With pulsed fluoroscopy the effective dose was reduced to 0.1 mSv. In this context new open high field MRI scanners offer the possibility of periradicular therapies without dose exposure and with superior tissue contrast. This is specifically of interest for young patients and patients who need repeated therapy cycles. Even low field MR may deliver satisfying image quality for PRT (Sequerios et al. 2002).

14.6.4 Complications

For informed consent, general and specific complications have to be considered. General complications such as bleeding, infection or abscesses may occur. Specific complications to be considered include meningitis, liquor leakage, or nerve root trauma with paresthesia or even paralysis. In PRT of the cervical level, damage to the vertebral artery must be considered as well as misinjection of crystalline corticoids in spinal arteries leading to infarction. However, complications are extremely rare in PRT, and none of those incidences considered are even described in most case series available in the literature. The most frequently seen minor complication may be a slight temporary weakness of the ipsilateral extremity or even a slight increase of pain caused by narrowing of the neuroforaminal space during drug administration. Allergic reactions to the non-ionic CT-contrast agent, local anesthetics and corticoid have to be considered.

Summary

CT guided periradicular therapy in patients with lumbar or cervical radiculopathy is a safe and effective therapy whilst minimizing the need for surgical intervention. PRT of the nerve root is the first step prior to operative intervention in patients with radiculopathy due to a herniated nucleus pulposus or spinal stenosis. Surgery on patients suffering from radiculopathy with or without minor sensory or motor deficit is only required if pain cannot be controlled by non-operative means.

Key Points

- The key to successful PRT is a careful preinterventional neurological assessment!

References

Blankenbaker D, De Smet A, Stanczak J et al. (2005) Lumbar radiculopathy: treatment with selective lumbar nerve blocks – comparison of effectiveness of triamcinolone and betamethasone injectable suspensions. Radiology 237:738–741

Boos N, Lander P (1996) Clinical efficacy of imaging modalitiesin the diagnosis of low back pain disorders. Eur Spine J 5:2–22

Groenemeyer DHW, Seibel R (1989) Interventionelle Computertomographie. Ueberreuter Wissenschaft, Vienna, Berlin, pp 92–135 [German]

Karppinen J, Malmivaara A, Kurunlathi M et al. (2001) Periradicular infiltration for sciatica – a randomized controlled trial. Spine 26:1059–1067

Lee K, Lin C, Hwang S et al. (2005) Transforaminal periradicular infiltration guided by CT for unilateral sciatica – an outcome study. Clin Imaging 29:211–214

Link S, el-Khoury G, Guilord W (1998) Percutaneous lumbar sympatholysis. Radiol Clin North Am 36:509–521

Macnab I (1971) Negative disc exploration. An analysis of the causes of nerve-root involvement in sixty-eight patients. J Bone Joint Surg Am 53(5):891–903

Narozny M, Zanetti M, Boos N (2001) Therapeutic efficacy of selective nerve root blocks in the treatment of lumbar radicular pain. Swiss Med Wkly 131:75–80

Nygaard OP, Mellgren SI, Osterud B (1997) The inflammatory properties of contained and noncontained lumbar disc herniation. Spine 22:2484–2488

Olmarker K, Blomquist J, Strömberg J et al. (1995) Inflammatogenic properties of nucleus pulposus. Spine 20:665–669

Peul W, Houwelingen H, Hout W et al. (2007) Surgery versus prolonged conservative treatment for sciatica. N Engl J Med 356:2245–2256

Riew KD, Park JB, Cho YS et al. (2006) Nerve root blocks in the treatment of lumbar radicular pain. A minimum five-year follow-up. J Bone Joint Surg Am 88:1722–1725

Saal JA, Saal JS (1989) Nonoperative treatment of herniated lumbar intervertebral disc with radiculopathy. An outcome study. Spine 14:431–437

Schmidt G, Schmitz A, Borchardt D et al. (2006) Effective dose of CT- and fluoroscopy-guided perineural/epidural injections of the lumbar spine: a comparative study. Cardiovasc Intervent Radiol 29:84–91

Sequeiros R, Ojala R, Klemola R et al. (2002) MRI-guided periradicular nerve root infiltration therapy in low-field (0.23-T) MRI system using optical instrument tracking. Eur Radiol 12:1331–1337

Silbergleit R, Mehta B, Sanders W et al. (2001) Imaging-guided injection techniques with fluoroscopy and CT for spinal pain management. Radiographics 21:927–939

Zennaro H, Dousset V, Viaud B et al. (1998) Periganglionic foraminal steroid injections performed under CT-control. Am J Neuoradiol 19:349–352

14.7 Discography

Oliver Beuing

14.7.1 Indications

Chronic back pain is one of the most common ailments in the industrialized nations (Milette et al. 1995). As various anatomic structures like facet joints, intervertebral discs, ligaments and muscles may contribute to pain, and innervation of these structures is complex and differs interindividually, it is crucial to identify the pain generating structure for optimal interventional or surgical treatment planning.

Defiant of advances in imaging technology, findings of physical examination and noninvasive imaging are still inconclusive in a substantial number of patients, especially in those with multilevel changes or without frank nerve root compression. The intervertebral disc may cause radiating pain to the hip, groin or even the leg and distribution of pain does not necessarily correlate with the level of the affected disc. The mechanisms of pain development are not yet fully clarified, but probably nerve roots are sensitive to chemical changes (inflammatory substances) in the direct surrounding of morphologically changed discs. However, there is also evidence that nociceptors sensitive to pressure and chemical changes may exist in the disc itself.

These are the major indications for discography (Resnick et al. 2002; Schellhas 2000):

- Chronic back pain with or without radicular pain and absence of documented nerve root compression in noninvasive tests.
- Disc or end plate changes are present, but clinical significance is unclear.
- Clinical findings suggest a specific level, but magnetic resonance (MR) imaging or computed tomography (CT) (-myelography) point to a different one.
- Disc protrusion in the suspected level is asymmetric and does not match the side where the patient indicates his pain.
- MR and CT-myelography already demonstrated instability in one segment, but the results concerning adjacent levels are equivocal.
- Percutaneous nucleotomy is planned.
- Exclusion of anular tears with potential epidural leakage in case chemonucleolysis is intended.

- Simulation of pain (exaggerated response may correlate with poor surgical outcome).
- Patients with previously fused segments develop pain after a symptom-free interval indicating affection of adjacent levels.

The contraindications for discography comprise of neurologic (motor) deficits, compression of the spinal cord with myelopathy, and if the patient has already undergone discectomy. Relative contraindications include coagulation disorders, allergies to substances used, and others.

14.7.2 Material

The list of materials and tools necessary comprises of:

- 22 G or 25 G – Needle (10 cm or longer), one for every level studied
- Non-ionic contrast media (CT) or Gd-DTPA (MR imaging)
- Local anesthesia
- Sterile drapes
- Sterile latex gloves
- Disinfection (e.g. povidone iodine)
- Intravenous antibiotics (effective against Staphylococcus epidermis like cefazolin)
- Intravenous access

14.7.3 Technique

14.7.3.1 Preinterventional Diagnostics

Prior to discography, clinical evaluation (history, physical examination) and noninvasive imaging (MR imaging, CT) with inconsistent results usually trigger the indication for the examination. In most patients, conservative pain management will already have failed. MR- or CT-scans are reviewed for abnormalities helping to determine which discs should be studied in further detail. Facet joints should have been excluded as the symptoms origin.

Discography may be performed under fluoroscopy as well as by employing CT or MR imaging.

14.7.3.2 Lumbar Discography

The patient is placed in prone position. A cushion placed under the patient's pelvis may help to reduce lordosis. If CT(-fluoroscopy) or MR imaging are used, the intended access route is planned in the same manner as customary for percutaneous abscess puncture or biopsy. Sterile preparation is accomplished by thorough cleansing with iodinated solutions and, after drying, isopropyl, followed by fixing the sterile drapes.

Then the solution for intradiscal injection is prepared. One mixes the antibiotic with the contrast material and, if desired, with local anesthesia. The entry point and the underlying tissue will then be anaesthetized. Application of sedatives is rarely required. Using (CT-)fluoroscopy- or MR-guidance, a 22–25 G needle is cautiously advanced to the disc space. Having placed the needle tip in the center of the disc nucleus (Fig. 14.26), injection of the solution (preferably under manometric control) begins (Fig. 14.27). Injection is terminated if a significantly increased pressure is needed for continuous application, after injecting a maximum of 6 ml of the solution, or if a concordant pain (> 6/10 on a scale from 0 to 10) has been provoked. Some authors recommend discography of adjacent levels in the latter cases.

14.7.3.3 Thoracic Discography

As with lumbar discography, the patient is placed in prone position. In the thoracic levels starting approximately at the middle third, it is often impossible to gain an unobscured access to the disc by standard fluoroscopy due to costovertebral or vertebral body osteophytes, low disc height or spinal deformity. Access

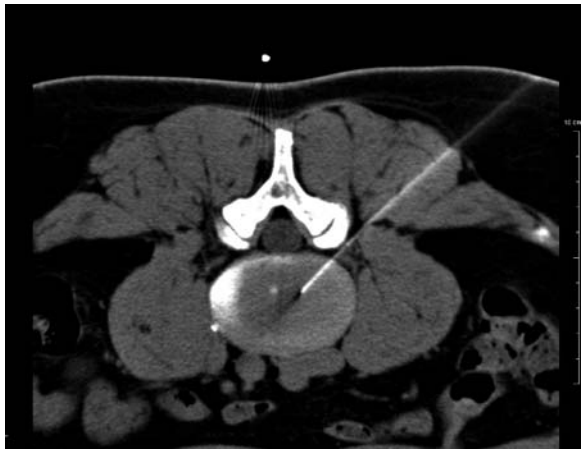

Fig. 14.26 CT-guided discography: positioning of the puncture needle

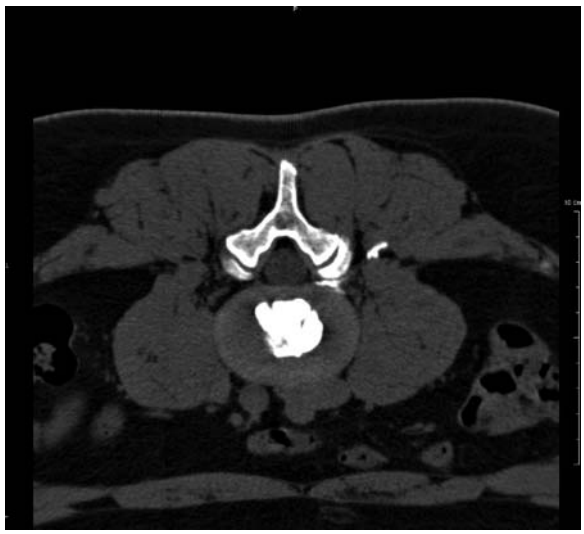

Fig. 14.27 Normal finding as obtained by CT-guided discography

is limited through the lung, which is anterior and lateral to the route and the spinal cord, which is medial and posterior. In these cases, CT or MR guidance is definitely advantageous.

14.7.3.4 Cervical Discography

The patient is placed in supine position with the shoulders slightly elevated. The cervical spine is palpated with two fingers and after shifting the carotid artery and the esophagus away the needle will be introduced from about 45° oblique and slightly below the disc.

Assessments reported should include (Sachs et al. 1987; Tomecek et al. 2002):

- Injected volume.
- Intensity of pain (i.e. visual analogue scale).
- Concordant pain during injection including its location.
- Disc morphology using the Dallas Discogram Description.
- Pain in adjacent levels and, if present, has it been concordant.
- If manometer has been used: opening pressure, pressure at pain onset.

14.7.4 Results

Results of discography are discussed controversially in the literature. Whereas some authors claim a sensitivity of pain provocative discography around 80%, others claim a best case positive predictive value of 50–60% only. False positive findings have been reported in up to 37%.

14.7.5 Complications

Complication rates generally vary between 0% and 2.5% (Pobiel et al. 2006; Guyer et al. 1997). The most serious complication is infection leading to discitis, spondylodiscitis or epidural abscesses with an incidence well below 5%. In case of discitis or spondylodiscitis, antibiotics must be administered intravenously. Microbiological assessments are often helpful. Epidural abscesses usually require instant surgical intervention.

Minor hematomas at the punction site may appear; massive hemorrhage is extremely rare. Persistent pain should be managed with analgesics. However, repeat MR imaging is recommended particularly in cases of neurologic deficits indicating disc herniation.

Allergic reactions may occur. Pneumothoraces after thoracic discography are usually asymptomatic and only incidentally require treatment. Pulmonary embolism through disc material is a very uncommon complication with only a few cases reported.

Summary

Discography has been proven to be highly sensitive in isolating discogenic pain. However, specificity is low, and false positive findings have been reported in up to 37% (Carragee et al. 1999). It has been shown that not only morphologic changes like internal disc disruption, disc degeneration or annular rupture influence the patient's report on pain, but also abnormal psychometric results. Improvement of specificity can only be achieved by selecting patients carefully and defining strict criteria for positive findings in discography. On the other hand, discography still remains the only diagnostic test potentially able to clearly identify disc pain and its origin.

Key Points

› Discography is an invasive, but safe diagnostic procedure.

- It provides excellent morphologic detail of degenerative disc changes and, even more important, information on clinical significance.
- Especially in the work-up of patients with chronic lumbar pain, discography should be considered as a preinterventional or presurgical test for optimal treatment planning, if clinical evaluation and non-invasive imaging do not conclusively explain the patient's pain.
- Strict criteria on the definition of a positive discogram must be used to avoid or lower false-positive results.

References

Carragee EJ, Tanner CM, Yang B et al. (1999) False-positive findings on lumbar discography. Reliability of subjective concordance assessment during provocative disc injection. Spine 24:2542–2547

Guyer RD, Ohnmeiss DD, Mason SL et al. (1997) Complications of cervical discography: findings in a large series. J Spinal Disord 10:95–101

Milette PC, Fontaine S, Lepanto L et al. (1995) Radiating pain to the lower extremities caused by lumbar disk rupture without spinal nerve root involvement. AJNR Am J Neuroradiol 16:1605–1615

Pobiel RS, Schellhas KP, Pollei SR et al. (2006) Diskography: infectious complications from a series of 12,634 cases. AJNR Am J Neuroradiol 27:1930–1932

Resnick DK, Malone DG, Ryken TC (2002) Guidelines for the use of discography for the diagnosis of painful degenerative lumbar disc disease. Neurosurg Focus 13:E12

Sachs BL, Vanharanta H, Spivey MA et al. (1987) Dallas discogram description. A new classification of CT/discography in low-back disorders. Spine 12:287–294

Schellhas KP (2000) Diskography. Neuroimaging Clin N Am 10(3):579–596

Tomecek FJ, Anthony CS, Boxell C et al. (2002) Discography interpretation and techniques in the lumbar spine. Neurosurg Focus 13:E13

Musculo-Skeletal Interventions

15

Philipp Bruners, Andreas H. Mahnken, Kai Wilhelm, Sebastian Kos, Peter Messmer, Deniz Bilecen, Augustinus L. Jacob and Gabriele A. Krombach

Contents

15.1 Interventional Therapy in Osteoid Osteoma

Philipp Bruners and Andreas H. Mahnken

15.1.1 Introduction

Osteoid osteoma is a benign bone tumor which was first described by Jaffe (1935). Histologically it consists of a centrally located nidus composed of osteoblasts and osteoid which is surrounded by an area of reactive sclerosis and/or periosteal new bone formation. Prostaglandins which are produced by the tumor induce a chronic inflammatory reaction and vasodilatation which results in stimulation of unmyelinated nerve endings in the nidus causing pain. This leads to the clinical symptoms of this lesion with local pain often worsening during the night, which is typically relieved by aspirin or other related nonsteroidal anti-inflammatory drugs. Osteoid osteomas occur more frequently in men than in women (2:1) and most patients, approximately 75%, suffering from osteoid osteomas are between 5 and 25 years old. Most commonly osteoid osteomas are found in the diaphysis of femur and tibia followed by humerus, radius, ulna, hand, and the verterbral spine. A malignant transformation of osteoid osteoma is not known.

The conventional X-ray typically shows a cortically located, sclerotic lesion with a central radiolucent area corresponding to the nidus (Fig. 15.1). In combination with the characteristic clinical symptoms these findings usually lead to further cross sectional imaging using

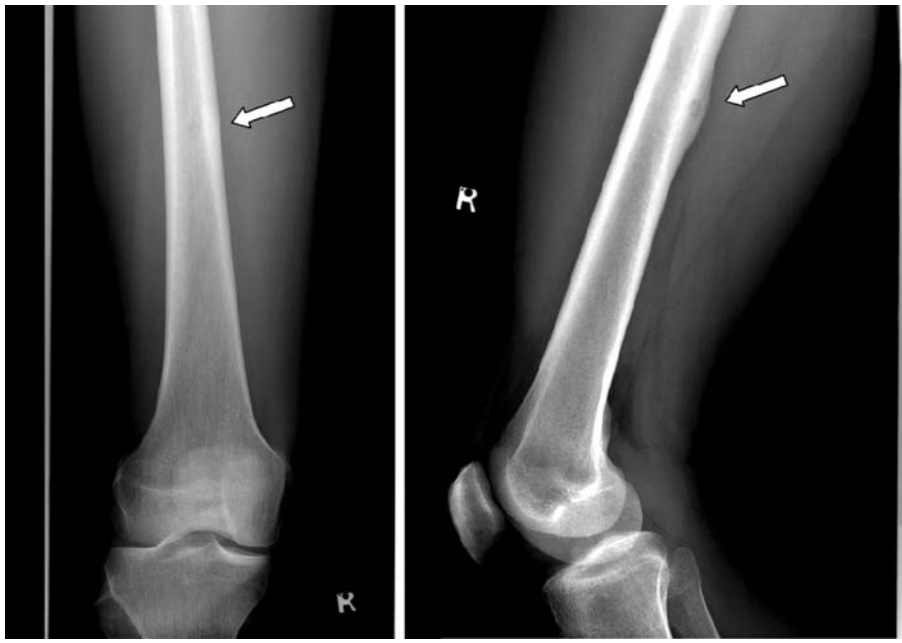

Fig. 15.1 Conventional X-ray of a 33-year-old male patient with pain in the right thigh. A thickening of the cortical bone with a round central radiolucent area in the femoral diaphysis can be depicted corresponding to an osteoid osteoma

computed tomography (CT) or magnetic resonance (MR) imaging. In MR imaging studies, especially the non-specific edema of the surrounding bone marrow and collateral soft tissue, alterations can be visualized which may result in a misleading aggressive appearance of the lesion, whereas the nidus is sometimes difficult to identify on MR imaging (Davies 2002). Native CT scans are more suitable to detect the central nidus and surrounding sclerotic bone (Fig. 15.2a).

Although the pain induced by osteoid osteomas often reacts promptly to anti-inflammatory drugs, a long-term conservative medical treatment may be unacceptable due to potentially severe side effects related to chronic use of nonsteroidal anti-inflammatory medication and sometimes refractory pain. Traditionally osteoid osteomas have been treated using surgical resection or open curettage but because of the difficult intraoperative localisation of the nidus, which needs to be completely removed, resection size sometimes is disproportional to the tumor size necessitating the use of cortical bone matrix transfer or internal fixation (Marcove et al. 1991). Therefore, different minimally-invasive techniques under image guidance have been developed to treat osteoid osteomas like drill trepanation with and without ethanol instillation, cryoablation and laser photocoagulation (Sans et al. 1999; Adam et al. 1995; Skjedal et al. 2000; Gebauer et al. 2006). The most commonly used local ablation technique for the treatment of osteoid osteoma is radiofrequency (RF)-ablation,, which was introduced by Rosenthal (1992) as an alternative minimal-invasive treatment and has found its way into clinical routine in the last decade. Therefore the following section focuses on the treatment of osteoid osteoma using RF-energy.

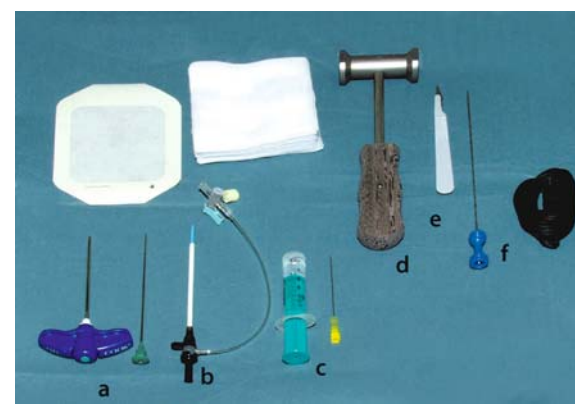

Fig. 15.2a–f Instruments recommended for CT-guided RF-ablation of osteoid osteomas. **a** 11 G hollow drill; **b** sterile angiographic introducer sheath; **c** spinal needle for injection of long-acting local anaesthetic agent; **d** sterile hammer; **e** single use scalpel; **f** needle shaped RF-probe

15.1.2 Indications

Minimally-invasive local ablation of an osteoid osteoma is indicated if:

- Typical clinical symptoms, particularly nocturnal pain are present.
- Characteristic bone lesion with a clearly identified nidus is detected.

There are no absolute contraindications for local ablation in osteoid osteoma. Relative contraindications for the local ablative therapy include:

- Impossibility to place the ablative device within the nidus at least 1 cm away from major nerves.
- Repeated (> 3) ineffective local ablations.

In these cases, surgical therapy should be considered. The use of RF-ablation in patients in patients with medical implants like cardiac pacemakers may lead to dysfunction although this has not yet been described as a complication in the literature.

15.1.3 Material

As mentioned above, there are several local ablative therapies for the minimal-invasive treatment of osteoid osteoma. Most techniques use thermal energy – either high (RF-ablation, LITT) or low temperature (cryoablation) – to destroy the nidus and all of these therapies require the image-guided placement of an ablation probe. Because RF-ablation is the most commonly used local ablative therapy the following text describes this technique in detail. Different RF-systems have been used for the successful ablation of osteoid osteomas commonly in combination with needle-shape RF-probes. In most published studies RF-ablation of osteoid osteomas is performed with monopolar RF-systems which need large grounding pads to draw current back to the radiofrequency system. Successful experience using a bipolar RF-ablation device which obviates the need for a neutral electrode and thereby reduces the risk of skin burns at the site of the grounding pads has also been reported (Mahnken et al. 2006). With regard to the ablation protocol (generator output, energy delivery, time), the recommendations of the vendor for the used RF-system should be carefully followed. Actually there is some evidence that the use of a high-energy delivery technique leads to increased post-procedural pain and a prolonged interval to symptom resolution (Cantwell et al. 2006). Besides the RF-generator, F-probe and grounding pads, a bone drill is also needed to penetrate the sclerotic cortical bone surrounding the nidus and thereby gain access for the placement of the RF-probe. Typically an 11–13 G hollow drill is used which allows performing biopsy of the bone lesion for histological confirmation of the diagnosis (Fig. 15.2). The use of a sterile angiographic introducer sheath is recommended to secure the puncture tract in the soft tissue. This technique provides an additional insulation of the RF-probe and therefore helps to avoid skin burns, which are the most common complication of RF-ablation in osteoid osteoma. A sterile single-use scalpel is needed for a stitch incision at the skin entry point. Furthermore, sterile drape sheets for the puncture site and disinfectant are required. Radiopaque markers, for example a grid made of parallel catheter pieces, which are fixed on the patient's skin, can be used as references for the planning of the access path. A small tube filled with formalin is used to store the drilled bone specimen before histological analysis. A long-acting local anaesthetic agent, e.g. bupivacaine 0.25%, can be applied into the nidus and along puncture tract after RF-ablation for post-interventional pain management.

15.1.4 Technique

15.1.4.1 Patient Preparation

Informed consent should be obtained from the patient at least 24 h prior to the intervention after discussion of alternative treatment options and possible complications of the local ablation procedure. This should include global complications of the puncture as bleeding, nerve injury or infection but also statements about a possible reintervention in case of recurrent symptoms and a possible damage of articular cartilage for the treatment of osteoid osteomas which are located near joints. Furthermore, patients should be advised that local pain may temporarily increase after the intervention. Because osteoid osteomas are often found in children and young underaged patients, informed consent of the patient's parents might be required.

In general it is possible to perform local ablation therapy with spinal or general anaesthesia. Especially

for the treatment of children, who might find the intervention frightening, the authors prefer general anaesthesia which provides optimal analgesia and compliance. Instead of an endotracheal tube a laryngeal airway mask can be used for the administration of anaesthetics. An exception is the local ablation of vertebral osteoid osteomas where analgesic sedation should be considered in order to be able to recognize a neural injury.

For the recovery of platelet function, pain medication with aspirin should be stopped one week prior to the intervention. The day before the intervention full blood count and coagulation should be obtained to identify inflammation or haemorrhagic diathesis. Due to the fact that most patients are young, a conventional chest radiograph is not routinely obtained.

A possible prophylactic antibiotic treatment would be the intravenous administration of 500 mg cefazolin during the procedure followed by two oral doses after the intervention (Peyser et al. 2007). Alternatively a single dose of Clindamycin (600 mg) can be administered intravenously.

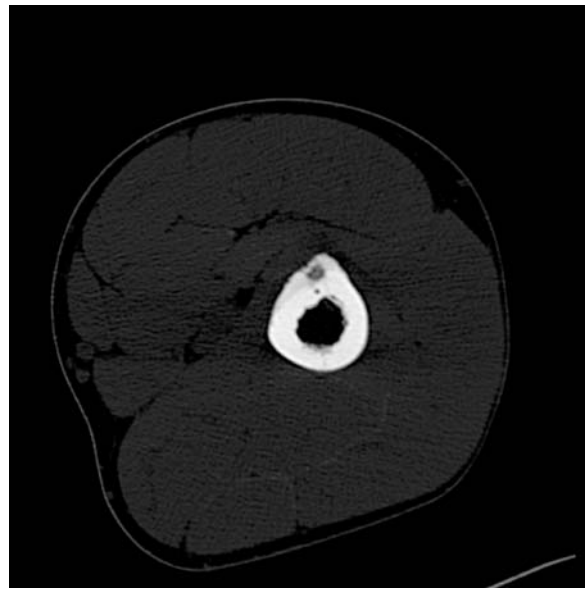

Fig. 15.3 CT-guided placement of a RF-probe in a patient suffering from osteoid osteoma of the femur. Corresponding to conventional radiography the unenhanced CT-scan reveals the thickening of the cortical bone with the centrally located nidus

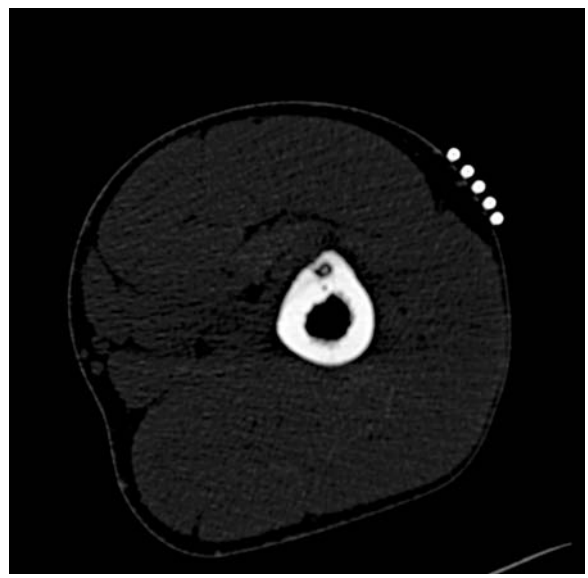

Fig. 15.4 For the planning of the access path and definition of the skin entry point a grid made of radiopaque material is fixed on the skin

15.1.4.2 Procedure

In general CT, MR imaging and conventional X-ray fluoroscopy can be used for image-guided placement of the biopsy drill and the ablation-probe, respectively. Due to the high spatial resolution and the mostly clear depiction of the nidus and the ablation-probe, the authors prefer CT as modality for image-guidance (Fig. 15.3). MR-guided local ablation requires the use of special MR-compatible tools.

In order to avoid pressure sites or damage of peripheral nerves during the procedure the patient under anaesthesia should be positioned carefully on the CT-table. Most patients with limb lesions can be treated in prone position. If necessary the limb can be internally or externally rotated and fixed with tape in order to afford optimal access. Spinal lesions often require the placement of the patient in supine position to achieve a dorsal access to the tumor. After acquisition of a thin section (collimation $\leqslant$ 3 mm, slice thickness 1–3 mm) unenhanced spiral scan of the region of interest, the access path for the placement of the ablation-probe is planned using the implemented software of the CT-scanner. If an in-plane access to the target lesion, which should be preferred, is not feasible, the reconstruction of multiplanar reformations may be helpful. RF-probe placement should be performed in a way that the risk for thermal damage of the skin or adjacent neural and vascular structures is avoided. Therefore, a safety distance of 1 cm should be kept between RF-

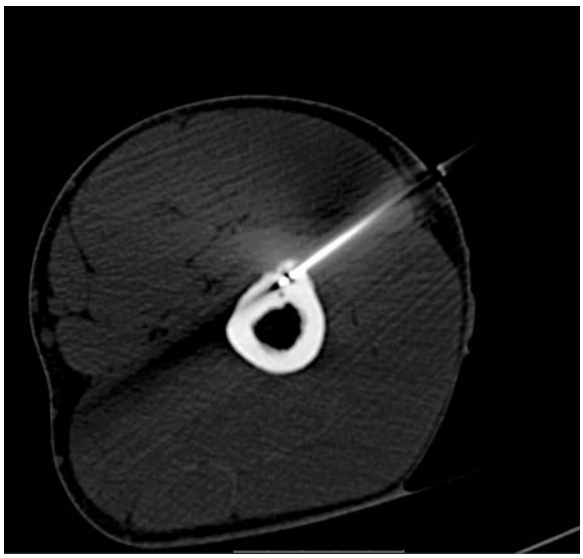

Fig. 15.5 After the skin entry point has been marked with a water-resistant pen the grid was removed. After a specimen has been obtained using the hollow drill the RF-probe was placed centrally in the nidus

Fig. 15.6 The MPR along the shaft of the RF-probe shows the placement within the center of the nidus

probe and critical structures especially nerves. A contralateral access to the target lesion passing through the normal cortex may be chosen if vulnerable structures omit the direct path. Osteoid osteomas being located near joints should be ablated using an extraarticular access in order to reduce the risk of infection and damage of the articular cartilage. An access path perpendicular to the bone surface avoids slipping of the drill and the RF-probe, respectively. Once the skin entry plane has been defined, the CT-table is moved to the corresponding slice position and radiopaque markers are fixed on the skin around the puncture site using the light shield of the CT-scanner as reference (Fig. 15.4). Thereafter another unenhanced CT-scan of the puncture site is performed and the skin entry point is defined using the radiopaque markers as landmarks. To optimally meet the lesion and to achieve a central drill hole in the relatively small lesion, a slice thickness of 3 mm or less is recommended for the interventional CT-imaging. After the skin entry point is marked with a water-resistant pen, radiopaque markers are removed and the skin is disinfected. Afterwards, the puncture site is draped in sterile fashion. First a stitch incision at the marked skin entry point is performed using a sterile single-use scalpel. In order to secure the puncture channel and to protect the surrounding soft tissue the hollow drill can be put through an appropriate sterile introducer sheath. Then the hollow drill is placed into the target lesion along the planned access path. Depending on the length of the access path control scans should be performed to verify the position of the drill. Thereafter the nidus of the osteoid osteoma is drilled out and the obtained bone specimen can be used for histological analysis. Therefore, it is put into a small tube containing formalin. The hollow drill is removed whereas the sheath is left in order to secure the puncture tract. After that the RF-probe is placed through the sheath into the target lesion. Another control scan should be performed to verify the correct placement of the RF-probe in the central area of the nidus with a maximum distance of 5 mm to edge of the nidus (Figs. 15.5 and 15.6). The RF-ablation of lesions larger than 1 cm requires more than one probe position due to the limited size of the ablation zone (Pinto et al. 2002). Therefore a second access tract may be necessary in order to create overlapping ablation zones which contain the whole nidus. Duration, output and total energy deposition strongly depend on the used RF-system and the vendor's recommendations. For commonly used monopolar RF-systems a tip temperature of 90 °C is maintained for 4–6 min. A second ablation cycle is recommended by some authors after rotation of the RF-probe in order improve heat conduction by removing carbonized tissue from the RF-probe (Mahnken et al. 2006). The injection of small volumes of 0.9% saline solution into the ablation site can also be used

to reduce impedance and avoid tissue carbonization especially in cortically located lesions (Rimondi et al. 2005). As heated saline may lead to thermal injuries along the puncture tracts, this approach should be limited to lesions with otherwise insufficient energy coupling. After the RF-ablation procedure the RF-probe is removed and a long-acting local anaesthetic agent can be applied into the lesion through the sheath to reduce post-interventional pain. Then the introducer sheath is removed and an adhesive sterile bandage is attached after the wound at the skin entry site is closed with elastic skin closures. Usually sutures are not necessary. In our experience between 90 and 120 min are required to perform the intervention including anaesthesia.

15.1.4.3 Post-interventional Management

Post-interventional imaging is not mandatory although the induced thermal necrosis can be visualized using contrast-enhanced MR imaging (Aschoff et al. 2002). Usually patients can be discharged from the hospital within 24 h after the ablation procedure so it is even possible to perform RF-ablation of osteoid osteomas on an outpatient basis. Although there is no proven evidence, patients with osteoid osteomas in weight-bearing bones should avoid strenuous activities including sports for an interval of two weeks. After this period a follow-up clinical assessment is helpful, especially to identify patients with persistent or recurrent pain. In these patients follow-up MR imaging is recommended to identify contrast enhancing and therefore viable parts of the lesion. In these patients up to two repeated interventions are recommended. Local ablation can be defined as successful if patients are free of pain without taking any pain medication. If follow-up imaging studies are performed, although this is not routinely recommended, a partial or complete replacement of the nidus by sclerotic bone can be expected over 2–27 months although only less or no changes of the ablation site may be found (Pinto et al. 2002).

15.1.5 Results

During the last few years several clinical studies investigated the benefit of RF-ablation of osteoid osteomas. Table 15.1 shows an overview of MEDLINE published studies sorted by publishing date. The cited studies include more than 700 percutaneous treatments of osteoid osteomas using RF-ablation with mean primary success of 87% (range: 56–100%). Mean secondary success rate ranged between 65% and 100% (mean: 82%) resulting in a total success rate of ~95%. Cantwell et al. (2004) reported slightly higher success rates for different surgical treatments varying between 88% and 100%. Nevertheless, surgical treatment of osteoid osteomas using curettage or resection is associated with a more extensive bone and soft tissue trauma which is reflected by higher complication rates compared to RF-ablation (Cantwell et al. 2004). The internal fixation rate after en-bloc resection can reach up to 56% (Cantwell et al. 2004). Using LITT as image-guided therapy for the treatment of osteoid osteoma, primary success rates range between 80% and 98% (Gangi et al. 2007; Sequeiros et al. 2003; Witt et al. 2000).

In a retrospective analysis of a case series including 110 patients, Vanderschueren et al. (2004) investigated factors for increased risk of unsuccessful thermal coagulation. Besides advanced age, an increased number of RF-probe positions during the ablation procedure was associated with a decreased risk of treatment failure. No evidence was found for an association between lesion location and increased risk for treatment failure.

15.1.6 Complications

In general, image-guided RF-ablation of osteoid osteomas is a safe minimally invasive treatment associated with only few complications as described above. Nevertheless, potential complications may occur due to the passage of the needle-shaped RF-probe and the hollow drill, respectively, including damage of neural and vascular structures or infection as it is known from other image-guided interventions.

Treatment related complications were found in 25/700 cases reported in the literature of which skin burns were the most common ones (Table 15.1). Donkol et al. (2007) reported a slightly higher complication rate in children treated with RF-ablation compared to adult patients. In a case series of 23 patients they described skin burns in two patients, a wound infection in one patient and hyperthermia in another two patients. They stated that this finding

Table 15.1 Published results of treatment of osteoid osteoma using RFA

Author(s)	Patients/ procedures	Primary success	Reablation/ success	Total success	Complications	Follow up (month)
Barei et al. 2000	11/11	10/11 (91%)	–	10/11 (91%)	–	18.7
Lindner et al. 2001	58/61	55/58 (95%)	3/3	58/58 (100%)	Skin burn ($n = 1$)	23 (4–41)
Woertler et al. 2001	47/50	44/47 (94%)	3/3	47/47 (100%)	–	22 (8–39)
Vanderschueren et al. 2002	97/121	74/97 (76%)	15/23	89/97 (92%)	Skin burn ($n = 1$); Probe defect ($n = 1$)	41 (5–81)
Ghanem et al. 2003	23/24	21/23 (91%)	1/1	22/23 (96%)	Calf atrophy ($n = 1$); asymmetry of joint mobility ($n = 2$)	42 (13–62)
Venbrux et al. 2003	9/13	5/9 (56%)	3/4	8/9 (89%)	Skin burn ($n = 1$); Transient paresthesia ($n = 1$)	10.3 (1–26)
Rosenthal et al. 2003	263/271	107/117 (91%)	–	107/117 (91%)	Cellulitis ($n = 1$); Vasomotor instability ($n = 1$)	24
Cioni et al. 2004	38/44	30/38 (79%)	5/6	35/38 (92%)	Skin burn ($n = 1$); Osteomyelitis ($n = 1$)	35.5 (12–66)
Mastrantuono et al. 2005	21/21	21/21 (100%)	–	21/21 (100%)	–	11.1 (0–24)
Martel et al. 2005	38/39	37/38 (94%)	1/1	38/38 (100%)	Skin burn ($n = 1$); Tendinitis ($n = 1$)	3–24
Rimondi et al. 2005	97/114	82/97 (85%)	13/15	95/97 (98%)	Skin burn ($n = 1$); Phlebitis ($n = 1$)	3–12
Mahnken et al. 2006	14/16	12/14 (86%)	1/1	13/14 (93%)	–	15.1 (5–31)
Cantwell et al. 2006	11/11	11/11 (100%)	–	11/11 (100%)	Muscle ablation ($n = 1$)	14.4 (6–27)
Soong et al. 2006	25/25	23/25 (92%)	–	23/25 (92%)	–	42 (12–136)
Kjar et al. 2006	24/32	16/24 (67%)	7/7	23/24 (96%)	Broken drill ($n = 1$)	26 (2–56)
Yip et al. 2006	6/7	5/6 (83%)	1/1	6/6 (100%)	Skin burn ($n = 1$)	40 (18–65)
Peyser et al. 2007	51/52	50/51 (98%)	1/1	51/51 (100%)	Wound infection ($n = 1$)	24 (5–91)
Donkol et al. 2007	23/24	18/23 (78%)	1/1	19/23 (83%)	Wound infection ($n = 1$); Skin burn ($n = 2$); Hyperthermia ($n = 2$)	30 (13–49)
Total	856/936	621/710 (87%)	55/67 (82%)	676/710 (95%)	($n = 25$)	–

might be due to the low body weight of the children resulting in higher applied energy per kilogram body weight.

Damage of neural structures can be avoided by the careful choice of an appropriate access path with at least 1 cm distance between neural structures and the active tip of the RF-probe. More common procedure-related complications of RF-ablation are skin burns which typically occur in patients with osteoid osteoma in superficially located bones due to contact of uninsulated parts of the RF-probe to the skin (Cioni et al. 2004). A severe skin burn could also lead to a skin fistula requiring surgical débridement or homologous skin transplant.

To minimize the risk of this complication the insulation of the RF-probe should be visually checked before probe placement. The use of an additional introducer sheath as described above helps to avoid skin burns at the entry point. Another typical site for skin burns are the grounding pads especially if high energy protocols are used.

Summary

In summary treatment local ablation of osteoid osteoma is safe and effective minimal-invasive treatment modality. Compared to surgical therapy, lower complication rates are described at comparable success rates. Furthermore, due to its minimal-invasive character, convalescence is quick after local ablation which leads to short hospitalisation. Because stability of the treated bone is not essentially altered, no internal fixation or cast is needed and therefore patients can quickly return to normal daily activities including sports. In addition, with regard to cost-effectiveness, RF-ablation is beneficial when compared to surgical therapy (Rosenthal et al. 1998; Lindner et al. 1997). Therefore, percutaneous RF-ablation nowadays has to be considered the method of choice for first and second line treatment of osteoid osteoma.

Key Points

- Indication: patients with typical symptoms of an osteoid osteoma and a clearly identified nidus in imaging studies.
- Contraindications: major neurovascular structures with less than 1 cm distance to the lesion intended to treat; repeated ($n > 3$) unsuccessful local ablation procedures.
- Needle placement: careful RF-probe placement in the central area of the nidus.
- Ablation technique: multiple ablation-probe positions if nidus larger than 1 cm.
- Complications: ~2.6% including skin burns, damage of neural and vascular structures adjacent to ablation zone, wound infection.
- Total success rate: ~95% (RF-ablation); ablation of recurrence possible.

References

Adam G, Keulers P, Vorwerk D et al. (1995) The percutaneous CT-guided treatment of osteoid osteomas: a combined procedure with a biopsy drill and subsequent ethanol injection. RoFo 162:232–235

Aschoff AJ, Merkle EM, Emancipator SN et al. (2002) Femur: MR imaging-guided radiofrequency-ablation in a porcine model – feasibility study. Radiology 225:471–478

Barei DP, Moreau G, Scarborough MT et al. (2000) Percutaneous radiofrequency ablation of osteoid osteoma. Clin Orthop Relat Res 373:115–124

Cantwell CP, Obyrne J, Eustace S (2004) Current trends in treatment of osteoid osteoma with an emphasis on radiofrequency ablation. Eur Radiol 14:607–617

Cantwell CP, O'Byrne J, Eustace S (2006) Radiofrequency ablation of osteoid osteoma with cooled probes and impedance-control energy delivery. AJR Am J Roentgenol 186 (Suppl 5):S244–248

Cioni R, Armilotta N, Bargellini I et al. (2004) CT-guided radiofrequency ablation of osteoid osteoma: long-term results. Eur Radiol 14:1203–1208

Davies M (2002) The diagnostic accuracy of MR imaging in osteoid osteoma. Skeletal Radiol 31:559–569

Donkol RH, Al-Nammi A, Moghazi K (2007) Efficacy of percutaneous radiofrequency ablation of osteoid osteoma in children. Pediatr Radiol Nov 27; [Epub ahead of print]

Gangi A, Alizadeh H, Wong L et al. (2007) Osteoid osteoma: percutaneous laser ablation and follow-up in 114 patients. Radiology 242:293–301

Gebauer B, Tunn PU, Gaffke G et al. (2006) Osteoid osteoma: experience with laser- and radiofrequency-induced ablation. Cardiovsc Intervent Radiol 29:210–215

Ghanem I, Collet LM, Kharrat K et al. (2003) Percutaneous radiofrequency coagulation of osteoid osteoma in children and adolescents. J Pediatr Orthop B 12:244–252

Jaffe HL (1935) "Osteoid osteoma", a benign osteoblastic tumor composed of osteoid and atypical bone. Arch Surg 31:709–728

Kjar RA, Powell GJ, Schilcht SM et al. (2006) Percutaneous radiofrequency ablation for osteoid osteoma: experience with a new treatment. Med J Aust 184:563–565

Lindner NJ, Scarborough M, Ciccarelli JM et al. (1997) CT-controlled thermocoagulation of osteoid osteoma in comparison with traditional methods. Z Orthop Ihre Grenzgeb 135:522–527

Lindner NJ, Ozaki T, Roedl R et al. (2001) Percutaneous radiofrequency ablation in osteoid osteoma.J Bone Joint Surg Br 83:391–396
Mahnken AH, Tacke JA, Wildberger JE et al. (2006) Radiofrequency ablation of osteoid osteoma: initial results with a bipolar ablation device. J Vasc Interv Radiol 17:1465–1470
Marcove RC, Heelan RT, Huvos AG et al. (1991) Osteoid osteoma. Diagnosis, localization, and treatment. Clin Orthop Relat Res 267:197–201
Martel J, Bueno A, Ortiz E (2005) Percutaneous radiofrequency treatment of osteoid osteoma using cool-tip electrodes. Eur J Radiol 56:403–408
Mastrantuono D, Martorano D, Verna V et al. (2005) Osteoid osteoma: our experience using radio-frequency (RF) treatment. Radiol Med (Torino) 109:220–228
Peyser A, Applbaum Y, Khoury A et al. (2007) Osteoid osteoma: CT-guided radiofrequency ablation using a water-cooled probe. Ann Surg Oncol 14:591–596
Pinto CH, Taminiau AHM, Vanderschueren GM et al. (2002) Technical considerations in CT-guided radiofrequency thermal ablation of osteoid osteoma: tricks of the trade. AJR Am J Roentgenol 179:1633–1642
Rimondi E, Bianchi G, Malaguti MC et al. (2005) Radiofrequency thermoablation of primary non-spinal osteoid osteoma: optimization of the procedure. Eur Radiol 15:1393–1399
Rosenthal DI, Alexander A, Rosenberg AE et al. (1992) Ablation of osteoid osteomas with percutaneously placed electrode: a new procedure. Radiology 183:29–33
Rosenthal DI, Hornicek FJ, Wolfe MW et al. (1998) Percutaneous radiofrequency coagulation of osteoid osteoma compared with operative treatment. J Bone Joint Surg Am 80:815–821
Rosenthal D, Hornicek FJ, Torriani M et al. (2003) Osteoid osteoma: percutaneous treatment with radiofrequency energy. Radiology 229:171–175
Sans N, Galy-Fourcade D, Assoun J et al. (1999) Osteoid osteoma: CT-guided percutaneous resection and follow up in 38 patients. Radiology 212:687–692
Sequeiros RB, Hyvonen P, Sequeiros AB et al. (2003) MR imaging guided laser ablation of osteoid osteomas with use of optical instrument guidance at 0.23 T. Eur Radiol 13(10):2309–2314
Skjedal S, Lilleås F, Follerås G et al. (2000) Real-time MRI-guided excision and cry-treatment of osteoid osteoma in os ischii: a case report. Acta Orthop Scand 71:637–638
Soong M, Jupiter J, Rosenthal D (2006) Radiofrequency ablation of osteoid osteoma in the upper extremity. J Hand Surg Am 31:279–283
Vanderschueren GM, Taminiau AHM, Obermann WR et al. (2002) Osteoid osteoma: clinical results with thermocoagulation. Radiology 224:82–86
Vanderschueren GM, Taminiau AH, Obermann WR et al. (2004) Osteoid osteoma: factors for increased risk of unsuccessful thermal coagulation. Radiology 233:757–762
Venbrux AC, Montague BJ, Murphy KPJ et al. (2003) Image-guided percutaneous radiofrequency ablation for osteoid osteomas. J Vasc Interv Radiol 14:375–380
Witt JD, Hall-Craggs MA, Ripley P et al. (2000) Interstitial laser photocoagulation for the treatment of osteoid osteoma. J Bone Joint Surg Br 82:1125–1128
Woertler K, Vestring T, Boettner F et al. (2001) Osteoid osteoma: CT-guided percutaneous radiofrequency ablation and follow-up in 47 patients. J Vasc Interv Radiol 12:717–722
Yip PS, Lam YL, Chan MK et al. (2006) Computed tomography-guided percutaneous radiofrequency ablation of osteoid osteoma: local experience. Hong Kong Med J 12:305–309

15.2 Vertebroplasty and Osteoplasty

Kai Wilhelm

15.2.1 Introduction

Percutaneous Vertebroplasty (PV) using PMMA (polymethylmethacrylate) was first described in 1987 by Gallibert and Deramond for treating vertebral body instability in patients with aggressive forms of vertebral hemangioma (Galibert et al. 1987). Other types of painful osteolytic bone lesions, such as osteoporotic vertebral fractures and vertebral metastases soon became more important in numbers (Weill et al. 1996; Deramond et al. 1998). Within the last few years this technique has become widely accepted and it is proposed for osteolytic bone lesions to regions difficult to approach surgically such as the pelvis and sacrum (Wetzel et al. 2002; Weill et al. 1998). The rapidity of analgesia and resulting stability has conferred an important role upon osteoplasty especially in palliative tumor treatment for patients with a shortened expected life span (Wetzel and Wilhelm 2006). Additionally, combined treatment of spinal metastases with image-guided radiofrequency (RF) ablation and percutaneous cement injection has been shown to be a safe modality in the therapy of nonresectable tumors of spine (Grönemeyer et al. 2002; Georgy and Wong 2007; Toyota et al. 2005).

15.2.2 Indications

The decision to perform PV should be made as a multidisciplinary approach. Patient evaluation should consider all available clinical information, and clinical examination should identify the focal pain that correlates to the lesion considered for PV. The patient's pain should be severe, altering activities of daily living or requiring substantial use of analgetics. This pain

should be documented with measurement instruments such as a visual analog scale (VAS) and a quality-of-life questionnaire before PV and during follow-up (Mathis 2006; Helmberger et al. 2003).

The principal indications for vertebroplasty are:

- Painful osteoporotic vertebral compression fracture refractory to medical therapy.
- Painful vertebral fracture or severe osteolysis with impending fracture related to benign or malignant tumor, such as hemangioma, myeloma or metastasis.

By now osteolytic metastases represent the most frequent indications for vertebroplasty and osteoplasty. The aim of cement injection is the consolidation of fractured or fragile vertebrae and pain treatment. The analgesic effect usually occurs within 24 h, and permits the reduction of major analgesic agents in most cases. Additionally, vertebral stabilization due to the consolidation effect decreases the risk of fracture and shortens patient's immobilization period.

There are several absolute and relative contraindications to PV that need to be considered when PV is planned.

15.2.2.1 Absolute Contraindications

Asymptomatic stable fracture:

- Patients clearly improving from pain treatment
- Prophylaxis in osteopenic patients with no evidence of acute fracture
- Osteomyelitis of target vertebra
- Acute traumatic fracture or non-osteoporotic vertebra
- Uncorrectable coagulopathy or hemorrhagic diasthesis
- Allergy to any component required for the procedure

15.2.2.2 Relative Contraindications

- Severe vertebral body collapse (vertebra plana).
- Stable fracture without pain and known to be more than 2 years old.
- Treatment of more than tree levels performed at one time.

Further relative contraindications in which PV may be indicated in combination with surgical spinal decompression procedure include:

- Radicular pain or radiculopathy and spinal compression significantly in excess of vertebral pain
- Rupture of the posterior wall, retropulsation of fracture fragments causing significant spinal canal compromise
- Tumor extension into the epidural space with severe spinal canal obstruction

15.2.3 Materials and Techniques

15.2.3.1 Imaging Guidance

Computed tomography (CT) is the established guidance technique for bone biopsies and collecting samples for histological evaluation. Since the first PV procedure, fluoroscopy has been the preferred method of imaging guidance for performing PV (Wetzel and Wilhelm 2006). Rotation C-arm fluoroscopy (C-arm CT) allows real time visualization for needle placement and cement injection and permits rapid alteration between imaging planes without complex equipment or patient movement. However, CT-guidance is especially valuable for osteoplasty and in deep-seated lesions and lesions that lie adjacent to vital structures. Although contrast resolution with CT is superior to that with fluoroscopy, the CT method does not include the ability to monitor cannula introduction and it is certainly not optimal for monitoring the injection of cement. Therefore the concept of using a combination of CT and single-plane C-arm fluoroscopy for PV is frequently used (Fig. 15.7) (Gangi et al. 1994). With the introduction of flat-panel detectors, it has also become possible to acquire CT-like images via a rotational C-arm fluoroscopy system in the angio suite. The feasibility of obtaining volumetric images immediately after or even during vertebroplasty procedures in the angio suite is clearly the key advantage over combined CT and single-plane C-arm fluoroscopy settings (Hodek-Wuerz et al. 2006). In addition, the use of flat-panel angiography systems provides the immediate possibility to perform cross sectional imaging without any changing of patients position, resulting in accelerate operational and organisational flow of VP procedures in all (Fig. 15.8) (Wilhelm and Babic 2006).

Magnetic resonance (MR) guidance for vertebroplasty is only at its beginning and not used now.

Fig. 15.7 Combined CT and mobile C-arm fluoroscopy setup for percutaneous vertebroplasty: CT guidance is used to choose puncture site and for needle placement while cement injection is performed under fluoroscopy control. This arrangement is preferred in the treatment of cervical or high thoracic vertebrae and sacroplasty where fluoroscopy alone is inadequate to visualize critical structures

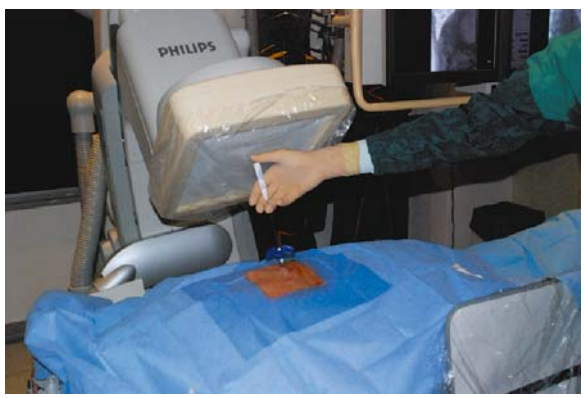

Fig. 15.8 Flat-panel detector angiography setup for vertebroplasty. The picture shows image-guided RF ablation prior to PV using a transpedicular access. Volumetric images can be obtained immediately after or even during fluoroscopically controlled intervention in the angio suite. Therefore acquisition of CT-like images acquired by a rotational c-arm system (C-arm CT) is possible

Nevertheless, pre-interventional obtained MR imaging is very helpful to detect vertebral body bone marrow edema to reveal acute vertebral fracture in osteoporosis (Tanigawa et al. 2006) and to detect exact tumor expansion and presence of multiple spinal lesions in patients with known cancer and back pain related to spinal metastases (Voormolen et al. 2006; Koh et al. 2007). Therefore pre-interventional obtained MR imaging should be available in all patients to assess vertebral fracture, the degree of collapse, osteolysis, extension of tumor into the epidural space and potential compression of the neural tissue.

15.2.3.2 Informed Consent

Written permission for the procedure is recommended following patients instruction about potential risks and complications of the procedure. The clinical history and findings, including the indication for PV, must be reviewed and recorded in the patient's medical record (Mathis 2006; Helmberger et al. 2003). The potential need for immediate surgical intervention should be discussed. Additionally, the probability that the procedure may not result in significant pain relief should also be noted.

15.2.3.3 Procedure

Several excellent detailed technical descriptions of the technique of vertebroplasty have been published (Mathis 2006). PV can be performed under local or general anesthesia. The choice of technique depends on the patient's general health status and the target region.

Using local anesthesia the skin, subcutaneous tissue along the expected needle tract, and especially the periosteal tissue at the target side must be infiltrated completely. Once this is carried out, the patient will tolerate the procedure without further i.v. sedation. However, general anesthesia may be necessary for patients with extreme pain and those who cannot tolerate the position necessary for the procedure or those who have problems with ventilation lying in prone position.

Most PV procedures are performed at the lumbar and lower thoracic spine levels following standard access routes (Fig. 15.9). For lumbar, thoracic and dorsal levels such as sacroplasty, the patient is positioned in prone position. For bone access an 11 Gauge needle is placed using a transpedicular approach (Fig 15.10). Penetration of the medial border of the pedicle must be avoided to prevent nerve root or spinal canal injury. In cases of small pedicels or intended unilateral access a parapedicular respectively posterolateral approach is possible (Wetzel and Wilhelm 2006).

In AP projection the needle is directed to the vertebral pedicle and entered through the cortical bone into

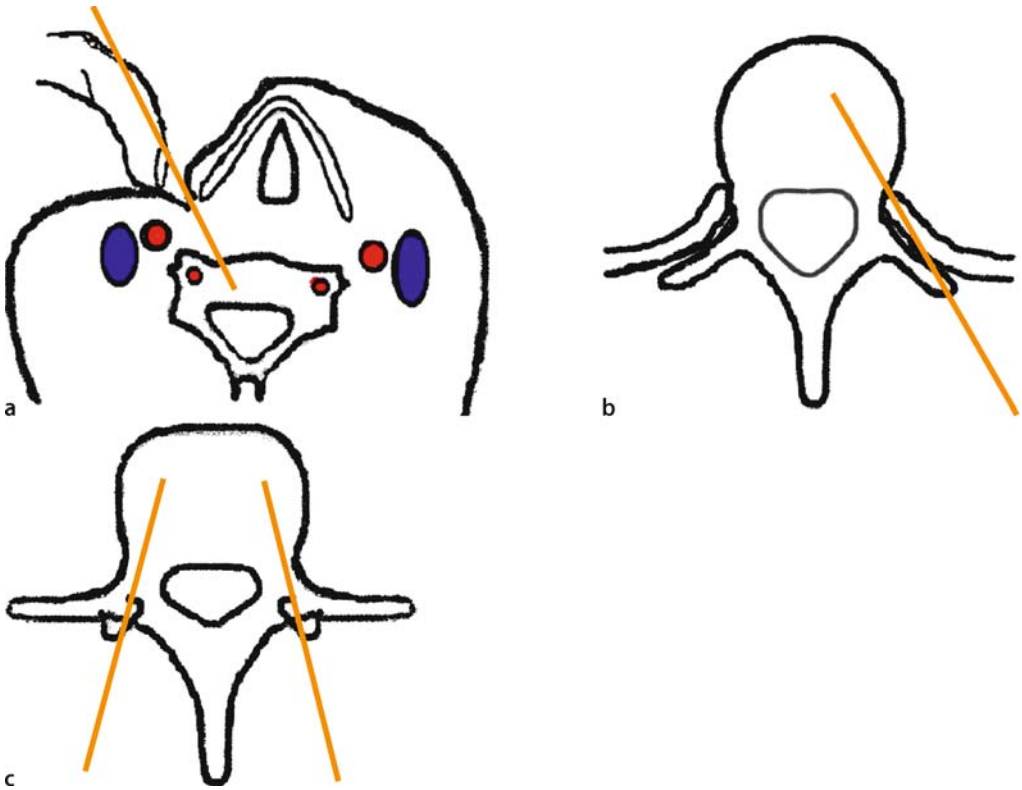

Fig. 15.9a–c Depending on the anatomic level, there are different commonly used access routes to the spine. The anterolateral approach is the most common approach for the treatment of cervical spine levels. Axial drawing demonstrates manual displacement of the carotid-jugular complex and subluxation of the larynx. The anterolateral oblique access for cervical spine levels allows to reach the central part of a vertebral body (**a**). Due to the orientation and small size of the pedicles, the parapedicular (transcostovertebral) approach is used for vertebroplasty of thoracic spine levels in most cases. The needle is placed through the junction of the rib and transverse process (**b**). The pedicles of the lumbar spine are large and allow transpedicular needle placement in almost all cases. The transpedicular approach using both pedicles is the most common and safest access (**c**)

the pedicle. Then, subsequently alternating from AP in lateral projection, the needle is pushed stepwise forward until the tip of the needle crosses the posterior wall of the vertebral body. Consecutively lateral projection is used for needle progression to reach the anterior third of the vertebral body and finalized cement filling.

Osteoplasty of lytic and deep-seated bone lesions is performed using direct CT guided access of the target region. Here harming of the adjacent vital structures has to be avoided (Fig. 15.11). Sacral insufficiency fractures and fractures due to osteoporosis and trauma as well as metastatic lesions of the sacrum may be augmented percutaneously using a posterior-oblique and transiliac approach (Fig. 15.12).

For the cervical spine the anterolateral approach is preferred. In these cases patients are positioned in supine position. For C2 vertebrae a posterolateral approach is possible if the vertebral body is affected (Wetzel et al. 2002). For the extremely rare treatment of the dens a transoral approach is possible, too (Martin et al. 2002). In these cases, 13 or 15 Gauge bone biopsy needles are used (Huegli et al. 2005). The foremost concern for cervical vertebroplasty is to avoid damage of the carotid artery and jugular vein.

Depending on the preference of the operator, a direct intra-osseous contrast injection under fluoroscopy in digital subtraction angiography (DSA) technique is performed (vertebrography). In most cases this will be helpful to learn about potentially dangerous leakage and to adapt the cement viscosity to the given injection conditions (Wetzel and Wilhelm 2006).

In cases of suspected malignancy a biopsy should precede cement injection (Mathis 2006). Appropri-

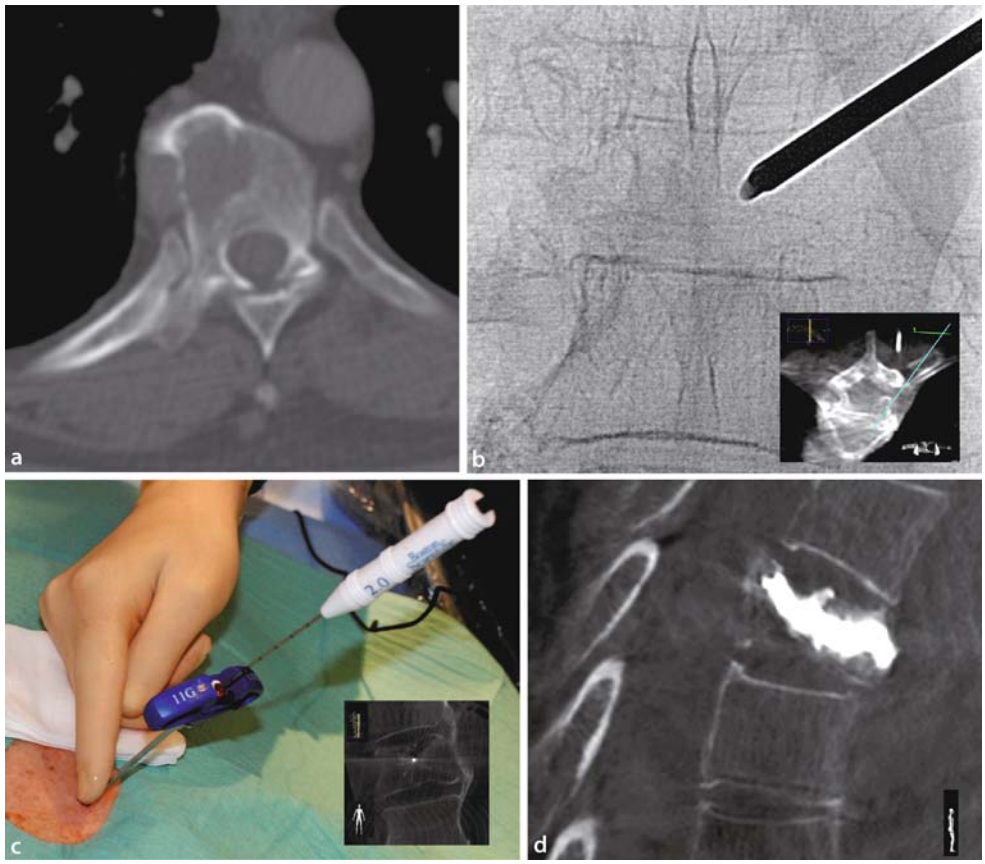

Fig. 15.10a–d Flat-panel C-arm CT in percutaneous vertebroplasty in a 74-year-old female patient who presented with severe and focal back pain related to osteolytic metastases of TH 5. Unilateral transpedicular approach was used for PV. Preinterventional axial CT image shows an osteolytic metastasis of the right hemivertebra (**a**). Fluoroscopy (pa projection) shows needle placement for unilateral transpedicular approach. *Insert image* demonstrates C-arm CT needle guidance (patient in prone position) for transpeducal access (**b**). The 11 Gauge bone biopsy needle in place (**c**). Prior to cement application, RF ablation is performed using a 2-cm LeVeen™ expandable needle electrode. *Insert image* shows correct positioning of the expandable needle electrode on C-arm CT obtained during RF ablation. Sagittal reformats from C-arm CT data obtained immediately after percutaneous vertebroplasty display the bony structures and cement filling without any cement extravasation (**d**)

ate biopsy devices are available. Using these devices biopsy can be performed in one session without the necessity to create a secondary approach. Additionally, RF ablation may be performed prior to cement application in osteolytic bone metastases using suitable needle electrodes (Grönemeyer et al. 2002; Georgy and Wong 2007; Toyota et al. 2005). As the combination of PV and RF ablation is a palliative procedure that does jet not prevent tumor growth for certain, it should be used in combination with radiation therapy and/or chemotherapy (Mathis 2006).

If the needle position is considered correct within the anterior third of the vertebral body, cement is injected under lateral fluoroscopic or CT-fluoroscopic control. There are several dedicated bone cements and applicator systems usable for vertebroplasty that allow safe and easy control of the cement injection. During cement filling particular attention is given to the epidural space and the posterior wall of the vertebral body (Mathis 2006). Usually 2–5 ml of cement per hemivertebra is adequate. Nevertheless, cement volume has to be adapted individually in order to avoid serious cement leakage, resulting in clinically significant complication. Any cement leakage outside the vertebral body gives a reason to interrupt the injection immediately. After about 1 min of waiting time, careful ce-

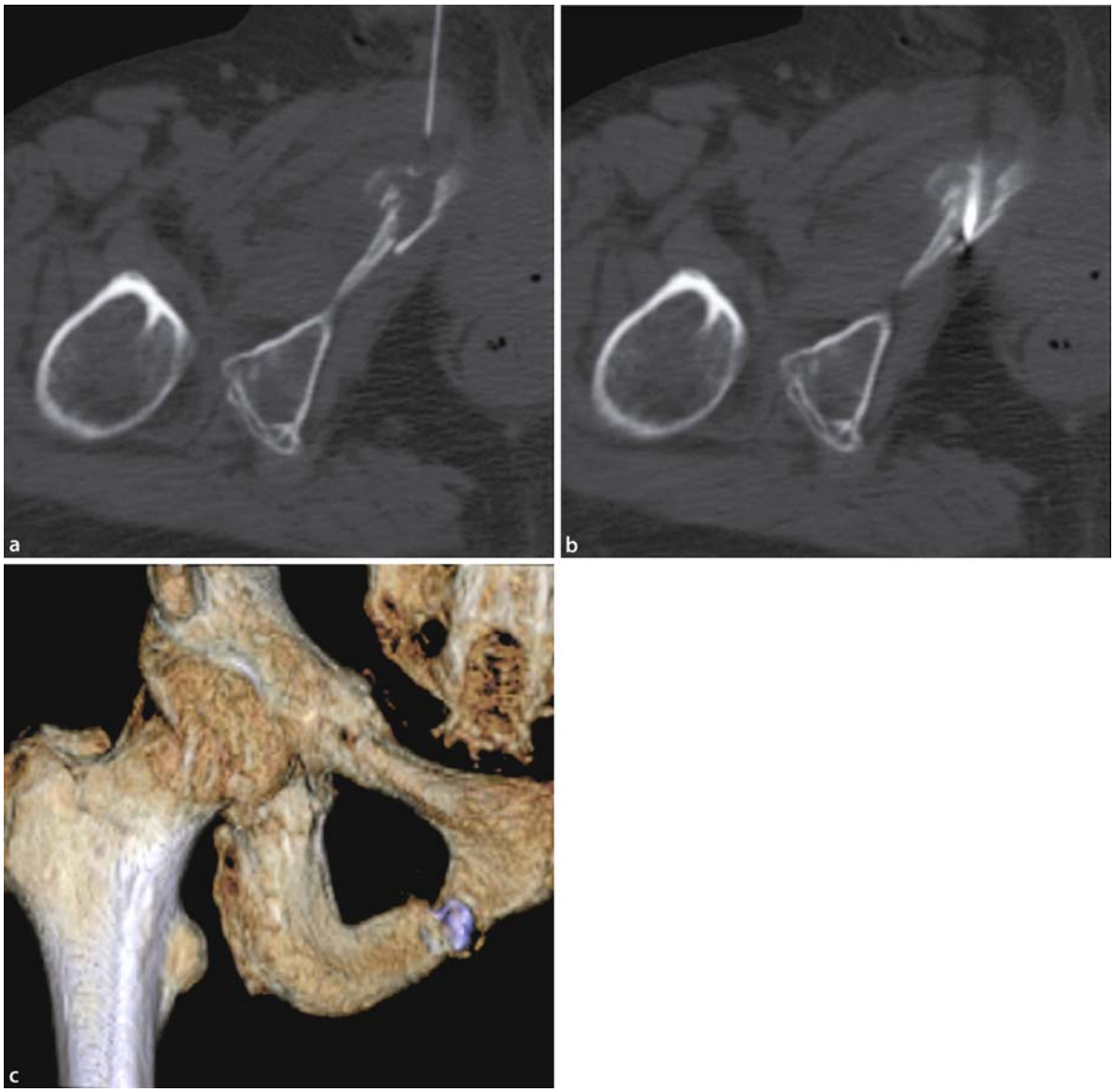

Fig. 15.11a–c Osteoplasty: axial CT scan of the pelvis shows painful osteolytic lesion of the right pubic bone associated with pathologic fracture (**a**). A 22 Gauge needle for local anesthesia is placed under CT guidance (**b**). An 11 Gauge trocar bone biopsy needle is inserted. CT image shows correct position of the needle within the lesion. Additionally biopsy is performed for histopathologic correlation of the lytic lesion. Three-dimensional reconstructed image (**c**) after osteoplasty reveals cement distribution

ment application may be continued under fluoroscopic control. Due to polymerization and cement hardening, cement filling might be achieved into other areas of the vertebra. Nevertheless, if leakage is still visible or even becomes larger, cement application is terminated. The amount of cement needed for stabilization and pain relief is very small; therefore filling of the entire vertebral body is not necessary at all. Finally, the trocars are withdrawn under fluoroscopic control to avoid cement tracking along the access site.

For PV, as for other surgical procedures that implant permanent devices, a single shot i.v. antibiotic prophylaxis is recommended (Mathis 2006). The most common antibiotic used is cephazolin (1–2 g), usually

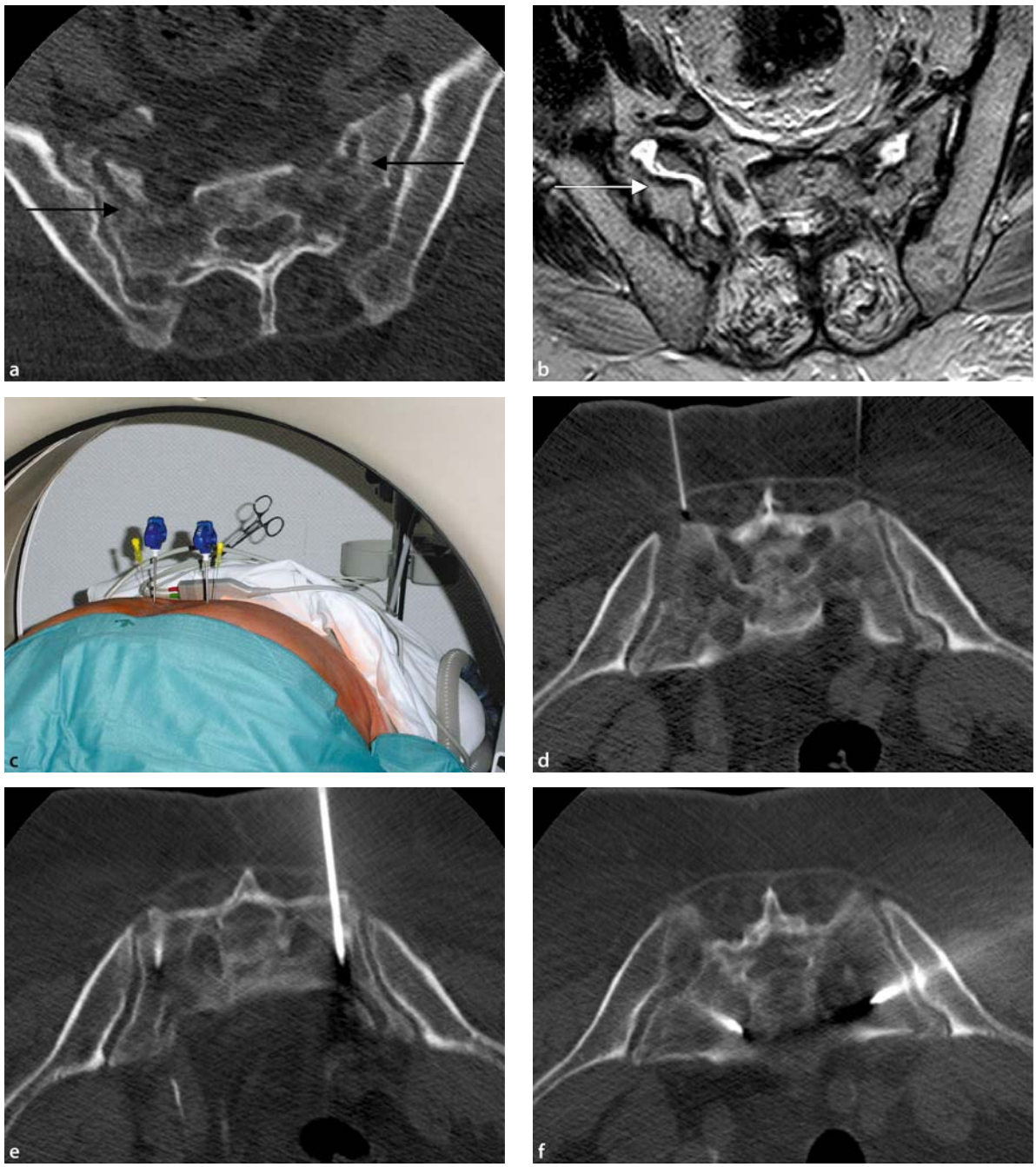

Fig. 15.12a–f Sacroplasty: pretreatment axial CT (**a**) and MR images demonstrate the fractures in both sacral alae (*black arrows*). The fractures are parallel to the sacroiliac joints and show edema on T2-weighted MRI images (*white arrows*) (**b**). CT setup is used for needle placement (**c**,**d**). Bilateral sacroplasty is performed using a both sided posterior (**e**) and transiliac approach (**f**)

30 min before starting the procedure. Working under strict aseptic conditions infections should be avoidable. Nevertheless, there are some reports about serious infections, most likely with preexisting spondylodiscitis or in high risk immunocompromised patients (Söyüncü et al. 2006; Lin et al. 2007).

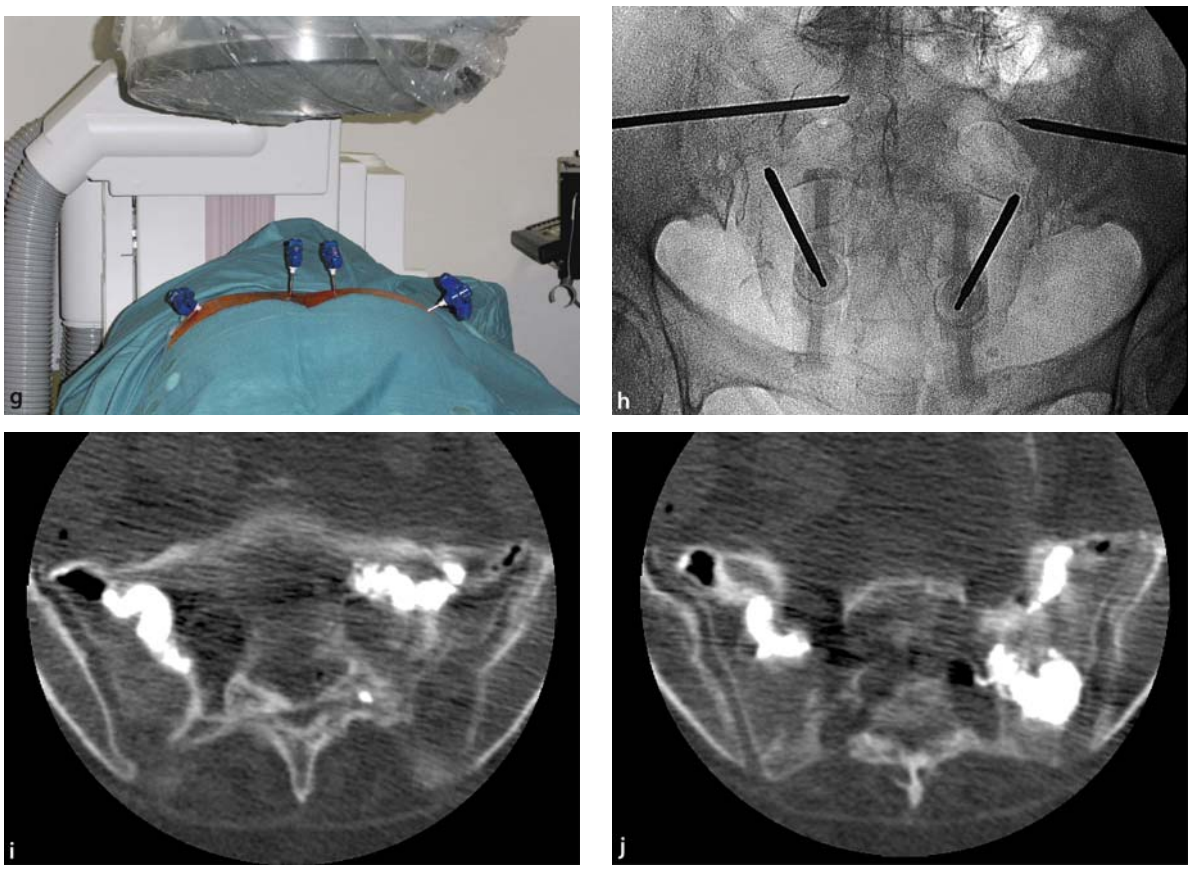

Fig. 15.12g–j Cement injection is performed under fluoroscopic control for optimal visualization of cement distribution (**g**,**h**). The cement is injected simultaneously in small amounts via the four injection sites. Post treatment CT (**i**,**j**) shows cement deposition within the fractures

Postinterventionally the assessment of cement distribution is best performed by CT; however, flat-panel detector CT and 3D reconstruction capabilities after rotational C-arm CT acquisition allow one to avoid an additional CT evaluation after vertebroplasty procedures and therefore accelerate proceedings (Fig. 15.11) (Hodek-Wuerz et al. 2006; Wilhelm and Babic 2006).

Clinical monitoring is performed after PV for 1–2 h for clinical changes in neurological function or for signs of any other change or side effects. During this time complete hardening of the cement is achieved and mobilization is possible. Appropriate to clinical follow-up discharge is conceded after 2–4 h if PV is performed on an outpatient basis.

15.2.4 Results

The efficacy of vertebroplasty and osteoplasty lies in its high potential in pain reduction and stabilization effect. Significant pain relief and improvement of mobility will be achieved in about 80–90% of patients.

When percutaneous vertebroplasty is performed for osteoporosis, success is defined as an achievement of significant pain relief and/or improvement mobility as measured by validated measurement tools with a threshold of 80%. For neoplastic involvement, success is classified as an achievement of significant pain relief and/or improvement mobility as measured by validated measurement tools with a threshold of 50–60% (Mathis 2006).

15.2.5 Complications

Clinical complications rates range from 1% to 10% (Wetzel and Wilhelm 2006). However, the number of publications reporting from unusual or rare complications associated with PV has increased as the method becomes more public and more procedures are being performed by less experienced physicians (Mathis 2006; Barragan-Campos et al. 2006).

The most dangerous complication is cement leakage because of the risk of spinal cord or nerve root compression. The clinical symptoms resulting from cement extravasation range from temporary nerve root irritation to permanent paraplegia. In most cases cement leakages are clinically asymptomatic.

Transient neurological deficit or radicular pain syndrome will occur in about 1% of osteoporotic and up to 10% of tumor patients. Although complications from vertebroplasty are uncommon, serious problems like death to pulmonary cement embolism, significant hemorrhage or vascular injury are reported in the literature (McGraw et al. 2003). Overall, cement leakage is seen more frequently in the treatment of metastatic lesions.

In the majority of cases with epidural leakage or cement leakage into the foramina, the symptoms will be transient because they are caused by an inflammatory reaction due to increased cement temperature during hardening. In these cases symptoms can be eased by administration of anti-inflammatory drugs or local steroid therapy (Mathis 2006; Kelekis and Martin 2005). On the other hand, spinal canal compression caused by a larger amount of cement extravasation resulting in paresis, paralysis, bowel or bladder dysfunction will require immediate surgical decompression (Wetzel and Wilhelm 2006).

Summary

PV is a safe and very effective tool in vertebral pain management that permits pain reduction and instantaneously improved bone stability.

Furthermore, in cancer patients PV and osteoplasty are palliative therapy options supplementing other antineoplastic therapies that result in patients comfort by giving them the possibility of re-establishing their daily activities in a short period of time. Both techniques may be combined with other tumor therapies including radiation therapy or RF ablation.

Key Points

- PV is safe and effective for managing a variety of painful bone lesions.
- Adequate image guidance for needle placement and during PMMA injection is the key to minimizing complications.
- Thorough peri-interventional patient surveillance is needed to detect and adequately deal in a timely fashion with potentially disabling complications.

References

Barragan-Campos HM, Vallee JN, Lo D et al. (2006) Percutaneous vertebroplasty for spinal metastases: complications. Radiology 238:354–362

Deramond H, Depriester C, Galibert P, Le Gars D (1998) Percutaneous vertebroplasty with polymethylmethacrylate. Technique, indications, and results. Radiol Clin North Am 36:533–546

Galibert P, Deramond H, Rosat P, Le Gars D (1987) Note préliminaire sur le traitement des angiomes vertébraux par vertébroplastie acrylique percutanée. Neurochirurgie 33:166–168

Gangi A, Kastler BA, Dietemann JL (1994) Percutaneous vertebroplasty guided by a combination of CT and fluoroscopy. Am J Neuroradiol 15:83–86

Georgy BA, Wong W (2007) Plasma-mediated radiofrequency ablation assisted percutaneous cement injection for treating advanced malignant vertebral compression fractures. Am J Neuroradiol 28:700–705

Grönemeyer DH, Schirp S, Gevargez A (2002) Image-guided radiofrequency ablation of spinal tumors: preliminary experience with an expandable array electrode. Cancer J 8:33–39

Helmberger T, Bohndorf K, Hierholzer J, Noldge G, Vorwerk D (2003) Guidelines of the German Radiological Society for percutaneous vertebroplasty. Radiologe 43:703–708 [German]

Hodek-Wuerz R, Martin JB, Wilhelm K, Lovblad KO, Babic D, Rufenacht DA, Wetzel SG (2006) Percutaneous vertebroplasty: preliminary experiences with rotational acquisitions and 3D reconstructions for therapy control. Cardiovasc Intervent Radiol 29:862–865

Huegli RW, Schaeren S, Jacob AL, Martin JB, Wetzel SG (2005) Percutaneous cervical vertebroplasty in a multifunctional image-guided therapy suite: hybrid lateral approach to C1 and C4 under CT and fluoroscopic guidance. Cardiovasc Intervent Radiol 28:649–452

Kelekis AD, Martin JB (2005) Radicular pain after vertebroplasty: complication and prevention. Skeletal Radiol 34:816

Koh YH, Han D, Cha JH, Seong CK, Kim J, Choi YH (2007) Vertebroplasty: magnetic resonance findings related to cement leakage risk. Acta Radiol 48:315–320

Lin WC, Lee CH, Chen SH, Lui CC (2007) Unusual presentation of infected vertebroplasty with delayed cement dislodgment in an immunocompromised patient: case report

and review of literature. Cardiovasc Intervent Radiol. Dec 13 [Epub ahead of print]
Martin JB, Gailloud P, Dietrich PY, Luciani ME, Somon T, Sappino PA, Rüfenach DA (2002) Direct transoral approach to C2 for percutaneous vertebroplasty. Cardiovasc Intervent Radiol 25:517–519
Mathis JM (2006) Percutaneous vertebroplasty: procedure technique. In: Mathis JM, Deramond H, Belkoff ST (eds) Percutaneous vertebroplasty and kyphoplasty, 2nd edn. Spinger, Berlin Heidelberg New York
McGraw JK, Cardella J, Barr JD et al. (2003) Society of interventional radiology quality improvement guidelines for percutaneous vertebroplasty. J Vasc Interv Radiol 14:S311–315
Söyüncü Y, Ozdemir H, Söyüncü S, Bigat Z, Gür S (2006) Posterior spinal epidural abscess: an unusual complication of vertebroplasty. Joint Bone Spine 73:753–755
Tanigawa N, Komemushi A, Kariya S, Kojima H, Shomura Y, Ikeda K, Omura N, Murakami T, Sawada S (2006) Percutaneous vertebroplasty: relationship between vertebral body bone marrow edema pattern on MR images and initial clinical response. Radiology 239:195–200
Toyota N, Naito A, Kakizawa H, Hieda M, Hirai N, Tachikake T, Kimura T, Fukuda H, Ito K (2005) Radiofrequency ablation therapy combined with cementoplasty for painful bone metastases: initial experience. Cardiovasc Intervent Radiol 28:578–583
Voormolen MH, van Rooij WJ, Sluzewski M, van der Graaf Y, Lampmann LE, Lohle PN, Juttmann JR (2006) Pain response in the first trimester after percutaneous vertebroplasty in patients with osteoporotic vertebral compression fractures with or without bone marrow edema. Am J Neuroradiol 27:1579–1585
Weill A, Chiras J, Simon JM, Rose M, Sola-Martinez T, Enkaoua E (1996) Spinal metastases: indications for and results of percutaneous injection of acrylic surgical cement. Radiology 199:241–247
Weill A, Kobaiter H, Chiras J (1998) Acetabulum malignacies: technique and impact on pain of percutaneous injection of acrylic surgical cement. Eur Radiol 8:123–129
Wetzel SG, Wilhelm KE (2006) Perkutane Vertebroplastie und Kyphoplastie. Radiol Up2Date 3:255–272
Wetzel SG, Martin JB, Somon T, Wilhelm K, Rufenacht DA (2002) Painful osteolytic metastasis of the atlas: treatment with percutaneous vertebroplasty. Spine 27:E493–495
Wilhelm K, Babic D (2006) 3D angiography in the interventional clinical routine. Med Mundi 12:24–31

15.3 Percutaneous Osteosynthesis of the Pelvis and the Acetabulum

Sebastian Kos, Peter Messmer, Deniz Bilecen and Augustinus L. Jacob

15.3.1 Indications

Mostly caused by high impact traumas, pelvic fracture account for about 0.3–8% of all fractures (Gansslen et al. 1996; Senst and Bida 2000), but in cases with multiple traumas, a pelvic ring injury is more frequent (20%). The trauma (Gansslen et al. 1996) may be lethal due to the injury itself (Kellam et al. 1987) or additional organ lesions (head, chest, abdomen and limbs) (Poole and Ward 1994). This is reflected by mortality rates between 10% and 31% (Pohlemann et al. 1994; Ben-Menachem et al. 1991; Hunter et al. 1997) and a high morbidity in survivors (Tile 2003). As a basic function the pelvic ring transmits forces from the lower extremities to the spine (Isler and Ganz 1996). Any therapy has to restore and preserve this ability, not so much to offer a high-precision anatomical reconstruction. In addition, the acetabular joint enables movement of the femoral head, which means that those fractures need a minute reduction and fixation to minimize the risk of post-traumatic osteoarthritis or at least allow a consecutive joint replacement (Starr et al. 2001).

15.3.1.1 Pelvic Fractures

As the osseous pelvic ring is a rigid structure an injury of, e.g. the posterior ring (ilium, sacroiliac joint, sacrum) rarely occurs without a concomitant interruption of the anterior ring (symphysis, obturator rings, acetabula). The AO/ASIF classification groups pelvic fractures according to its severity (Fig. 15.13) (AC) (Tile 1996, 2003; Isler and Ganz 1996).

The most common Type “A” injuries (50–60%) are isolated fractures of the anterior pelvic ring with intact posterior stability. They are often treated conservatively with partial load bearing using crutches. Rare indications for open or percutaneous surgery may be muscle avulsion fractures, fragment dislocation, persistent pain and a prolonged rehabilitation.

Type “B” fractures (20–30%) preserve a partial posterior stability but are unstable towards rotational forces. This may occur in cases with complete anterior plus partial posterior disruptions. Those are usually treated conservatively (Tile 2003). Nevertheless, due to partial but clinically disabling functional pelvic ring instability, certain types of B fractures, e.g. open book lesions with symphyseal disruption of more than 2–3 cm (AO B2.2), frequently undergo surgery. Other indications for surgery may be potentially unstable intermediate type B/C lesions to prevent secondary dislocation and malunion. In rotationally unstable frac-

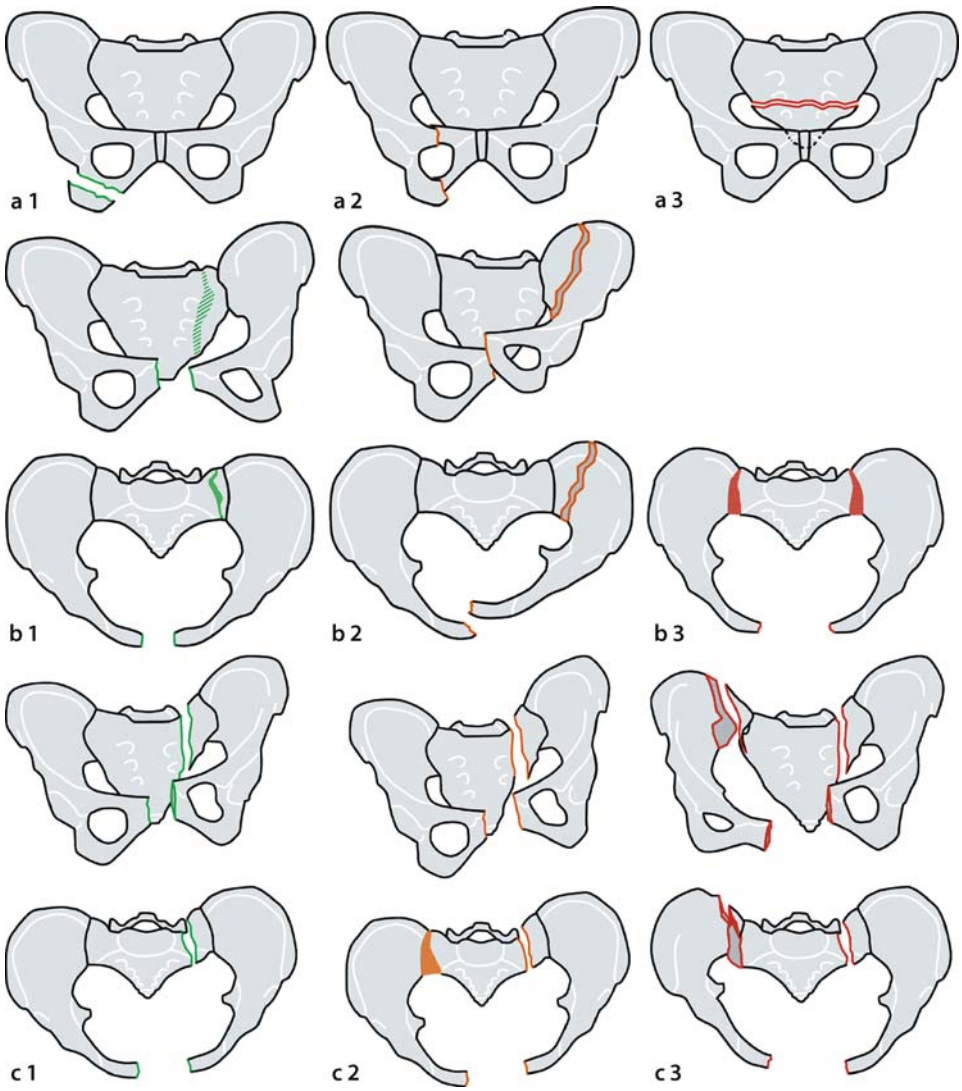

Fig. 15.13a1–c3 AO classification of pelvic fractures (AO 61). Examples for fracture types A1C3 are given. Modified according to Tscherne H. and Pohlemann T. Becken and Acetabulum. Springer, New York 1998

tures an anterior stabilization,in combination with the preserved posterior sacroiliac ligament complex, provides sufficient stability. For simple cases with non-displaced fractures either antegrade or retrograde superior pubic ramus screws or reconstruction plates can be used. Reconstruction plates may be used in displaced, comminuted and/or complex cases (Simonian et al. 1994a).

Type "C" fractures (10–20%) show a complete loss of posterior stability, are rotationally and vertically unstable and should be treated surgically. An approach with initially anterior plating normally reduces the posterior pelvic ring sufficiently for a subsequent percutaneous ilio-sacral screw fixation.

15.3.1.2 Acetabular Fractures

The Letournel classification (Fig. 15.14) discriminates between simple fracture types of the posterior wall (1), posterior column (2), anterior wall (3), anterior column (4), and transverse fractures (5) and associated fracture types. The latter are a variety of combinations of the simple types (6–10). As mentioned, the

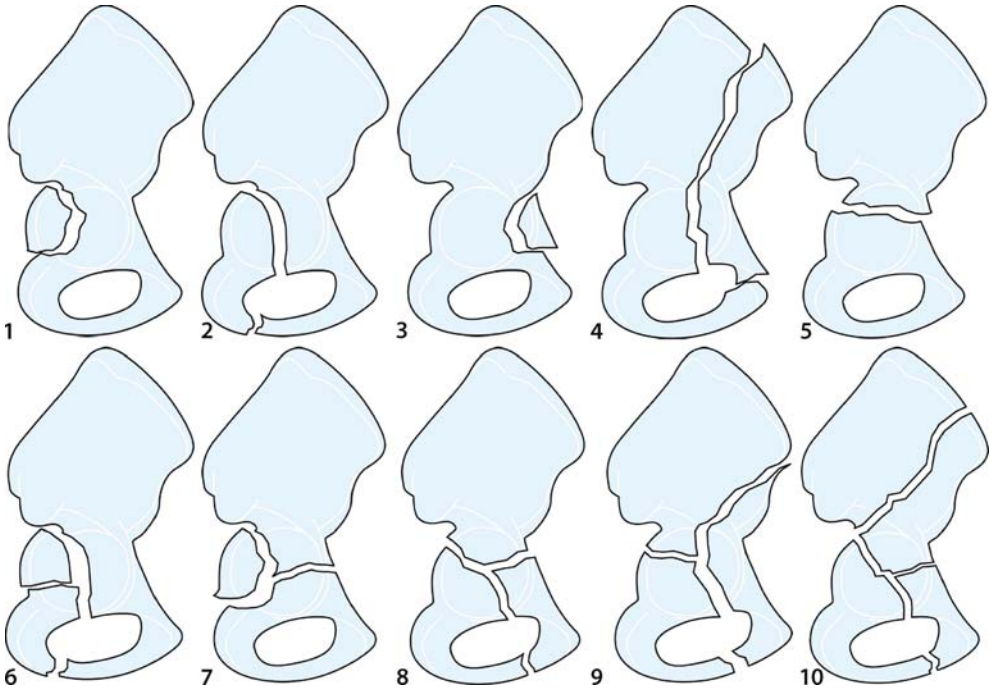

Fig. 15.14 Letournel classification of acetabular fractures. Simple types (1–5) and associated types (6–10). Modified according to Tscherne H. and Pohlemann T. Becken and Acetabulum. Springer, New York 1998

main goal of treatment is the precise reconstruction of joint surface integrity. Insufficient reduction may lead to posttraumatic osteoarthritis in up to 1/3 of the cases, whereas this only occurs in about 10% after a good reduction (Letournel 1993).

Accepted treatment is an open surgical reduction of the fracture itself and an internal fixation (ORIF) with screws and plates (Letournel 1993; Judet et al. 1964; Qureshi et al. 2004). In selected cases a minimally-invasive therapy is possible (Gay et al. 1992; Jacob et al. 2000a; Gross et al. 2004; Starr et al. 1998).

15.3.2 Material

15.3.2.1 Pre-interventional Diagnostics

As both pelvic and acetabular fractures are usually complex, the exact fracture morphology is hard to detect by routine radiographs alone (Falchi and Rollandi 2004). False negative rates regarding the detection of pelvic fractures in conventional a.p. views reach 32% and in up to 55% of cases with a fracture detected on plain film, computed tomography (CT) reveals either additional fractures or an upgrade in fracture classification (Guillamondegui et al. 2002). In general, multislice spiral CT (MSCT) is superior regarding the depiction of the spatial fracture fragment arrangement and the fracture extent, particularly when using three-dimensional reformations and is therefore the actual gold standard for pelvic fracture assessment (Wedegartner et al. 2003). For the standard CT-protocol we use 3 mm slice thickness and 1.5 mm slice increment. Multiplanar reformations are obtained adapted to the individual fracture pattern.

15.3.2.2 Image Guidance Methods

The main task of percutaneous fixation is the safe placement of an implant well adapted to the fracture morphology. Such guidance is performed like in any standard CT or CT fluoroscopy-guided procedure. As an advantage, by the end of the procedure, the postoperative control is already done. In strictly percutaneous procedures a normal CT suite may be sufficient from a hygienic point of view, which nevertheless has to be approved by the local authorities. For any open or hybrid procedure a sterile operating room is mandatory

(Jacob et al. 2000c). Until today, MR-guidance for percutaneous osteosynthesis is neither used for the preinterventional procedure planning, nor for its guidance.

15.3.2.3 Robotic Assistance

As ambitious robotic projects failed within the last decade (Glauser et al. 1995; Schrader 2005; Siebert et al. 2002), at our institution we use a more conservative approach. With good results, we use a robotic assisted device (Fig. 15.15) (Innomotion, Innomedic, Herxheim, Germany) that leaves the medical act of introducing instruments and implants into the body to the physician (Cleary et al. 2006) instead of an "active" robot performing the procedure. Of course, procedure guidance could be performed without robotic assistance either, but in our opinion precise device positioning is hereby facilitated.

15.3.2.4 Hardware

To date there is no dedicated hardware for closed reduction combined with percutaneous fixation (CRPF) available on the market. These procedures therefore rely on standard surgical tools (e.g. Schanz screws, external fixators, guide wires, cannulated screws, screwdriver, drill) (Fig. 15.16). From our experience we want to emphasize some specific points for percutaneous osteoysyntheses. We use 2.8-mm AO/ASIF guide wires (Synthes, Solothurn, Switzerland) which are both rigid and sharp (Fig. 15.17). Rigidity is needed for navigation where the near end of the instrument is guided and the tip is extrapolated assuming linearity of the device. Acuity avoids the guidepin sliding off a bone entry site with an obtuse angle between device and cortex. We use self-cutting self-tapping AO/ASIF 7.3-mm set and lag screws (Synthes, Solothurn, Switzerland) without the need for additional drilling and tapping (Fig. 15.18). These are inserted immediately after correct placement of the guide wire is documented. Fully threaded set screws are needed in cases where additive compression is unwanted or dangerous (e.g. foraminal comminution) to fix the fragments in their current relative position. Those fully threaded set screws do not compress the fracture and therefore are biomechanically not as strong as lag screws. Lag screws are threaded in a defined region, from their tip backwards, leading to fracture compression and are used in all other indications. The threaded portion is chosen by the interventionalist, in such a way that it lies entirely in the far fragment. In some cases a lag screw may be inserted first to gain controlled compression, which is than held using a set screw.

15.3.3 Technique

15.3.3.1 Placement, Immobilization, Patient Preparation

Procedures are performed with a written informed consent obtained at least 24 h prior to the procedure. All procedures are performed under general anesthesia and sterile conditions in an operation suite. In navigated procedures and using robotic assist devices it is necessary to immobilize the patient. We routinely use a setup with a vacuum mattress and broad adhesive tape. The patient is fixed in a position where the screw trajectory envisioned runs either vertically or horizontally and "as orthogonal as possible", especially when a navigation or robotic assistance system is not used.

15.3.3.2 Minimally-Invasive Reduction Methods

Imaging may identify different types of dislocation as, e.g. seen in translation, joint step, gap and rotation (Wedegartner et al. 2003). In cases with a fracture or luxation *gap*, ideally all points of the bone fragments have the same distance to their counterparts. The reduction may be achieved by a fixation, applied perpendicular to the gap plane. Fragment *translation* may be seen in all directions. In most cases an external manipulation alone is sufficient, but in cases with a craniocaudal component an additional fragment extension may be needed. *Rotated fragments* may be reduced with a percutaneously inserted guide-pin or Schanz screw which is used as a handle. *Joint steps* (e.g. acetabular) are most difficult and least likely to be treatable by minimal invasive means alone.

A good reduction is an important prerequisite for further fixation and a reduction in general should be attempted as early as possible to prevent complicating haematoma consolidation and soft tissue fibrosis

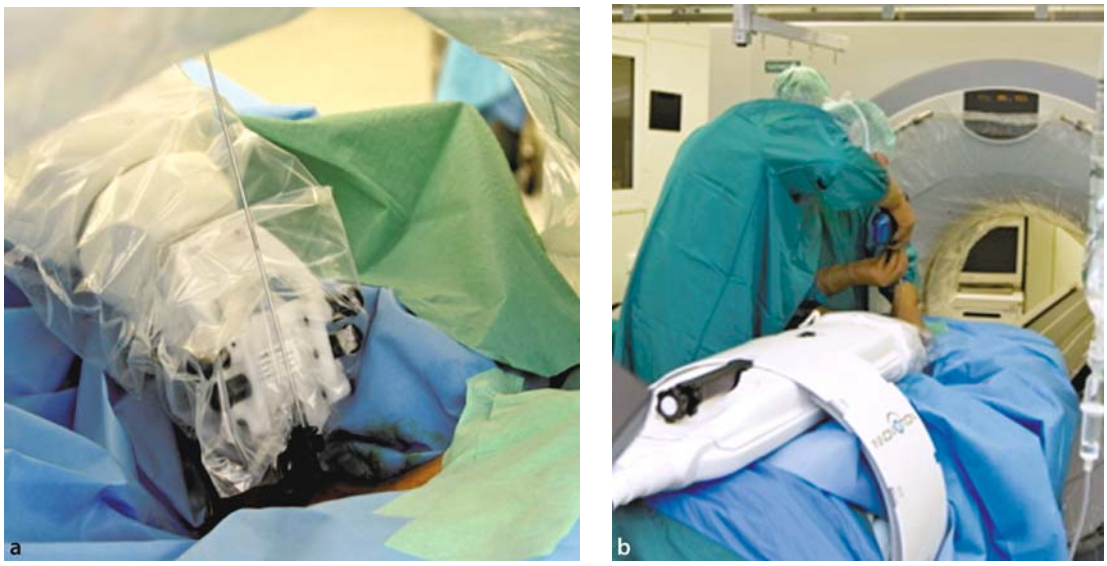

Fig. 15.15a,b Using robotic assistance (Innomotion, Innomedic, Herxheim, Germany); the operative device insertion is directed by the robotic system along a prior planned trajectory (**a**). The osteosynthesis is finally performed by the operator (**b**)

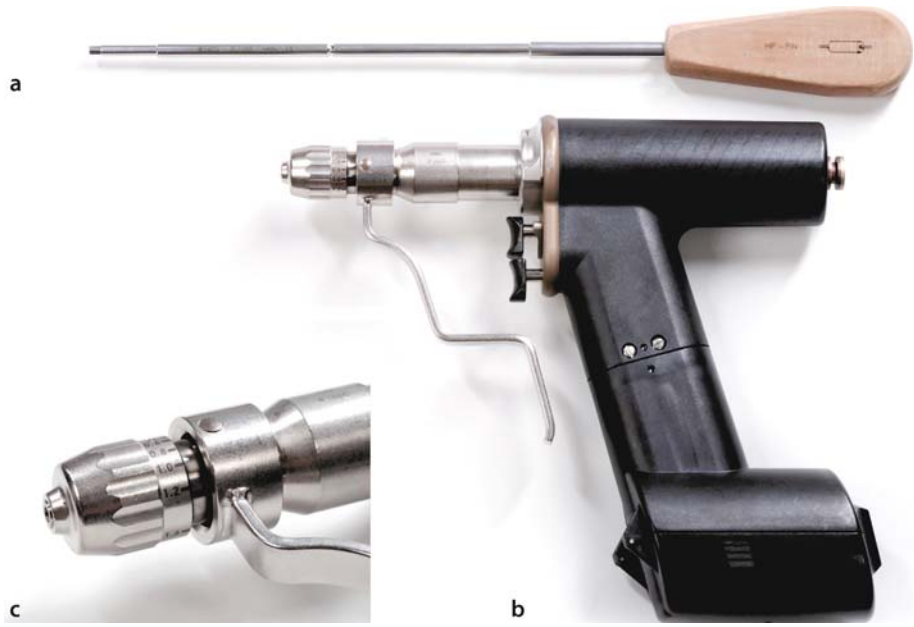

Fig. 15.16a–c Hand screwdriver used for screw drilling (**a**). Electric drill (**b**) with a drill chuck for placement of the 2.8-mm AO/ASIF guide wires (**c**)

which may occur within two days. Open, percutaneous and open or limited access types of reduction are feasible, each having its own limitations (Jacob et al. 1997, 2000a; Gross et al. 2004; Gansslen et al. 2006; Gay et al. 1992).

Open reduction (OR) or possibly *Limited* access reduction (LAR) needing a posterior surgical exposure has been complicated by wound problems. Regarding this a *closed* reduction (CR) as the least invasive method is preferred whenever possible. CR may be ap-

Fig. 15.17a,b A 2.8-mm AO/ASIF guide wire (Synthes, Solothurn, Switzerland) which is both rigid and sharp (**a**). Enlarged guide wire tip (**b**)

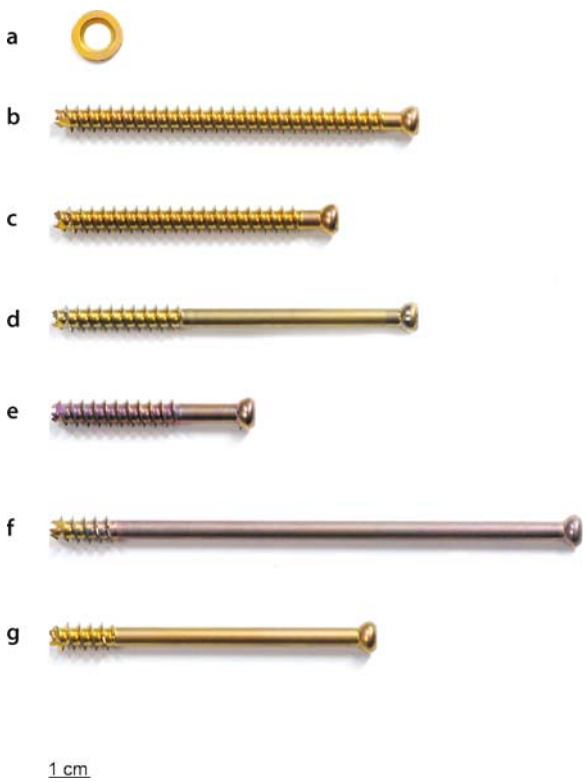

Fig. 15.18a–g Washer for use with self-cutting self-tapping AO/ASIF 7.3-mm set and lag screws (Synthes, Solothurn, Switzerland) (**a**). Fully threaded 7.3-mm set screws (**b**,**c**). Partially threaded 7.3-mm lag screws with the threaded portion being 32 mm (**d**,**e**) or 16 mm (**f**,**g**)

plied by 1) gravity, 2) external manipulation and 3) extension, depending on type and degree of dislocation, fracture age, involvement of joint surfaces and/or adjacent (e.g. neural) structures. CR outcome is usually evaluated by control imaging.

Using *percutaneous* reduction (PR) handles, most often Schanz screws are percutaneously attached to the fragments, which are than manipulated through the inserted devices. Examples are seen in the:

1. Application of a pelvic clamp in cases with pelvic haemorrhage to close a gap in the posterior pelvic ring, reducing the internal pelvic volume and assisting spontaneous tamponade.
2. Schanz screws used in the pelvic girdle for force transmission safeguarding neurovascular structures. These are often inserted into the anterior superior iliac spine or the iliac crest, whereas screw insertion into deeper structures may necessitate image guidance.
3. The use of external fixators allow precise movements and in addition the ability to retain the achieved osseous reduction (Kellam 1989).

15.3.3.3 Minimally-Invasive Percutaneous Therapy

The fixation methods should be image-guided in cases where a planned and image based linear trajectory is to be reproduced as precisely as possible, to allow exact placement of compression and positioning screws. The linear trajectory is planned by the interventionalist according mainly to the individual fracture pattern, disregarding anything like surgical access, anatomy or dissection plans. In a targeting step a guide wire is placed and within a fixation step the active element, mostly a cannulated screw, is slid over the guide wire through the interjacent tissues (crossing, e.g. skin, fat, fascia and muscles). The following indications for minimally-invasive percutaneous therapy of pelvic injuries are given according to the literature and our own experience.

Superior Pubic Ramus Fracture

The superior pubic ramus screw, described in 1995, can be used in cases with non-displaced and non-comminuted fractures of the anterior acetabular pillar or the midportion of the superior pubic ramus (Routt et al. 1995a). It can replace an anterior reconstruction plate applied either through a formal or reduced ilioinguinal approach. It may be introduced in an antegrade (craniodorsal to caudoventral) fashion or in the retrograde direction with the insertion point near the pubic symphysis. The antegrade access requires a high targeting precision as it uses a long guiding trajectory while the retrograde approach may be made impossible through interference with the genitals. The cannulated screws used (7.3-mm) are big, providing a firm fixation, but may therefore interfere with the narrow isthmic portion above and in front of the hip joint. Indication can be seen in stabilization of the anterior compartment of an unstable pelvic ring fracture. For that a straight and wide trajectory for the passage of the screw, distant from the hip joint, has to be found, as seen in cases with small primary displacement or a good primary reduction (Routt et al. 1995a).

Sacrum, Ilium and Ilio-sacral Joint

Ilio-sacral screws inserted from the lateral ilium, crossing the sacroiliac joint, reaching into the first sacral vertebral body, are broadly accepted for internal fixation of posterior pelvic ring and sacroiliac joint disruptions and sacral fractures (Fig. 15.19) (Nelson and Duwelius 1991; Routt et al. 1995b; Simonian et al. 1994b). Techniques for ilio-sacral screw insertion using fluoroscopy, CT, or even direct visual guidance have been described. Screws may be inserted with the patient in the supine, prone, or lateral position (Routt et al. 1995b; Ebraheim et al. 1987; Matta and Saucedo 1989). At our institution we usually place and immobilize the patient on the side contralateral to the injury for a good reduction by gravity and an appropriate target path. This may necessitate two consecutive placements in cases with bilateral pathologies. In contrast supine and prone positions both offer bilateral access. However fixation in a supine position may be limited as the oblique trajectory may interfere with the OR-table and draping as well as the scanner gantry. Prone placement may be associated with problems of mechanical ventilation and rotation of the iliac wings if prior anterior fixation is not performed yet. Ilio-sacral screws are biomechanically at least equal to common sacral bars and open or local plating (Pohlemann et al. 1993), and with double ilio-sacral screw fixation the strongest fixation of posterior pelvic ring disruptions is achieved (Yinger et al. 2003). Indications are the stabilization of the posterior component of unstable pelvic ring fractures, with either a small primary displacement or a good reduction achieved. For the treatment of comminuted fractures affecting the neural foramina or the spinal canal, set screws should be used either alone, or after an initial controlled compression using lag screws. Position and complication control in such cases may be performed intraoperatively either visually by CT or less commonly functionally by somatosensory evoked potentials (Moed et al. 1998). A few reports exist about the use of ilio-sacral screws in SI-joint arthritis and even metastatic bone destruction (Ebraheim and Biyani 2003) as well as in cases with postpartum pelvic pain and sacral non-union (van den Bosch et al. 2002; Huegli et al. 2003). These indications have to be considered experimental.

Acetabulum

In 1992 computed tomography was already used to guide the percutaneous placement of 6.5-mm cannulated screws (Gay et al. 1992). Starr et al. (1998, 2001) guided the placement of percutaneous screws in cases with non-displaced or minimally displaced acetabular fractures by fluoroscopy. This may also be used in terms of a supplemental fixation when combined with an open reduction and internal fixation of complex acetabular fractures. In cases of “simple” acetabular fractures lacking relevant steps or comminution the acetabular roof screw alone may close the fracture gap and restore mechanical stability. We usually apply two screws, one adjacent to the joint and another a little more cranially. As the trajectory is dictated by the fracture course, sometimes a limited access to pull aside vital structures like the femoral nerve may be needed (Gross et al. 2004). Unlike others, we commonly use an anterior approach, as in a posterior access the sciatic nerve often disables the optimal screw trajectory (Jacob et al. 2000a). For the decision to treat percutaneously an acetabular fracture by osteosynthe-

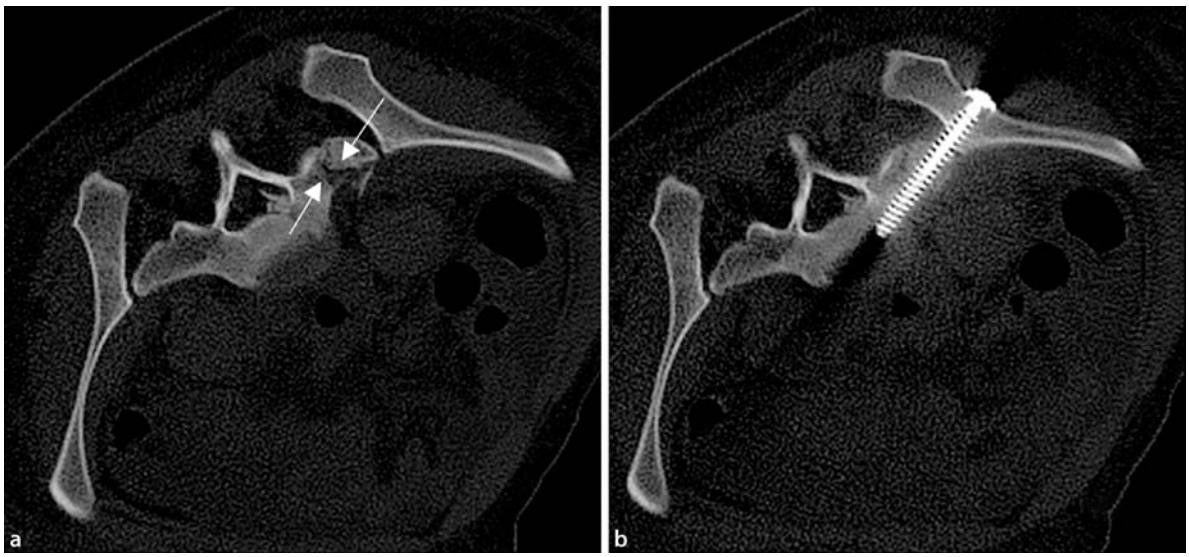

Fig. 15.19 Fracture of the right lateral mass of the sacral bone (*arrows*), with a bony fragment in the sacral canal (**a**). Therefore a fully threaded set screw is inserted for fixation, with adequate postoperative fracture adaptation (**b**)

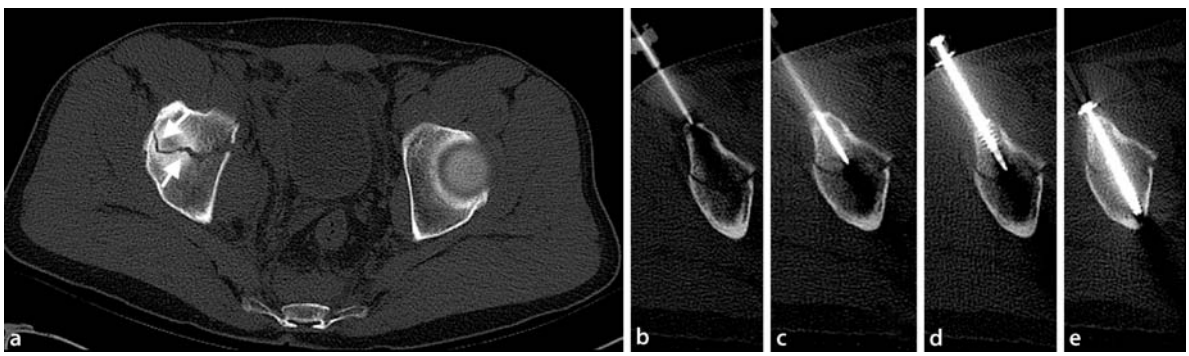

Fig. 15.20 Fracture of the right acetabulum (*arrows*) (**a**). A guide wire is inserted under CT-fluoroscopy guidance (**b**,**c**). Over the guide wire a lag screw is then inserted to reduce the fracture, with the threaded screw part lying completely on the far side of the fracture

sis (Fig. 15.20), we apply the following criteria (Gay et al. 1992; Gross et al. 2004; Jacob et al. 2000a):

1. Two or very few fragments of the load bearing acetabulum portion.
2. The far fragment needs to be big enough to host the threaded portion of the inserted lag screw.
3. Intraarticular fragments not present.
4. At the most a very small articular step-off or impression is present.

In selected cases variant approaches, like a "bottom-up" screw in transverse fractures of the posterior acetabular pillar or an iliac wing screw to close a gaping iliac crest, may be applied. The paths are chosen at the discretion of the operator and according to the situation at hand. The reduction and fixation methods outlined above can of course well be used in combined approaches:

1. Open or limited access reduction and internal fixation *(ORIF/LARIF)* as a standard or less invasive surgery.
2. Open or limited access reduction and percutaneous fixation *(ORPF/LARPF)* if percutaneous fixation is possible after open reduction or an open release of neural compression combined with percutaneous fixation is wanted.
3. Closed or percutaneous reduction combined with percutaneous fixation *(CRPF/PRPF)* is a standard

minimally invasive technique in non-displaced or externally reducible fractures.
4. Closed or percutaneous reduction and limited access fixation (CRLAF/PRLAF) may be used for guided insertion of an implant in cases with a limited surgical access due to vital structures disabling the optimal trajectory.

15.3.3.4 Follow-up

Patients with surgically treated fractures of the pelvis and acetabulum at our institution undergo immediate postoperative CT control (Müller et al. 1991; Jacob et al. 1997). Further follow up imaging should be performed according to the individual clinical symptoms, most often with conventional radiographies. Within clinical studies, e.g. CT, controls were obtained up to 1 year after the operation (Jacob et al. 1997).

15.3.4 Results

The following quality criteria are presented according to the literature and our own experience. If these criteria are fulfilled a decent morphological and clinical result as well as a minimum of complications can be expected. Regarding clinical criteria:

1. Good indication adapted to the individual situation
2. Infection rate $< 1\%$
3. Pain relief
4. Function
5. Rehabilitation and return to work

should be achieved and quality assured.

Regarding imaging criteria we assess by CT:

1. Screws should lie as close as possible perpendicular to the fracture gap.
2. The thread of lag screws should completely lie in the distant fragment.
3. There should be no additional compression when compared with the preoperative images using set screws.
4. In posterior ring fractures, the maximum offset should be < 10 mm.
5. Superior pubic ramus screws should splint both fragments centrally in the marrow canal through a sufficiently long distance.
6. Residual gaps in the articular surface of the hip joint should be $\leqslant 3$ mm, steps $\leqslant 1$ mm.
7. No hardware perforation into the hip joint itself should be visible.

Table 15.2 provides an overview of published results regarding ilio-sacral screw fixation. With 85–100% of the screws being positioned adequately, the results are well acceptable. In essence, for acetabular fractures excellent results have been published for 2D fluoroscopy guidance by Starr et al. (1998, 2001). Very precise (above 90% adequate positioning) results have been obtained for CT guidance by several groups for ilio-sacral as well as acetabular screw fixation (Jacob et al. 1997, 2000a). Excellent results have been reported for both two-dimensional (2D) fluoroscopy and CT-based navigation systems (Jacob et al. 1997; Peng et al. 2006).

15.3.5 Complications

Considering the quality criteria mentioned above, and with appropriate procedure experience, the complication rate is extremely low with CT-guidance and/or navigation. According to the literature, complications of ilio-sacral screw usage include fixation failures, misplaced screws, nerve injuries, infections, and poor posterior pelvic reduction, among others (Routt et al. 1995b; Keating et al. 1999). In reports on 2D-fluoroscopy guidance in type B fractures up to 8% (7/88) of all patients and 19% (6/31) of the subgroup with a screw into the second sacral body exhibited neurological complaints and needed re-operation in ilio-sacral screw fixation, making the latter a potential risk factor. In addition, 7% (15/220) malpositioned screws were detected in all patients who underwent postoperative CT and even 44% (4/9) in the subgroup with neurological complaints (van den Bosch et al. 2002). Although this is in contrast to better results reported earlier, it nevertheless emphasizes that patients with malpositioned screws are at higher risk to develop iatrogenic neurological injury. Keating et al. (1999) reported unusually high rates of pulmonary embolism, deep infection, late loss of reduction and pain within a series with 58% (22/38) of the patients undergoing ORIF and not CRPF.

Table 15.2 Synopsis of literature on ilio-sacral screw fixation

Authors	Patients (n)	Screws (n)	Implant	Guidance method	Adequate positioning	Malpositioned screws	Complications
van den Bosch et al. (2002)	88	285	7.3 mm cannulated screws	2-D fluoroscopy	93%	– 7% (15/220) @ CT – 44% (4/9) in pts with neurologic complaints	– Neurologic complications in 8% (7/88 pts) necessitating re-operation. – 19% (6/31 pts) with screw in second sacral body had neurologic complications
Peng et al. (2006)	18	n. k.	Cannulated screws	Single-plane vs. biplane 2-D fluoroscopy	100%	0% @ radiography	– 5% (1/18) superficial wound infection
Arand et al. (2004)	10	10	22 cannulated screws – 11: 7.5 mm – 11: 6.5mm	2D-fluoroscopy based navigation	95%	5% (1/22) @ CT due to bending of guidewire	n. k.
Stöckle et al. (2004)	28	28	7.3 mm cannulated screws	2D-fluoroscopy based navigation	96%	(4%) 1/28 @ CT	1 malreduction of the posterior pelvic ring (4%)
Grützner et al. (2002)	7	7	7.3 mm cannulated screws	Optoelectronic navigation	86%	(14%) 2/14 @ CT	None
Jacob et al. (1997)	13	27	7 mm cannulated screws	CT-navigation	93%	(7%) 2/27	– 8% (1/13) pulmonary embolism – 8% (1/13) superficial wound infection – 8% (1/13) broken screw after 1 year
Keating et al. (1999)	38	85	Cannulated screws	2D-fluoroscopy	87%	13% (5/38) pts @ radiography	Early Complications: – 13% (5/38) pulmonary embolism – 14% (3/22) deep infection in pts with ORIF, – 0% (0/16) with CRPF¨ Malunions: – 44% (15/34) malunions – 57% (4/7) malunions in pts without anterior fixation Late Complications: – 26% (10/38) ‘gradual loss of reduction’ @ 2 mos – 85% (22/26) troublesome pain

Summary

Minimally-invasive percutaneous screw fixation of the pelvic ring in combination with closed, minimal-access or open reduction can be safe and successfully applied to a variety of sacral, iliac and pubic fractures and combinations thereof. The placement of sacroiliac and superior pubic ramus screws are the most widely used examples of this technique. Treatment of acetabular fractures is also well feasible, with the restriction that a precise reduction of joint surfaces has to be achieved before percutaneous fixation is attempted to reduce the risk of developing secondary osteoarthritis. A critical and rational interdisciplinary selection of the best treatment modality for every patient is of extraordinary importance and may often be the most difficult part within the treatment process. An excellent quality of pre-and intra-operative imaging, image-guidance, navigation or robotic-assistance is crucial for a good outcome.

Key Points

- Closed reduction and percutaneous osteosynthesis of the pelvic ring under image guidance is well feasible.
- Closed reduction and percutaneous osteosynthesis of the acetabulum is well feasible in selected cases.
- Radiologists performing percutaneous osteosynthesis of the pelvis need to know the capabilities and limitations of other open and minimal invasive operation techniques.
- A close cooperation between orthopedic surgeon and interventional radiologist is mandatory.

References

Arand M, Kinzl L, Gebhard F (2004) Computer-guidance in percutaneous screw stabilization of the iliosacral joint. Clin Orthop Relat Res 422:201–207

Ben-Menachem Y, Coldwell DM, Young JW, Burgess AR (1991) Hemorrhage associated with pelvic fractures: causes, diagnosis, and emergent management. AJR Am J Roentgenol 157:1005–1014

Bosch EW van den, Zwienen CM van, Vugt AB van (2002) Fluoroscopic positioning of sacroiliac screws in 88 patients. J Trauma 53:44–48

Cleary K, Melzer A, Watson V, Kronreif G, Stoianovici D (2006) Interventional robotic systems: applications and technology state-of-the-art. Minim Invas Ther Allied Technol 15:101–113

Ebraheim NA, Biyani A (2003) Percutaneous computed tomographic stabilization of the pathologic sacroiliac joint. Clinical Orthop Relat Res 252–255

Ebraheim NA, Rusin JJ, Coombs RJ, Jackson WT, Holiday B (1987) Percutaneous computed-tomography-stabilization of pelvic fractures: preliminary report. J Orthop Trauma 1:197–204

Falchi M, Rollandi GA (2004) CT of pelvic fractures. Eur J Radiol 50:96–105

Gansslen A, Pohlemann T, Paul C, Lobenhoffer P, Tscherne H (1996) Epidemiology of pelvic ring injuries. Injury 27(Suppl 1):S-A13–20

Gansslen A, Hufner T, Krettek C (2006) Percutaneous iliosacral screw fixation of unstable pelvic injuries by conventional fluoroscopy. Oper Orthop Traumatol 18:225–244

Gay SB, Sistrom C, Wang GJ, Kahler DA, Boman T, McHugh N, Goitz HT (1992) Percutaneous screw fixation of acetabular fractures with CT guidance: preliminary results of a new technique. AJR Am J Roentgenol 158:819–822

Glauser D, Fankhauser H, Epitaux M, Hefti JL, Jaccottet A (1995) Neurosurgical robot Minerva: first results and current developments. J Image Guided Surg 1:266–272

Gross T, Jacob AL, Messmer P, Regazzoni P, Steinbrich W, Huegli RW (2004) Transverse acetabular fracture: hybrid minimal access and percutaneous CT navigated fixation. AJR Am J Roentgenol 183:1000–1002

Grützner PA, Rose E, Vock B, Holz F, Nolte LP, Wentzensen A (2002). Computerassisted screw osteosynthesis of the posterior pelvic ring. Initial experiences with an image reconstruction based optoelectronic navigation system. Unfallchirurgie 105:254–260 [German]

Guillamondegui OD, Pryor JP, Gracias VH, Gupta R, Reilly PM, Schwab CW (2002) Pelvic radiography in blunt trauma resuscitation: a diminishing role. J Trauma 53:1043–1047

Huegli RW, Messmer P, Jacob AL, Regazzoni P, Styger S, Gross T (2003) Delayed union of a sacral fracture: percutaneous navigated autologous cancellous bone grafting and screw fixation. Cardiovasc Intervent Radiol 26:502–505

Hunter JC, Brandser EA, Tran KA (1997) Pelvic and acetabular trauma. Radiol Clin North Am 35:559–590

Isler B, Ganz R (1996) Classification of pelvic ring injuries. Injury 27(Suppl 1):S-A3–12

Jacob AL, Messmer P, Stock KW, Suhm N, Baumann B, Regazzoni P, Steinbrich W (1997) Posterior pelvic ring fractures: closed reduction and percutaneous CT guided sacroiliac screw fixation. Cardiovasc Intervent Radiol 20:285–294

Jacob AL, Suhm N, Kaim A, Regazzoni P, Steinbrich W, Messmer P (2000a). Coronal acetabular fractures: the anterior approach in computed tomography-navigated minimally invasive percutaneous fixation. Cardiovasc Intervent Radiol 23:327–331

Jacob AL, Kaim A, Baumann B, Suhm N, Messmer P (2000b) A simple device for continuous leg extension during CT-guided interventions. 174:1687–1688

Jacob AL, Regazzoni P, Steinbrich W, Messmer P (2000c) The multifunctional therapy room of the future: image guidance, interdisciplinarity, integration and impact on patient pathways. Eur Radiol 10:1763–1769

Judet R, Judet J, Letournel E (1964) Fracture of the acetabulum: classification and surgical approaches for open reduction. Preliminary report. J Bone Joint Surg 46:1615–1646

Keating JF, Werier J, Blachut P, Broekhuyse H, Meek RN, O'Brien PJ (1999) Early fixation of the vertically unstable

pelvis: the role of iliosacral screw fixation of the posterior lesion. J Orthop Trauma 13:107–113
Kellam JF (1989) The role of external fixation in pelvic disruptions. Clin Orthop Relat Res 66–82
Kellam JF, McMurtry RY, Paley D, Tile M (1987) The unstable pelvic fracture. Operative treatment. Orthop Clin North Am 18:25–41
Letournel E (1993) The treatment of acetabular fractures through the ilioinguinal approach. Clin Orthop Relat Res 62–76
Matta JM, Saucedo T (1989) Internal fixation of pelvic ring fractures. Clin Orthop Relat Res 83–97
Moed BR, Ahmad BK, Craig JG, Jacobson GP, Anders MJ (1998) Intraoperative monitoring with stimulus-evoked electromyography during placement of iliosacral screws. An initial clinical study. J Bone Joint Surg 80:537–546
Müller ME, Perren SM, Allgöwer M (1991) Manual of internal fixation: techniques recommended by the AO-ASIF Group, 3rd edn, expanded and completely revised. Arbeitsgemeinschaft für Osteosynthesefragen. Springer, Berlin Heidelberg New York
Nelson DW, Duwelius PJ (1991) CT-guided fixation of sacral fractures and sacroiliac joint disruptions. Radiology 180:527–532
Peng KT, Huang KC, Chen MC, Li YY, Hsu RW (2006) Percutaneous placement of iliosacral screws for unstable pelvic ring injuries: comparison between one and two C-arm fluoroscopic techniques. Trauma 60:602–608
Pohlemann T, Angst M, Schneider E, Ganz R, Tscherne H (1993) Fixation of transforaminal sacrum fractures: a biomechanical study. J Orthop Trauma 7:107–117
Pohlemann T, Bosch U, Gansslen A, Tscherne H (1994) The Hannover experience in management of pelvic fractures. Clin Orthop Relat Res 305:69–80
Poole GV, Ward EF (1994) Causes of mortality in patients with pelvic fractures. Orthopedics 17:691–696
Qureshi AA, Archdeacon MT, Jenkins MA, Infante A, DiPasquale T, Bolhofner BR (2004) Infrapectineal plating for acetabular fractures: a technical adjunct to internal fixation. J Orthop Trauma 18:175–178
Routt ML Jr, Kregor PJ, Simonian PT, Mayo K (1995a) Early results of percutaneous iliosacral screws placed with the patient in the supine position. J Orthop Trauma 9:207–214
Routt ML Jr, Simonian PT, Grujic L (1995b) The retrograde medullary superior pubic ramus screw for the treatment of anterior pelvic ring disruptions: a new technique. J Orthop Trauma 9:35–44
Schrader P (2005) Technique evaluation for orthopedic use of Robodoc. Z Orthop Ihre Grenzgeb 143:329–336
Senst W, Bida B (2000) Expert assessment of pelvic injuries. Zentralbl Chirurg 125:737–743
Siebert W, Mai S, Kober R, Heeckt PF (2002) Technique and first clinical results of robot-assisted total knee replacement. Knee 9:173–180
Simonian PT, Routt ML Jr, Harrington RM, Mayo KA, Tencer AF (1994a) Biomechanical simulation of the anteroposterior compression injury of the pelvis. An understanding of instability and fixation. Clin Orthop Relat Res 245–256
Simonian PT, Routt ML Jr, Harrington RM, Tencer AF (1994b) Internal fixation of the unstable anterior pelvic ring: a biomechanical comparison of standard plating techniques and the retrograde medullary superior pubic ramus screw. J Orthop Trauma 8:476–482
Starr AJ, Reinert CM, Jones AL (1998) Percutaneous fixation of the columns of the acetabulum: a new technique. J Orthop Trauma 12:51–58
Starr AJ, Jones AL, Reinert CM, Borer DS (2001) Preliminary results and complications following limited open reduction and percutaneous screw fixation of displaced fractures of the acetabulum. Injury 32(Suppl 1):SA45–50
Stöckle U, Krettek C, Pohlemann T, Messmer P (2004) Clinical applications – pelvis. Injury 35(Suppl 1):S-A46–56
Tile M (1996) Acute pelvic fractures: I. Causation and classification. J Am Acad Orthop Surg 4:143–151
Tile M (2003) Fractures of the pelvis and acetabulum, 3rd edn. Williams and Wilkins, Baltimore
Wedegartner U, Gatzka C, Rueger JM, Adam G (2003) Multislice CT (MSCT) in the detection and classification of pelvic and acetabular fractures. RoFo 175:105–111
Yinger K, Scalise J, Olson SA, Bay BK, Finkemeier CG (2003) Biomechanical comparison of posterior pelvic ring fixation. J Orthop Trauma 17:481–487

15.4 CT- and MR-Guided Arthrography

Gabriele A. Krombach

15.4.1 Introduction

Computed tomography (CT)- and magnetic resonance (MR)-arthrography are nowadays routinely used for evaluation of many joint disorders. MRI offers an inherent good contrast between skeletal muscle, cartilage and ligaments. However, the subtle anomalies searched for in chronic joint disorders are difficult to assess on conventional MR images. It was soon recognized that the presence of intra-articular fluid improves visualization of the complex anatomical structures and subtle injuries, owing to the distension of the joint capsule. This finding has been termed the “arthrogram effect”. Since intra-articular fluid is seldom present in subacute or chronic injury, direct injection of fluid has been introduced into clinical routine imaging to increase the sensitivity of the MR study in patients, in whom intra-articular pathologies are suspected. In order to allow for differentiation between leakage of fluid from the articular space and bursal effusion, diluted contrast medium is used instead of pure saline solution, which does not allow for this differentiation.

On CT skeletal muscle has a density of approximately 50 Hounsfield units (HU), while cartilage, ligaments and menisci have a slightly higher density,

ranging from 79 to 90 HU. These small differences do not allow differentiation of these structures from each other. In CT-arthrography distension of the joint capsule as well as enabling delineation of ligaments and cartilage due to enhanced contrast is obtained from injection of diluted iodinated contrast medium.

15.4.2 Indications

In general, CT- or MR-arthrography can be performed in any joint in which conventional arthrography is possible:

- In the shoulder arthrography is commonly performed if a rotator cuff tear is suspected and in order to asses shoulder instability or injuries of the glenoid labrum. In the elbow arthrography is carried out if collateral ligament tears are suspected. Arthrography of the wrist is applied for evaluation of the ligaments and triangular fibrocartilage.
- In the hip arthrography can detect and differentiate CAM and PINCER femoroacetabular impingement.
- Arthrography of the knee is indicated if a residual or recurrent meniscal tear is suspected following meniscal surgery.
- In the ankle arthrography can be used in patients in whom ligamentous damage is suspected but not assessable with conventional imaging.
- In all joints direct arthrography can also be helpful in the assessment of loose bodies and cartilage lesions.

Arthrography is contraindicated if bacterial arthritis is suspected or if the overlying soft tissue is infected. Some authors refuse to carry out arthrographies if conventional MR imaging has not been obtained.

Written informed consent must be obtained at minimum 24 h prior to the intervention and coagulation disorders must be excluded.

15.4.3 Material

Usually a standard 20 G puncture needle with an end-hole (7–12 cm spinal needle for shoulder, hip or knee, shorter needle for wrist and ankle) is used. In addition, a connecting tube, a stop cock and a 10 or 20-ml syringe are required (Fig. 15.21). If double contrast is used, a bacterial filter is connected to the connecting tube before the injection of air is started.

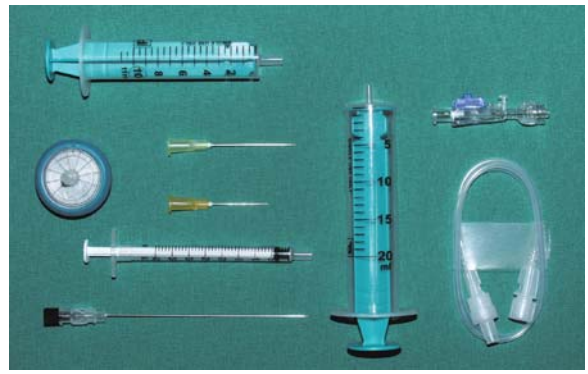

Fig. 15.21 Self assembled sterile set for arthrography, containing syringes for local anesthesia (10-ml syringe), mixture of contrast medium (20 ml) and dosing of small amounts of MR contrast medium (1 ml), a connecting tube, a stopcock, a bacterial filter (used if air is injected), a 20 G spinal needle, a 22 G needle for local anesthesia and an 18 G needle for filling the syringe with local anesthesia

15.4.3.1 Contrast Medium

CT-Arthrography

For big joints, such as the shoulder and hip, either the double contrast or the monocontrast technique might be applied, while in small joints (wrist, elbow) only the monocontrast technique is possible. In order to obtain double contrast, the intra-artricular injection of 2–3 ml contrast material is followed by injecting 12–15 ml air. Usually a contrast medium containing 240–300 mg of iodine per ml is applied. Nonionic iso-osmolar contrast material is preferred, since the osmotic effect and consecutive dilution of the contrast material as well as resorption from the articular space are less pronounced compared to hyperosmolar contrast medium. For the monocontrast technique, 10 ml contrast medium can be diluted with 5 ml saline solution and 5 ml lidocaine 1%.

MR-Arthrography

Monocontrast is used for all joints, since intra-articular air would cause susceptibility artifacts arising from the fluid air interface. The signal intensity, obtained from

the injected diluted contrast medium, depends on the concentration of gadolinium and the field strength. At 1.5 T, concentrations ranging from 1:200 to 1:250 render optimal signal intensity on T1-weighted images. Several ways to obtain this concentration are possible. For example, 0.8 ml gadopentetate dimeglumine can be added to 100 ml of saline solution. Next 10 ml of this solution can be mixed with 5 ml of iodinated contrast medium and 5 ml of lidocaine 1%. The resulting solution has a dilution ratio of 1 : 250 gadolinium. In Europe and Australia a precast preparation for intraarticular injection, containing 0.0025 mmol/ml Gd-DOTA (Gadoterate meglumine) can be purchased (Artirem, Guerbet). The concentration of gadolinium of this solution is less than 1 : 200; however, it does not contain an anesthetic or iodinated contrast medium.

15.4.4 Technique

15.4.4.1 Shoulder

Many investigators still prefer fluoroscopic guidance for needle placement (Fig. 15.22). However, arthrography in general can be performed using solely MR- or CT-guidance. A clear advantage of applying only one modality for puncture and imaging is easier patient scheduling and workflow. For MR-guidance, real-time imaging can be applied (Fig. 15.23). In this case, advancing the needle into the joint space is directly visible. This technique usually allows accessing of the joint space fast and reliably. Furthermore, the joints can be punctured using the widely established approach of stepwise CT- or MR-guidance. In this case, an external marker is placed over the possible entry site on the patient's skin and a scan is obtained for planning the puncture. The target can then be chosen and the puncture path planned on the images. In the next step, the needle tip is placed on the selected entry point on the patient's skin and the angle of the needle adjusted according to the path obtained from the planning scan. Next the needle can be advanced stepwise and the respective position of the needle tip repeatedly controlled.

Regardless of which modality and technique has been chosen for the puncture, before arthrography of the shoulder is performed, anteroposterior radiographs in external and internal rotation of the shoulder should be obtained to assessing calcifications in the rotator cuff tendons. If calcifications have not been identified prior to CT-arthrography, they can be misinterpreted as leakage of contrast medium on the CT-images, suggestive of a tear. On MR-arthrography they are usually overlooked, owing to similar signal of tendons and calcifications (Zubler et al. 2007). Supine positioning of the patient with the shoulder in external rotation allows for best access to the joint via the anterior approach. The optimal entry point is located at the upper inner quadrant of the humeral head or at the junction of the middle and inferior thirds of the humeral head just lateral to the medial cortex (Fig. 15.22). After this entry point has been marked on the skin, the region is prepped and draped with sterile cover sheds, and local anesthesia is administered. Puncture and injection of contrast medium solution must be performed under sterile conditions. The needle can then be inserted. If fluoroscopy is used, the needle hub is centered over the tip of the needle on the images in order to ensure that the path is perpendicular to the fluoroscopic beam. If MR- or CT-guidance has been chosen the puncture is planned and performed as described above. The needle should be inserted and advanced together with the stylet, so that injury of the tissue is minimized and clotting of the needle avoided. However, it has to be kept in mind that the joint capsule is pain-sensitive and small amounts of local anesthesia might repeatedly be injected as the needle is advanced if the patient complains about pain. As soon as bone is reached, the needle can be pulled back slightly. Usually a test injection of 2 ml of local anesthetic confirms needle position in a compartment (low resistance) and further anesthetizes the joint. If joint effusion is present, the fluid should be aspirated. With injection, care must be taken to avoid air bubbles and fluid should be dripped into the hub of the needle so that a wet-to-wet connection can be performed with the prefilled connecting tube and the syringe. By this means, injecting air bubbles can be avoided. One can inject 2 ml of the contrast medium solution in order to verify intra-articular position of the needle. If the intra-articular position has been verified, either 12 ml of the respective contrast medium solution are injected for monocontrast, or air for CT-arthrography with double contrast. Arthrography should be performed within a time frame of 40 min after injection of the contrast medium solution. Otherwise resorption of con-

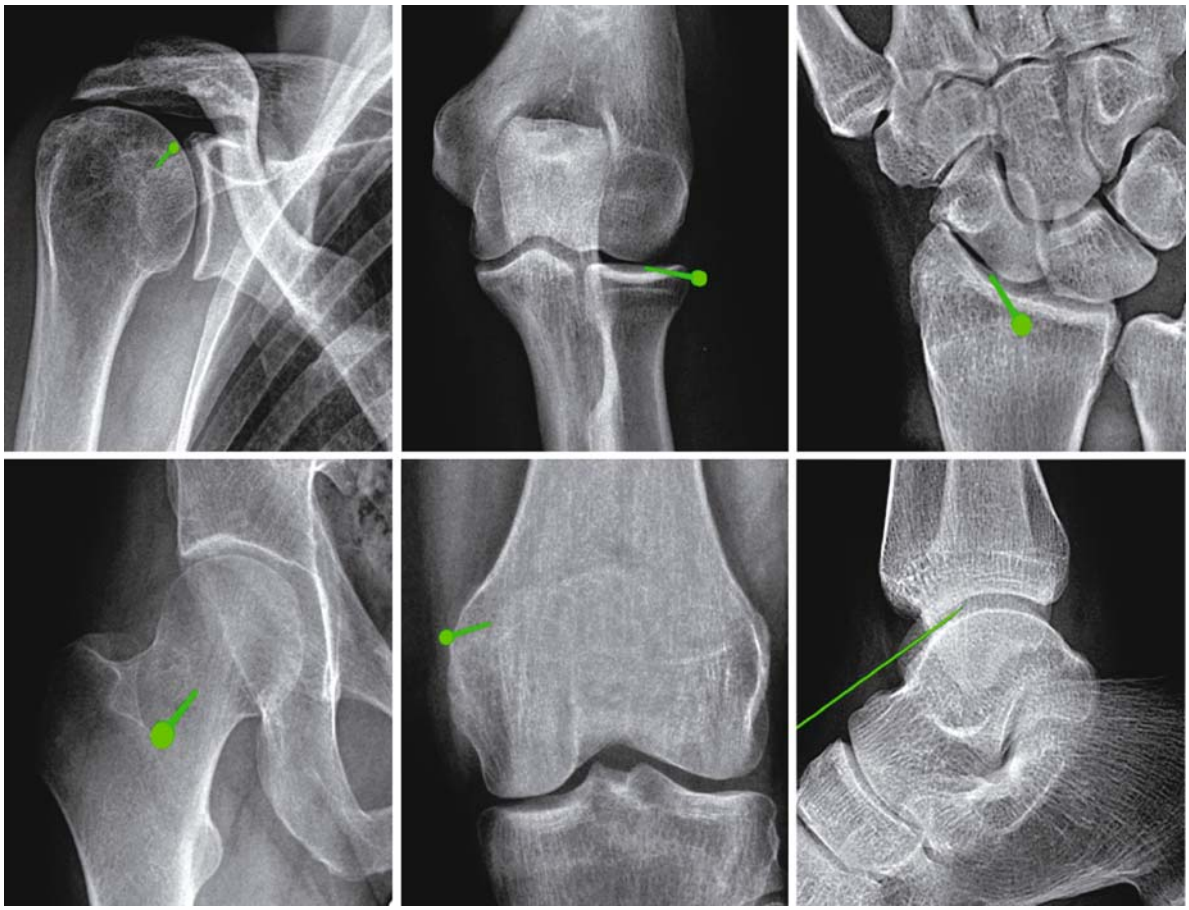

Fig. 15.22 Injection sites at the different joints for fluoroscopically guided puncture. With CT- and MR-guidance identical approaches should be used

trast medium and air will result in inadequate distension of the joint capsule and insufficient image quality.

The shoulder is imaged with the arm placed in neutral position. If the antero-inferior labrum must be assessed, sensitivity of arthrography can be further increased by imaging in abduction and external rotation (ABER position) of the shoulder. The ABER position is achieved by elevating the patient's arm, flexing the elbow and placing the patient's hand posterior to the contralateral aspect of the head.

In CT, thin axial slices are obtained and multiplanar reconstructions performed. In MR imaging preferably a 3D T1-weighted (gradient-echo) sequence with fat suppression should be obtained in an axial and paracoronal imaging plane, the later running perpendicular to the glenoid. A small field of view and a surface coil should be used for MR-arthrography in order to obtain images with high resolution and increased signal-to-noise ratio. If isovolumetric voxel are obtained, multiplanar reformations can be obtained.

15.4.4.2 Elbow

The patient is placed prone, the arm elevated and the elbow flexed. The joint can either be entered laterally over the radial head or posterolaterally between olegranon, humerus and radial head. The posterolateral approach has the advantage of avoiding the lateral collateral ligament complex on the puncture path. A total of up to 10 ml contrast medium solution can be injected into this joint. The ulnar and radial collateral ligaments are best visualized in a coronal plane tilted 20° posteriorly.

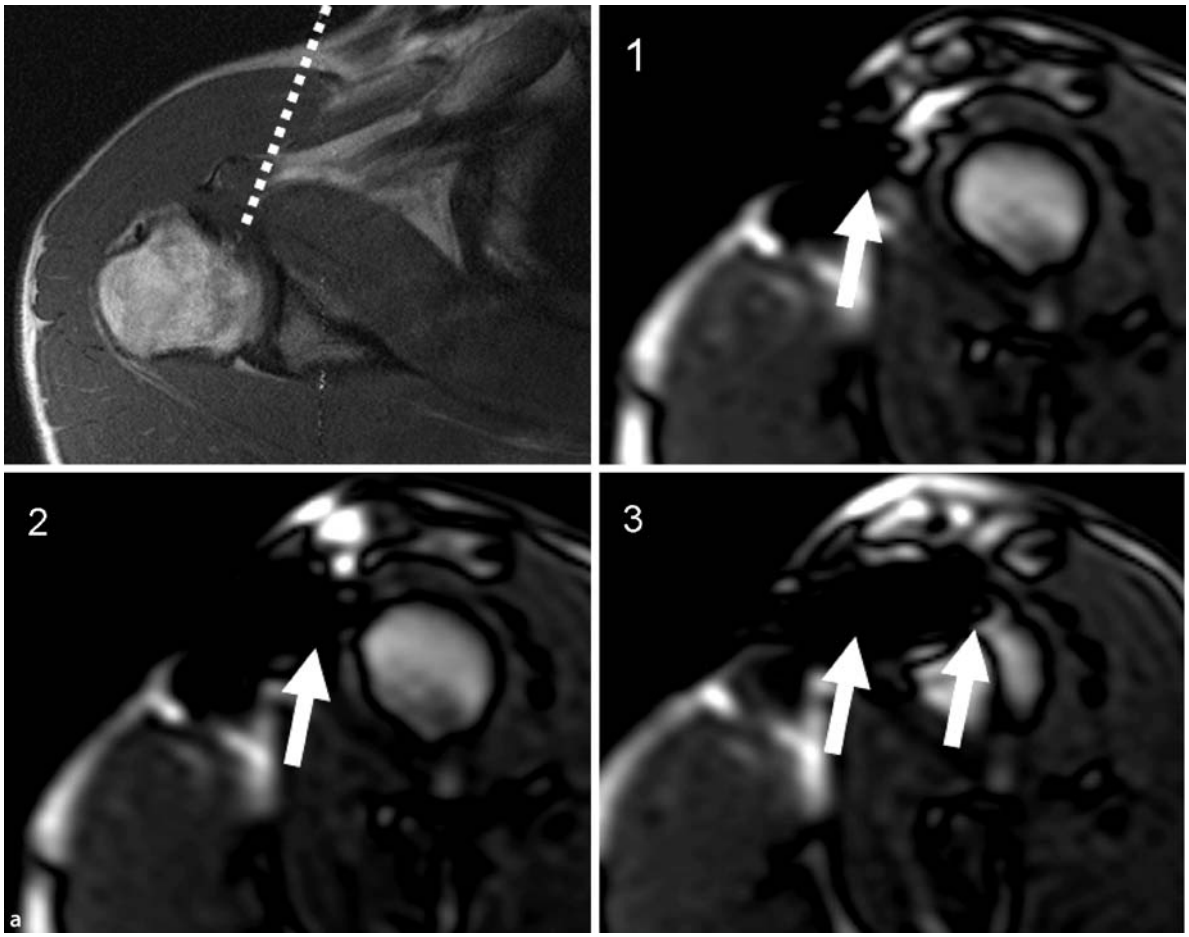

Fig. 15.23 (**a**) MR-guided arthrography. The puncture path can be planned on an axial slice (*top row left image, dotted line*). In the next step, a real-time sequence is planned in the course of the desired puncture path, so that insertion of the needle can be visualized and guided with these images (*1–3*, the *arrows* mark needle artifact)

15.4.4.3 Wrist

Arthrography of the wrist can be performed with single- (radiocarpal), double- (interarpal and radioulnar), or triple-compartment injection. The patient is in prone position, the arm elevated and the palm pointing downwards. The needle is introduced between the middle of the scaphoid and the radius for filling of the radiocarpal compartment. For carpal injection the needle is inserted between lunate, capitate, hamate and triquetrum or at the distal scapoid. For injection into the radioulnar joint space, the distal part of the ulnar head just lateral of the medial cortical bone is targeted. Approximately 3–5 ml of fluid can be in each of the three compartments. Coronal and axial images should be obtained. For assessment of the cartilage coronal and sagittal images should be obtained.

15.4.4.4 Hip

The patient is placed supine, a bolster placed under the knees and the leg positioned in internal rotation. The symptomatic side can be elevated to 10−15°. This position increases the distance from the puncture path to the neurovascular bundle, which than decreases the probability of infiltration of the femoral nerve. Anesthesia of

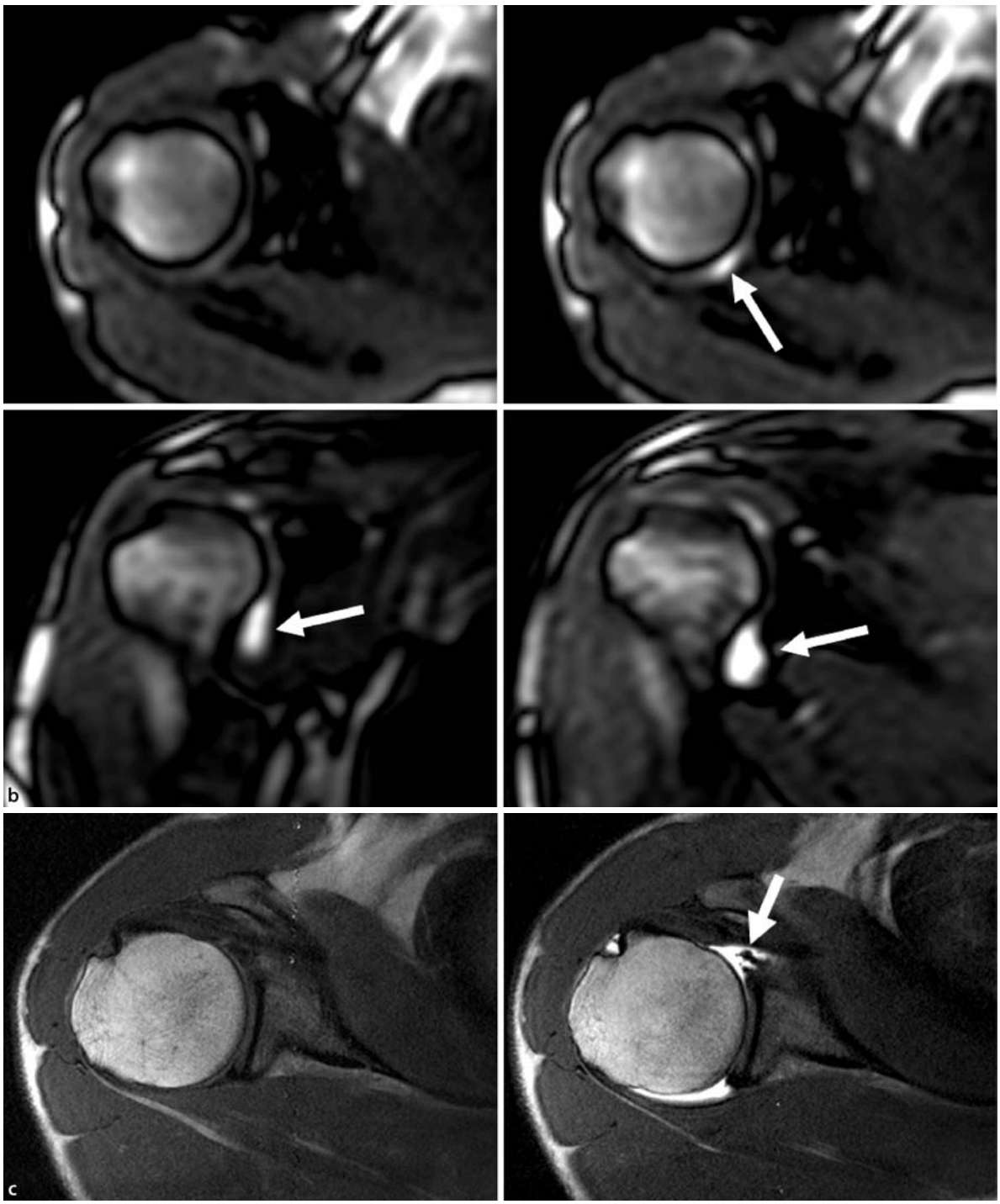

Fig. 15.23 (**b**) Injection of contrast medium doped solution, visualized on real-time true-FISP images. The increasing filling of the joint space is visible from *the top left to bottom right image* (*arrows*). (**c**) Axial true FISP prior (*left*) and after MR-guided injection of contrast solution into the articular space (*right*). The tear of the labrum can not be visualized on the conventional MR-image, but is clearly visible on MR-arthrograpy (*arrow*)

the femoral nerve can cause fall of the patient when trying to get up after the procedure. To maintain internal rotation of the hips, the feet may be taped together. Mainly either the superior lateral quadrant of the femoral head or the middle of the femoral neck are used to enter the joint. The imaging plane should be axial and coronal. If sports related labral tears are suspected oblique images, oriented parallel to the femoral neck on coronal images should be acquired. The anterosuperior labrum is best visualized in this imaging plane.

15.4.4.5 Knee

In supine position of the patient, the joint is accessed medially between patella and femur. The injection can safely be performed without fluoroscopy guidance. Axial and sagittal images should be acquired or reconstructed.

15.4.4.6 Ankle

The patient is in supine position and the X-ray tube angled laterally. The needle is introduced from anterior, medial to the extensor hallucis longus muscle and slightly tilted cranially. To avoid the dorsalis pedis artery, it should be palpated prior to needle placement. Approximately 6 ml fluid can be injected into this joint. Images should be acquired in the sagittal and coronal plane.

15.4.5 Results

15.4.5.1 Shoulder

For the diagnosis of full thickness tears of the rotator cuff, both sensitivity and specificity approach 100% for MR-arthrography. For partial tears the corresponding values are 80% and $>$ 95%, respectively (Waldt et al. 2007). Sensitivity of CT-arthrography is 73% for full thickness tears of the rotator cuff (Bachmann et al. 1998). The characteristic imaging finding for a full thickness tear is presence of extra-articular contrast medium. Partial tears fill with contrast medium.

Labral tears present as defects within the labrum that fill with contrast medium. Anatomical variants represent possible pitfalls in assessing labral integrity. A small normal labrum can be difficult to differentiate from a blunted, deficient labrum. At two locations, a sublabral sulcus separates the normal labrum from the interface of the articular cartilage: anterosuperior between the origins of the inferior and middle glenohumeral ligament and superior, at the junction of the labrum with the bicipital tendon. Sulci can increase in size with age and then fill with contrast medium. This finding can be misinterpreted for a labral tear. However, sensitivity for detecting labral tears was 96% for MR- and 76% for CT-arthrography and specificity 96% (MR-) and 92% (CT-arthrography) respectively (Blitzer et al. 2004). Lesions of the cartilage are more difficult to assess, due to the concave shape of the articular facet. In a recent study sensitivity for glenoidal cartilage lesions was 75% and specificity 63% on MR-arthrography (Guntern et al. 2003) and 80% and 94% on CT-arthrography (Lecouvet et al. 2007)

15.4.5.2 Elbow

Although detailed description of all pathologic findings is beyond the scope of this chapter, tears of the ulnar collateral ligament present as defects that fill with contrast medium. Complete rupture causes extravasation of the contrast medium into the surrounding soft tissue. For tears of the ulnar collateral ligament a comparative study using findings at surgery as the gold standard, found a sensitivity of 86% and a specificity of 100% for CT-arthrography (Timmerman et al. 1994). For MR-arthrography sensitivity is 86% for partial and 95% for complete tears of the ulnar collateral ligament and specificity for both lesion types 100% (Schwartz et al. 1995). Lesions of the radial collateral ligament are extremely rare.

Cartilage lesions present as indentations, filling with contrast medium. For detection of cartilage lesions, CT-arthrography had a sensitivity of 80% and MR-arthrography 78% in a study, conducted on cadaver specimen (Waldt et al. 2005). Specificity was 93% for CT- and 95% for MR-arthrography.

Loose bodies become visible as round to oval shaped hypointense or hypodense regions within the contrast medium filled joint space. Care has to be taken to not misinterpret injected air bubbles for loose bodies on MR-arthrography. Regarding the detection of

loose bodies, a sensitivity of 88% and 100% has been reported for MR- and CT-arthrography, respectively (Dubberley et al. 2005). Specificity was 20% for MR- and 70% for CT-arthrography and did not exceed that of plain film radiography (specificity 71%, sensitivity 84%). Synovial plicae may cause locking of the elbow joint. However, plicae are a common finding in the elbow and clinical correlation of such a finding is thus of utterly importance.

15.4.5.3 Wrist

A full tear of the triangular fibrocartilage becomes evident as presence of contrast medium in the distal radio-ulnar joint. Extrinsic ligament tears are not accessible on arthrography. In the interosseous ligaments, surface irregularity is a sign for partial tear. In the evaluation of CT-arthrography sensitivity and specificity of 94% and 86% have been found for detecting tears of the scapholunate ligament, 85% and 79% for detecting tears of the lunotriquetral ligament and 30% and 94% for diagnosing tears of the triangular fibrocartilage complex, compared to arthroscopy (Bille et al. 2007). In another study a direct comparison of MR imaging, CT- and MR-arthrography has been performed (Moser et al. 2007). Sensitivity and specificity were 59% and 70% (MR imaging), 95% and 96% (CT-arthrography), 68% and 87% (MR-arthrography) for tears of the scapholunate ligament, and 30% and 94% (MR imaging), 100% and 94% (CT-arthrography), 60% and 97% (MR-arthrography) for tears of the lunotriquetral ligament, 27% and 100% (MR imaging), 100% and 100% (CT-arthrography), 82% and 100% (MR-arthrography) for tears of the triangular fibrocartilage complex and 30% and 100% (MR imaging), 100% and 100% (CT-arthrography) and 40% and 100% (MR-arthrography) for cartilage abnormalities. In this study, partial tears of the ligaments were better visualized with CT-arthrography.

15.4.5.4 Hip

Femoro-acetabular impingement is a cause for labral tears and cartilage lesions. CAM and PINCER impingement can be differentiated. In PINCER acetabular overcoverage of the femur leads to restricted motion and consecutive labral tear. In CAM a nonspherical shape of the femur in combination with a reduced depth of the femoral waist lead to labral tears (Pfirrmann et al. 2006). For treatment the differentiation of cam and pincer is important, in addition to the diagnosis of a labral tear. Sensitivity and specificity of CT-arthrography compared to arthroscopy are reported to approach 97% and 87% for labral tears and 88% and 82% for acetabular cartilage lesions (Nishii et al. 2007). Sensitivity and specificity were found to be 92% and 100% respectively for detection of labral tears on MR-arthrography, compared to arthroscopy (Toomayan et al. 2006). The sensitivity and specificity in the diagnosis of cartilage lesions reach 79% and 77% (Schmid et al. 2003).

15.4.5.5 Knee

Recurrent meniscal tears might be difficult to differentiate from degenerative changes after partial resection of menisci. On direct arthrography tears fill with contrast medium, while degenerative changes and scars do not. In a recent study sensitivity and specificity of MR-arthrography were 90% and 78% and that of conventional MR imaging 86% and 67% (White et al. 2002). For CT-arthrography sensitivity and specificity have been reported to approach 100% and 78% for detection of meniscal tears (Mutschler et al. 2003). Arthrography has also been demonstrated being useful in the diagnosis of intra-articular bodies and cartilage lesions (Brossmann et al. 1996).

15.4.5.6 Ankle

MR-arthrography has a sensitivity of 71% and specificity of 96% for detection of ligament tears (second- and third degree sprains) (van Dijk et al. 1998). First degree sprains are not associated with a tear and cannot be diagnosed on MR-arthrography. In this instance a region of high signal intensity is visible within the ligament on T2-weighted images. Second degree sprains present as a contrast medium filled defect of the ligament and third degree sprains are characterized by leakage of the contrast medium into the periarticular space.

In a current study accuracy of MR-arthrography for detection of cartilage lesions in the talus/tibia/fibula

was 88%/88%/94% and for CT-arthrography 90%/94%/92% (Schmid et al. 2003).

15.4.6 Complications

Complications following direct arthrography are rare. The most feared complication is infection (septic arthritis) of the joint, which has an incidence of 0.003–0.01% (Schulte-Altedorneburg et al. 2003). The leading symptoms are increasing pain in the affected joint, especially when moving, and swelling and redness. Onset of symptoms is usually several days after the injection. This major complication must be immediately treated with antibiotics and eventually joint drainage, in order to avoid destruction of the cartilage. Hematoma or hemarthrosis is also possible as a sequel of arthrography, especially in patients with coagulopathy.

Summary

Direct arthrography extents the diagnostic capabilities of conventional imaging by far. It is the method of choice in patients with suspected partial tear of the rotator cuff, for the diagnosis of meniscal tears in the postoperative knee and for assessment of the labrum in the hip. In the other above mentioned indications, it increases the sensitivity and specificity of MR imaging, and enables surveying ligaments and cartilage in CT. In the hand of the experienced radiologist, complications are extremely rare. However, it turns a non-invasive examination into a mildly invasive procedure. Accordingly, the indication for direct arthrography has to be critically reviewed in each patient. In general, MR-arthrography should be preferred, if MR is available and contraindications for MR imaging are not present, in order to limit radiation exposure. Joint puncture with cross-sectional image guidance, particularly MR-guidance allows for a safe direct puncture of the joint and helps to reduce paravasation that might mimic pathology. Moreover, this technique permits online monitoring of intra-articular contrast injection, providing additional information.

Key Points

- Direct arthrography extends the diagnostic capabilities of CT and MR imaging.
- CT- and MR-guided joint puncture is safely feasible
- Complications are extremely rare, if the procedure is carried out under strict sterile conditions.

References

Bachmann G, Bauer T, Jürgens I et al. (1998) The diagnostic accuracy and therapeutic relevance of CT arthrography and MR arthrography of the shoulder. RoFo 168(2):149–156 [German]

Bille B, Harley B, Cohen H (2007) A comparison of CT arthrography of the frist to findings during wrist arthroscopy. J Hand Surg Am 32:834–841

Blitzer M, Nasko M, Krackhardt T et al. (2004) Direct CT-arthrography versus direct MR-arthrography in chronic shoulder instability: comparison of modalities after the introduction of multidetector-CT technology. Rofo 176(12):1770–1775 [German]

Brossmann J, Preidler KW, Daenen B et al. (1996) Imaging of osseous and cartilaginous intraarticular bodies in the knee: comparison of MR imaging and MR arthrography with CT and CT arthrography in cadavers. Radiology 200(2):509–517

Dubberley JH, Faber KJ, Patterson SD et al. (2005) The detection of loose bodies in the elbow: the value of MRI and CT arthrography. J Bone Joint Surg Br 87(5):684–686

Guntern DV, Pfirrmann CW, Schmid MR et al. (2003) Articular cartilage lesions of the glenohumeral joint: diagnostic effectiveness of MR arthrography and prevalence in patients with subacrominal impingement syndrome. Radiology 226:165–170

Lecouvet FE, Dorzee B, Dubuc JE et al. (2007) Cartilage lesions of the glenohumeral joint: diagnostic effectiveness of multidetector spiral CT arthrography and comparison with arthroscopy. Eur Radiol 17(7):1763–1771

Moser T, Dosch JC, Moussaoui A, Dietemann JL (2007) Wrist ligament tears: evaluation of MRI and combined MDCT and MR arthrography. AJR Am J Roentgenol 188(5):1278–1286

Mutschler C, Vande Berg BC, Lecouvet FE et al. (2003) Postoperative meniscus: assessment of dual-detector row spiral CT arthrography of the knee. Radiology 228(3):635–641

Nishii T, Tanaka H, Sugano N et al. (2007) Disorders of acetabular labrum and articular cartilage in hip dysplasia: evaluation using isotropic high-resolution CT arthrography with sequential radial reformation. Osteoarthr Cartil 15(3):251–257

Pfirrmann CWA, Mengiardi B, Dora C et al. (2006) Cam and pincer femoroacetabular impingement. Radiology 240(3):778–785

Schmid MR, Nötzli HP, Zanetti M et al. (2003) Cartilage lesions in the hip: diagnostic effectiveness of MR arthrography. Radiology 226(2):282–286

Schulte-Altedorneburg G, Gebhard M, Wohlgemuth WA et al. (2003) MR arthrography: pharmacology, efficacy and safety in clinical trials. Skeletal Radiol 32:1–12

Schwartz ML, al-Zahrani S, Morwessel RM et al. (1995) Ulnar collateral ligament injury in the throwing athlete: evaluation with saline-enhanced MR-arthrography. Radiology 197(1):297–299

Timmerman LA, Schwartz ML, Andrews JR (1994) Preoperative evaluation of the ulnar collateral ligament by magnetic resonance imaging and computed tomography arthrography. Am J Sports Med 22(1):26–31

Toomayan GA, Holman WR, Major NM et al. (2006) Sensitivity of MR arthrography in the evaluation of acetabular labral tears. Am J Roentgenol 186(2):449–453

van Dijk CN, Molenaar AH, Cohnen RH et al. (1998) Value of arthrography after supinator trauma of the ankle. Skeletal Radiol 27(5):256–261

Waldt S, Bruegel M, Ganter K et al. (2005) Comparison of multisclice CT arthrography and MR arthrography in the detection of articular cartilage lesions. Eur Radiol 15(4):784–791

Waldt S, Bruegel M, Mueller D et al. (2007) Rotator cuff tears: assessment with MR arthrography in 275 patients with arthroscopic correlation. Eur Radiol 17:491–498

White LM, Schweitzer ME, Weishaupt D et al. (2002) Diagnosis of recurrent meniscal tears: prospective evaluation of conventional MR imaging, indirect MR arthrography, and direct MR arthrography. Radiology 222(2):421–429

Zubler C, Mengiardi B, Hodler J et al. (2007) MR arthrography in calcific tendinitis of the shoulder: diagnostic performance and pitfalls. Eur Radiol 17:1603–1610

Special Techniques

16

Jens-Peter Staub, Andreas H. Mahnken, Markus Völk,
Frank K. Wacker, and Bernhard Meyer

Contents

16.1 Sclerosing Therapy in Cysts and Parasites

Jens-Peter Staub

16.1.1 Introduction

Due to the increasing utilization of cross-sectional imaging techniques like computed tomography (CT), magnetic resonance (MR) imaging, and ultrasound (US), cysts, in particular those of the abdominal organs like kidneys, liver and spleen, are frequently diagnosed. Therapeutic consequences can only be driven if the cysts become symptomatic because of their position, increasing size, hemorrhage or superinfection. The surgical excision, resection or fenestration of the cyst by laparatomy or laparoscopic deroofing, with widest possible excision of the wall and coagulation, show high success rates and were regarded to be the standard procedure for a long time. However, during the last two decades, following the first description by Bean (1981), the percutaneous interventional therapy has gained more and more importance as a safe and low invasive procedure.

Cysts of the abdominal organs are histologically classified into true cysts or pseudocysts. While true cysts are surrounded by a single-layer epithelium wall and often congenital, pseudocysts originate from a trauma, an operation or an infection. Hydatid cysts are acquired, true cysts which are surrounded by a multilayer membrane and thus require a different treatment.

Mahnken/Ricke (Eds.), *CT- and MR-Guided Interventions in Radiology*

16.1.2 Indications

16.1.2.1 Renal Cysts

The most frequent form of the renal cyst is the cortical cyst which is surrounded by a single epithelial layer. It originates from dilated tubules in the nephrons, detaches by increasing growth and can reach enormous size. More than half of the adults over 50 years have renal cysts which are in general asymptomatic. Large cysts can cause flank pain by distension of the capsule, and a further complication is compression of the calices or the proximal ureter with the result of obstruction or renal hypertension. Infected renal cysts are treated like abscesses in other organs by percutaneous drainage and antibiotics.

16.1.2.2 Splenic Cysts

As many as 75% of all splenic cysts are posttraumatic pseudocysts (Fig. 16.1), developed out of hematomas, whereas congenital splenic cysts are a rare finding (Klee et al. 1996). Splenic cysts can reach substantial sizes before they become symptomatic by their space-demanding effect on surrounding organs. Pain is the most often described complaint. Since the surgical standard therapy of splenectomy is associated with an increased risk of septic complications, especially the overwhelming postsplenectomy syndrome (OPSI syndrome), sclerotherapy is an alternative, safe option with high success rates (Akhan et al. 1997; Völk et al. 1999).

16.1.2.3 Hepatic Cysts

True hepatic cysts are often solitary and are found sonographically in 4.65% of the normal population (Caremani et al. 1993). They originate in utero from a malformation of intrahepatic bile ducts and are lined by a cuboidal epithelium. Large cysts can cause hepatomegaly, pain and sense of fullness; other possible complaints are feeling of sickness, nausea and dyspnea. Compression of the biliary tree leads to intrahepatic cholestasis with jaundice. Cases of leg and scrotal edema by obstruction of the inferior vena cava were described (Frisell et al. 1979).

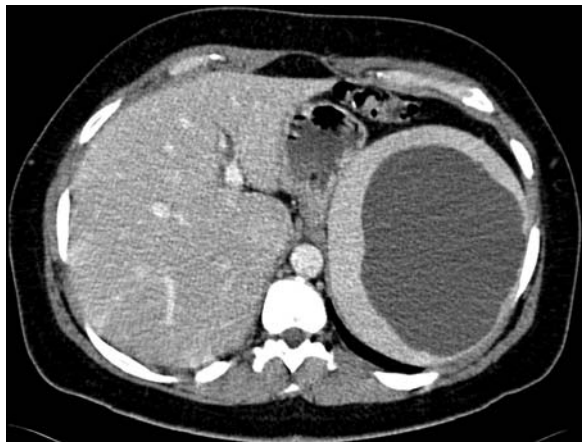

Fig. 16.1 Huge, asymptomatic cyst of the spleen: no indication for sclerotherapy

16.1.2.4 Pancreatic Cysts

Up to 85% of the cystic lesions in the pancreas are pseudocysts. Sclerotherapy is contraindicated in half of all pseudocysts because of a communication with the pancreatic duct and a subsequent risk of pancreatitis. Non-communicating pseudocysts have a low recurrence rate, so that a simple drainage can be performed. Congenital cysts of the pancreas are rare and often occur in patients with polycystic diseases. They seldom become symptomatic due to large size or their position; in these cases a percutaneous drainage and sclerotherapy can be indicated.

16.1.2.5 Lymphoceles

In contrast to true cysts, lymphoceles are not surrounded by an epithelium but by fibromembranous tissue. They are a postoperational complication, following surgery in areas of lymphatic trajectories in the abdomen or pelvis. Often existing septations and locules complicate the entire drainage of many lymphoceles. If lymphocele recurrence appears after simple percutaneous aspiration, sclerotherapy can be an effective alternative to surgical treatment with a low complication risk (Sawhney et al. 1996).

16.1.2.6 Hydatid Cysts

Sclerosing therapy of hydatid cysts is performed percutaneously with the PAIR technique (puncture, aspi-

ration (drainage), injection, and reaspiration of a scolicidal solution). Infections with *Echinococcus granulosus* occur worldwide, most especially in the Mediterranean region of Europe, the Middle East, Asia, South America and North Africa as well as endemically in Australia in areas of intensive sheep breed. Ingested embryos from slipped eggs penetrate the intestinal mucosal wall and proceed to the capillary filters of the parenchymal organs via the venous system. The most frequent affected organ is the liver in about 80% of cases, followed by the lung (20%). The peritoneum, kidney and the spleen are affected less (WHO Informal Working Group on Echinococcosis 1996).

Hydatid cysts are composed of three layers: the inner germinal layer with brood capsules and thousands of protoscolices, the ectocyst, a thin, chitinlike membrane and the outer pericyst which consists of host cells and compressed fibrous tissue. Due to the multilayer structure and subsequent enhancement of cyst walls and septations, CT as well as MR imaging have a high sensitivity and specificity in detecting hydatid disease. The sonographic appearance of the cysts, according to the classification by Gharbi et al. (1981), has different therapeutic consequences: percutaneous therapy is only effective in cysts of the type I and II, and in some cysts of type III (Table 16.1), that have only a small amount of daughter cysts (Kabaalioglu et al. 2006).

16.1.2.7 Summary of Indications and Contraindications

As emphasized above, sclerotherapy is only indicated in symptomatic cysts. The most frequent symptom is pain. Compression of the biliary tree by liver cysts can lead to cholestasis. Space demanding cysts in the pancreas duct system may cause pancreatitis, close to vascular structures there is a risk of ischemia or impaired venous drainage. Renal cysts can lead to a compression of the renal collecting system, microhematuria or renal hypertension (Table 16.2).

Hydatid cysts of the type I and II according to Gharbi (pure fluid collection and fluid collection with a split/wall) can be treated alternatively to the surgical procedure by sclerotherapy. Because every single subsidiary cyst must be treated, surgery should be preferred in multiseptated, honeycomb-like cysts of type III and in cysts of type IV. Calcified, inactive type V cysts (Fig. 16.2) are not treated (WHO Informal Working Group on Echinococcosis 1996).

Table 16.1 The Gharbi classification of hydatid cysts based on ultrasound appearance (Gharbi et al. 1981)

Gharbi classification	Lesion features	Sclerosing therapy
Type I	Pure fluid collection	+
Type II	Fluid collection with a split wall	+
Type III	Fluid collection with septa	(+)
Type IV	Heterogeneous echo patterns	–
Type V	Reflecting thick walls	–

Table 16.2 Indications and contraindications for sclerosing therapy in cysts and hydatid disease

Indications	
Cysts	Symptomatic cysts (e.g. pain, nausea, vomitus, jaundice, shortness of breath, obstruction of collecting system)
Hydatid disease	Cysts types I and II according to Gharbi classification, type III if not of honeycomb appearance
Contraindications	
Cysts	No informed consent Coagulation disorders Inaccessible location Communication with bile or pancreatic duct, blood vessels, renal collecting system or free peritoneal cavity
Hydatid disease	Cysts types IV and V, type III with honeycomb appearance

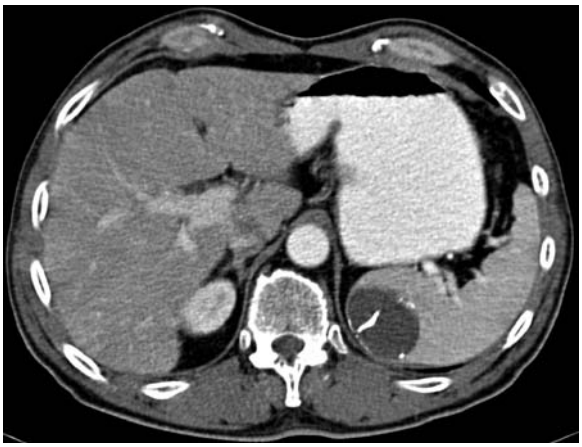

Fig. 16.2 Calcified, inactive hydatid cyst of the spleen type V acc. Gharbi classification: no indication for sclerotherapy

Contraindications for sclerotherapy are the favoring of surgical procedures, absence of patients consent or uncorrectable coagulation disorders. The platelet level should be at least 50,000/ml, the partial thrombin time (PTT) should be less than 50 s and the international normalized ration (INR) should be below 1.3. Lower values can be substituted by transfusion of thrombocytes or fresh frozen plasma (FFP). Difficult access routes with a high risk of vascular injury or injury of abdominal organs should be avoided as well as alcoholic sclerotherapy of cysts, which communicate with the biliary tree, vascular system or the free peritoneal space.

16.1.3 Material

16.1.3.1 Sclerosing Agents

As secretion of the endocystic epithelium remains, sole puncture of a cyst shows a high recurrence rate and should only be performed for diagnostic reasons. A large number of different agents (glucose, formalin, phenol, povidone-iodine, pantopaque, tetracycline, doxycycline, bleomycin) were used for sclerosing therapy of cysts and had either a high failure rate or were highly toxic. Ethanol is also a highly toxic agent, but is proved to be an effective agent in treatment of abdominal cysts. The injected solution leads within 1–3 min to a fixation of the epithelium cells, so that secretion is interrupted. Cyst recurrences are related to an insufficient contact of alcohol with the epithelium. As a consequence an adequate amount of alcohol (30–50% of the cyst volume) has to be injected after complete evacuation of the cyst, and the patient has to be moved in supine, prone and in both decubitus positions during sclerotherapy.

Because ethanol can cause serious side effects, if it is injected intravasally, in the free peritoneal space, the biliary tree system or the renal collecting system, a communication must be excluded by fluoroscopy or CT after injection of diluted contrast medium. With an injected ethanol amount of up to 200 ml and a maximum exposition time of 20 min, no side effects are to be expected by systemically absorbed alcohol. Developing pain symptoms should be treated by intravenous injection of analgesics like fentanyl citrate.

Hypertonic saline (20–30%) is the second most common scolicidal substance in hydatid cysts. The osmotic gradient of highly concentrated saline results in a destruction of the infectious protoscolices and a delamination of the ecto- from the pericyst.

16.1.3.2 Needles, Wires and Catheters

The required material is defined by the selected technique which depends on the size and location of the cyst, access way, and preferences of the performing radiologist. Larger cysts with a size of more than 5 cm should be drained with a pigtail catheter which guarantees a safe position in the cyst cavity while evacuation, injection and reaspiration can be performed even if the patient's position is changed during sclerotherapy. Due to the low viscosity of the serous cyst content a catheter size of 5- to 8-gauge is sufficient. Pigtail catheters have multiple side holes along the distal shaft which allow drainage of large cysts up to 1000 ml content. They are mounted on a rigid trocar to allow direct puncture of a superficial located cyst (e.g. 8 F Flexima regular ADP all purpose drainage catheter set, 27-129, Boston Scientific Corporation, Miami, FL, USA).

If a difficult access route requires it, the less traumatic Seldinger technique is used for puncture with 20- to 22-gauge biopsy needles (e.g. R-5-C2220, 22 G/20 Chiba biopsy fine needle, Peter Pflugbeil GmbH, Zomeding, G). A 0.018-inch guidewire (e.g. PMG-18-60-COPE, 0.018″/60 Cope Mandril Wire Guide, William Cook Europe, Bjaeverskov, DK) is inserted through the biopsy needle and is finally replaced by a 5-French sheath (e.g. R-51100, 5F/27 DILPLUS, Peter Pflugbeil GmbH, Zomeding, G). After coiling a rigid, 0.035-inch guidewire (e.g. 46-453, 0.035″/75 Amplatz Super Stiff, Boston Scientific Corporation, Miami, FL, USA) within the cyst, Teflon coated dilatators of 6- and 8-French size are used to dilatate the access way of the final catheter (e.g. JCD6.0-35-20, 6 F/20 Puncture site dilatator, JCD8.0-35-20, 8 F/20 Puncture site dilatator, William Cook Europe, Bjaeverskov, DK).

Smaller cysts may be punctured directly with a long angiography or trocar needle (e.g. ADN-18-18.0, 18 G/20 Vascular access catheter needle, William Cook Europe, Bjaeverskov, DK), 0.035-inch guidewires can be inserted through the needle sheath for further dilatation maneuvers and final pigtail replacement (Figs. 16.3b,c and 16.4a,b).

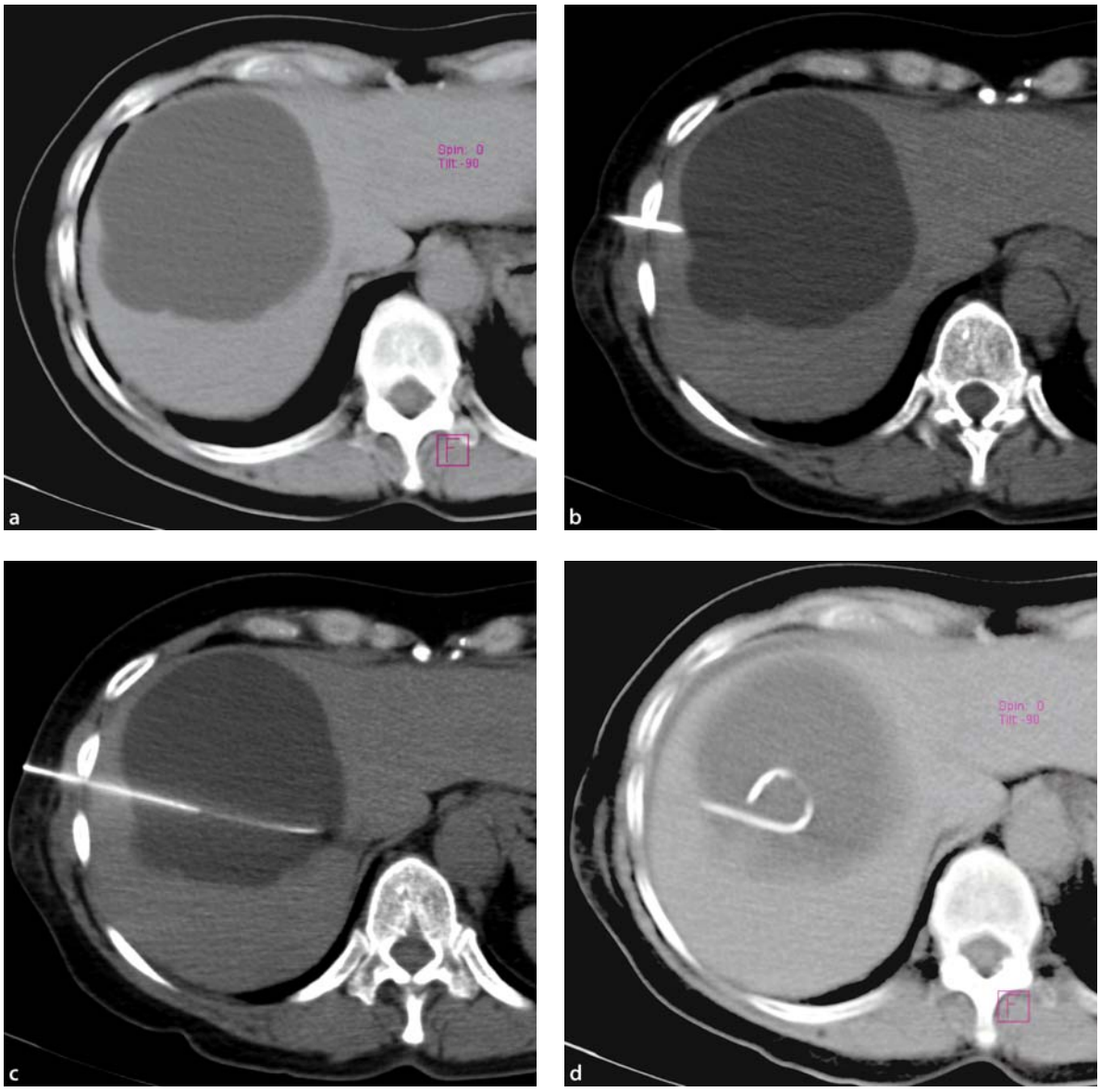

Fig. 16.3a–d Alcohol sclerotherapy of a 10-cm symptomatic hepatic cyst. Preprocedure scan to choose entry site shows the large fluid isodense lesion in right liver lobe (**a**). Puncture with 18 G angiography needle (**b**). Removal of the trocar and insertion of a 0.035-inch wire (*arrow*) through the needle sheath (**c**). Control scan of pigtail position (**d**)

16.1.4 Technique

16.1.4.1 Pre-interventional Imaging

Before sclerotherapy is performed, true cysts must be differentiated from septated cysts, infected cysts, parasitic cysts and cystic carcinomas. Communication with the biliary tree, the urinary tract, the vascular system or the peritoneal cavity must be excluded. Contrast enhanced CT as well as MR imaging are superior imaging modalities compared to US, besides, they permit the planning of difficult access routes by precise visualization of blood vessels and the bowel.

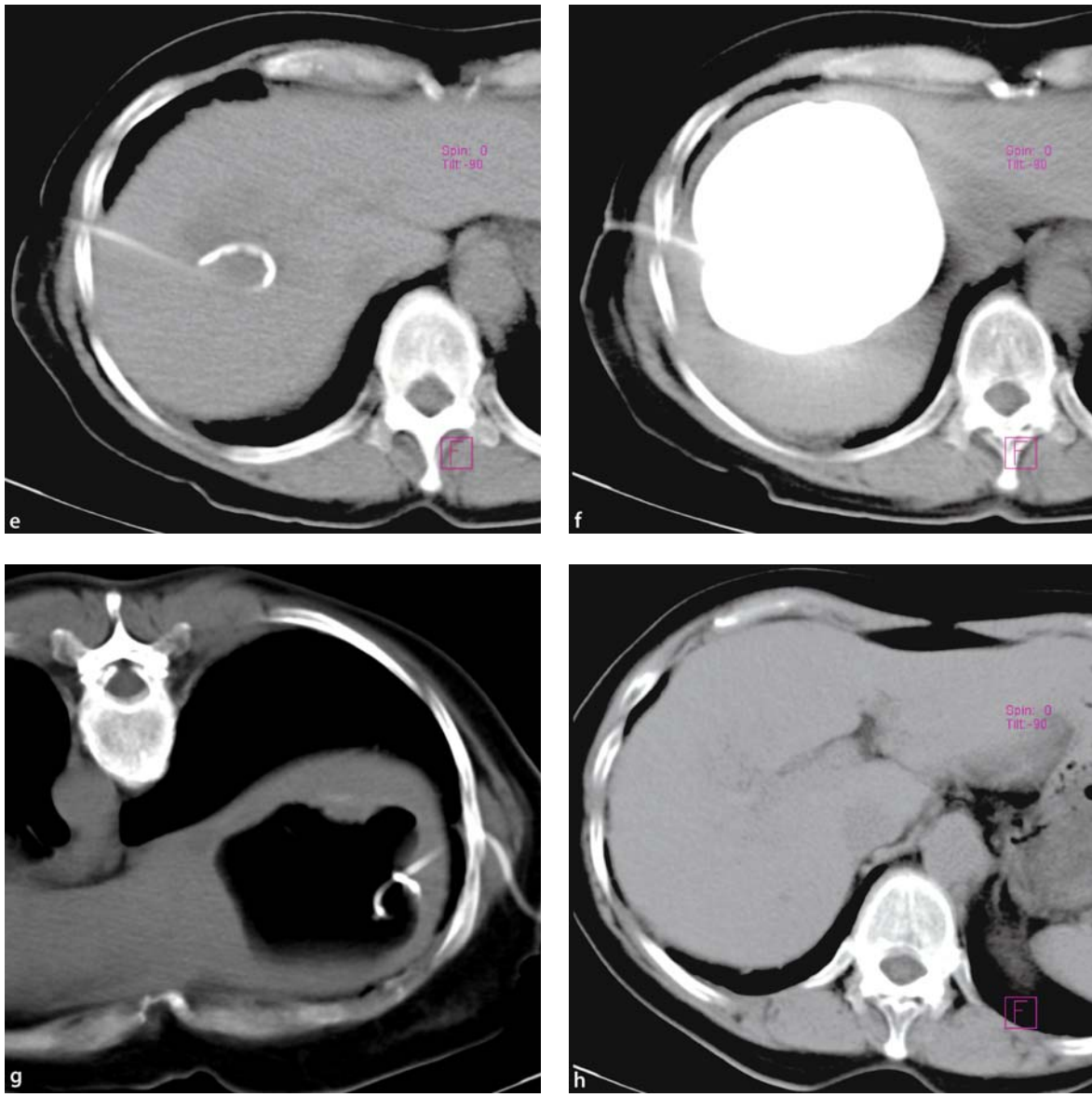

Fig. 16.3e–h Complete evacuation of the cyst (**e**). No leakage after injection of diluted contrast media (**f**). Scan in prone position after injection of 160 ml ethanol 95% (measured intracystic attenuation was −160 HU) (**g**). Postprocedure scan after reaspiration and removal of pigtail catheter (**h**)

When compared with MR imaging and US, CT is the imaging modality of choice for guiding sclerotherapy in cysts due to its quick acquisition time, low movement artifacts, a high spatial resolution with better detection of blood vessels, available space and the more precise visualization of the used puncture needles, guidewires and catheters.

16.1.4.2 Non-parasitic Cysts

Before intervention is performed, the whole procedure is explained in detail to the patient, who has to agree the procedure by signing the consent papers. Coagulation parameters have to be determined and checked. Monitoring of oxygen saturation, ECG and blood pres-

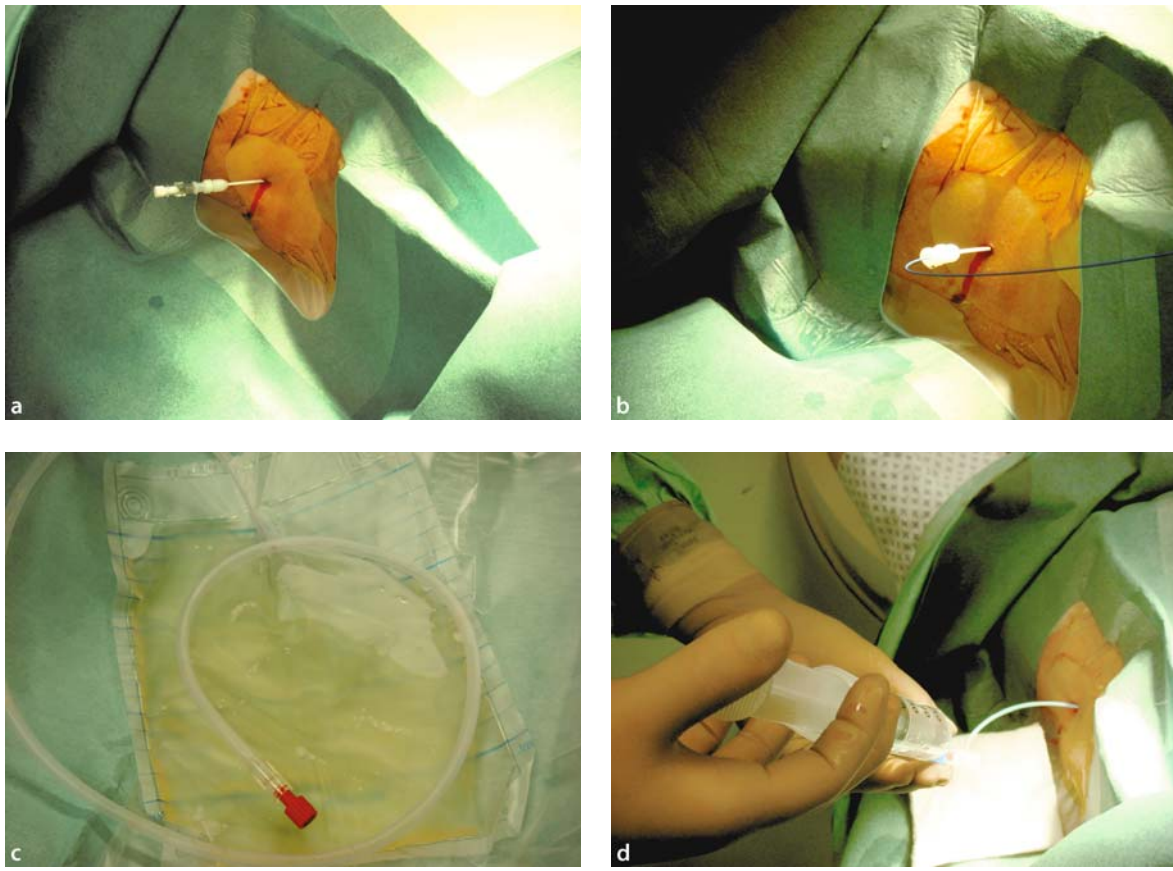

Fig. 16.4a–d Sclerotherapy of a benign hepatic cyst. A 10-cm 18 G angiography needle is placed in the cyst (**a**). A 0.035-inch guide wire is coiled in the cyst after removal of the trocar (**b**). Clear cyst fluid in the drainage bag (**c**). Injection of 95% ethanol, using a 60-ml syringe (**d**)

sure should be available if the intervention is performed under conscious sedation of the patient.

The patient is placed comfortably in supine, prone or lateral position, depending on the planned access route. In principle the approach should be as atraumatically as possible. In order to avoid spilling of cyst content into peritoneal space, the puncture should reach through about 1–2 cm of normal parenchyma.

In general un-enhanced CT scans are performed prior to the procedure (Fig. 16.3a). However, there may be cases that require intravenous contrast media to visualize the blood vessels. The access is planned on the CT console, the skin is disinfected and a local anesthetic like 5–20 ml lidocaine 1% is injected subcutaneously by a 25-gauge needle. The needle is left in situ to check its position on a control CT scan. Moderate conscious sedation may be achieved by intravenous injection of 1–2 mg midazolam in combination with opioid analgetics like fentanyl (0.025–0.05 mg) and piritamide (1.875–3.75 mg) or esketamine (6.25–12.5 mg). Standard initial doses of the listed agents have to be adapted to patients body-mass, age and disease, and can be repeated every 3–5 min (see Chap. 5).

The anesthesia needle is removed and the skin carefully disinfected and draped. The further procedure depends on the location and size of the cyst, the access way and experience of the performing radiologist. Small cysts with a size of <5 cm can be aspirated and sclerosed directly with an 18-gauge needle, large cysts should be drained with a pigtail catheter. Technically difficult access routes like a deep cyst position or ad-

jacent vessels require the Seldinger technique instead of the direct puncture.

Small Cysts

Smaller (< 5 cm) and superficially located cysts can be punctured directly with an 18-gauge angiography or trocar needle. After a small skin incision the needle is directed into the cyst until the centre of the cyst cavity is reached. Controlling CT scans can be necessary if the access route is long or very angulated. After checking the correct needle position the trocar is removed and the cyst content is sampled for laboratory analysis.

Trocar Technique

The trocar technique allows a quick and safe insertion of an indwelling catheter in superficially located cysts of more than 5 cm diameter. After straightening the catheter by inserting the trocar and stiffening cannula, the assembled drainage set is placed into the cyst cavity. The trocar stylet is removed, the stiffening cannula unlocked and held stationary, and the pigtail catheter is fully advanced into the cystic cavity. After removal of the cannula, the correct pigtail catheter position is checked by a control CT scan. The cyst content is sent to laboratory for analysis.

Seldinger Technique

Technically difficult approaches like a deep parenchyma location of the cyst or risk of injuring blood vessels or bowel require the Seldinger technique. A 22-gauge needle is positioned in the proximal cyst cavity under controlling CT scans. After aspiration of cyst fluid a 0.018-inch guidewire is inserted in the sheath and coiled into the cyst. The puncture needle is replaced by an 18-gauge trocar-dilatator-combination and a stiff 0.035-inch guidewire is positioned. Teflon dilatators are passed over the guidewire and the straightened pigtail catheter is advanced into the proximal cyst. The stiffening cannula is unlocked and held stationary while the catheter is fully advanced into the cavity. Stiffening cannula and guidewire are removed; samples of the cyst fluid are obtained.

Sclerosing Therapy

Prior to sclerosing therapy the correct position of the pigtail tip is checked by CT scanning. In order to avoid displacement of the sclerosing agent it is important to ensure that all sideholes of the catheter are located within the cyst. After checking the correct position of the needle or pigtail tip within the cyst cavity (Fig. 16.3d) samples of the cyst content are taken for cytological, microbiological and biochemical analysis. The catheter is fixed and a three-way stopcock is attached. The cyst is drained completely with a large syringe (e.g. 60 ml) and a drainage bag (Figs. 16.3e and 16.4c). The obtained volume should correspond to the CT calculation of the cystic content ($d_1 \times d_2 \times d_3 \times 0.5232$); if necessary a control scan is performed to ensure complete evacuation of the cysts content. After complete evacuation, diluted contrast medium (300 mg iodine/ml mixed with 0.9% NaCl 1:10) is injected and a CT scan is performed to exclude leakage out of the cyst (Fig. 16.3f). If the contrast medium spreads into blood or lymphatic vessels, the biliary tree, the renal collecting system or into peritoneum, sclerotherapy is contraindicated and the pigtail catheter has to be removed after complete reaspiration.

If there is no leakage, the contrast medium is aspirated completely and 95% alcohol is injected (Fig. 16.4d). The amount of alcohol should be 30–50% of the previous cyst content and not exceed 200 ml, even if the cyst size is larger than 600 ml. Because patients develop pain under injection of alcohol, additional application of analgesics are generally required. The alcohol remains for approximately 20 min in the cyst, during this time the patient has to be moved into supine, prone, left and right decubitus position in order to guarantee a sufficient alcohol contact to the cystic epithelial layer (Fig. 16.3g). After sclerotherapy the alcohol is removed completely, together with the catheter and a postprocedure CT scan is performed to rule out possible complications (Fig 16.3h).

Patients have to rest in bed for about 4 h, but can be dismissed on the same day if there are no suspicious clinical symptoms. After 3 months a follow-up by US, CT or MR imaging examination should be performed. US typically shows a small, irregular shaped residual cyst with thick walls (Fig. 16.5a), CT normally depicts a higher density of the residual cyst than before the sclerotherapy, and can show an enhancement of the

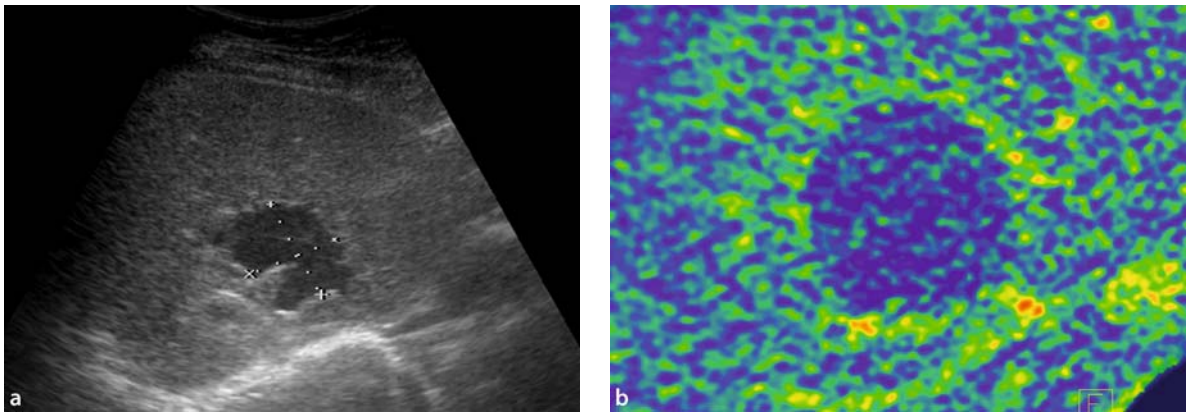

Fig. 16.5a,b Follow-up of hepatic cysts after sclerotherapy. Residual small cyst with thick, irregular walls at US (**a**). Slight enhancement of cyst wall in Dual-Energy CT scan, volume reduction was −98% (**b**)

cyst wall (Fig. 16.5b). Recurrent symptomatic cysts require a repeated drainage or a surgical procedure.

16.1.4.3 Hydatid Cysts

Sclerosing therapy of hydatid cysts is performed applying the PAIR technique (percutaneous drainage consisting of puncture, aspiration, injection, and reaspiration of a scolicidal solution). Besides alcohol, hypertonic saline is the most common scolicidal substance. Because of the high density of hypertonic saline on CT scans the entire filling of the cyst and a communication with vessels or the biliary tree can be demonstrated. In contrast to alcohol saline solution does not cause a chemical cholangitis.

To minimize the risk of anaphylaxia and secondary echinococcosis, sclerotherapy of hydatid cysts must be accompanied by an antihelminthic chemotherapy with mebendazole or albendazole. Medical treatment begins 4–7 days before the planned intervention and should last for 4 weeks. Because of the risk of anaphylaxia, the attendance of a radiologist experienced in emergency medicine or an anesthetist is advisable.

Sclerotherapy is only performed in liquid-filled cysts of the type I and II according to Gharbi, and in cysts type III if there is no honeycomb appearance (Table 16.2). The technique of needle or catheter positioning is the same as described above in non-parasitic cysts. Hydatid cysts are evacuated completely after sampling 20 ml cyst content for microbiological analysis, protoscolices and fragments of the membrane can

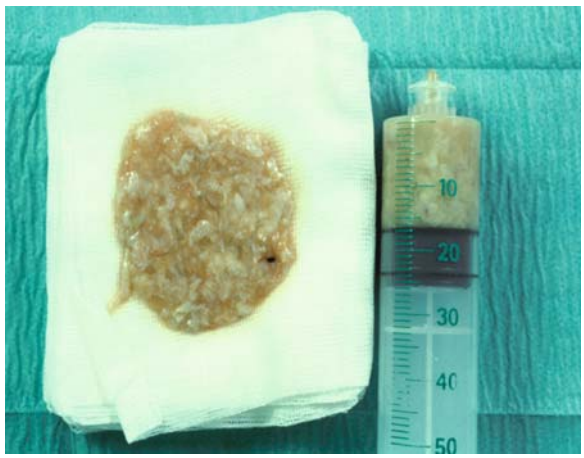

Fig. 16.6 Contents of a hydatid cyst (Courtesy of Prof. Feuerbach, Regensburg)

be seen in the aspirated liquid (Fig. 16.6). The cyst is filled with hypertonic saline (20%); the amount should be 50% of the totally aspirated cystic volume. The saline remains 10–20 min within the cyst and the delamination of the endocyst can be shown in a controlling CT scan. Particular cysts larger than 6 cm and septated cysts can be treated by injection of 95% alcohol, after leakage is excluded. After sclerotherapy, the cyst is evacuated completely, and the catheter is removed.

Patients can be dismissed after resting for 4 h in bed if US control shows no hematoma. Follow-up should be performed closely including serology, immunology analysis, and US examinations every week during the

first month, once a month during the first year, and once a year in the following 10 years.

16.1.5 Results

16.1.5.1 Non-parasitic Cysts

While aspiration of the cyst content alone shows a high recurrence rate up to 100% (Saini et al. 1983), the sclerotherapy of simple cysts with alcohol by percutaneous approach has proved to be a safe and effective procedure shown by the first description by Bean (1981). Akinici et al. (2005) noted in 98 renal cysts treated with sclerotherapy a volume reduction of 93% at the end of the first year of follow-up. Of the 74 patients with flank pain, 90% reported a reduction or a complete disappearance of complaints. Hydronephrosis disappeared in 10 of 12 patients (83%), and blood pressure values normalized in 7 of 8 patients (87.5%). After an alcohol exposition time of only 10 min Larssen et al. (2003) were able to achieve a volume reduction of 95% in symptomatic liver cysts after a follow-up period of 12–47 months. All of the seven treated patients experienced total relief of the clinical symptoms. Tikkakoski et al. (1996) published earlier a larger study with 59 treated liver cysts and a technical success rate of 97%, the follow-up time was up to 4 years. Interventional treatment of congenital liver cysts has similar results like laparoscopic fenestration and is associated with a lower mortality (Gigot et al. 1996).

There are only a few reports on the percutaneous sclerotherapy of splenic cysts using alcohol, describing a high technical success rate by a low risk of complications (Anon et al. 2006; Thanos et al. 2005; Akhan et al. 1997; Völk et al. 1999).

16.1.5.2 Hydatid Cysts

Since the first description of percutaneous drainage of a hydatid cyst (Mueller et al. 1985) the safety and efficacy of the method could be documented in more than 2500 patients. Different procedures, primarily with hypertonic saline or with 90–96% ethanol as a scolicidal substance achieved similar results. In a worldwide survey of the WHO Informal Group on Echinococcosis, the treatment of 765 hydatid cysts, primarily in the liver, with the PAIR method was evaluated (WHO Informal Working Group on Echinococcosis 2000). Positive response was achieved in 763 cases (99.7%) with a reduction of size about at least 50%. Recurrent cysts were observed in 12 cases (1.6%); in 8 cases recurrence was related to an insufficient amount of the injected scolicidal agent.

In a metaanalysis (Smego et al. 2003), 21 studies with 769 patients treated with PAIR and chemotherapy with mebendazole or albendazole were compared with a total amount of 962 patients from 14 studies undergoing surgical intervention (Table 16.3). The clinical and parasitological outcome was significantly better, in 95.8% of the patients undergoing PAIR compared with 89.8% of the patients with surgical procedure alone. The recurrence rate was 1.6% of patients in the PAIR group compared to 6.3% ($p < 0.0001$) in the other group. The rate of complications was significantly higher in the surgical control objects.

Table 16.3 Clinical outcomes and complications in patients undergoing PAIR plus chemotherapy ($n = 769$) or surgical intervention ($n = 952$) for hepatic echinococcosis appearance (Smego et al. 2003)

Clinical outcomes	PAIR + chemotherapy No. (%)	Surgical intervention No. (%)	p value
Cure	737 (95.8)	855 (89.8)	< 0.0001
Died	1 (0.1)	7 (0.7)	< 0.0827
Insufficient response	15 (2.0)	30 (3.2)	< 0.1249
Recurrence	12 (1.6)	60 (6.3)	< 0.0001
Major complications	61 (7.9)	239 (25.1)	< 0.0001
Cyst infection	16 (2)	63 (6.6)	< 0.0001
Abscess	3 (0.4)	34 (3.6)	< 0.0001
Biliary fistula	34 (4.4)	140 (14.7)	< 0.0001
Anaphylaxis	8 (1.0)	1 (0.1)	n.s.
Minor complications	101 (13.1)	314 (33.0)	< 0.0001
Fever	42 (5.5)	24 (2.5)	< 0.002
Allergic reactions	37 (4.8)	1 (0.1)	< 0.0001
Wound infection/ dehiscence	–	63 (6.6)	< 0.0001
Pleural effusions	4 (0.5)	67 (7.0)	< 0.0001
Hemorrhage	1 (0.1)	12 (1.3)	< 0.008
Peritonitis	–	61 (6.4)	< 0.0001
Intraperitoneal leakage	1 (0.1)	–	n.s.

Long time observations after percutaneous treatment of hydatid cysts for a period from up to 6 years confirmed the results that percutaneous aspiration, injection and reaspiration is a safe and effective alternative to surgical procedures (Üstünsöz et al. 1999; Kabaalioglu et al. 2006).

16.1.6 Complications

16.1.6.1 Non-parasitic Cysts

The complications regarding puncture and positioning of the pigtail catheter ranges between 3% and 4% of all cases, and depends on the access way, position of the cyst and utilized material. It includes infection, the risk of pneumothorax by transgressing the pleura, and in particular hemorrhage. The injection of alcohol does not seem to increase the risk of intracystic bleeding. Because alcohol is a toxic substance, spilling along the catheter, via iatrogenic fistulas or through an existing communication with the biliary tree or the renal collecting system must be excluded by cystography.

Because of the pain during injection of alcohol, sufficient conscious sedation should be guaranteed in order not to interrupt or terminate the procedure. Pain immediately recedes after reaspiration of alcohol. If measured, the blood-alcohol level rises regularly, but does not reach values in the toxic range with amounts up to 200 ml and a maximum sclerosing time of 20 min, so that bed rest of 4 h and monitoring is sufficient after the procedure. Patients have to be advised not to drive for 24 h after intervention. Postprocedurally the body temperature can rise up to 38.5 °C. However, if there are no further signs of infection, no therapy is required.

16.1.6.2 Hydatid Cysts

Beside the general puncture complications listed above like infection, bleeding and pneumothorax, the additional risk of an anaphylaxia and the peritoneal spilling of infectious cystic liquid exists in sclerotherapy of hydatid cysts. Periprocedural chemotherapy with mebendazole or albendazol is therefore necessary; the access to the cyst should lead through about 1–2 cm of normal parenchyma. Anaphylactic reactions appear in 0.5–1.0% of cases (Simego et al. 2003), a mortal outcome due to anaphylaxia in 0.1–0.2% (Akhan and Özmen 1999). Minor allergic reactions like urticaria, itching and hypotension appear in up to 5% of the cases and require a therapy with antihistaminics and infusion of volume. Fever up to 38.5 °C is another frequent symptom which is treated symptomatically in case of absent infection.

The rate of infected cysts and biliary fistulas is higher with hydatid cysts of the liver than with simple liver cysts. In comparison to surgical procedures the rate of major (7.9% compared with 25.1%) as well as minor complications (13.1% instead of 33.0%) is significantly lower with PAIR, so that the percutaneous treatment of hydatid cysts with hypertonic saline or alcohol is considered to be a safe procedure (Table 16.3).

Summary

Percutaneous sclerotherapy of non-parasitic cysts with alcohol is a technically simple and approved procedure. Only symptomatic cysts should be treated. Due to the quick acquisition time, the available space for intervention and the precise visualization of the inserted puncture systems, CT is the imaging modality of choice for guiding the intervention. Considering indications and contraindications, the technical and clinical success rate is high and comparable with the traditional surgical procedures. However, complications and mortality is clearly lower in comparison to surgical procedures, in addition, the method can be performed on outpatients with considerably lower costs.

The risk of anaphylaxia or spreading of protoscolices into peritoneum has been overestimated; however, it should not be neglected. Careful planning of the access route and periprocedural chemotherapy with mebendazole or albendazole is indispensable in percutaneous treatment of hydatid cysts. Considering the right indication (Table 16.2), sclerotherapy of hydatid cysts with hypertonic saline or alcohol has a high success rate of up to 95.8% with a clearly lower morbidity (Smego et al. 2003) compared to surgical procedures.

Key Points

- Because alcohol is a toxic substance, a communication of the cyst with vessels, the biliary tree, the renal collecting system or the peritoneal space must be excluded by cystography before sclerotherapy is applied.
- Patients often develop pain under the injection of alcohol, so that sufficient conscious sedation should be guaranteed.
- The success of sclerotherapy depends decisively on a sufficient intracystic concentration of alcohol which must have contact to the whole cystic epithelial layer. Hence, beside the entire emptying of the cyst an amount of 30–50% (max. 200 ml) of the aspirated volume has to be injected, and the patient must be turned into different positions including the prone position.
- In hydatid cysts, an adjuvant chemotherapy with mebendazole or albendazole must be carried out due to the danger of anaphylaxia and spilling of protoscolioces. Because anaphylactic reactions appear with a rate from up to 1% and the mortality ranges from 0.1% to 0.2%, sufficient monitoring of the patient should be guaranteed and the attendance of a radiologist, competent in emergency medicine or an anesthetist should be guaranteed.

References

Akhan O, Özmen MN (1999) Percutaneous treatment of liver hydatid cysts. Eur J Radiol 32:76–85

Akhan O, Baykan Z, Oguzkurt L, Sayek I, Özmen MN (1997) Percutaneous treatment of a congenital splenic cyst with alcohol: a new therapeutic approach. Eur Radiol 7:1067–1070

Akinci D, Akhan O, Ozmen M, Gumus B, Ozkan O, Karcaaltincaba M, Cil B, Haliloglu M (2005) Long-term results of single session percutaneous drainage and ethanol sclerotherapy in simple renal cysts. Eur J Radiol 54:298–302

Anon R, Guijarro J, Amoros C, Gil J, Bosca MM, Palmero J, Benages A (2006) Congenital splenic cyst treated with percutaneous sclerosis using alcohol. Cardiovasc Intervent Radiol 29:691–693

Bean WJ (1981) Renal cysts: treatment with alcohol. Radiology 138:329–331

Caremani M, Vincenti A, Benci A, Sassoli S, Tacconi D (1993) Ecographic epidemiology of non-parasitic hepatic cysts. J Clin Ultrasound 21:115–118

Frisell J, Rojdmark S, Arvidsson H, Lundh G (1979) Compression of the inferior caval vein – a rare complication of a large non-parasitic liver cyst. Acta Med Scand 205:541–542

Gharbi HA, Hassine W, Brauner MW, Dupuch K (1981) Ultrasound examination of the hydatic liver. Radiology 139:459–463

Gigot JF, Legrand M, Hubens G, de Canniere L, Wibin E, Deweer F, Druart ML, Bertrand C, Devriendt H, Droissart R, Tugilimana M, Hauters P, Vereecken L (1996) Laparoscopic treatment of nonparasitic liver cysts: adequate selection of patients and surgical technique. World J Surg 20:556–561

Kabaalioglu A, Ceken K, Alimoglu E, Apaydin A (2006) Percutaneous imaging-guided treatment of hydatid liver cysts: do long-term results make it a first choice? Eur J Radiol 59:65–73

Klee FE, Osswald BR, Wysocki S (1996) Splenic cyst – a classical "incidental finding". Zentralbl Chir 121:805–816

Larssen TB, Rosendahl K, Horn A, Jensen DK, Roervik J (2003) Single-session alcohol sclerotherapy in symptomatic benign hepatic cysts performed with a time of exposure to alcohol of 10 min: initial results. Eur Radiol 13:2627–2632

Mueller PR, Dawson SL, Ferrucci JT, Nardi GL (1985) Hepatic echinococcal cyst: successful percutaneous drainage. Radiology 155:627–628

Saini S, Mueller PR, Ferrucci JT Jr, Simeone JF, Wittenberg J, Butch RJ (1983) Percutaneous aspiration of hepatic cysts does not provide definitive therapy. AJR Am J Roentgenol 141:559–560

Sawhney R, D'Agostino HB, Zinck S, Rose SC, Kinney TB, Oglevie SB, Stapakis JC, Fishbach TJ (1996) Treatment of postoperative lymphoceles with percutaneous drainage and alcohol sclerotherapy. J Vasc Interv Radiol 7:241–245

Smego RA, Bhatti S, Khaliq AA, Beg MA (2003) Percutaneous aspiration-injection-reaspiration drainage plus albendazole or mebendazole for hepatic cystic echinococcosis: a meta-analysis. Clin Infect Dis 37:1073–1083

Thanos L, Mylona S, Ntai S, Pomoni M, Batalkis N (2005) Percutaneous treatment of true splenic cysts: report of two cases. Abdom Imaging 30:773–776

Tikkakoski T, Mäkelä JT, Leinonen S, Päivänsalo M, Merikanto J, Karttunen A, Siniluoto T, Kairaluoma MI (1996) Treatment of symptomatic congenital hepatic cysts with single-session percutaneous drainage and ethanol sclerosis: technique and outcome. J Vasc Intervent Radiol 7:235–239

Üstünsöz B, Akhan O, Kamiloglu MA, Somuncu I, Ugurel MS, Cetiner S (1999) Percutaneous treatment of hydatid cysts of the liver: long-term results. Am J Roentgenol 172:91–96

Völk M, Rogler G, Strotzer M, Lock G, Manke C, Feuerbach S (1999) Post-traumatic pseudocyst of the spleen: sclerotherapy with ethanol. Cardiovasc Intervent Radiol 22:246–248

WHO Informal Working Group on Echinococcosis – PAIR network (1996) Guidelines for treatment of cystic and alveolar echinococcosis in humans. Bull World Health Organ 74:231–242

WHO Informal Working Group on Echinococcosis (2000) Percutaneous drainage of echinococcal cysts (PAIR—puncture, aspiration, injection, reaspiration): results of a worldwide survey for assessment of its safety and efficacy. Gut 47:156–157

16.2 Percutaneous Management of Endoleaks

Andreas H. Mahnken

16.2.1 Introduction

Endovascular treatment of aortic aneurysms is an increasingly used technique in patients with favorable vascular anatomy. With an incidence in the range from 10% to 50%, endoleak is the most common complication arising after endovascular treatment (Cuypers et al. 1999; Parent et al. 2002). Endoleaks are defined as persistent flow within the aneurysm sac but outside the graft. In case of persistent endoleakage the aneurysm sac remains pressurized and those aneurysms may rupture due to continued arterial pressure on the aneurysm wall.

Within the first 30 days after implantation leaks are called "primary endoleaks", while "secondary endoleaks" occur more than 30 days after the procedure. Leaks are classified according to their origin (Table 16.4).

Computed tomography (CT) angiography with additional acquisition of a second delayed phase is considered the imaging technique of choice for the detection of endoleaks (Gorich et al. 1999; Rosenblit et al. 2003). Alternative techniques for diagnosing endoleaks include (Doppler) ultrasound (US) and magnetic resonance (MR) imaging. While various studies on US showed a variable sensitivity and specificity for the detection of endoleaks (Golzarian et al. 2002), contrast enhanced MR imaging may yield a higher sensitivity to detect slow flow type II endoleaks when compared to CT angiography (Ayuso et al. 2004).

16.2.2 Indications

Among the different types of leaks, type II endoleaks are the only group that is currently considered suited for percutaneous treatment. While there is a clear indication to treat types I and III endoleaks, management of type II endoleaks is considered controversial. As type II endoleaks are associated with a lower risk of rupture than types I and III (0.5% vs. 3.4%) and many of these endoleaks seal spontaneously, treatment might be limited to the point of aneurysm growth (Zarins et al. 2000; van Marrewijk et al. 2002). However, type II endoleaks also present with an elevated aneurysm sac pressure and aggressive treatment may be advocated.

Considering currently published recommendations as well as our own experience, percutaneous management of endoleaks after endovascular aortic aneurysm repair is indicated in:

- Type II endoleak and aneurysm growth
- Persistent (> 6 month) type II endoleak
- Type II endoleaks not suited for embolization

16.2.3 Material

For percutaneous embolization of type II endoleaks, all the materials needed for a CT-guided puncture have to be on hand, including:

- Sterile draping
- Povidone-iodine for skin disinfection
- Local anesthetics for skin infiltration
- Scalpel
- 5-, 10- and 20-ml syringes with Luer-Lock adapter
- 18–20 G fine needle with end-hole

For embolization, different materials may be used including:

- Coils as for endovascular treatment
- Onyx
- Ethibloc
- Thrombin (500 IU/ml)
- Cyanoacrylate

Depending on the choice of the embolic agent, additional materials are needed, e.g. glucose for flushing lines and needle in order to avoid premature precipitation in cyanoacrylate.

Considering the different embolic agents cyanoacrylate provides some advantages. Unlike thrombin, its effectiveness does not depend on the patient's coagulation system and is not affected by adding contrast agents for better visualization. Moreover, its radiopacity facilitates embolization. It does not hamper future endoleak detection during the follow-up of patients as long as an unenhanced CT-scan is performed before intravenous contrast is administered.

Table 16.4 Classification of endoleaks

Type	Subtype	Location/details	Mechanism
I	A	Proximal	Separation from the arterial wall with insufficient seal at the fixation zones
	B	Distal	
	C	Iliac occluder	
II	A	Single vessel	Retrograde flow in the aneurysm sac from branching vessels
	B	Multiple vessels	
III	A	Junctional separation	tears, junctional leaks or modular disconnection
	B	Endograft fracture or holes	
IV			Graft porosity
V			Endotension – elevated pressure levels in the aneurysm sac without visible endoleak

16.2.4 Technique

The patient is positioned in a way that allows reaching the feeding vessel. For most interventions the patient will be put in the prone position for a translumbar approach. Alternatively a transabdominal route may be used. Ideally, the left-side access is used for the translumbar approach to avoid the inferior vena cava. For a transabdominal route any bowel interposition needs to be avoided. After infiltration of the puncture site with local anesthetics, the tip of the fine needle is brought into the endoleak, either using CT-fluoroscopy or a stepwise puncture technique as described in Chap. 9.

Once the needle is placed in the aneurysm sac an angiogram of the sac might be performed via the puncture needle. It will show the extent of the endoleak including the draining vessels. Particularly in the case of multiple vessels (type IIB), the endoleak can be compared with an arteriovenous malformation, with the sac forming the lesions nidus (Baum et al. 2002). To achieve good results in these complex lesions it is crucial to disrupt the channel that connects the different feeding and draining vessels (Fig. 16.7). In addition, the feeding vessels should be occluded by injection of the embolic agent directly at the origin of these vessels.

Using cyanoacrylate, the viscosity of the embolic agent can be individually adapted by adding a variable amount of Lipiodol® (Guerbet, Aulnay-sous-Bois, France). As a contrast agent it provides good visualization of the embolic agent during injection and by adapting the viscosity the spread of the agent within the aneurysm sac can be adapted to the size of the lesion. This is particularly helpful for occluding the feeding vessels. When using thrombin, not more than 1000–1500 IU should be injected for the initial treatment, as its local control is difficult and a high amount of thrombin has been reported to cause colonic ischemia (Gambaro et al. 2004). In general any embolizing agent should be injected slowly.

Additional pressure measurements are recommended before and after injection of the embolic agent. Reduction of the intrasac pressure proves efficacy of the procedure.

16.2.5 Results

Currently there is only sporadic data on the use of percutaneous embolization of type II endoleaks (van den Berg et al. 2000; Schmid et al. 2002; Rial et al. 2004). Baum et al. (2002) compared the use of the transarterial and the translumbar approach for dealing with endoleaks after endovascular aneurysm repair. The results were favorable for the translumbar approach being effective in 92% of patients vs. 20% in the transarterial approach. This was likely due to the fact that the network between the different feeding and draining vessels was disrupted using the percutaneous technique.

16.2.6 Complications

In general, percutaneous injection therapy for treating type II endoleaks has to be considered safe if

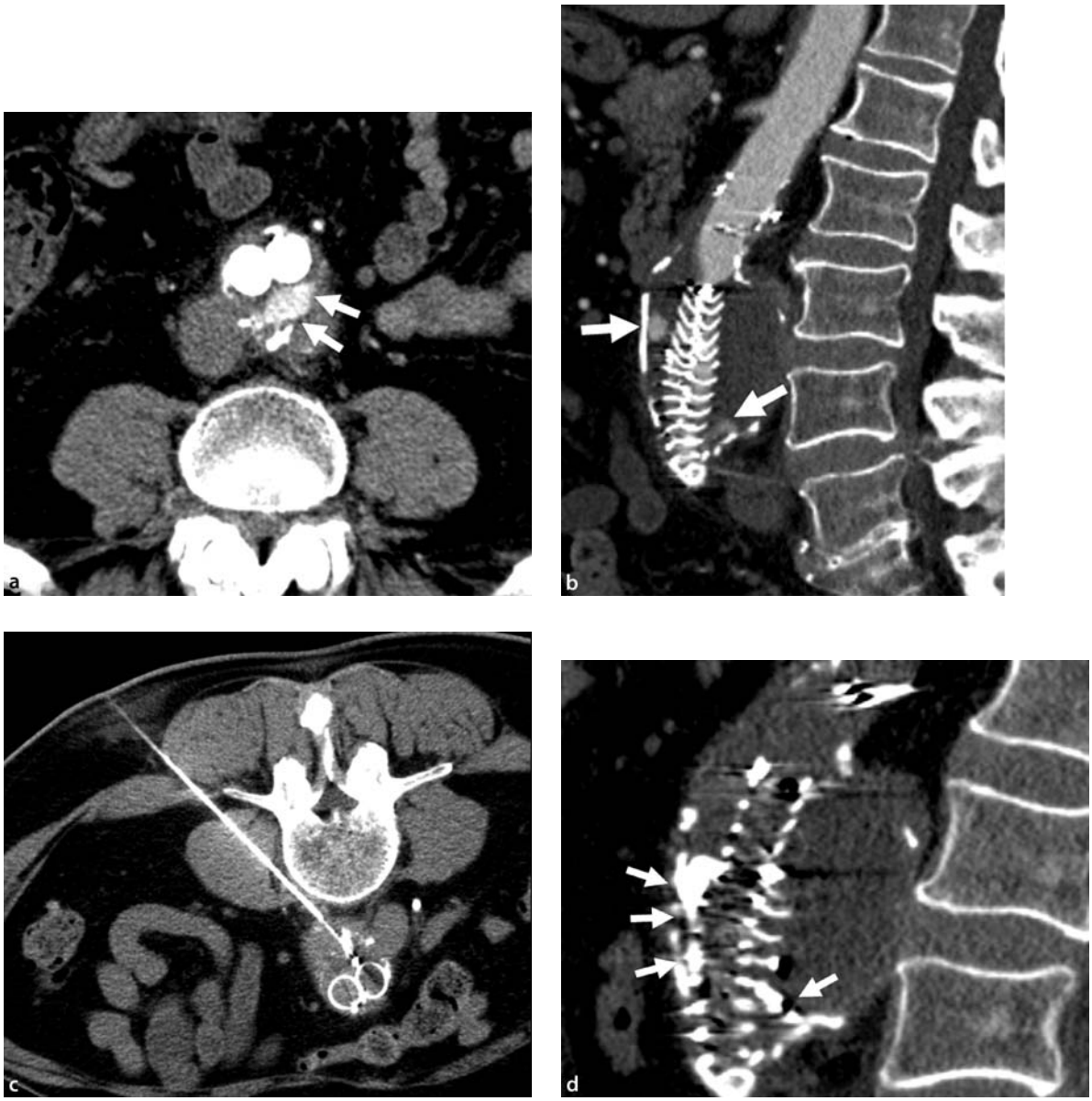

Fig. 16.7a–d A 72-year-old patient with endovascular repair of an abdominal aortic aneurysm. Six months after the procedure there was still a persistent endoleak (*arrows*) (**a**,**b**) that was thought to be caused by retrograde filling of the aneurysm sac from the inferior mesenteric artery (type II). The aneurysm sac was punctured with a 20 G fine needle (**c**) and after aneurysm angiogram (not shown) 1.5 ml of a mixture of cyanoacrylate and Lipiodol® were slowly injected. Control CT shows the cyanoacrylate distribution with in the aneurysm sac following a preformed channel that connected the different vessels involved in the endoleak (*arrows*) (**d**). Treatment was successful and the aneurysm size gradually decreased after the procedure

properly performed and monitored. The risk of infection is considered minor when working under sterile conditions and if bowel passage is avoided in case of a transabdominal route. Potential complications include thrombotic graft occlusion and peripheral embolism. Gambaro et al. reported a case of colonic ischemia which was considered to be due to embolization of the inferior mesenteric artery after thrombin injection in the aneurysm sac (Gambaro et al. 2004).

Summary

Endoleak is still an unsolved problem associated with endovascular repair of aortic aneurysms. Percutaneous treatment of type II endoleaks after endovascular repair of abdominal or thoracic aneurysms is feasible and effective. Although there is only very limited data available, this technique appears to be at least as effective as the endovascular approach. As this is a straightforward procedure, which is much less time consuming when compared with the endovascular approach, the indication for using this technique may expand in the future.

Key Points

- CT-angiography with additional delayed image acquisition is the first line diagnostic modality for the detection of endoleaks.
- There are endovascular and percutaneous treatment options. Optimal therapy depends on the type of the endoleak.
- Thrombin and cyanoacrylate are most commonly used for percutaneous treatment of type II endoleaks.
- Disruption of the network between the involved vessels by embolizing the connecting channel is mandatory to ensure treatment success.

References

Ayuso JR, de Caralt TM, Pages M, Riambau V et al. (2004) MRA is useful as a follow–up technique after endovascular repair of aortic aneurysms with nitinol endoprostheses. J Magn Reson Imaging 20:803–810

Baum RA, Carpenter JP, Golden MA et al. (2002) Treatment of type 2 endoleaks after endovascular repair of abdominal aortic aneurysms: comparison of transarterial and translumbar techniques. J Vasc Surg 35:23–29

Cuypers P, Buth J, Harris PL et al. (1999) Realistic expectations for patients with stent-graft treatment of abdominal aortic aneurysms. Results of a European multicentre registry. Eur J Vasc Endovasc Surg 17:507–516

Gambaro E, Abou-Zamzam AM Jr, Teruya TH et al. (2004) Ischemic colitis following translumbar thrombin injection for treatment of endoleak. Ann Vasc Surg 18:74–78

Golzarian J, Murgo S, Dussaussois L et al. (2002) Evaluation of abdominal aortic aneurysm after endoluminal treatment: comparison of color Doppler sonography with biphasic helical CT. AJR Am J Roentgenol 178:623–628

Gorich J, Rilinger N, Sokiranski R et al. (1999) Leakages after endovascular repair of aortic aneurysms: classification based on findings at CT, angiography, and radiography. Radiology 213:767–772

Parent FN, Meier GH, Godziachvili V et al. (2002) The incidence and natural history of Type I and II endoleak: a 5-year follow-up assessment with color duplex ultrasound scan. J Vasc Surg 35:474–481

Rial R, Serrano FJ, Vega M et al. (2004) Treatment of type II endoleaks after endovascular repair of abdominal aortic aneurysms: translumbar punture and injection of thrombin into the aneurysm sac. Eur J Endovasc Surg 27:333–335

Rosenblit AM, Patlas M, Rosenbaum AT et al. (2003) Detection of endoleaks after endovascular repair of abdominal aortic aneurysms: value of unenhanced and delayed CT acquisitions. Radiology 227:426–433

Schmid R, Gurke L, Aschwanden M et al. (2002) CT-guided percutaneous embolization of a lumbar artery maintaining a Type II endoleak. J Endovasc Ther 9:198–202

van den Berg JC, Nolthenius RP, Casparie JW et al. (2000) CT-guided thrombin injection into aneurysm sac in a patient with endoleak after endovascular abdominal aortic aneurysm repair. AJR Am J Roentgenol 175:1649–1651

van Marrewijk C, Buth J, Harris PL et al. (2002) Significance of endoleaks after endovascular repair of abdominal aortic aneurysms: the Eurostar experience. J Vasc Surg 35:461–473

Zarins CK, White RA, Hodgson KJ et al. (2000) Endoleak as a predictor of outcome after endovascular aneurysm repair: AneuRx multicenter clinical trial. J Vasc Surg 32:90–107

16.3 Percutaneous Gastrostomy

Markus Völk

16.3.1 Introduction

Pershaw (1981) reported the first percutaneous radiological gastrostomy (PRG) using fluoroscopy for image guidance. About one year before, the first percutaneous endoscopic gastrostomy (PEG) was performed (Gauderer et al. 1980).

16.3.2 Indications

PRG or PEG is indicated in those patients who require nutritional support with an intact, functional gastrointestinal tract, but who are unable to process a sufficient amount of calories. Enteral feeding is generally preferred to parenteral feeding, due to preservation of gastrointestinal integrity, associated risks, and economical reasons. PRG is especially indicated when PEG is impossible or unavailable. Among others, this includes:

- Chilaiditi-syndrome
- Previous gastrectomy

- Excessive hepatomegaly
- Inadequate transillumination in PEG
- High grade upper digestive tract obstruction

For PRG there are only a few contraindications. A normal coagulation screen and platelet count is necessary. Massive ascites has been described as a contraindication for PRG; however mild ascites is not a contraindication. In patients with markedly more ascites, pre-procedural paracentesis is helpful. Gastric neoplasm is a contraindication for any kind of gastrostomy; here a jejunostomy may be an alternative. For fluoroscopic-guided PRG and PEG relatively, contraindications are colonic interposition (Chilaiditi-syndrome), hepatomegaly, previous gastrectomy, and not-passable stenosis of the esophagus for a nasogastric tube; in these cases CT-guided PRG is a special technique which allows an exact anatomical demonstration to avoid organ injury.

16.3.3 Material

For PRG a T-fastener set (e.g. Cope Gastrointestinal T-fastener set of Cook, Bjaeverskov, Denmark) for gastropexy and the gastrostomy-tray (e.g. Cook, William Cook Europe, Bjaeverskov, Denmark) are commonly used devices (Fig. 16.8). However, there are various gastrostomy sets available for image-guided PRG (Table 16.5).

16.3.4 Technique

16.3.4.1 Patient Preparation and Aftercare

If possible, the patient should give his informed consent for the procedure at least one day before. The most important complications during the procedure are organ perforation and bleeding. That's why a recent coagulation screen must be performed. A nasogastric tube should be placed in the stomach the evening before. If a nasogastric tube cannot be placed, it should be tried under fluoroscopic guidance or direct puncture of the stomach under CT guidance (Gottschalk et al. 2007; Seitz et al 1997). Some authors recommend the oral application of 200 ml dilute barium 12 h before the procedure to identify the colon (Given et al. 2004).

The patient should fast from the night before. An intravenous access is necessary for the administration of sedative and analgesics (e.g. combination of midazolam hydrochloride and fentanyl citrate). All patients should be monitored for cardiac function (heart rate and rhythm, blood pressure) and oxygen saturation. The patient is placed in the CT-scanner in supine position and draped with a sterile cover. Immediately before the localization diagnostic 500–1000 ml of compartment air should be applied over the nasogastric tube and 40 mg butylscopolamin respectively 1 mg glucagon should be given intravenously for distention of the stomach. To localize the optimal access only a few scans (10–15 cm) through the stomach are necessary. After selecting the slice for the puncture the tract is anesthetized with 20 ml lidocaine (1%). Routine antibiotic prophylaxis for PRG tube placement is not necessary due to infrequent severe infectious complications following PRG (David et al. 1998; McDermott et al. 1997).

After the procedure the patient remains fastening for 12–24 h and then enteral feeding can be started beginning with tea. Normally no further aftercare is needed. The catheter should be changed in case of blockage and leakage; a routine exchange is not necessary.

16.3.4.2 Procedure

CT-guided PRG consists of gastrostomy using a T-fastener set for gastropexy and placement of the gastrostomy catheter (Fig. 16.9). The principle of gastropexy is to accelerate tract formation. With the stomach and abdominal walls closely apposed, the risk of peritoneal leakage is reduced. In addition, it is felt that gastropexy might reduce the risk of hemorrhage due to a tamponading affect (Given et al. 2005). That is why gastropexy is recommended for the PRG by fixing the anterior gastric wall to the anterior abdominal wall. This is performed with an 18-G hollow needle, containing a T-fastener which is inserted into the distended stomach (Fig. 16.9a). An alternative method is to use four T-fasteners in a quadratic order, leave the T-fasteners for about 10 days before the nylon thread is cut. An intragastric position can be confirmed by aspirating air into the syringe containing sterile water. After controlling the intragastric position a 0.035-inch guidewire is inserted

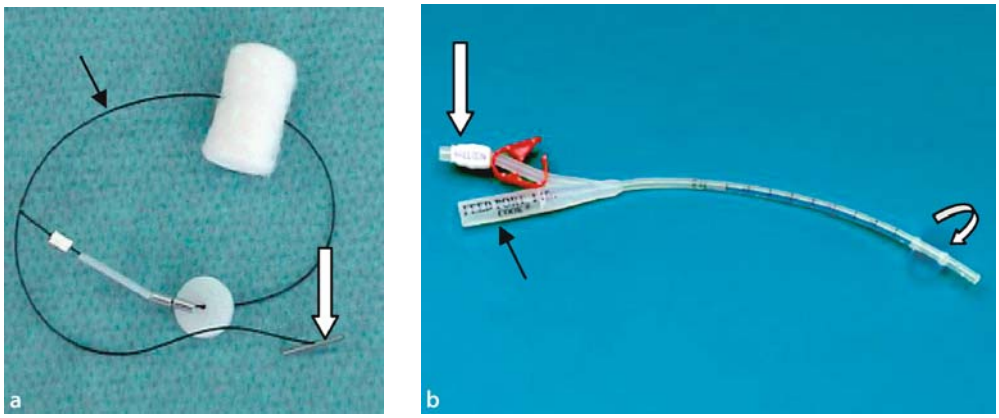

Fig. 16.8a,b T-fastener with fiber (*white arrow*) and T-bar (*black arrow*) (**a**). Example for a gastrostomy-set (Russell Gastrostomy tray; Copyright by Cook, William Cook Europe, Bjaeverskov, Denmark). Feeding lumen (*black arrow*), balloon inflation lumen (*white arrow*), and blocking balloon (*curved arrow*) (**b**)

Table 16.5 Available gastrostomy sets. (This list is not exhaustive)

Type	Manufacturer
1. Russell gastrostomy tray 2. Carey-Alzate-Coons Gastrojejunostomy Set	Cook, William Cook Europe, A Cook Group Company, Sandet 6, 4632 Bjaeverskov, Denmark
1. Corflo Cubby 2. Corflo Dual and Triple G-tubes	CORPAK 100 Chaddick Dr., Wheeling IL 60090, USA
1. EndoVive Standard PEG	Boston Scientific Corporate Headquarters, One Boston Scientific Place, Natick, MA, USA
1. Tri-Funnel Replacement Gastrostomy Tube 2. Button Replacement Gastrostomy Devices	C.R. Bard Inc., 730 Central Avenue, Murray Hill, New Jersey, 07974, USA
MIC-KEY Low-Profile Gastrostomy Tube Kit MIC* Gastrostomy	Kimberly-Clark, Belgicastraat 13, 1930 Zaventem, Belgium

through the needle into the stomach (Fig. 16.9b). While the guidewire is pushed forward, the T-fastener in the stomach has to be held by a nylon thread. Next the needle is removed and the anterior gastric wall is temporary fixed to the anterior abdominal wall by gentle tension on the T-fastener fiber. The guidewire is kept in intragastric position. Now the tract is dilated over the lying guidewire up to the size of the chosen gastrostomy catheter (Table 16.5). The Russell-Gastrostomy-tray requires insertion through a peel-away sheath (Fig. 16.9c). After placement the balloon is blocked with 5 ml of diluted contrast agent. The catheter is fixed by an extra corporal fastening plate (Fig. 16.9d). After this the T-fastener fiber is cut and the T-fastener leaves the body through the intestinal tract. Correct intragastric position must be documented (Fig. 16.9e).

16.3.5 Results

The reported technical success rate for PRG vary between 95% and 100% (Gottschalk et al. 2007; Neeff et al. 2003; Beaver et al. 1998; Wollmann et al. 1995). The largest series is a meta-analysis by Wollmann et al. (Table 16.6); they compared PEG, fluoroscopic PRG and surgical gastrostomy for technical success rate and found 99.2% for PRG, 95.7% for PEG and 100% for surgical gastrostomy.

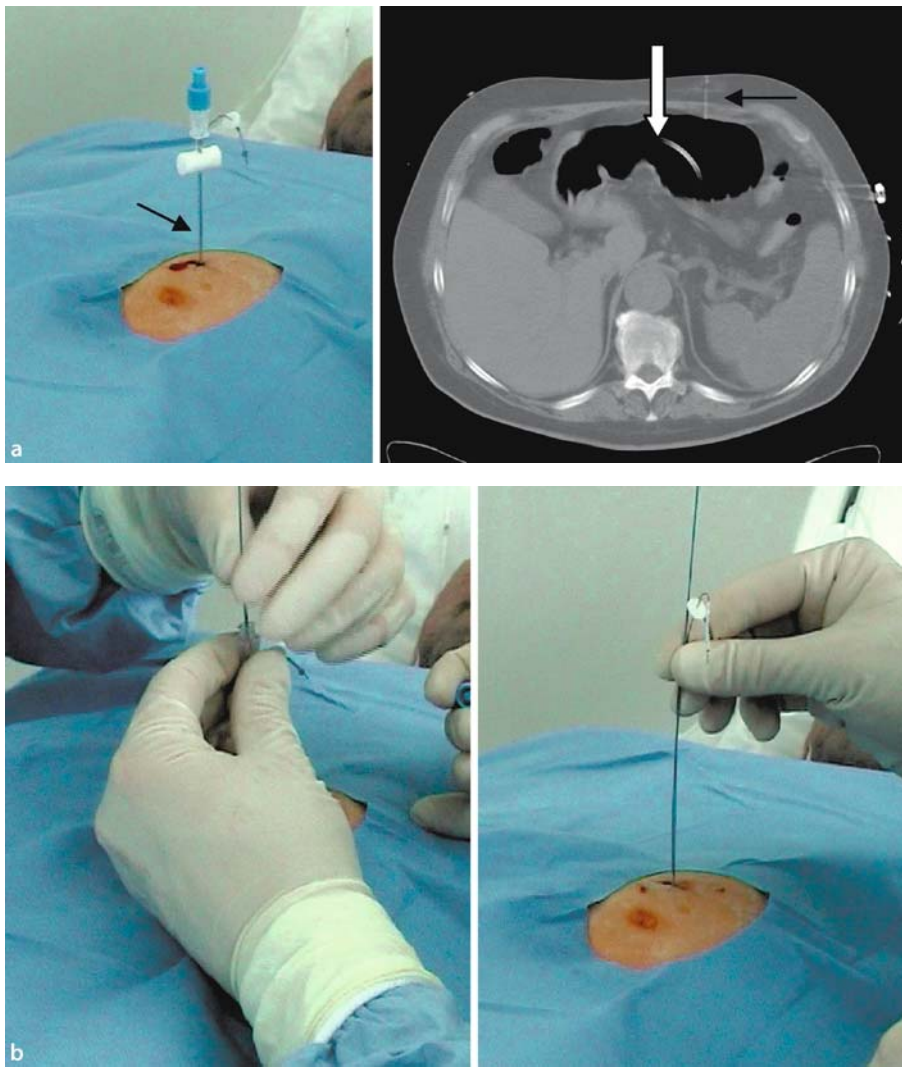

Fig. 16.9a,b Step-by-step illustration of a CT-guided gastrostomy: Percutaneous puncture with an 18-G hollow needle, containing a T-fastener. CT-scan with the needle (*black arrow*) in the distended stomach with lying nasogastric tube (*white arrow*) (**a**). A 0.0035-inch guide wire is inserted through the 18-G hollow needle in the stomach. Afterwards the 18-G hollow needle is removed. Then the fiber of the T-fastener is held under careful strain to fix the anterior gastric wall to the anterior abdominal wall (**b**)

16.3.6 Complications

The mortality and major complications with PEG and PRG are significantly lower than in the surgical group (Table 16.6). According to a recent study complications can be classified in minor (early and late) and major (early and late) complications (Gottschalk et al. 2007):

1. Early complications (within the first 3 days after gastrostomy)
   a) Major complications:
      - Dislocation of the feeding tube or required surgical intervention
      - Peritonitis
      - Hemorrhage requiring blood transfusion
      - Perforation

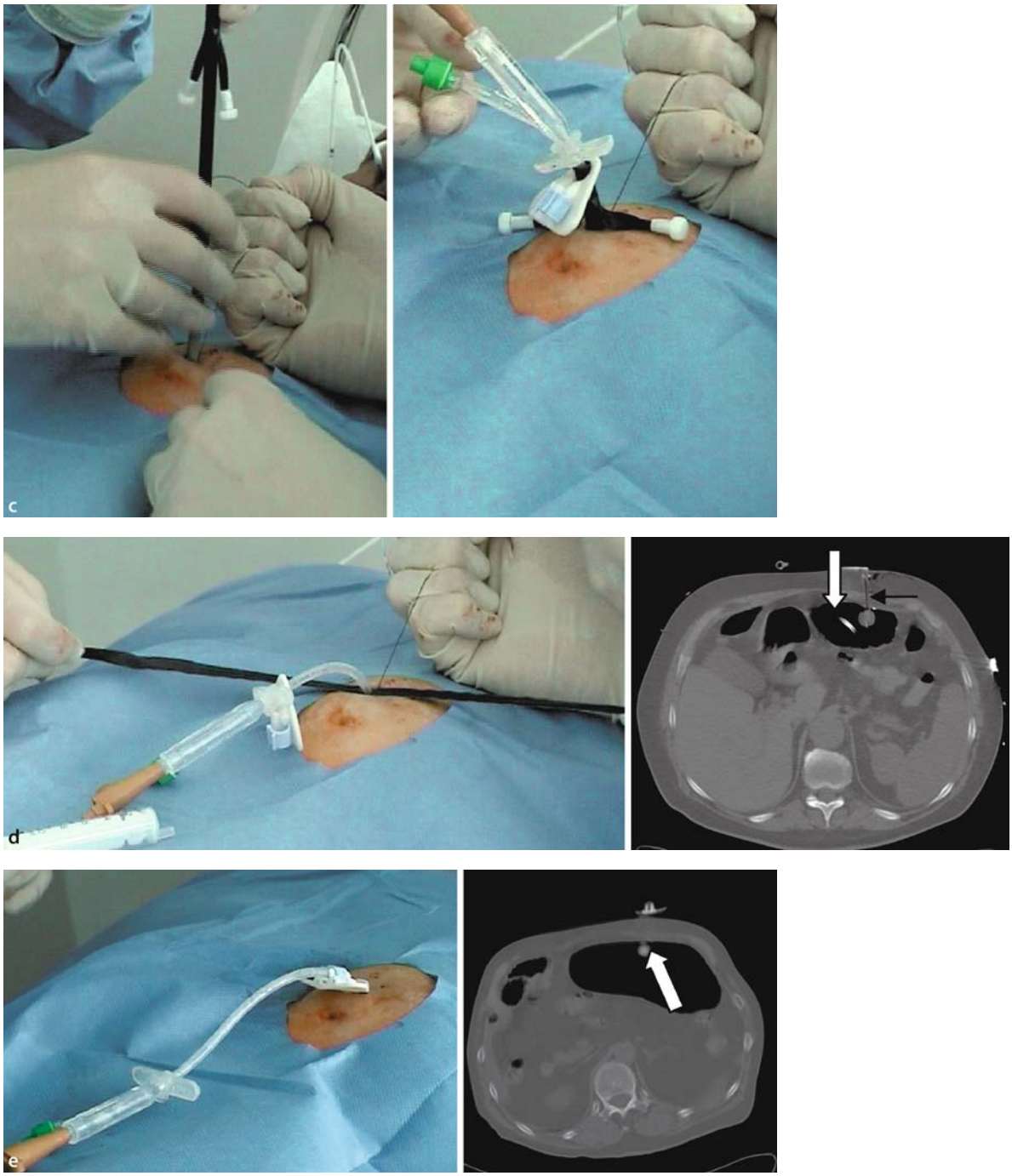

Fig. 16.9c–e The tract is dilated over the lying guide wire up to the size of the chosen gastrostomy catheter, and then the peel-away sheath is inserted. The gastrostomy set is inserted through a peel-away sheath (**c**). The peel-away sheath is removed. CT-scan with the blocked balloon of the gastrostomy-set (*black arrow*) and the nasogastric tube (*white arrow*). The T-fastener fiber is cut (**d**). The catheter is fixed by an extracorporal fastening plate. CT-scan to document the correct intragastric position of the catheter and the balloon (*white arrow*) (**e**)

Table 16.6 Meta-analysis of complication rates according to Wollmann et al. (1995)

	Surgical gastrostomy	PEG	PRG
Number of patients	721	4194	837
Technical success rate	100%	95.7%	99.2%
Procedural mortality rate	2.5%	0.5%	0.3%
Major complication rate	19.9%	9.4%	5.9%
Minor complication rate	9.0%	5.9%	7.8%

- Wound infection requiring systemic antibiosis
- Death associated with complication

b) Minor complications
- Wound infection requiring no systemic antibiosis
- Bellyache
- Peritubal leakages

2. Late complications (as from 4th day after gastrostomy)

a) Major complications
- Dislocation of the feeding tube or required surgical intervention
- Peritonitis
- Hemorrhage requiring blood transfusion
- Perforation
- Wound infection requiring systemic antibiosis
- Gastroparesis
- Death associated with complication

b) Minor complications
- Dislocation of the feeding tube in case of granulated puncture canal
- Bellyache
- Peritubal leakages
- Local irritations and self-limiting wound infections

Summary

PEG is in most cases the method of choice. The technical success rate is almost the same for PEG and PRG; even the complication rates are comparable. CT-guided PRG is a safe and helpful method when PEG is not possible due to anatomical reasons, for example Chilaiditi-syndrome, previous gastrectomy, and hepatomegaly or inadequate transillumination in PEG. Another special indication for CT-guided PRG is a high grade obstruction of the upper digestive tract with a gastroscopically not passable stenosis, because direct gastric puncture is feasible with CT guidance.

Key Points

- Consider the correct indication and contraindications.
- Use adequate materials.
- Ensure adequate gastropexy.
- Thorough watch and treat early and late complications.

References

Beaver ME, Myers JN, Griffenberg L, Kimberly W (1998) Percutaneous fluoroscopic gastrostomy tube placement in patients with head and neck cancer. Arch Otolaryngol Head Neck Surg 124:1141–1144

David VS, Gupta A, Zegel HG et al. (1998) Investigation of antibiotic propylaxis usage for vascular and nonvascular interventional procedures. J Vasc Interv Radiol 9:401–406

Gauderer MW, Ponsky JL, Izant RJ (1980) Gastrostomy without lapratomy: a percutaneous endoscopic technique. J Pediatr Surg 15:872–875

Given MF, Lyon SM, Lee MJ (2004) The role of the interventional radiologist in enteral alimentation. Eur Radiol 14:38–47

Given MF, Hanson JJ, Lee MJ (2005) Interventional radiology techniques for provision of enteral feeding. Cardiovasc Intervent Radiol 28:692–703

Gottschalk A, Strotzer M, Feuerbach S et al. (2007) CT-guided percutaneous gastrostomy: success rate, early and late complications. Fortschr Röntgenstr 179:387–395

McDermott VG, Schuster MG, Smith TP (1997) Antibiotic prophylaxis in vascular and interventional radiology. AJR Am J Roentgenol 169:31–38

Neeff M, Crowder VL, McIvor NP et al. (2003) Comparison of the use of endoscopic and radiologic gastrostomy in a single head and neck unit. ANZ J Surg 73:590–593

Pershaw RM (1981) A percutaneous method for inserting a feeding gastrostomy tube. Surg Gynaecol Obstet 152:659–660

Seitz J, Gmeinwieser M, Strotzer M et al. (1997) CT-guided gastrostomy and gastreoenterostomy: a reliable nonsurgical method also when percutaneous endoscopic gastrostomy is contraindicated or has failed. Dtsch Med Wschr 122:1337–1342

Wollmann B, D'Agostino HB, Walus-Wigle JR et al. (1995) Radiologic, endoscopic, and surgical gastrostomy: an institutional evaluation and meta-analysis of the literature. Radiology 197:699–704

16.4 Interventions Using C-Arm Computed Tomography

Frank K. Wacker and Bernard Meyer

16.4.1 Indications

Over the past 25 years, ultrasound (US)- and computed tomography (CT)-guided procedures and more recently magnetic resonance (MR)-guided interventions have proven to be safe, reliable, and provided accurate targeting of lesions for biopsy, drainage and therapy. As outlined in the previous chapters, CT is often chosen as a guidance modality over the less expensive and more flexible ultrasound, if the loss of an acoustic window attributable to air, bone, or artifacts prevents a sonographically guided intervention. Known disadvantages of CT guidance include limited possible scan plane orientations for puncture guidance, small gantry diameter limiting the needle length, low soft tissue resolution without intravenous contrast, and lack of availability of a CT scanner dedicated for interventional procedures.

Another challenge in an economically driven hospital environment is that lengthy procedures might occupy the CT suite that could otherwise be used for diagnostic studies. On the other hand, angiography suites are no longer busy with diagnostic angiograms as they are performed using CT angiography and MR angiography. Hence in many interventional suites there might be time slots that can be used for biopsies and drainage procedures. Since fluoroscopy alone does not provide sufficient soft tissue resolution, punctures had to be performed based on landmarks or in combination with ultrasound guidance. With the recent advent of C-arm CT (CACT), three-dimensional (3D) image acquisition can be performed in the angiography suite using the C-arm. Performing such procedures in the angiography room has several advantages:

1. Angiography suites are usually well equipped and staffed for interventional procedures allowing for easy patient handling and management.
2. C-arms with free floating tables facilitate easy patient movement in three directions and easy access to the patient without the need to bring the patient in and out of a scanner gantry for local anesthesia or needle advancement.
3. With a C-arm fluoroscopy is always at hand during the procedure for controlling needle position or guidewire and catheter placement, e.g. for drainage procedures.
4. CACT permits one to switch immediately to endovascular procedures, e.g. for managing complications of percutaneous interventions such as bleeding.

CACT has evolved from 3D rotational angiography. Digital flat panel detector (FD) angiographic systems with high frame rates and high contrast resolution facilitate 3D tomographic reconstructions, thereby resulting in a new class of hybrid C-arm systems capable of producing conventional, projectional fluoroscopy and angiography images as well as CT-like soft tissue images. As CACT is a relatively new technique, the full range of indications is not jet defined and depends largely on the imaging properties of this new modality. When compared to multislice spiral CT (MSCT), CACT provides higher spatial resolution, but encompasses a number of disadvantages, such as a slightly lower contrast resolution, a limited field of view and a lower temporal resolution. CACT is therefore not aimed at challenging standard clinical CT with regard to the typical diagnostic studies. Nevertheless, it can be seamlessly used for peri-interventional imaging in those procedures, in which current limitations are acceptable.

In percutaneous punctures, CACT can act as a mere replacement for conventional CT as it also acquires axial slices similar to CT images. Furthermore, it provides the ability to use fluoroscopic controls, e.g. for needle propagation or contrast injections in drainages and therefore adds pertinent intraprocedural imaging options.

Another range of applications for CACT are catheter-based endoluminal interventions, which are usually done in the angiography suite based on 2D images alone. In those interventions, CACT bridges the gap between rotational 3D angiography and conventional CT and allows for imaging beyond blood vessels, visualizing soft tissue and thus alleviating complex procedures such as TIPSS placement (Sze et al. 2006), transarterial embolization and chemoembolization (Meyer et al. 2007a) and complication management in challenging neurointerventional cases (Heran et al. 2006).

16.4.2 Materials and Techniques

16.4.2.1 Technical Background of C-Arm CT

The idea to use a C-arm for acquisition of projection data over a partial circle-scan trajectory comprising at least 180° was first pursued in the early 1990s using C-arms equipped with image intensifier. That setup facilitated 3D imaging of high-contrast objects such as osseous structures and blood vessels during intra-arterial contrast injections. A few yeas ago, FD technology, initially developed for radiography, started replacing image intensifiers on angiography C-arm systems (Fahrig et al. 2004). FDs can dispense with image intensifiers distortion correction, provide a wider dynamic range and high image quality at high frame rates. When mounted on C-arm gantries facilitating at least 200° partial circle-scans, they provide a two-dimensional (2D) data acquisition setup for subsequent 3D reconstruction of CT-like images (Kalender 2006) Terms such as C-arm CT (CACT), FD-CT, cone-beam CT, angiographic CT, DynaCT® (Siemens Medical Solutions), Innova CT® (GE Healthcare) or XperCT® (Philips Medical Systems) are used to describe this relatively new technology.

The current basic principle of FD still relies on the conversion of X-rays to light using a fluorescence scintillator screen. The light emitted is then recorded by an array of photodiodes. Direct-conversion detectors, e.g., based on photon counting principles, are not yet commercially available. The standard detector frame rate for 2D clinical radiographic X-ray imaging on C-arm systems typically ranges between 1 to 6 frames per second but can be increased to 15 images per second if needed. For CT-like image acquisition in a C-arm system, higher readout rates of up to 60 images per second are desirable. This can be achieved with an FD using detector pixel binning that combines 2×2 or 4×4 pixels to be read out as one pixel. This enables faster readout rates up to 60 images per second by reducing the amount of data acquired. Noise and spatial resolution are also reduced. It is important to note that even with 2×2 binning, the spatial resolution of CACT still exceeds that of most current MSCT scanners. The reduction of noise is also beneficial to the contrast resolution which is known to be slightly inferior with CACT in comparison to MSCT at any given dose level.

Since CACT is an optional feature with angiography systems, the basic system design including X-ray source is still optimized for fluoroscopy and digital subtraction angiography applications. In contrast to MSCT, the X-ray source usually has a smaller focal spot, lower power limits, and it operates at voltage levels below 90 kV. As far as the mechanical properties of the C-arm are concerned, a circular scan range over 180−240° is needed together with a stable, reproducible gantry motion behavior. Thus the system can be calibrated for 3D image acquisition facilitating 3D images.

Due to the special geometry of non-ideal orbits based on the mechanic instability of a C-arm, accurate knowledge of the source and detector positions at each projection view and reproducibility of the positions is required for high-quality CACT image reconstruction. Techniques for geometric calibration of CACT systems have been previously reported (Fahrig and Holdsworth 2000). They usually provide removal of misalignment artifacts implicitly assuming a non-stable but reproducible imaging geometry (Wiesent et al. 2000). It remains to be seen, if more stable C-arm geometries such as the previously launched angiography system mounted on an industrial grade robotic arm by one vendor has the potential to further overcome misalignment artifacts.

In addition to mechanical instabilities, CACT is also characterized by smaller cone angles which results in artifacts due to data truncation and high scatter intensities. Truncation artifacts occur when the currently limited field of view of the CACT scanner does not cover the volume of a patient. Tomographic reconstruction from truncated projections impact the accuracy of the reconstructed CT values and it disturbs the quantitative diagnostic quality of the images. Correction algorithms have been developed to restore image quality and improve the accuracy of the CT values in the field of view (Ohnesorge et al. 2000). The high scatter-to-primary ratios in the acquired input projections are due to its 2D character with 30 cm height and 40 cm width, e.g., comprising around 1000 rows in a typical 2×2 binning configuration. This can induce a drop in CT values towards the centre of the patients. Scatter correction algorithms are available to improve CT value accuracy. The use of anti-scatter grids can also decrease the scatter artifact, but it results in a higher radiation dose due to its presence in

front of the detector. In addition to CACT specific artifacts, other well known tomographic imaging artifacts also occur, including beam hardening, e.g. due to metal within the scan range or detector element malfunction.

Dose considerations for CACT are largely the same as in MSCT. Traditional CT dose metrics such as the computed tomography dose index, CTDI, which represents a dose inside a standard phantom, are no longer applicable for both, MSCT and CACT, since the beam coverage in the z direction has increased to up to 30 cm in both techniques. As a result, standard CTDI phantoms and ionization chambers with a length of 150 mm and 100 mm, respectively, only measure a poor approximation of the true dose. Therefore comparisons of modern MSCT and CACT systems, including their dose characteristics, are challenging. Different approaches are currently being pursued and a consensus on how to proceed exactly is yet to be found. The relationship between tube voltage, image noise, dose, and contrast perception are discussed in great detail by Fahrig et al. (2006) and Kalender and Kyriakou (2007).

Although it is beyond the scope of this chapter to provide exact details on how to perform a CACT scan, we want to provide typical guideline values for the acquisition of CACT images of the abdomen or pelvis. The data are taken from an Axiom-Artis angiography flat detector C-arm (Siemens Medical Solutions, Forchheim, Germany). Usually an 8-s rotation with a total scan angle of 240°, a projection angle increment of 0.5°, and a system dose per pulse of 0.36 μGy is performed. The scan range that can be covered with the biggest detector currently available has a cylindrical shape with a cranio-caudal coverage of 185 mm and a transverse and sagittal scan range of 225 mm. For image reconstruction the raw data set is sent to a dedicated 3D image reconstruction workstation. It generates an isotropic voxel data set with typical voxel sizes of around 0.4 mm which can be viewed using multiplanar cross-sectional images as well as maximum intensity projection as well as volume rendering techniques. The generation of a 3D data set with 512×512 matrix size takes usually less than 1 min when a fast network connection between the C-arm system and the reconstruction workstation is used.

16.4.2.2 Percutaneous Puncture Technique Using C-Arm CT

CACT guided punctures in the angiography suite have several advantages: equipment and staff are dedicated to performing interventional procedures, and easy patient access and fluoroscopic as well as US guidance are available if needed. With the current C-arm systems there are different techniques that facilitate percutaneous punctures in the angiography suite. Punctures can be performed using intermittent acquisition of CACT images. This is similar to the traditional CT puncture technique that uses intermittent control scans allowing for a stepwise control of the actual needle position. Since repeated confirmation of the needle path is necessary, this requires the acquisition of multiple CACT volumes resulting in relatively long procedure times and radiation exposure. To reduce the patient radiation dose, the volume of interest can be collimated from top and bottom leaving open a slab that covers only the needle and the immediate surroundings. Finding the entry point is more difficult in a C-arm than in CT, where the slice selection is usually done using the positioning laser in combination with an external marker grid. In a C-arm there is no laser provided that could be used to find the entry point. Therefore an external grid has to be placed based on external landmarks, which makes the definition of the needle entry point less intuitive.

To overcome boundaries that are associated with intermittent CACT control scans during the puncture, fluoroscopy can be used to control the needle advancement. Since most targets are not visible under fluoroscopy and fluoroscopy offers only one projection image at a time, additional features are needed to facilitate safe and reliable puncture. One approach is, to use a graphic overlay on top of the live fluoroscopic image that helps outlining the needle entry point and the needle path with different C-arm angulations. The initial planning of the needle path has to be performed prior to starting the puncture on CACT images. Once the skin entry has been made, the C-arm can be brought in a position perpendicular to the needle and the depth can be determined based on live images, the graphic representation of the target and a virtual needle path superimposed on the live fluoroscopic image. In addition to overlaying the live fluoroscopic image with

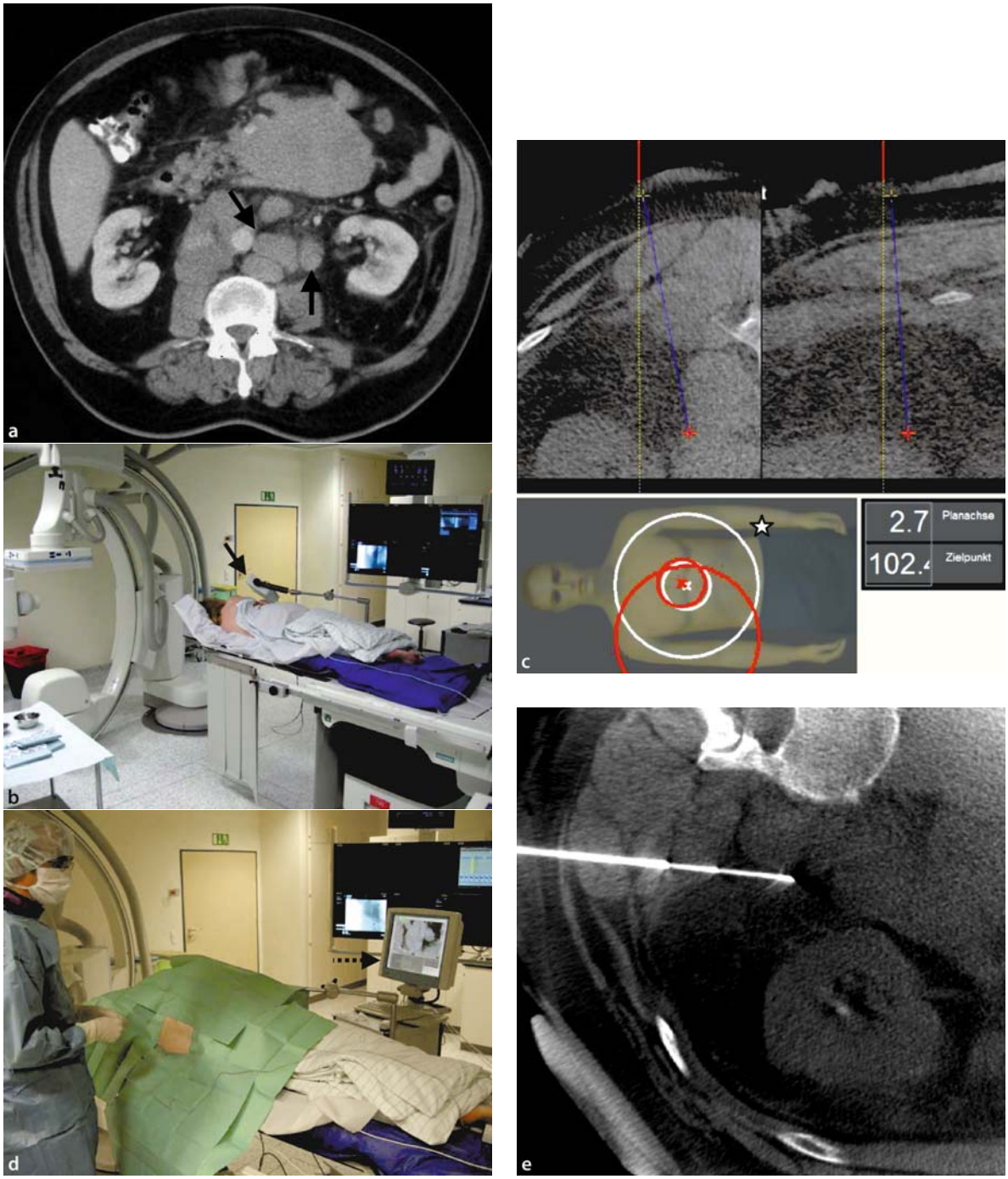

Fig. 16.10a–e Biopsy of an enlarged retroperitoneal lymph node. **a** MPR of the upper abdomen MDCT shows multiple enlarged retroperitoneal lymph nodes (*arrow*). **b** Photograph of the setting of an electromagnetic field-based navigation device (ND). The patient is bedded on a vacuum mattress to avoid movements during baseline CACT scan and intervention. **c** Initial phase of the puncture. Screen-shot shows two preprocedural CACT images that are displayed orthogonal to the needle (*red line*) in real time. The virtual needle extension (*yellow dotted line*) eases the correct angulation of the needle. The selected skin entry point (*yellow cross*) and the puncture target (*red cross*) are also superimposed on the MPR images. The schematic ring figure (*asterisk*) summarizes both the depth of the needle tip as well as the needle orientation. **d** The sterile covered field generator (*arrow in **b***) is attached to the patient table and connected to the ND (*dotted arrow*). **e** The transversal MPR image of the post-interventional CACT scan confirms the correct needle placement

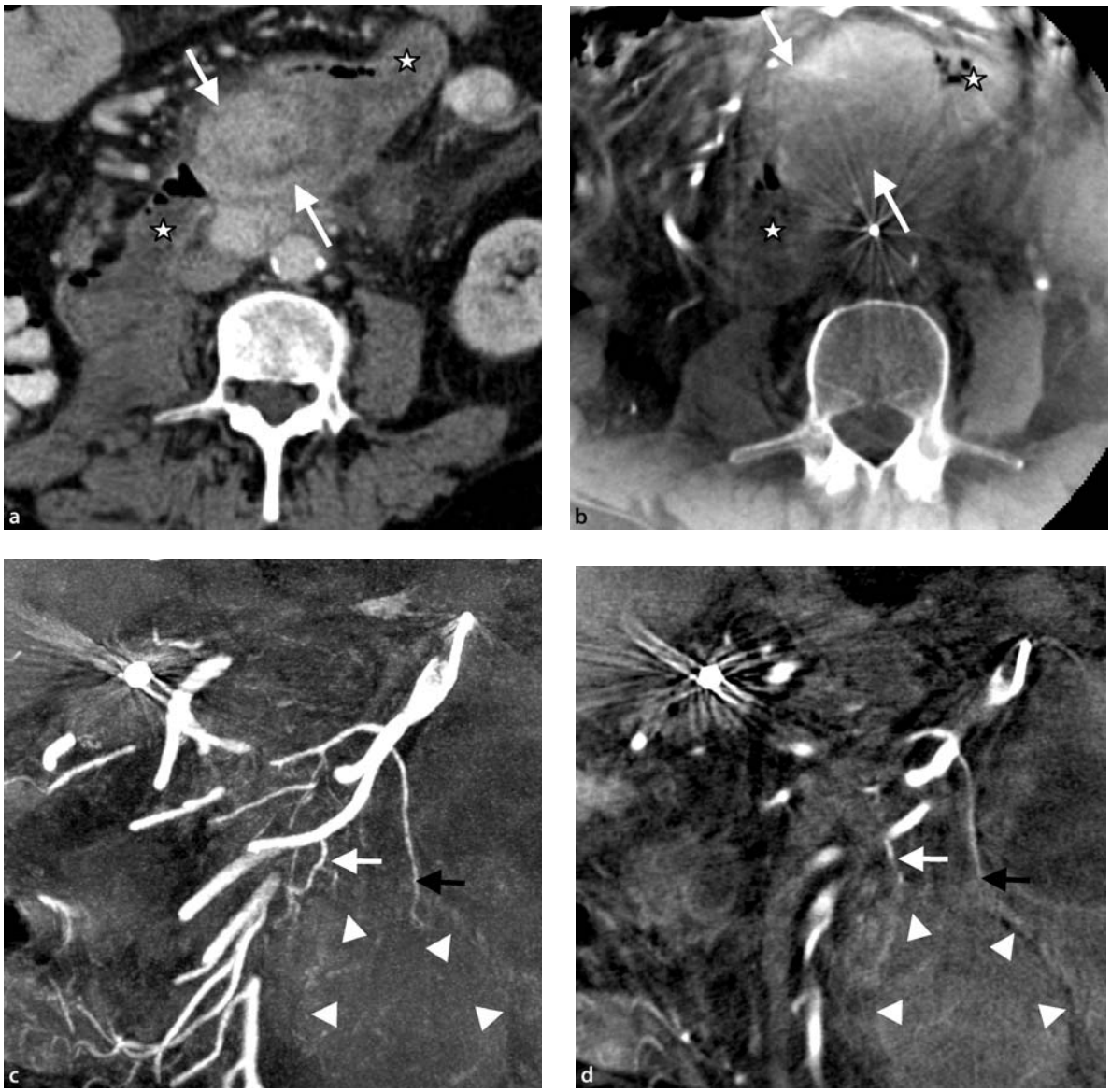

Fig. 16.11a–d Embolization of a liposarcoma infiltrating the duodenum. **a**,**b** MDCT and CACT of the abdomen show a large tumor (*arrows*) infiltrating the duodenum (*asterisk*). **c**,**d** MIP (15 mm, **c**) and MPR (5 mm, **d**) of the CACT in the arterial phase provides information on both, feeding vessels as well as soft tissue of the tumor (*arrowheads*) and the surrounding structures. This enables clear-cut identification of two tumor feeding arteries (*white and black arrow*)

graphic features representing the target and the virtual needle trajectory, the actual CACT images (and any other information that can be fused with the CACT mages) can be displayed as an overlay. With both methods, however, it is important to avoid any patient movement between acquisition of the planning CACT and the actual procedure.

The need for both repeated CACT as well as intermittent fluoroscopy can be overcome by using navigation systems for needle tracking. Such systems provide navigation information visualizing the puncture needle and roadmap information based on imaging obtained prior to the puncture. Careful trajectory planning within the 3D roadmap allows the physician to

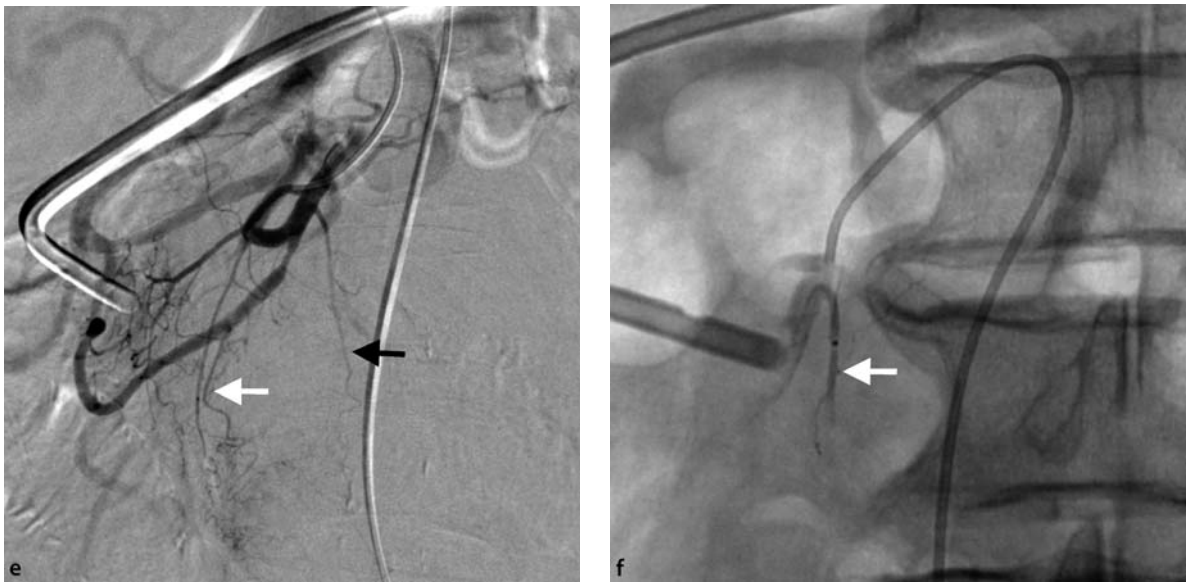

Fig. 16.11 **e** DSA of the SMA shows multiple small branches but conclusive identification of tumor feeding vessels is not provided. **f** Selective angiogram proves successful embolization of one of the feeding vessels (*white arrow*, same vessel as in **c–e**) (from Meyer et al. 2007a)

"see" nearby anatomy when planning the procedure as well as during needle advancement without any additional radiation exposure. Advantages are free needle angulations, use of additional image information such as MR imaging, CT, or positron emission tomography (PET) that can be coregistered with the 3D roadmap for virtual navigation, and, as mentioned before, reduction of radiation exposure to the patient and interventionalist. Disadvantages are need for coregistration of the patient's body with the 3D space of the navigation system, respiratory, bowel and patient motion error as well as organ shift during the needle advancement. There are optical as well as electromagnetic tracking systems available on the market. With optical needle tracking methods, known limitations are line-of-sight problems with the optical markers at the needle end and positioning errors due to needle bending. These problems have more recently been overcome with electromagnetic tracking. Here an electromagnetic field generator (Fig. 16.10) is placed in proximity to the patient. The field generator produces an ultra-low electromagnetic field that induces very weak currents in the sensor coils in the needle tip as well as the reference frame. The current strength in these coils is dependent on the location, the position and the orientation of the detector and can thus be measured and localized within the electromagnetic space. The main advantage over optical navigation is that the actual needle tip position is electromagnetically tracked in real time, whereas with optical systems the needle tip must be calculated from the position and orientation of the needle end outside the body. The precision of electromagnetic navigation systems however may be limited if relevant amount of ferromagnetic metal such as a CT gantry is present in the proximity of the field generator.

Most needle tracking systems have been developed for use in CT. However, most CT guided procedures are currently performed without a navigation system. Among other reasons this is because ease of use of such navigation systems is often limited by lengthy software setups, tedious registration processes and lack of seamless integration with the imaging system. With the advent of CACT, however, navigation systems have gained increased interest. This is mainly because finding the optimal skin entry point in relation to the deeper laying target is more difficult with CACT than with conventional CT. In addition, the acquisition of a CACT takes longer than the acquisition of a CT scan, at least with the currently available

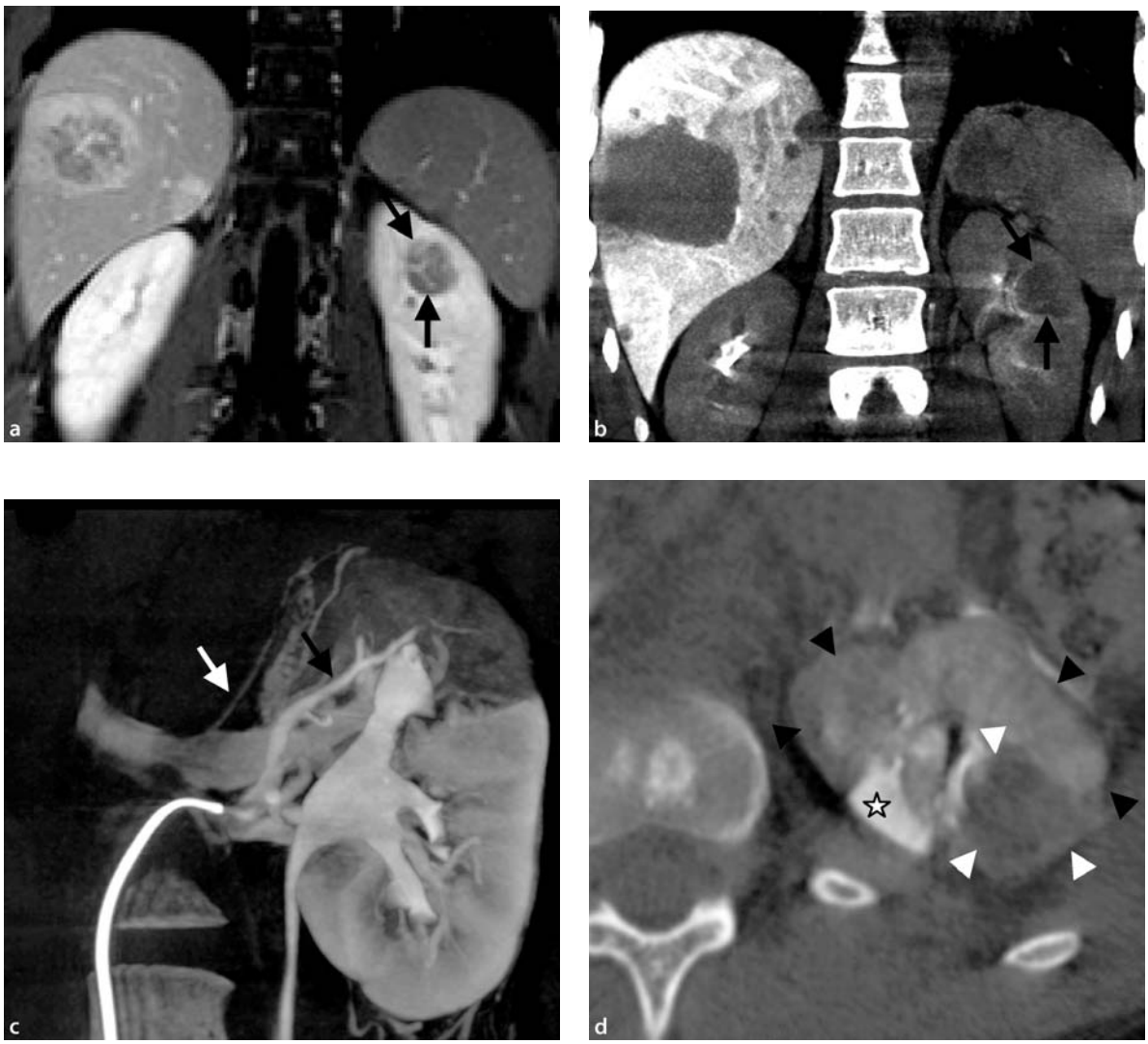

Fig. 16.12a–d Embolization of a renal metastasis for pain management. **a** Coronal T1-weighted fat-saturated post-contrast MRI acquired prior to the intervention, shows hepatic metastases and renal metastasis in the upper third of the left kidney (*arrow*). **b** CACT of the upper abdomen in the portalvenous phase. Disseminated hepatic metastases and renal metastasis in the upper third of the left kidney (*arrow*). **c,d** CACT images acquired after chemoembolization of the left kidney. The perfusion defect in the upper pole of the kidney can clearly be appreciated. A segmental artery feeding the upper pole is still opacified (*black arrow*). CACT allows differentiation of the perfusion defect (*black arrowhead*), metastasis (*white arrowhead*), and the normally perfused renal parenchyma (*asterisk*). Note: Excellent visualization of the small left adrenal gland vein (*white arrow*) (from Meyer et al. 2007a)

C-arms. Therefore, a well integrated navigation system could provide more time saving in percutaneous CACT interventions when compared with conventionally CT-guided interventions.

Although the use of electromagnetic navigational systems with multiple other modalities has been performed, the use of such a system with CACT is new. In general, pre-procedural imaging has to be performed before the puncture. After data acquisition and image reconstruction, the 3D data set is sent to the navigation system using a local area network Ethernet connection. Coregistration of the tracking space

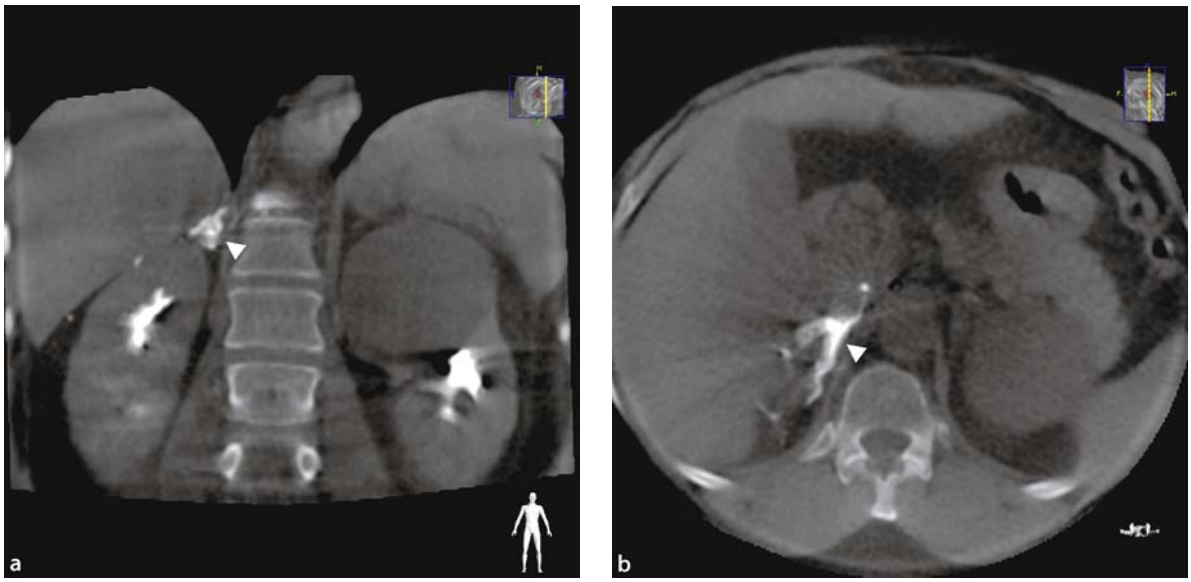

Fig. 16.13a,b CACT of the adrenal gland. **a,b** Coronal and axial MPR of C-arm CT performed during hand-injection of contrast medium via a catheter in the adrenal vein demonstrate opacification of the right adrenal gland (*white arrowhead*), confirming proper catheter position. The medial and lateral limbs of the gland are clearly identified. (Images courtesy of Christos Georgiadis, Johns Hopkins School of Mecicine, The Russell H. Morgan Department of Radiology and Radiological Science)

and the CACT image space can be performed using skin or anatomic fiducial markers. In one system a reference frame inside the scan range with radiopaque markers and two sensor coils allow for automatic coregistration. After successful registration, real-time tracking of the needle within the electromagnetic space is performed. This is facilitated through a small coil embedded in the tip of the needle which is connected to the interface of the navigation system. Based on the current in the coil, the position of the needle tip is displayed in real time on the CACT images.

16.4.2.3 Catheter Based Interventions Using C-Arm CT

Vascular interventions are usually performed in an angiography suite relying on 2D real time projection radiography with poor soft tissue contrast and no 3D information. This problem led to installation of the first combined suites or hybrid suites with both CT and digital subtraction angiography (DSA) units a decade ago (Capasso et al. 1996). These suites were used for various clinical indications, such as selective arterially enhanced CT examinations, organ and lesion perfusion studies before embolization and local chemotherapy, and combined CT- and fluoroscopy-guided interventions such as percutaneous biopsy and catheter drainage, bone interventions, and CT arthrography (Capasso et al. 1996; Froelich et al. 2000a,b; Vanderschelden et al. 1998). More recently, hybrid units combining DSA and MR imaging systems have been developed (Vogl et al. 2002; Dick et al. 2005). However, such suites require higher investment cost and spacious room for equipment installation in comparison to a single fluoroscopy C-arm angiography. In contrast to such hybrid suites, modern FD-C-arms with CACT capability offer unrestricted availability of both, digital subtraction angiography and cone-beam volume CT. Risky and time-consuming patient transfer from the angiography table to other imaging modalities such as MR or CT can be avoided. Since CACT is a relatively new technique, only few reports exist on clinical applications of CACT during catheter based interventions and many of the potential benefits of CACT mentioned earlier (in the "Indications" section) have not yet been evaluated.

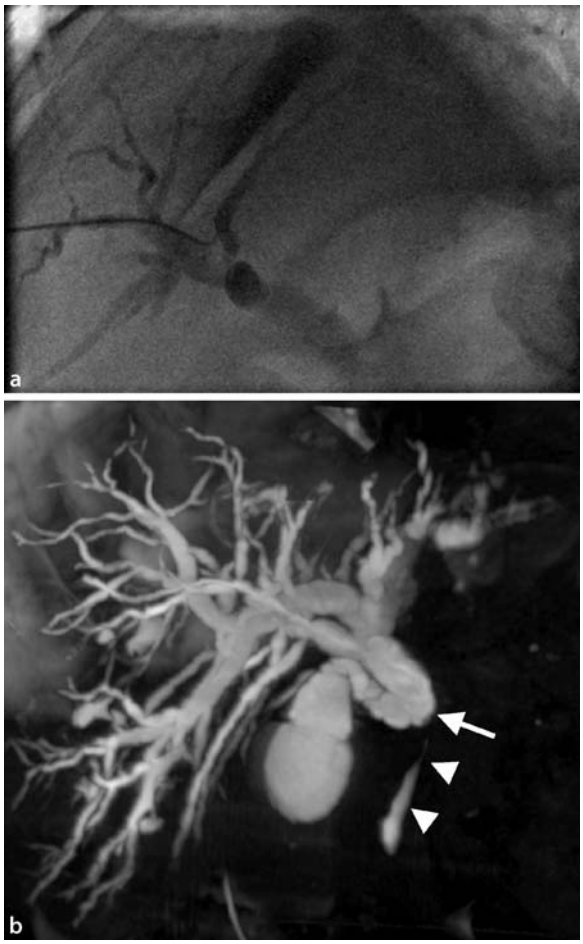

Fig. 16.14a,b PTC and direct CACT-cholangiography. **a** Fluoroscopic image after puncture of a right hepatic bile duct, contrast injection and insertion of a guidewire. **b** CACT-cholangiography after injection of diluted contrast material through the drainage catheter shows the subtotal stenosis of the common bile duct (*arrow*) followed by a filiform stenosis of the subsequent segment (*arrowhead*) caused by a tumor in the pancreas head. Due to the high endoluminal contrast, a high window level allows for a clear delineation of the small bile duct branches even with MIP

Fig. 16.15a–f ► TACE of the liver. **a**,**b** Coronal MPR (3 mm) of the MDCT (**a**) and the CACT (**b**), both in the portal venous phase. The disseminated hepatic metastasis as well as the segmental partial thrombosis of the portal vein (*arrow*) can be better appreciated with CACT. **c** DSA shows the left hepatic artery feeding liver segments 2, 3, and 4 (*arrow*) coming off the prominent left gastric artery. **d** Enlarged view of the DSA shown in **c**. Clear classification of the three proximal side branches of the left gastric artery could not be achieved on a single projection. **e**,**f** Coronal curved-MPR of the CACT with simultaneous presentation of both the soft tissue as well as the arteries, facilitates clear identification of the gastric branches (white arrowhead in d and e), a phrenic branch (*black arrowhead* in **d** and **e**), and a hepatic branch (*black arrow* in **d** and **f**) feeding liver segments 2 and 3. Based on these findings, the catheter for chemoembolisation of the left liver lobe was positioned at the arrowhead shown in **c**. St = Stomach, Ao = Aorta, L = Liver, Sp = Spleen, H = Heart (from Meyer et al. 2007a)

16.4.3 Results

16.4.3.1 Results of Percutaneous Punctures Using C-Arm CT

Currently only preliminary results are available on CACT guided percutaneous interventions. In an accuracy evaluation based on a 3D rotational X-ray system with an image intensifier rather than an FD and a camera based optical navigation system, an error below 3 mm was obtained in cadavers (van de Kraats et al. 2002). In a preclinical evaluation of the accuracy of an electromagnetic tracking system (CAPPA IRAD EMT, CAS innovations AG, Erlangen, Germany) in combination with an FD-CACT, our group reported a technical error of 1.0–1.4 mm. In phantoms, targeting a lesion 7 mm in diameter was successful in 97% of the punctures with a mean error of 2.6 mm using the same system (Meyer et al. 2007b). Initial clinical applications of the electromagnetic tracking system are promising. In a pilot study at our institution the needle deviation was less than 10 mm for targets as deep as 20 cm. So far we have targeted only lesions that were not prone to breathing motion such as retroperitoneal lymph nodes or abscesses.

For needle guidance using virtual graphic overlay there is a recent pictorial essay presenting seven cases that were done using this technique (Racadio et al. 2007). The authors state that this technique ensured accurate needle advancement following user defined trajectories in all cases. In this essay no data on precision of needle placement is given. In our own experience, with phantoms, animals, and patients using a similar technique on a different platform, the mean error was below 2 mm for phantoms and below 10 mm for animals and patients. Based on the experience in our own group and on the results in the literature, CACT guided punctures have the ability to expand the range of procedures that can be performed in an angiography suite. One of the main advantages is the seamless transition from a CACT guided to a fluoroscopy guided

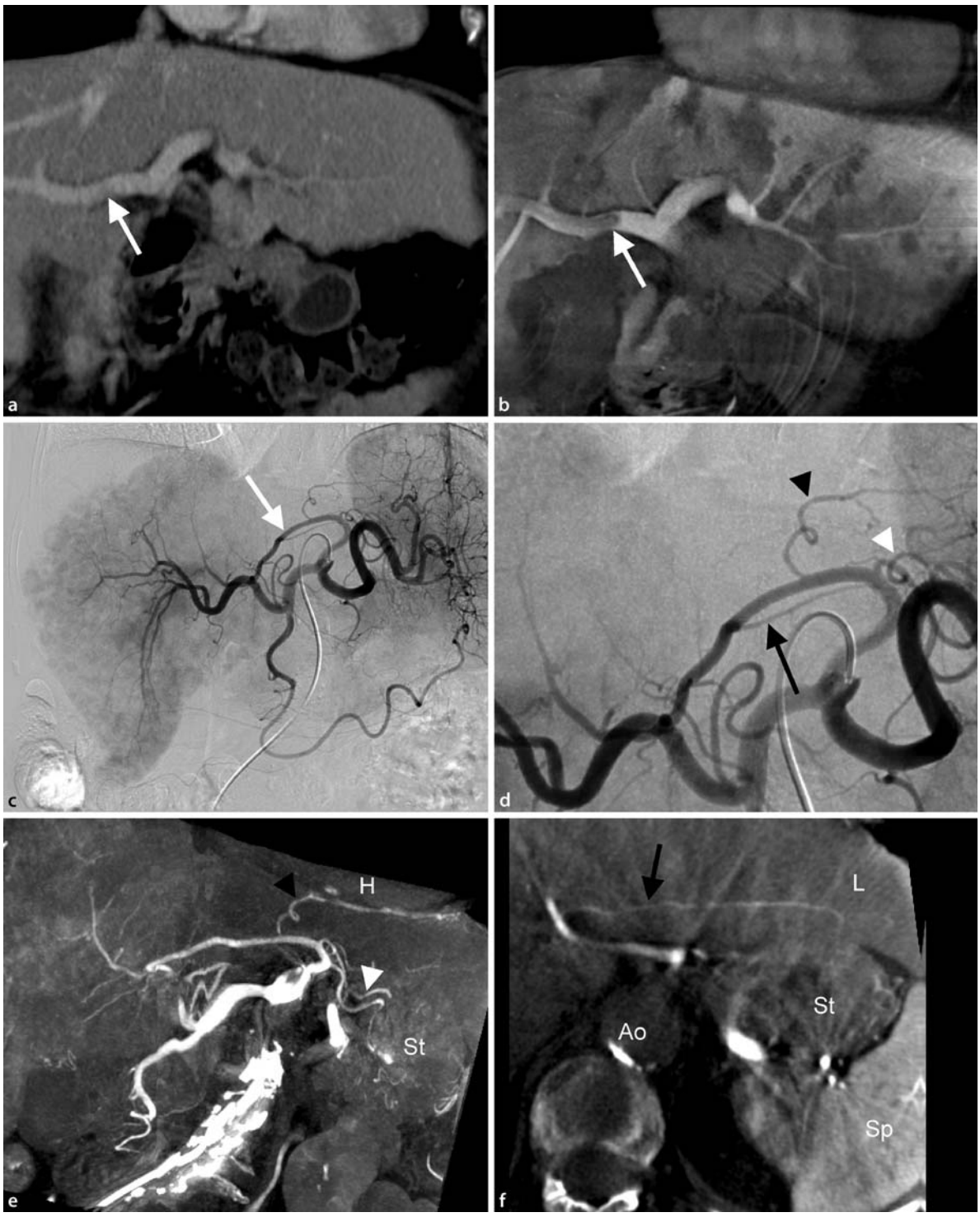
a
b
c
d
H
St
e
L
St
Ao
Sp
f

intervention for procedures such as percutaneous biliary drainage (Fig. 16.11), percutaneous nephrostomy, abscess drainage or percutaneous endoleak embolization.

16.4.3.2 Results of Catheter Based Interventions Using C-Arm CT

One major benefit of 3 D information provided by CACT during angiography was found to be the identification of tumor feeding arteries in cases with a complex anatomy or multiple feeding arteries (Figs. 16.12 and 16.13). In one study the anatomic detail on continuous cross-sectional CACT imaging was advantageous over DSA alone in patients with advanced head and neck tumors for superselective intra-arterial chemotherapy thus enabling higher concentrations of chemotherapeutic agents into the tumor bed with fewer systemic toxic effects than normally seen with systemic chemotherapy (Kakeda et al. 2007). The same was true for embolization procedures in abdominal tumors (Meyer et al. 2008). Here, CACT in combination with the intraarterial contrast injection leads to improved visualization of smaller vessels that compares favorably to MSCT during intravenous administration of contrast medium.

In other small series, CACT was instrumental for the creation of TIPS (Sze et al. 2006), for the detection of intracranial hemorrhage (Heran et al. 2006), and for the confirmation of the catheter position during adrenal vein gland blood sampling (Fig. 16.14) (Georgiades et al. 2007). In a study in patients undergoing transarterial chemoembolization of the liver from our group, the angiographic C-arm was used to perform the procedure under fluoroscopic control as well as to acquire CACT images during contrast injection into the hepatic and superior mesenteric artery (Fig. 16.13b). This is comparable to CTHA and CTAP using conventional CT, which rely on selective delivery of contrast material to the liver via the hepatic artery and the portal vein and are known to have sensitivities around 90% for the detection of hypervascular liver lesions (Spreafico et al. 1997). Triggered by the cumbersome patient handling the success of MR imaging with liver specific contrast agents led to a sustained decline in usage of CTHA and CTAP over the last decade. With CACT, however, no patient transfer is necessary and inter-observer agreement for segmental tumor involvement in the liver was very good during intraarterial contrast administration and compared favorably to that of MDCT (Meyer et al. 2008).

Potential disadvantages of CACT include increased amount of contrast agent, additional radiation exposure and additional time required for setup, CACT run and reconstruction. In our experience however the detailed information on vascular anatomy provided by CACT helps to avoid additional oblique DSA runs thus reducing radiation and amount of contrast with the interventional procedure. It remains to be seen if this compensates for the time, dose and contrast agent used for CACT during catheter based interventions.

16.4.4 Complications

CACT is a relatively new technique with only few reports on clinical applications. Most of them use CACT during catheter based interventions and only few papers exist on percutaneous punctures using CACT. Complications are more likely to be related to the procedure itself and specific complications of CACT have, to the best of our knowledge, not yet been reported.

Summary

The increasing complexity of minimally invasive procedures requires a continuous improvement in imaging technologies that guide and monitor such procedures. Modern FD-C-arms with CACT technology combine 3D soft tissue imaging, real time fluoroscopy and high resolution angiography without the need for transferring the patient to another imaging modality. Since CACT is a relatively new technique, the workflow is not yet established, its benefits for interventional procedures have not been fully determined and only few reports exist on actual clinical applications. However, based on the preliminary results obtained so far, its potential goes beyond just copying existing procedures currently performed in an angiography or CT suite towards the guidance of minimally invasive techniques that need the full breadth of information available in an C-arm with CACT capabilities.

Key Points

- CACT requires FD angiographic systems to produce CT-like soft tissue images.
- CACT currently provides slightly higher spatial and lower contrast and temporal resolution, and a limited field of view when compared to MSCT.
- CACT is beneficial for percutaneous as well as endovascular procedures.
- In the course of an interventional procedure, CACT provides 3D soft tissue information similar to MSCT without the need for transferring the patient.

References

Capasso P, Trotteur G, Flandroy P, Dondelinger RF (1996) A combined CT and angiography suite with a pivoting table. Radiology 199(2):561–563

Dick A, Raman V, Raval A et al. (2005) Invasive human magnetic resonance imaging during angioplasty: feasibility in a combined X-ray/MRI suite. Catheter Cardiovasc Intervent 64(3):265–274

Fahrig R, Holdsworth DW (2000) Three-dimensional computed tomographic reconstruction using a C-arm mounted XRII: image-based correction of gantry motion nonidealities. Med Phys 27(1):30–38

Fahrig R, Ganguly A, Starman JD, Strobel N (2004) C-arm CT with XRIIs and digital flat panels: a review. SPIE, Denver, CO, USA, pp 400–409

Fahrig R, Dixon R, Payne T, Morin RL, Ganguly A, Strobel N (2006) Dose and image quality for a cone-beam C-arm CT system. Med Phys 33(12):4541–4550

Froelich JJ, El-Sheik M, Wagner HJ, Achenbach S, Scherf C, Klose KJ (2000a) Feasibility of C-arm-supported CT fluoroscopy in percutaneous abscess drainage procedures. Cardiovasc Intervent Radiol 23(6):423–430

Froelich JJ, Wagner HJ, Ishaque N, Alfke H, Scherf C, Klose KJ (2000b) Comparison of C-arm CT fluoroscopy and conventional fluoroscopy for percutaneous biliary drainage procedures. J Vasc Interv Radiol 11(4):477–482

Georgiades CS, Hong K, Geschwind JF et al. (2007) Adjunctive use of C-arm CT may eliminate technical failure in adrenal vein sampling. J Vasc Interv Radiol 18(9):1102–1105

Heran NS, Song JK, Namba K, Smith W, Niimi Y, Berenstein A (2006) The utility of DynaCT in neuroendovascular procedures. AJNR Am J Neuroradiol 27(2):330–332

Kakeda S, Korogi Y, Miyaguni Y et al. (2007) A cone-beam volume CT using a 3D angiography system with a flat panel detector of direct conversion type: usefulness for superselective intra-arterial chemotherapy for head and neck tumors. AJNR Am J Neuroradiol 28(9):1783–1788

Kalender WA (2006) X-ray computed tomography. Phys Med Biol 51(13):R29–43

Kalender WA, Kyriakou Y (2007) Flat-detector computed tomography (FD-CT). Eur Radiol 17(11):2767–2779

Meyer BC, Frericks BB, Albrecht T, Wolf KJ, Wacker FK (2007a) Contrast-enhanced abdominal angiographic CT for intra-abdominal tumor embolization: a new tool for vessel and soft tissue visualization. Cardiovasc Intervent Radiol 30(4):743–749

Meyer BC, Nagel MH, Peter O et al. (2007b) Evaluation of an electromagnetic field-based navigation device for angiographic cone beam CT. Eur Radiol 17(Suppl 1):320

Meyer BC, Frericks BB, Voges M et al. (2008) Visualization of hypervascular liver lesions during TACE: comparison of C-Arm CT and MDCT. AJR Am J Roentgenol (in press)

Ohnesorge B, Flohr T, Schwarz K, Heiken JP, Bae KT (2000) Efficient correction for CT image artifacts caused by objects extending outside the scan field of view. Med Phys 27(1):39–46

Racadio JM, Babic D, Homan R et al. (2007) Live 3D guidance in the interventional radiology suite. AJR Am J Roentgenol 189(6):W357–364

Spreafico C, Marchiano A, Mazzaferro V et al. (1997) Hepatocellular carcinoma in patients who undergo liver transplantation: sensitivity of CT with iodized oil. Radiology 203(2):457–460

Sze DY, Strobel N, Fahrig R, Moore T, Busque S, Frisoli JK (2006) Transjugular intrahepatic portosystemic shunt creation in a polycystic liver facilitated by hybrid cross-sectional/angiographic imaging. J Vasc Interv Radiol 17(4):711–715

van de Kraats EB, van Walsum T, Kendrick L, Noordhoek NJ, Niessen WJ (2006) Accuracy evaluation of direct navigation with an isocentric 3D rotational X-ray system. Med Image Anal 10(2):113–124

Vanderschelden P, Flandroy P, Dondelinger RF, Martin D, Lenelle J (1998) Comparative evaluation of cerebral aneurysms with selective arterially enhanced CT and DSA. Eur Radiol 8(7):1181–1186

Vogl TJ, Balzer JO, Mack MG, Bett G, Oppelt A (2002) Hybrid MR interventional imaging system: combined MR and angiography suites with single interactive table. Feasibility study in vascular liver tumor procedures. Eur Radiol 12(6):1394–1400

Wiesent K, Barth K, Navab N et al. (2000) Enhanced 3-D-reconstruction algorithm for C-arm systems suitable for interventional procedures. IEEE Trans Med Imaging 19(5):391–403

Part IV
Economics in Interventional Radiology

Quality Management in Interventional Radiology

17

Joachim Ernst Wildberger

Contents

17.1 Introduction

Quality in everyday life and business, engineering and manufacturing is defined as "the non-inferiority, superiority or usefulness of something" (http://en.wikipedia.org/wiki/Quality 2008).

The first question that might come up with this rather theoretical definition is whether a quality management (QM) is really needed for interventional radiology. The answer to that question – from my side – certainly is "yes". Each of us has faced situations where a certain device was needed and was not available at that time. Subsequent searching, nervous acting and even misunderstanding may lead to hazardous situations and will endanger the patient. Another example out of the clinical practice is the misunderstanding between the referring physician and the interventional radiologist by not following standardized pathways; e.g. a certain laboratory test is requested in the forefront of the procedure and personally addressed. On the day of the intervention, the results of the test are not available and the colleague is not on duty. Therefore, the whole procedure has to be postponed, or the intervention will become some kind of a risky "off-label procedure".

One of the primary ambitions of QM is to set up standards, e.g. by establishing "standard operating procedures (SOP)" or clinical pathways. Standardization is helpful in many respects: It facilitates comparability, appropriate treatment and reporting as well as effective communication. This may lead to an effective usage of time and will improve the cost-benefit ratio. A critical incident reporting system (IRS) might be useful as well. For instance, the latter is implemented in nuclear power plants, aviation and the North American Search Authority (NASA). It increases awareness of actual and potential problems, even before harmful events and critical endpoints for the patient are met. On the other hand, however, the variety and complexity of human conditions make it impossible to always reach the most appropriate diagnosis or to predict with certainty a particular response to treatment (American College of Radiology 2005). Nevertheless, internal review and structured audits will help to understand potential risks and lead to further optimization of workflow issues. Therefore, QM is a prerequisite in modern radiology.

Probably everyone is practicing QM, even without trying to get to the bottom of the question. Most of us do procedures according to an (individual) guideline. According to Donabedian (Donabedian 1980) three objective dimensions always have to be met:

1. Quality of structure
2. Quality of process
3. Quality of outcome

Mahnken/Ricke (Eds.), *CT- and MR-Guided Interventions in Radiology*

Major interventional radiological societies like the "Society of Interventional Radiology (SIR)" and the "Cardiovascular Interventional Radiological Society of Europe (CIRSE)" have published practical guidelines and standards of clinical practice on the web (http://www.sirweb.org/clinical/all.shtml 2008; http://www.cirse.org/index.php?pid=88#1 2008). Standards of practice are currently available on different issues for imaging-guided interventions. It should be stressed that these guidelines have to be adapted individually according to the local facilities and profiles, as these are some kind of "minimal consensus". Some recommendations deal with this issue in a comprehensive manner, e.g. establishing a quality assurance program in vascular and interventional radiology (Society of Interventional Radiology Standards of Practice Committee 2003) and establishing a general practice guideline for interventional clinical practice (American College of Radiology 2005). Other standards refer to terminology and reporting criteria for radiofrequency ablation and renal cell carcinoma (Goldberg et al. 2005; Clark et al. 2006), the quality improvement guidelines for percutaneous nephrostomy (Brountzos 2008), quality improvement guidelines for adult percutaneous abscess and fluid drainage (Bakal et al. 2004) as well as for image-guided percutaneous biopsy in adults (Cardella et al. 2003).

Evidence-based medicine will play an important role; however, there is also a tendency for too much evaluation, with a new term arising, the so-called "evaluitis" (http://papers.ssrn.com/sol3/papers.cfm?abstract_id=914123 (2008)). Therefore, the main goal is to keep it simple, rational and productive. Applying the triad of structure, process and outcome according to Donabedian (1980) is one of various possible approaches to QM that should be applied also to interventional radiology.

17.2 Quality of Structure

Quality of structure describes all infrastructural measures in an interventional radiology department. One striking example is the organization of logistics, which is particularly complex due to the broad variability of medical devices needed for interventional procedures. A standardized logistic division and stock-keeping is advantageous for all kinds of interventions. Even staff members without expert knowledge will profit from SOPs and the computer-based supply of materials under emergency conditions. In addition, an intelligent stock-keeping will provide information such as remaining periods of use and adequate stockage on the basis of a valid estimate. Compiling emergency kits with the necessary interventional devices are modules that have delivered an optimal performance in practice, e.g. for abscess drainage procedures and aortic interventions. Customized checklists with the individual preferences are favorable, and should be updated on a regular basis.

Setting up individual SOPs again works best in a team approach, with technicians, interventional radiologists and all other member of staff available that are responsible for the patient. A decision tree in terms of good medical practice avoids time consuming discussions and may serve as a guiding line for less experienced colleagues, e.g. for on-call procedures.

17.3 Quality of Process

At first the indication for the intervention should be checked. Usually imaging diagnostics, the clinical course of the patient and all additional information available (laboratory tests, previous results, etc.) form the basis for a rational decision-making ("assessment" and "decision to treat"). Especially cross-sectional image guided procedures have profited from the tremendous technical development over the past years. Complex and challenging procedures have become technically feasible on the basis of 3D-data acquisition. A standardized examination protocol will guarantee a consistent image quality and will allow for proper decision. This course of action is nearly indispensable for follow-up studies in interventional oncology. Standardization of contrast material (CM) delivery as well as standardization of the examination protocol are the real challenges in clinical routine. Therefore, you first have to agree on whether CM is needed or not. If you are going to administer CM, for instance, you will check for the appropriate CM itself, the optimal amount, the flow rate and delay for the scanning procedure. Different examination phases, e.g. late-arterial phase, portal-venous phase, late phase scanning as

well as perfusion studies (4D-studies) will be selected according to the clinical request given.

Nowadays, the usage and the specification of an interventional procedure will be discussed by an internal review board, for instance a tumor board or a local reference centre for certain diseases. It is the responsibility of the interventional radiologist to advice the other members of the committee. Opportunities and potential drawbacks of the anticipated technique should be reflected so that the best decision for the individual patient can be put on a firm footing (central question: Is there enough evidence in order to allow for a clear cut indication management that meets objective criteria (treatment selection)?

Also the anticipated pathology is of major importance, as this will influence the intervention itself; e.g. a core biopsy will be mandatory if a lymphoma is the most likely diagnosis, while a fine-needle aspiration biopsy will be adequate for suspected bronchial cancer (Böcking 1991).

The patient's informed consent has to be taken in the forefront of the intervention, usually requiring a written education. A pre-printed *standardized* form can be used as a starting basis for an *individual* preoperative interview and customizing. The whole spectrum of therapeutic options including interventional diagnostics and therapy should be reflected from this perspective as well ("patient related factors").

When it comes to the procedure itself, one has to consider that interventional radiology is an individual and interactive supply of service. Therefore, the demands and personal skills of the interventional radiologist also have to be part of the process negotiation and delivery. To guarantee an acceptable quality of process the interventional procedure also needs to be performed in a standardized manner, according to the local conditions (imaging techniques, availability of staff, etc.) and the individual experience of the interventional radiologist. This also includes the management of the corporate and the individual knowledge within the interventional team (Fig. 17.1).

17.4 Quality of Outcome

Finally, the outcome of the interventional procedure should also be reflected and this type of policy must also be put into practice, e.g. by cross-checking the results. Typical questions that might be answered by a standardized questionnaire include:

- Has the anticipated pathology been met by the intervention?
- Must this type of policy also be put into practice, e.g. by cross-checking the results (anticipated pathology met)?
- Is additional imaging needed?
- Did the chosen method prove to be feasible in terms of outcome?
- Is another therapeutic option mandatory yet?
- Are there alternate options?
- Can the procedure itself be changed for the better?

A clear-cut responsibility assignment will optimize post-operative treatment and prevent patients from falling through the cracks (especially in oncologic patients). This ensures fulfillment in treatment and diagnostics with continuity and sustainability in patient management.

Many sequences of action have become established over time and are not dealt with critically any more. This is regarded problematic, as radiology and interventional options are substantially advancing over time. Therefore, prospective implementation of an individually customized QM profile usually starts with an analysis of the present situation.

17.5 Set-Up of Individual Guidelines

The following nine step proposition of quality aspects according to the "Joint Commission on Accreditation of Healthcare Organizations (JCAHO 1990)" might serve as a basis for further discussion if the reader wants to set-up an individual guideline for image-guided interventions or wants to reflect on the existing workflow within a department:

Accessibility of care: The ease with which patients can obtain the care that they need when they need it.

Appropriateness of care: The degree to which the correct care is provided, given the current state of the art.

Continuity of care: The degree to which the care needed by patients is coordinated among practitioners and across organization and time.

Effectiveness of care: The degree to which care (e.g. an interventional procedure) is provided in

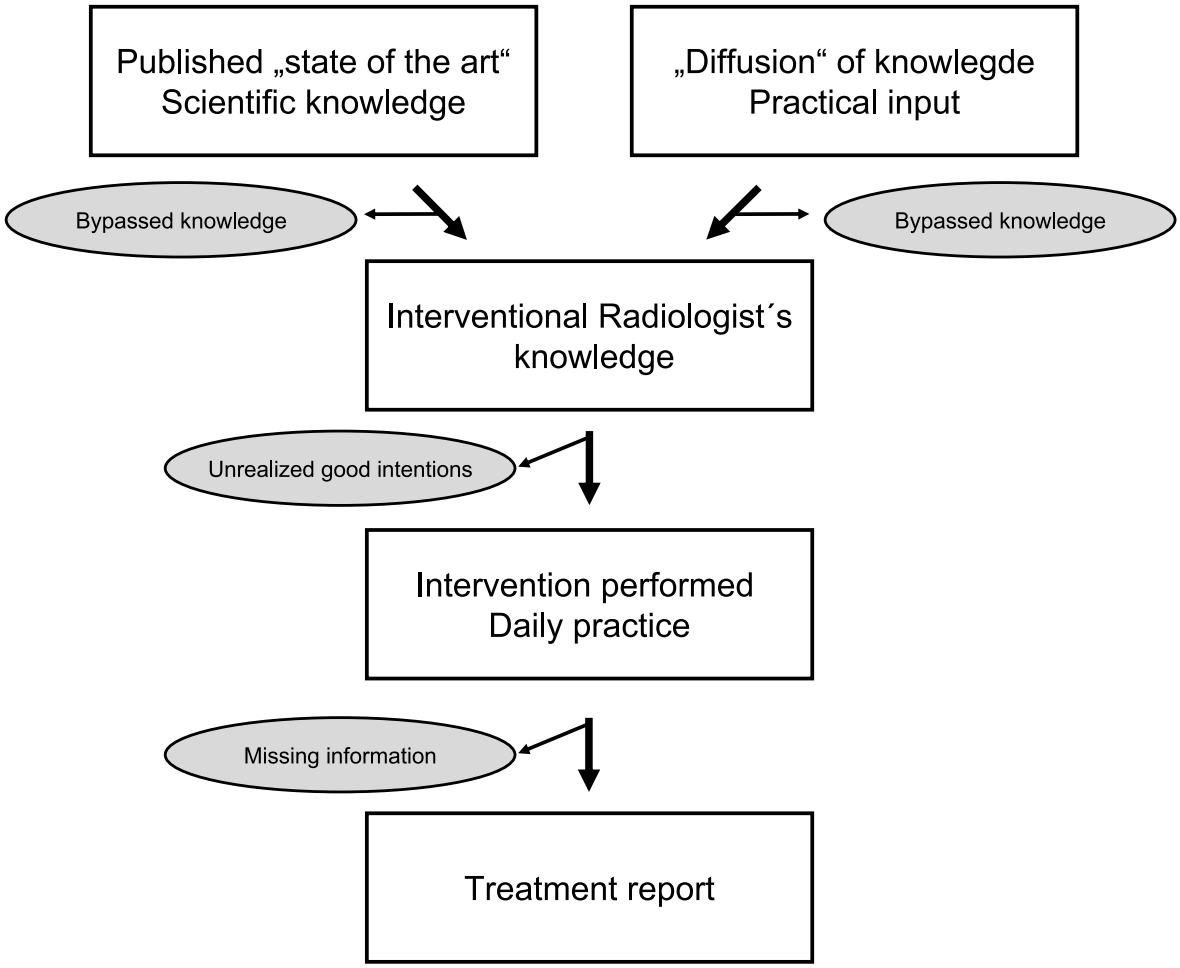

Fig. 17.1 Managing the explicit (e.g. literature) and the implicit knowledge (e.g. personal experience) is an inherent part of QM in interventional radiology

the correct manner given the current state of the art.

Efficacy of care: The degree to which a service has the potential to meet the need for which it was used.

Efficiency of care: The degree to which the care received has the desired effect with a minimum of effort, expense or wast.

Patient perspective issues: The degree to which patients (and their families) are involved in the decision-making processes in matters pertaining to their health, and the degree to which the care received has the desired effect with a minimum of effect, expense or waste.

Safety of the care environment: The degree to which the environment is free from hazard or danger.

Timeliness of care: The degree to which care is provided to patients when it is needed.

Standardization can also be achieved by an internal or external certification and helps to structure the specified pathway in the particular setting. Some of these certificates are valid throughout the US/Europe and even worldwide (http://www.efqm.org/ 2008; http://www.din.de/cmd?level=tpl-home&contextid=din 2008; http://www.jointcommissioninternational.org/ 2008).

Development of training charters for interventional radiology, including non-invasive vascular imaging,

diagnostic angiography/venography and vascular as well as non-vascular interventions, will be beneficial as well. Such guidelines have been set up, e.g. in a detailed curriculum for sub-specialty training by the European Society of Radiology (ESR Board 2005a,b). These might also serve as a good starting point for internal discussions, in combination with a proper definition of required technical, communication and decision-making skills.

Summary

In summary, prospectively organized quality management should become an integrated part of interventional radiology. Standardization as its primary tool will have valuable advantages: it makes examination techniques, procedures, outcome and the long-time course of the patients more comparable and will, therefore, be beneficial for interventional radiology in the long run. Moreover, QM establishes a beneficial link between the quality of the procedure and its efficiency. Therefore, QM has also important economic impact. Lapses in the standards of care may lead to harm to the patient and will be avoided in many cases by a functioning QM system. Completely unexpected errors, however, cannot be avoided in all cases. Finally, the main aim of risk management will be to reduce and, where possible, to safeguard the patient, the radiologist and the organization in which the radiologist works (ESR Board 2004).

Key Points

- Prospectively organized QM is needed in interventional radiology.
- The triad of structure, process and outcome is well suited to establish QM in interventional radiology.
- SOPs and clinical pathways are effective tools of QM that can also be used in interventional radiology.
- QM improves the clinical as well as the economic outcome of interventional therapy.

References

American College of Radiology (2005) American College of Radiology; American Society of Interventional and Therapeutic Neuroradiology; Society of Interventional Radiology. Practice guideline for interventional clinical practice. J Vasc Interv Radiol 16:149–155

Bakal CW, Sacks D, Burke DR, Cardella JF, Chopra PS, Dawson SL, Drooz AT, Freeman N, Meranze SG, Van Moore A Jr, Palestrant AM, Roberts AC, Spies JB, Stein EJ, Towbin R (2003) For the Society of Interventional Radiology Standards of Practice Committee. Quality improvement guidelines for adult percutaneous abscess and fluid drainage. J Vasc Interv Radiol 14:S223–S225

Böcking A (1991) Cytological vs histological evaluation of percutaneous biopsies. Cardiovasc Intervent Radiol 14:5–12

Brountzos EN (2008) Quality improvement guidelines for percutaneous nephrostomies. http://www.cirse.org/files/File/05_qig.pdf (access on: March, 2nd, 2008)

Cardella JF, Bakal CW, Bertino RE, Burke DR, Drooz A, Haskal Z, Lewis CA, Malloy PC, Meranze SG, Oglevie SB, Sacks D, Towbin RB (2003) For the Society of Interventional Radiology Standards of Practice Committee. Quality improvement guidelines for image-guided percutaneous biopsy in adults. J Vasc Interv Radiol 14:S227–S230

Clark TW, Millward SF, Gervais DA, Goldberg SN, Grassi CJ, Kinney TB, Phillips DA, Sacks D, Cardella JF (2006) For the Technical Assessment Committee of the Society of Interventional Radiology. Reporting standards for percutaneous thermal ablation of renal cell carcinoma. J Vasc Interv Radiol 17:1563–1570

Donabedian A (1980) Explorations in quality assessment and monitoring. Volume 1. The definition of quality and approaches to its assessment. Health Administration Press, Ann Arbor, Michigan

ESR Board (2004) Risk management in radiology in Europe. Publications and Media, IV, European Society of Radiology, Vienna

ESR Board (2005a) Interventional radiology. In: Detailed curriculum for the initial structured common programme. Publications and Media, VI, European Society of Radiology, Vienna, pp 28–30

ESR Board (2005b) Interventional radiology. In: Detailed curriculum for subspeciality training. Publications and Media, VI, European Society of Radiology, Vienna, pp 58–60

Goldberg SN, Grassi CJ, Cardella JF, Charboneau JW, Dodd GD III, Dupuy DE, Gervais D, Gillams AR, Kane RA, Lee FT Jr, Livraghi T, McGahan J, Phillips DA, Rhim H, Silverman SG (2005) For the Society of Interventional Radiology Technology Assessment Committee; International Working Group on Image-Guided Tumor Ablation. Image-guided tumor ablation: standardization of terminology and reporting criteria. Radiology 235:728–739

http://en.wikipedia.org/wiki/Quality (2008) (Access on: March, 2nd, 2008)

http://papers.ssrn.com/sol3/papers.cfm?abstract_id=914123 (2008) (access on: March, 2nd, 2008)

http://www.cirse.org/index.php?pid=88#1 (2008) (access on: March, 2nd, 2008)

http://www.din.de/cmd?level=tpl-home&contextid=din (2008) (access on: March, 2nd, 2008)

http://www.efqm.org/ (2008) (access on: March, 2nd, 2008)

http://www.jointcommissioninternational.org/ (2008) (access on: March, 2nd, 2008)

http://www.sirweb.org/clinical/all.shtml (2008) (access on: March, 2nd, 2008)

JCAHO (1990) Primer on indicator development and application. Joint Commission on Accreditation of Healthcare Organizations. One Renaissance Bvld, Oakbrouk Terrace, ILL

Society of Interventional Radiology Standards of Practice Committee (2003) Guidelines for establishing a quality assurance program in vascular and interventional radiology. J Vasc Interv Radiol 14:S203–S207

Cost Effectiveness in Interventional Radiology

18

Mathias Bosch

Contents

18.1 Introduction

Cost effectiveness is a term most medical doctors didn't know some years ago and some of them still don't! However, it will become more and more important in the future and physicians can no longer afford to leave this field to economists and controllers only!

In most other areas of life it is accepted that resources are limited and therefore a lot of effort is made to use it optimally, to "produce" at minimal costs. Only in medicine where the well-being (and sometimes indeed the life) of patients is at stake does this seem to be unethical whilst in fact it is unethical to waste resources thoughtlessly which are missing to treat another patient who much needs it.

Before we proceed, let me quickly explain what you can and cannot expect in this short chapter.

Certainly you will be disappointed if you just want to know whether, for example, radiofrequency ablation of the liver is cost-effective. The answer to this complex question depends on so many variables (such as: What other procedure do you compare it with? What are the local costs and outcomes of both procedures? What time horizon do you chose? At what rate do you discount future costs and health benefits?) that it just cannot be answered globally.

On the other hand you will learn:

- What the difference is between efficacy, effectiveness and cost effectiveness.
- What the definition of cost effectiveness is.
- An easy graphic model of cost effectiveness.
- What kind of resource allocations have to be identified, collected and valued.
- How the systematic cost calculation is done in the German DRG system.
- How important the point of view (society as a whole, sickness fund, hospital, private practice, patient) as well as the time horizon chosen is for the result of a cost effectiveness analysis.
- Why we have to discount future costs.
- Why models can help you in assessing cost effectiveness.
- How to ask the right questions.

Mahnken/Ricke (Eds.), *CT- and MR-Guided Interventions in Radiology*

18.2 Hurdles on the Way to the Market

Here are the three consecutive steps every pharmaceutical drug or interventional procedure normally has to go through:

1. The evaluation of a new procedure (or drug) starts with clinical studies to prove its *efficacy*. The patient group in those clinical studies on purpose is made very homogenous by strict inclusion and exclusion criteria. The question which can be answered after this step is: "Does it work?" Only if the answer to this question is a clear "yes" it will be approved and put on the market.
2. The evaluation typically continues with registries or all-comer studies to prove its *effectiveness*. This step is important in order to come closer to real world conditions. The patient population in this stage has to be as inhomogeneous as the patients a doctor sees every day. At the end it is clear, whether the intervention is effective, i.e. whether it works in regular patients under regular conditions (which among others also means "in the hands of average physician") and therefore has an advantage for them.
3. Only after these first two steps have been made successfully the question of *cost-effectiveness* (or efficiency) comes up. Now the question to be answered is: "How much effect do we get at what cost?" Unfortunately, for most interventions, valid data on cost-effectiveness in real-world patients are still lacking, but much needed.

It is the constant price pressure of every national healthcare system (due to various factors such as an aging population, costly innovations, less revenue of the sickness funds due to unemployment in countries where their revenue is defined as a percentage of wage) that put cost effectiveness on the forefront of health political discussions with organizations like NICE (National Institute for Health and Clinical Excellence) in the UK or IQWiG (Institut für Qualität und Wirtschaftlichkeit im Gesundheitswesen) in Germany. For them, cost effectiveness is a means of ensuring that the least cost interventions are utilized given the allocated budget. An economic evaluation informs what additional costs society has to spend for an additional improvement in medical benefits (Aidelsburger et al. 2007).

Clearly, policy makers cannot and should not scrutinize every minor change in medical practice. In the United States, the Centers for Medicare and Medicaid Services (CMS), for example, reserves its national coverage determinations for types of technologies that (Hollingworth and Jarvik 2006):

1. Affect a large number of beneficiaries.
2. Represent a significant medical advantage.
3. Have a potential for rapid diffusion or overuse.
4. Are subject to substantial controversy.
5. Local carriers have inconsistent coverage policies for.

It is generally accepted that minimally invasive procedures such as they are performed in interventional radiology do have many advantages in comparison to, e.g. open surgery. This is true for the patient (less trauma, shorter stay in hospital, quicker recovery), the sickness fund (shorter stay in hospital, sooner back to work), and the hospital/doctor, if adequately reimbursed (good image, high patient satisfaction). Therefore, their number is growing in virtually all medical fields. However, according to evidence based medicine, their superiority needs to be shown in well made cost effectiveness studies.

18.3 Definition of Cost-Effectiveness

Since there are various similar terms, let's start by defining what cost-effectiveness is. Cost-effectiveness analysis (CEA) is a form of economic analysis that compares the relative expenditure (costs) and outcomes (effects) of two or more courses of action (Wikipedia 2007). It is important which procedure is chosen as the comparator: this can be the most frequently performed procedure, the most effective or the most cost-effective procedure. Sometimes it is also essential to compare a new procedure to doing nothing ("watchful waiting" as, e.g. in the case of prostate cancer).

The difference between the effects (E) of an intervention (I) and an alternative intervention (A) in relation to the difference of cost (C) results in the incremental cost-effectiveness ratio (ICER) (Drummond et al. 1997; Gold et al. 1996):

$$\mathrm{ICER} = (C_I - C_A)/(E_I - E_A) \qquad (1)$$

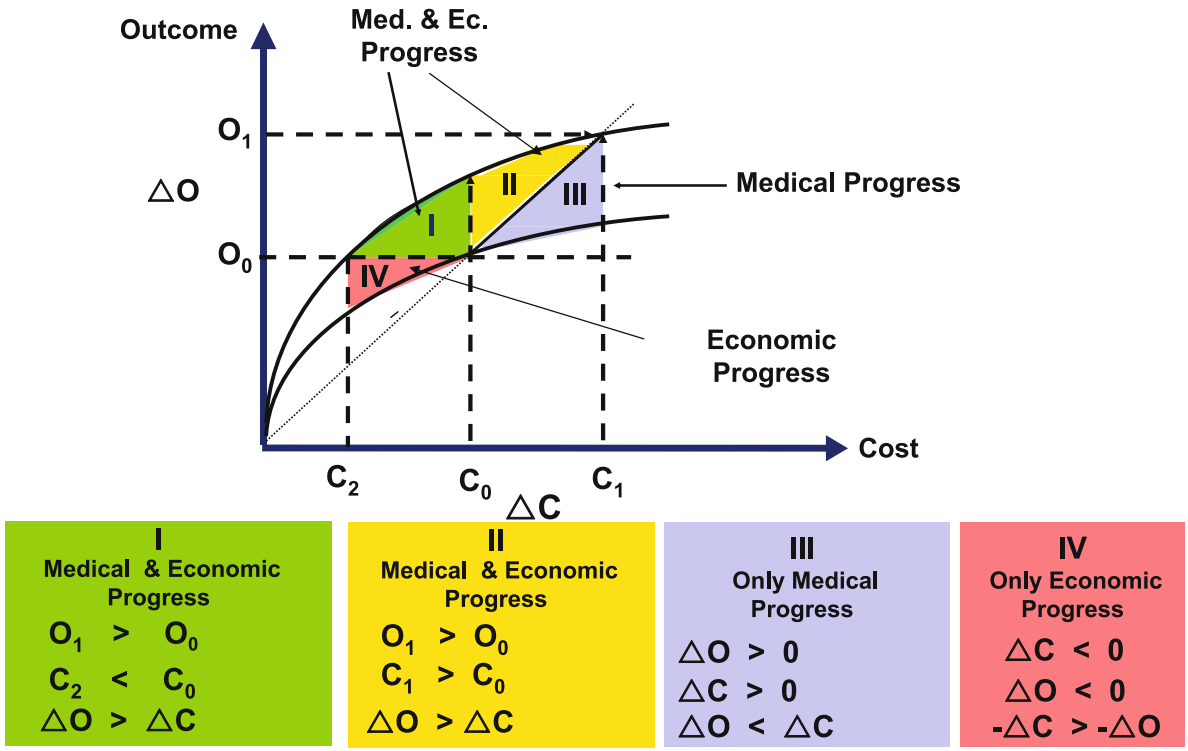

Fig. 18.1 Model of cost-effectiveness: the two production functions (*upper one*: with the innovation; *lower one*: conventional procedure for comparison) show the relationship between the different inputs (i.e. costs, C) and the outcomes (O) of the intervention. I = "ideal situation"; II = typical "cost effective" innovation; III = typical "costly" innovation; IV = only economic progress (modified according to Bundesverband Medizintechnologie e.V. 2003)

The four general results which a cost-effectiveness analysis can potentially have are illustrated in Fig. 18.1. The two production functions show the relationship between the different inputs (i.e. costs, C) and the outcomes (O) of the intervention.

I – "Ideal situation" which probably is rare in the real world. The new procedure (blue curve) is a medical progress since its outcome (O_1) is higher (better) than the outcome of the compared procedure (O_0). At the same time, it is also an economic progress since its costs (C_2) are lower than the costs of the compared procedure (C_0).

II – Typical "cost effective" innovation. Again, it is a medical progress since its outcome (O_1) is higher (better) than the outcome of the compared procedure (O_0). However, this time there is a price to pay for this progress, its costs (C_1) are somewhat higher than the costs of the compared procedure (C_0). Please note that additional outcome is greater (*above* the 45° line) than the additional costs ($\Delta O > \Delta C$). Such a procedure should be acceptable to most health-economists.

III – Typical "costly" innovation. Here we have almost the same situation as in case No. II: a higher outcome ($\Delta O > 0$) at higher costs ($\Delta C > 0$). The minor however important difference is that the additional outcome is smaller (*below* the 45° line) than the additional costs ($\Delta O < \Delta C$). Such a procedure will be looked at very intensely by health-economists who will ask: Should we pay this higher price for this amount of better outcome or should be better spend this money in other fields where we can get more additional outcome for it?

IV – Only economic progress. Here is a result not many physicians and patients will like: The outcome is worse ($\Delta O < 0$)! Why then is it still considered to be an economic progress? Simply because costs are more reduced that outcome ($-\Delta C > -\Delta O$). In cases of very scarce resources

one therefore might decide to go for a procedure which "only" brings economic progress.

18.4 What Kind of Resource Allocations Have to Be Identified, Collected and Valued?

If we look at the costs of an intervention, the challenge is to identify, measure and value all resources which are needed for a certain intervention. Obviously there are various groups of costs as far as the time is concerned: costs incurred before the intervention (e.g. before hospital), in hospital, after hospital. The same applies to the various benefits. The general difficulty of collecting cost/benefit data is partly due to that fact. If a country (like Germany) has two totally separated sectors, hospitals (inpatient) and private practices (outpatient), the task of collecting cost data becomes almost impossible.

Costs and benefits may be separated in direct and indirect costs which can be divided in tangible and intangible. Figure 18.2 summarizes some (by far not exhaustive) examples of what costs and benefits we could think of.

On the other hand, there are various cost categories which you will have to look at when calculating the cost of a procedure:

- Material costs (such as implants, catheters, contrast medium, etc.)
- Drugs
- Labor costs (time of physicians, assistant medical technicians, nurses, etc.)
- (Virtual) renting costs of, e.g. a computed tomography (CT) or magnetic resonance (MR) scanner
- Overhead costs (e.g. for the hospital administration)

If you don't restrict your view to the time in hospital you might also have the following costs:

- Future medical costs that are a consequence of the intervention (such as certain medication the patient has to take for a certain time or adjuvant medical devices such as crutches or a wheelchair).
- Rehabilitation.
- Medical treatment in private practice.
- Lack of work due to sick certificate (indirect cost).
- Home care by professionals or family members (indirect cost).
- Invalidity pension (indirect cost).
- Time losses from activities which might not receive a wage, but which may be valued by society or the individual none the less (intangible cost).

There is one more outcome parameter which needs to be measured (by questionnaires which have proven their effectiveness such as the SF-36): quality of life (QoL) (Ware and Sherbourne 1992). It is obvious that one of the main advantages of (minimally invasive) interventional radiology is that QoL in most cases should be better than in the case of open (and more invasive) surgery.

But how can you measure and compare the lifetime gained by different procedures if the QoL is different because of the different procedures (e.g. bypass vs percutaneous coronary intervention). The answer is quality-adjusted life years, or QALYs, a way of measuring both the quality and the quantity of life lived, as a means of quantifying the benefit of a medical intervention. They are based on the number of years of life that would be added by the intervention. Each year in perfect health is assigned the value of 1.0 down to a value of 0 for death. If the extra years would not be lived in full health, for example if the patient would lose a limb, or be blind or be confined to a wheelchair, then the extra life-years are given a value between 0 and 1 to account for this (e.g. major stroke ~ 0.35, post-MI ~ 0.683). The calculation of QALY therefore depends on the health state (QoL score) and time spent in that state.

Example:

- 1 year in perfect health = 1 QALY
- 1 year after major stroke = 0.35 QALY
- 0.5 year in perfect health + 0.5 year dead = 0.5 QALY

QALYs are used in cost-utility analyses to calculate the ratio of cost to QALYs saved for a particular health care intervention. This is then used to allocate healthcare resources, with an intervention with a lower cost to QALY saved ratio being preferred over an intervention with a higher ratio. This method is controversial because it means that some people will not receive treatment as it is calculated that cost of the intervention is not warranted by the benefit to their quality of life. However, its supporters argue that, since health care resources are inevitably limited, this method enables

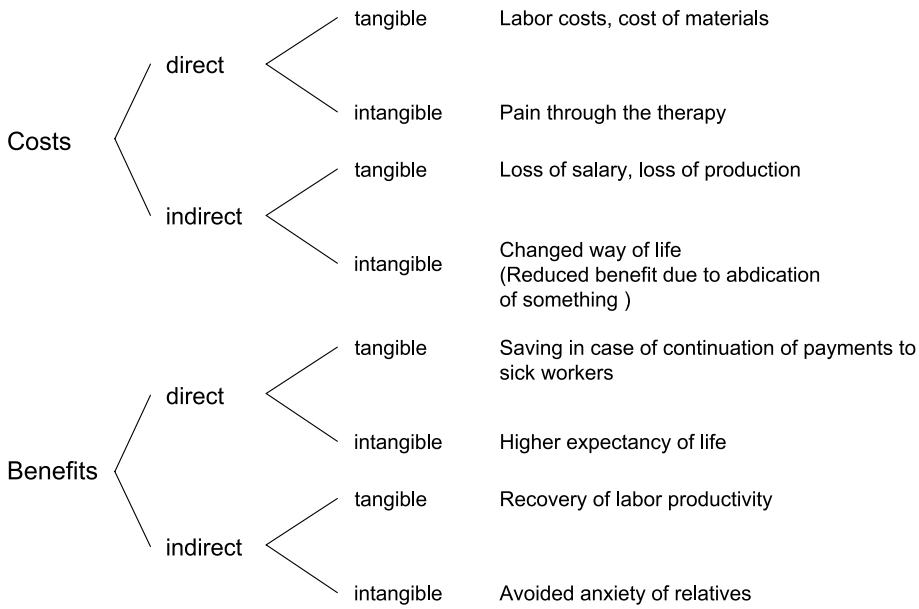

Fig. 18.2 Various costs and benefits (Ujlaky 2005)

them to be allocated in the way that is most beneficial to society.

The meaning and usefulness of QALY is debated for some other reason too. Perfect health is hard, if not impossible, to define. (The WHO has tried to do so but its definition is of no practical use.) Some argue that there are health states worse than death, and that therefore there should be negative values possible on the health spectrum (indeed, some health economists have incorporated negative values into calculations). Determining the level of health depends on measures that some argue places disproportionate importance on physical pain or disability over mental health. The effects of a patient's health on the quality of life of others – caregivers, family, etc. – also do not figure in these calculations.

18.5 Systematic Cost Calculation in the German DRG System

The various kinds of costs become much more practical if we look for a moment at the German DRG system where costs are calculated every year anew.

Although relatively new and "imported" from Australia, the German DRG (diagnosis related groups) system which is mandatory for all German acute hospitals is already rather refined and (in contrast to, for example, the USA and Italy) updated every year. The basis for cost calculations are about 250 hospitals which collect their full year cost data (according to the specifications of a detailed calculation handbook) and give it to the German DRG institute (called InEK). InEK makes a quality check, annually calculates the roughly 1000 various DRGs and publishes the aggregated data afterwards.

Let's demonstrate this point with radiofrequency ablation of the liver. In 2007 this leads to the DRG H41A (Table 18.1) if the patient has so many side diagnoses that he has a PCCL (patient clinical complexity level, i.e. the total weight of all his side diagnoses) of 4.

The different columns show the different cost categories:

1. Doctors
2. Nurses
3. Assistant medical technicians
4. Drugs
5. Implants
6. Other medical equipment
7. Medical infrastructure
8. Non-medical infrastructure

Cost categories 1–3 obviously are labor costs, 4–6 are material costs, 7 and 8 are a mixture of both.

Table 18.1 Cost matrix of the DRG H41A (InEK 2007)

	Labor costs			Cost of materials				Labor and material		
Cost Center	Physicians 1	Nurses 2	Medical/technical assistants 3	Drugs 4	4b	Implantats/ transplants 5	Other medical demand 6a	6b	Med. infra-structure 7	Non-med. infrastructure 8	Total
01. Normal ward	422.82	1021.35	100.78	149.4	67.93	0	96.19	18.43	189.64	802.71	2869.26
02. Intensive care	36.67	95.69	4.67	18.3	4.83	0.14	16.55	0.65	10.93	34.23	222.66
04. Operating room	18.06	0	18.83	0.94	0.06	4.4	15.4	3.13	6.14	10.93	77.9
05. Anesthesia	15.73	0	10.93	1.33	0.02	0	3.37	0.06	1.29	3.76	36.48
07. Cardilogic diagnosis/therapy	1.37	0	1.39	0.06	0.03	0.66	0.38	0.42	0.26	0.65	5.22
08. Endoscopic diagnosis/therapy	185.31	0	195.71	11.4	4.44	26.68	119.38	26.34	58.74	108.13	736.15
09. Radiology	**62.9**	**0**	**87.22**	**1.67**	**0.12**	**10.69**	**37.81**	**36.06**	**41.31**	**56.72**	**334.49**
10. Laboratories	25.82	0	128.97	4.26	45.96	0	98.52	17.54	12.68	46.59	380.34
11. Other diagnostic and therapeutic areas	60.51	0.65	93.08	3.04	0.06	0.45	15.32	7.98	12.68	38.5	232.26
12. Basic cost center	0	0	0	0	0	0	0	0	0	309.06	309.06
Total	**829.19**	**1117.69**	**641.58**	**190.4**	**123.45**	**43.02**	**402.92**	**110.61**	**333.67**	**1411.28**	**5203.82**

The different lines outline the various *cost centres*:

1. Regular ward
2. Intensive care unit
3. Operating room
4. Anesthesia
5. Cardiologic diagnosis and therapy
6. Endoscopic diagnosis and therapy
7. Radiology
8. Laboratory
9. Other diagnosis and therapy
10. Basic cost centre

Total costs of the DRG add up to € 5203.80, € 334.50 of this being in radiology.

Despite the fact that this DRG (called "Complex therapeutic ERCP with extremely severe clinical complexity or photodynamic therapy") contains many more patients than just those who received a radiofrequency ablation of the liver, these costs are considered more and more as norm costs. The consequence is that many heads of radiology departments in Germany are confronted with the norm costs of their department given all the various DRGs of a hospital. This figure is then compared with the actual costs of the radiology department in order to assess its overall "cost-effectiveness".

A rough calculation of all DRGs (weighting the costs of each DRG with its number in the calculation data) shows this picture (own data on file): the cost of radiology (cost centre No. 9) in 2007 was € 206 000 000 representing 3.8% of all costs € 5 400 000 000. Since in 2006 the percentage was 3.5% and in 2008 4.0%, this percentage seems to be pretty stable although slightly rising.

18.6 The Importance of the Point of View and the Time Horizon of a Cost-effectiveness Analysis

Although it is useful in cost-effectiveness analyses to take the overall societal point of view in evaluating alternative allocations of health resources (i.e. by measuring aggregate health cost and aggregate health benefits across all members of society), it is also important that the particular objectives of the actual decision maker be considered. For example, total costs

might be of concern to a sickness fund or health maintenance organization, whereas only in-hospital costs might concern a hospital administrator receiving a certain DRG reimbursement. Society as a whole bears all the costs, whether through insurance premiums or out-of-pocket payments, but the organizations and individuals who actually make resource-allocation decisions usually have varying objectives that should be recognized in a realistic cost-effectiveness analysis (Weinstein and Stason 1977).

It is also vital to choose the right time horizon for the study. As all effects and costs related to an intervention should be included into the economic evaluation, a long-term time horizon for the evaluation might become necessary. In these cases the usage of data from randomized clinical trials (RCT) are not sufficient (even if they should contain cost data) as they usually do not cover this long-term time horizon for cost containment reasons. Mathematical models which utilize data from different sources can be applied to overcome this limitation.

The importance of the time horizon chosen can be easily illustrated by the following example. If you compare the cost effectiveness of an arrhythmic drug with the cost-effectiveness of a pacemaker or internal defibrillator, no doubt the drug will be superior in a short time frame. However, if you set the end point of the study at 7–8 years, the result might be the opposite. (Aidelsburger et al. 2007)

A totally different question to cost-effectiveness is whether the costs of an intervention (the total stay of a patient in hospital) are adequately reimbursed.

Literature about the cost-effectiveness of certain interventions is not easily found; the number of patients included is generally too low (e.g. 7 and 6 respectively in a study comparing the cost of MRI-guided laser ablation and surgery in the treatment of osteoid osteoma) and its quality is not satisfactory (Ronkainen et al. 2006). Blackmore and Smith (1998) have evaluated the methodological quality of economic analyses of radiological procedures published in the non-radiology medical literature during the years 1990–1995. Of the 56 articles, only 8 (14%) conformed to all 10 methodological criteria:

1. Comparative options stated
2. Perspective of analysis defined
3. Outcome measure identified
4. Cost data included
5. Source of cost data stated
6. Long term costs included
7. Discounting employed
8. Summary measure provided
9. Incremental computation method used
10. Sensitivity analysis used

One of the peculiarities in comparison to clinical studies is that cost-effectiveness studies should be national (since the healthcare systems and their incurred costs vary so much across different countries) and recent (since prices vary considerably over time).

This can be demonstrated by a recent cardiologic cost-effectiveness study (Brunner-La Rocca et al. 2007) from Switzerland which was intended to find out whether in percutaneous coronary interventions and stenting the use of drug-eluting stents (DES) instead of bare metal stents (BMS) is cost effective. They found that overall costs were higher for patients with drug-eluting stents (€ 11 808) than for patients with bare-metal stents (€ 10 450) due to higher stent costs. They calculated an incremental cost effectiveness ratio (ICER) of € 64 732 to prevent one major adverse cardiac event and stated that an unrealistic reduction of the cost of DES of about 29% would have been required to achieve the arbitrary threshold ICER of € 10 000. Sounds logical; however, what prices did they assume? Swiss list prices of 2004 are certainly more that 29% higher than, for example, present DES prices in Germany. Therefore, their findings are only valid for Switzerland in 2004 and cannot be extrapolated to all of Europe, let alone across the whole world.

18.7 Why We Have to Discount Future Costs

In finance and economics, discounting is the process of finding the present value of an amount of cash at some future date. To calculate the present value of a single cash flow, it is divided by one plus the interest rate for each period of time that will pass. If we assume a 12% per year interest rate, the present value of € 100 that will be received in five years time is only about € 56.74. Therefore, a procedure which incurs exactly the same costs as an alternative proce-

dure – but does it at a later point in time – is more cost effective.

However, not only do costs have to be discounted. Benefits have to be discounted too for at least three reasons (Cairns 2001):

- Diminished marginal utility (in the temporal context).
- The risk that, whether as a result of death or some other circumstances, future consumption opportunities may not be available.
- Individuals simply have a preference for earlier consumption compared to later consumption.

18.8 Why Models Can Help You in Assessing Cost Effectiveness

Economic evaluations (such as cost effectiveness) depend on the evidence on cost and health effects of medical and public health interventions. This evidence can be derived from clinical studies, registries, meta-analysis, databases, administrative records (e.g. from sickness funds) and case reports. Of course the level of evidence found in these various sources is quite different.

Because the evidence required on consequences, cost of interventions is never present in a single source, and the time horizon of most clinical studies is far too short, practitioners of cost-effectiveness analysis use mathematical models to synthesize data on costs and benefits of alternative clinical strategies. Economic evaluations that have been piggy-backed on clinical trials often require almost as much modeling in order to extend the time horizon. If one fails to consider health and economic outcomes that may occur beyond the time frame of the observed data, there is an implicit assumption being made that all arms of the trial are equivalent.

A model makes explicit assumptions about the incidence and/or prognosis of a disease, the magnitude and duration of risks and benefits of prevention and/or treatment, the determinants of utilization of health care resources, and health related quality-of-life. Of particular value to clinicians and policy makers it that the models allow one to investigate how cost effectiveness ratios might change if the values of key parameters in a model are changed (Kunz and Weinstein 2001).

Models often used are decision trees (or probability trees), Markov models, and state-transition models (Gazelle et al. 2004). A decision tree has one decision node at the root. The branches of the initial decision node represent all interventions that are to be compared. Markov models are analytical structures that represent key elements of a disease and are commonly used in economic evaluations. They are particularly useful for diseases in which events can occur repeatedly over time such as acute myocardial infarction for patients with stable angina, or cancer recurrence. For more detailed information see Sonnenberg and Beck 1993.

In both cases there is a trade-off between building a complicated model that accurately reflects all the important aspects of a disease and its treatment, and building a simple model that is more transparent. At any rate, the input probabilities, utilities, and costs, as well as the key assumptions that underlie the model should be carefully documented.

Summary

Economic questions (such as cost-effectiveness of alternative procedures) become more and more important in medicine due to increasing pressure to curb health care costs. Every radiologist is well advised to open his mind to such questions and to start finding what the costs of his clinical pathway are. In countries with a fixed payment (DRG) per patient this is a must anyhow.

Learn how to ask the right questions when building up an interventional radiology program. These questions could be:

- What are the alternatives to my intervention (including wait and see)?
- What are the cost and the outcome of my intervention and the alternatives?
- What is the cost per QALY gained?
- What is the perspective of the patient, provider, payer, health maintenance organization, health care system, society?

Should the radiologist initiate a clinical study, it is generally a good idea to include cost data in order to be able to answer economic questions which might arise later. As with clinical studies, the design of which has improved over the last few years, so will cost effectiveness studies improve as more physicians become aware of the methodological standards of such studies.

Key Points

- Health economics become more and more important due to limited resources for health care.
- Cost-effectiveness analyses are generally complex studies requiring a multidisciplinary team with expertise in the clinical problem, clinical epidemiology, decision analysis, economics, and statistics.
- Collecting the various cost and asking the right questions is a reasonable first step.
- In order to improve our knowledge about the cost-effectiveness of interventional radiological procedures, cost data (and well made cost-effectiveness analyses) should be included in all future clinical studies.

References

Aidelsburger P, Grabein K, Klauss V et al. (2007) Cost effectiveness of cardiac resynchronization therapy in combination with an implantable cardioverter defibrillator (CRT-D) for the treatment of chronic heart failure from a German health care system perspective. Clin Res Cardiol 97:89–97

Blackmore CC, Smith WJ (1998) Economic analyses of radiological procedures: A methodological evaluation of the medical literature. Eur J Radiol 27:123–130

Brunner-La Rocca HP, Kaiser C, Bernheim A et al. (2007) Cost-effectiveness of drug-eluting stents in patients at high or low risk of major cardiac events in the Basel Stent KostenEffektivitäts trial (BASKET): an 18-month analysis. Lancet 370:1552–1559

Bundesverband Medizintechnologie e.V. (2003) Leitfaden für eine lokale und dezentrale Marktetablierung innovativer und neuer Medizinprodukte, Berlin

Cairns J (2001) Discounting in economic evaluations. In: Drummond M, McGuire A (eds) Economic evaluation in health care, merging theory with practice. Oxford University Press, Oxford, p 236

Drummond M et al. (1997) Methods for the economic evaluation of health care programmes. Oxford University Press, New York

Gazelle GS, McMahon PM, Beinfeld MT et al. (2004) Metastatic colorectal carcinoma: cost-effectiveness of percutaneous radiofrequency ablation versus that of hepatic resection. Radiology 233:729–739

Gold MR, Siegel JE, Weinstein MC (1996) Cost-effectiveness in health and medicine. Oxford University Press, New York

Hollingworth W, Jarvik JG (2006) Evidence on the effectiveness and cost-effectiveness of vertebroplasty: a review of policy makers' responses. Acad Radiol 13:550–555

InEK (2007) Institut für das Entgeltsystem im Krankenhaus. Homepage (http://www.g-drg.de). Report Browser 2005/2007, published Dec. 15, 2006

Kuntz KM, Weinstein MC (2001) Modelling in economic evaluation. In: Drummond M, McGuire A (2001) Economic evaluation in health care, merging theory with practice, Oxford University Press, Oxford, p 141

Ronkainen J, Blanco Sequeiros R, Tervonen O (2006) Cost comparison of low-field (0.23 T) MRI-guided laser ablation and surgery in the treatment of osteoid osteoma. Eur Radiol 16:2858–2865

Sonnenberg FA, Beck JR (1993) Markov models in medical decision making: a practical guide. Med Decis Making 13:322–338

Ujlaky R (2005) Innovations-Risikomanagement im Krankenhaus, Frankfurt/Main, p 133

Ware JE, Sherbourne CD (1992) The MOS 36-item short-form health survey (SF-36): conceptual framework and item selection. Med Care 30:473–483

Weinstein MC, Stason WB (1977) Foundations of cost-effectiveness analysis for health and mental practices. N Engl J Med 296:716–721

Wikipedia (2007): http://de.wikipedia.org/wiki/Hauptseite; search for "cost-effectiveness"

Building an Interventional Department

19

Jens Ricke

Contents

19.1 Introduction

Interventional radiology's unique selling point is non-invasive imaging and the ability of radiologists to understand better principles and technologies of image guidance as compared to specialists from other medical areas. During the past few decades, radiology has always been evolution-driven for the simple fact that, as soon as a radiological technology was suitable for routine use, it had to be defended against competing clinicians – often without success, e.g. in ultrasound, coronary arteriography, and likely even in magnetic resonance (MR) imaging. Hence, the key to survival of radiology is:

1. Continuous innovation in radiology which is only possible if key imaging technologies are best understood by radiologists.
2. Evidence-based data derived from GCP (good clinical practice) conformant studies performed by radiologists – proving their competence.
3. Enhanced clinical abilities and patient orientation by improved clinical training of radiologists.

Increasing problems in billing of radiological procedures by radiologists themselves are in some ways only symptoms, not necessarily the underlying cause. In interventional radiology, status today is as follows:

1. Interventionalists often separate themselves from general radiology; as a result, their competence in image guidance declines, and a decline of knowledge will inevitably ruin the ability to develop visions and vision-based research. Interstitial intervention is a good example – MR-intervention will definitely not be further developed in interventional radiology centers without general radiology knowledge.
2. More than 80% of publications in the field of angioplasty of the periphery are authored by cardiologists and angiologists. The small remaining portion is shared by vascular surgeons and radiologists. Randomized prospective trials designed and performed by radiologists are extremely rare. An objective observer (such as the ministry of health in your country) will easily draw his conclusion where the competence for intervention really is.
3. Waiting for the patient to be transferred by a surgeon, cardiologist or oncologist is deadly (see Sect. 19.2). Undoubtedly the key to success for an interventional radiologist is clinical competence, passion for the patient, an own outpatient department and beds in the hospital under his own full responsibility. In such a situation, optimal treatment for each individual patient may be and must be discussed between equal partners from various clinical faculties – which is not the case in a partnership of dependency.

Mahnken/Ricke (Eds.), *CT- and MR-Guided Interventions in Radiology*

19.2 Cost and Revenues

It is impossible to discuss extensively financial compensation in countries with different cultures of their health care system in the frame of this chapter. However, as a general statement, one may say that under the circumstances of a Diagnosis Related Groups (DRG)-based healthcare system, interventional radiology is extremely attractive since minimal-invasive interventions decrease the length of the hospital stay as well as cost driving associated morbidities. This leads to the situation that a variety of interventions may well be performed on an outpatient basis – a concept that is well supported by health care sponsors due to its cost effectiveness. However, material costs in interventional radiology are generally extensively higher than in competitive techniques such as open surgery. They are usually hard to balance against, e.g. much higher costs of the operation theatre needed by the surgeon. However, it is extremely helpful to prepare diligently costs and revenues of each specific intervention intended to be introduced in a hospital environment – in essence, support by the hospital administration will very much help to establish a successful interventional department, and all hospital administrations are financially driven.

19.3 Marketing and Motivation

The key to successful marketing is the key message to get across. This message can only be based on competence and optimal use of methods and techniques offered to the patients – by a competent physician, not a fancy machine. In addition, a patient-centered approach is usually easily sensed and well taken by help seeking patients – who in an interventional department tend to be well informed since many of them have found the interventional specialist through their own initiative. In that situation, previously mentioned aspects return in the game: presence and knowledge of evidence, as well as the possibility to discuss optimal treatment options with other clinicians among equals. Finally, to be very clear, the best motivation to build and run a successful interventional radiology department probably is honest passion to deliver the best treatment available for your patient – be it delivered by the interventional radiologist or anybody else.

Key Points

The following key points greatly help to make an interventional department successful:

- Interventional competence (including the unique selling point of radiologists: to better understand and use image guidance).
- Clinical competence (including the ability to manage your patients from the outpatient clinic until hospital discharge).
- Evidence-based, GCP-conformant data at hand (also generated by radiologists).
- No patient comes to be treated by a high tech machine. All patients I know want to be treated by a competent human being.
- Passion and care for the patient are success guarantors.

Index